Design and Synthesis of Novel Inhibitors of the p53-Mdm2 Interaction and the Development of Novel Inhibitors of Cyclin Dependent Kinases

Kevin Roy Bailey

The University of Edinburgh

A thesis submitted for the degree of Doctor of Philosophy

September 2004

Acknowledgements

I would like to take this opportunity to thank my supervisor Professor Nicholas J. Turner for his continual support, encouragement and optimism throughout my PhD studies. I'd also like to thank Drs. Peter Fischer, Daniella Zheleva and Shudong Wang at Cyclacel Ltd. for their help and guidance and for the opportunity to work on two extremely interesting projects. Many thanks also to Dr. Campbell McInnes who has provided remote tutoring and advice on visualizing some of the protein-ligand structures contained in this work. I'd like to acknowledge the University of Edinburgh and Cyclacel Ltd. for their funding during the period of my studies.

I would also like to express my thanks to the technical staff at the School of Chemistry, University of Edinburgh, in particular John Millar for NMR spectroscopy and Alan Taylor for mass spectrometry, both of whom were not phased when I approached them with large numbers of samples.

For making the last three years enjoyable and also for providing numerous useful suggestions, I'd like to thank past and present members of the Turner-Flitsch group, in particular Bface, The Pig and Tentacles for providing not so useful, but perhaps more amusing suggestions.

Finally, I'd like to thank my parents for their constant support and Claire, Ella and Emily for their love and helping me keep in touch with reality.

Abstract

The research contained in this thesis concerns two distinctly separate approaches to the design of novel drugs that can be used to treat cancer.

The disruption of the p53-Mdm2 interaction is an attractive therapeutic strategy for activating p53 tumour supressor activity in tumours expressing wild type p53. One such strategy for the disruption of the P53-Mdm2 interaction is the design of low molecular weight ligands that bind at the p53-Mdm2 interface. The molecular docking programme LIDAEUS has identified a sulfonamide scaffold that has the potential to bind at the p53-Mdm2 interface. Adopting a high-throughput, combinatorial chemistry approach, a number of sulfonamides and amides have been synthesized and screened *in vitro* for their ability to disrupt the p53-Mdm2 interaction.

Cyclin dependent kinases (CDKs) are important in cell cycle regulation as they control the transition between the four primary phases. The association of a cyclin dependent kinase with a cyclin subunit, and subsequent phosphorylation of the complex formed, is essential for CDK activity. Therefore, the design of ATP antagonists that inhibit the activity of CDKs is an attractive strategy for the treatment of proliferative disorders. Using microwave assisted organic synthesis, a high-throughput synthetic sequence has been developed to afford a series of 6-anilino-4-aryl-pyrimidines (**I**) that have been subsequently screened *in vitro* against a panel of kinases. Several of these compounds have been shown to be low micromolar inhibitors of the CDK2/cyclin E complex.

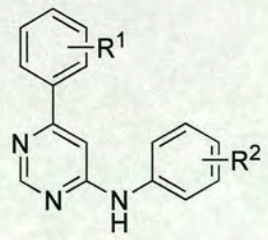

I

Abbreviations

Ac	acetyl
AC3C	1-amino-cyclopropanecarboxylic acid
ADDP	1,1-(azodicarbonyl)dipiperidine
AIB	α-amino isobutyric acid
ATP	adenosine triphosphate
Boc	*tert*-butoxycarbonyl
Bu	butyl
CDK	cyclin-dependent kinase
CKI	cyclin-dependent kinase inhibitor
d	doublet
DCM	dichloromethane
DEAD	diethylazodicarboxylate
DIPEA	*N,N*'-diisopropylethylamine
DMAP	*4-N,N*'-(dimethylamino)pyridine
DMF	*N,N*'-dimethylformamide
DMSO	dimethyl sulfoxide
EI	electron impact
ELISA	enzyme-linked immunosorbent assay
ES	electrospray
ESI	electrospray ionization
Et	ethyl
EtOAc	ethyl acetate
FAB	fast atom bombardment
FP	fluorescence polarisation
Hdm2	human double minute 2
HPLC	high performance liquid chromatography
KIP	kinase inhibitor protein
m	multiplet
Mdm2	murine double minute 2

Me	methyl
MeCN	acetonitrile
MS	mass spectrometry
NMM	*N*-methyl morpholine
NMR	nuclear magnetic resonance
PMP	phosphonomethylphenylalanine
ppm	parts per million
Pr	propyl
pRb	retinoblastoma protein
PS	polystyrene
q	quartet
R_f	retention factor
RT	room temperature
s	singlet
t	triplet
TFA	trifluoroacetic acid
THF	tetrahydrofuran
TLC	thin-layer chromatography
TMAD	*N,N,N,N*-tetramethylazodicarboxamide
TMS	tetramethylsilane
TOSIC	*para*-toluenesulfonic acid
t_R	retention time
UV	ultraviolet
v/v	volume per volume
w/v	weight per volume
wt	wild type

Table of Contents

1 An introduction to the p53-Mdm2 interaction

1.1 The cell cycle

In eukaryotic cells, the process of DNA replication and cell division follows a series of coordinated events known as a cell cycle. The cell cycle is composed of five distinct stages, as illustrated in Figure 1.1.

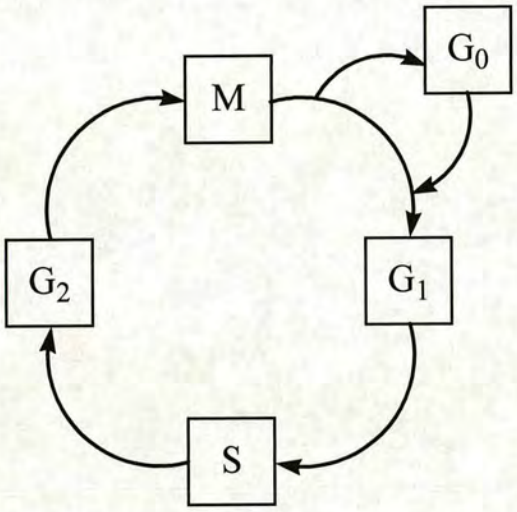

Figure 1.1: The cell cycle.

In each cell cycle, the chromosomes of the cell are replicated once in what is termed the synthesis phase (S-phase) and segregated, to create two genetically identical daughter cells during mitosis (M-phase). The interval between mitosis and synthesis is called the G_1 gap phase, and the interval between synthesis and mitosis is called the G_2 gap phase. Both gap phases are periods of cell growth and reorganisation, during which, various mRNAs and proteins are synthesized that are required for either DNA synthesis or mitosis. When a cell is in any phase of the cell cycle other than mitosis, it is often said to be in interphase. Cells can leave the cell cycle, either temporarily or permanently, exiting the cycle at G_1 and entering the G_0 phase, during which period the cell is often called 'quiescent'. G_0 cells can carry out their functions within the organism until they die. However, with proper stimulation, some G_0 cells can reenter into the cell cycle at the late G_1 stage and proceed onto new rounds of

alternating S phase and mitosis. Crucially, cancer cells cannot enter G_0 and therefore repeat the cell cycle indefinitely.[1]

The cell cycle is controlled by at least two mechanisms. The first mechanism of control involves a highly regulated kinase family called the cyclins.[2] Activation of a transiently expressed cyclin through association with a second protein subunit, a cyclin-dependant kinase (CDK), generates a complex with unique substrate specificity. Regulatory phosphorylation and dephosphorylation fine-tune the activity of the CDK-cyclin complex, allowing the progression of the cell through well-delineated transitions between cell cycle stages.[3] The cyclins and cyclin-dependent kinases are the subject of discussion in Chapter 3.

A second regulatory mechanism in the cell cycle involves cell cycle checkpoints that monitor completion of critical events such as DNA replication and chromosome segregation.[4] The primary cell cycle checkpoint is the restriction point at the G_1-S phase transition after which, the cell is generally committed to a further round of DNA replication and division. There is also a checkpoint at the G_2-M phase transition, which prevents cells with incompletely replicated or damaged DNA from entering mitosis.[5] The activation of these checkpoints causes a delay in cell cycle progression, thus averting the danger of mutation.

1.2 Oncogenes and tumour supressors

Human cancer can be defined as a disease that is characterized by deregulation of the cell cycle and increased genetic instability.[6] Two classes of genes, oncogenes and tumour supressors, play crucial roles in the development and progression of cancer. A proto-oncogene is a gene whose products function in signal transduction pathways that promote cell proliferation. The activation of proto-oncogenes, through genetic mutation, can promote or allow the uncontrolled growth of cancer.[7] Genetic mutations of oncogenes can be inherited or caused by an environmental exposure to carcinogens. A tumour suppressor is a gene whose function is to inhibit cell growth or proliferation. This can be achieved through cell cycle arrest and induction of

apoptosis. Although inactivation of both copies of a tumour suppressor gene is required for loss of function, mutation, inactivation or deletion of part or all of one allele of a tumour suppressor gene predisposes that individual to increased risk of tumour development because only one mutational event is required to prevent synthesis of any functional gene product.[3] Activation of proto-oncogenes that promote cell proliferation, and inactivation of tumour suppressor genes that inhibit cell proliferation leads to tumour formation, growth and progression.

This chapter will focus on the tumour suppressor gene p53; discussing its role in the cell cycle, highlighting its structure and provide an introduction to current strategies which target p53 with the aim of providing effective cancer therapy.

1.3 p53 and the cell cycle

1.3.1 The role of p53

The p53 protein was first identified as a cellular protein that could be immunoprecipitated with the simian virus 40 (SV40) large T-antigen.[8] The human p53 tumour suppressor gene encodes a 393 amino acid nuclear phosphoprotein that acts as a tetrameric sequence-specific DNA-binding protein that regulates the transcription of a number of genes involved in cell cycle arrest or apoptosis.[9] Wild type p53 (wt-p53) is present at low concentrations in normal cells, but, in response to cellular stress, such as DNA damage[10] or hypoxia,[11] p53 accumulates in the nucleus of cells where it is active.[12] The activation of p53 can lead to various responses, depending on the nature of the stress and the cell type, with a common aim to prevent damaged cells from proliferating and passing mutations on to the next generation.[13] The p53 protein can halt the progression of the cell cycle in both the G_1/S and G_2 checkpoints.

1.3.2 p53 regulation of the G_1/S checkpoint

Cell cycle progression is halted at the G_1/S checkpoint in response to DNA damage. After exposure of cells containing wild-type p53 to genotoxic agents, p53 is activated and transcriptionally upregulates the CDK inhibitor p21.[14] p21 can inhibit the binding of either cyclin and CDK subunits or the activated cyclin-CDK complexes that mediate G_1 phase progression, resulting in pRB hypophosphorylation. In its hypophosphorylated state, pRB binds to E2F to inhibit S phase entry. Once hyperphosphorylated, pRB releases E2F that results in the activation of genes required for S phase entry (Figure 1.2).[15]

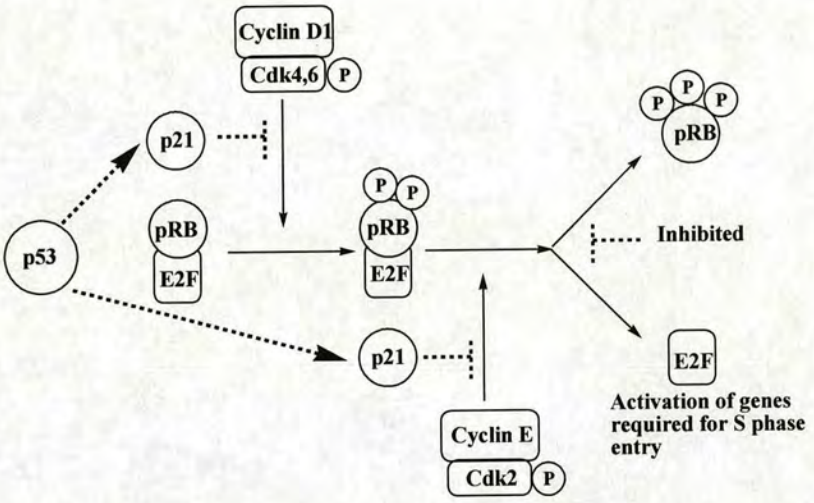

Figure 1.2: Regulation of the G_1/S checkpoint.

1.3.3 p53 regulation of the G_2/M checkpoint

During S and G_2 phases, cells accumulate the cyclin B1-Cdc2 complex in an inactive form due to inhibitory phosphorylations by Weel and Myt1 kinases. Cdc25c phosphatase mediates the conversion of Cdc2 from an inactive to an active form and, in doing so, stimulates mitosis. In response to genotoxic stress, the Chk1 and Chk2 kinases are activated and phosphorylate Cdc25c.[16] This phosphorylation promotes the interaction of Cdc25c with 14-3-3 adaptor proteins and inhibits the ability of Cdc25c to activate the cyclin B1-Cdc2 complex, resulting in cell cycle arrest at the

G_2/M checkpoint. Furthermore, in response to genotoxic stress, activated Chk1 and Chk2 also phosphorylate p53, resulting in stabilization and activation of the protein.[17] In turn, p53 activation upregulates the 14-3-3σ protein that causes G_2 arrest via sequestration of Cdc25c in the cytoplasm and G_2/M arrest due to inhibition of Cdc2 activity.[18] The transcription of p21 is also upregulated by p53.[14] P21 binds to cyclin-Cdk complexes to reduce the level of phosphorylation of pRB. Hypophosphorylated pRB sequesters E2F, and, in doing so, prevents E2F from mediating the biosynthesis of cyclin B1 and Cdc2 (Figure 1.3).[15]

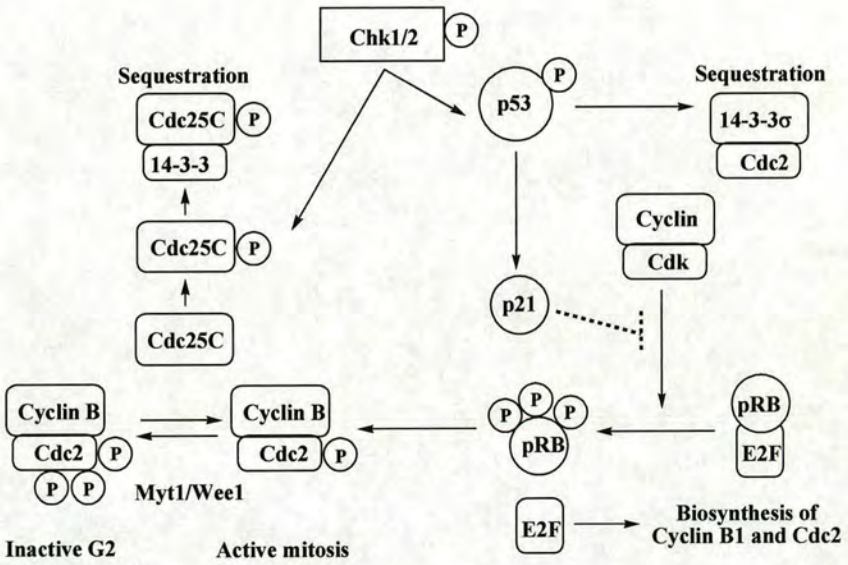

Figure 1.3: Regulation of the G_2/M checkpoint.

1.3.4 p53 and cancer

Most human cancers have a defect in the p53 pathway. Indeed, it has been reported that p53 is inactivated by mutations and other genomic alterations in about one half of all human cancer cases.[19] These genomic alterations include, for example, mutational inactivation of upstream activating enzymes of p53, or amplification of cellular or viral oncogenes responsible for the inhibition of the activity of p53.[20] Cells that lack functional p53 can accumulate mutations that favour the development of cancer as they are unable to respond appropriately to stress. *In vivo* studies in mice

have shown that inactivation of the Trp53 gene, which encodes p53, has no effect on the development of the mouse but renders it more prone to tumours, with death occurring in all cases within 10 months.[21] It has been shown that tumour derived p53 mutants are defective in DNA binding[22] and cannot function as a transcription factor.[23]

1.3.5 The structure of p53

The p53 protein can be divided into a number of domains, including the *N*-terminal transactivation domain;[24] the core DNA-binding domain;[25] a tetramerisation domain that facilitates sequence specific DNA binding;[26] and the C-terminal domain that is involved in regulation of the sequence-specific DNA-binding function.[27] The crystal structure of p53, resolved by Pavletich,[28] is shown in Figure 1.4.

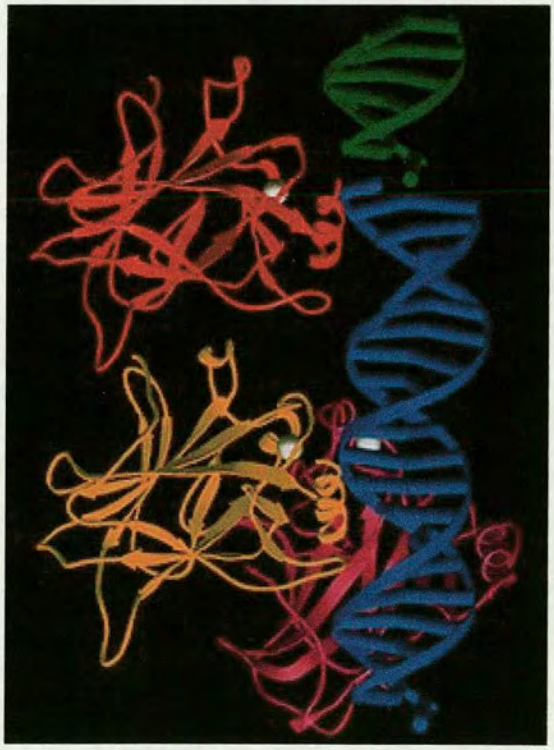

Figure 1.4: The crystal structure of a p53-DNA complex (PDB code 1TSR).[28]

Several *in vivo* phosphorylation sites have been mapped to the *N*- and *C*- termini of the p53 protein. A number of residues located in the core DNA-binding domain,

namely Arg175, Gly245, Arg248, Arg249, Arg273 and Arg282, are often mutated in human tumours.[28] These mutations destroy p53's sequence-specific DNA-binding activity, suggesting that this function is critical for tumour supression. A schematic of the structure of p53 is illustrated in Figure 1.5.

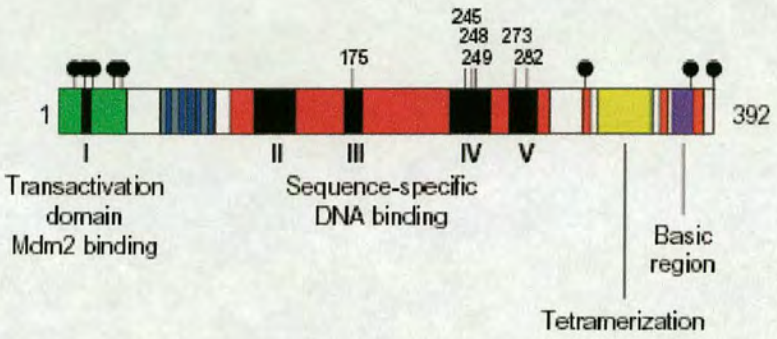

Figure 1.5: A schematic of the structure of p53.[29]

1.4 Mdm2

An important step in tumourgenesis is the targeting and inactivation of p53 by a number of viral oncogenes. The gene encoding Mdm2 (murine double-minute) was first identified on a mouse double minute chromosome.[30] Later, Mdm2 was rediscovered as a p53 binding protein in several transformed rat fibroblast cell lines overexpressing a mutant p53 protein.[31] The Hdm2 gene, the human homologue of Mdm2, encodes a 491-amino acid polypeptide that contains several functional domains, namely, a N-terminus which contains the p53 binding site and a DNA-dependent protein kinase (DNA-PK) phosphorylation site which can affect binding to p53;[32] an acidic domain; a zinc-binding domain; and a ring-finger domain at its *C*-terminus that can mediate protein-protein and protein-DNA interactions (Figure 1.6).[29] Hdm2 has been shown to be overexpressed in a number of human tumours, particularly sarcomas.[33]

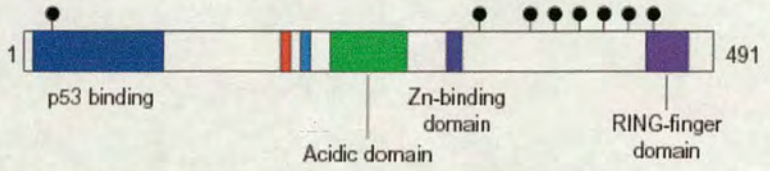

Figure 1.6: A schematic of the structure of Mdm2.[29]

1.5 Strategies to restore the tumour supressor activity of mutant p53

Restoring the tumour suppressor activity of mutant p53 can be achieved in a number of ways. Gene therapy with wt-p53 has been evaluated in both clinical and preclinical models.[34] Another strategy is the pharmacological rescue of mutant p53 function, although this strategy requires various approaches owing to the number of different mutations of the p53 gene. Studies have identified a number of second-site mutations in p53 that can suppress natural deactivating mutations,[35] and one approach would be to mimic these suppressor mutations with small-molecule pharmaceutical agents. A third strategy involves the mimicking of downstream p53-dependent gene products, such as p21,[14] to replace the tumour suppressor function of p53. Indeed, it has been reported that short peptides derived form the *N*- and *C*-terminal domains of p21 inhibit pRB phosphorylation and induce G_1/S growth arrest when introduced into cells through conjugation with a membrane-penetrating peptide.[36]

1.6 Strategies to increase the tumour supressor function of wild type p53

Strategies for activating the transcriptional activity of wild type p53, and in doing so its tumour supressor function, include inhibition of the nuclear export of p53; inhibition of Mdm2 ubiquitin ligase activity; and disruption of the Mdm2-p53 interaction.[37]

1.6.1 The p53-Mdm2 interaction

The binding site for Mdm2 on p53 has been mapped to a small region in the N-terminus of p53.[38] The binding of Mdm2 to p53, interferes with p53's transcriptional activity as it conceals the DNA-binding domain of the p53 protein.[39] Studies have shown that the interaction between p53 and Mdm2 forms an autoregulatory negative feedback loop, keeping the activity of p53 and levels of Mdm2 in a cell in balance. In healthy cells, wt-p53 stimulates the synthesis of Mdm2 which, in turn, through its binding to p53, inhibits the transcriptional activity and growth-supressing activity of p53.[40] Mdm2 also contains a signal sequence that is similar to the nuclear export signal of various viral proteins.[41] After binding to p53, Mdm2 induces its nuclear export to the cytoplasm, thereby inhibiting the ability of p53 as a transcription factor.[42] Mdm2 is an ubiquitin ligase[43] and studies have shown that the binding of Mdm2 to p53, targets p53 for ubiquitin mediated degradation.[44] In tumour cells, accumulation of mutant p53 is a result of its inability to activate Mdm2 transcription. Furthermore, Mdm2 is unable to bind to mutant p53, and consequently there is no Mdm2-mediated p53 degradation.[45]

Although, embryos of Mdm2 gene-knockout mice die early during gestation, it has been shown that death is prevented by additional deletion of Trp53, which encodes p53, signifying the importance of Mdm2 in the down-regulation of the activity of p53.[46] Mdm2 overexpression has been shown to block p53-mediated cell cycle arrest and apoptosis.[47] The activation of p53 tumour suppressor activity therefore depends on its association with Mdm2, and several activation pathways have been reported. For example, p53's association with Mdm2 is prevented by the phosphorylation of several different p53 residues (Ser15, Thr18 or Ser20) that is induced by DNA damage.[48] Alternatively, Mdm2-mediated degradation of p53 can be prevented by the expression of ARF, which can be stimulated by the activation of oncogenes such as c-MYC or RAS.[49] Mdm2 has also been shown to interact physically and functionally with several other regulators of the cell cycle, such as pRb, E2F1 and p107[50] and TAF250/CCG1.[51]

The disruption of the Hdm2-p53 interaction is therefore an attractive therapeutic strategy for activating p53 tumour supressor activity in tumours expressing wild type p53. Two different approaches have so far been reported; the design of Mdm2 antisense oligodeoxynucleotides, which knock down the expression of Mdm2 and, in doing so, stabilize p53; and the design of low-molecular-weight ligands that bind at the p53-Mdm2 interface, and, in doing so, prevent their association.

1.7 Properties of the p53-Mdm2 complex

There have been many studies on the characterisation of the p53-Mdm2 interface. In a yeast two-hybrid screen, the Mdm2-binding domain of p53 was identified on the amino-terminus from residues 1-41 and the p53-binding domain of Mdm2 was identified at the amino terminus from residues 1-118.[39] Similarly, immunoprecipitation experiments identified residues 1-52, on p53, and 19-102, on Mdm2, as being at the p53-Mdm2 interface.[52] The six residue sequence ^{18}TFSDLW^{23} was identified as being the minimal Mdm2-binding site on the p53 protein using synthetic peptides,[38] and the importance of residues Leu14, Phe19, Leu22 and Trp23 in the binding of p53 to Mdm2 was confirmed following mutation studies. Leu22 and Trp23 have been shown to be responsible for transactivation.[53]

1.7.1 The Mdm2 cleft

The region that corresponds to residues 13 – 119 of *Xenopus laevis* Mmd2 and residues 17-125 of Hdm2 have been crystallized in complex with a peptide that corresponds to residues 15-29 of p53.[54] The Mdm2 *N*-terminal domain has been shown to contain two structurally similar portions, 45 and 38 amino acids long. The repeat structure consists of a β strand, an α helix, a β strand, a longer α helix and a β strand as illustrated in Figure 1.7.

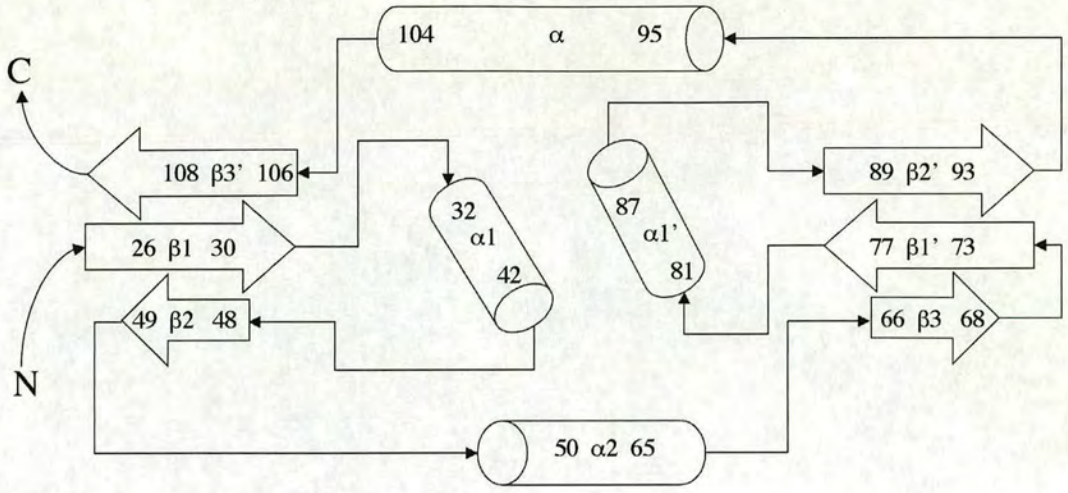

Figure 1.7: The Mdm2 *N*-terminal domain.

The two longer helices of the repeat and the first two β strands form a small globular structure, similar to a twisted trough, containing a hydrophobic cleft, the bottom of which is formed by the two shorter helices (α1 and α1'). The cleft is capped at each end with a pair of three stranded β sheets, one of which contains the amino and carboxylic termini of the polypeptide (Figure 1.8). The cleft is about 25 Å long, 10 Å wide near the surface, but narrows towards the bottom, which is up to 10 Å deep. The cleft is lined with 14 hydrophobic and aromatic amino acids, namely Met50, Leu54, Leu57, Gly58, Ile61 and Met62 from the α2 helix; Tyr67, His73, Val75, Phe91 and Val93 from the β-strands β3, β1' and β2'; and His96, Ile99 and Tyr100 from the α2' helix.[54]

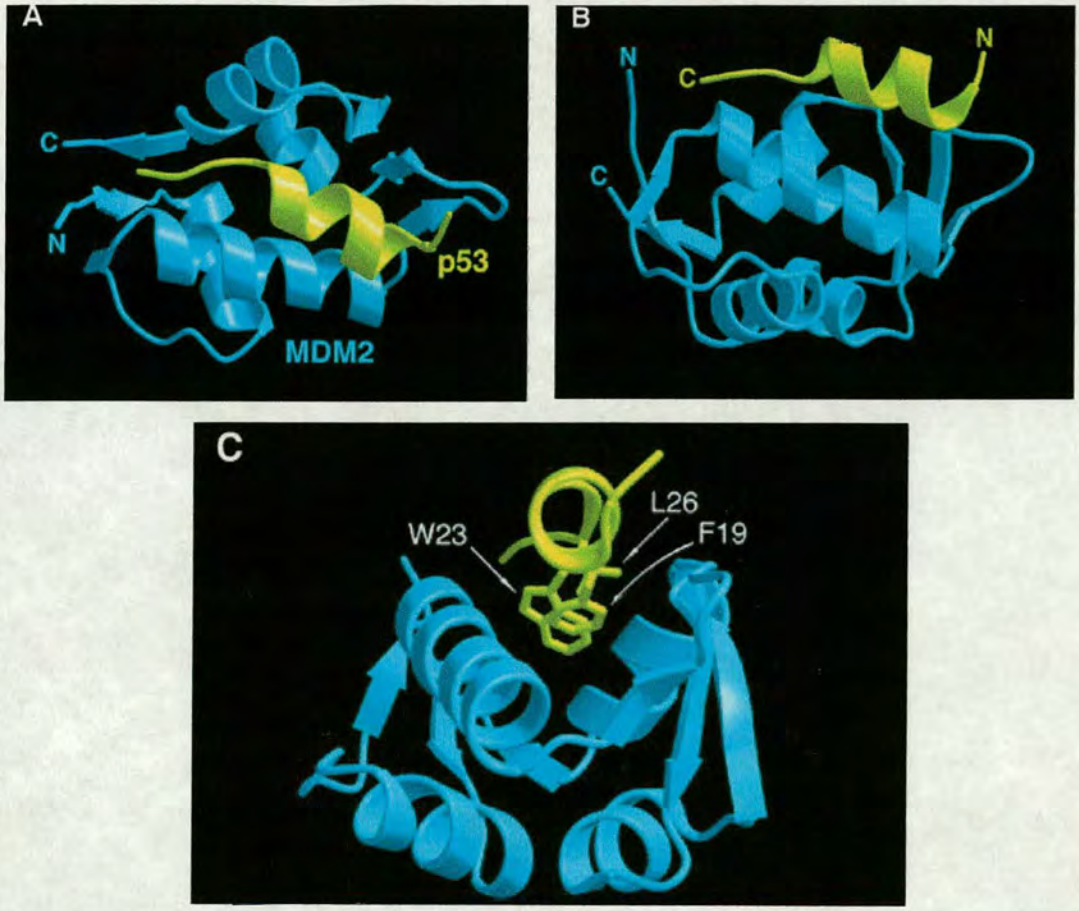

Figure 1.8: Three approximately orthogonal views of the p53-Mdm2 complex. The Mdm2 amino terminal domain is shown in cyan, whereas the p53 peptide is coloured yellow. The NH_2- and COOH- termini of p53 and Mdm2 are labeled N and C respectively. (**A**) The floor of the Mdm2 cleft in the plane of the figure. (**B**) The complex rotated approximately 90° about the horizontal axis of (A). (**C**) The complex rotated approximately 90° about the vertical axis of (B), looking down the helix of p53. Also shown are Phe19, Trp23 and Leu26 of p53, which insert deep into the Mdm2 cleft.[54]

1.7.2 The p53 binding domain

It was shown that $p53_{15\text{-}29}$ binds to the hydrophobic cleft that is present at the surface of Mdm2. Residues 18 to 26 of p53 were reported to form an amphipathic α helix, initiated by a network of hydrogen bonds formed by residues Thr18 and Asp21, with

one 3_{10} helical hydrogen bond at its *C*-terminal. Thr18 has also been reported to be particularly important in the regulation of the p53-Mdm2 interaction by phosphorylation.[48] The triad of key amino acid residues; Phe19, Trp23 and Leu26; make sequential Van der Waals contacts and have extended side-chain conformations inserting deeply into the Mdm2 cleft.[54] Consequently these three residues contribute to a large extent to the binding energy of the p53 peptide.[55] These three residues have been reported to be involved in transactivation, supporting the hypothesis that Mdm2 inactivates p53 by restricting access to its transactivation domain. The aromatic side chains of Phe19 and Trp23 have been shown to stack face to face in a staggered arrangement (Figure 1.9). The two charged amino acids of the helix; Asp21 and Lys24; are within salt bridge distance. Immediately after the α helix is Pro-27, which is likely to contribute to its termination. NMR studies have shown that the p53 protein is loosely folded in solution,[56] suggesting that the α helix is stabilized by Mdm2 binding. The α helix is readily digested by proteases in the absence of Mdm2, in particular by cleavage at Trp23.[57]

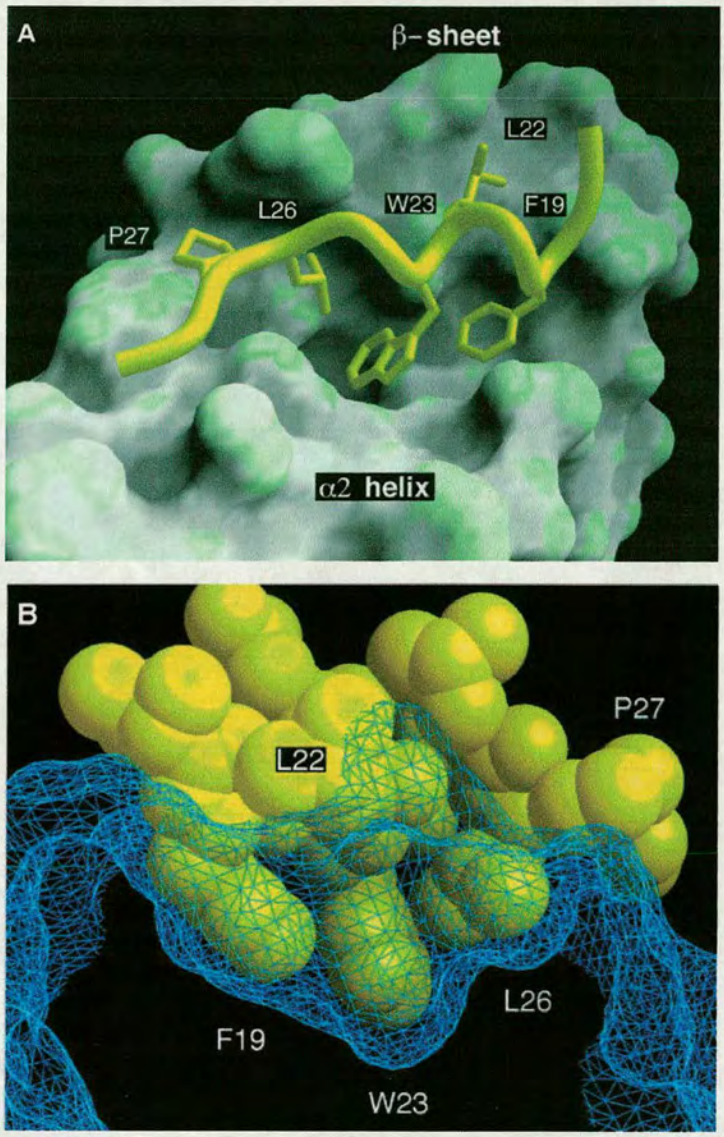

Figure 1.9: (**A**) Surface representation of the Mdm2 binding cleft, coloured grey. The p53 amino acids that interact with this surface are shown in yellow, and are labeled. (**B**) A cross section of the Mdm2-p53 interface showing that the residues Phe19, Trp23 and Leu26 pf p53 fit tightly in the Mdm2 pocket. The Mdm2 surface is represented as a blue wire mesh and p53 residues 18 – 27 are in space filling representation.[54]

The peptide-protein interface relies primarily on Van der Waals contacts between the hydrophobic and aromatic amino acids that line the Mdm2 cleft and p53. The p53 α-

helix makes its primary Van der Waals contacts along about three-quarters the length of the cleft over a portion that resembles a wide deep pocket. Where the cleft is narrower and shallower, it has little hydrophobic character and there are only a few Van der Waals contacts in this region, primarily involving the Phe19 side chain of p53. Van der Waals contacts are made between Phe19 and the residues Gly58 and Ile61 on Mdm2. These two residues on Mdm2 are also involved in Van der Waals contacts to Trp23 on p53. Additional Van der Waals contacts occur between Leu22 and the side of the Mdm2 cleft. Only two intermolecular hydrogen bonds have been identified at the p53-Mdm2 interface, these being between the p53 Trp23 indole group and the Mdm2 Leu54 backbone carbonyl deep inside the cleft, and between the Phe19 backbone amide of p53 and the Gln72 side chain of Mdm2 at the entrance of the cleft. Preservation of one or both of these hydrogen bonds should obviously be a key feature in the design of low molecular weight inhibitors to ensure sufficient affinity.[54] The p53-Mdm2 interaction is illustrated in more detail in Figure 1.10.

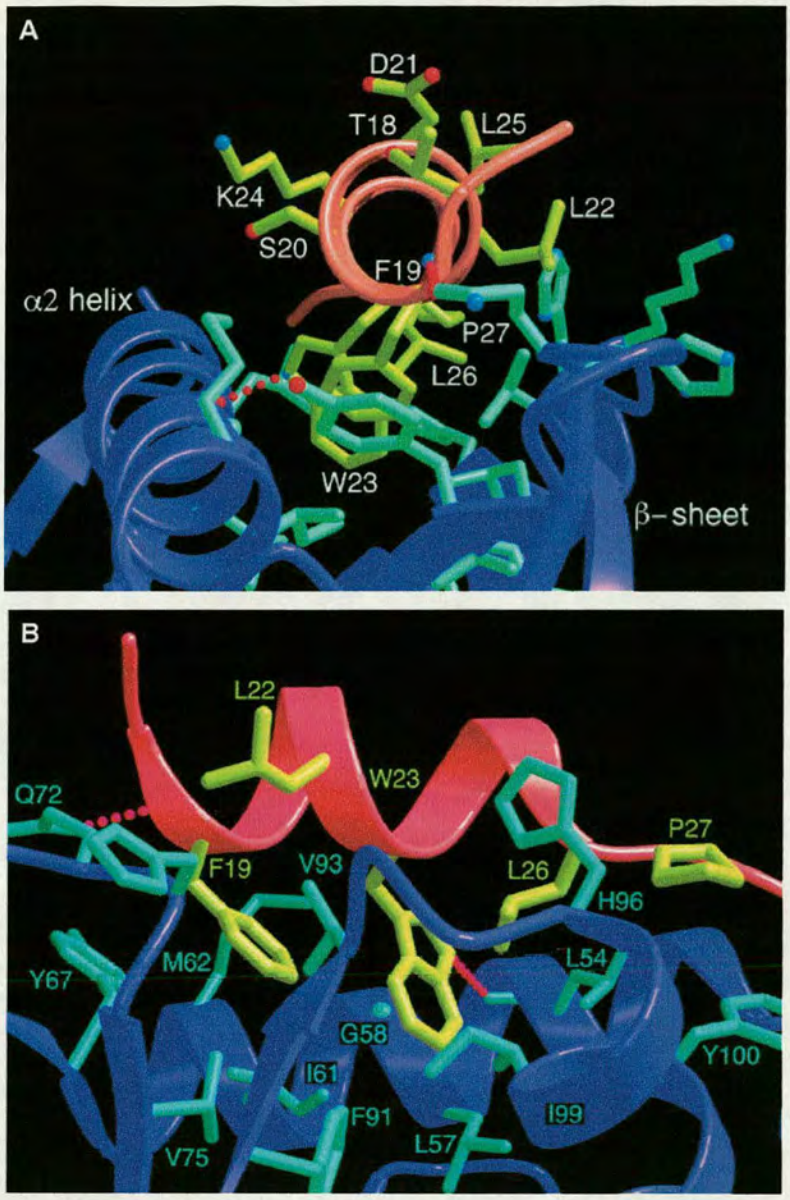

Figure 1.10: The p53-Mdm2 interaction in more detail. (**A**) The Mdm2 cleft is coloured blue, with Mdm2 amino acid residues at the interface coloured cyan. The amphipathic □ helix of p53 is coloured pink, with residues at the Mdm2-p53 interface coloured yellow. Blue and red spheres represent nitrogen and oxygen atoms respectively. For simplicity, only the p53 amino acids are labeled. The two intermolecular hydrogen bonds at the interface are shown as red dotted lines. (**B**) The interface rotated 90° about the vertical axis of (A). The Mdm2 □2 helix is below the plane of the figure, its β sheet is above the plane, and p53 is between the two. Only the interacting amino acids at the interface are shown, and they are labelled.[54]

The small size of the p53-Mdm2 interface and the combined molecular mass of the sidechains of Phe19, Trp23 and Leu26 of around 300 Da makes the design of low molecular weight molecules that can inhibit the Mdm2-p53 interaction a very attractive strategy. This would stabilize the p53 protein and lead to a direct pharmaceutical activation of the p53 tumour supressor response in cells expressing wild type p53.

1.8 Current research into the inhibition of the p53-Mdm2 interaction

A number of groups have examined the feasibility of the p53-Mdm2 model. Lane *et al.* have shown that p53 accumulation and activation are induced by the expression of a modified thioredoxin containing a peptidic homologue of p53 on its surface.[58] The induction of activity of p53 in some tumour cells by the same peptidic homologue of p53 fused to the glutathione S-transferase protein (GST) has also been reported.[59] Furthermore, it has been shown that inhibition of the p53-Mdm2 interaction, through microinjection of normal human fibroblasts with 3G5 antibody (directed against the p53-binding domain of Mdm2), induces expression of p53 responsive genes.[60] However, it has also been reported that inhibition of the p53-Mdm2 interaction prevents the normal cell proliferation.[61] This raises the issue of toxicity of inhibitors of the p53-Mdm2 interaction to healthy tissue.

It has been reported that three synthetic peptides derived from wild-type p53 ($p53_{12\text{-}20}$, $p53_{17\text{-}26}$ and $p53_{12\text{-}26}$), and coupled to the leader sequence of the antennapedia protein, are toxic to various p53-null tumour cell lines in addition to cell lines that express wild-type or mutant p53, but are not toxic to normal cells. The induction of apoptosis via a p53-independent mechanism was suggested as no p53-apoptotic markers, such as Bax and p21, were identified after treatment with the peptides. It was postulated that the common sequence Glu-Thr-Phe-Ser, contained in each of the three peptides, was attributable for the observed cytotoxicity.[62]

1.9 Other members of the p53 and Mdm2 families

Recently, two p53-related genes, p63 and p73, were identified. The primary sequence of p53 has a similarity of 62% with p63 and 69% with p73. Although structurally similar to p53, each of these two genes has distinct physiological function.[63] There is evidence to suggest that p53 is involved more with tumour suppression whereas p73 and p63 are more important during development and differentiation respectively.[64] One Mdm2 related gene, MdmX, has been identified.[65] The primary sequence of Mdm2 has a 37% similarity with MdmX.

The homology between p53, Mdm2 and their respective family members suggest that cross association may be a possibility. Indeed, MdmX has been reported to bind to p53, p63[65] and p73.[66] Mdm2 has also been reported to associate with p63[67] and p73.[66] Also, inhibitors of the p53-Mdm2 interaction have been demonstrated to disrupt the p53-MdmX interaction.[68] This presents the challenge of the design of selective inhibitors that specifically only disrupts one of these interactions.

1.10 The design of inhibitors of the p53-Mdm2 interaction

The short sequence of contiguous amino acids on p53, shown to be essential for Mdm2 binding, allow the design of small peptidic inhibitors which would mimic the interaction of p53. However, the significant Van der Waals character of the Mdm2-p53 interaction differentiates it from most other known protein-peptide interactions in which there are extensive hydrogen bonding contacts. In these complexes, a significant proportion of the buried surface is polar, whereas in the Mdm2-p53 complex the majority of the buried surface, amounting to some 1498 $Å^2$ of surface area, is hydrophobic. Indeed, as approximately 70% of the interfacial atoms are non-polar, a key feature of inhibitors of the p53-Mdm2 interaction would be the presence of lipophilic groups, which, although having a negative effect on the oral bioavailability of the inhibitors, may provide a favourable entropic contribution to the binding energy upon interaction with Mdm2.[13] However, it is important to

conserve the key hydrogen bond in the p53-Mdm2 complex, that between Trp23 on p53 and Leu54 on Mdm2, in order to ensure sufficient affinity of the inhibitors.

1.10.1 Peptidic Mdm2 inhibitors and peptidomimetics

The identification of the minimal Mdm2 binding site on p53 as a contiguous six-residue sequence (^{18}TFSDLW^{23}) induced the design of small peptides to inhibit the p53-Mdm2 interaction. Initial studies on the hexapeptide $p53_{18-23}$ indicated it had little affinity.[58] Further studies, involving the screening of phage-displayed peptide libraries allowed the identification of more potent peptides, including the 12mer peptide (Table 1.1, **2**) that was 28-fold more potent *in vitro* than the corresponding p53 wild-type peptide (Table 1.1, **1**). Truncation studies on the 12mer peptide, **1**, revealed that its size could be reduced to eight residues whilst retaining micromolar affinity (Table 1.1, **3**).[69]

To further increase the potency of peptide **3**, the residues Asp21 and Gly25 were substituted with the non-natural amino acids α-amino isobutyric acid (AIB) and 1-amino-cyclopropanecarboxylic acid (AC3C) to favour the pre-organisation of a helical structure of the peptide in solution, thereby hoping to mimic that observed in the p53-Mdm2 crystal structure reported by Kussie *et al.*[54] These modifications resulted in a > 4-fold increase in potency of peptide **3** (Table 1.1, **4**).[69]

To enhance the affinity of peptide **4**, and in doing so provide a positive enthalpic contribution to the peptide's binding to Mdm2, two modifications were made. The residue corresponding to Tyr22 on p53 was replaced with phosphonomethyl-phenylalanine (PMP) to favour the formation of a salt bridge with the Lys94 residue of Mdm2. Also, the residue corresponding to Trp23 on p53 was replaced with 6-chloro-tryptophan, with the aim being to fill a small hydrophobic cavity left unoccupied by wild-type p53 in the Mdm2 cleft. The result of these modifications was to increase the affinity of peptide **4** 440-fold (Table 1.1, **6**).[69]

Cmpd	Structure	IC_{50} (μM)
1	Ac-Gln-Glu-Thr-Phe[19]-Ser-Asp-Leu-Trp[23]-Lys-Leu-Leu[26]-Asn-NH2	8.7
2	Ac-Met-Pro-Arg-Phe[19]-Met-Asp-Tyr-Trp[23]-Glu-Gly-Leu[26]-Asn-NH2	0.3
3	Ac-Phe[19]-Met-Asp-Tyr-Trp[23]-Glu-Gly-Leu[26]-Asn-NH2	8.9
4	Ac-Phe[19]-Met-AIB-Tyr-Trp[23]-Glu-AC3C-Leu[26]-Asn-NH2	2.2
5	Ac-Phe[19]-Met-AIB-PMP-Trp[23]-Glu-AC3C-Leu[26]-Asn-NH2	0.3
6	Ac-Phe[19]-Met-AIB-Tyr-6ClTrp[23]-Glu-AC3C-Leu[26]-Asn-NH2	0.005

Table 1.1: Peptidic inhibitors of the p53-Mdm2 interaction; IC_{50} values shown represent inhibition of wild type p53 binding to GST-Hdm2.

1.10.2 Non-peptidic small-molecule Mdm2 inhibitors

There has been very little reported to date on non-peptidic or natural inhibitors of the p53-Mdm2 interaction. The discovery and structure determination of chlorofusin, **7**, a fungal metabolite that antagonizes the p53-Mdm2 interaction has been reported.[70] Chlorofusin has been shown to have an IC_{50} of 4.6μM in an enzyme-linked immunosorbent assay (ELISA). However, it is not known whether chlorofusin binds at the p53-Mdm2 interface.

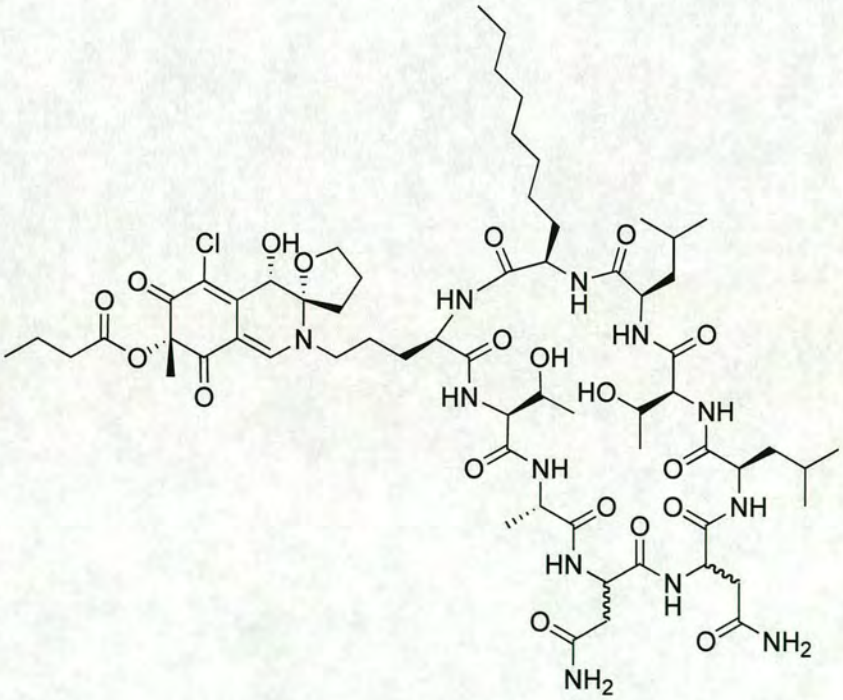

7

Recently, Zhao *et al.* have reported on the initial evaluation of non-peptidic small-molecule Mdm2 inhibitors selected from a virtual screen based on the p53-Mdm2 complex structure.[71] The advantages associated with non-peptidic small molecules are that they generally have higher cell permeability than peptides and can also be synthesized more cost effectively by chemical methods. In this study, of the 23 synthetic small molecules and nine intermediate products evaluated, five showed affinity with Hdm2 and were shown to affect the viability of several tumour cells lines that express wt-p53. More importantly, one of these compounds, syc-7, **8**, was shown to activate the p53 pathway and induce apoptosis in cells with wild type p53.[71]

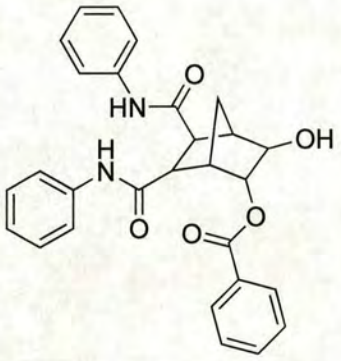

8

A number of chalcones (1,3-diphenyl-2-propene-1-ones) have been reported to inhibit the p53-Mdm2 interaction *in vitro* on ELISA and gel-shift assays. NMR studies have indicated that these compounds, exemplified by the chalcone B-1, **9**, interact with the p53 Trp23 binding pocket subsite on the Mdm2 protein and, therefore, do not fully occupy the p53 binding cleft of Hdm2, which is perhaps reflected in their low potency of between 50 μM and 250 μM.[72]

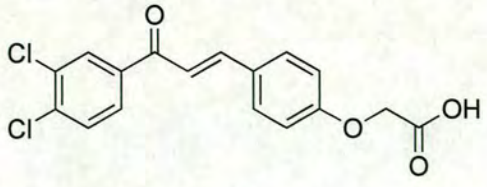

9

Significantly and more recently, a series of small-molecule antagonists of Mdm2 have been reported based around a cis-imidazoline scaffold.[73] These antagonists, named 'Nutlins' and exemplified by Nutlin-2, **10**, have been shown to bind to Mdm2 in the p53 binding pocket, leading to p53 accumulation, through decreased degradation of the protein, and subsequent cell cycle arrest and apoptosis in tumour cells expressing wt-p53. The IC_{50} value of **10,** representing the inhibition of wild type p53 binding to Hdm2, was determined to be 0.14 μM.

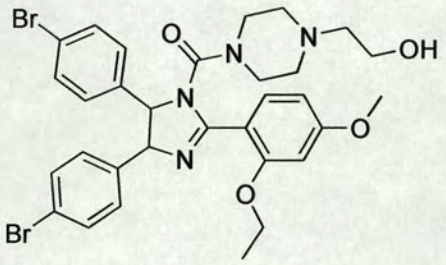

10

Furthermore, it was shown that the Nutlin **10** mimics the interaction of the p53 peptide to a high degree with the imidazoline scaffold successfully replacing the helical backbone of p53, as illustrated by Figure 1.11.

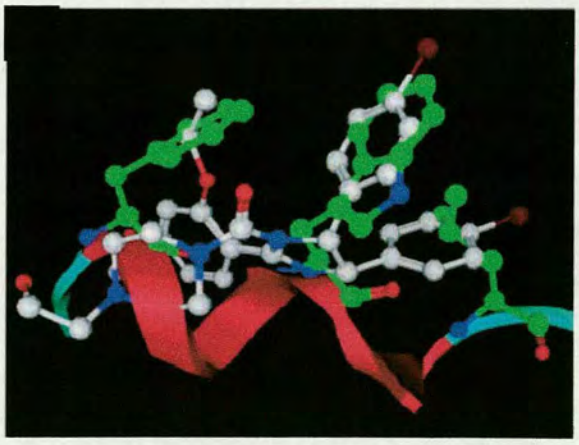

Figure 1.11: An overlay of Nutlin-2 with the peptide side chains of Phe19, Trp23 and Leu26 of p53. For the inhibitor atoms are coloured as follows: C, white; N, blue; O, red; Br, brown. For the protein atoms are coloured C, green; N, blue, O, red.[73]

The crystal structure of the Hdm2-Nutlin2 complex was solved (Figure 1.12) that revealed one bromophenyl moiety of the ligand extending deeply into the pocket normally occupied by Trp23, one bromophenyl moiety occupying the Leu26 pocket, and the ethyl ether moiety directed towards the Phe19 pocket.

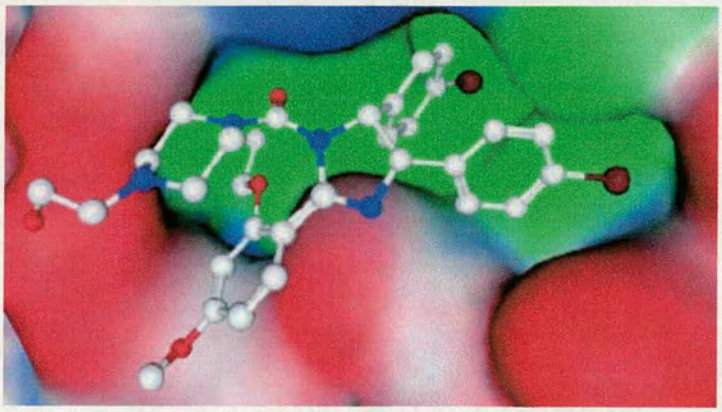

Figure 1.12: Nutlin-2 located in the p53 binding pocket of Mdm2. The surface of the protein has been coloured as follows: Buried regions, green; Exposed portions, red. The inhibitor is coloured: C, white, N, blue; O, red; Br, brown.[73]

2 The development of novel inhibitors of the p53-Mdm2 interaction

2.1 An introduction to structure based ligand design

2.1.1 An overview of structure based design

This chapter concerns the design and synthesis of high affinity ligands that disrupt the p53-Mdm2 interaction. By way of introduction, certain aspects of ligand design within the drug discovery process have been discussed.

For binding to occur between a drug and receptor, both must have a complementary shape and charge distribution to achieve the required negative interaction energy. A small increase in binding energy can lead to an almost tenfold increase in potency, as shown by Equation 2.1, which relates the binding energy (ΔG) to the binding constant, K. The binding energy of a ligand can be influenced by various factors including molecular shape, electrostatic interactions, Van der Waals (hydrophobic) interactions and hydrogen bonding.[75]

$$\Delta G = -RT\ln K \qquad \textbf{(Equation 2.1)}$$

A combination of these factors is considered in the rational design of a ligand for a particular receptor site. Molecular modelling software enables the factors that contribute to the binding energy of a ligand to be evaluated, and, through the calculation of these factors at many points around the surface of a receptor, a picture of the binding site can be generated showing where particular atoms will bind most strongly. Subsequently, a ligand can be built and docked in the binding site and visualized using modelling software, providing an effective tool for the synthetic chemist.

Thus, structure based design is an iterative process of computational design, synthesis, screening, testing, structure elucidation and data analysis illustrated by Figure 2.1. 3D structures can be used for the design of *de novo* ligands, if the structure of a protein, or protein-ligand complexes are known which may involve the screening of 3D databases of small molecules for predicted binding to a known protein target (computational virtual screening). Molecular modelling also enables the optimization of existing leads for affinity and selectivity, by examining the effect of modifications or extension to the ligand in the binding site.

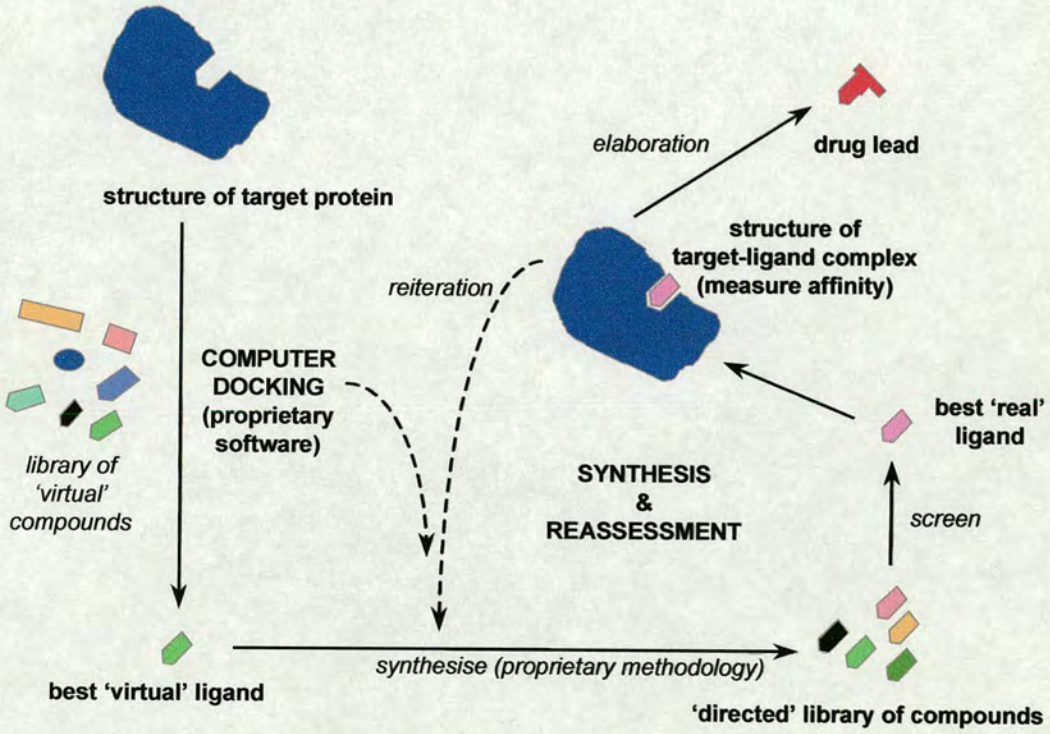

Figure 2.1: An overview of the structure based design of ligands.

2.1.2 Protein-ligand interactions

The contribution of non-bonded protein-ligand interactions to binding affinity is difficult to quantify. However, several structure-activity relationship studies have shown that enhanced binding affinity is frequently observed by enlargement of the lipophilic contact

surface of the ligand by addition of a lipophilic substituent, capable of forming hydrophobic interactions with the protein surface. Conformationally constrained ligands often bind more strongly than flexible ligands because the binding of a ligand to a protein results in a loss of entropy due to freezing of internal degrees of freedom. Furthermore, additional hydrogen bonds between polar groups may improve selectivity and make the ligand more water soluble, although this may not necessarily improve binding affinity. One further contribution to the enhancement of the binding affinity of a ligand to a protein can be achieved through the displacement of water molecules at the binding site. If the ligand forms more hydrogen bonds than the number of water molecules released, strong binding can be achieved.[76]

2.2 Project background – lead discovery

For the current work, no crystal structure existed for a small ligand bound to the Mdm2 cleft. However much was known about the structure of p53 and Mdm2.[54] At the Institute of Cell and Molecular Biology at Edinburgh University, Paul Taylor used the docking programme LIDAEUS, developed by himself, to generate the ligand template for the current work. Using the available structural information about the p53-Mdm2 complex, the LIDAEUS programme screened the 46,000 membered Maybridge compound library for small molecules able to bind to the hydrophobic cleft of Mdm2. To achieve this, the LIDAEUS programme calculates the interaction energy between a "probe atom" and the protein on a 3D grid of site points around the protein active site. In the calculation, carbon and oxygen atoms are used as probe atoms, with favoured hydrophilic interactions mapped out by the carbon atoms, to generate areas of low energy in the protein active site. A negative template of the active site of the target protein can then be generated, by turning the areas of low energy into site points. The template obtained contains information on the geometrical and chemical properties of putative ligands and the data can then be used to search the Maybridge Fine Chemicals database to select the best-fitting ligand for the site points. The list of commercially available compounds obtained is subjected to a second selection process on the basis of molecular weight and

hydrophobicity. The most hydrophobic ligands with molecular weight less than 500 are chosen, since smaller, hydrophobic ligands can more easily penetrate the crystal to reach the binding site.

The LIDAEUS hits were further visualised by Campbell McInnes at Cyclacel Ltd., resulting in the selection of 78 compounds for purchase and their subsequent screening using *in vitro* Mdm2 competitive binding assays developed by Cyclacel Ltd. From this screen, two sulfonate esters, KM05076, **11**, (IC_{50} = 106 μM) and KM05658, **12**, (IC_{50} = 95 μM), were both identified as being novel inhibitors of the p53-HdM2 binding interaction in a fluorescein-labelled peptide fluorescence polarisation (FP) assay and also were active in an immobilised biotin-peptide assay, with IC_{50}'s of 12 μM and 13 μM respectively. Furthermore, the benzothiazole *N*-oxides CD03683, **13**, and CD09069, **14**, were shown to be active in the immobilised biotin-peptide assay, with respective IC_{50} values of 112μM and 200 μM, although they exhibited no activity in the FP assay.

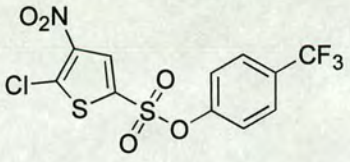

11

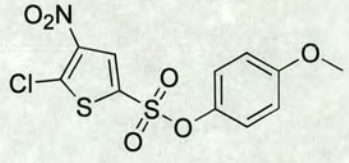

12

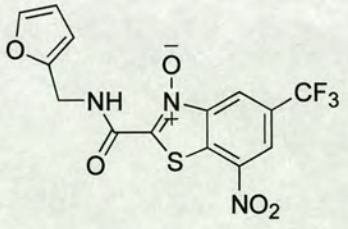

13

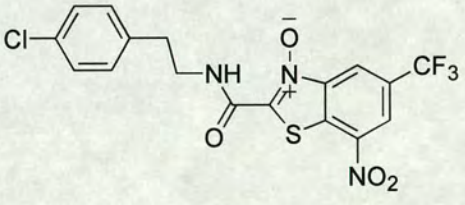

14

Two hit expansion libraries were purchased from the Maybridge and Chembridge commercial compound database based on the two substructures of these 4 hits (Figure 2.2).

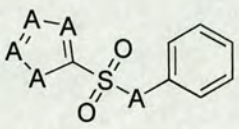

Substructure 1

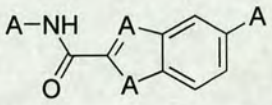

Substructure 2

Figure 2.2: Substructures forming the basis of a hit expansion library for inhibitors of the p53-Mdm2 interaction.

Of the 191 compounds purchased with Substructure 1, 27 compounds were active in the primary screen using the FP p53-Mdm2 competitive binding assay, resulting in >50% inhibition of p53-Mdm2 binding at 500 μM concentration. Of these 27 ligands, IC_{50} values were determined for 16 compounds in a secondary screen using the FP p53-Mdm2 competitive binding assay. Of the 174 compounds purchased with substructure 2, there were no hits in the primary screen.

Early structure activity relationship studies deducible from the 191 membered hit expansion library of substructure 1 were limited. Of this library, a subset of 172 members had thiophene functionality, and activity in the primary screen was confined to this group. All 65 members that contained an unsubstituted thiophene moiety were shown to be inactive in the primary screen. There were five 5-chloro-4-nitro-thiophene-2-sulfonamide analogues in the expansion library and, in the secondary screening assay, the IC_{50} values of each were shown to be in the range of 107 – 181 μM. A further 4 ligands from a subset of 24 5-halo-thiophene-2-sulfonamides or sulfonate esters were shown to exhibit activity in the secondary screen. Those ligands with the greatest activity in the hit expansion library, as determined by the secondary screen, were shown

to be 2-sulfonyl-3-chloro-5-trifluoromethyl-pyridine analogues exemplified by KM5576, **15**, and KM5582, **16**, with IC_{50} values of 123 μM and 69 μM respectively.

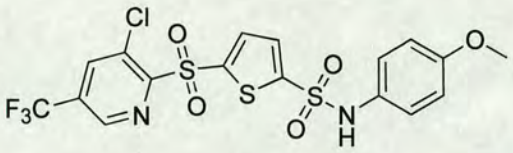

15

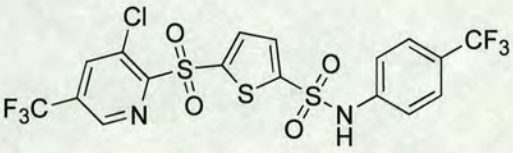

16

2.3 Initial expansion libraries

Given the activity of sulfonamides **15** and **16** in the FP p53-Mdm2 competitive binding assay, it was desirable to screen further compounds that contained this pharmacophore in order to generate and gather more structure-activity relationship (SAR) data and also to discover analogues with improved binding. The initial aim of this project was to investigate this pharmacophore with an expansion library of *N*-substituted sulfonamides, synthesized using solution phase combinatorial techniques. From an early molecular modelling study of an *N*-alkylated sulfonamide ligand, **17**, docked in the binding site of Mdm2 (Figure 2.3), undertaken by scientists at Cyclacel Ltd., it was envisaged that the introduction of a third substituent off the sulfonamide nitrogen atom had the potential to generate new contacts with the Leu26 pocket in the receptor binding site. Furthermore, this would address whether a hydrogen bond donor at this site was essential for ligand activity. The initial modelling studies also suggested that the thiophene moiety was placed in the Phe19-binding pocket of Mdm2, with the aromatic group of the ligand probing deep into the Trp23 pocket. Following the synthesis of novel libraries of sulfonamides and favourable first round screening in the FP assay, those ligands found to be active could then form the basis of a second-generation library of *N*-alkylated sulfonamides.

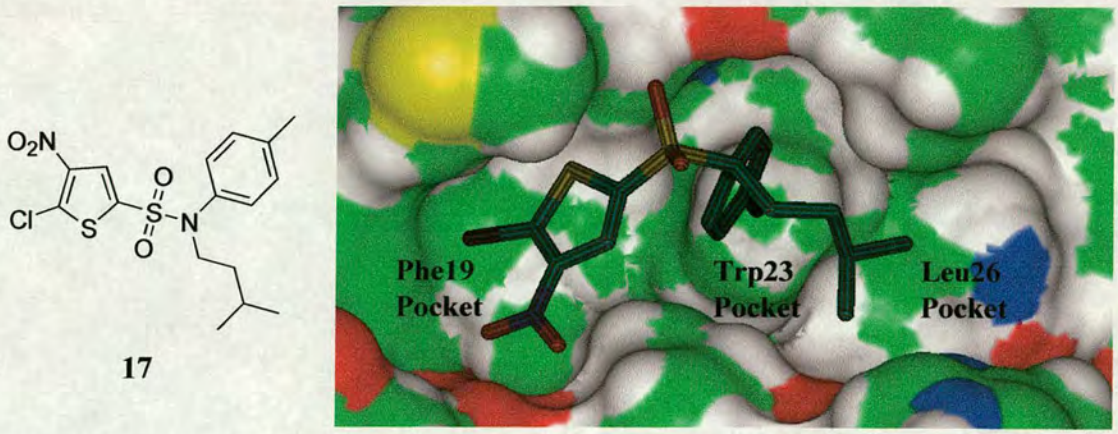

17

Figure 2.3: An early modelling study of **17** docked in the p53-binding site of Mdm2 undertaken by Cyclacel Ltd.

2.3.1 Strategies for the synthesis of *N*-substituted sulfonamides.

An obvious disconnection of the template exhibited by **15** and **16** was the sulfonamide linker to obtain the sulfonyl chloride and aniline synthons. A library of *N*-substituted sulfonamides could be generated by initial coupling of a sulfonyl chloride with an amine, followed by *N*-alkylation, which could be achieved through a number of strategies such as direct alkylation with an alkyl halide or using the Tsunoda modification of the Mitsunobu reaction.[77] Owing to the commercial availability of a large number of sulfonyl chlorides, anilines, primary alcohols and alkyl halides, this strategy had the potential to produce diverse sets of combinatorial libraries fairly rapidly, without resorting to the synthesis of building blocks.

2.3.2 The Tsunoda modification of the Mitsunobu reaction.

Sulfonamides are relatively weak acids and require activation via conversion to their conjugate base before they can react with alkyl halides. The alkylation of both amides and sulfonamides under phase transfer conditions has been reported.[78] *N*-alkylation can

also be achieved through the Mitsunobu reaction[79,80] in which an amide or imide is treated with equimolar amounts of an alcohol in the presence of triphenylphosphine and diethyl azodicarboxylate at room temperature, as illustrated in Scheme 2.1. As reviewed by Mitsunobu, the reaction proceeds via formation of a zwittionic P-N adduct, **18**, which is protonated in the presence of an acidic component, **19**, to form an alkoxyphosphonium salt, **20**, and the reduced hydrazine by-product, **21**. Finally, the deprotonated acidic component reacts with the alkoxyphosphonium salt in an S_N2 manner to provide the alkylated acidic species, **22**, and triphenylphosphine oxide.

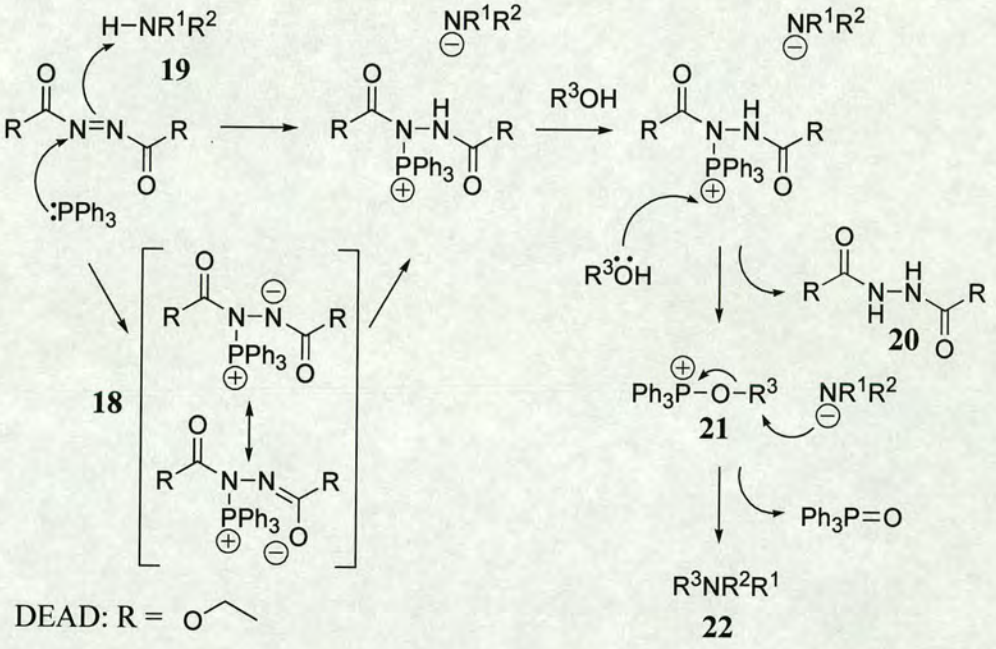

Scheme 2.1: Mechanism of the Mitsunobu *N*-alkylation reaction.

A number of factors are crucial to the success of the Mitsunobu reaction, namely the pK_a of the acidic component,[81] **19**, which needs to be acidic enough to protonate the zwittionic adduct, **18**. However, the deprotonated acidic species must be less nucleophilic than the alcohol in order to prevent a competing reaction with the phosphonium salt, which would prevent formation of the alkoxyphosphonium intermediate, **21**. It has been reported that the maximum pK_a of the acidic component for

the reaction to proceed is approximately 11 – 13 and much lower yields are obtained with acidic components with pK_a's 13 – 14.[82]

Tsunoda *et al.* have reported a number of modifications to the Mitsunobu system namely replacement of DEAD with either of the more basic, and thereby activating, diazo compounds *N*, *N*, *N'*, *N'*-tetramethylazo-dicarboxamide (TMAD, **23**) or 1,1'-(azodicarbonyl)-dipiperidine (ADDP, **24**), both of which are commercially available, and replacement of triphenylphosphine with the less bulky, more nucleophilic, tributylphosphine, that has the effect of localizing the positive charge exclusively on the phosphorus atom facilitating activation of the alcohol and attack of the deprotonated acidic component on the alkyloxyphosphonium salt.[77]

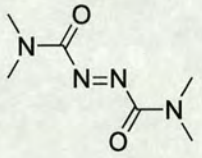

23

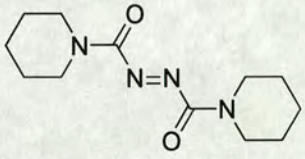

24

2.3.3 *N*-Alkylation of sulfonamides

Initial efforts were focussed on the synthesis of sulfonamide **26** following a previously reported method by Arcoria *et al.*[83] Treatment of a methanolic solution of aniline with 2-thienyl sulfonyl chloride, **25**, followed by stirring the solution at room temperature for 24 hours afforded the sulfonamide **26**, in 75% yield (Scheme 2.2).

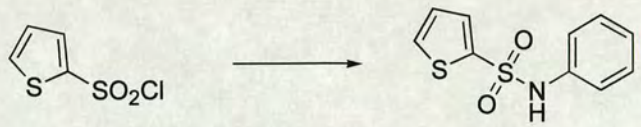

25 **26**

Scheme 2.2: *Reagents and conditions*: aniline, methanol, room temperature, 24h.

N-Methylation of **26**, following the protocol developed by Tsunoda *et al.*[77] using TMAD, TBP and methanol, using benzene as solvent and under an atmosphere of nitrogen and at 0 °C, afforded **27** in 30% yield (Scheme 2.3).

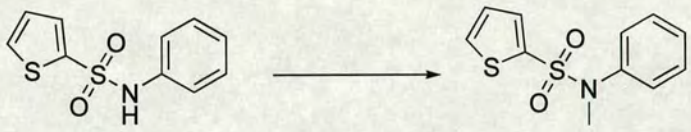

26 **27**

Scheme 2.3: *Reagents and conditions*: methanol, TMAD, TBP, benzene, room temperature, 24h.

Using the Tsunoda protocol, subsequent *N*-alkylation of **26**, using either ethanol, n-butanol, benzyl alcohol or allyl alcohol respectively, and conducted at room temperature afforded **28**, (49%), **29**, (45%), **30**, (35%) and **31**, (66%). It was postulated that the lower yield obtained from the *N*-benzylation reaction was attributable to increasing steric demands at the S_N2 reaction site. The isolated yields of **28** – **31** were lower than expected and at this stage it was considered that the reaction temperature could have an effect on the outcome of the reaction, although this was not investigated.

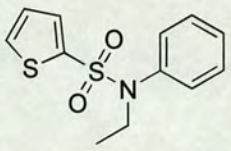

28

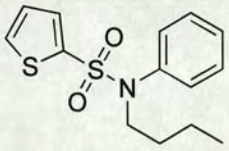

29

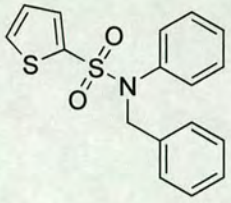

30

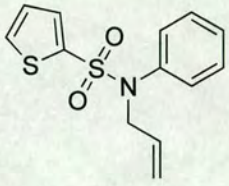

31

2.3.4 The attempted synthesis of 2-sulfonyl-3-chloro-5-trifluoromethyl-pyridine analogues

Given the initial success of the Tsunoda *N*-alkylation reaction, the *N*-alkylation of the commercially available KM5576, **15**, and KM5582, **16**, was attempted using allyl alcohol and following the protocol used for the synthesis of **31**. However, after 24 hours, analysis of both reaction mixtures by TLC revealed no reaction had taken place. Similarly, there was no evidence of *N*-allylation after addition of a further 1.5 equivalents of allyl alcohol and allowing each reaction mixture to stir at room temperature for a further 66 hours. Both reactions were repeated using 'fresh' TMAD, although, again, this resulted in the recovery of either **15** or **16**. In instances where no *N*-alkylated product was isolated, Tsunoda had reported the isolation of the oxadiazole, **34**, through rearrangement of the zwittionic P-N adduct, **32**, via the pathway illustrated in Scheme 2.4. However the oxadiazole, **34**, was not isolated in the above study.

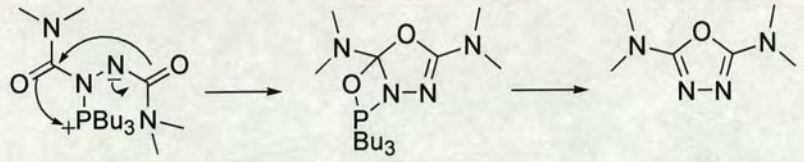

32 **33** **34**

Scheme 2.4: Proposed formation of oxadiazole, **34**, in the Tsunoda modification of the Mitsunobu alkylation reaction.[77]

Although Tsunoda *et al.* had shown that TMAD was more versatile in the Mitsunobu reaction than ADDP when used in conjunction with tributylphosphine in benzene, it was decided to investigate the allylation of **15** and **16** using ADDP for completeness. In both cases, no evidence of the *N*-allylated **15** and **16** species was identified upon work up.

A short study was undertaken varying the reaction solvent from benzene. The *N*-allylation of **26** was carried out using either THF, toluene and, again, benzene. Apart from the *N*-alkylation performed in THF, which afforded **31** in 44% yield, each reaction resulted in the recovery of **26** with no *N*-allylated species detected by TLC. Results from this study highlighted the capricious nature of the reaction and not only pointed to the reaction solvent having an effect on the outcome of the reaction, but also questioned its reproducibility using the current protocol.

In order to address the synthesis of *N*-alkylated **15** and **16** analogues, another strategy had to be found. It was thought that the coupling of 5-chloro-thiophene-2-sulfonyl chloride, **35**, with either the 4-trifluoromethyl or 4-methoxy substituted aniline to yield the sulfonamide **36** or **37** could then be followed by *N*-allylation, under Tsunoda conditions, to afford **38** or **39**. Subsequent nucleophilic displacement of the 5-chloro functionality with the commercially available 3-chloro-5-(trifluoromethyl)-pyridine-2-thiol, **40**, to yield the thioether, **41**, adopting similar conditions to those reported by Barnish *et al.*[84] for the synthesis of 5-(arylthio)- and 5-(arylsulfonyl)-thiophene-2-

sulfonamides from 5-bromo-thiophene-2-sulfonamide, would then be followed by oxidation of the thioether to afford the sulfone, **42** (Scheme 2.5).

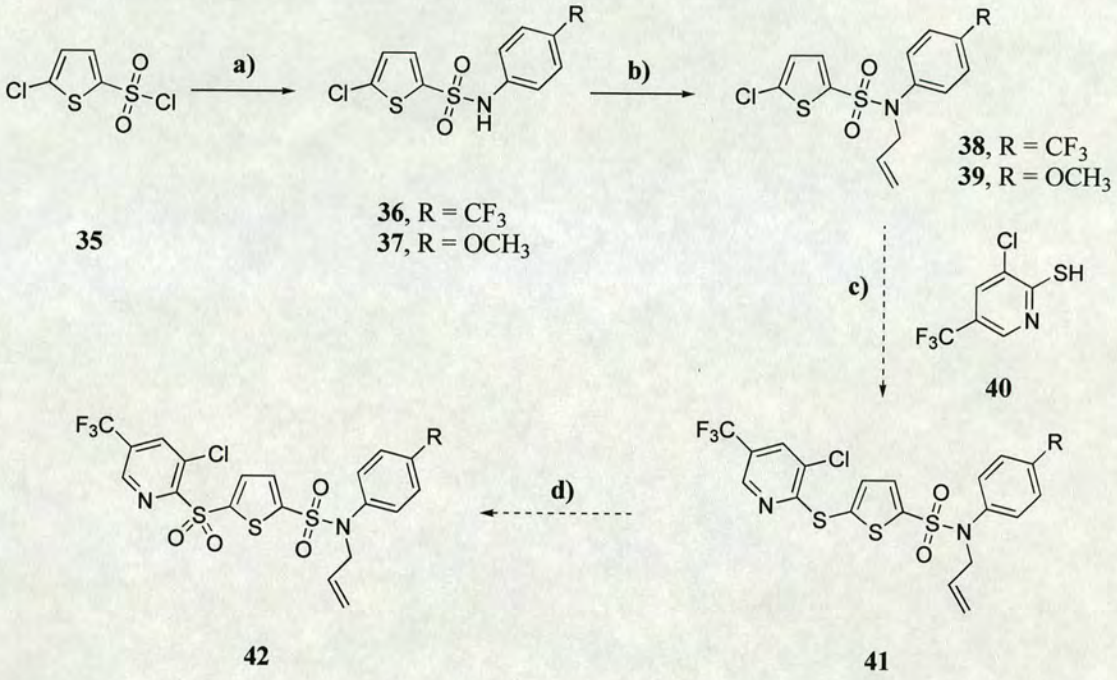

Scheme 2.5: *Reagents and conditions*: **a**) 4-substituted aniline, DIPEA, THF, room temperature, 24 h. **b**) allyl alcohol, TMAD, TBP, benzene, room temperature, 4, days. **c**) NaOH (aq.), DMF. **d**) H_2O_2, AcOH, 100 °C, 1 h.

The synthesis of sulfonamide **37** using DIPEA (1.0 eq.) to activate the sulfonyl chloride, proceeded in quantitative yields. However, adopting a similar procedure for the synthesis of **36**, the bis-sulfonamide **43** (Scheme 2.6) was isolated in 23% yield and the sulfonamide **36** was not identified. This result was unexpected as it was envisaged that the electron withdrawing effect of the sulfonyl group would decrease the nucleophilicity of the sulfonamide nitrogen compared with that of the aniline. However, formation of the bis-sulfone species, **43**, suggests a greater reactivity of the sulfonamide compared with that of the aniline.

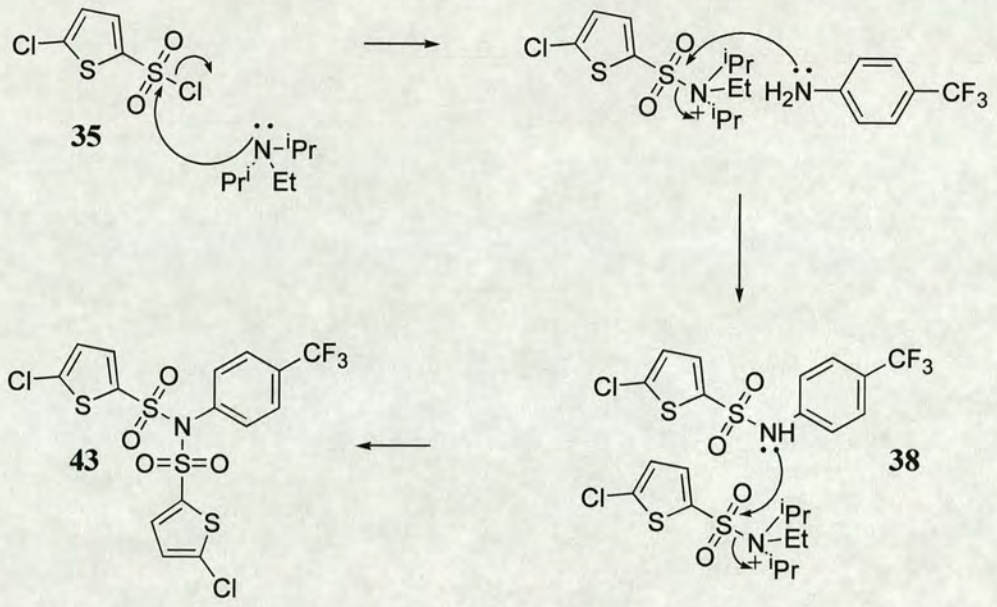

Scheme 2.6: Proposed mechanism for the formation of bis-sulfonamide species **43**.

N-Allylation of sulfonamide **37** afforded **39** in 92% yield. Nucleophilic displacement of the 5-chloro functionality with the commercially available 3-chloro-5-(trifluoromethyl)-pyridine-2-thiol, **40**, was unsuccessful, resulting in the recovery of **39**. It was postulated that conversion of the chloro group to either a bromo- or iodinated species would activate **39** for reaction. However, as the halogen exchange reaction has not been reported for chlorothiophenes, it would be necessary to resynthesize the *N*-alkylated sulfonamide from 5-bromo-thiophene-2-sulfonyl chloride.

An alternative strategy (Scheme 2.7) was the conversion of sulfonamide **39** to the α-lithio species, **45**, and subsequent reaction with the sulfonyl chloride, **44**, to afford **42**. It was envisaged that **44** could be prepared directly from the thiol, **41**, following a method reported by Park *et al.*[85] However, two attempts to synthesize the sulfonyl chloride **44** were not successful and afforded a complex mixture of products. Clearly this strategy required further work and ultimately it would only yield one ligand, **42**, for screening in the p53-Mdm2 competitive binding assay. It was therefore decided that the best strategy

would be to synthesize a number of combinatorial libraries containing novel sulfonamides that could be submitted for screening in the p53-Mdm2 competitive binding assay. In turn this would generate a valuable SAR picture of the Mdm2 binding cleft with regards to sulfonamide ligands.

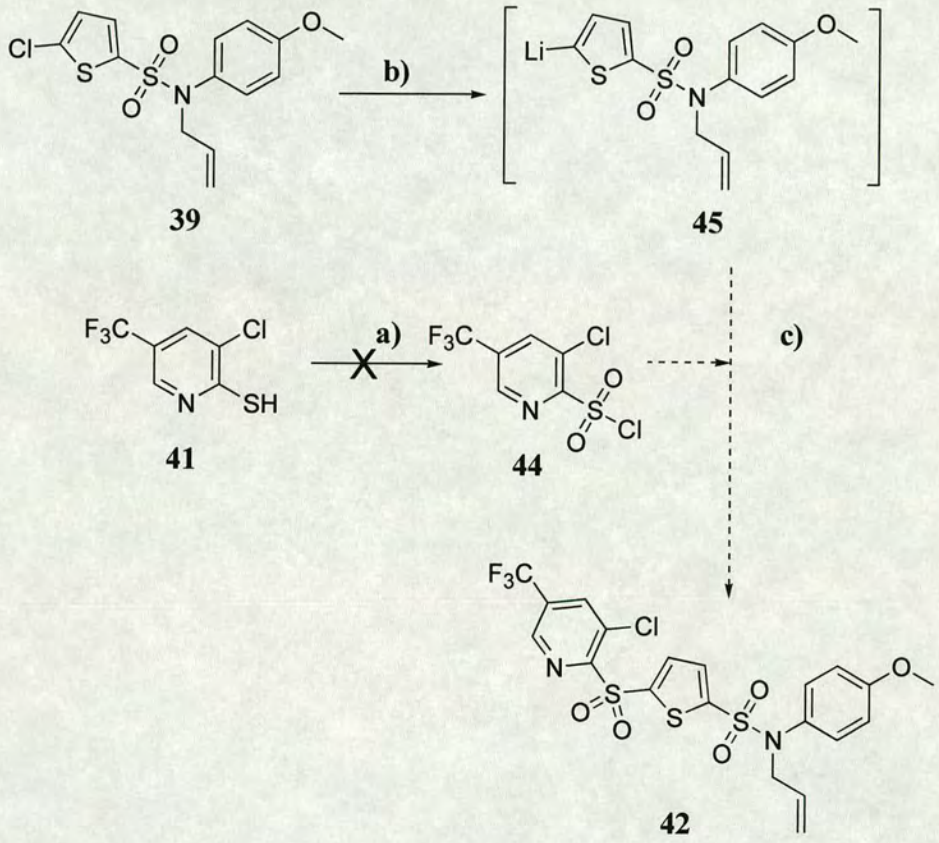

Scheme 2.7: Alternative strategy for the synthesis of 2-sulfonyl-3-chloro-5-trifluoromethyl-pyridine analogues. *Reagents and conditions*: **a**) SO_2Cl_2, KNO_3, DCM (anhydrous), room temperature, 24 h. **b**) BuLi, Et_2O, -78 °C, 30 mins. c) **44**, room temperature, 2 days.

Sulfonamides **37**, **39** and **43** were submitted for screening in the FP p53-Mdm2 competitive binding assay, the IC_{50} values determined for these sulfonamides are

presented in Table 2.1. Details of each assay are given in Section 5.2. A discussion of the biological assay results is presented in Section 2.10.

Compound No	IC_{50} μM	IC_{50} μM
37	338	>500
39	>500	407
43	156	>500

Table 2.1: IC_{50} values (μM) determined in FP assay 1 (blue) and 2 (red) for sulfonamides **37**, **39** and **43**.

2.4 Combinatorial synthesis of sulfonamide libraries

2.4.1 Equipment

Figure 2.4 is a representation of the robotic equipment available at Edinburgh University for parallel array preparation, synthesis, purification and analysis of combinatorial libraries. After the time-consuming installation and training on each piece of equipment had been completed, the aim was to prepare a small library of sulfonamide analogues in order to become familiar with the operation of each system, and to illustrate the application of the full range of equipment to the synthesis of combinatorial libraries in the ligand design process.

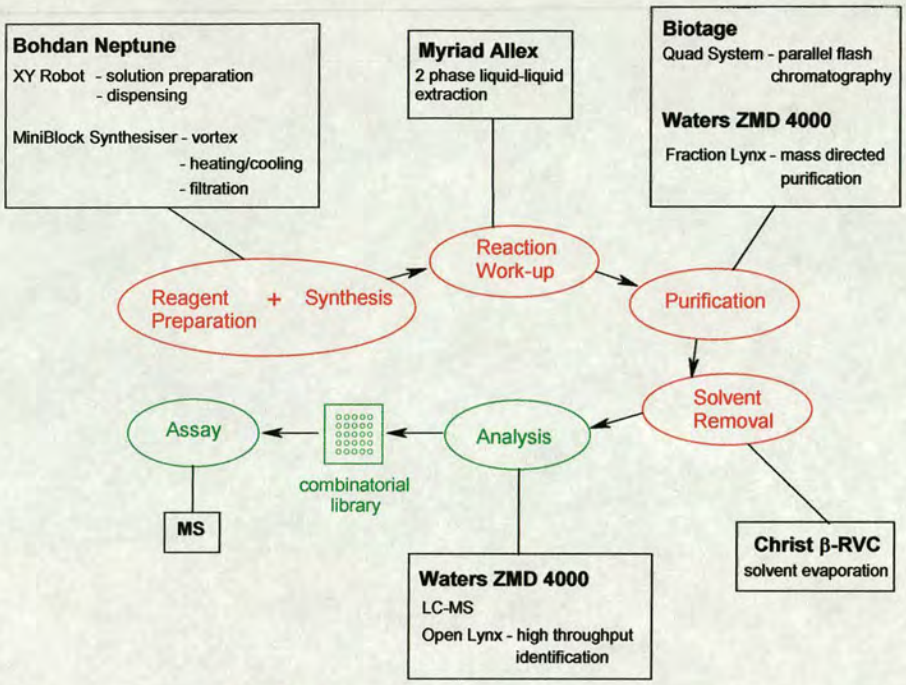

Figure 2.4 Parallel Array Synthesis and Analysis

The first step in library preparation was development of a synthetic route to the desired sulfonamide analogues. In order to minimise the possibility of the formation of the bis-sulfonamide species that had been reported using the protocol adopted for the synthesis of sulfonamide **36,** and also to make the sulfonamide condensation reaction more suited to an automated approach by dispensing with the requirement of a separate addition of base to each reaction vessel, it was decided to investigate whether the sulfonamide coupling would proceed using pyridine as the reaction solvent, rather than using THF and small volumes of *N,N*-diisopropylethylamine. Indeed, this was found to be the case, with the sulfonamide **36** being synthesized in good yield, with no evidence of the bis-sulfonamide side reaction (Scheme 2.8). Consequently, this protocol was adopted for the synthesis of pilot sulfonamide Library **L1**.

The choice of an appropriate solvent is often crucial to the success of an automated synthesis of an array of compounds, formed using common building blocks, as it is an important requirement to be able to dispense all of the required reagents as solutions, in

order to minimize manual input. Furthermore, a problem associated with the poor solubility of a reagent could not only manifest itself in inadequate transferral of that reagent to a number of reaction vessels, resulting in poor yields, but could potentially block the cannula of the Bodhan Neptune™-MB Automated Workstation causing termination of the automated synthesis.

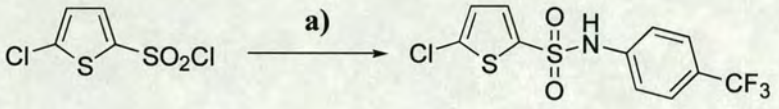

Scheme 2.8: *Reagents and conditions*: a) 4-trifluoromethyl-aniline, pyridine, room temperature, 24 h.

The Neptune™ is capable of tare weighing vials and dispensing solvent to prepare solutions of known concentration, when the compound molecular weights and required solution volumes have been entered. Thus, although the accurate weights and volumes are calculated by the computer, all solid reagents must be weighed out approximately by hand. Considering that a 48-membered library would commonly consist of a 6 x 8 array of building blocks, only 14 stock solutions would be required. Therefore it was decided to prepare these manually rather than with the Neptune™. The Neptune™ would then be used to dispense a fixed volume of each stock solution to designated reaction vessels contained in a MiniBlock™.

The next challenge proved to be adaptation of the chosen synthetic route to make it suitable for automation. Using MiniBlock™ technology, it was neither possible nor desirable to perform each sulfonamide synthesis on a 2.8 mmole scale, as for sulfonamide **36**. Furthermore, there was an economic factor associated with some of the commercially available sulfonyl chloride building blocks. It was hoped to synthesize ca. 50 mg of each sulfonamide, not only to provide ample quantities of ligand for screening at Cyclacel Ltd., but also to provide enough material for full characterization. Anticipating a 70% yield for each reaction in the pilot library, a reaction scale of 0.15

mmole was set, based on a 50 mg scale of the 4,5-dibromo-thiophene-2-sulfonyl chloride building block.

Prior to purification of the library, each reaction mixture had to undergo an acidic wash and an extraction into organic solvent to remove excess pyridine from the reaction mixture. It was anticipated that the Myriad® Allex liquid-liquid extraction system could be used for this purpose. The Allex is capable of separating a two-phase system (aqueous and organic layers) by sensing the change in dielectric constant at the meniscus. It can then be programmed to transfer either the top or bottom layer to a different reaction vessel, with separation just above or just below the meniscus depending on the layer required. Two-phase systems can also be mixed before separation, through aspiration of the mixture.

Clearly, there was also an issue associated with the scale of each reaction when addressing the subject of parallel purification. Too high a concentration of a sample in a given solution had the potential to overload a column and give poor separation. Although this could be addressed by multiple injections of the sample, this was not considered attractive, as it would lengthen the time required to purify a library. Equipment available in the laboratory suitable for parallel, automated purification consisted of the Biotage Quad3™, the Biotage Parallex Flex™ and the Waters ZMD 4000 LCMS system.

Potentially, the Quad3™ can purify up to 12 compounds, at a scale of around 0.250 g, in around 30 minutes, using normal-phase flash chromatography techniques. It is limited to elution using an isocratic solvent system, unless additional solvent systems are prepared and loaded onto the system manually. Owing to the need to monitor the purification by thin layer chromatography and to combine and then concentrate desired fractions *in vacuo*, its maximum output is, however, probably limited to 24 compounds per day. It was thought that the quantities of sulfonamides synthesized in each library would be at the lower end of the scale with respect to the purification range of this machine.

One further option was to use the Biotage Parallex Flex™ reverse phase HPLC. Potentially, the Flex™ has the capacity to purify up to 0.250 g of injected sample on a Supercosil ABZ+Plus reverse-phase column, of dimension 25 cm x 21.2 mm, particle size 12 μM, although, in practice following subsequent work on CDK inhibitor programme as discussed in Chapter 4, this was found to be around 0.050 g. The threshold for collection of a peak in the chromatogram can be lowered, allowing ligands present in small concentrations to be collected. Samples may be queued to allow for sequential automated purification. The main disadvantage to using this system was that it was envisaged that a considerable amount of time would have to be spent developing reverse-phase purification methods.

Perhaps the most attractive option was the use of an automated mass directed purification system, such as the Waters ZMD 4000 reverse-phase LCMS system. This equipment has the potential of sequentially purifying compounds in concentrations up to 50 mg ml^{-1}, with typical methods of around 20 minutes duration and maximum injection volumes of 1 mL. Although a commitment of time would be required to develop reverse-phase purification methods on this system, the use of the ZMD would provide identification of the sulfonamides by ESI-MS and furthermore to give a reasonable indication of the reaction progress, including reagents remaining and product formation.

2.4.2 Pilot sulfonamide library L1 and early SAR

The sulfonamide combinatorial chemistry programme was initiated with a test library of 12 sulfonamides (Table 2.2) consisting of 2-sufonyl chloride building blocks dropped from a proposed initial 'full-scale' (48 member) library, and 6 anilines. The rationale for the design of both this library was based on the review of the 191-membered hit expansion library based on the sulfonamide and sulfonate ester template. From this hit expansion library, both thiophene and aniline part of those ligands shown as being active in either the FP or ELISA assay were identified and considered separately for inclusion within the combinatorial library.

For the pilot library **L1** two sulfonyl chlorides were selected, both of which contained a 5-halo substituent at the thiophene ring. Of the 10 ligands containing these building blocks in the initial hit expansion library, 2 were shown to have IC_{50} values <500 μM in the FP assay. Notably, of the 6 anilines selected as building blocks for library **L1**, 3,5-bis-trifluoromethylaniline had been represented by 2 ligands in the hit expansion library, both of which were active in the FP assay. Of the 6 anilines selected, only 3,5-dichloroaniline had not been represented in the initial hit expansion library, its inclusion in library **L1** was based on the activity of a sulfonate ester containing the 3,5-dichlorobenzene moiety.

	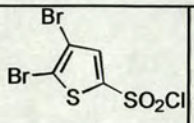	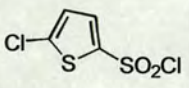
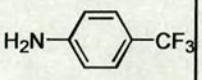	**46** Sample Not Recovered	**52** 1% 477 358
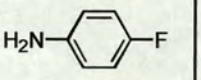	**47** Sample Not Recovered	**53** Reaction Failed
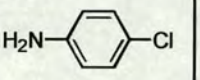	**48** Reaction Failed	**54** 1% >500 320
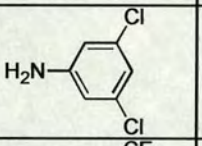	**49** 1% 194 -	**55** 1% >500 >500
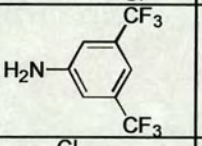	**50** 1% 103 102	**56** 1% 88 435
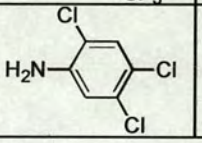	**51** 1%	**57** Reaction Failed

Table 2.2: Library **L1**. Compound numbers are given in bold, together with percentage yields. IC_{50}'s (μM) in the FP assay are given in blue (FP assay 1) and red (FP assay 2).

Library **L1** was synthesized on the Neptune™ adopting the protocol used for the synthesis of **36**, on a 0.15 mmole scale. Stock solutions of each reagent were prepared in 20 ml reagent vials, 2 containing a 0.15M concentration of either 4,5-dibromo- or 5-chloro-thiophene-2-sulfonyl chloride in pyridine, and 6 containing a 0.16M concentration of the selected substituted aniline in pyridine. The reagents were dispensed into a MiniBlock™ (the MiniBlock consists of 48 fritted tubes, each reversibly sealed at the narrow tube end by a pinching mechanism, and encased in an

insulated block which may be heated or cooled) that was shaken at room temperature for a period of 24 hours. The reactions were carried out in 2.0 mL total volume of solution.

The first problem encountered in performing the library synthesis was in the transferral of the reaction mixtures from the MiniBlock™ to the test tubes used on the Allex system, owing to the limited compatibility of the volume and format of reagent vessels used in the MiniBlock™ and Allex systems. Although MiniBlock tubes can be drained into the commercially available 48-well microtitre plates, which are compatible with the Allex, these plates have a well volume of 5 ml and the Allex requires at least 2 mL of solvent in each layer to facilitate accurate separation. This meant that the solutions contained in the MiniBlock would first have to be transferred to larger test tubes on the Allex. To each test tube would then be added a solution of HCl (3 mL), followed by a 1:1 mixture of Et_2O: EtOAc (3 mL), the mixture would then be aspirated and the organic layers transferred to a separate test tube, to which brine (3 mL) would be added. Following the aspiration of this second mixture, the organic layer (approximately 3 mL) would finally be transferred to a 48-well microtitre plate for solvent concentration using the Christ evaporation system. Even using these larger volumes of solvent, problems were encountered during the separation steps, with approximately 0.5 mL of organic solvent not being transferred to either the second test tube or the 48-well microtitre plate. However, increasing the volume of solvent used in each liquid-liquid extraction step would be counterproductive as each sample had to be contained in a format suitable for parallel sample concentration using the Christ system. Another problem encountered when using the Allex system was that, following aspiration, some mixtures had a tendency to emulsify. Although, in some instances, this could be addressed by programming a number of wait cycles between the aspirate and dispense steps, the problem could not be completely solved and, in some instances, resulted in no detection of a liquid-liquid interface and consequently the organic solutions were not transferred to the 48-well microtitre plate for concentration. In these cases manual separation techniques had to be employed.

Further problems were encountered during purification of library **L1**. Sulfonamides **46** and **47** were used as test samples for mass directed purification on the ZMD 4000. Unfortunately, the molecular ions of these two sulfonamides were not detected and consequently, despite further attempts to identify the molecular ions of these species by ESI-MS, it was decided to undertake the remaining purifications on the Flex™ HPLC system. It is postulated that failure to detect the molecular ions of these species may have been attributable to the presence of the pyridinium ion in the samples.

Library **L1** yielded 6 sulfonamides for screening with failures resulting from 2 compounds lost at the purification stage (**46** and **47**), 3 failed reactions (**48**, **53** and **57**) and 1 compound, **51**, cross-contaminated. Yields were disappointingly low, with only trace amounts of sulfonamide being isolated and identified by ESI-MS. It was thought that the low yields obtained were mostly attributable to problems encountered with the use of the Allex. Of the 6 compounds isolated and subsequently submitted for screening, 4 displayed <500 μM activity in the FP assay (with **56** (88 μM) acting as a control and previously tested as KM01046 (199 μM) in the screening of the hit expansion library). Significantly, both **50** and **56** were shown have good activity in the FP assay, and perhaps suggested a favourable interaction between the 3,5-trifluoromethylanilino moiety and the Mdm2 protein. Sulfonamide **49**, exhibiting a 3,5-dichloroanilino moiety was also shown to have good activity in the FP assay, with an IC_{50} value of 194 μM. Both **49** and **50** containing the 4,5-dibromothiophene moiety were active in the FP assay.

2.4.3 Library L2.

A 48-membered library, as shown in Tables 2.3.1 and 2.3.2, followed library **L1**. Again, library **L2** was selected based on review of the hit expansion library screened by Cyclacel Ltd. A decision was made not to include the 5-chloro-4-nitro-thiophene-2-sulfonyl chloride building block in the combinatorial library for a number of reasons, despite the favourable activity of analogues containing this functionality screened from the hit expansion library. Firstly, scientists at Cyclacel Ltd. had found that the reactivity

of the 5-chloro- substituent to nucleophilic substitution was high, owing to the electron withdrawing effect of the adjacent 4-nitro- group. Consequently, reaction of the 5-chloro-4-nitro-thiophene-2-sulfonyl chloride with an aniline often afforded either the 5-anilino-4-nitro-thiophene sulfonic acid or the 5-anilino-4-nitro-thiophene-2-sulfanilide upon work up. Secondly, scientists at Cyclacel were focussing on the synthesis of further 5-chloro-4-nitro thiophene analogues and it was felt that the main objective of the combinatorial programme was to identify novel ligands. To address this issue, 4-oxazol-2-yl-benzenesulfonyl chloride and 3-nitrobenzene-sulfonyl chloride were included as building blocks for library **L2** to increase its diversity; to investigate whether the thiophene ring could be replaced by a benzene moiety; and to probe for additional non-covalent interaction in the Mdm2 binding cleft. Also, 5-benzenesulfonyl-thiophene-2-sulfonyl chloride was included as a building block to investigate whether sulfonamides containing this moiety would have similar activity to the 2-sulfonyl-3-chloro-5-trifluoromethyl-pyridine analogues, exemplified by **15** and **16**. Of the 8 anilines selected for inclusion within the library, 3 contained a substitution pattern that had not been screened in the hit expansion library. The unsubstituted aniline was selected to investigate whether functionality off the anilino ring was required for activity. 4-Methylaniline was selected to examine the effect of an electron-donating group in the anilino ring. 2,4-Dichloroaniline was selected for comparison with the 3,5-dichloroaniline analogues to gain insight into a preferred substitution pattern on the anilino ring.

	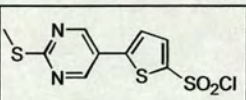	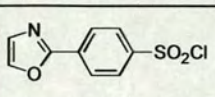	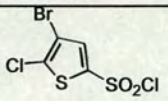
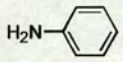	**58** 4% >500 >500	**66** Reaction Failed	**74** 1% 450 >500
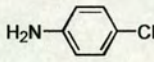	**59** 2% >500 >500	**67** 10% 416 494	**75** 1% 274 218
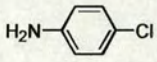	**60** 4% >500 >500	**68** 10% >500 >500	**76** 1% >500 >500
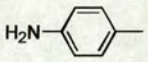	**61** 1% >500 >500	**69** 1% >500 >500	**77** 2% >500 >500
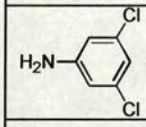	**62** 1% 455 374	**70** 1% 246 -	**78** Reaction Failed
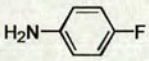	**63** 1% >500 >500	**71** 2% >500 >500	**79** Reaction Failed
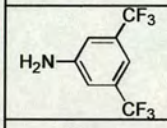	**64** 2% 159 >500	**72** 1% 437 448	**80** 1% 293 -
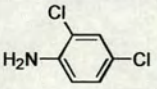	**65** 1% >500 >500	**73** Reaction Failed	**81** 1% 431 -

Table 2.3.1: Library **L2**. Compound numbers are shown in bold, with percentage yields given. IC_{50}'s (μM) in the FP assay are given in blue (FP assay 1) and red (FP assay 2).

	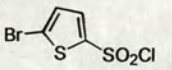	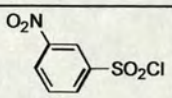	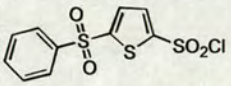
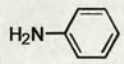	**82** 3% >500 >500	**90** 28% >500 >500	**98** 16% >500 >500
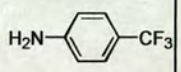	**83** 2% 152 -	**91** 25% >500 482	**99** 6% 241 146
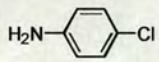	**84** 2% 424 290	**92** 30% 392 295	**100** 6% 395 243
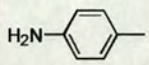	**85** 1% >500 >500	**93** 29% >500 >500	**101** 13% >500 >500
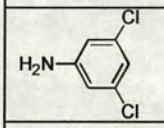	**86** 1% 290 291	**94** 30% >500 >500	**102** 2% 480 288
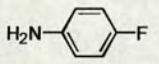	**87** Reaction Failed	**95** 29% >500 >500	**103** 19% >500 >500
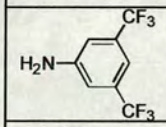	**88** 1% 209 172	**96** 15% 292 209	**104** 3% 147 -
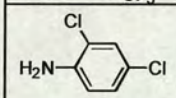	**89** 1% >500 -	**97** 6% >500 441	**105** 3% 305 -

Table 2.3.2: Library **L2**. Compound numbers are shown in bold, with percentage yields given. IC_{50}'s (μM) in the FP assay are given in blue (FP assay 1) and red (FP assay 2).

Owing to the poor yields of sulfonamides obtained for library **L1**, the synthetic protocol was adjusted, with the scale of each reaction being increased from 0.15 mmole to 0.20 mmole. However, similar problems to those reported for library **L1** were still encountered when performing the automated work-up of the library, despite having inserted additional wait cycles into the work-up programme.

It was still envisaged to purify the library members using the ZMD and therefore 16 reactions (**90** - **105**) were used as test samples for mass directed purification. Unfortunately, for each sample the molecular ion of the sulfonamide was not detected and the majority of the samples were dispensed to waste. Consequently, a further 16 membered library was planned to resynthesize samples **90** - **105** lost at the purification stage. Where some residual crude mixture had been recovered and for subsequent library members **58** - **89**, the sample was dissolved in methanol (1 mL) and injected directly onto the Biotage Parallex Flex™ HPLC.

Despite these difficulties library **L2** afforded 30 novel sulfonamides for screening, with failures resulting from 13 compounds being lost at the purification stage on the ZMD and 5 failed reactions where only the sulfonic acid was identified by ESI-MS. Again, the isolated yields of sulfonamides recovered from the HPLC was extremely low compared to those sulfonamide condensations synthesized and purified by conventional techniques. To address this, an attempt was made to resynthesize library **L1** using triethylamine as opposed to pyridine as a reaction solvent. However, this was not successful as it was found that in the majority of cases, activation of the sulfonyl chloride with triethylamine precipitated the species out of solution, rendering automated transfer impossible.

A small 2 x 2 array was undertaken using the 5-bromo-thiophene- and 3-nitrobenzene-sulfonyl chlorides and 3,5-dichloro- and 2,4-dichloro- anilines. The reactions were performed at 0.20 mmole scale using DCM as the reaction solvent. A solution of DIPEA (2.0 eq.) in DCM was added to each reaction vessel and the mixtures allowed to stir for 64 hours at room temperature. NMR and ESI-MS analysis of the unpurified reaction mixtures failed to identify the presence of the sulfonamide products.

The protocol adopted for the synthesis of library **L2** was slightly modified for the resynthesis of sulfonamides **90** - **105** (Table 2.3.2). Prior to the liquid-liquid extraction step on the Allex, the samples were transferred from MiniBlock to a 48-well microtitre

plate and concentrated *in vacuo* on the Christ system in order to remove excess pyridine. Rather than using a 1:1 mixture of EtOAc:Et_2O, solely EtOAc was used for extraction. An additional aqueous wash was performed on each sample prior to washing each with brine. More significantly, a decision was made to purify each reaction manually, using small scale, normal phase column chromatography techniques. In doing so, it was expected that the added attention to each individual purification would result in a higher recovery of isolated sulfonamide. Indeed, for most reactions this was found to be the case, with isolated yields from the reactions purified manually ranging from 2 – 30 %, with an average yield of 16 % for the 16 reactions, compared to 1 – 10%, with an average yield of 2%, for the reactions from library **L2,** purified using automated purification techniques. However, isolated yields were clearly still significantly lower than those anticipated based on the manual synthesis of **36** (71 %) and clearly further work was required on developing the existing protocol. Furthermore, although manual purification of sulfonamides **90** - **105** had resulted in an overall increase in isolated yields, it would not be practical to adopt this approach if larger combinatorial libraries were required to be synthesized nor if throughput was an issue.

The biological assay results obtained from library **L2** are presented in Tables 2.3.1 and 2.3.2 and are discussed in detail in Subsection 2.9. However, some general trends were immediately observed from the data. Those sulfonamides containing either a 3,5-dichloro- or 3,5-bis-trifluoromethyl- substitution pattern on the anilino aromatic ring generally had good activity in the FP assay, demonstrated by ligands **64** and **70** with IC_{50} values of 159 μM and 246 μM respectively. Furthermore, assay results indicated that the thiophene ring could be replaced by an aromatic ring and afford compounds with some activity.

2.4.4 Library L3

To address the resynthesis of 2 sulfonamides, **50** and **56**, to provide additional ligand for further *in vitro* screening, library **L3** (Table 2.4) was planned. Additionally, this library

aimed to investigate a small number of sulfonamides made from 4-chloro-3-nitro-benzene sulfonyl chloride. Only 2 ligands, **106** and **107**, had been screened prior to the generation of this library that contained the 4-chloro-3-nitro-benzene moiety. Both **106** and **107** exhibited moderate activity in the FP assay, with IC_{50} values of 192 μM and 232 μM respectively. It was postulated that the 4-chloro-3-nitro-benzene moiety could interact with Mdm2 in a similar manner to the 5-chloro-4-nitro-thiophene moiety. Finally, the benzoyl chloride building block was included to investigate whether an amide linker could replace the sulfonamide linker. Of the anilines chosen for inclusion within the library, both the 3,5-bis-trifluoromethyl-aniline and 3-trifluoromethyl-aniline moieties had been present in hits from the initial hit expansion library; the 3-chloro-benzene moiety had been present in the form of an active sulfonate ester from the hit expansion library; and the 3,4-dichlorobenzene moiety had been present in the form of an inactive sulfonate ester in the hit expansion library.

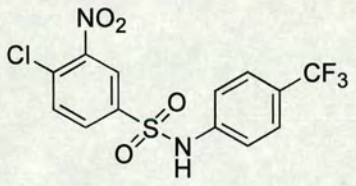

106

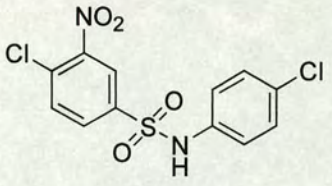

107

	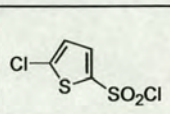	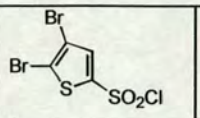	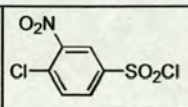	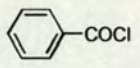
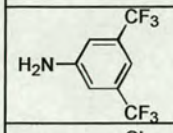	**56** 2% 88 435	**50** 7% 103 102	**114** 11% - 129	**118** 14% - >500
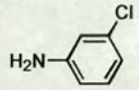	**108** 13% >500 >500	**111** Reaction Failed	**115** 5% - >500	**119** 31% - >500
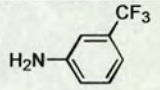	**109** 38% >500 >500	**112** 12% - 199	**116** 3% - 335	**120** 36% - >500
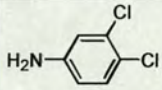	**110** 7% - 295	**113** 8% - 160	**117** 4% - 427	**121** 24% - >500

Table 2.4: Library **L3**. Compound numbers are shown in bold, with percentage yields given. IC_{50}'s (μM) in the FP assay are given in blue (FP assay 1) and red (FP assay 2).

Adopting identical protocol to that used for the resynthesis of sulfonamides **90** - **105**, library **L3** yielded 15 compounds for screening, with 1 failed reaction. A minimal amount of **56** was isolated (2%) owing to the majority of the sample being transferred to waste during the liquid-liquid extraction stage. Otherwise, yields of isolated sulfonamides were in the range 3 – 38%, with an average yield of 15%.

FP assay results obtained from library **L3** suggested that the amide linker was not tolerated in the Mdm2 binding pocket. However, given the IC_{50} value obtained for **114** of 129 μM, it was decided that a more suitable comparison could be made by adding 4-chloro-3-nitro- substitution pattern to the benzene carbonyl chloride. The novel ligands **112** and **113**, both containing the 4,5-dibromothiophene moiety, were shown to be active in the FP assay, with IC_{50} values of 199 μM and 160 μM respectively.

2.4.5 Library L4

A further sulfonamide library, Library **L4** (Tables 2.5.1 and 2.5.2), was planned to explore a number of novel sulfonyl chloride building blocks that had been made available from Maybridge. 4,5-dibromo-thiophene-2-sulfonyl chloride was included as this building block had exhibited activity in the form of ligand **50**. The anilines selected for this library included the 3,5-bis-trifluoromethyl-, 4-trifluoromethyl- and 4-chloro-substitution patterns, featured in ligands from library **L2**, that had been shown to have good activity in the FP assay. It was decided to investigate whether an additional CH_2 spacer would be tolerated between the sulfonamide linker and the aromatic ring, and to address this issue, 3,5-bis-trifluoromethyl-benzylamine, 4-trifluoromethyl-benzylamine and 4-chloro-benzylamine were selected for inclusion within the library. Furthermore, to continue the investigation of whether an additional interaction could be found between the ligand and the Leu26 pocket, both (*R*)- and (*S*)- enantiomers of 1-(4-chlorophenyl)-ethylamine were included as building blocks.

The protocol adopted for the synthesis of library **L4** was based on that established for the manual synthesis of sulfonamides shown in Table 2.7, detailed in 2.6.1, with only one equivalent of pyridine, in a solution of DCM, being added to each reaction vessel. The library was synthesized on the Neptune and the scale of each reaction increased from 0.20 mmole to 0.40 mmole. Owing to mechanical downtime of the Allex, each work-up was to be performed manually, again using the protocol adopted for the sulfonamides shown in Table 2.7. It was envisaged that Library **L4** would be purified using the normal phase column chromatography techniques on the Quad3.

	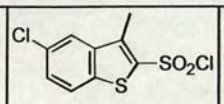	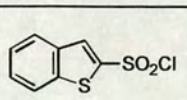	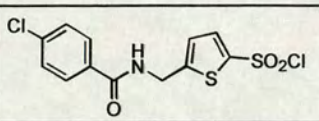
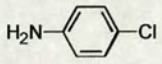	**122** 10% >500	**130** 17% >500	**138** Reaction Failed
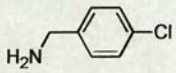	**123** Reaction Failed	**131** 12% >500	**139** Reaction Failed
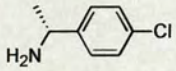	**124** 5 % >500	**132** 10% >500	**140** Reaction Failed
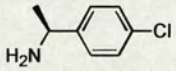	**125** Reaction Failed	**133** 3% >500	**141** Reaction Failed
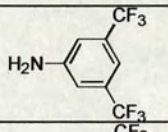	**126** 7% 106	**134** 29% 193	**142** Reaction Failed
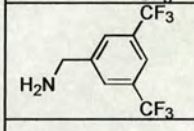	**127** 33% >500	**135** 30% >500	**143** Reaction Failed
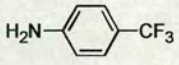	**128** 8% >500	**136** 18% >500	**144** Reaction Failed
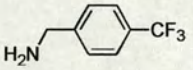	**129** Reaction Failed	**137** 9% >500	**145** Reaction Failed

Table 2.5.1: Library **L4**. IC_{50} values determined for each ligand in the (new) FP assay are shown in red.

	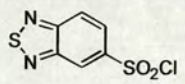	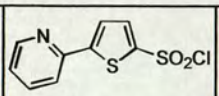	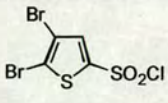
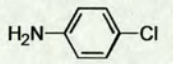	**146** 4% 314	**154** 29% >500	**48** 5% 198
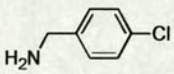	**147** 7% >500	**155** 2% >500	**162** 16% >500
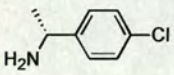	**148** 5% >500	**156** 8% >500	**163** 18% >500
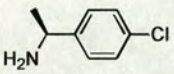	**149** 13% >500	**157** 3% >500	**164** Reaction Failed
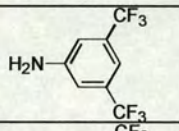	**150** 28% 165	**158** 29% 265	**50** 2% 102
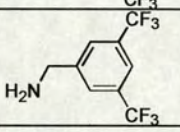	**151** 44% >500	**159** 33% >500	**165** 33% >500
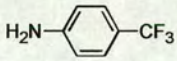	**152** 8% 329	**160** 8% >500	**46** 38% 163
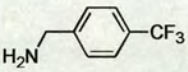	**153** 32% >500	**161** 19% >500	**166** 13% >500

Table 2.5.2: Library **L4**. IC_{50} values (μM) determined for each ligand in FP assay 2 are shown in red.

Library **L4** afforded 36 sulfonamides for screening, 35 of which were novel. 8 reactions failed owing to poor solubility of the building block containing the benzoylaminomethyl moiety that resulted in minimal transferral of the reagent to the reaction vessels. Isolated yields were in the range 2% - 44%, with an average yield of 16%, comparable to that of 15% for library **L3**.

Assay results obtained from members of Library **L4** indicated that an additional CH_2 spacer between the sulfonamide functionality and the aromatic ring was not tolerated in the Mdm2 binding cleft, demonstrated by **150** (IC_{50} 165 μM) and **151** (IC_{50} >500 μM). Furthermore, the activity of sulfonamides **126**, **134** and **150**, with IC_{50} values in the FP assay of 106 μM, 193 μM and 165 μM respectively, suggested that the benzothiazole and benzothiadiazole ring systems could potentially replace the thiophene ring. The significance of the biological data is discussed in detail in Section 2.10.

2.5 Exploratory solid phase work

To attempt to optimize the synthesis of sulfonamide libraries, whilst still retaining a high-throughput approach, some exploratory work was undertaken focussing on the use of 'catch and release' resins. The applicability of polymer supported DMAP as a catch and release resin of acid chlorides and sulfonyl chlorides to synthesize a variety of acyl and sulfonyl derivatives, including esters, amides and sulfonamides, has been reported.[86] The electrophilic acyl or sulfonyl chloride can be reacted with PS-DMAP, **167**, to form an *N*-substituted pyridinium salt, **168**, which can then be reacted with various nucleophiles such as alcohols, amines and thiols, without the requirement of a tertiary amine base (Scheme 2.9).

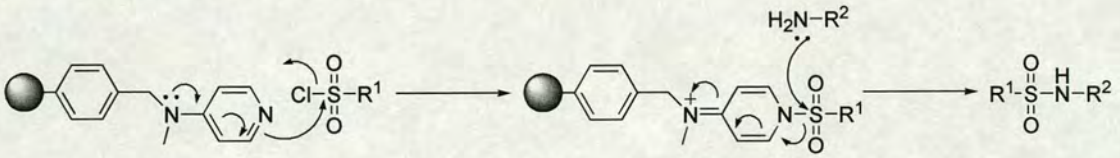

167 **168**

Scheme 2.9: The use of PS-DMAP as a catch and release resin.

The perceived advantage of using a catch and release strategy was that by using the nucleophile as the limiting reagent, the product could be isolated in high purity by filtration, with the excess electrophile remaining bound to the resin. This strategy would not only remove the problematic liquid-liquid extraction steps on the Allex but also

eradicate the need for purification of each sample by HPLC or normal phase column chromatography. In turn, an increase in throughput was expected. One disadvantage to using the catch and release strategy was that the scale of each reaction would be required to be decreased owing to the small volume of the reaction vessels used by the MiniBlock (3 mL) and the relatively low loading of the resin (0.35 mmole g^{-1}). Also, the resin would have to be washed prior to addition of the nucleophile to remove excess unbound sulfonyl chloride.

Seven trial reactions were undertaken using this strategy. Typically, the resin (1.0 eq.) was mixed with a solution of the sulfonyl chloride (1.5 eq.) in anhydrous DCM and allowed to stir at room temperature for 2 hours. After thorough washing of the resin with DCM to remove excess sulfonyl chloride, a solution of the aniline (0.7 eq.) in the chosen reaction solvent was added. The mixture was allowed to stir at room temperature for a period of 1-3 days before being filtered, washed with DCM and the filtrate and washings concentrated *in vacuo*. Analysis of the residue by TLC and ESI-MS revealed, in the majority of cases, little sulfonamide, with the unreacted aniline being detected in all cases. Preliminary results from this study (Table 2.6) suggested that either the sulfonyl chlorides were not being successfully loaded onto the resin or failure of the anilines to react with the bound sulfone owing to the poor nucleophilicity of the aniline species. This question could have been addressed by collection and concentration of the resin washings after the loading of the sulfonyl chloride. However, with only 1 sulfonamide being recovered in from 6 reactions, in low yield and after purification by column chromatography, the catch and release protocol in its current form was deemed not as successful as the methodology developed for libraries **L2** and **L3** and, consequently, it was decided not to continue with this strategy.

	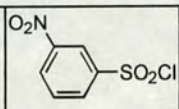	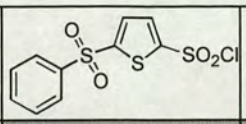	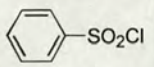	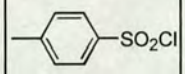
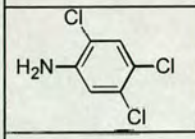	**169** Aniline isolated			
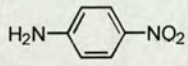	**170** Aniline isolated			
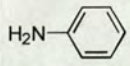		**98** Sulfonamide identified by ESI-MS		
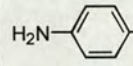	**171** Aniline isolated		**172** 23%	**173** Aniline isolated

Table 2.6: Exploratory reactions examining a catch and release strategy using PS-DMAP, **167**. Compound numbers are shown in bold, with the isolated yield of **172** shown. Shaded boxes represent those reactions not undertaken.

2.6 Synthesis of *N*-alkylated sulfonamides

2.6.1 Manual scale up of sulfonamide synthesis to allow second-generation library

Given that a number of sulfonamides synthesized in libraries **L1** - **L4** had been shown to be active in the FP assay, it was decided to resynthesize a number of these (Table 2.7) on a larger scale, ranging from 1.9 – 3.1 mmole, and, in doing so, not only satisfy a demand for further *in vitro* screening but also to allow the synthesis of a second generation library of *N*-alkylated sulfonamides. To facilitate work-up and purification of the ligands, it was decided to use a stoichiometric amount of pyridine in the synthesis, rather than an excess. The isolated yields obtained for each sulfonamide synthesis shown in Table 2.7 were encouraging and significantly better than those obtained using the same method utilizing the combinatorial equipment for the synthesis of library **L4**, although it should be noted that library **L4** was performed on a 0.4 mmole scale.

	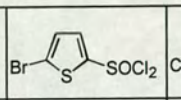	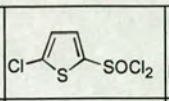	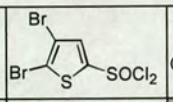	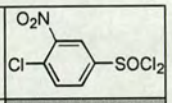
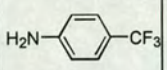	**83** 89%	**56** 81%	**50** 97%	
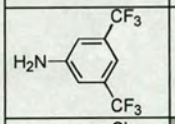	**88** 72%	**52** 77%	**46** 80%	**114** 94%
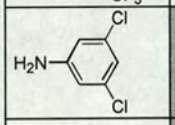				**174** 74%
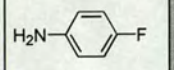				**175** 86%

Table 2.7: Manual resynthesis of a selection of sulfonamides active in the FP assay. Compound numbers are shown in bold, with percentage yields of isolated sulfonamides given. Shaded boxes represent those reactions not undertaken.

2.6.2 *N*-Alkylation of sulfonamides

Screening results of two ligands synthesized by Shudong Wang at Cyclacel Ltd., CY12258 (IC_{50} 42 μM, FP assay 1), **176**, and CYC12263 (IC_{50} 15 μM, FP assay 1), **177**, suggested that *N*-alkylation of the sulfonamide moiety resulted in an increase in potency of thiophene sulfonamides *in vitro*.

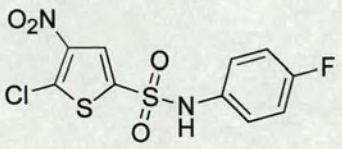

176

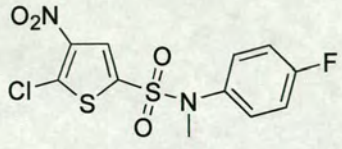

177

This observation was supported by screening data obtained from the FP assay for several *N*-benzylated sulfonamides, synthesized by chemists at Cyclacel Ltd., and exemplified

by CYC12444, **178**, and CYC42919, **179**, with IC_{50} values of 15 μM and 7 μM respectively.

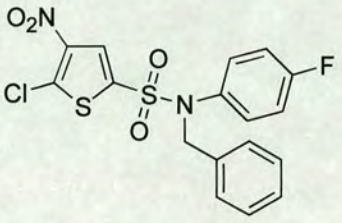

178

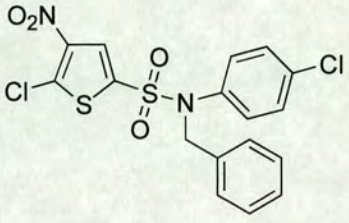

179

Furthermore, a modelling study undertaken by Mark Thomas at Cyclacel Ltd., which built on earlier work detailed in Chapter 2.3, had suggested that potentially an *N-alkyl-* or *N-benzyl-* substituent could fill the Leu26 binding pocket of Mdm2.

With the aim of generating a small library of *N*-alkylated **56** analogues, 3 reactions were undertaken to evaluate the applicability of the Tsunoda reaction performed under perceived optimal conditions based on unpublished work undertaken by Mascio within the group. In each case the *N*-alkylated sulfonamides **180**, **181** and **182** were not isolated, and only unreacted **56** was recovered. Clearly this reaction did not lend itself well to library synthesis in its current form, and consequently, other methods of *N*-alkylation were sought.

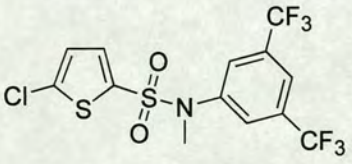

180

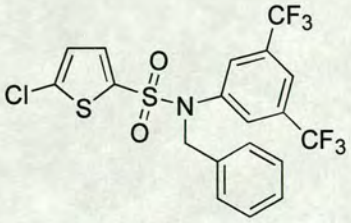

181

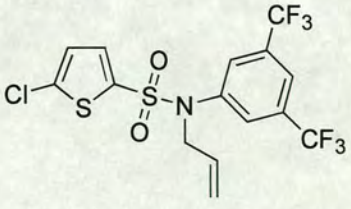

182

Selective synthesis of *N*-alkylanilines via direct alkylation with excess aniline in the presence of an alkyl halide is often problematic due to the difficulty in preventing the

formation of the corresponding *N*-*N*-dialkylaniline and the quaternary ammonium salt. One convenient method for the synthesis of a secondary amine is via reductive amination of an aniline, **183**, with an aldehyde, **184**, using the Borch reduction.[87] The reductive animation can be regarded as proceeding via a hemiaminal intermediate, **185**, that can undergo conversion to an imine, **186**, followed by reduction, using $NaBH_3CN$, **187**, to the *N*-alkylated anilino moiety, **188**. Again, overalkylation is often a problem associated with this reaction. It was expected that subsequent reaction of the *N*-alkylated anilino species, **188**, with a sulfonyl chloride, **189**, would afford the *N*-alkylated sulfonamide, **190**, as illustrated by Scheme 2.10.

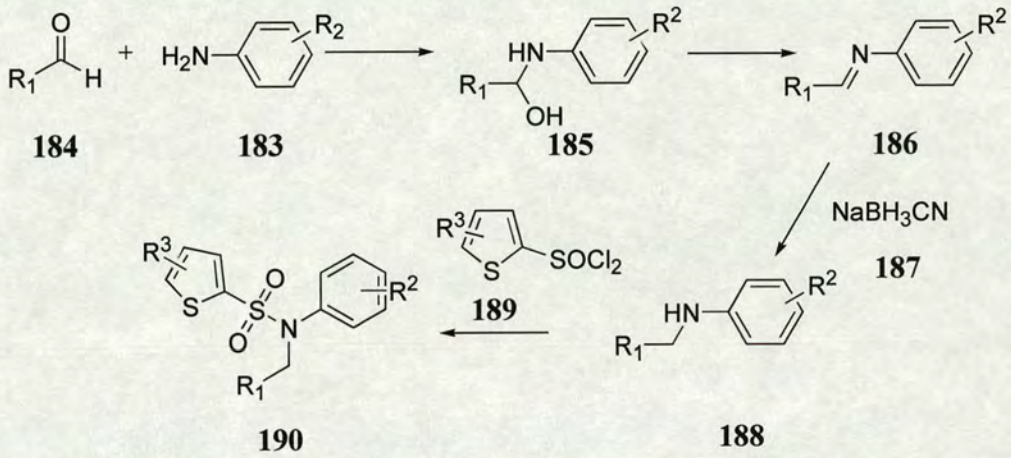

Scheme 2.10: Reductive amination and subsequent condensation to afford a sulfonamide.

The perceived advantage associated with this strategy was that, by fixing the sulfonyl chloride species and varying the aldehyde, a diverse 1-dimensional library could be generated, based on an existing mono-substituted sulfonamide that had shown good activity in the FP assay. The library would therefore directly examine the effect of *N*-alkylation. However, this strategy would require the generation of two novel libraries as opposed to only the one – one of secondary amines, which were not likely to be useful for screening purposes, and one of *N*-alkylated sulfonamides. Also, the perceived

difficulty of purification of secondary amines and inherent stability issues associated with this species was potentially a challenge.

Given that a number of sulfonamides had been isolated in good yield (Table 2.7) a convenient strategy to generate a library of *N*-alkylated sulfonamides would be by S_N2 alkylation of the sulfonamide with an alkyl halide. Table 2.8 shows those reactions undertaken. Typically, for each alkylation, the alkyl halide (5.0 eq.) was added to a stirring solution of the sulfonamide (1.0 eq.) in acetone and sufficient triethylamine was added to make the reaction mixture basic. For alkylation **192** the reaction mixture was allowed to stir at room temperature for 24 hours. For alkylation **196** the reaction mixture was subjected to microwave irradiation at 150 °C for 5 minutes. Other alkylations shown in Table 2.8 were performed under microwave irradiation at 60 °C for 10 minutes. The isolated yields of *N*-alkylated sulfonamides obtained, following manual purification using normal phase column chromatography, were generally moderate. In those reactions where the *N*-alkylated sulfonamide was not isolated this was attributable to poor separation, in the case of the methylation reactions, or in the instance of isobutyl iodide, steric demands.

	—I	Br	Br	I	I
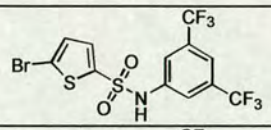	**191** Not Isolated	**197** 38% >500	**204** 48% >500	**211** 35% >500	**218** Not Isolated
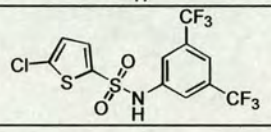	**192** 12 % >500	**198** 47% >500	**205** 45% >500	**212** 46% >500	**219** Not Isolated
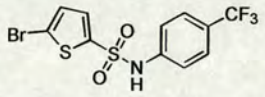	**193** Not Isolated	**199** 64% >500	**206** 57% >500	**213** 51% >500	**220** Not Isolated
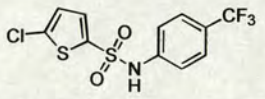	**194** Not Isolated	**200** 87% >500	**207** 84% >500	**214** 38% >500	**221** 8% >500
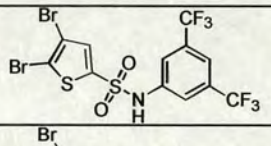	**195** Not Isolated	**201** 75% >500	**208** 36% >500	**215** 26% >500	**222** 3% >500
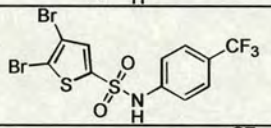	**196** 20% >500	**202** 81% >500	**209** 39% >500	**216** 35% >500	**223** 6% >500
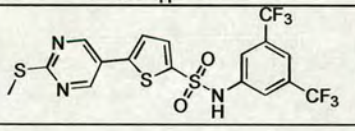		**203** 57% >500	**210** Not Isolated	**217** Not Isolated	**224** Not Isolated

Table 2.8: *N*-alkylated sulfonamides synthesized. Compound numbers are in bold, with percentage yields given. Shaded boxes represent reactions not undertaken. IC_{50} (μM) values as determined in FP assay 1 are shown in red.

As a result of this chemistry, 24 novel ligands were submitted for screening in the FP assay, although, disappointingly, all were shown to have >500 μM activity. Following further investigation, it was postulated that the absence of the *4-nitro-* group on the thiophene ring removes the potential for the formation of a hydrogen bond to the side chain of Gln59, and consequently the thiophene sulfonamide may adopt a different binding mode than that modelled for the 5-chloro-4-nitro-thiophene series.

2.7 Replacement of the sulfonamide linker

Using molecular docking, Mark Thomas at Cyclacel Ltd. investigated the replacement of the sulfonamide linker with an amide linker in the context of nine 5-chloro-4-nitro-thiophene sulfonamides and concluded that all molecules examined had the potential to dock in a similar manner to that observed in the sulfonamide series. Consequently it was decided that it would be useful to prepare a library of amides that could be screened in the FP p53-Mdm2 competitive binding assay.

Amides synthesized are shown in Tables 2.9.1 and 2.9.2. A key feature of the aromatic amides shown in Table 2.9.1 is the 3-nitro- functionality. It was hoped that the 4-chloro-3-nitro- substitution pattern would either mimic the 5-chloro-4-nitro- substitution pattern in the thiophene analogues or afford amides of comparable activity to the sulfonamides **114** – **117** synthesized in library **L3**. Furthermore the 4-methyl-3-nitro- substitution pattern had been investigated in the sulfonamide series and was present in a number of ligands shown to be active in the FP assay.

Amides shown in Table 2.9.2 contain heterocyclic functionality. Of the 5 acid chloride building blocks selected, 4 contained a thiophene ring. The 5-chloro-4-nitro-, 4-nitro- and 5-nitro- substitution patterns were selected on the basis of demonstrated activity exhibited by ligands synthesized by chemists at Cyclacel Ltd. for the sulfonamide series. Benzo[*b*]thiophene-2-carbonyl chloride was selected for inclusion within the array as a result of the IC_{50} value obtained for ligand **134** in the sulfonamide series. Only 9 ligands containing a furan ring had been screened in the hit expansion library, and, although all 9 were shown to be inactive in the FP assay, it was considered worthwhile to include 5-(4-chloro-phenyl)-2-methyl-furan-3-carbonyl chloride as a building block for the array to generate a number of novel ligands for screening.

	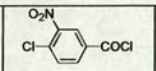	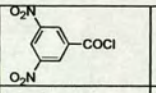	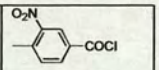
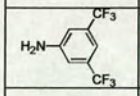	**225** 79% >500	**239** 23% >500	**241** 40% >500
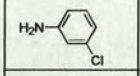	**226** 92% >167		**242** 81%
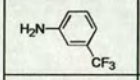			**243** 59%
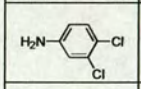	**227** 71% >167		
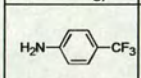	**228** 66% >500		**244** 59%
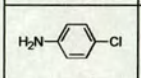	**229** 83% >500	**240** 26% >500	**245** 61% >500
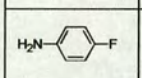	**230** 59% >167		**246** 53%
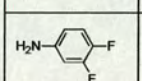	**231** 57% >500		**247** 61% >56
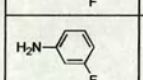	**232** 66% >167		
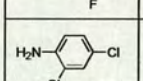	**233** 92% >56		
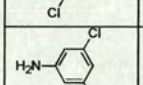	**234** 93% >56		**248** 34%
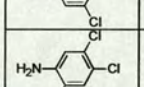	**235** 62% >56		
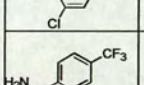	**236** 94% >167		**249** 76% >500
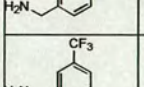	**237** 58%		**250** 73%
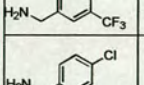	**238** 74% >167		**251** 78% >500
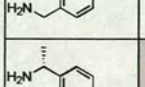			**252** 61% >56
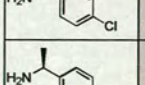			**253** 60% >56

Table 2.9.1: Aromatic amides synthesized. Percentage yields are given. Figures in red indicate the concentration (μM) at which the amide precipitated out of the FP assay.

	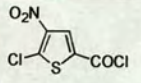	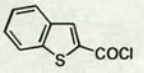	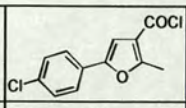	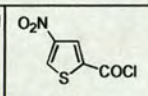	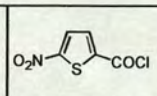
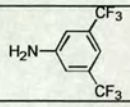	**254** 17%	**260** 60% >500	**268** 74% >167	**274** mixture of isomers	**278** 18%
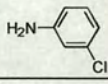					**279** 59%
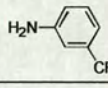		**261** 97% >167			**280** 48%
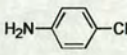	**255** 27%	**262** 34% >500	**269** 70%		**281** 45%
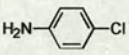	**256** 30%	**263** 51% >56	**270** 66% >167	**275** mixture of isomers	**282** 31%
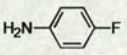	**257** 21%	**264** 55% >56	**271** 83% >167		**283** 59%
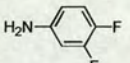		**265** 52% >500			**284** 51%
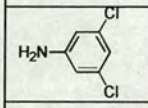					**285** 43%
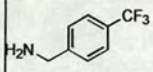	**258** 48%	**266** 72% >56	**272** 70% >56		
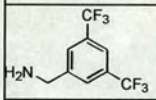				**276** mixture of isomers	**286** 76%
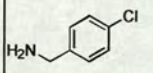	**259** 58%	**267** 46% >56	**273** 83% >500	**277** mixture of isomers	**287** 47%
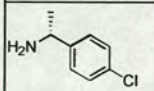					**288** 74%
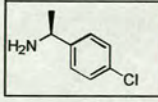					**289** 69%

Table 2.9.2: Heterocyclic amides synthesized. Percentage yields are given. Figures in red indicate the concentration (μM) at which the amide precipitated out of the FP assay.

A number of the acid chloride starting materials required to be synthesized, owing to their lack of commercial availability. Nitration of the commercially available 5-chloro-thiophene-2-carboxylic acid, **290**, using procedure reported by Fu *et al.*[88] afforded the mono-nitrated thiophene, **291**, exclusively in moderate yield (36%). It is postulated that the 3-position is deactivated to nitration owing to the presence of the 2-carboxyl group. Conversion of **291** to the carbonyl chloride, **292**, was achieved using oxalyl chloride and a catalytic amount of DMF (Scheme 2.11). **292** was used directly, without purification, for the synthesis of **254** – **259**.

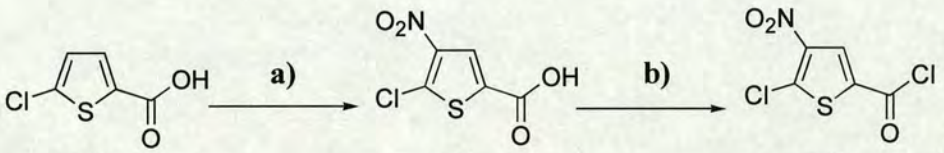

290 **291** **292**

Scheme 2.11: *Reagents and conditions:* **a**) HNO_3, HOAc, Ac_2O, room temperature, 24 h. **b**) $(COCl)_2$, DMF, DCM, room temperature, 24 h.

Nitration of the commercially available thiophene-2-carboxylic acid afforded a mixture of 5-nitro- and 4-nitro-thiophene-2-carboxylic acids that was converted to the respective isomeric mixture of carbonyl chlorides without purification. It was planned to isolate both isomers following reaction of the mixture of carbonyl chlorides with a selection of anilines, (Table 2.9.2, **274** – **277**) and, in doing so, provide 2 novel amides per anilino coupling, for screening in the FP assay. However, owing to the suspension of the p53-Mdm2 inhibitor programme, these purifications were not performed.

5-Nitro-thiophene-2-carboxylic acid **294** was synthesized by treating the commercially available 5-nitro-thiophene-2-carbaldehyde, **293**, with silver oxide, according to protocol reported by Satonaka[89] (Scheme 2.12). The acid **294** was converted to the carbonyl chloride **295**, which was used, without isolation, for amide couplings **278** – **289**.

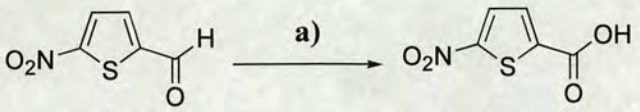

293 **294**

Scheme 2.12: *Reagents and conditions:* a) NaOH, $AgNO_3$, H_2O, room temperature, 2 h.

The general procedure used for the synthesis of amides **225 - 238** involved the addition of the substituted benzoyl chloride (1.1 eq) to a solution of the aniline (1.0 eq.) in anhydrous DCM. The reaction mixture was subjected to microwave irradiation at 110 °C for 5 minutes, before being extracted into EtOAc; washed with water, dried over anhydrous Na_2SO_4 and concentrated *in vacuo* to afford the amide in good purity.

One further method investigated for the synthesis of amides was based on work reported by Booth that employs the use of polymer-bound quenching reagents for high-throughput parallel purification.[90] Owing to its simplicity and efficiency, this methodology enables the rapid, parallel purification of crude reaction products obtained via solution phase synthesis and is therefore an attractive alternative to solid-phase organic synthesis in the application of combinatorial chemistry. The modified procedure, used for the synthesis of amides **239 - 289**, involved reacting an excess of a substituted benzoyl chloride (1.2 eq.) with an aniline (1.0 eq.) in anhydrous DCM, in the presence of resin bound morpholine. Following stirring overnight at room temperature, the reaction was then quenched by the addition of tris-(2-aminoethyl)amine resin. After a period of 4 hours, the resin was filtered and washed with DCM, the filtrate being collected and concentrated *in vacuo* to afford the amide in excellent purity.

Recently, Perreux *et al.* reported the synthesis of amides via pyrolysis of the salts obtained by mixing neat primary amines and carboxylic acids under solvent free conditions and under microwave irradiation.[91] Although the reported yields were low when reacting either aniline or 4-methoxyaniline with benzoic acid, this was considered an attractive strategy owing to the wide commercial availability of benzoic acid

analogues. Three exploratory reactions were undertaken using 4-nitro-benzoic acid and either 3,5-bis-trifluoromethyl-, **295**, 4-trifluoromethyl-, **296**, or 4-chloro-aniline **297**, of which only **296** was successful, affording 4-nitro-*N*-(4-trifluoromethyl-phenyl)-benzamide in 15% yield (Scheme 2.13). Although this one result was encouraging, this strategy was not pursued as it was apparent that time would have to be spent optimizing the reaction conditions.

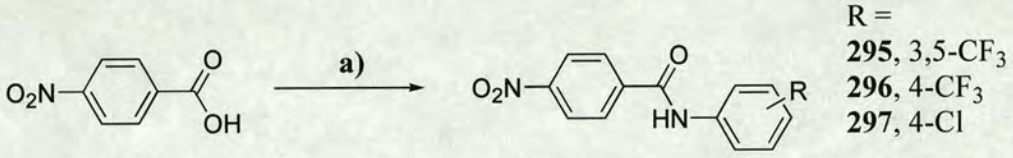

Scheme 2.13: *Reagents and Conditions:* a) Substituted aniline, solvent free, microwave irradiation, 160 °C, 15 mins.

Amides **225** – **289** were submitted for screening in the FP p53-Mdm2 competitive binding assay. Unfortunately all amides screened suffered from poor solubility in the assay, and consequently, IC_{50} values for each of the ligands could not be determined. This result was extremely disappointing and, owing to the subsequent suspension of the p53-Mdm2 programme, time did not permit the modification of the assay conditions.

2.8 Reversed amides and sulfonamides

Intriguingly, the effect of reversal of the sulfonamide or amide linker on the binding of a ligand to Mdm2 had not been addressed. Biological assay data had been collected for only one example of a pair of sulfonamides, namely sulfonamides **114** and CYC-0043560, **298**, which had IC_{50} values of 128 μM and 153 μM respectively, in the FP p53-Mdm2 competitive binding assay. This suggested that the reversal of the sulfonamide linker was tolerated in the p53-binding pocket of Mdm2 for aromatic sulfonamides. Therefore, it was desirable to see if a similar modification could be made in the thiophene sulfonamide series.

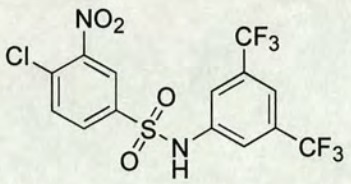

114

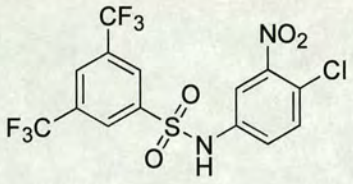

298

Using protocol reported by Galvez *et al.*,[92] reaction of the acid, **291**, with diphenylphosphorylazide, **299**, would afford the azide, **300**, that would undergo the Curtius rearrangement[93] to afford the isocyanate, **301**. Using *tert*-butanol as the reaction solvent would afford the carbamate, **302** (Scheme 2.14). It was envisaged that subsequent deprotection of **302** and reaction with a benzoyl or benzene sulfonyl chloride would afford an amide or sulfonamide respectively.

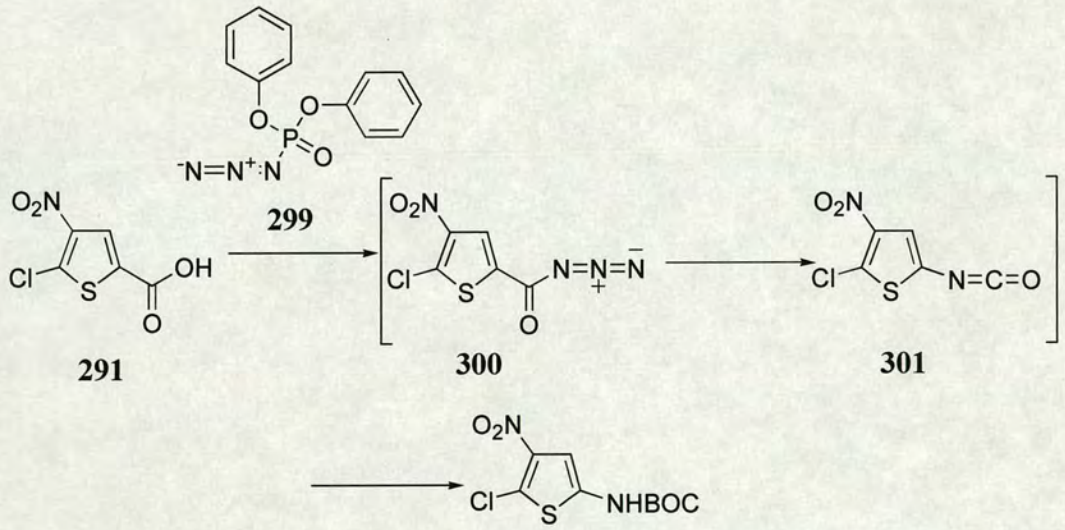

299

291 **300** **301**

302

Scheme 2.14: *Reagents and conditions: tert*-butanol, triethylamine, reflux, 20 h.

Unfortunately, the reaction between **291** and **299** afforded a brown oil that was polymeric in character. Subsequent ESI-MS analysis of this oil did not reveal the isotopic distribution pattern expected for chloro- containing molecules. Therefore, it was

postulated that incomplete reaction of the isocyanate, **301**, with *tert*-butanol lead to the formation of the carbaminic acid, **303**, upon aqueous work up which immediately underwent decarboxylation to afford the amine, **304** (Scheme 2.15). Subsequent nucleophilic displacement of the 5-chloro group by the amine, **304**, may have taken place affording a polymeric material. Subsequently, however, the suspension of the p53-Mdm2 programme prohibited further investigation.

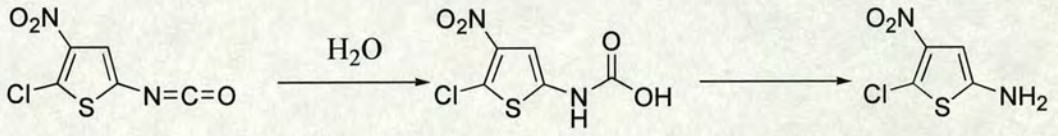

301 **303** **304**

Scheme 2.15

2.9 Discussion of biological data

Analysis of the biological assay data obtained for those ligands screened in the FP assay has enabled an understanding of the SAR of these ligands. Firstly, the majority of sulfonamides with activity <100 μM in the FP assay are 5-chloro-4-nitro-thiophenes, illustrated by CYC12100, **305** (IC_{50} 26 μM). In this series, the 4-nitro group was considered essential to activity, interacting with the sidechain amino group of the Gln59 residue of Mdm2. Removal of the 4-nitro group to afford **54** resulted in a decrease in potency (IC_{50} 319 μM). Similarly, the 5-nitro analogue CYC43275, **306**, exhibited a decrease in potency in the FP assay (IC_{50} 430 μM). Removal of the 5-chloro group to afford CYC43279, **307**, resulted in a less marked reduction in potency (IC_{50} 151 μM).

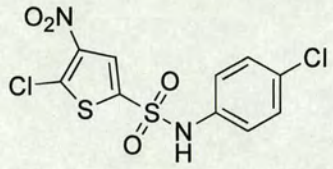

305

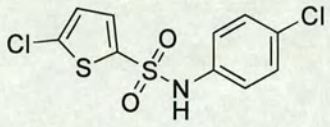

54

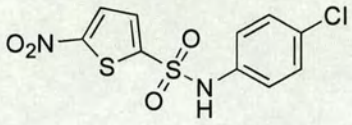

306

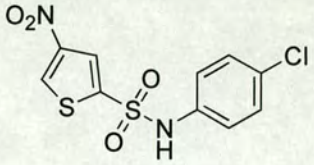

307

N-methylation of 5-chloro-4-nitro-thiophene sulfonamides has been shown to lead to an increase in potency, exemplified by CYC12262, **308**, (IC_{50} 20 μM) and CYC12441, **309**, (IC_{50} 7 μM). However, it has been shown that thiophene sulfonamides not containing this substitution pattern have their activity removed following *N*-methylation, exemplified by **50** (IC_{50} 163 μM) and **196** (IC_{50} > 500 μM).

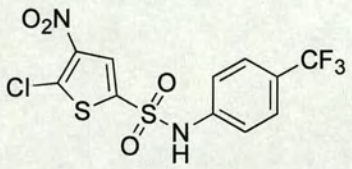

308

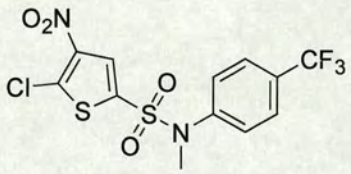

309

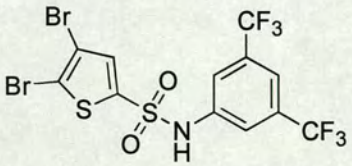

50

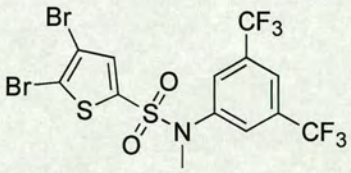

196

Similarly, the activity of CYC12258 (IC_{50} 42 μM), **176**, was enhanced following *N*-benzylation, illustrated by CYC12444 (IC_{50} 15 μM), **178**, whereas the activity of **50**

(IC_{50} 163 μM) was supressed, illustrated by **202** (IC_{50} >500 μM). Clearly, the effect of a hydrogen bond acceptor on the 4-position of the thiophene ring is crucial for direction of the *N*-substituent into the Leu26 pocket.

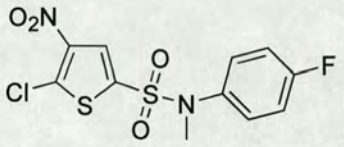

176

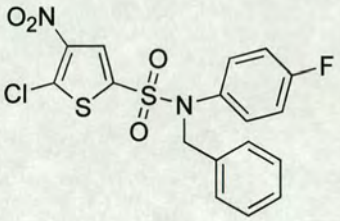

178

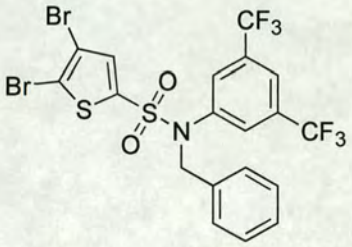

202

The insertion of a CH_2 spacer between the sulfonamide group and the aromatic ring results in a slight increase in potency in the 5-chloro-4-nitro-thiophene series, exemplified by CYC12262 (IC_{50} 20 μM), **308**, and CYC12429 (IC_{50} 11 μM), **310**, but again removes activity in thiophene sulfonamides that do not exhibit this substitution pattern, illustrated by **50** (IC_{50} 163 μM) and **166** (IC_{50} >500 μM).

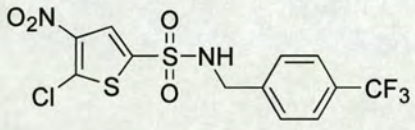

310

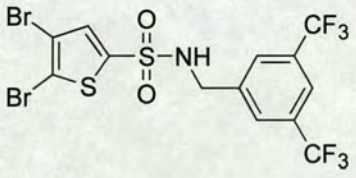

166

Research at Cyclacel Ltd. has shown that the half-life of CYC12100, **305**, in whole mouse blood at 37°C was less than 30 minutes. Analysis of LC/MS spectra obtained from plasma samples identified a degradation product with overall mass 2 Da less than the parent compound. LC/MS analysis of 5-chloro-4-nitro-thiophene sulfonamides in 0.05% glutathione, **311**, showed that these compounds degraded very quickly under these conditions and confirmed the formation of a degradant, postulated to be species **312** (Scheme 2.16). Furthermore, both the *in vitro* activity and cytotoxicity of **305** in the

presence of 0.05% glutathione were significantly reduced. However, chloro-/bromo- and chloro substituted thiophenes and aromatic sulfonamides, including one substituted with both a chloro and a nitro group, were stable at the conditions used (0.05% glutathione at 37 °C, incubation for 3 hours).

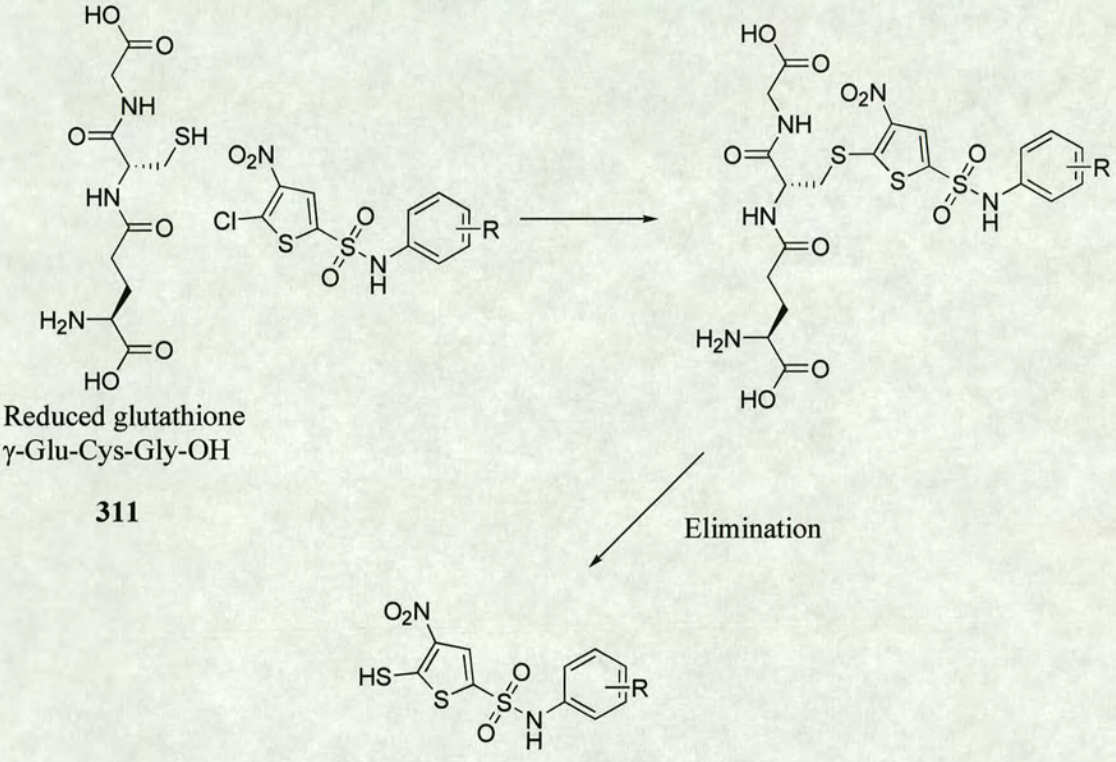

Scheme 2.16

The role of the 5-chloro group with regards to the activity of the ligand is not clear. Replacement of the chloro group with thioacetate has been shown to be tolerated, illustrated by CYC43751, **313** (IC_{50} 16 μM). However, the 5-ethyl analogue, CYC43572, **314**, (IC_{50} 237 μM) was shown to be less potent than the corresponding unsubstituted sulfonamide **307**.

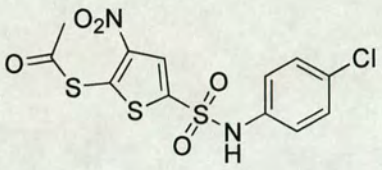

313

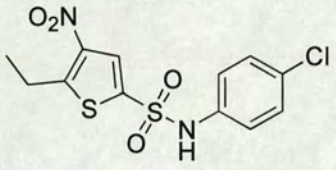

314

Replacement of the 5-chloro-4-nitro-thiophene moiety has been shown to significantly reduce the activity of the sulfonamide in the FP assay. Aromatic sulfonamides CYC12203 (IC_{50} 192 μM), **315**, CYC16745 (IC_{50} 119 μM), **316**, and **114** (IC_{50} 129 μM), each containing a 4-chloro-3-nitro substitution pattern have been shown to exhibit moderate activity. Similarly, CYC43547, **317**, has exhibited moderate activity in the FP assay, with an IC_{50} value of 151 μM.

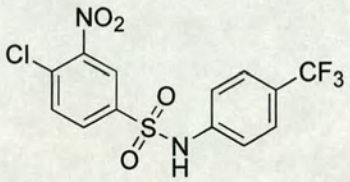

315

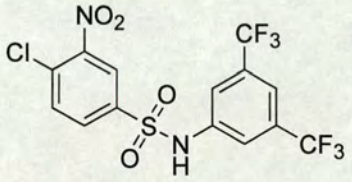

114

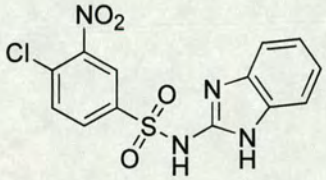

316

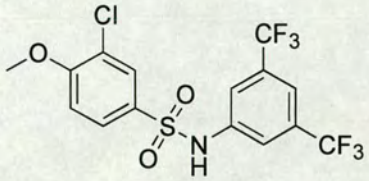

317

Furthermore, the benzothiophenes **126** (IC_{50} 106 μM) and **134** (IC_{50} 193 μM) and the benzothiadiazole **150** (IC_{50} 165 μM) have moderate inhibitory activity of the p53-Mdm2 interaction *in vitro*.

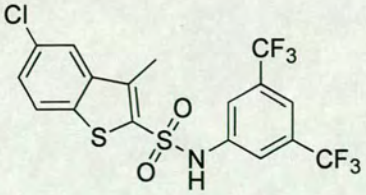

126

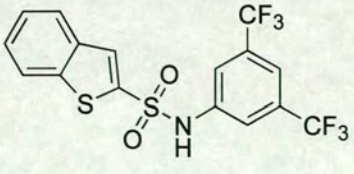

134

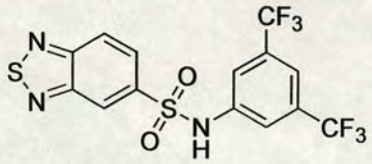

150

Unfortunately, crystalization studies of Hdm2 (17-125) and Hdm2 (1-118), undertaken by Iain McNae at the Institute of Cell and Molecular Biology at Edinburgh University, have not been successful to date. However, analysis by Paul Barlow of NMR data collected for several chloro/nitro containing sulfonamides in complex with Mdm2 has shown that the amino acid residues shifts generated by NMR are not inconsistent with the binding mode predicted by molecular docking experiments undertaken by Thomas and McInnes at Cyclacel Ltd. (Figures 2.5 and 2.6).

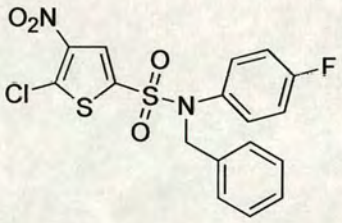

178

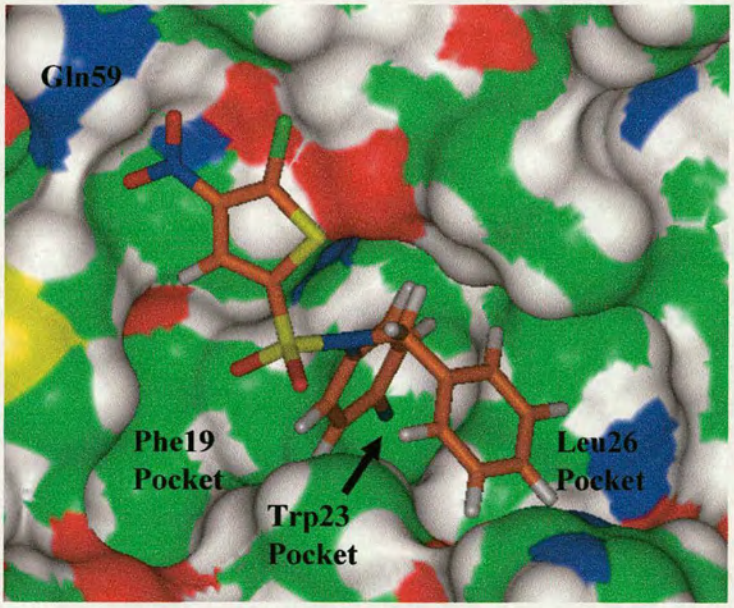

Figure 2.5: The thiophene sulfonamide **178** docked in the Mdm2 binding cleft.

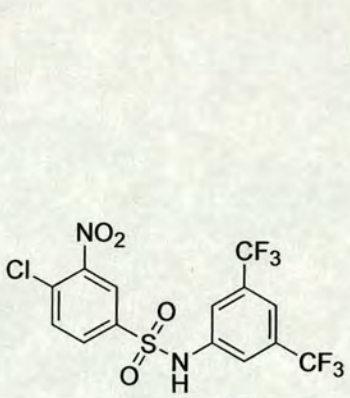

114

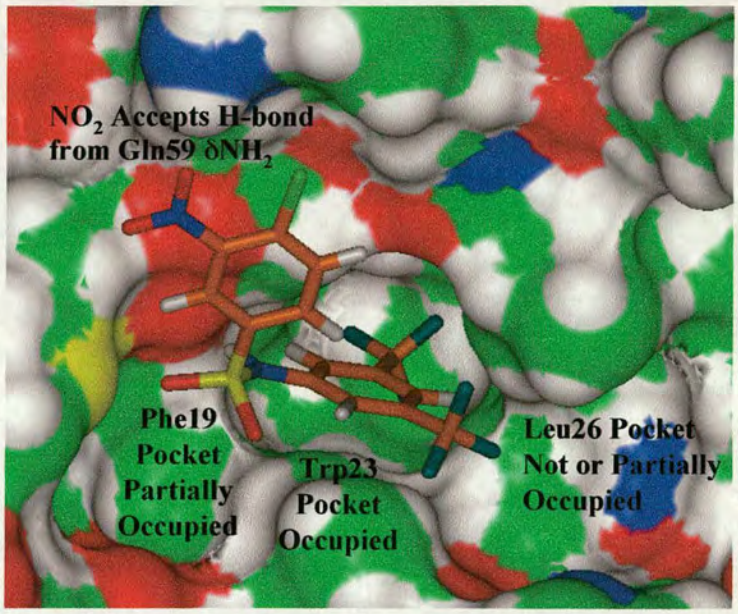

Figure 2.6: The aromatic sulfonamide **114** docked in the Mdm2 binding cleft.

The generation of novel ligands for the inhibition of the p53-Mdm2 interaction was suspended to allow the focus of research into the development of novel inhibitors of the CDK family of enzymes, discussed in Chapters 3 and 4. NMR and crystalization studies of Mdm2 in complex with sulfonamide ligands are ongoing, to allow for the resumption of synthetic chemistry once further structural evidence and rationale for Mdm2 inhibition by current leads is obtained.

2.10 Conclusions and Future work

A number of aromatic and thiophene sulfonamides have been shown to be moderate to potent inhibitors of the p53-Mdm2 interaction *in vitro*. The most active sulfonamides in the series, containing a 5-chloro-4-nitro-thiophene moiety, have been shown to suffer from poor stability in whole mouse blood. Other thiophene and aromatic sulfonamides not containing a chloro/nitro substitution have been shown to be stable in whole blood,

although exhibit only moderate inhibitory activity of the p53-Mdm2 interaction with IC_{50} values >100 μM. Although molecular modelling and NMR studies of several sulfonamides in complex with Mdm2 have shown that in the majority of cases, the 3 p53-binding pockets in the Mdm2 cleft are not fully occupied by the sulfonamide ligands, the determination of a crystal structure of a sulfonamide bound to Mdm2 is of paramount importance to the advancement of this programme. A solid foundation for structure-based ligand design would enable the further investigation into the replacement of the thiophene ring; replacement of the 5-chloro substituent to improve ligand stability in whole blood; and *N*-benzylation of sulfonamide ligands containing a nitro group which can hydrogen bond to the side chain amino group of Gln59.

3 Cyclin dependent kinases

3.1 Introduction

Protein kinases have become attractive targets for low-molecular weight therapeutic agents to treat cancers as they have been shown to be important regulators of intracellular signal transduction pathways.[94] Abnormalities in, and deregulation of, these signaling pathways have been identified in the majority of cancers. The development of selective protein kinase inhibitors is therefore an attractive and promising approach for the treatment of proliferative disorders.[95] The following discussion will introduce the reader to protein kinases, specifically focusing on the cyclin dependent kinases (CDKs), and highlight strategies taken to target these proteins with a view to improving cancer treatment. Particular attention will be made to reviewing the efforts made to discover potent and selective small molecular weight inhibitors of the CDKs.

3.2 Protein kinases

3.2.1 An introduction to protein kinases

As a result of the Human Genome Project, in excess of 800 protein kinases and 130 protein phosphatases are thought to be present in the human genome.[96] Both of these enzyme classes can be subdivided into three categories based upon their catalytic specificity; those specific for Ser/Thr; those specific for Tyr; and those specific for both Ser/Thr and Tyr.

Mutations that lead to activated kinase activity;[94] deregulation of kinase activity by activation of oncogenes[97] or loss of tumour suppressor functions;[98] or deregulation of kinase activity by over-expression[99] have all been shown to play a role in the development and maintenance of human malignancies.

There are a number of approaches available to generate protein kinase inhibitors. One approach is to design low molecular weight peptidic compounds capable of interfering with either ligand or protein substrate binding. This bisubstrate inhibitor approach has to date proven difficult and little progress has been made in transforming these peptides into cell-permeable peptidomimetics.[100] Another approach is to generate allosteric inhibitors, although this approach has been met with little success.[101] The most successful strategy to date has been to target the catalytic site of kinases to generate antagonists of ATP, **318**. Recently, this strategy has been aided by progress made in the crystallization of protein kinases, with a significant number of crystal structures of protein kinases complexed with ATP site directed inhibitors. However, the synthesis of low molecular weight protein kinase inhibitors that display both selectivity and specificity for a target protein kinase is a considerable challenge as each cell will have a complement of between 50 and 100 different protein kinases.[95]

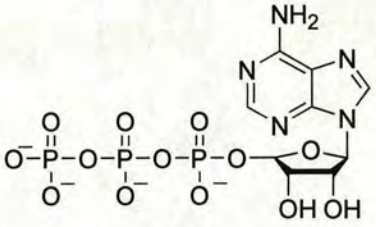

318

3.2.2 Similarities of the ATP binding site amongst protein kinases

The ATP binding site is highly conserved among the protein kinases and contains a number of key features, two of which, an adenine region and a hydrophobic pocket, have been exploited to achieve selectivity in a number of protein kinase inhibitors. The adenine region of the ATP binding site is hydrophobic in character and contains two key hydrogen bonds formed between the *N*-1 and *N*-6 amino groups of the adenine ring and the backbone NH and carbonyl of the adenine anchoring hinge region of the protein kinase. The hinge region also contains a number of backbone carbonyls that can serve as hydrogen bonds acceptors for some inhibitors. The selectivity of most protein kinase

inhibitors is achieved through exploitation of the hydrophobic pocket region in the ATP-binding site of the kinase. Other distinct regions in the ATP-binding site are the sugar region, a region that is hydrophilic in the majority of protein kinases, and a phosphate binding region that appears to contribute little in terms of binding affinity. The ATP-binding site also contains a hydrophobic channel which opens to solvent, and, as it is not occupied by ATP, could be exploited to achieve further binding affinity.[95]

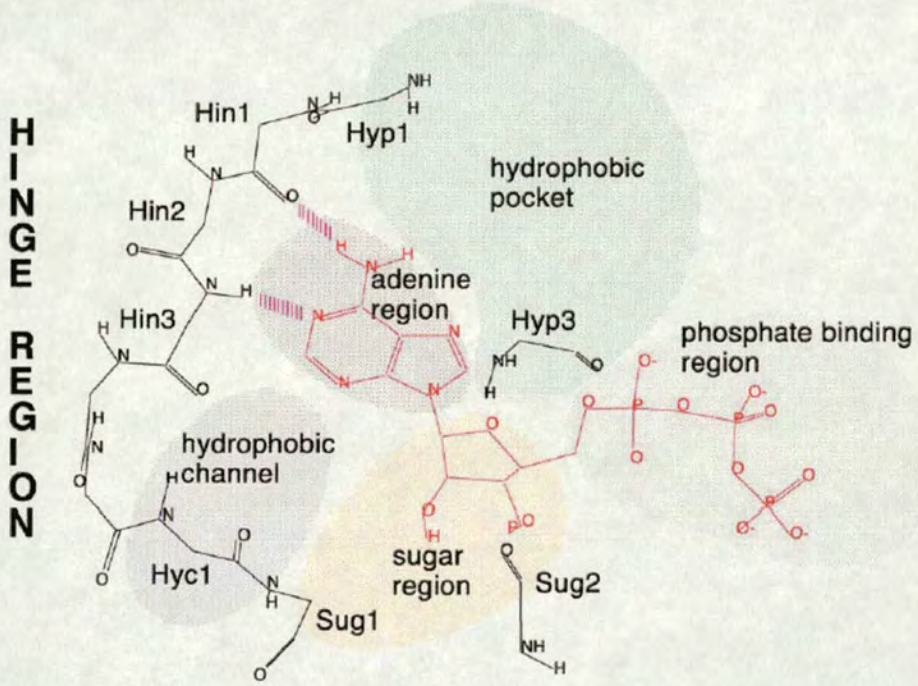

Figure 3.1: Schematic showing the ATP binding site of protein kinases. ATP is in red. sug1, Hyp1, and Hyc1 are residues lining the sugar region (Sug), hydrophobic pocket (Hyp), and hydrophobic channel (Huc), respectively. Hin, hinge region.[95]

3.3 The cyclin dependent kinases

3.3.1 Introduction

Cyclin dependent kinases (CDKs) are of paramount importance in cell cycle regulation as they control the transition between the four primary phases.[102] Cyclin dependent kinases are low molecular weight serine-threonine kinases, between 34–40 kDa, that constitute a catalytic subunit and require association to a regulatory subunit, a cyclin, to be activated. Cyclins are synthesized and destroyed during the cell cycle, during which their levels of expression fluctuate. For example, cyclins A and B accumulate during the S and late G_2 phase and undergo proteolysis during mitosis, whereas cyclins C, D, and E function mainly during the G_1 phase and the G_1-S transition, before undergoing ubiquitin mediated degradation. In contrast, CDK expression remains relatively constant during the cell cycle.

To date, at least 9 CDKs and 15 cyclins have been identified, although the relationship between some cyclins, namely cyclins F, G and I, and the CDKs is still to be characterized. (Figure 3.1). There are also several CDK-related kinases, recognized by their sequence homology to known CDKs, with no identified cyclin partner. CDKs positively regulate the cell cycle by catalyzing the transfer of phosphate from ATP to specific protein substrates.

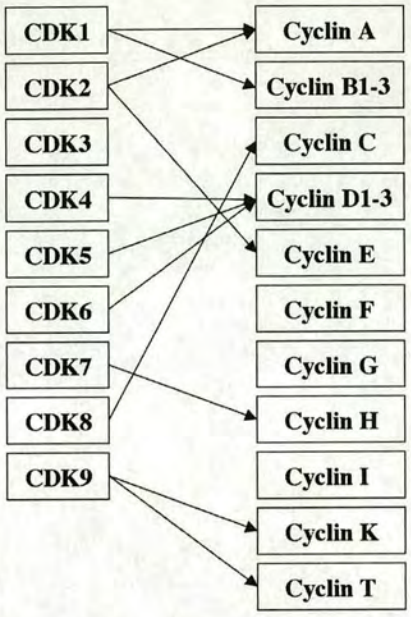

Figure 3.1: Schematic showing the known relationships between the CDKs and the cyclins.

The principal function of the cell cycle is to bring about the duplication of DNA and to distribute this DNA to newly divided daughter cells. Specific CDK/cyclin complexes are known to operate in distinct phases of the cell cycle as illustrated by Figure 3.2.[103] For example, CDK4/cyclin D and CDK6/cyclin D are responsible for progression of the cell through the G_1 phase and the G_1- to S- phase transition by phosphorylation and inactivation of the retinoblastoma phosphoprotein, Rb.[104] As a consequence of Rb phosphorylation, the phosphorylated Rb (pRb) is unable to bind and inactivate the transcription factor E2F1, which leads to the transactivation of E2F-dependent genes and progression to S phase.[105] CDK2/cyclin E is required for progression from G_1 to S, CDK2/cyclin A is required for progression through the S phase and CDK1/cyclin B (also known as Cdc2/cyclin B) is required for the transition through G_2 to M.[106] Deregulation of CDKs and their activators or inhibitors are frequently observed in cancers. CDKs are therefore attractive targets for anticancer therapy.

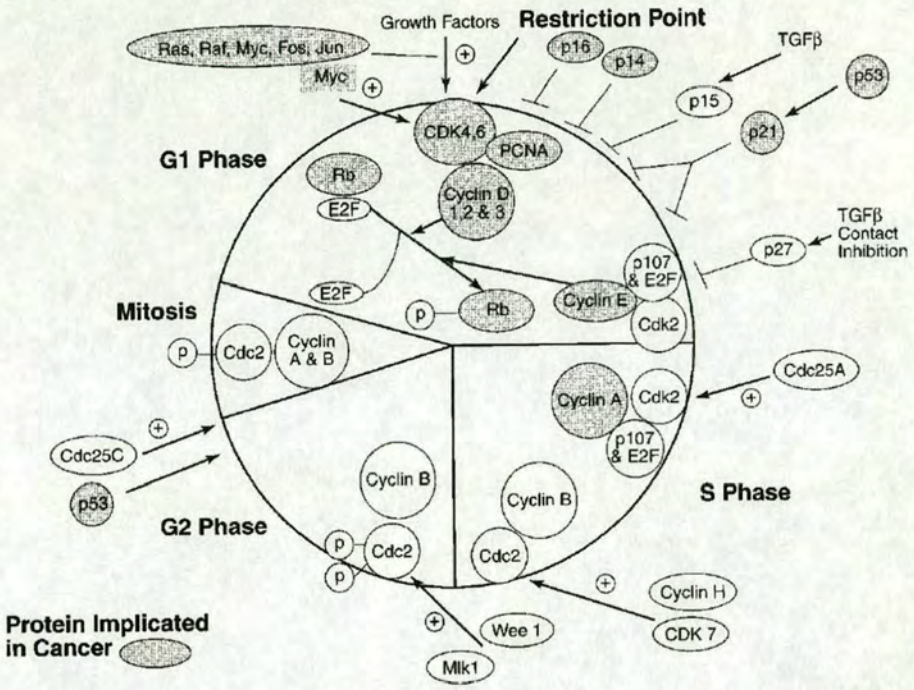

Figure 3.2: Cell cycle regulatory components determined to be altered in human cancers.[103]

In additional to playing a role in the regulation of the cell cycle, CDKs have also been reported to have additional functionality. Some members of the CDK family, known as CDK-activating kinases or CAKs, play a regulatory role in controlling the activity of cell cycle CDKs by phosphorylation of critical serine and threonine residues needed for activity.[108] More recently, several other cellular functions of CDKs have been identified. CDKs have been reported to be involved in apoptosis (CDK2, CDK5), in neuronal functions (CDK5), in transcription (CDK7, CDK8, CDK9) and in differentiation (CDK4, CDK5, CDK9).[109]

3.3.2 Regulation of CDK activity

Monomeric CDK is inactive, its activation being dependent on a two-step process namely association with a cyclin subunit[110] and subsequent phosphorylation of the CDK/cyclin complex by the CDK-activating kinase (CAK).[111] This two-step activation

process is illustrated in Figure 3.3. Association of the CDK to the cyclin imparts partial activity to the complex, although this activity is increased 100-fold following phosphorylation.[112]

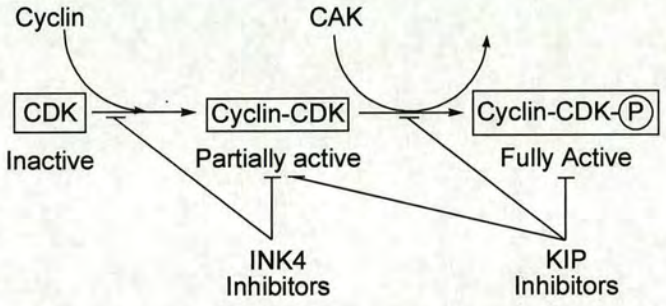

Figure 3.3: Regulation of CDKs and CDK/cyclin complexes.

A family of small inhibitory proteins called cyclin-dependent kinase inhibitors (CKIs) have been shown to regulate CDKs and CDK/cyclin complexes. There are two families of CKIs; the INK4 family, whose members are $p15^{INK4B}$, $p16^{INK4A}$, $p18^{INK4C}$ and $p19^{INK4}$;[113] and the kinase inhibitor protein (CIP/KIP) family, whose members are $p21^{WAF1}$, $p27^{KIP1}$, and $p57^{KIP2}$.[114] The INK4 family inhibits the CDK4/Cyclin D and CDK6/Cyclin D complexes by binding directly with the CDK and preventing its association and subsequent activation, causing cells to accumulate in the late G_1 phase. The INK4 family can also bind to the CDK/cyclin complex.[113] The CIP/KIP family has a broader CDK preference, regulating the complexes CDK2/cyclin E, CDK2/cyclin A and CDK1/cyclin B by binding directly to the CDK/cyclin complex.[114]

3.3.3 Activation of CDKs

Structural studies of the CDKs have revealed the catalytic centre includes a core of approximately 300 amino acid residues that possesses a high degree of homology between the different members of this protein kinase family.[115] The majority of crystal structures of CDK/inhibitor complexes studied to date focus on the monomeric,

inactivated form of CDK2. The N-terminal domain of CDK2 consists of five anti-parallel β-strands that form a β-sheet, and one helix. The C-terminal domain of CDK2 is larger and predominantly α-helical. A flexible hinge links these two domains and the deep cleft formed by the classic bi-lobal kinase fold contains the ATP-binding site.[116] CDK2 contains two unique regions that regulate its activity. Firstly, CDK2 contains an α-helix located in its N-terminal domain that has a unique PSTAIRE sequence found only in cyclin-dependent kinases. Secondly, CDK2 contains a regulatory loop known as the 'T-loop', consisting of residues 150-165, that blocks access of the polypeptide substrate to the ATP-binding site. The structure of monomeric CDK2 in ribbon representation is shown in Figure 3.4.

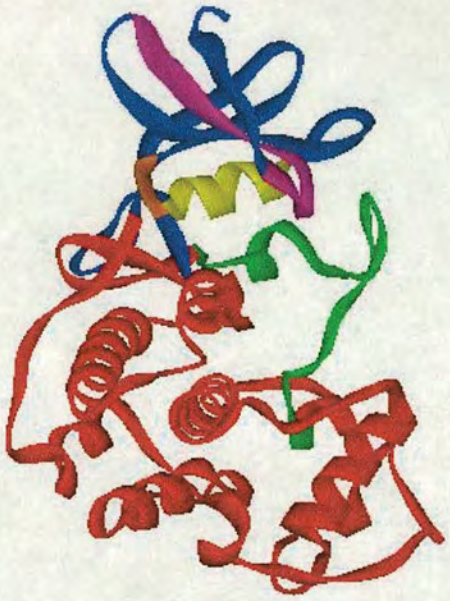

Figure 3.4: The structure of monomeric CDK2 shown in ribbon representation. The N terminal domains (residues 1 – 86) are shown in blue with the exception of the glycine-rich loop (residues 11 – 24) coloured magenta, the hinge region (residues 81-84) coloured orange and the C-helix (PSTAIRE helix, residues 46 –55) coloured yellow. The C-terminal domain is coloured red, with the activation segment (residues 145 – 172) that contains the T loop highlighted in green (PDB code - 1HCL).

Upon cyclin binding, the cyclin forms contacts to both lobes of the CDK, with key interfacial contacts being made with the C-helix, which contains the PSTAIRE sequence. Cyclin binding causes the C-helix to swing in towards the ATP-binding site, a key conformational change that facilitates coordination of the α-phosphate of ATP for phosphotransfer, directed partially by the residue Glu51, contained in the PSTAIRE helix. The residues Lys33 and Asp145 together with a magnesium ion are also involved in the phosphorylation step.[117] Another consequence of cyclin binding is the movement of the T loop away from the entrance of the ATP-binding cleft, an event which also exposes the phosphorylation site on the T loop (Thr160). Subsequent phosphorylation of

Thr160 invokes an additional conformational change of the T loop, with the phosphate group coordinating to three arginine side-chains, one from the N-terminal domain, one from the C-terminal domain and one from the T loop of the CDK. In turn, the arginine residues hydrogen bond to other CDK and cyclin groups, and in doing so stabilize the CDK/cyclin complex.[112]

3.3.4 The CDK2/ATP complex

The X-ray crystal structure of a CDK2/ATP complex has been reported and reveals a number of key interactions between the kinase and the ligand, providing a solid foundation for further structure-based design of low molecular weight, ATP-competitive inhibitors. The crystal structure of ATP bound to CDK2 is shown in Figure 3.5.

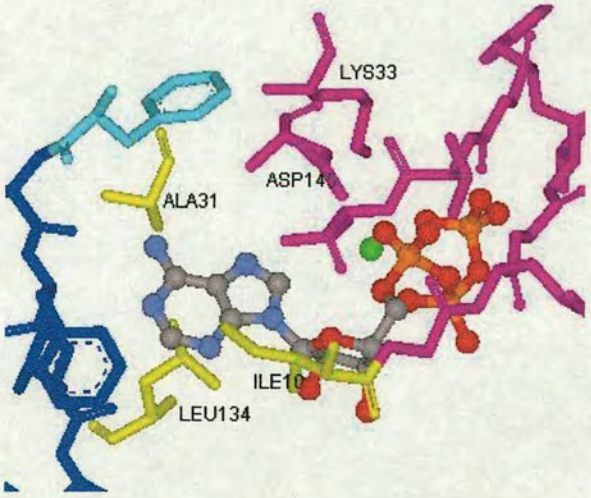

Figure 3.5: Crystal structure of ATP bound to CDK2 (PDB Code 1HCK). ATP is coloured as follows; C grey, N light blue, O red, P orange. Mg^{2+} is coloured green. CDK2 is coloured as follows; the hinge region (residues 81-84) is coloured dark blue; the ribose/phosphate binding region (residues 11 – 18) and residues Lys33 and Asp145, which form a salt bridge, are coloured magenta; residues Ile10, Ala31 and Leu134, that dictate the width of the ATP binding cleft, are coloured yellow; and Phe80 is coloured cyan.

Hydrogen bonds have been identified between Leu83 and *N*-1 of ATP, between Glu81 and N(6)H_2 and between Asp86 and O(2')H, and the phosphate chain of ATP interacts with the pocket at Lys33, Asn132, Asp145, Lys129, Thr14 and Wat558.[118] A schematic of these key interaction is illustrated in Figure 3.6.

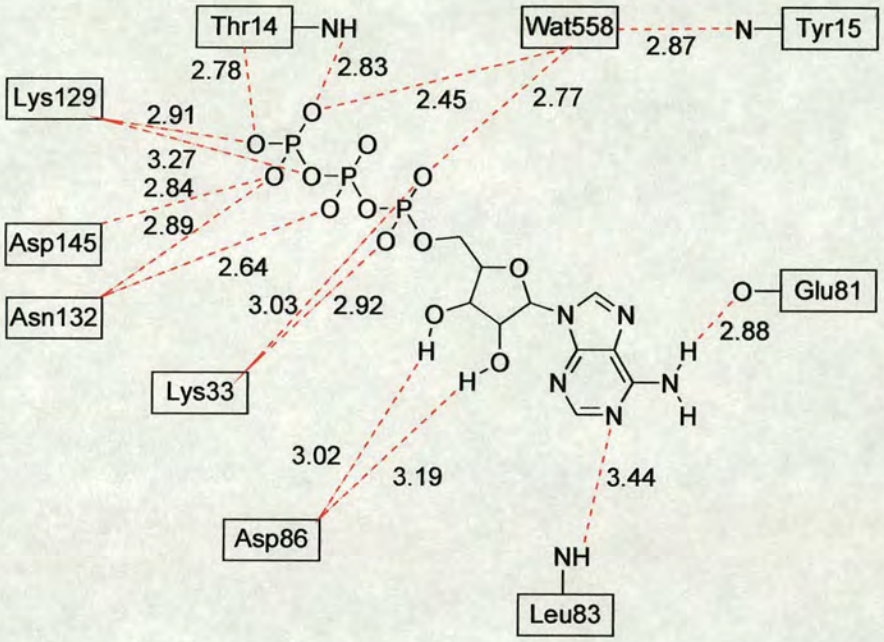

Figure 3.6: Schematic showing interactions between ATP and CDK2 at the ATP-binding site.[118]

3.3.5 CDK2 ATP antagonist binding modes

There have been a number of reports in the literature of X-ray crystal structures of small molecule inhibitors complexed with monomeric CDK2. The majority of these show inhibitors bound at the site occupied by the adenine ring in the CDK2/ATP complex. This site resembles a narrow cleft, formed between the N- and C- terminal domains of CDK2, the width of which is determined by the hydrophobic side chains of Ile10, Val18, Ala31 and Leu134. A β–strand, containing the residues Phe80, Glu81, Leu83 and His84, forms the boundary wall of the cleft and links the N- and C- terminal domains. In all cases, the backbone amide groups of Glu81 and Leu83 make key hydrogen bond

interactions with the inhibitors, although two distinct hydrogen bonding patterns have been observed; one where the NH of Leu83 and the carbonyl of Glu81 act as a donor-acceptor pair for a complimentary hydrogen bond donor and acceptor on the inhibitor with an additional interaction between the carbonyl of Leu83 and a CH on the inhibitor; and one where the NH and carbonyl of Leu83 acts as a donor and acceptor to a complimentary acceptor and donor pair on the inhibitor, with an additional interaction between an aromatic proton on the ligand and the carbonyl of Glu81. The former binding mode has been observed in CDK2 complexes with ATP,[119] flavopiridol,[120] **319**, and the 4-heteroaryl-2-amino-pyrimidines CYC1, **320**, and CYC2,[121] **321**, whereas the latter binding mode has been observed for purvalanol B,[122] **322**, roscovitine,[123] **323**, and OL567, **324**.[124]

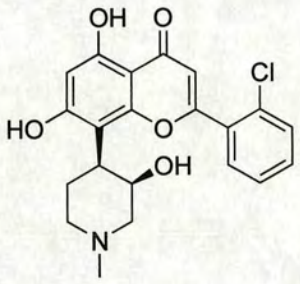

319

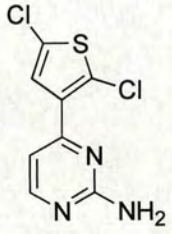

320

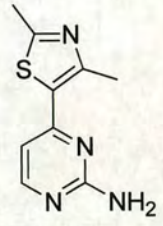

321

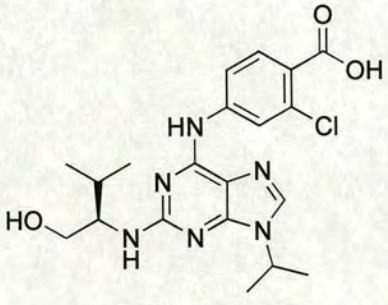

322

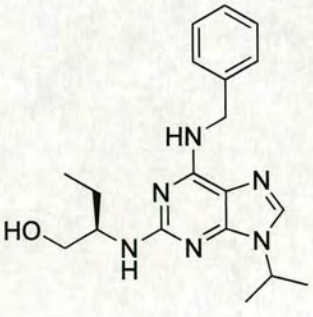

323

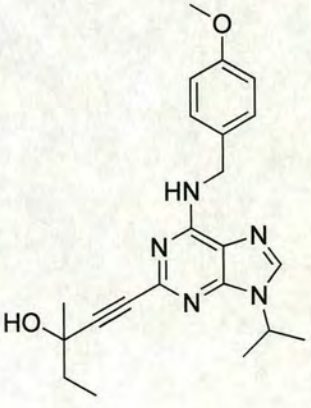

324

3.3.6 The validity of using structure based design to target monomeric CDK2

Activation of CDK2 has two main effects on the ATP-binding site. Firstly it causes a rotation of the N- and C- terminal domains by approximately 5° about the hinge region and a slight widening of the ATP cleft. Secondly, as a result of the movement of the C-helix and subsequent reorganization of the residues involved in coordination to ATP, the phosphate-binding site is reshaped, the ATP cleft is deepened and an additional pocket is formed.[125] These conformational changes raise the question of the validity of using monomeric CDK2 to design inhibitors of the active kinase and, indeed, to interpret the structure-activity relationships of inhibitors arising from biological assays on the active complex. Indeed, a recent analysis of the binding of the inhibitor indirubin-5-sulfonate, **325**, to both active and inactive forms of CDK2 revealed that on activation, the interactions between the inhibitor and the kinase at the ribose site were considerably altered owing to movements of the glycine loop, suggesting that the accuracy of monomeric CDK2 as a inhibitor design template is restricted to the adenine binding site (Figure 3.7).[126]

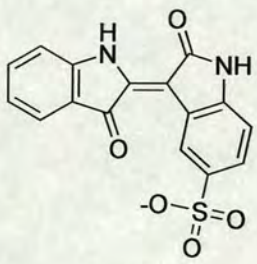

325

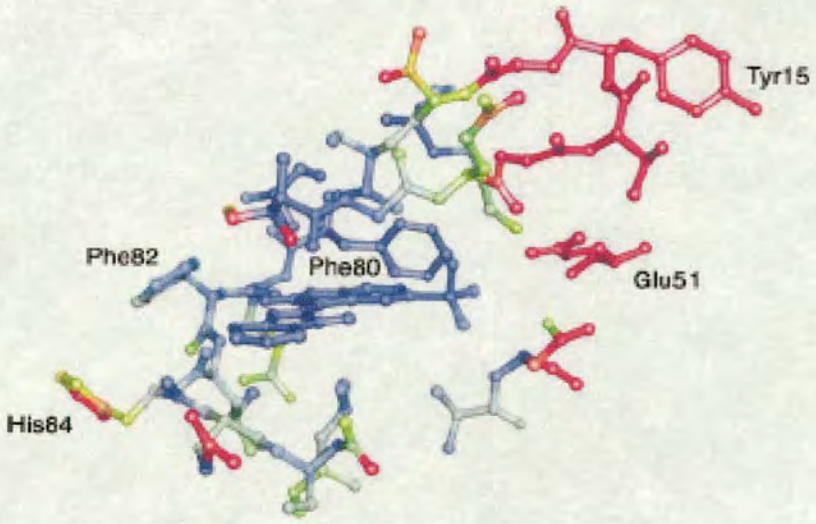

Figure 3.7: Active site detail of CDK2 in complex with indirubin-5-sulphonate, **325**, coloured by structural displacement between monomeric and binary complexes. The structures were superimposed on the basis of the inhibitor. Atoms are coloured from blue (displacement <0.5 Å) through yellow to red (displacement > 2.5 Å).

3.4 A review of ATP-competitive CDK inhibitors

3.4.1 Introduction

All CDK inhibitors identified so far share a common mechanism of action, acting at the ATP-binding pocket of the kinase and, in doing so, competing with ATP for binding. CDK inhibitors display antiproliferative properties, terminating the cell cycle in G_1 and G_2/M phases depending on the conditions and cell type. This section attempts to provide an overview of the key pharmacophores that have been reported to inhibit the CDKs. Where possible, attention is drawn to crystal structures of the inhibitor/CDK complex and key protein-ligand interactions are exemplified in the text. Next generation inhibitors based around the particular scaffold, where reported in the literature, are discussed, and a current understanding of the structure activity relationship of the pharmacophore is presented together with key features of the inhibitors selectivity profile.

3.4.2 Staurosporine and analogues

The natural product staurosporine, **326**, isolated from *Streptomyces staurosporeus*, is an ATP-competitive inhibitor of a numbers of CDKs.[127] Staurosporine exhibits an IC_{50} of 7 nM against CDK2/cyclin A[128] and 3-10 μM against CDK4/cyclin D,[129] but also inhibits PKC and cAPK. The crystal structure of staurosporine bound to CDK2 (Figure 3.8) revealed a similar hydrogen-bonding pattern to that observed in the CDK2/ATP complex, namely a hydrogen bond donor interaction to the oxygen of Glu81 and a hydrogen bond acceptor interaction to the nitrogen of Leu83. Additional hydrogen bonds were reported between the methylamino group of staurosporine and the carbonyls of Gln131 and the side chain of Asp86, located in the ribose binding site.[130]

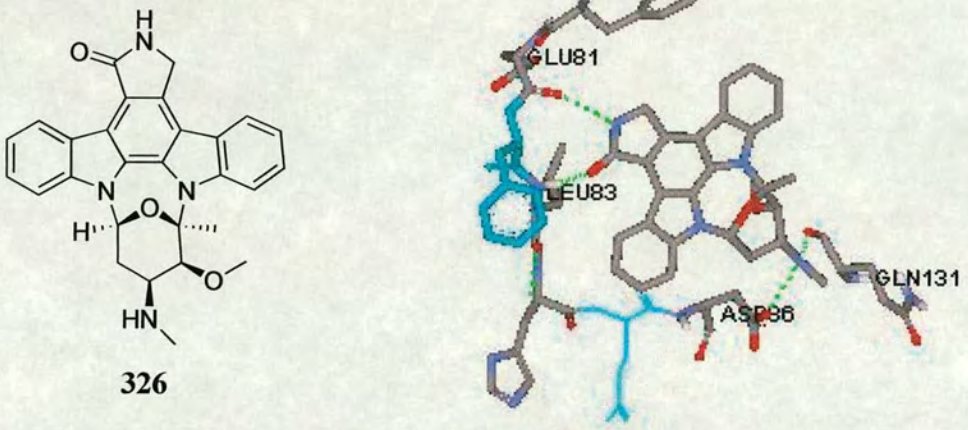

326

Figure 3.8: Staurosporine bound to CDK2 (PDB code 1AQ1).

The hydroxystaurosporine analogue UCN-01, **327**, has been reported as a non-specific kinase inhibitor against PKC, CDK1 and CDK2 and is currently undergoing clinical trials.[131]

327

A series of indolo[6,7-*a*]pyrrolo[3,4-*c*]carbazoles, as illustrated by the scaffold shown in Figure 3.9, have been reported as potent, nanomolar inhibitors of CDK2 and CDK4.[132] It was shown that the C-11 position, and to a lesser extent C-12, tolerated the greatest diversity of substituents in terms of CDK inhibition although those inhibitors incorporating an aminoalkyl sidechain at C-12 exhibited the highest selectivity and

activity in the series with IC_{50}'s against CDK4/cyclin D1 < 69 nM. Scaffolds bearing aminoethanol at C-12 generally showed the greatest inhibition of CDK2. These inhibitors have been shown to induce strong G1 arrest in two human cell lines and to inhibit Rb phosphorylation at Ser780 consistent with inhibition of CDK4/cyclin D1.[132]

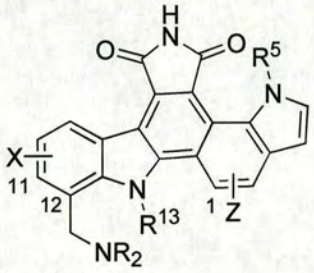

Figure 3.9: The indolo[6,7-*a*]pyrrolo[3,4-*c*]carbazole scaffold.

3.4.3 Flavonoids

Quercetin, **328**, a naturally occurring flavonoid, has been reported as a relatively weak CDK inhibitor that exhibits antiproliferative effects at the G_0/G_1 interface of the cell cycle.[133] Another flavonoid, flavopiridol, **319**, has also been reported as an effective CDK inhibitor and is the most advanced in terms of clinical development.[131] *In vitro*, flavopiridol has been shown to be a relatively non-selective kinase inhibitor, exhibiting nanomolar activity against CDK1,[134] CDK2, CDK4 and CAK,[135] and PKC.[136]

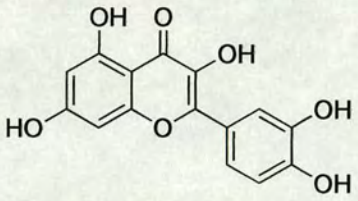

328

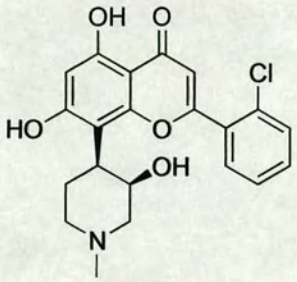

319

The crystal structure of deschloroflavopiridol (Figure 3.10) cocrystallized with CDK2 has been reported which revealed the core hydrogen bonds between O(5)H and Glu81, and between O(4) and Leu83.[137] In addition to these two interactions, key hydrogen bonds were identified between O(3) of the hydroxypiperidine moiety and the residues Lys33 and Wat384, and between O(3)H and N(11)H of the hydroxypiperidine moiety and the residue Asp145.

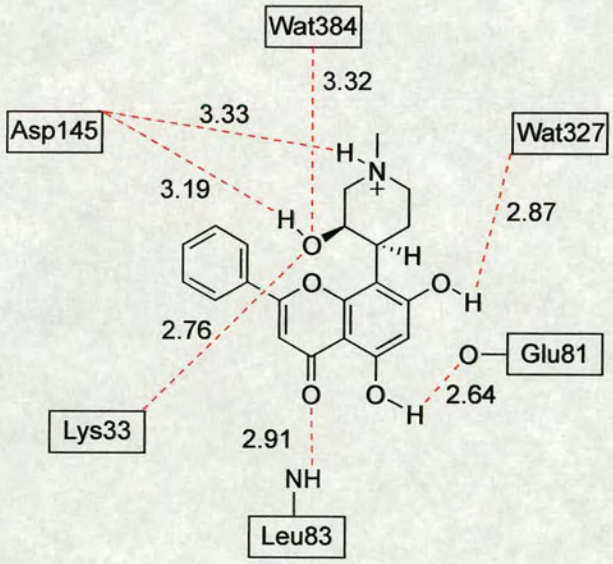

Figure 3.10: Schematic showing interactions between CDK2 and deschloroflavopiridol.

Flavopiridol analogues, thio- and oxoflavopiridols, **329** and **330**, that contain a sulfur or oxygen between a piperidylchromone ring and a hydrophobic side chain, have been

reported as selective CDK1 inhibitors with potencies of 110 and 130 nM respectively.[120] Flavopiridol analogues **329** and **330** exhibit selectivity over CDK2 by approximately 20-fold and 50-150-fold over CDK4. Analogues with hydrophilic side chains, such as pyrimidine or aniline, were shown to cause a severe reduction in CDK inhibitory activity. X-ray crystal studies of ligand-protein complexes formed between flavopiridol or thioflavopiridol and CDK2, together with a comparison of the sequences of CDK1, CDK2 and CDK4, revealed the basis for CDK1 selectivity in these compounds. The CDK1 selectivity of thioflavopiridol compared to flavopiridol was attributed to a relative decrease in CDK2 binding resulting from a less-than-optimal interaction between the chlorophenyl ring and Ile10, a residue conserved in CDK1, CDK2 and CDK4. A compensating interaction was reported between the chlorophenyl ring and Lys89 in the thioflavopiridol-CDK2 complex. Lys89 is common to both CDK1 and CDK2 but not to CDK4. In CDK1, sequence differences near Lys89 (Met85 in CDK1 versus Gln85 in CDK2) increase the hydrophobic nature of this region and alter packing preferences, and impose a change in the orientation of Lys89, directing it towards the chlorophenyl ring of thioflavopiridol.

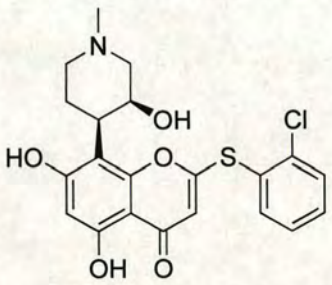

329

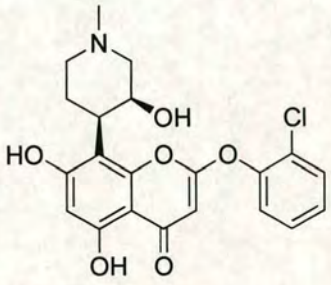

330

3.4.4 Paullones and analogues

Zaharevitz *et al.* reported the identification of 9-bromo-7,12-dihydro-indolo[3,2-*d*][1]benzazepin-6(5*H*)-one, kenpaullone, **331**, through analysis of the National Cancer Institute Human Tumor Cell Line Anti-Cancer Drug Screen data using the COMPARE

algorithm[138] to detect similarities in the pattern of compound activity to flavopiridol. Kenpaullone is a potent inhibitor of CDK1/cyclin B (IC_{50}, 400 nm) and also shows some activity against CDK2/cyclin A (IC_{50}, 680 nm), CDK2/cyclin E (IC_{50}, 7.5 μM), and CDK5/p25 (IC_{50}, 850 nm). Significantly, kenpaullone has little activity against CDK4. Molecular modeling studies have suggested that kenpaullone can bind in the ATP-binding site of CDK2, with similar binding interactions to those observed in other CDK2 inhibitors, namely hydrogen bonds to both the backbone and carbonyl amide of Leu83 and positioning of ring atoms between the Leu134 and Ile10 hydrophobic sidechains. Furthermore it was shown that analogues of kenpaullone, notably 10-bromopaullone, **332**, were reported to lead to a reduction in kinase specificity inhibiting various protein kinases including CDKs, several protein kinase C isozymes and casein kinase 2.[139]

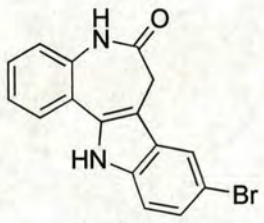

331

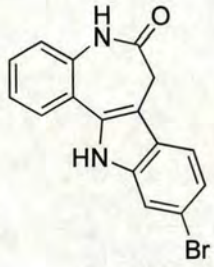

332

A further study, focusing on derivatives of kenpaullone provided useful information concerning the structure-activity relationship of this new class of pharmacophore against CDK1/cyclin B. Electron withdrawing substituents at the 9-position were shown to be favourable. A 9-trifluormethyl substituent was found to give comparable activity to the 9-bromo substituent of kenpaullone (IC_{50} 400 nM), whereas a substantial increase in potency was observed following replacement of the 9-bromo substituent with 9-cyano (IC_{50} 24 nM) or 9-nitro (IC_{50} 35 nM). With the exception of a 2,3-dimethoxy substitution on the paullone basic scaffold, substitutions at the 2-, 3-, 4-, and 11-positions were not well-tolerated and led to decreased CDK1 inhibition. Evaluation of the paullone derivatives in a cancer cell line screening showed, surprisingly, that the antiproliferative activity of the compounds was not directly related to CDK1 inhibition.

Indeed, the 9-cyano paullone displayed no *in vitro* antitumour activity, despite having an IC_{50} of 24 nM against CDK1. The 9-nitropaullone, alsterpaullone, **333**, exhibited excellent in vitro antitumour in addition to greater activity against CDK1 than both flavopiridol and roscovitine and was therefore selected for preclinical development.[140] Further work on the paullone series of CDK inhibitors has shown that 2-substitution of the paullone scaffold with a 2-cyanoethyl substituent, **334**, significantly enhanced CDK1/cyclin B inhibition and in vitro antiproliferative activity. Molecular modeling indicated that 2-substitution of the paullone scaffold with carbon chains containing polar terminal groups resulted in partial occupancy of the access channel of the ATP binding site, forming favourable interactions with solvent molecules or amino acid side chains in the vicinity of the ATP binding site.[141] However, data collected on the paullone series of inhibitors shows that cellular activity does not parallel CDK activity, suggesting alternative mechanisms for cellular antiproliferative effects for some of the compounds.[140]

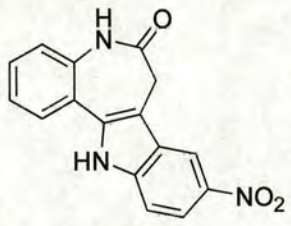

333

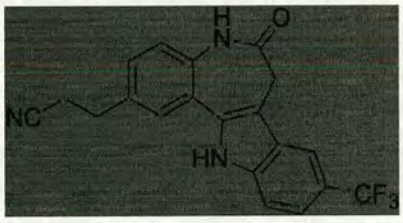

334

A later study revealed that paullones act as potent inhibitors of glycogen synthase kinase-3β(GSK-3β), □□□4 – 80 □□ in addition to the neuronal CDK5/p25 (IC_{50} 20 – 200 nM).[142] Both GSK-3β and CDK5 are responsible for hyperphosphorylation of the microtubule-binding protein tau, a feature observed in the brains of patients with many pathological conditions, including Alzheimer's disease, Down's syndrome and Pick's disease.[143] It was shown that alsterpaullone acts by competing with ATP for binding to GSK-3β. The binding of alsterpaullone to GSK-3β inhibits the phosphorylation of tau *in vivo* at sites that are typically phosphorylated by tau in Alzheimer's disease. Although

results obtained from a screen of some 50 paullones against GSK-3β, CDK1 and CDK5 indicate that GSK-3β appears to be more sensitive to paullones than CDKs, there exists the potential to develop paullone derivatives selective for either GSK-3β or CDKs. Indeed, from the screen, it was shown that CDK5 activity appears to be very sensitive to substitution at the 12-position of the paullone ring, as exemplified by the ligand **335**, whose IC_{50} values against GSK3, CDK1 and CDK5 were shown to be 0.4 μM, 6.2 μM and 400 μM respectively.[142]

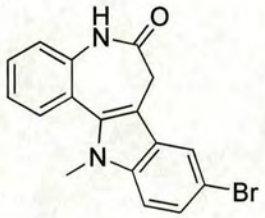

335

3.4.5 Purines

The purine derivative olomoucine, **336**, has been developed as a selective inhibitor of both CDK1 and CDK2.[144] In addition to two key hydrogen bonds between *N*-7 and NH of Leu83, and between *N*-6 and the carbonyl of Leu83, it was shown that an additional hydrogen bond exists between the hydroxy group of the amino alcohol and Gln131.

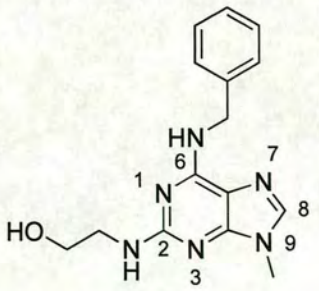

336

A novel purine derivative, (*R*)-roscovitine, **323**, was identified as a selective, orally bioavailable CDK2 inhibitor that targets the ATP-binding site.[123] (*R*)-Roscovitine has IC_{50}'s of 80 nM, 390 nM, 1.1 μM and 12 μM against CDK2, CDK7, CDK1 and CDK4 respectively and has been shown to induce apoptotic cell death from all phases of the cell cycle. (*R*)-Roscovitine is currently in Phase II clinical trials.

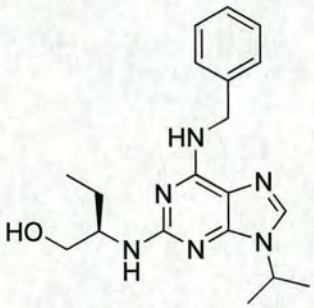

323

Whilst olomoucine lacked the potency required of a suitable drug candidate, with an IC_{50} against CDK2 of 4.5 μM, it has been a useful tool for further structure-based design. Adopting a combinatorial approach, other work on the olomoucine scaffold, involving amination at the 2- and 6-positions and Mitsunobu alkylation at *N*-9, has afforded several diverse libraries of compounds that have been used to examine the effects of a range of substituents on the purine ring.[122] A number of benzylamine and aniline substituents at the 6-position were reported to lead to significant improvements in CDK2 binding compared to olomoucine. At the 2-position, amino alcohols derived from alanine, valine and isoleucine were shown to improve binding affinity by up to 6.5-fold relative to the hydroxyethyl substituent of olomoucine. Purines with small alkyl or hydroxyalkyl substituents at *N*-9 were shown to be more potent CDK2 inhibitors than those purines with larger substituents at this position. X-ray studies have revealed that substituents at the *N*-9 position of the purine ring occupy a small hydrophobic pocket formed by the side chains Val18, Ala31, Phe80, Leu134 and Ala144. This pocket is unoccupied in the CDK2/ATP complex and, in other kinases, is much larger owing to a smaller residue at its entrance. Consequently, this feature has been exploited by many

other purine-based inhibitors to achieve selectivity.[145] This study resulted in the identification of the CDK2 inhibitor purvalanol B, **322**, which has an IC_{50} of 6 nM against the CDK2/cyclin A complex, a 100-fold increase over olomoucine. Significantly, purvalanol B has an IC_{50} against CDK4/cyclin D1 of >10,000 nM.[122] X-ray studies have shown that purvalanol B has a similar binding mode to olomoucine in the ATP-binding site of CDK2, although exhibits improved packing interactions resulting from the tight packing of the 3-chloroanilino group at *N*-6 of the purine ring of the inhibitor against the side chains of Ile10 and Phe82, with additional stabilization coming from polar interactions between the chloro group and the side chain of Asp86 and between the carboxy aniline group and the amino portion of the Lys89 side chain, which notably is a threonine residue in CDK4. The increased binding affinity of purvalanol B compared to olomoucine may also result from steric constraints imposed by the purine and the chlorinated aniline ring systems that limit the number of conformations of purvalanol B compared to olomoucine. Furthermore, the region occupied by the substituent at *N*-6 of the purine ring is empty in the CDK2-ATP complex, an observation that may account for the higher binding affinity and selectivity of purvalanol B and olomoucine compared to ATP.

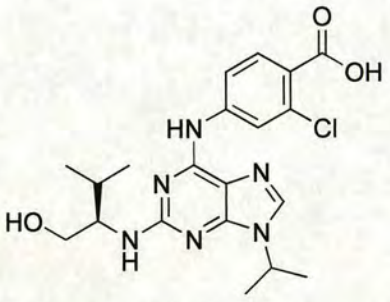

322

Similar increases in potency against CDK2 compared to olomoucine have been observed for other 2,6,9-trisubsitituted purine systems, illustrated by CGP 74514, **337**, which has been shown to have an IC_{50} against CDK2 of 9 nM.[146]

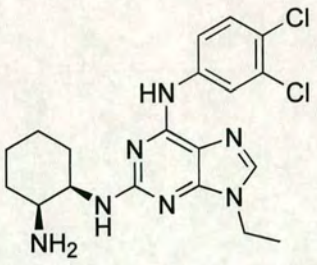

337

The 2,6,9-trisubstituted purine derivative H717 (Figure 3.11), has been shown to adopt a slightly different binding mode in complex with CDK2 than that observed for olomoucine and purvalanol, as illustrated in Figure 3.11. It was shown that the orientation of the *C*2-*p*-diaminocyclohexyl portion of the inhibitor generated two novel interactions generated by the amino group, namely a salt bridge to Asp145-Oδ1 and a hydrogen bond with Asn132-Oδ1. Interestingly, this charged amino group was shown to be in close proximity to the Mg^{2+} ion that binds to the phosphates and to Asp145 of CDK2 in the CDK2/ATP complex. The retention of this ionic interaction may contribute favourably to the binding affinity of H717 with CDK2. The *N*-9 cyclopentyl ring was shown to fully occupy a space formed predominantly by the residues Phe80, Val18 and Val64, a region only partially occupied in the complexes formed between CDK2 and the homologous inhibitor olomoucine. H717 was shown to have selectivity for CDKs 1 and 2 with IC_{50} values of 52 nM and 48 nM respectively.[147]

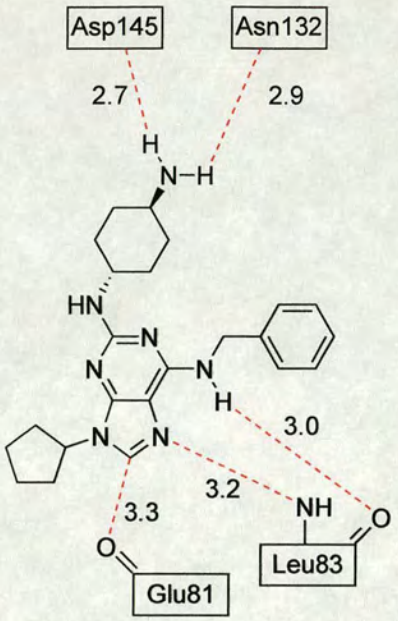

Figure 3.11: Schematic showing the polar interactions between the inhibitor H717 and CDK2 with distances given in Å. Only interactions up to 4.0 Å are shown. Contacts to CDK side chain atoms are indicated by lines to the respective box boundaries, whereas interactions to main chain atoms are shown as lines to the specified atoms.[147]

Other CDK inhibitors based around a purine scaffold have been described in the literature. These include isopentenyladenine,[123] **338**, bohemine,[148] **339**, CVT 313,[149] **340**, and a number of 2-alkynylated purines, exemplified by OL567,[150] **324**.

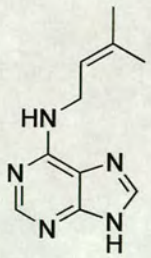

338

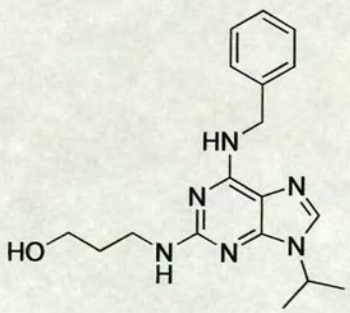

339

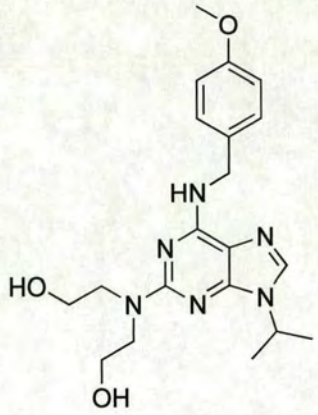

340

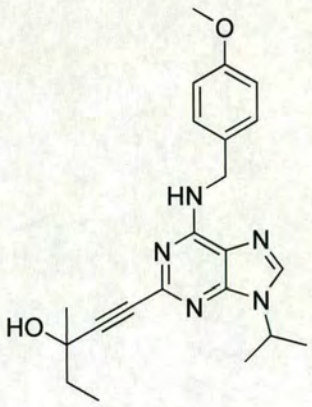

324

Recently, a series of 2,6,8,9-tetrasubstituted purines have been reported as novel CDK1 inhibitors, exemplified by **341**.[151] This research built on the work undertaken on the roscovitine pharmacophore and extended it further by introducing a novel modification at the C-8 position of the purine ring. A screen of this series of tetrasubstituted purines against CDK1 revealed that introduction of a C-8 substituent lowered the CDK1 inhibitory activity of roscovitine, an observation that was later confirmed by molecular modeling studies which revealed some degree of steric repulsion between the C-8 substituents and the fairly rigid hinge region at the 'back' of the ATP-binding site.

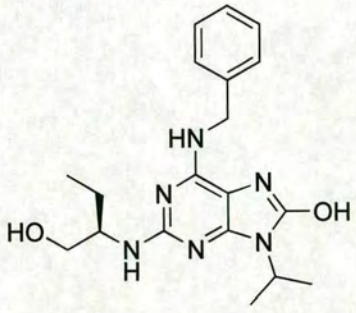

341

3.4.6 Quinoxalines

Several pyrazolo[3,4-*b*]quinoxalines, exemplified by **342**, have been reported to be sub-micromolar inhibitors of CDK1/cyclin B. These pyrazolo[3,4-*b*]quinoxalines are structurally similar to some purine inhibitors reported, such as roscovitine and olomoucine and, although the synthesis of further analogues is required to explore the kinase selectivity of this class of inhibitors, it has been shown that even minor modifications at the 6- and 7-positions, such as the introduction of a methyl group, leads to a significant reduction in kinase inhibition.[152]

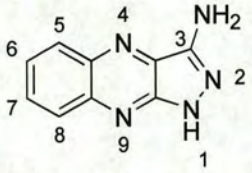

342

3.4.7 Oxindoles

The oxindole **343** has been reported as a modestly potent CDK inhibitor, with some selectivity towards CDK4/cyclin D (IC50 4.9 μM).[153] A slight modification of the oxindole scaffold, incorporating a pyridine ring, afforded compounds, illustrated by **344**, with submicromolar activity against CDK2, although, in some cases, CDK selectivity was not achieved. It was shown that a number of substitutions at the 5-position of the pyridine ring were tolerated, in addition to alkyl- or aryl-substitution on the pendant aryl ring.[154]

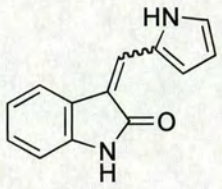

343

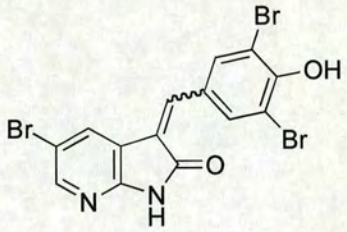

344

Two classes of compounds, 1*H*-indole-2,3-dione 3-phenylhydrazones and 3-(anilinomethylene)-1,3-dihydro-2*H*-indol-2-ones, based on the oxindole scaffold, have been reported that are low nanomolar ATP-competitive inhibitors of both CDK2 and CDK1, with approximately 10-fold selectivity for CDK2.[155] Analysis of X-ray crystal structures of CDK2/ligand **345** complex (Figure 3.12) revealed two hydrogen bonds analogous to hydrogen bonds between ATP and CDK2, namely between the amide NH of the inhibitor and the backbone carbonyl of Glu81 and between the amide carbonyl oxygen with the backbone NH of Leu83. Replacement of the hydrazone linker in the lead compound, **345**, with an enamine was shown to be inconsequential to enzyme binding.

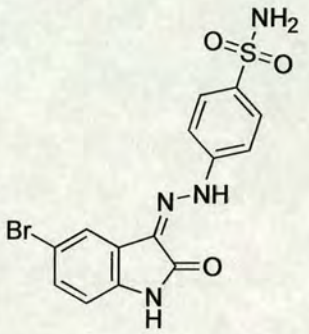

345

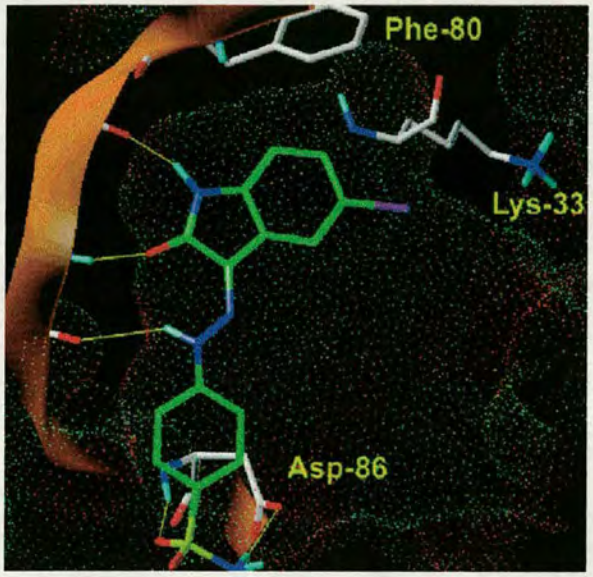

Figure 3.12: The 1*H*-indole-2,3-dione 3-phenylhydrazone inhibitor **345** bound to CDK2 The binding cavity is illustrated with a dot surface. Hydrogen bonds between the inhibitor and CDK2 are shown as yellow lines. Atoms are coloured as follows: C, green; H, light blue; N, dark blue; O, red; S, yellow; Br, purple.[155]

Further structure based design focused on variation of the substituents off the oxindole ring. It was shown that 4-substitution with small lipophilic groups, such as ethyl, isopropyl and isobutyl, afforded potent CDK2 inhibitors with IC_{50} values in the range 1 – 8 nM, the enhancement in affinity attributable to the 4-susbstituent occupying a relatively hydrophobic region of the protein formed by the residues Val18 and Leu134. Substitution at the 5-position with a hydrogen bond acceptor, such as a carboxylic ester, was shown to enhance inhibitor affinity by the hydrogen bonding to the side chain of Lys33 and/or the backbone NH of Asp145. Disubstitution at the 4- and 5-positions afforded highly potent inhibitors, exemplified by **346**, particularly in the case of compounds with 4,5-fused heterocycles with a hydrogen bond acceptor at the 5-position and hydrophobic character at the 4-position. It was hoped that variation of the substituent at the 6-position would probe CDK2 selectivity as the substituent would be

projected towards the small Phe80 pocket. However, although no measurable inhibition was reported for compounds containing larger substituents at the 6-position, such as *tert*-butyl and phenoxy, only a moderate enhancement of binding affinity was observed for those inhibitors containing smaller substituents such as ethyl, isopropyl and hydroxymethyl. Substitution at the 7-position was shown to decrease inhibitor activity owing to unfavourable steric interactions between the substituent and the side chain of Phe80.[155]

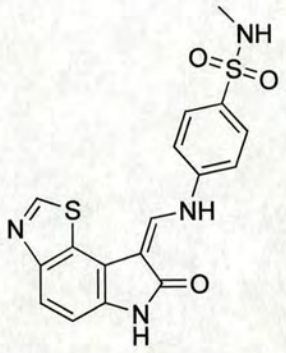

346

3.4.8 Pyrazoles

Recently a novel series of indenopyrazole-based ATP competitive CDK inhibitors have been disclosed, which display remarkable selectivity for CDK4 over CDK2. Using the crystal structure of CDK2/cyclin A as a starting point, a homology model of the CDK4/cyclin D complex was constructed and the indenopyrazole, **347**, with IC_{50} values of 460 nM and 510 nM against CDK4 and CDK2 respectively, was docked in the ATP binding pocket of the enzyme (Figure 3.13). Several observations were made that supported the SAR observed in this series of inhibitors. Firstly, the key interactions seen between the inhibitor and the kinase were similar to those reported in the X-ray crystal structure of olomucine bound to CDK2, namely the pyrazole NH interacting with the backbone carbonyl of Val96 (Leu83 in CDK2), and the adjacent pyrazole nitrogen acting as a hydrogen bond acceptor from the backbone NH of Val96. Additionally,

another key interaction was observed between the 5-substituted acetamide carbonyl and the side chain amino group of Lys35. Indeed, those inhibitors in the series that did not possess a hydrogen bond acceptor at the 5-position were reported to suffer from a significant decrease in potency against both CDK2 and CDK4. Although no significant interactions were observed between the indeno ring carbonyl and the kinase, it was suggested that the indeno ring carbonyl allowed the formation of an intramolecular hydrogen bond with the adjacent amide NH and, in doing so, aligned the acetamide group for more favourable interaction with the kinase.

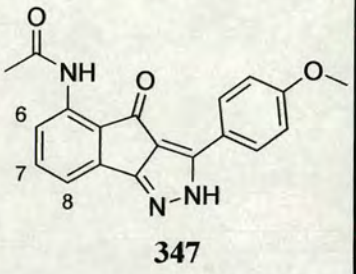

347

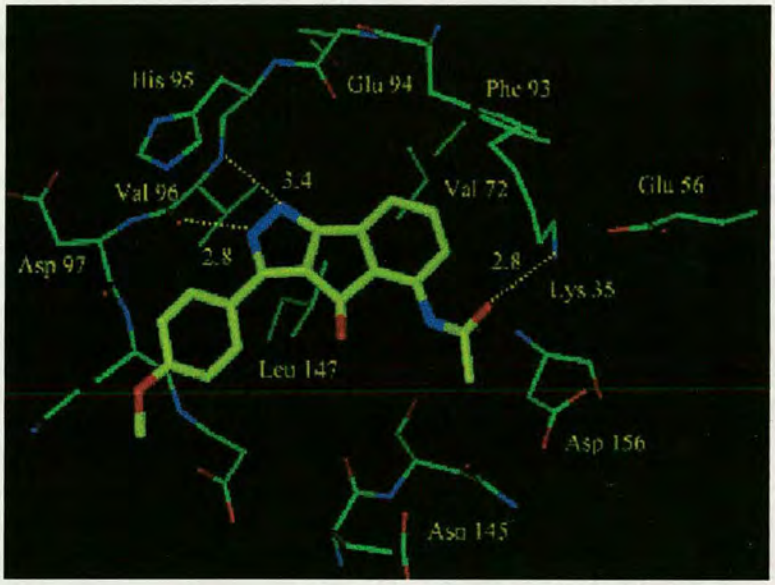

Figure 3.13: Molecular model of **347** docked to the ATP binding pocket of a CDK4/D1 homology model. Protein carbons are coloured light green and inhibitor carbons yellow.

Further increases in activity against CDKs 2 and 4 were achieved through the preparation of a number of glycinamide analogues of **347**, which revealed that substitution at the α-carbon with a six-membered saturated ring containing an additional nitrogen at the 4-position afforded compounds, such as the inhibitor **348** (IC_{50} 125 nM CDK4; 12 nM CDK2), which were some 10-fold more potent. Branching α to the amide carbonyl was not tolerated, but replacing the α-carbon with an sp^2 hybridized nitrogen

introduced an additional hydrogen bond donating element into the molecule, which, in conjunction with further substitution at the nitrogen, generated a series of urea/semicarbazide analogues. Crucially it was reported that those inhibitors containing the semicarbazide moiety displayed a 10-fold increase in activity against CDK4 when compared to their corresponding glycinamide analogues, as the inhibitor **349** demonstrates (IC_{50} 9nM CDK4; 12 nM CDK2). It was suggested that the improved activity of the semicarbazide series, compared to the glycinamide series, is attributable to the interaction of the semicarbazide N*H* with the side chain carbonyl of Asp156. The improved selectivity of the semicarbazide series against CDK4 could not be explained by molecular modeling, as Asp156 is conserved in both CDK2 and CDK4, and further structural studies are required to resolve this matter.[156]

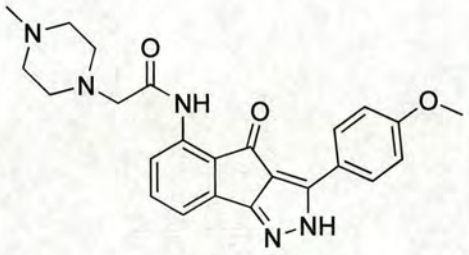

348

349

A further study by Yue and co-workers focused on the effects of substitution at the *C*3 of the indeno[1,2-*c*]pyrazol-4-one core with alkyls heterocycles and substituted phenyls and concluded, following analysis of a crystal structure of the CDK2/ligand **350** complex (Figure 3.14), that substituents at *C*3 were positioned towards the exterior of the kinase and partially exposed to solvent. It was suggested that bulkier groups that fill the binding pocket and maximize Van der Waals interactions could be less exposed to solvent than linear alkyl or large hydrophobic groups and therefore exhibit increased binding with the protein. In general, heterocycles at *C*3, particularly a thienyl moiety, gave the most potent analogues.[157]

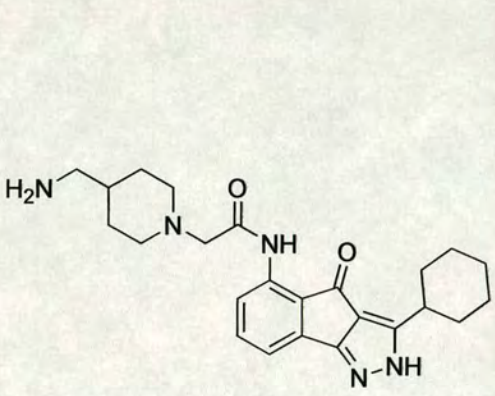

350

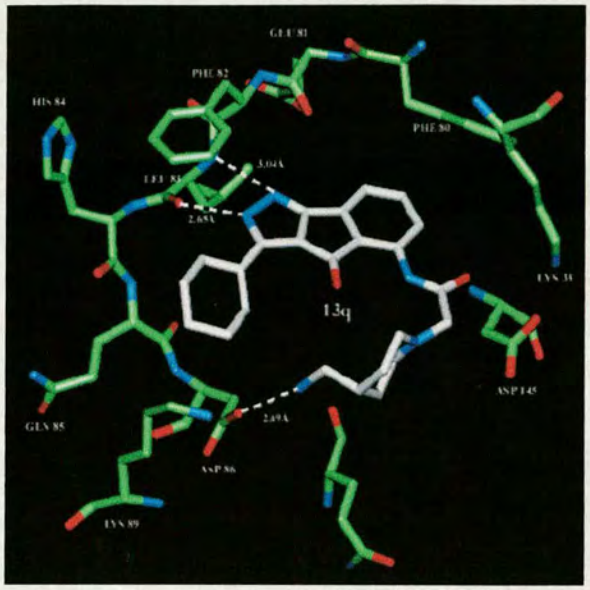

Figure 3.14: The inhibitor **350** bound to CDK2. Protein carbons are coloured green and inhibitor carbons white.[157]

Tang *et al.* have reported the synthesis of a novel series of anilinopyrazoles based on **351** that have been shown to be about 100-fold more potent as inhibitors of CDK2 than other kinases. An essential feature of this series of anilinopyrazoles was shown to be a para-sulfonamide on the 3-anilino moiety, which was shown to hydrogen bond with Asp86, and a small hydrophilic substituent at 3' of the bromophenyl ring which is projected towards a cavity formed by Lys33.[158]

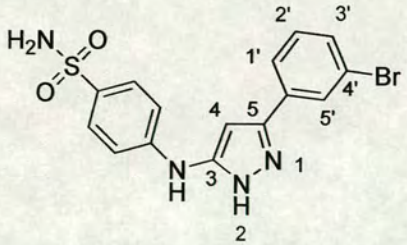

351

3.4.9 Pyrimidines

A number of phenylaminopyrimidines (PAPs) have been identified as potent inhibitors of various protein kinases, including CDK1 and CDK2. The PAP, CGP 60474, **352**, has been shown to bind to the hinged region of CDK2, forming two hydrogen bonds between the pyrimidine *N*-1 and the amide-N*H* of Leu83 and between the anilino nitrogen and the carbonyl group of Leu83.[146]

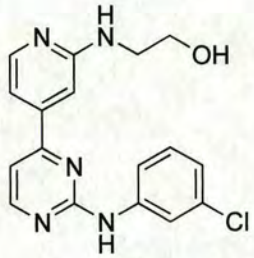

352

The identification of a series of guanines and pyrimidines that acted as ATP competitive inhibitors of CDK1/cyclin B1 and CDK2/cyclin A3 has been reported.[159] An X-ray crystal structure of the inhibitor O^6-cyclohexylmethyguanine (NU2058), **353**, bound to CDK2 (Figure 3.15) revealed three key hydrogen bonds between the inhibitor and the protein, these being between NH-9 and Glu81, N-3 and Leu83 and 2-NH_2 and Leu83. NU2058 was shown to have an IC_{50} value of 5 μM against CDK1 and 12 μM against CDK2. This novel hydrogen-bonding pattern was also observed in the crystal structure of the inhibitor NU6027, **354**, and CDK2. NU6027 was shown to have an IC_{50} value of 2.5 μM against CDK1 and 1.3 μM against CDK2.[159] Crystal structures of four additional guanidines based around this template bound to monomeric CDK2 were reported which revealed that optimum binding with the kinase was achieved with moderately sized non-polar alkyl or cycloalkyl O^6 substituents packing against a hydrophobic region of the glycine loop, centered on Val18. In this study, no compound was identified that was markedly more potent or selective than the initial lead compound **353**, which led to the conclusion that exploitation of the ribose binding pocket for the development of potent

and selective CDK2 inhibitors would be difficult owing to its hydrated nature and high degree of flexibility.[160]

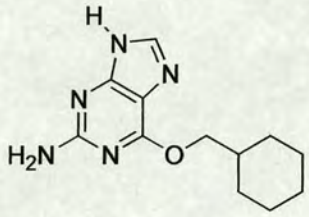

353

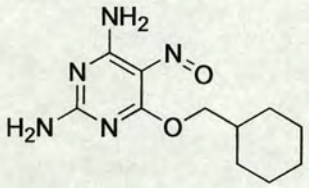

354

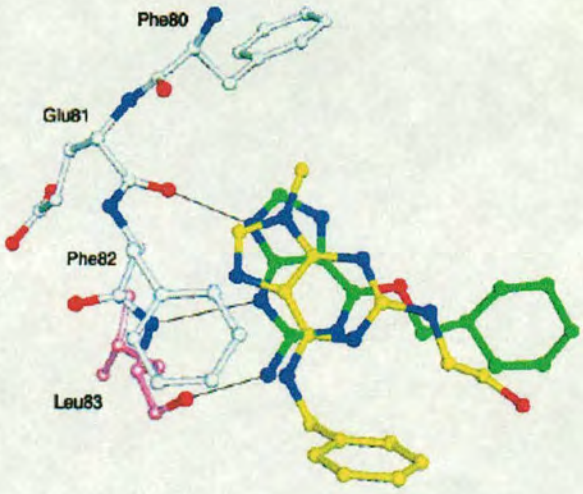

Figure 3.15: Overlay of the CDK2/olomoucine structure with that of the CDK2/**353** complex in the vicinities of the inhibitor binding sites. Olomoucine carbon atoms are coloured yellow and **353** carbon atoms are coloured green. Conserved hydrogen bonds between the CDK2 backbone, at residues Glu81and Leu83, and NU2058 are shown as thin lines. Only CDK2 residues Phe80 to Leu83 in the CDK2/NU2058 complex are included for clarity.[159]

An extension to this work reports on the structure-based design of a series of O^4-cyclohexylmethyl-5-nitroso-6-aminopyrimidines containing a range of 2-arylamino substituents that are potent inhibitors of both CDK1 and CDK2.[161] 2-Arylaminopyrimdines with a sulfonamide or carboxamide group at the 4'-position were shown to be potent inhibitors of CDK2 with nanomolar potency. A crystal structure of the 4'-carboxamide derivative, **355**, in complex with Thr160 CDK2/cyclin A (Figure 3.15) revealed 4 hydrogen bonds between the inhibitor and CDK2. In addition to hydrogen bonds formed between the amino group at the 6-position of the pyrimidine ring and the carbonyl of Glu81; between *N*-1 of the pyrimidine ring and the amide

backbone of Leu83; and between the anilino nitrogen at the 2-position of the pyrimidine ring and the carbonyl of Leu83; a further interaction between the carboxamide group and Asp86 was suggested (Figure 3.16).[161]

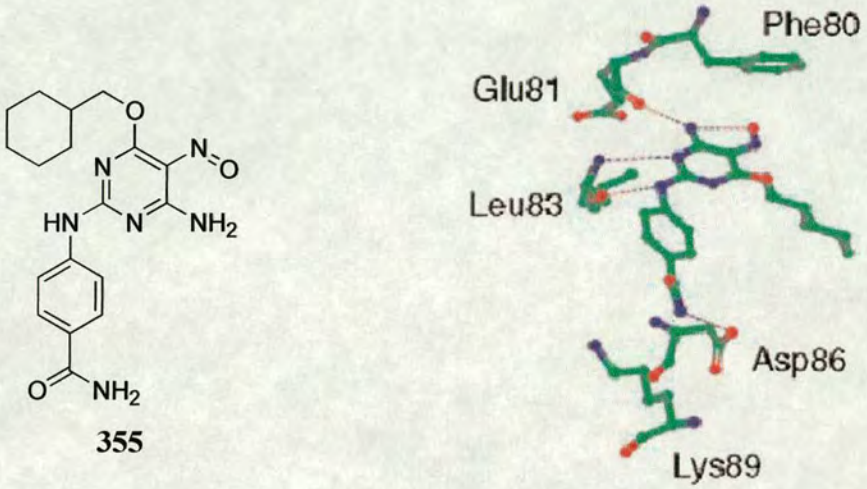

355

Figure 3.16: Interaction of **355** with active site of phospho-Thr160 CDK2/cyclin A.

The identification of a series of 3,7 disubstituted pyrazolo[4,3-*d*]pyrimidines as novel inhibitors of CDK1/cyclin B has been reported.[162] In contrast to *C*-2, *C*-6, and *N*-9 trisubstituted purine inhibitors, such as olomoucine, the pyrazolo[4,3-d]pyrimidines, illustrated by **356**, demonstrate a comparable inhibitory effect against CDK1 with only two substituents off the central ring. Focusing on a variety of amines at the 7-position of the ring, a series of pyrazolo[4,3-*d*]pyrimidines was synthesized and screened against CDK1/cyclin B together with their 6,9-disubstituted purine analogues. It was shown that members of the pyrimidine series were approximately 2-10 times more potent as inhibitors of CDK1 than the respective 6,9-disubstituted purines.

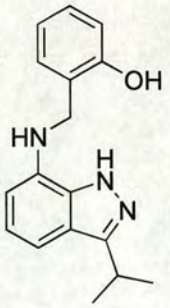

356

A class of compounds, based on the pyrido[2,3-*d*]pyrimidin-7-one moiety, have been described that exhibit modest selectivity for CDK4.[163] The most potent of these inhibitors, **357**, has an IC50 of 4 nM, compared with an IC_{50} of 25 μM for ATP. X-ray crystallographic analysis of an analogous inhibitor, **358**, bound to CDK2 (Figure 3.17) indicated that the ligand occupied the ATP binding site, and kinetic studies indicated that the binding was competitive. Again, the key features of this phamacophore are the aromatic amine at the *C*-2 position that generates a hydrogen bond from the anilino N*H* to the carbonyl of Leu83 in CDK2 (Val-96 in CDK4), and the pyrimidine *N*-3 nitrogen, which forms a hydrogen bond to the N*H* of Leu83. The electronic properties of the aromatic amine were shown to have a significant effect on the potency of the compound, with electron poor anilines being generally less potent than the initial lead. Mixed results were observed with electron rich anilines and amine-substituted anilines were generally more potent than oxy- or halo-substituted anilines. Substitution at the *N*-8 position of the ring was shown to allow occupancy of a fairly large and predominantly hydrophobic region on the binding site. Consequently, alkyl groups were reported to be preferred to aryl groups, with cycloaryl groups affording the highest potency.[163]

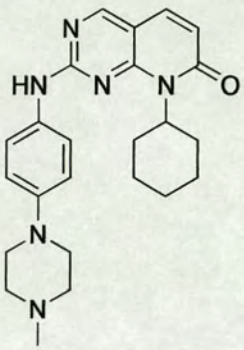

357

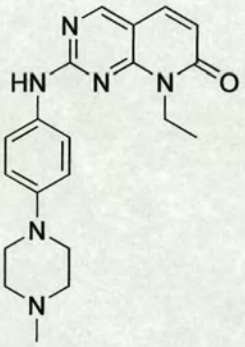

358

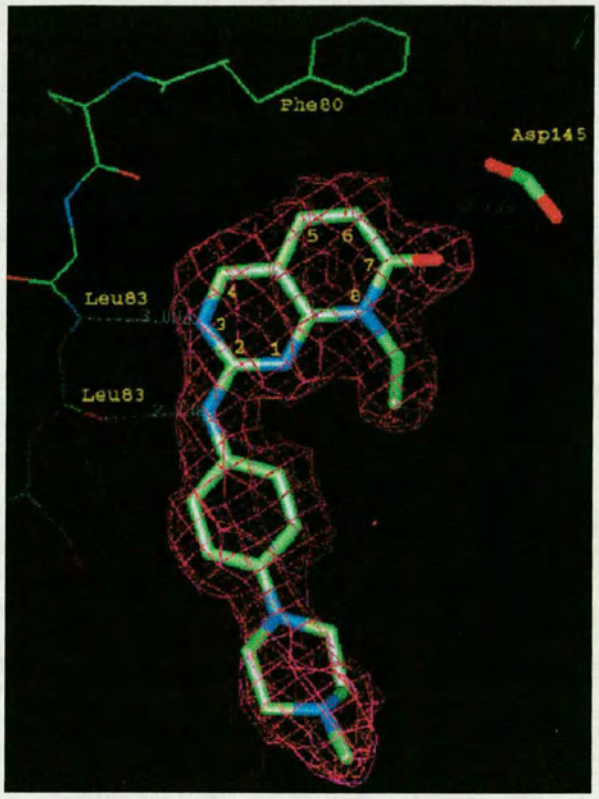

Figure 3.17: Crystal structure of the inhibitor **358** bound to CDK2.[163]

A potent series of inhibitors based around the imidazo[1,2-*a*]pyridine template has been reported.[164] Analysis of a crystal structure of the imidazo[1,2-*a*]pyridine **359** bound with inactivated, monomeric CDK2 revealed three key hydrogen-bonding interactions. Two hydrogen bonds were observed between the pyrimidine *N*-1 and Leu83 backbone N*H*, and the 2-amido NH and Leu83 backbone carbonyl oxygen atom and are consistent with the accepted kinase-purine mimetic pharmacophore and were also observed in a bisanilinopyrimidine/CDK2 complex. A third, previously unreported, hydrogen bond was observed between the imidazo[1,2-*a*]pyridine *N*-1 and the Lys33 amino group (Figure 3.18).

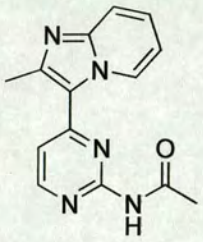

359

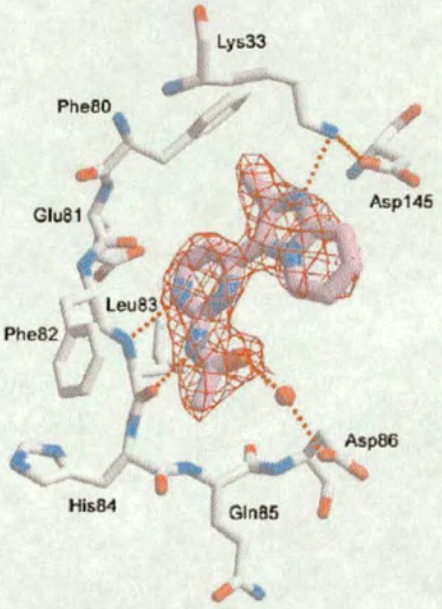

Figure 3.18: Crystal structure of CDK2 complexed with the imidazo[1,2-a]pyridine inhibitor **359**.[164]

It was shown that a para-sulphonamoyl substituted aniline **360**, at the 2-position of the pyrimidine ring, not only improved potency against both CDK2 and CDK4, attributable to the generation of hydrogen bonds with the Asp86 backbone N*H* and with its carbocylic side chain, but also highly improved selectivity for CDK2, presumably as a result of more favourable packing interactions between the aniline ring and the kinase (Figure 3.19).

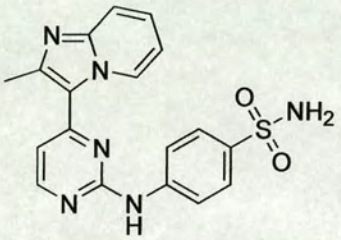

360

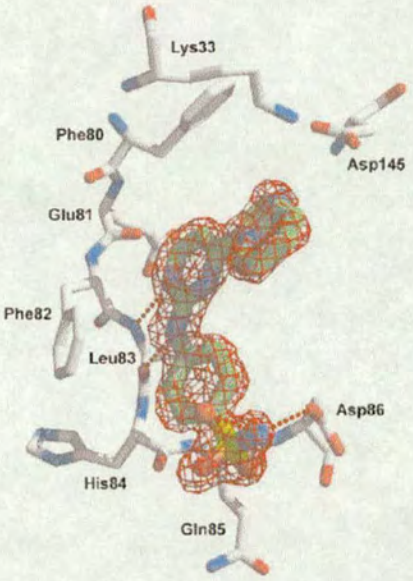

Figure 3.19: Crystal structure of CDK2 complexed with the inhibitor **360**.[164]

More recently, 2-phenylamino-4-thiazolopyrimidines have been identified as potent *in vitro* and *in vivo* CDK2 inhibitors.[165] This series of ligands, exemplified by **361** which is the most potent CDK2 inhibitor reported to date with an IC_{50} <1 nM, forms the basis of further discussion in Chapter 4.

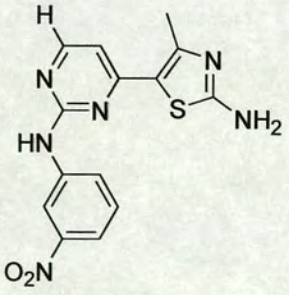

361

Notably, the introduction of an aromatic substituent to the amino group of ligand CYC2, **321**, has been shown to result in a different binding mode between the ligand **362** and the protein, one where the pyrimidine ring had been flipped 180°C (Figure 3.20).[121]

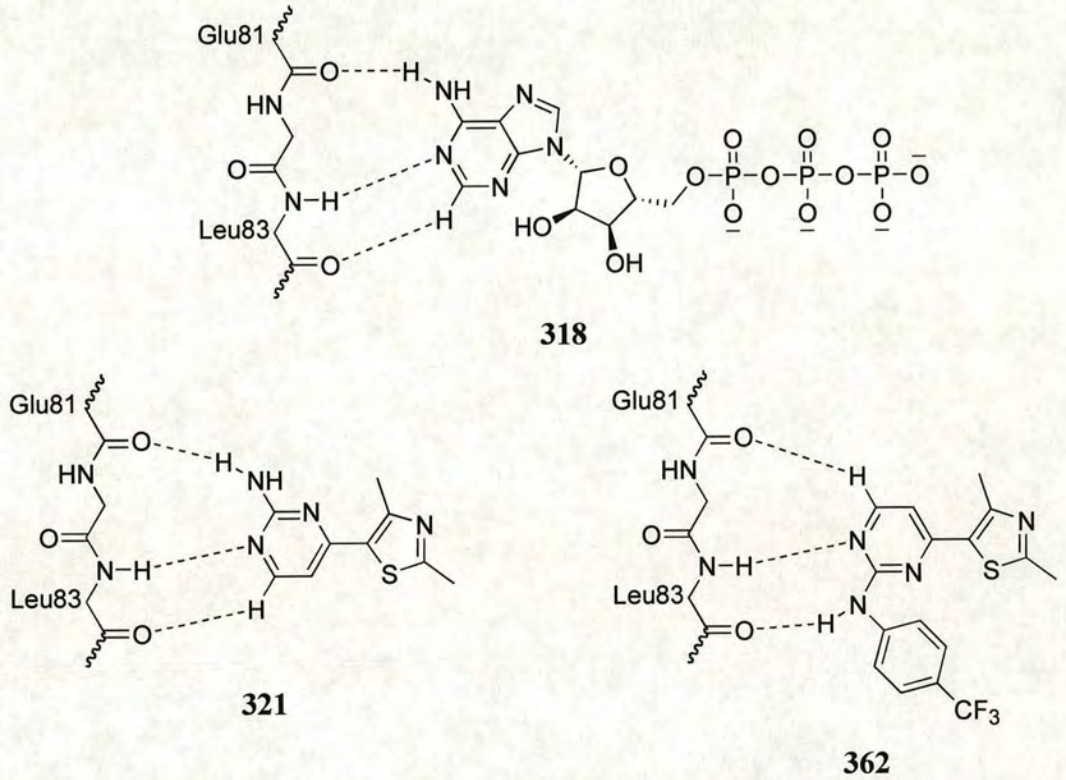

Figure 3.20: H-bonding interactions of ATP, **318**, and ligands **321** and **362** with the backbone of CDK2 residues Glu81 and Leu83.

Furthermore, the application of computational methods to this series of 2-phenylamino-4-thiazolopyrimidines has enabled the derivation of a structural basis for specific, high-affinity binding of inhibitors to the CDK4 active site.[166] It was postulated that appropriate incorporation of an ionizable function into a CDK2 inhibitor results in a more favourable binding to CDK4, owing to a favourable interaction between the ATP cleft of CDK4 (Asp99, Glu144), whereas the inhibitor is repulsed from the active site of CDK2 owing to the presence of Lys89.

Lastly, and of particular significance to the discussion presented in Chapter 4, a series of 4,6-bis-anilino pyrimidines[167] and 2,4-bis-anilino pyrimidines[168] have been reported as inhibitors of CDK4. Given demonstrated activity in the 4,6-bis-anilino series[167] it was postulated that the pyrimidine 5H (Figure 3.21) could be crucial to activity as it would contribute to the twisting of the aniline rings out of the plane of the pyrimidine in the bioactive conformation. However, crystal structures obtained of members of both series of ligands bound to CDK2 indicated that both series adopted the same binding mode that was consistent with the accepted kinase purine-mimetic pharmacophore, namely the pyrimidine *N*-1 acting as a hydrogen bond acceptor and the 6-aniline NH acting as a hydrogen bond donor with the amide NH and amide carbonyl oxygen of Leu83 respectively. However, it was reported that the tilt in the B ring (Figure 3.21) with respect to the pyrimidine varied substantially between different enzyme/inhibitor complex structures both within and between the two series. Furthermore, it was shown that the 2,4-disubstituted pyrimidine series was generally more potent than the equivalent 4,6-series, with improvements in IC_{50} values against CDK2 and CDK4 approximately 10-fold.[168]

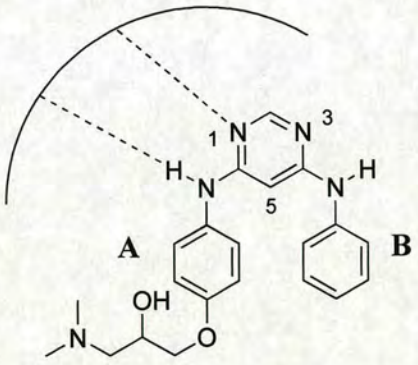

Figure 3.21: General scaffold for reported 4,6-bis-anilino pyrimidine inhibitors of CDK4.

4 The development of novel inhibitors of cyclin dependent kinases

4.1 Introduction

Research carried out at Cyclacel Ltd. has provided a solid foundation for the development of a number of novel series of inhibitors of cyclin dependent kinases. The CYC-202 programme, focusing on the purine analogue (*R*)-roscovitine, **323**, has entered Phase II clinical trials in cancer and also Phase I clinical trials in glomerulonephritis has been initiated.

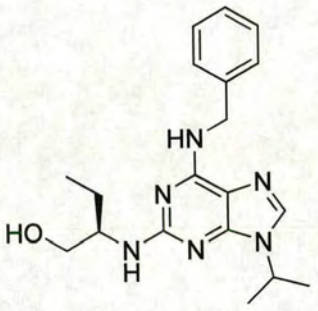

323

Cyclacel Ltd. have also developed a second generation family of CDK2 inhibitors based around a 2-anilino-4-(thiazol-5-yl)-pyrimidine scaffold exemplified by the inhibitor CYC4223, **363**.[165]

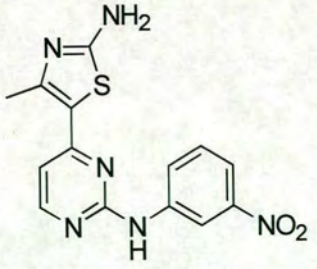

363

The general synthetic route to 2-anilino-4-heteroaryl-pyrimidines is shown in Scheme 4.1. Reaction of an *N*-substituted alkylthiourea, **364**, with 3-chloro-2,4-pentanedione **365** affords the thiazole **366** which is subsequently refluxed in *N*-*N*-dimethylformamide dimethylacetal to yield the enaminone **367**. Cyclisation of the enaminone **367** with a guanidine **369**, synthesized from a substituted aniline **368** and cyanamide, affords the pyrimidine **370**.[165]

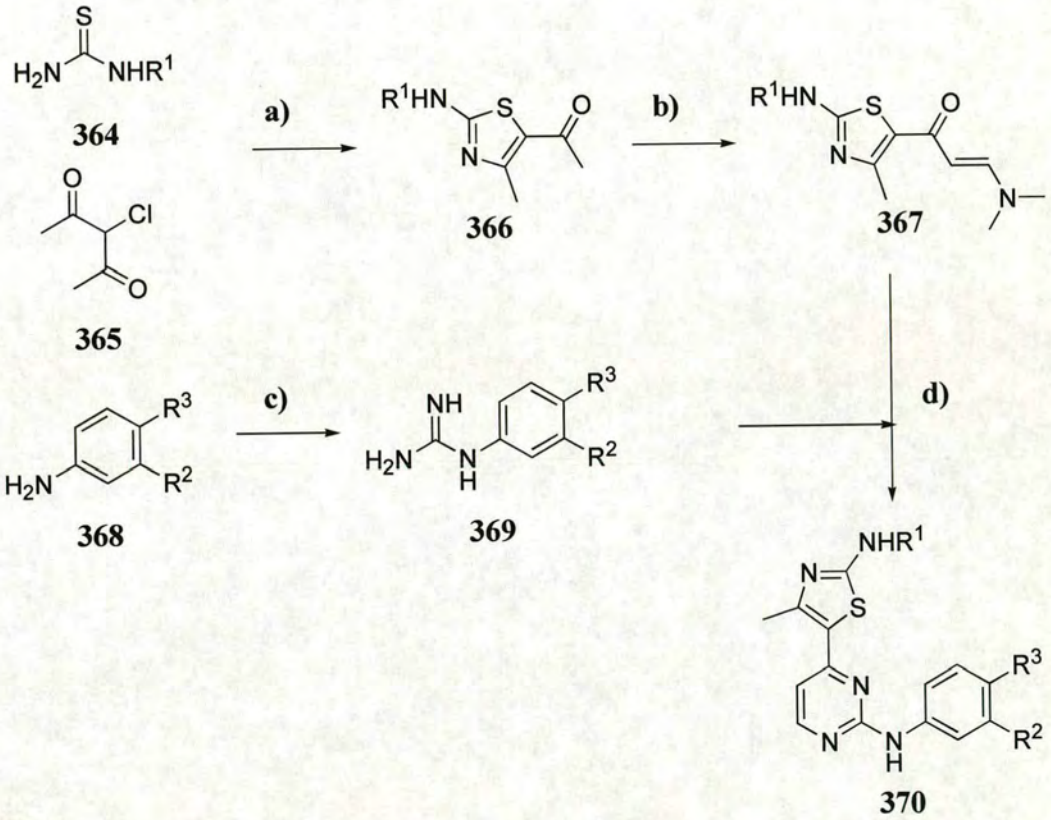

Scheme 4.1: *Reagents and conditions:* **a**) methanol, pyridine; **b**) *N*,*N*-dimethylformamide dimethyl acetal, 120 °C; **c**) HNO_3, cyanamide (aq.), 100°C, reflux, 24 h; **d**) NaOH, 2-methoxyethanol, 125 °C.

The X-ray crystal structure of the inhibitor **363** bound to CDK2 has been solved by McNae and is shown in Figure 4.1.[121]

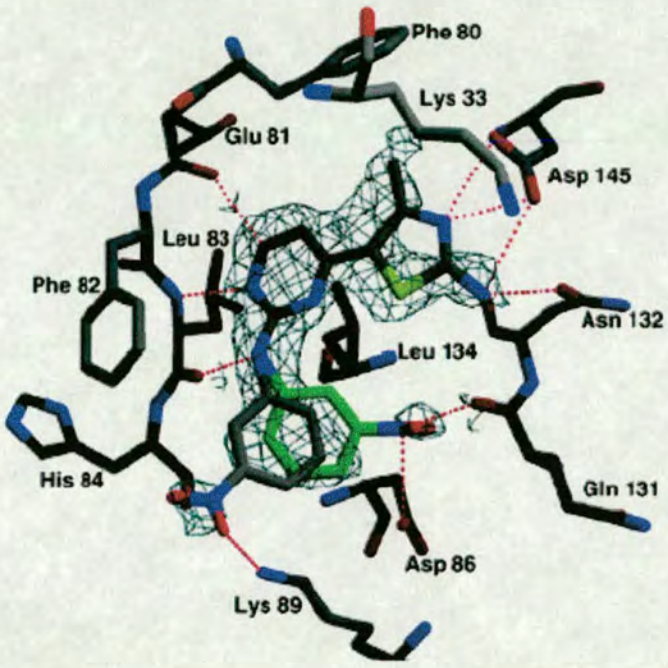

Figure 4.1: The X-ray crystal structure of the inhibitor CYC4223, **363**, bound to CDK2. The two positions of the nitro group are distinguished from each other by one of the rings being coloured green. Key hydrogen-bonding interactions between the inhibitor and the protein are shown as red broken lines. Carbon atoms are coloured black and green; nitrogen blue; sulfur yellow; and oxygen red. CDK2 residues are labeled (PDB Code 1PXO).

Notably, the crystal structure of the CDK2/ligand **363** complex showed that *N*1 of the pyrimidine ring acts as a hydrogen-bond acceptor and interacts with the backbone N*H* of Leu83, and the aniliño-N*H* of the inhibitor acts as a hydrogen-bond donor and interacts with the carbonyl of Leu83. There was some ambiguity in the electron density of the anilino moiety of **363** that suggested the aromatic ring of the aniline could adopt one of two different binding modes. The nitrogen of the nitrophenyl group was shown to form weak but favourable electrostatic interactions to Asp86 and a close contact with the

backbone carbonyl of Gln131. In the alternative conformation, the nitro group was shown to be weakly hydrogen-bonded to the side chain of Lys89. The nitrogen of the thiazole ring was shown to be within hydrogen-bonding distance to the carboxylic acid of Asp145. The primary amino group at the 2-position of the thiazole ring was shown to interact with the side chains of Asp145 and Asn132.[121] Significantly, the nitrogen at the 3-position of the pyrimidine ring did not appear to be involved in any binding interactions with the protein. This observation raised the question of whether the pyrimidine ring could be substituted with other aromatic ring systems, such as a pyridine or a pyrazine, whilst still retaining CDK inhibitory activity. Modifications to the central ring system would also have a subtle effect on the pK_a of the hydrogen-bond acceptor at *N*-1, deemed to be essential for CDK binding, and, as such, would merit further investigation.

A further challenge of CDK inhibitors targeting the ATP binding pocket is achieving selectivity between the protein kinases. Consequently, CDK inhibitors synthesized are routinely screened against other protein kinases, for example glycogen synthase kinase (GSK-3β). A recent study[169] argues that selectivity between GSK-3β and CDK2 may be achieved through exploitation of one of the main structural differences between the two kinases, namely the residues Phe80 in CDK2 and Leu132 in GSK-3β. In the context of the CDK2 inhibitor **363**, it has been shown that the thiazol-4-yl methyl group is directed towards the Phe80 phenyl ring in CDK2.[165] It is postulated that this favourable hydrophobic interaction in not present in the GSK-3β/ligand **363** complex (Figure 4.2).[170] Substitution studies at the 4-position of the thiazole ring may give rise to **363** analogues with increased selectivity.

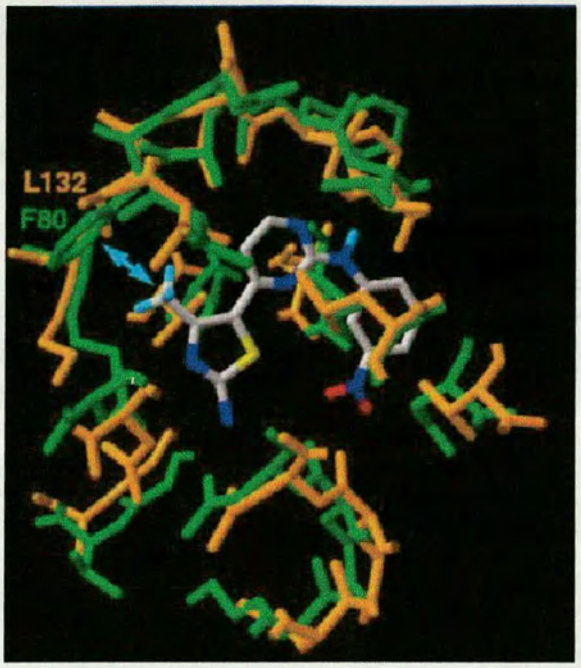

Figure 4.2: Comparison of the ATP-binding pockets in CDK2 and GSK-3β. The residues involved in direct interactions between CDK2 and ATP are shown in green, whereas the corresponding residues in GSK-3β are shown in orange. The CDK2 binding modes of the inhibitor CYC-4223 are shown in CPK colouring (PDB Code 1HCK and 1I09).[170]

To date there are no examples in the literature of CDK inhibitors based around a pyrimidine scaffold that contains a 4-aryl substituent. Furthermore, the replacement of the pyrimidine scaffold present in the 2-anilino-4-(thiazol-5-yl)-pyrimidine with a 4,6-disubstituted pyrimidine warranted further investigation. Therefore, the primary aim of the research discussed in this chapter was to develop a number of novel CDK inhibitors based around a 4-aryl-6-anilino-pyrimidine template, **371**, using high-throughput synthesis techniques.

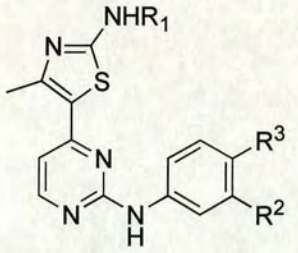

362

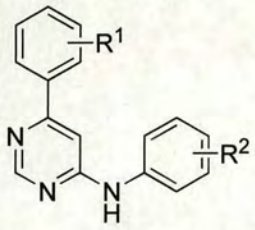

371

4.2 Synthetic strategy

Ultimately, as it was desirable to generate a large number of inhibitors based around the 4-aryl-6-anilino-pyrimidine template that contained some functional diversity, it was perceived that the synthetic route selected would need to be simple, efficient and amenable to combinatorial chemistry. Alternatively, it was envisaged that if microwave-assisted organic synthesis could be utilized to shorten reaction times, the automated serial synthesis of ligands would be possible.

Retrosynthetic analysis of the 4-aryl-6-anilino-pyrimidine template revealed that the simplest synthetic strategy would be to leave the central pyrimidine ring intact and to make two disconnections, a carbon-carbon disconnection at *C*-4 and a carbon-nitrogen disconnection at *C*-6, thereby rendering the template into three synthons, each of which could contain some structural diversity. It was envisaged that the Suzuki reaction could be employed to couple a substituted phenylboronic acid to the commercially available 4,6-dichloropyrimidine. Similarly, nucleophilic substitution of an aniline with the chloropyrimidine could be used to generate the carbon-nitrogen bond at *C*-6 (Scheme 4.2).

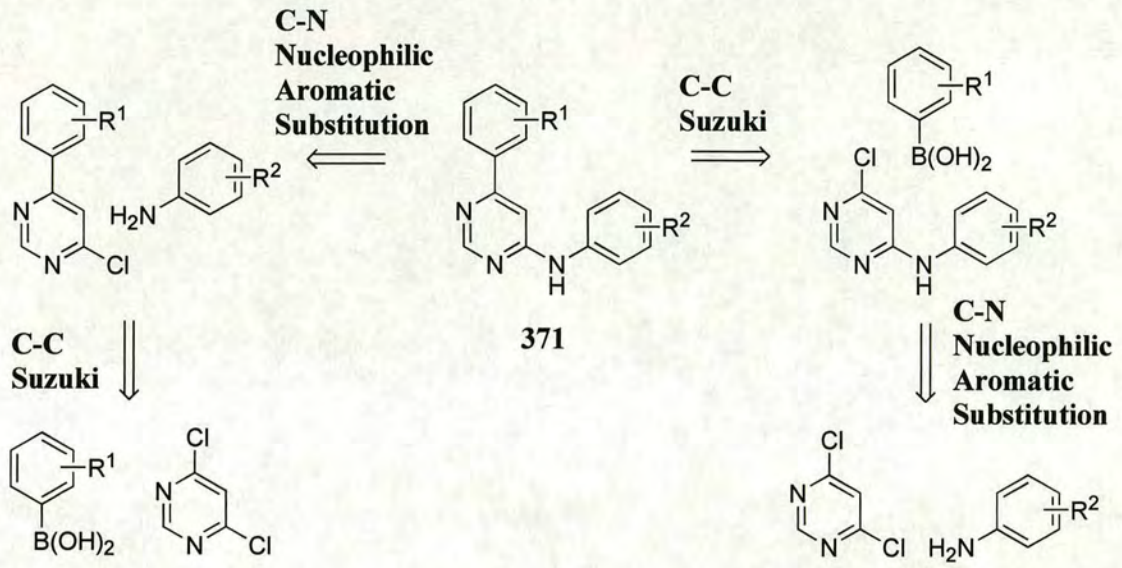

Scheme 4.2: Retrosynthetic analysis of the 4-aryl-6-anilino-pyrimidine template **371**.

4.2.1 The Suzuki Reaction

The Suzuki reaction[171] is only one of the reactions available to the synthetic organic chemist that enables the synthesis of new carbon-carbon bonds. Other methods include the Stille,[172] Negishi,[173] Heck,[174] Kumada,[175] Sonogashira[176] and Hiyama reactions.[177] The generally accepted reaction mechanism for the Suzuki reaction is shown in Scheme 4.3. Oxidative addition of an aryl, alkenyl or alkynyl halide, **372**, with a palladium (0) complex, **373**, affords a palladium (II) species, **374**. Activation of an organoboron compound, usually a boronic acid, by reaction with a base, to afford **375** and subsequent reaction with the palladium (II) species results in transmetallation to afford a palladium (II) species, **376**, that undergoes reductive elimination to yield the coupling product, **377**, and the regenerated catalytically active palladium (0) complex, **373**.[171]

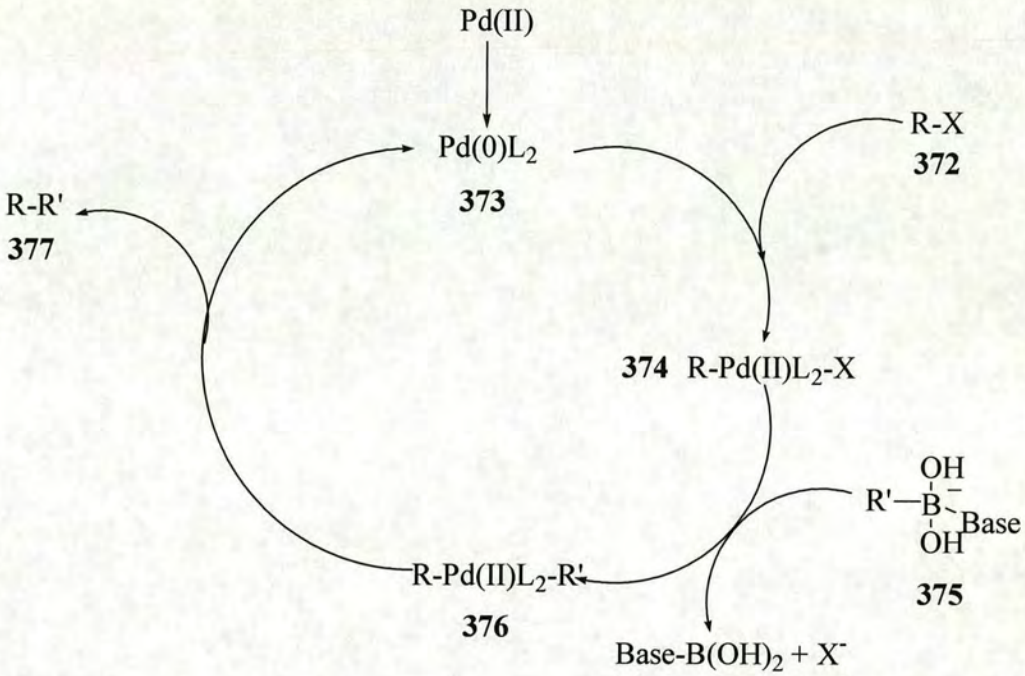

Scheme 4.3: The general catalytic cycle for the Suzuki reaction.

A wide range of palladium (0) catalysts can be used for the cross-coupling reaction, such as $Pd(dba)_2$ or, more commonly, $Pd(PPh_3)_4$ although $PdCl_2(PPh_3)_2$ or $Pd(OAc)_2$ plus PPh_3 or other phosphine ligands can be used as they are readily reduced to the active palladium (0) complexes.[171]

Often, the rate-limiting step of the Suzuki reaction is the oxidative addition of the halide or triflate to the palladium (0) complex, **373**, with the relative reactivity decreasing in the order of I > OTf > Br >> Cl.[178] Although there are many literature examples of palladium catalyzed cross-coupling reactions involving the use of aryl bromides and iodides, it is only recently that examples of palladium-catalyzed cross-coupling reactions involving organic chlorides have been reported. The bond dissociation energy of Ph-Cl (96 kcal mol^{-1}) is significantly higher than that of the Ph-Br (81 kcal mol^{-1}) and Ph-I (65 kcal mol^{-1}) bonds, reflecting the relative strength of the C-Cl bond.[179] Certain aryl chlorides, in particular electron-poor aryl chlorides that are activated towards oxidative

addition, have been shown to be suitable substrates for the Suzuki cross-coupling reaction. Furthermore, the successful use of the Suzuki reaction has been reported for other chloro-substituted nitrogen heterocycles including pyridines, pyrazines, pyridazines, triazines, quinolines, isoquinolines, quinazolines and purines.[180]

The choice of phosphine ligand is often of paramount importance to the success of the Suzuki coupling of activated aryl chlorides. Shen reported that palladium complexes that include a bulky, electron-rich trialkylphosphine were effective at catalyzing the cross-couplings of activated aryl chlorides and proposed that the electron-richness of the ligand might aid the oxidative addition of the Ar-Cl bond to the palladium (0) centre and, furthermore, steric crowding of the ligand around the palladium centre may favour its dissociation to afford an active monophosphine palladium catalyst.[181]

The decision to employ the Suzuki reaction for the formation of the carbon-carbon bond at *C*-4 of the pyrimidine ring was made based on the commercial availability of 4,6-dichloropyrimidine and a relatively large number of aryl-boronic acids, which could be used to develop an understanding of the SAR based around the 4-aryl-pyrimidine pharmacophore. It was envisaged that a study of various substitutions off the 4-aryl substituent would probe the region around the Asp145 and Phe80 residues of CDK2 and, following the subsequent screening of ligands against a panel of kinases, provide an insight into the selectivity preferences between the CDK family and GSK-3β. Furthermore, the stability of boronic acids to heat, air and moisture as well as their non-toxic nature warranted the use of this strategy over other cross-coupling methods.

The electron deficient nature of the pyrimidine ring makes this system far more reactive to Suzuki couplings compared to analogous benzenoid halides. Gronowitz *et al.* reported the coupling of 2,4-dichloropyrimidine with 2-thienylboronic acid and showed that the reaction selectively took place at the 4-position of the pyrimidine ring, as opposed to the more electron-rich 2-position (Scheme 4.4).[182]

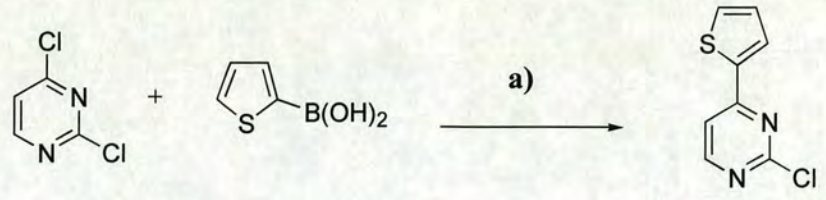

59 %

Scheme 4.4: *Reagents and conditions*: **a)** $Pd(PPh_3)_4$ (3 %), Na_2CO_3 (aq.), DME, reflux.

More recent examples of the Suzuki coupling of 2,4-dichloropyrimidine that show selectivity at the 4-position as opposed to the 2-position have been reported by Jiang *et al.*[183] and Gong *et al.*[184] Schomaker *et al.* have reported the Suzuki cross-coupling reaction between 2,4-dibromopyrimidine and phenylboronic acid,[185] isolating both the 2-bromo-4-phenyl-pyrimidine and 2,4-diphenylpyrimidine in 58% and 22% yield respectively. An analogous coupling, using 4,6-dibromopyrimidine afforded both 6-bromo-4-phenyl-pyrimidine and 4,6-diphenylpyrimidine in respective yields of 56% and 23%. The palladium catalyzed cross-coupling of 4,6-dichloro-2-methyl-5-nitropyrimidine with *o*-(trifluoromethyl)-phenylboronic acid to afford the 4-aryl-substituted pyrimidine as the major product has been reported by Cocuzza *et al.*[186]

4.2.2 Microwave assisted organic synthesis

In the electromagnetic spectrum, the microwave radiation region is located between infrared radiation and radio waves, with microwaves having wavelengths ranging from 1mm – 1m. The use of microwaves to heat materials is not a novel concept, dating back some 50 years. In chemistry, studies using microwave technology have been undertaken since the late 1970s, initially within the field of inorganic chemistry, and, during the mid-1980s, within organic chemistry. Although microwave chemistry has been slow to develop, hampered primarily because of its lack of reproducibility and controllability, recently, it is evident from the increasing number of publications in the field that there has been renewed interest in the technology. This interest has emerged as a result of the

recent influx of availability of commercial microwave equipment, the development of novel solvent-free techniques, and as a reaction to increasing pressure in the pharmaceutical industry to seek shorter reaction times to aid in the synthesis of a greater number of novel chemical entities.

Microwave dielectric heating has a number of advantages over traditional heating techniques, such as oil baths and heating jackets. Firstly, the microwave radiation heats only the reactants and solvents, and not the reaction vessel itself. Secondly, the use of correctly designed single mode cavity microwave reactors ensures the uniform heating of samples, unlike traditional heating techniques, where local hot spots or temperature gradients can sometimes develop. One further advantage gained by the use of microwave technology in chemistry is that it is possible to heat reactions to a temperature far greater than the conventional boiling point of the reaction solvent used, as reaction mixtures are heated in sealed tubes which, when heated, act as pressurized systems.[187]

The main advantage of using microwave assisted organic synthesis is the shorter reaction times. The rate of reaction can be described by the Arrhenius equation (Equation 4.1).

$$k = A\, e^{-\Delta G/RT} \qquad \textbf{(Equation 4.1)}$$

The pre-exponential factor, A, describes molecular mobility and is related to the frequency of vibrations of the molecules at the reaction interface. Microwaves induce an increase in molecular vibrations, and it has been proposed that this can affect the pre-exponential factor, in turn, leading to an increase in rate of reaction, k.[188] It has also been proposed that microwave irradiation can affect alter the exponential factor by affecting the free energy of activation.[189]

Recently, microwave technology has been successfully applied to many different aspects of synthetic organic chemistry including heterocyclic synthesis,[190] solvent free reactions,[191] phase transfer catalysis,[192] cycloaddition reactions,[193] and transition metal catalyzed processes.[194] Kappe and co-workers have extended the application of microwave-assisted chemistry to parallel synthesis using reactors with suitable multimode microwave cavities.[195] Furthermore, it has been shown that high-speed serial microwave-assisted organic synthesis can offer an attractive alternative to parallel synthesis using conventional combinatorial chemistry apparatus.[196]

4.3 Results and discussion

4.3.1 Initial Strategy

Exploratory research in the group by Causton[197] had shown that a number of substituted aryl boronic acids could be selectively coupled to the 4-position of the commercially available 2,4-dichloropyrimidine, **378**, under Suzuki conditions using microwave assisted organic synthesis. Optimized reactions conditions were determined to be the irradiation of a solution of 2,4-dichloropyrimidine in MeCN/H_2O with a stoichiometric amount of the aryl boronic acid, **379**, at 110°C for 10 minutes in the presence of $Pd(OAc)_2$ and Cs_2CO_3. Furthermore, Causton had demonstrated that the reaction mixture containing the mono-substituted Suzuki intermediate, **380**, could then undergo subsequent coupling with an aniline, **381**, under acidic conditions, to afford a range of 2-anilino-4-aryl-pyrimidines, **382**, (Scheme 4.5).[197] This strategy was very attractive, allowing the high-throughput synthesis of novel CDK inhibitors, from commercially available building blocks, with only one purification step required at the end of the synthetic sequence. Research was still ongoing in this area upon the initiation of the chemistry discussed in the remainder of this chapter.

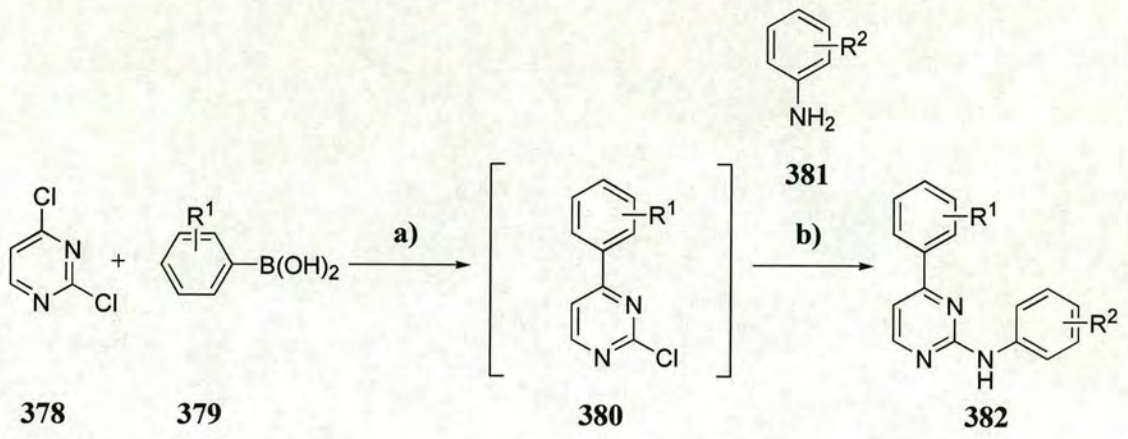

Scheme 4.5: *Reagents and conditions:* **a)** $Pd(OAc)_2$, Cs_2CO_3 (3 eq.), $MeCN/H_2O$, μwave, 110 °C, 15 min. **b)** HCl (2M), μwave, 110 °C, 5 min.

Initially, it was envisaged that the synthetic route developed in the group by Causton to afford 2-anilino-4-aryl-pyrimidines could be employed to synthesize 6-aryl-4-anilino analogues. Prior to obtaining Causton's method, 3 trial two-step reactions were undertaken, illustrated in Scheme 4.6. Reaction of 2,4-dichloropyrimidine with either 4-chloro-, 4-methyl- or 3,5-bis-trifluoromethyl-aniline under basic conditions afforded anilino-pyrimidines **384** – **386**, identified by ESI-MS. Analysis of the mass spectra of **385** and **386** also confirmed the presence of the bis-anilino pyrimidine. Subsequent palladium catalyzed cross-coupling of **384** – **386** with phenylboronic acid afforded the 4-aryl-6-anilino-pyrimidines **387** – **389** in very low yields. Analysis of the mass spectrum of **387** also revealed the presence of triphenylphosphine oxide. However, it was encouraging that in just two steps, each consisting of very short reaction times, and with only one final purification step, two novel ligands, **388** and **389**, had been synthesized which could be subsequently screened against the CDKs.

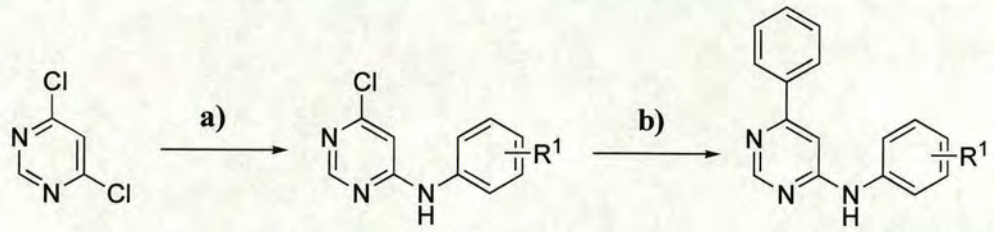

383

384 R^1 = 4-Cl
385 R^1 = 4-CH_3
386 R^1 = 3,5-CF_3

387 R^1 = 4-Cl
388 R^1 = 4-CH_3
389 R^1 = 3,5-CF_3

Scheme 4.6: *Reagents and conditions:* **a**) R^1-Substituted aniline, NaOH (2M), μwave, 110 °C, 5 min. **b**) Phenylboronic acid, $Pd(OAc)_2$ (5%), PPh_3 (10%), Cs_2CO_3 (3 eq.), THF, μwave, 110 °C, 15 mins.

It was postulated that the poor yields of **387** – **389** were attributable to formation of the bis-anilino species and consequently it was decided to reverse the steps, i.e.to perform the Suzuki coupling initially, followed by the amination reaction for subsequent syntheses of ligands. Recently, Qing *et al.* have reported that treatment of 4,6-dichloropyrimidine with two equivalents of boronic acids under Suzuki coupling conditions resulted in the formation of 4,6-disubstituted pyrimidines in high yield with no evidence of the homo-coupling of the boronic acid.[198] However, it has been shown that the trichloropyrimidine **390** can couple with phenylboronic acid under Suzuki conditions to afford 2,4-dichloro-6-phenylpyrimidine, **391**, in excellent yield (Scheme 4.7).[185] Therefore, it was envisaged that the treatment of **383** with one equivalent of boronic acid would afford the primarily the mono-substituted pyrimidine as the greater electron-richness of the 4-aryl-6-chloropyrimidine compared with that of the 4,6-dichloropyrimidine would prevent the bis-Suzuki coupling from taking place. Furthermore, given Causton's success employing a Suzuki coupling and subsequent anilino coupling in the 2,4-dichloropyrimidine series, it seemed prudent to adopt this strategy for future syntheses.

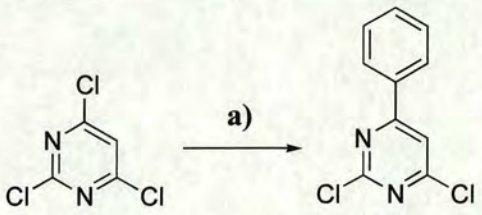

390 **391** (88%)

Scheme 4.7: *Reagents and conditions:* Phenylboronic acid (1 eq.), $Pd(OAc)_2$, PPh_3, glyme/H_2O, Na_2CO_3, reflux, 18 h.[185]

The Suzuki coupling between 4,6-dichloropyrimidine and 3-nitrophenyl boronic acid using the protocol developed by Causton for the 2,4-dichloropyrimidine series (Table 4.1) was adopted, and ran in triplicate on a 4.0 mmole scale. Following the Suzuki coupling step, the reaction mixture was apportioned into three aliquots and to each aliquot was added an aniline followed by HCl (2M, 4.0 eq.). Each sample was sealed and irradiated in the microwave at 110 °C for 5 minutes. From each reaction vessel, 1 mL organic solvent was taken and injected directly onto the Flex™ (1 mL is the maximum injection volume on this system). Following purification, a sample was taken from each well corresponding to a discrete peak on the chromatogram and analysed by ESI-MS. Appropriate wells, corresponding to peaks shown to represent product, were combined and concentrated *in vacuo* to afford the 4-(3-nitrophenyl)-6-anilino pyrimidines **392 - 400**. Of the 9 samples injected, only four pyrimidines, **392, 393, 395** and **396** were recovered, and in approximately 1% yield. However, a further 4 pyrimidines, **394**, and **398 - 400**, were identified by ESI-MS, although their mass spectra indicated the presence of other species. Only one ligand, **397**, was not detected by ESI-MS. Although it was planned to perform multiple injections onto the Flex™ for each of the remaining reaction mixtures **392 - 400**, given that the isolated yields of each ligand from the first injection was low, it was considered more worthwhile to pursue the synthesis of further libraries, with the aim of improving the reaction conditions.

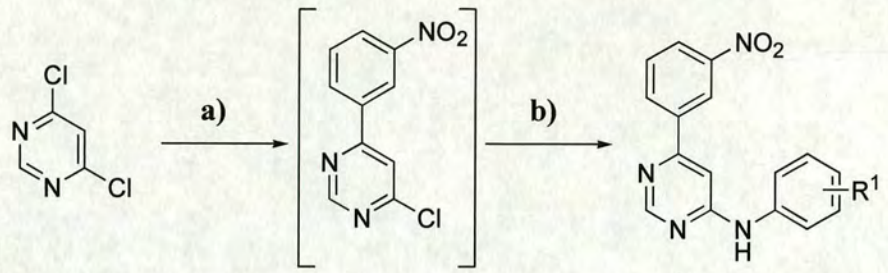

383 **392 - 400**

No.	R^1
392	3,5-CF_3
393	4-Cl
394	4-NO_2
395	4-CH_3
396	4-CF_3
397	3,5-Cl
398	3-Cl
399	3,4-F
400	3,4-Cl

Table 4.1: *Reagents and conditions:* **a**) 3-nitrophenylboronic acid, $Pd(OAc)_2$, Cs_2CO_3 (3 eq.), $MeCN/H_2O$, μwave, 110 °C, 15 min. **b**) R^1-Substituted aniline, HCl (2M), μwave, 110 °C, 5 min.

Causton had found that using *p*-toluenesulfonic acid to catalyse the nucleophilic aromatic substitution of the unreacted chloro moiety of the 2,4-substituted pyrimidine led to increased yields for the two-step reaction sequence. Consequently this was explored in the 4,6-disubstituted pyrimidine series, with a 5 x 5 array of boronic acids and amines. The scale of the Suzuki reaction was increased from 4.0 to 6.7 mmole to allow for the generation of sufficient 4-aryl-6-chloropyrimidine to be subsequently reacted in 5 amine coupling reactions. Unfortunately, this strategy was found to be less successful than using HCl for the anilino-coupling step, resulting in the recovery of only one ligand, **401** (Scheme 4.8). For the majority of these reactions, HPLC analysis revealed the presence of unreacted amine and 4-aryl-6-chloro-pyrimidine among other species.

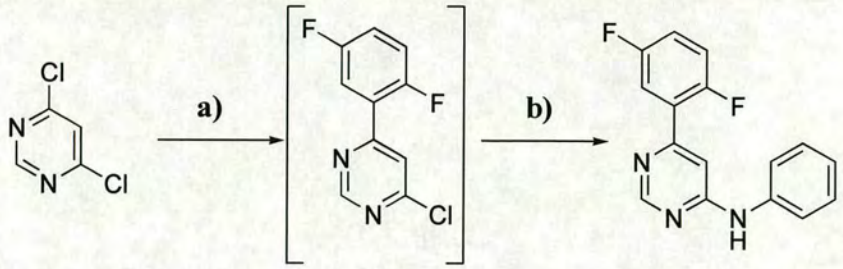

383 **401**

Scheme 4.8: *Reagents and conditions:* **a**) 2,5-difluoro-phenylboronic acid, $Pd(OAc)_2$ (5%), PPh_3 (10%), Cs_2CO_3 (1.5 eq.), MeCN, μwave, 130 °C, 15 mins. **b**) Aniline, *p*-toluenesulfonic acid (2 eq.), μwave, 110 °C, 5 mins.

It was postulated that the low recovery of ligand **401** could be attributable to poor solubility of Cs_2CO_3, hindering transmetallation in the Suzuki coupling step. Therefore the concentration of the Suzuki coupling step was reduced from 1.34 M, as used for the synthesis of **401**, to 0.22 M. A 3 x 2 array was synthesized to afford the ligands **402** – **407** (Table 4.2). Following Suzuki coupling, a sample of each reaction mixture was analysed by ESI-MS and the presence of 4-aryl-6-chloropyrimidine was confirmed. Evidence of bis-Suzuki coupled pyrimidine was found in the mass spectrum of 4-(2,5-difluorophenyl)-6-chloropyrimidine. Anilino couplings were performed using HCl (4 eq.).

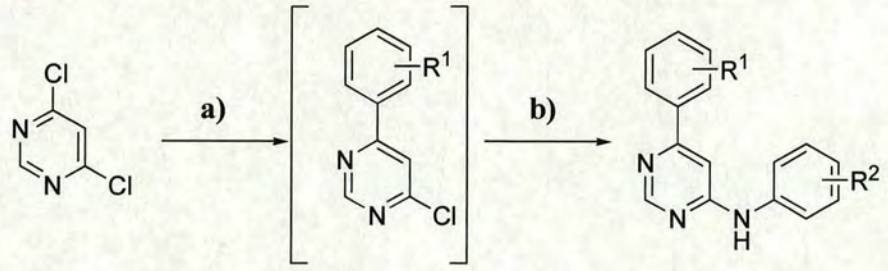

383 **402 - 407**

No.	R^1	R^2
402	2,5-F	3,5-CF_3
403	2,5-F	4-CF_3
404	2-OCH_3, 5-F	3,5-CF_3
405	2-OCH_3, 5-F	4-CF_3
406	3-CF_3	3,5-CF_3
407	3-CF_3	4-CF_3

Table 4.2: *Reagents and conditions:* **a)** R^1-substituted-phenyl boronic acid, $Pd(OAc)_2$ (5%), PPh_3 (10%), Cs_2CO_3 (1.5 eq.), MeCN, μwave, 130 °C, 15 mins. **b)** R^2-Substituted aniline, HCl (4.0 eq.), μwave, 110 °C, 5 mins.

Again the quantity of product recovered from each reaction was low, with the estimated recovery of each ligand in the range 1 – 4 %, based on the injection volume of each sample compared to the total reaction volume. Clearly this was not satisfactory. However, each of the pyrimidines **402** – **407** had been isolated, purified and identified by ESI-MS, and were subsequently submitted for screening.

The protocol used for the synthesis of pyrimidines **402** – **407** was adopted for the synthesis of pyrimidines **408** – **423** (Table 4.3). Again, these pyrimidines contained either a 3,5-bis-trifluoromethyl- or 4-trifluoromethyl-anilino moiety at *C*-6 of the pyrimidine ring. It was hoped that by fixing the *C*-6 substituent some insight could be gained into the nature of the 4-aryl moiety required for potent CDK inhibitory activity

following subsequent screening of each ligand. The isolated yields of **408** – **423** whilst still low, were generally an improvement over those obtained for **402** – **407**.

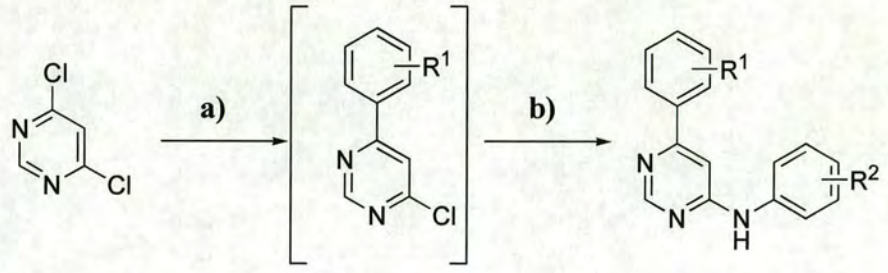

383 **408 - 423**

No.	R^1	R^2	% Yield
408	4-F	3,5-CF_3	8
409	3,5-CH_3	3,5-CF_3	23
410	4-CF_3	3,5-CF_3	10
411	2-NO_2	3,5-CF_3	1
412	4-OH	3,5-CF_3	3
413	4-OCH_3	3,5-CF_3	6
414	3-NH_2	3,5-CF_3	1
415	4-F	4-CF_3	9
416	2-Br	4-CF_3	7
417	3,5-CH_3	4-CF_3	18
418	4-CF_3	4-CF_3	7
419	2-NO_2	4-CF_3	2
420	4-OH	4-CF_3	8
421	4-OCH_3	4-CF_3	15
422	3-NH_2	4-CF_3	1
423	thiophene-5-carbaldehyde	4-CF_3	2

Table 4.3: *Reagents and conditions:* **a)** R^1-substituted-phenylboronic acid, $Pd(OAc)_2$ (5%), PPh_3 (10%), Cs_2CO_3 (1.5 eq.), MeCN, μwave, 130 °C, 15 mins. **b)** R^2-substituted aniline, HCl (4.0 eq.), μwave, 110 °C, 5 mins. **Note:** For the synthesis of ligand **423**, 5-formyl-thiophene-2-boronic acid was used for (**a**).

Work continued on the synthesis of further pyrimidines for screening against CDK2, whilst modifying reactions conditions for both the Suzuki cross-coupling and the anilino substitution reaction. Unfortunately, however, results were inconsistent, depending not only on the conditions applied but also both the boronic acid and the aniline used. Other bases were investigated for the Suzuki coupling step including Na_2CO_3, K_2CO_3, $KOBu^t$ and TBAB but no real improvements were made on the outcome of the two-step sequence. Similarly, several Suzuki couplings were performed using $Pd(OAc)_2$ in the absence of triphenylphosphine; $Pd(OAc)_2$ in the presence of tri-*o*-tolylphosphine; and $Pd(PPh_3)_4$ alone, however, again, consistently good results for the two-step synthetic sequence were not attainable. Reactions were also performed in alternative solvent systems, including THF, dioxane and glyme, as it has been reported that the solvent system used in the Suzuki coupling step can affect the selectivity of the cross-coupling.[185] Those pyrimidines synthesised are presented in Table 4.4.

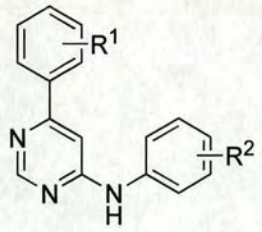

No.	R^1	R^2	% Yield
424	3-NO_2	4-OH	15
425	3-$(CH)_4$-4	4-OH	2
393	3-NO_2	4-Cl	31
426	3-$(CH)_4$-4	4-NO_2	33
427	3-$NHCOCH_3$	3,5-OCH_3	6
428	3-NO_2	3-OH	15
429	3-OH	3-OH	32
430	2,5-F	3-OH, 4-OCH_3	9
431	2,5-F	3,4-OCH_3	29
432	2,5-F	3-OH	63
433	2,5-F	4-OH	22
434	3-NH_2	3,5-OCH_3	16
435	2,5-F	3,5-OCH_3	20
436	3-OH	H	31
437	3-OH	3-NO_2	15
438	3-OH	3-F	13
439	2,5-CH_3	3-CH_2OH	4
440	2,5-CH_3	3-F	8

Table 4.4: 4-aryl-6-anilino-pyrimidines synthesized from 4,6-dichloropyrimidine via Suzuki cross-coupling and subsequent nucleophilic substitution by an aniline.

ESI-MS analysis of products obtained from several two-step synthetic sequences identified the mono-arylated pyrimidine species in addition to the mono- and bis-aminated pyrimidine species. It is postulated that in the 4,6-dichloropyrimidine species arylation at the 4-position of the pyrimidine ring increases the pK_a of the *N*-3 pyrimidyl

nitrogen compared to the pK_a of the *N*-1 pyrimidyl nitrogen. However, in the 2,4-dichloropyrimidine series, it is postulated that *N*-3 is less basic than *N*-1 owing to two α-chloro groups. It is postulated that in the 2,4-dichloropyrimidine species, arylation at the 4-position increases the basicity of at *N*-3 rendering it similar in character to the *N*-1 pyrimidyl nitrogen. Furthermore, it is postulated that in the 4-aryl-2-chloropyrimidine system, **441**, the acid catalysed nucleophilic displacement reaction is easier than the analogous 4-aryl-6-chloropyrimidine system, **442**, as both sites available for protonation are adjacent to the chloro group to be displaced.

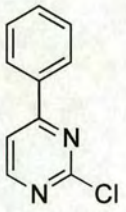

441

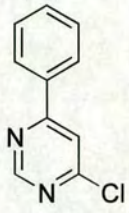

442

4.3.2 2-Amino-4-aryl-6-anilino pyrimidines

Upon reviewing the crystal structure of the pyrimidine **363** bound to CDK2, it was considered worthwhile to investigate whether a small substituent at the 2-position of the pyrimidine ring would lead to enhanced affinity of the pyrimidine as a result of interaction with the backbone carbonyl of residue Glu81 of CDK2.

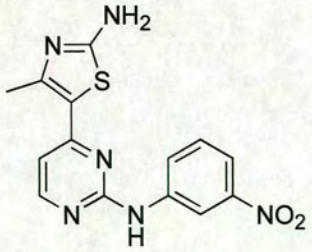

363

The commercially available 2-amino-4,6-dichloropyrimidine was an ideal building block that could be used to address this question as it was envisaged that 2-amino-4-aryl-6-anilino-pyrimidines, illustrated by **443**, could be synthesized using identical chemistry to that being used in the 4-aryl-6-anilino-pyrimidine series. Consequently, work was initiated to synthesize several pyrimidines based around template **443**, although this was met with similar problems as to those experienced in the 4,6-disubstituted series. Those pyrimidines that were successfully synthesized are presented in Table 4.5.

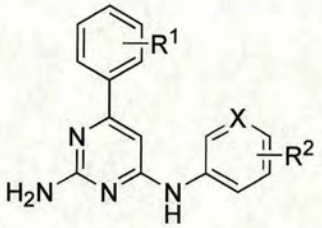

443

	R^1	R^2	X	% Yield
444	3,5-CH_3	4-OH	C	39
445	3,5-CH_3	4-Cl	C	38
446	3-$NHCOCH_3$	3,5-OCH_3	C	19
447	3-$NHCOCH_3$	3-NO_2	C	15
448	3-NO_2	3-OH	C	16
449	3-OH	3-NO_2	C	5
450	3-OH	3-OH	C	22
451	2,5-CH_3	3-NO_2	C	7
452	2,5-CH_3	3-OH	C	10
453	2,5-F	3,5-NO_2	C	23
454	2,5-F	H	N	20
455	2,5-F	3,5-OCH_3	C	32

Table 4.5: Synthesis of 2-amino-4-aryl-6-anilino-pyrimidines

Assay data obtained for the 2-amino pyrimidines submitted for screening is presented in Table 4.15 and discussed in Section 4.4. Analysis of the data presented in Table 4.16 revealed that 2-amino-substituted pyrimidines were less active than their unsubstituted

analogues and consequently further work on the 2-amino substituted series was abandoned.

4.3.3 Further investigation into the Suzuki cross-coupling reaction

Initially, it was hypothesized that 4,6-dichloropyrimidine may have been decomposing under Suzuki conditions, as TLC analysis of the reaction mixtures after the two step synthetic sequence showed that the 4,6-dichloropyrimidine species had been consumed. To examine this hypothesis, three reactions were set up in series, each containing a solution of 4,6-dichloropyrimidine, $Pd(OAc)_2$ (0.05 eq.) and Cs_2CO_3 (1.5 eq.) in 10:1 acetonitrile: water (2.2 mL) in the absence of a boronic acid. Each reaction mixture was irradiated in the microwave for 15 minutes at either 90 °C, 110 °C or 130 °C. TLC analysis of the reaction mixtures after microwave irradiation showed no evidence of decomposition of the dichloropyrimidine.

Subsequently, it was postulated that the poor recovery of ligand from the two-step synthesis was attributable to formation of the bis-arylated species in the Suzuki cross-coupling reaction. Consequently, a short study was undertaken focussing on the optimization of the cross-coupling reaction between 4,6-dichloropyrimidine and phenyl boronic acid. The various conditions examined are presented in Table 4.6 together with the isolated yields of both the 4-phenyl-6-chloropyrimidine species, **456**, and 4,6-diphenyl-pyrimidine species, **457**, after purification by HPLC.

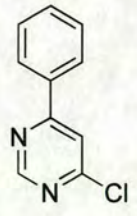

456

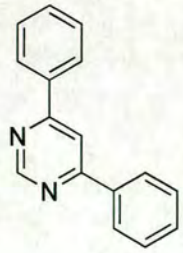

457

Entry	Catalyst	Solvent	Base	Time / min	Temp / ¼C	Yield 457 / %	Yield 458 / %
1	C1 (10%)	S1	B1 (1.2 eq.)	25	110	30	5
2	C2 (10%)	S1	B1 (1.2 eq.)	25	110	30	5
3	C3 (10%)	S1	B1 (1.2 eq.)	25	110	3	47
4	C4 (1%)	S1	B1 (1.2 eq.)	25	110	3	16
5	C1 (10%)	S2	B1 (1.2 eq.)	25	110	3	5
6	C1 (10%)	S3	B1 (1.2 eq.)	25	110	3	5
7	C1 (10%)	S4	B1 (1.2 eq.)	25	110	15	5
8	C1 (10%)	S5	B1 (1.2 eq.)	25	110	18	5
9	C1 (10%)	S4	B2 (1.2 eq.)	25	110	3	-
10	C1(10%)	S4	B3 (1.2 eq.)	25	110	3	3
11	C1 (10%)	S4	B4 (1.2 eq.)	25	110	9	3
12	C1 (10%)	S4	B5 (1.2 eq.)	25	110	-	3
13	C1 (10%)	S4	B4 (1.2 eq.)	25	50	27	3
14	C1 (10%)	S4	B4 (1.2 eq.)	25	90	24	3
15	C1 (10%)	S4	B4 (1.2 eq.)	25	110	21	-
16	C1 (10%)	S4	B4 (1.2 eq.)	25	140	24	3
17	C1 (10%)	S4	B4 (1.2 eq.)	5	50	3	-
18	C1 (10%)	S4	B4 (1.2 eq.)	10	50	3	3
19	C1 (10%)	S4	B4 (1.2 eq.)	15	50	9	3
20	C1 (10%)	S4	B4 (1.2 eq.)	20	50	9	3
21	C1 (1%)	S4	B4 (1.2 eq.)	10	50	3	3
22	C1 (5%)	S4	B4 (1.2 eq.)	10	50	12	3
23	C1 (5%)	S4	B4 (2.0 eq.)	10	50	12	6
24	C1 (5%)	S4	B4 (3.0 eq.)	10	50	15	3

Table 4.6: *Reagents and standard conditions*: 4,6-dichloropyrimidine (0.17 mmole, 1.0 eq.), phenylboronic acid (1.0 eq.), catalyst C1 - $Pd(dppf)_2$, C2 – $Pd(PPh_3)_4$, C3 – $Pd_2(dba)_3$, C4 – POPd; solvent (1 mL reaction volume) S1 – MeCN, S2 – EtOH, S3 – H_2O, S4 – Dioxane, S5 – THF; base B1 - Cs_2CO_3, B2 – Na_2CO_3, B3 – K_2CO_3, B4 – KO^tBu, B5 – TBAB, K_2CO_3; H_2O (0.1 mL) added to each reaction to solubilize the base, μwave.

It was hoped that conditions could be found to maximize the formation of species **456** and minimize the formation of species **457** but, unfortunately, no strong conclusions can be drawn from the results presented in Table 4.6. The conditions examined in Table 4.6 are by no means exhaustive, adopting a single point optimization strategy. Entries 1-4 shows that the chosen catalyst can have a significant affect on the products formed during the Suzuki coupling, with $Pd_2(dba)_3$ enhancing the formation of **457** over **456**. $Pd(dppf)_2$ was shown to be as affective as the catalyst $Pd(PPh_3)_4$ in the synthesis of the mono-arylated species **456** and consequently was selected for further studies over $Pd(PPh_3)_4$ which had been shown to form triphenylphosphine oxide in the Suzuki cross-coupling reaction. Entries 1 and 5 – 8 examine the effect of solvent on the cross-coupling reaction and show that a non-polar solvent affords a greater yield of **456** in comparison with a polar solvent. Entries 8 –12 examine the effect of various bases and show that the strong base KO^tBu could be used in the Suzuki reaction. It has been postulated that the halogen ligand on organopalladium(II) halide can be readily displaced by an alkoxy anion to provide a reactive alkoxopalladium(II) intermediate that is involved in the transmetallation process.[199] Entries 13 – 16 show that the reaction temperature does not have a significant influence on the outcome of the Suzuki coupling, with comparable results obtained at both 50 °C and 140 °C. However, direct comparison of entries 11 and 15 suggest there is some variability in the ratio of **456** and **457** obtained under identical conditions. If time had allowed, it would have been prudent to repeat the experiments listed in Table 4.6 to obtain average yields of **456** and **457** for each set of conditions. Entries 17 – 20 show that a reaction time in excess of 10 min increases the quantity of **456** isolated in the reaction. Entries 21 – 24 show that the use of 3 equivalents of base and 5% catalyst affords a greater ratio of **456**:**457** in the reaction. It should be noted that unreacted 4,6-dichloropyrimidine was present in all samples listed in Table 4.6 following the Suzuki coupling, which, unfortunately, could not be isolated as it was found to undergo sublimation upon solvent evaporation. Clearly, no conditions were found that gave significant yields of **456** and minimal formation of **457**, although, in the majority of conditions examined in the study, and illustrated in Table 4.6, species **457** was not isolated in significant quantity.

4.3.4 Isolation of 4-aryl-6-chloro-pyrimidines

To ease purification of the 6-anilino-4-aryl-pyrimidine it was decided to isolate the 4-aryl-6-chloro-pyrimidine intermediate following the Suzuki coupling. Although in doing so this would considerably lengthen the synthetic procedure, it would provide some indication of how well the Suzuki couplings were proceeding and possibly explain the low isolated yields of 6-anilino-4-aryl-pyrimidine ligands. 5 Suzuki couplings were performed using the boronic acids shown in Table 4.7. It was decided to use the electron rich 3-methoxy-, 4-methoxy- and 3,4-methoxyphenylboronic acids as building blocks as it was envisaged that the 4-aryl-6-chloropyrimidines generated would be more reactive to the subsequent acid catalysed nucleophilic substitution reaction. After microwave irradiation of the sample, each sample was divided in 3 aliquots and injected onto the Flex^{TM} HPLC (Method A). Following identification of the 4-aryl-6-chloropyrimidine by ESI-MS, appropriate fractions were combined and concentrated *in vacuo*. Isolated yields for the Suzuki couplings were 66 – 93%, considerably higher than those yields reported in Table 4.6 for the cross-coupling between 4,6-dichloropyrimidine and phenylboronic acid, although a direct comparison of conditions cannot be made. Each intermediate was used directly in the anilino couplings shown in Table 4.7, without further characterization. For the synthesis of ligands **458**, **459**, **463**, **464** and **468**, KO^{t}Bu was used for the nucleophilic aromatic substitution reaction between the 4-aryl-6-chloro-pyrimidine species and the aniline.

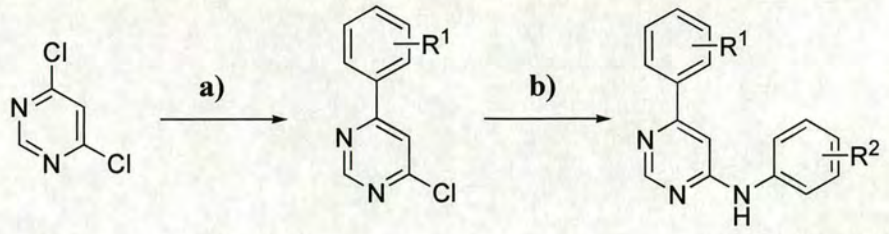

383 **458 - 470**

No.	X	Y	R^1	R^2	% Yield
458	N	C	4-OCH_3	H	-
459	N	N	4-OCH_3	H	-
460	C	C	4-OCH_3	3-NO_2	33
461	C	C	4-OCH_3	4-OH	33
462	C	C	4-OCH_3	3-OH	13
463	N	C	3-OCH_3	H	42
464	N	N	3-OCH_3	H	-
465	C	C	3-OCH_3	3-NO_2	-
466	C	C	3-OCH_3	4-OH	42
467	C	C	3-OCH_3	3-OH	36
468	N	C	3,4-OCH_3	H	-
469	C	C	3,4-OCH_3	4-OH	14
470	C	C	3,4-OCH_3	3-OH	38

Table 4.7: *Reagents and conditions*: a) Cs_2CO_3 (3.0 eq.), $Pd(OAc)_2$ (5%), PPh_3 (10%), R^1-substituted phenyl boronic acid (1.0 eq.), dioxane/H_2O (10:1, 3.3 mL), μwave, 130 °C, 20 min. b) R^2-substituted aniline (1.0 – 1.6 eq.), HCl (4.0 eq.), dioxane (1 mL), μwave, 130 °C, 20 min.

The results presented in Table 4.7 were generally an improvement over those obtained from previous syntheses of 4-aryl-6-anilino-pyrimidine ligands reported in this chapter. It is postulated that this is attributable to two factors, namely the use of electron rich phenyl boronic acids in the Suzuki cross-coupling reaction and electron rich anilines in the nucleophilic aromatic substitution of the 4-aryl-6-chloropyrimidine intermediate.

Nucleophilic aromatic substitution reactions involving either 2-aminopyrimidine, illustrated by **459** and **464**, or 2-aminopyridine, illustrated by **458** and **468**, were largely unsuccessful, presumably owing to the poor nucleophilicity of these species.

4.3.5 Isolation of 6-anilino-4-chloropyrimidines

It was now apparent that the Suzuki cross-coupling reaction was deactivating the pyrimidine system to subsequent nucleophilic aromatic substitution. However, initial studies reported for the synthesis of ligands **387** – **389** in which the anilino coupling reaction had been performed prior to the Suzuki cross-coupling reaction had also been unsatisfactory in terms of isolated yields of desired ligands, with evidence of the bis-anilino pyrimidine species being identified in the ESI-MS of the intermediates **385** and **386**. Consequently, a short study was performed investigating the nucleophilic substitution reaction under both acidic and basic conditions. 3-Fluoroaniline (0.13 mmole, 1.0 eq.) was added to a solution of 4,6-dichloropyrimidine (1.0 eq.) in acetonitrile in the presence of 2 equivalents of acid or base (Table 4.8). Each sample was subjected to microwave irradiation for 5 minutes at 100 °C. TLC analysis of each sample indicated the presence of 4,6-dichloropyrimidine and consequently, each sample was irradiated for a further 10 minutes at 100 °C. ESI-MS analysis of each sample indicated the presence of the 6-anilino-4-chloro-pyrimidine, **471**, in all cases and subsequently each sample was purified by HPLC. Significantly, no evidence of di-substituted pyrimidine was found in each case. Unfortunately, owing to mechanical failure of the Christ RVC during solvent evaporation, only two samples were recovered. Although the study was not repeated, it had shown that Cs_2CO_3 could be used to effect the nucleophilic substitution reaction. However, when Cs_2CO_3 was employed to effect the nucleophilic substitution reaction between a selection of anilines and 4-aryl-6-chloro-pyrimidines it was found to be unsuccessful, again providing evidence of the deactivating effect of a 4-aryl group on the pyrimidine species to the nucleophilic aromatic substitution reaction.

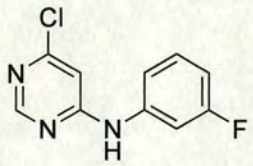

471

Acid/Base (2.0 eq.)
p -Toluenesulfonic acid
HCl (2M)
Triethylamine
N ,*N* -diisopropylethylamine
Cesium carbonate

Table 4.8: Acids and bases used to effect the nucleophilic aromatic substitution reaction between 3-fluoroaniline and 4,6-dichloropyrimidine.

Given that no evidence of bis-anilino substitution had been found in the reaction between 3-fluoroaniline and 4,6-dichloropyrimidine, it was decided to undertake the nucleophilic substitution reaction prior to the Suzuki coupling step. Indeed, this approach had been reported by Schultz *et al.* in the development of a combinatorial scaffold approach toward kinase-directed heterocycle libraries.[200] The first step of the synthesis was the reductive amination of 4-formyl-3,5-dimethoxyphenoxymethyl resin **472** with a primary alkyl- or benzyl- amine **473** to afford a resin supported secondary amine **474**. Significantly, subsequent nucleophilic aromatic substitution of **474** with 4,6-dichloropyrimidine in butanol using *N,N*-diisopropylethylamine at 90 °C afforded the solid-supported pyrimidine **475** that was coupled with an aryl boronic acid, **477**, under Suzuki conditions (Scheme 4.9) to afford the 6-anilino-4-aryl-pyrimidine, **477** in excellent yield (>85%) and purity.

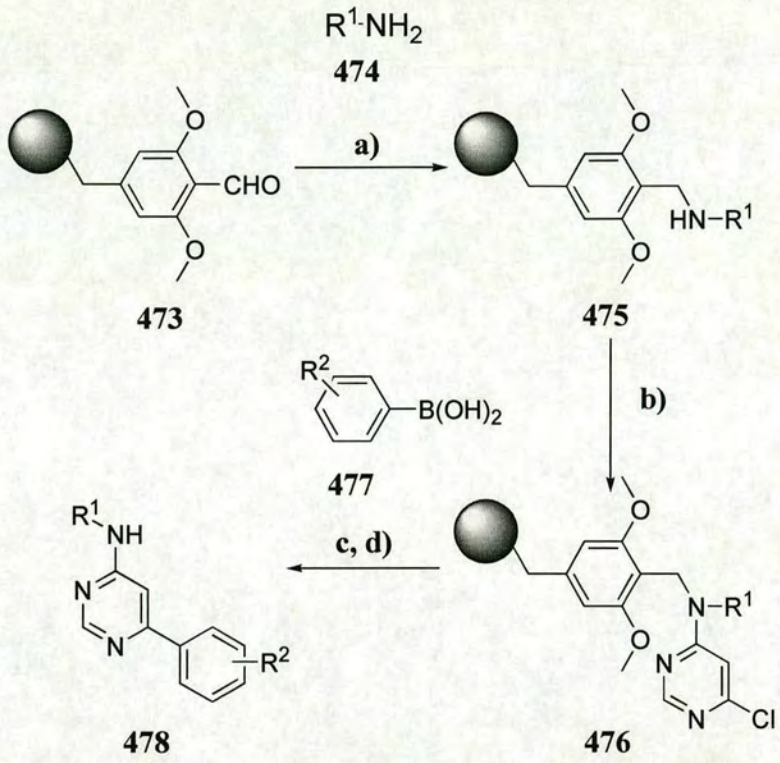

Scheme 4.9: *Reagents and conditions*: **a)** $NaBH(OAc)_3$, HOAc (1%), THF. **b)** 4,6-dichloropyrimidine, *N,N*-diisopropylethylamine, butanol, 90 °C, 24 h. **c)** boronic acid (5.0 eq.), $Pd_2(dba)_3$ (7%), carbene ligand (14%), Cs_2CO_3 (6.0 eq.), 1,4-dioxane, 90 °C, 12 h. **d)** DCM:TFA:Me_2S:H_2O (45:45:5:5).[200]

Furthermore, during the period of our investigation into the 6-anilino-4-aryl-pyrimidine scaffold, a method was published by Wade *et al.*, adopting a similar solid-supported approach to that reported by Schultz *et al.*, that specifically focussed on the 4,6-dichloropyrimidine system. (Scheme 4.10).[201] The 4,6-disubstituted pyrimidines synthesized and reported therein were isolated in moderate yields (25 – 48%) although in excellent purity.

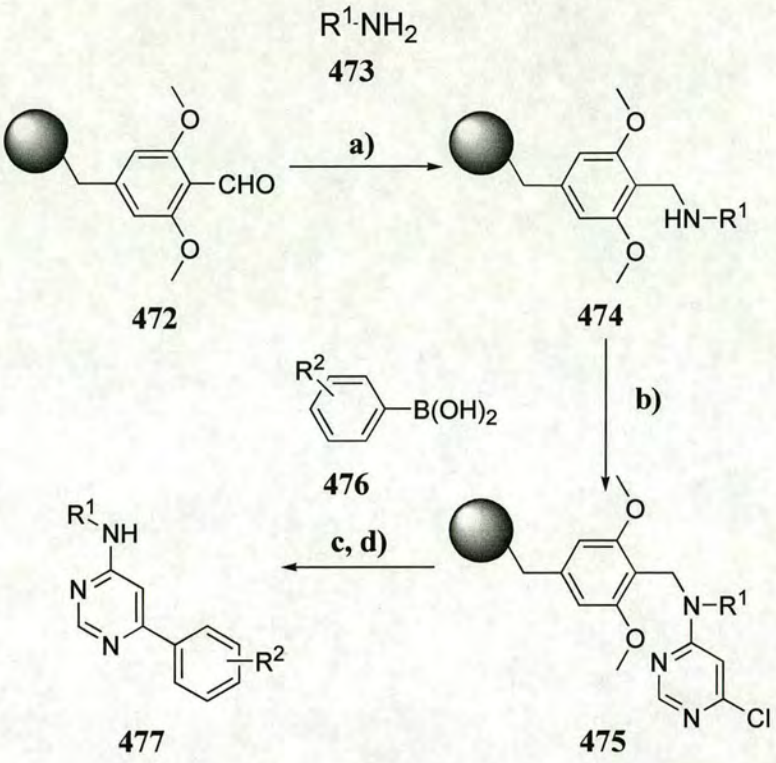

Scheme 4.10: *Reagents and conditions*: **a) 473** (5.0 eq.), $NaBH(OAc)_3$ (3.0 eq.), HOAc (10.0 eq), THF, room temperature, 15 h. **b)** 4,6-dichloropyrimidine (4.5 eq.), *N,N*-diisopropylethylamine (4.5 eq.), DMF, 50 °C, 18 h. **c)** R^2-substituted boronic acid (4.0 eq.), $Pd_2(dba)_3$ (10 %), $P(^tBu)_3$ (20%), spray dried KF (10.0 eq.), 1,4-dioxane, 50 °C, 18 - 22 h. **d)** DCM:TFA (4:1).[201]

Initially it was thought that the use of an excess of 4,6-dichloropyrimidine to react with the resin supported secondary amine, **474**, was minimizing the formation of bis-aminated pyrimidine. However, further investigation of the literature revealed a report by Luo *et al.* that showed 4,6-dichloropyrimidine could be reacted with benzylamine, utilizing solution phase microwave assisted organic synthesis, to afford the mono-aminated product, **478**, in excellent yield. Furthermore, it was reported that the first addition of benzylamine was substantially easier than the addition of a second amino group.[202] The Suzuki cross-coupling reaction between **478** and phenylboronic acid to afford the 6-amino-4-aryl-pyrimidine **479** was also reported (Scheme 4.11).[202]

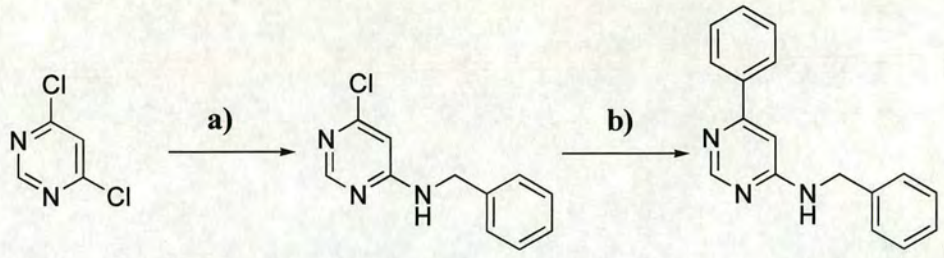

94% 87%

383 **478** **479**

Scheme 4.11: *Reagents and conditions*: a) benzylamine (0.9 eq.), 2-propanol, *N,N*-diisopropylethylamine (2.0 eq.), μwave, 130 °C, 20 min. b) phenylboronic acid (1.4 eq.), $Pd(PPh_3)_4$ (4%), K_2CO_3 (2.0 M in water), toluene/ethanol (4:1, 0.13 M), μwave, 140 °C, 10 min.[202]

A series of 6 two-step reactions were undertaken as illustrated in Table 4.9. Following the two nucleophilic aromatic substitution reactions between 4,6-dichloropyrimidine and either 3-hydroxy- or 3-nitroaniline, which were isolated in 28% and 31% yield respectively, the Suzuki cross-coupling reaction was performed using a modification of the protocol reported by Luo *et al.*[202] K_2CO_3 (4.0 eq.) was used as the base, dissolved in the minimum amount of water. The reactions were performed in a solution of 4:1 toluene: EtOH (1 mL), each sample being irradiated in the microwave at 140 °C for 15 minutes. Pyrimidines **480**, **462** and **460** were isolated in low yields, primarily as a consequence of incomplete conversion of the pyrimidine to the 6-anilino-4-chloro-pyrimidine species.

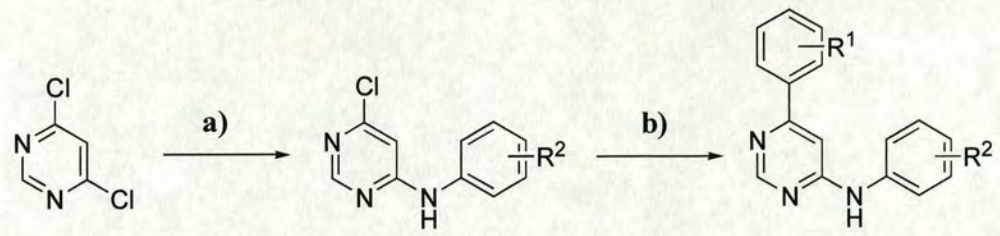

383

No.	R^1	R^2	% Yield
480	3-OCH_3	3-OH	12
481	3-OCH_3	3-NO_2	-
462	4-OCH_3	3-OH	23
460	4-OCH_3	3-NO_2	10
482	3,4-OCH_3	3-OH	-
483	3,4-OCH_3	3-NO_2	-

Table 4.9: *Reagents and conditions*: a) R^2-substituted aniline (1.0 eq.), HCl (4.0 eq.), 1,4-dioxane, μwave, 130 °C, 30 min. b) R^1-substituted phenylboronic acid (1.4 eq.), $Pd(PPh_3)_4$ (4%), K_2CO_3 (4.0 eq.), toluene/ethanol (4:1), H_2O (0.1 mL), μwave, 140 °C, 15 min.

Adopting the method reported by Luo *et al.*,[202] a number of pyrimidines were synthesized, as illustrated by Table 4.10. It was found that it was necessary to reduce the reaction temperature from 130 °C, reported for the substitution reaction between benzylamine and 4,6-dichloropyrimidine, to 120 °C in order to prevent the safety pressure limited of 300 psi being exceeded on the microwave reactor. Consequently, the reaction time was increased from 20 minutes to 30 minutes. For synthesis of the 6-anilino-4-aryl-pyrimidines shown in Table 4.10, the mono-aminated pyrimidine species was isolated following HPLC purification before subsequent Suzuki coupling with a substituted phenyl boronic acid, its presence being confirmed by ESI-MS.

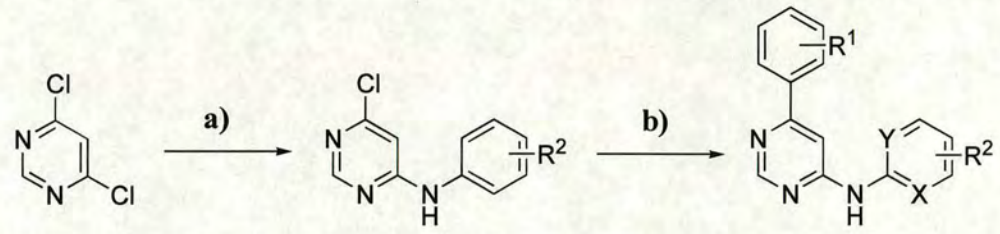

383

No.	X	Y	R^1	R^2	% Yield
484	C	C	3-OCH_3	3-NO_2	-
480	C	C	3-OCH_3	3-OH	15
462	C	C	4-OCH_3	3-OH	20
470	C	C	3,4-OCH_3	3-OH	19
485	C	C	3-OCH_3	3,4-OCH_3	72
486	C	C	4-OCH_3	3,4-OCH_3	29
487	C	C	3,4-OCH_3	3,4-OCH_3	40
466	C	C	3-OCH_3	4-OH	55
461	C	C	4-OCH_3	4-OH	9
488	N	N	3-OCH_3	H	-
463	N	C	3-OCH_3	H	5
489	C	C	3-OCH_3	F	6
469	C	C	3,4-OCH_3	4-OH	25
490	C	C	2,5-CH_3	3-OH	51
491	C	C	H	3-OH	49
492	C	C	3-OH	4-OH	1
493	C	C	2,5-CH_3	4-OH	16
494	C	C	4-OCH_3	3-F	-
495	C	C	4-OCH_3	3-NO_2	-
467	C	C	3-OCH_3	H	20
496	C	C	4-OCH_3	H	40
497	C	C	2,5-CH_3	3,4-OCH_3	32
498	C	C	3-OH	3,4-OCH_3	51

Table 4.10: *Reagents and conditions:* a) R^2-substituted aniline (1.0 eq.), 2-propanol, *N,N*-diisopropylethylamine, (2.0 eq.), μwave, 120 °C, 30 min. b) R^1-Substituted phenylboronic acid (1.4 eq.), $Pd(PPh_3)_4$ (4%), K_2CO_3 (4.0 eq.), toluene/ethanol (4:1, 1 mL), H_2O (0.1 mL), μwave, 140 °C, 15 min.

The results from this library were encouraging as not only were the isolated yields of each ligand generally higher than those obtained when performing the Suzuki coupling first, the recovery rate of ligand had increased with 19 novel ligands being isolated from 23 two-step reactions. Pyrimidines **484** and **495** could not be isolated owing to the small scale of the Suzuki coupling, with the nucleophilic aromatic substitution reaction between 4,6-dichloropyrimidine and the electron poor 3-nitroaniline proceeding in very poor yield (3%). Similarly, the nucleophilic substitution reactions between 4,6-dichloropyrimidine and either 3-fluoroaniline or 2-aminopyrimidine resulted in poor recovery of mono-aminated species.

To investigate whether both the anilino and Suzuki couplings could be performed in a two-step, one-pot manner, pyrimidines **499 - 518** were synthesized using the synthetic protocol adopted for the synthesis of pyrimidines shown in Table 4.10. Propan-2-ol was used as the reaction solvent for both the nucleophilic substitution reaction and the Suzuki cross-coupling. Following each anilino coupling, the crude reaction mixture was apportioned into four equal aliquots, each aliquot transferred to a microwave tube and the reagents for the Suzuki coupling added. The library, together with isolated yields for each two-step reaction, is shown in Table 4.11.

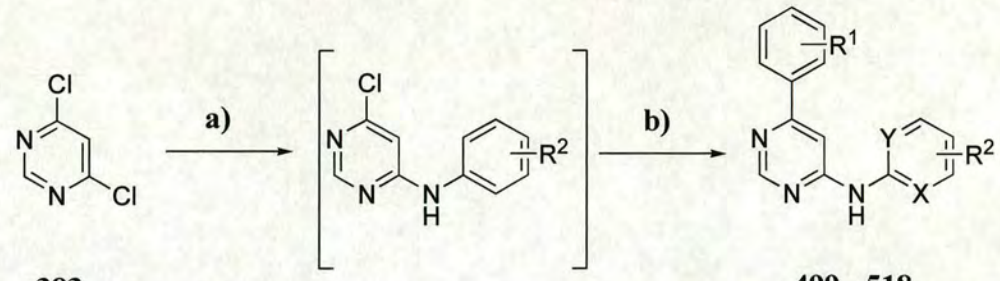

383 **499 - 518**

No.	R^1	R^2	% Yield
499	3-OCH_3	4-F, 3-CH_3	57
500	3-OCH_3	4-OH, 2-NO_2	-
501	3-OCH_3	3-CN	-
502	3-OCH_3	3-OH, 4-OCH_3	67
503	3-OCH_3	3,5-OCH_3	24
504	4-OCH_3	4-F, 3-CH_3	66
505	4-OCH_3	4-OH, 2-NO_2	30
506	4-OCH_3	3-CN	-
507	4-OCH_3	3-OH, 4-OCH_3	37
508	4-OCH_3	3,5-OCH_3	14
509	2,5-CH_3	4-F, 3-CH_3	54
510	2,5-CH_3	4-OH, 2-NO_2	-
511	2,5-CH_3	3-CN	-
512	2,5-CH_3	3-OH, 4-OCH_3	21
513	2,5-CH_3	3,5-OCH_3	20
514	3-OH	4-F, 3-CH_3	45
515	3-OH	4-OH, 2-NO_2	-
516	3-OH	3-CN	3
517	3-OH	3-OH, 4-OCH_3	6
518	3-OH	3,5-OCH_3	8

Table 4.11: *Reagents and conditions:* a) R^2-substituted aniline (1.0 eq.), 2-propanol, *N,N*-diisopropylethylamine, (2.0 eq.), μwave, 120 °C, 30 min. b) R^1-substituted phenylboronic acid (1.4 eq.), $Pd(PPh_3)_4$ (4%), K_2CO_3 (4.0 eq.), H_2O (0.1 mL), μwave, 140 °C, 15 min.

Table 4.11 shows that 14 novel ligands were isolated from 20 reactions and demonstrates that a two-step, one-pot strategy can be adopted in favour of a two-step reaction sequence, with purification of the 6-anilino-4-chloropyrimidine intermediate, with no apparent drop in yields. Failures from this library featured electron deficient anilines containing either 3-cyano- or 4-hydroxy-2-nitro- substitution patterns. Ligands **500** and **510** were identified by ESI-MS but were not isolated in sufficient purity for screening.

4.4 Summary of biological results and conclusions

Summaries of primary biological results received for pyrimidines submitted to Cyclacel Ltd. for screening are shown in Tables 4.12 – 4.16. These results are discussed in the light of the crystal structure of the CDK2/ligand **363** complex [PDB Code 1PXO], shown again in Figure 4.3, that was solved during the period of the research discussed in this chapter. It must be stressed that the results presented in Tables 4.12 – 4.16 are from a primary screen, and, as such, have an associated error that renders them open to interpretation. The main purpose of the primary screen is to reduce the numbers of ligands for secondary screening.

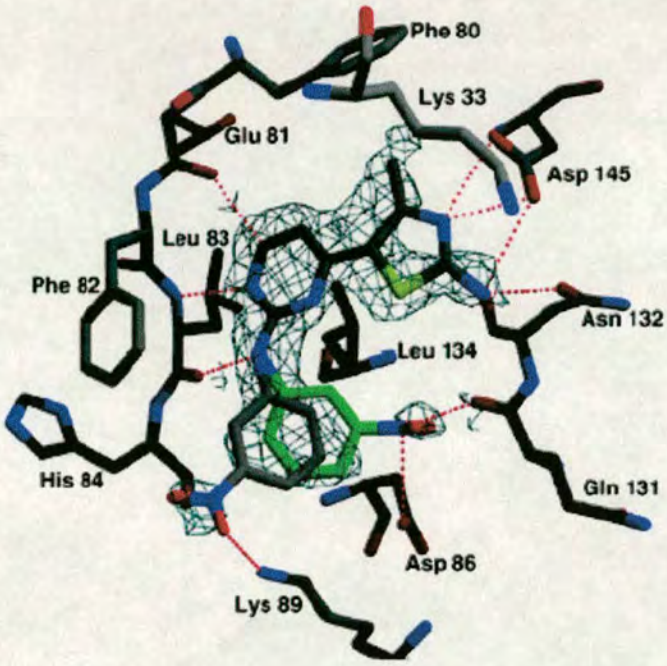

Figure 4.3: The X-ray crystal structure of the inhibitor CYC4223, **363**, bound to CDK2 (PDB Code 1PXO).

Table 4.12 shows that greatest inhibition of the CDK2/E complex of those ligands listed in the table is with 3,5-dimethyl- aryl and 3,5-bis-trifluoromethyl- anilino substitution patterns. However, comparison of the primary screening data of pyrimidines **403** with **402**; **407** with **406**; **405** with **404**; and **415** with **408**; show that pyrimidines with a 4-trifluoromethyl- anilino substitution pattern are generally more potent than their 3,5-bis-trifluoromethyl- analogues. It is postulated that the steric bulk of the 3,5-bis-trifluoromethyl-anilino moiety is not well tolerated in the ATP binding pocket owing to the proximity of the residues Gln131, Asp86 and Lys89. Indeed, this trend is also apparent for ligands **428**, **412**, **413** and **410** listed in Table 4.13. Focussing on the 4-aryl substituent, the 3,5-dimethyl- substitution pattern affords ligands with reasonably potency, exemplified by pyrimidines **409** and **417**. This result is surprising as it appears from the crystal structure of the CDK2/ligand **363** complex that a hydrophobic group at the 3- or 5-position of the aromatic ring would be directed towards the residues Asp145

or Asn132 of CDK2. However, it is possible that a favourable hydrophobic interaction may occur between the ligand and the Phe80 residue of CDK2.

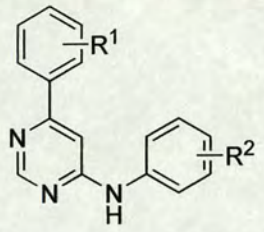

No.	R^1	R^2	CDK2/E % I @ 100 μM	CDK9/T1 % I @ 50 μM
409	3,5-CH_3	3,5-CF_3	81.2	17.8
416	2-Br	4-CF_3	67.1	16.2
417	3,5-CH_3	4-CF_3	64.8	-2.0
420	4-OH	4-CF_3	62.7	15.9
403	2,5-F	4-CF_3	57.9	13.9
405	2-OCH_3, 5-F	4-CF_3	46.8	25.0
407	3-CF_3	4-CF_3	41.1	-8.7
388	H	4-CH_3	38.4	59.7
402	2,5-F	3,5-CF_3	36.0	19.7
406	3-CF_3	3,5-CF_3	35.8	16.9
418	4-CF_3	4-CF_3	27.0	7.2
404	2-OCH_3, 5-F	3,5-CF_3	17.5	6.8
411	2-NO_2	3,5-CF_3	12.8	20.5
389	H	3,5-CF_3	8.6	19.3
419	2-NO_2	4-CF_3	7.6	23.2
415	4-F	4-CF_3	7.2	0.6
423	2-thienyl-5-carbaldehyde	4-CF_3	6.8	16.9
395	3-NO_2	4-CH_3	5.2	32.5
396	3-NO_2	4-CF_3	-1.3	21.9
408	4-F	3,5-CF_3	-7.9	20.4

Table 4.12: Primary screening data of a number of 4-aryl-6-anilino-pyrimidines, tabulated in descending order of CDK2/cyclin E inhibitory activity. % I = percentage inhibition at the ligand concentration shown in the table. Entries highlighted in blue are discussed in the text.

Table 4.13 shows that the introduction of a hydrogen bond donor at the 3-position of the 4-aryl moiety, afforded ligands with good potency against CDK2/E at 25 μM. It is envisaged that a hydrogen bond donor at the 3-position of the 4-aryl moiety can interact favourably with the carbonyl of Asp145 or the carbonyl of Asn132, in an analogous manner to the primary amino group of the inhibitor **363**. Furthermore, a 3-hydroxy substituent off the anilino moiety also appears to afford ligands with reasonable potency, exemplified by **429** and **428**. Again, it is postulated that a hydrogen bond donor at the 3-position of the anilino moiety would be well placed to interact with the backbone carbonyl of Gln131.

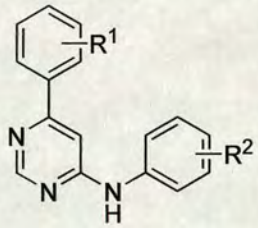

			CDK2/E	CDK9/T1	GSK3
No.	**R^1**	**R^2**	% I @ 25 μM	% I @ 5 μM	% I @ 25 μM
429	3-OH	3-OH	80.8	55.6	58.5
414	3-NH_2	3,5-CF_3	68.0	7.2	94.1
422	3-NH_2	4-CF_3	60.6	35.2	94.6
428	3-NO_2	3-OH	52.6	28.0	66.2
440	2,5-CH_3	3-F	47.7	-25.8	32.3
427	3-NHAc	3,5-OCH_3	33.8	16.9	29.7
452	2,5-CH_3	3-OH	26.7	4.9	2.5
421	4-OCH_3	4-CF_3	24.8	16.1	34.4
412	4-OH	3,5-CF_3	21.8	20.8	45.5
413	4-OCH_3	3,5-CF_3	16.8	20.1	71.9
410	4-CF_3	3,5-CF_3	-3.0	15.0	19.4

Table 4.13: Primary screening data of a number of 4-aryl-6-anilino-pyrimidines, tabulated in descending order of CDK2/cyclin E inhibitory activity. % I = percentage inhibition at the ligand concentration shown in the table. Entries highlighted in blue are discussed in the text.

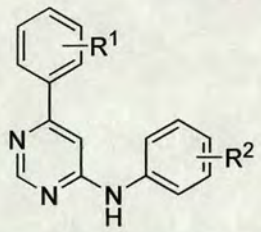

No.	R^1	R^2	CDK2/E % I @ 0.5μM	CDK2/E % I @ 10μM	CDK9/T1 % I @ 1μM	CDK9/T1 % I @ 10μM	GSK3 % I @ 1μM
461	4-OCH_3	4-OH	8.8	74.9	30.6	64.7	17.0
490	2,5-CH_3	3-OH	-9.2	63.7	13.4	57.4	-0.3
491	H	3-OH	-2.8	60.3	25.7	64.1	5.3
463	3-OCH_3	2-Aminopyridine	-2.8	58.3	59.9	87.5	18.2
496	4-OCH_3	H	-5.4	52.6	23.6	56.1	21.7
507	4-OCH_3	3-OH, 4-OCH_3	13.0	52.4	22.3	69.7	5.7
469	3,4-OCH_3	4-OH	-7.9	49.9	10.5	25.9	14.5
504	4-OCH_3	4-F, 3-CH_3	9.2	48.3	14.6	33.3	2.0
502	3-OCH_3	3-OH, 4-OCH_3	10.5	47.5	16.6	50.0	1.0
514	3-OH	4-F, 3-CH_3	4.1	45.0	20.4	59.8	13.8
498	3-OH	3,4-OCH_3	-6.7	40.8	22.5	55.7	8.8
512	2,5-CH_3	3-OH, 4-OCH_3	13.7	38.9	20.5	52.6	-11.2
509	2,5-CH_3	4-F, 3-CH_3	10.2	35.5	12.3	34.5	-12.7
467	3-OCH_3	H	6.9	33.8	26.7	45.6	-4.9
497	2,5-CH_3	3,4-OCH_3	14.2	30.1	19.8	37.2	19.9
466	3-OCH_3	4-OH	13.6	29.7	19.7	50.7	-17.9
489	3-OCH_3	3-F	0.5	28.6	13.5	49.5	-4.1
480	3-OCH_3	3-OH	11.7	28.4	21.9	58.5	7.7
505	4-OCH_3	4-OH, 2-NO_2	-2.3	27.5	9.5	-2.0	4.3
516	3-OH	3-CN	9.7	27.1	26.0	68.7	16.5
513	2,5-CH_3	3,5-OCH_3	-10.7	26.8	12.4	33.9	2.2
503	3-OCH_3	3,5-OCH_3	8.0	20.6	5.7	20.4	-10.9
485	3-OCH_3	3,4-OCH_3	6.9	16.9	9.7	30.0	-3.5
493	2,5-CH_3	4-OH	8.3	12.3	15.1	54.7	0.4
462	4-OCH_3	3-OH	6.7	10.5	23.8	39.4	3.8
518	3-OH	3,5-OCH_3	28.1	1.6	25.0	58.6	4.3
499	3-OCH_3	4-F, 3-CH_3	12.0	-1.5	17.7	30.4	1.2
517	3-OH	3-OH, 4-OCH_3	14.5	-15.5	27.1	64.3	1.8

Table 4.14: Primary screening data of a number of 4-aryl-6-anilino-pyrimidines, tabulated in descending order of CDK2/cyclin E inhibitory activity at a ligand concentration of 10 μM. % I = percentage inhibition at the ligand concentration shown in the table. Entries highlighted in blue are discussed in the text.

It is difficult to draw any conclusions from the primary screening data presented in Table 4.14 as there appears to be no correlation between various 4-aryl and 6-anilino substituents and the potency of the ligand against CDK2 at 10 μM. Furthermore, at a ligand concentration of 0.5 μM, the ligands presented in Table 4.14 show neglible inhibition of CDK2. Table 4.14 shows that ligand **461** inhibits CDK2/cylin E and CDK9/T1 with modest potency. Replacement of its 4-hydroxy substituent on the anilino ring with a 3-hydroxy group, as exemplified by ligand **462**, destroys activity. However, several ligands are shown to have activity against CDK2/Cyclin E and CDK9/T1 that contain a 3-hydroxy substituted aniline, illustrated by ligands **490** and **491**.

Table 4.15 shows the primary screening data received for several 2-amino-4-aryl-6-anilino-pyrimidines. A direct comparison is made between this data and data obtained from analogous ligands not containing a 2-amino substituent in Table 4.16.

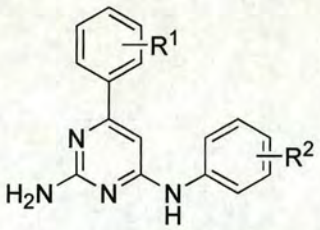

			CDK2/E	CDK9/T1	GSK3
No.	**4-Aryl**	**6-Anilino**	% I @ 25 μM	% I @ 5 μM	% I @ 25 μM
448	3-NO_2	3-OH	44.8	22.3	22.9
449	3-OH	3-NO_2	38.7	24.4	15.9
451	2,5-CH_3	3-NO_2	37.6	18.8	11.5
450	3-OH	3-OH	36.9	19.7	7.1
447	3-NHAc	3-NO_2	28.6	9.1	0.6
446	3-NHAc	3,5-OCH_3	14.4	19.9	6.3

Table 4.15: Primary screening data of a number of 2-amino-4-aryl-6-anilino-pyrimidines. % I = percentage inhibition at the ligand concentration shown in the table.

No.	4-Aryl	6-Anilino	CDK2/E % I @ 25 μM	CDK9/T1 % I @ 5 μM	GSK3 % I @ 25 μM
429	3-OH	3-OH	80.8	55.6	58.5
450	3-OH	3-OH	36.9	19.7	7.1
428	3-NO_2	3-OH	52.6	28.0	66.2
448	3-NO_2	3-OH	44.8	22.3	22.9
427	3-NHAc	3,5-OCH_3	33.8	16.9	29.7
446	3-NHAc	3,5-OCH_3	14.4	19.9	6.3

Table 4.16: Direct comparison of primary screening data of a number of 4-aryl-6-anilino-pyrimidines (blue) and 2-amino-4-aryl-6-anilino-pyrimidines. % I = percentage inhibition at the ligand concentration shown in the table.

Table 4.16 shows that the introduction of a 2-amino group to the 4-aryl-6-anilino-pyrimidine scaffold results in a reduction in ligand potency against the CDK2/E, CDK9/T1 and GSK3. It was envisaged that the 2-amino group could potentially hydrogen bond with the backbone carbonyl of Glu81, in an analogous manner to that observed in the CDK2/ATP complex (PDB Code 1HCK) and CDK2/ligand **321** complex (PDB Code 1PXJ). Analysis of the crystal structure of ligand **363** bound to CDK2 revealed that the size of the pocket that would accommodate the 2-amino group is small. It is therefore postulated that the introduction of a 2-amino group off the central pyrimidine ring disrupts the donor-acceptor pair interactions between the *N*-1 of the pyrimidine ring and the backbone N*H* of Leu83, and the anilino-N*H* of the ligand and the backbone carbonyl of Leu83.

Those ligands that exhibited 50% or greater inhibition of CDK2/E in the primary screen were put forward for a secondary screen and their IC_{50} values against CDK2/E were determined. The secondary screen consisted of a full 10 point IC_{50} determination, performed twice, using 2 independent dilution series. The IC_{50} values of compounds submitted for screening against CDK2/Cyclin E that have been received are shown in Table 4.17. The dilution series for the IC_{50} determination of ligands **413**, **414** and **422**

had a highest ligand concentration of 12.5 μM. These three ligands failed to give 50% inhibition at 12.5 μM are therefore listed in Table 4.17 as having an IC_{50} > 12.5 μM.

No.	CDK2/E IC50 μM	GSK3 IC50 μM
413	>12.5	>12.5
414	>12.5	>12.5
422	>12.5	>12.5
428	18.313	23.953
429	8.051	20.645
424	10.690	-

Table 4.17: Secondary screening data for 4,6-disubstituted pyrimidines tested.

What is evident from the data presented in Tables 4.12 – 4.17 is that 4-aryl-6-aniliino-pyrimidines are modest inhibitors of CDK2/E, CDK9/T1 and GSK3. Eight direct comparisons of results obtained from the CDK2/Cyclin E assay for both the 4,6- and 2,4-disubstituted pyrimidine series are shown in Table 4.18. These comparisons show that in most cases the 4,6-disubstituted-pyrimidine analogue is less potent an inhibitor of CDK2/E than its 2,4-disubstituted-pyrimidine analogue.

No.	Aryl	Anilino	CDK2/E % I	CDK2/E IC50 μM
ASCII-202/1	3-OCH_3	3-F	67.5	-
489			28.6	-
ASC11-191	3-OH	3,5-OCH_3	13.7	-
518			1.6	-
ASC11-85	4-OCH_3	3-OH	98.3	0.0015
462			10.5	-
ASC1-174A	3-NO_2	4-OH	-	3.300
424			-	10.690
ASC11-16	2,5-CH_3	3-OH	91.8	3.654
452			26.7	-
ASC11-17	2,5-CH_3	3-F	80.4	>12.5
440			47.7	-
ASC11-19	3-OH	3-OH	97.0	0.491
429			80.8	8.051
ASC11-22	3-NO_2	3-OH	93.8	1.396
428			52.6	18.313
ASC11-36	3-NHAc	3,5-OCH_3	90.4	5.427
427			33.8	-
ASC11-45	3,4-OCH_3	4-OH	8.7	-
469			49.9	-

Table 4.18: Comparison of assay results obtained from the CDK2/E assay. Figures in red represent % inhibition at 25 μM; figures in blue represent % inhibition at 10 μM.

The comparison of three sets of pyrimidines is worthy of further discussion. Pyrimidine ASC11-85 was shown to be an extremely potent inhibitor of CDK2/E with an IC_{50} of 1.5 nM. Disappointingly, this activity was not reflected in the analogous 4,6-disubstituted pyrimidine series, with ligand **462** exhibiting neglible inhibition of CDK2/E at 10 μM. Furthermore, the poor activity of ligand **462** is difficult to justify when compared with the potency of ligand **461** shown in Table 4.14. Repetition of the primary screen of ligand **462** is therefore desirable. Pyrimidine **429**, exhibiting a *meta*-hydroxy group on both the 4-aryl and 6-anilino aromatic rings, was shown to be very potent against the CDK2/cyclin E complex at 25 μM and compared favourably with the percentage inhibition of CDK2/cyclin E complex measured for the 2,4-disubstituted pyrimidine

analogue. However, secondary screening data received for pyrimidine **429** revealed it was 20-fold less potent than the pyrimidine ASC11-19, again highlighting the danger in overinterpretation of data from the primary screen. Intriguingly, the ligand **469** was shown to be more potent than the corresponding 2,4-disubstituted analogue, ASC11-45, although its activity in the primary screen was below the threshold for full IC_{50} determination.

In the absence of crystal structures of a ligand from both the 4-aryl-6-anilino- and 2-anilino-4-aryl- pyrimidine series bound to CDK2 it is difficult to justify the significant difference in potency shown in Table 4.17 of these two series of ligands. However, it is likely that the 6-anilino ring system is unable to adopt a similar conformation to those ring systems in the analogous 2-anilino substituted series owing to unfavourable steric interactions between the pyrimidyl *C*-5 proton and a proton at the *ortho*-position on the anilino ring, as illustrated in Figure 4.4. This issue could be investigated further by either the synthesis of a series of 2,4-disubstituted triazines, or by replacement of the 6-anilino moiety in the 4,6-disubstituted pyrimidine series with either a functionalised 2-amino pyridine or 2-amino-pyrimidine. Indeed, primary screening data presented in Table 4.16 for ligands **463** and **467** shows that replacement of the 6-anilino moiety with 2-aminopyridine resulted in an increase in inhibition of CDK2/E and CDK9/T1 at a ligand concentration of 25 μM. Clearly, however, replacement of the anilino moiety requires further investigation before firm conclusions can be drawn. It is also worthy of note that the co-planarity of the anilino and pyrimidyl ring systems feature in the majority of crystal structures reported of 2-anilino-4-(thiazol-5-yl)-pyrimidines bound to CDK2 (PDB Codes 1PXL, 1PXM, 1PXP), with the crystal structure of the CDK2/ligand **363** complex being the exception (Figure 4.3).

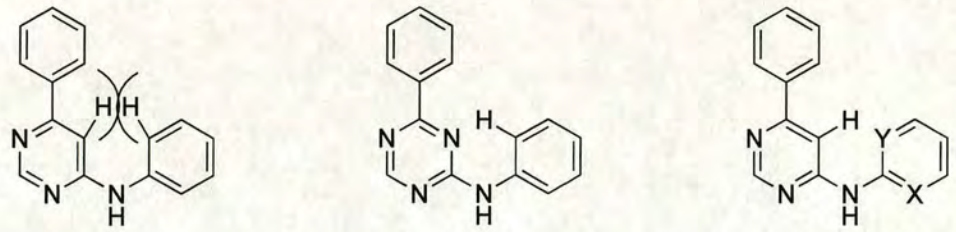

Figure 4.4: Possible explanation for decrease in ligand potency against CDK2 when moving from 2-anilino-4-aryl- to 6-anilino-4-aryl- substituted pyrimidines.

4.5 Future work

Unfortunately, time constraints did not allow further work on the 4-aryl-6-anilino-pyrimidine series. However, given that the synthetic route to these ligands has now been established, it would be desirable to prepare further analogues of the 2-anilino-4-aryl-pyrimidine series that have been shown to be potent inhibitors of the CDK2/cyclin E complex, namely containing either a 3-nitro-, 3-hydroxy-, 3-hydroxymethyl- or 4-hydroxy- substituent on the anilino-ring system and either a 3-hydroxy- or 3-nitro-substituent on the aryl ring. Furthermore, the resolution of crystal structures of ligands from both these series bound to CDK2 should provide an explanation of the marked difference in inhibitory activity seen between them.

It would also be worthwhile to investigate other ring systems that could replace the central pyrimidine scaffold whilst retaining activity. The synthesis of a series of 2-anilino-4-aryl-pyridine analogues would be worthy of merit, as it is expected that the hydrogen bond donor-acceptor pair between Leu83 and the anilino nitrogen and *N*-1 of the pyridyl ring would be conserved. Furthermore, if the decrease in potency of the 4,6-disubstituted series compared to the 2,4-disubstituted pyrimidine series is attributable to the inability of the ligand to bind in the ATP-binding pocket in a co-planar conformation, this could be addressed by the synthesis of a series of 2-anilino-4-aryl-triazines. It is envisaged that 2,4-dichloro-1,3,5-triazine **521**, which can be synthesised

from *N*-cyanochloroformamidine **519** and the chloromethyleniminium salt **520**, generated *in situ* from the reaction between phosphoryl chloride and *N,N*-dimethylformamide, following protocol reported by Harris (Scheme 4.12),[203] could serve as a useful building block for this series of compounds.

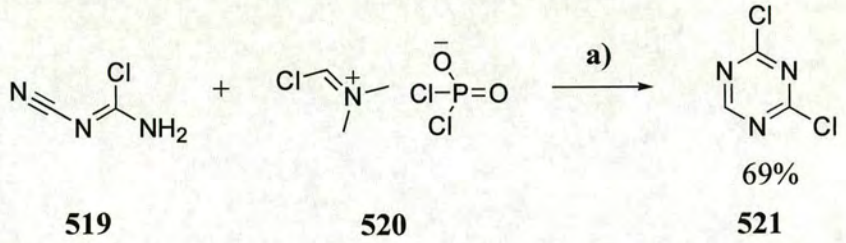

69%

519 **520** **521**

Scheme 4.12: *Reagents and conditions*: a) DCM, room temperature, 18 h.

5 Experimental procedures

5.1 General techniques

5.1.1 Instrumentation and basis of characterization of compounds

All microwave irradiation experiments were carried out using the Discover and Explorer systems from CEM Corporation, Buckingham, UK including Chemdriver software (versions 2.22 – 3.6). The reactions were performed in heavy-walled Pyrex tubes (10 ml, length = 150 mm) sealed with a septum utilizing the standard absorbance level (300 W maximum power). ^{1}H and ^{13}C NMR spectra were recorded on Brüker ARX250, DPX-360, ARX-500, Varian Inova-300 or Varian Gemini-200 instruments. The following abbreviations are used: δ, chemical shift; d, doublet; dd, doublet of doublets; dt, doublet of triplets; dq, doublet of quartets; *J*, coupling constant; m, multiplet; q, quartet; s, singlet; t, triplet. Chemical shifts (δ) are reported in parts per million (ppm) and coupling constants (*J*) in Hz. Residual protic solvent, $CHCl_3$ (δ_H 7.27, s), CH_3OH (δ_H 3.35, s) or $(CH_3)_2SO$ (δ_H 2.52, m), was used as the internal standard in ^{1}H NMR spectra, and ^{13}C NMR shifts at either 63 or 75 MHz were referenced using $CHCl_3$ (δ_C 77.0, t), CH_3OH (δ_C 49.0, m) or $(CH_3)_2SO$ (δ_C 39.7, m) with broad band decoupling. Electrospray (ES) nominal mass spectra were recorded using a Micromass Platform II mass spectrometer. Fast Atom Bombardment (FAB) high resolution mass spectra were recorded on a Kratos MS50TC instrument. Infra-red absorption spectroscopy was performed on a Jasco FT-IR 450 plus spectrometer, and ν_{max} values are quoted in cm^{-1}.

All experiments detailed in this chapter were undertaken using a combinatorial, high-throughput approach with the aim of providing novel ligands for biological screening. The adoption this approach, and time constraints imposed, rendered it imprudent to obtain full characterization of all compounds and, therefore, where possible, a representative proportion of each library has been fully characterized (in excess of 10%).

5.1.2 Chromatography

Analytical TLC was carried out on Merck aluminium-backed plates coated with silica gel 60 F_{254}, 0.25 mm. Components were visualised using quenching of ultra-violet fluorescence (254 nm), and ammonium molybdate or permanganate dips. Flash chromatography was carried out using silica gel 60H (Merck 9385, 0.04-0.063 mm, 230-400 mesh).

All HPLC purifications were performed on the Parallex Flex™ purification system manufactured by Biotage. This system detects at 254 and 280 nm. The column used was a Supercosil ABZ+Plus reverse-phase column, of dimension 25cm x 21.2 mm, particle size12 μM. The flow rate used for each method was 20 ml min^{-1}, unless otherwise specified. Methods used are shown in Tables 5.1 – 5.17, with solvents A and B being water and acetonitrile respectively.

Starting A%	Ending A %	Starting B%	Ending B%	Duration /min
90	90	10	10	2
90	90	10	10	0.5
90	90	10	10	2
90	30	10	70	15
30	5	70	95	2
5	5	95	95	3
5	90	95	10	2

Table 5.1: HPLC Method A

Starting A%	Ending A %	Starting B%	Ending B%	Duration /min
90	90	10	10	2
90	90	10	10	0.5
90	90	10	10	2
90	10	10	90	20
10	5	90	95	1
5	5	95	95	3
5	90	95	10	2

Table 5.2: HPLC Method B

Starting A%	Ending A %	Starting B%	Ending B%	Duration /min
65	65	35	35	2
65	65	35	35	0.5
65	65	35	35	2
65	35	35	65	20
35	5	65	95	2
5	5	95	95	3
5	65	95	35	2

Table 5.3: HPLC Method C

Starting A%	Ending A %	Starting B%	Ending B%	Duration /min
90	90	10	10	2
90	90	10	10	0.5
90	90	10	10	2
90	45	10	55	18
45	5	55	95	2
5	5	95	95	3
5	90	95	10	2

Table 5.4: HPLC Method D

Starting A%	Ending A %	Starting B%	Ending B%	Duration /min
90	90	10	10	2
90	90	10	10	0.5
90	90	10	10	2
90	45	10	55	24
45	5	55	95	2
5	5	95	95	3
5	90	95	10	2

Table 5.5: HPLC Method E

Starting A%	Ending A %	Starting B%	Ending B%	Duration /min
90	90	10	10	2
90	90	10	10	0.5
90	90	10	10	2
90	20	10	80	20
20	5	80	95	2
5	5	95	95	3
5	90	95	10	2

Table 5.6: HPLC Method F

Starting A%	Ending A %	Starting B%	Ending B%	Duration /min
85	85	15	15	2
85	85	15	15	0.5
85	85	15	15	2
85	35	15	65	27
35	5	65	95	2
5	5	95	95	3
5	85	95	15	2

Table 5.7: HPLC Method G

Starting A%	Ending A %	Starting B%	Ending B%	Duration /min
85	85	15	15	4
85	85	15	15	1
85	85	15	15	4
85	35	15	65	40
35	5	65	95	4
5	5	95	95	6
5	85	95	15	4

Table 5.8: HPLC Method H, Flow rate 10 ml min^{-1}.

Starting A%	Ending A %	Starting B%	Ending B%	Duration /min
85	85	15	15	2
85	85	15	15	0.5
85	85	15	15	2
85	35	15	65	17
35	5	65	95	2
5	5	95	95	3
5	85	95	15	2

Table 5.9: HPLC Method I

Starting A%	Ending A %	Starting B%	Ending B%	Duration /min
65	65	35	35	2
65	65	35	35	0.5
65	65	35	35	2
65	35	35	65	15
35	5	65	95	2
5	5	95	95	3
5	65	95	35	2

Table 5.10: HPLC Method J

Starting A%	Ending A %	Starting B%	Ending B%	Duration /min
65	65	35	35	2
65	65	35	35	0.5
65	65	35	35	2
65	35	35	65	15
35	5	65	95	2
5	5	95	95	3
5	65	95	35	2

Table 5.11: HPLC Method K

Starting A%	Ending A %	Starting B%	Ending B%	Duration /min
65	65	35	35	2
65	65	35	35	0.5
65	65	35	35	2
65	35	35	65	15
35	5	65	95	2
5	5	95	95	3
5	65	95	35	2

Table 5.12: HPLC Method L

Starting A%	Ending A %	Starting B%	Ending B%	Duration /min
95	95	5	5	2
95	95	5	5	0.5
95	95	5	5	2
95	65	5	35	27
65	5	35	95	2
5	5	95	95	3
5	95	95	5	2

Table 5.13: HPLC Method M

Starting A%	Ending A %	Starting B%	Ending B%	Duration /min
95	95	5	5	4
95	95	5	5	1
95	95	5	5	4
95	35	5	65	40
35	5	65	95	4
5	5	95	95	6
5	95	95	5	4

Table 5.14: HPLC Method N, Flow rate 10 ml min^{-1}.

Starting A%	Ending A %	Starting B%	Ending B%	Duration /min
70	70	30	30	2
70	70	30	30	0.5
70	70	30	30	2
70	10	30	90	15
10	5	90	95	1
5	5	95	95	3
5	90	95	10	2

Table 5.15: HPLC Method P

Starting A%	Ending A %	Starting B%	Ending B%	Duration /min
70	70	30	30	2
70	70	30	30	0.5
70	40	30	60	15
40	5	60	95	15
98	5	2	95	2
5	70	95	30	2

Table 5.16: HPLC Method Q

Starting A%	Ending A %	Starting B%	Ending B%	Duration /min
95	95	5	5	2
95	95	5	5	0.5
95	5	5	95	10
5	5	95	95	3
5	95	95	5	1
95	95	5	5	1

Table 5.17: HPLC Method R

Starting A%	Ending A %	Starting B%	Ending B%	Duration /min
90	90	10	10	2
90	90	10	10	0.5
90	75	10	25	1
75	65	25	35	15
65	5	35	95	2
5	5	95	95	3
5	90	95	10	2

Table 5.18: HPLC Method S

5.1.3 Solvents and reagents

All reagents and solvents were standard laboratory grade and were used as supplied unless otherwise stated. DMF refers to peptide synthesis grade.

5.2 Assay protocol

5.2.1 Fluorescence polarisation assay 1

A fluorescence polarisation competitive binding assay was carried out by Cyclacel Ltd. using a 96-well microtiter plate (Costar) format. Recombinant Hdm2 (1.5 μg per well) in TBS-BSA buffer (50 mM Tris pH 7.4, 150 mM NaCl, and 0.1 % BSA) was incubated for 5 minutes at room temperature in the presence of serially diluted test compound (in

TBS-BSA buffer with a final concentration of 5 % DMSO). Fluorescently labelled 12/1-peptide (fluorescein-Met-Pro-Arg-Phe-Met-Asp-Tyr-Trp-Glu-Gly-Leu-Asn-NH_2, 0.2 μM) was added to each well and the plate was incubated at room temperature for 45 minutes. The fluorescence polarisation (excitation 485 nm, emission 520 nm) of the peptide was measured. IC_{50} values were calculated from dose-response curves.

5.2.2 Fluorescence polarisation assay 2

The protocol as detailed for Fluoresence Polarisation Assay 1 was followed, although the quantity of Hdm2 used per reaction was reduced from 1.5 μg to 20 ng.

5.2.3 CDK2/Cyclin E Assay

The CDK2/E kinase assay was performed by Cyclacel Ltd. with a 96-well plate format with recombinant CDK/cyclin complexes (His_6-tagged recombinant human CDK2/cyclin E was expressed in sf9 cells with a baculovirus expression system, proteins were purified by metal chelate affinity chromatography to > 90% homogeneity). The assay buffers consisted of 25 mM β-glycerophosphate, 20 mM MOPS, 5 mM EGTA, 1 mM DTT, and 1 mM Na_3VO_3 (pH 7.4) into which were added 2-4 μg of active enzyme with purified histone H1. Inhibitors were made up in 10% aq. DMSO, and 10 μL of the solutions was added to the wells. Final reaction volume was 50 μL. The reaction was initiated by addition of Mg/ATP mix (15 mM $MgCl_2$, plus 100 μM ATP with 30-50 kBq per well of [γ-^{32}P]-ATP), and the mixtures were incubated for 10 min at 30 °C. Reactions were stopped on ice, and then the mixtures were filtered through p81 filterplates. After washing three times with 75 mM aq. orthophosphoric acid, plates were dried, scintillant (Microscint 40) was added, and incorporated radioactivity was measured with a scintillation counter (TopCount; Packard Instruments, Pangbourne, Berks., UK). Data was analysed with curve fitting software (GraphPad Prism version

3.00 for Windows; GraphPad Software, San Diego, CA) to determine IC_{50} values (concentration of test compound that inhibits kinase activity by 50%).

5.2.4 CDK9/T1 and GSK3β assays

The CDK9/T1 kinase assay was performed by Cyclacel Ltd. Peptide substrate (biotinyl-Ahx-(Tyr-Ser-Pro-Thr-Ser-Pro-Ser)$_4$-NH_2; 1 – 2 mg/mL) and recombinant human CDK9/cyclin T1 (0.5 – 2 μg) were incubated at 45 min at 30 °C in the presence of varying amounts of test compound in 20 mM MOPS pH 7.2, 25 mM β-glycerophosphate, 5 mM EGTA, 1 mM DTT, 1 mM Na_3VO_3, 15 mM $MgCl_2$, and 100 μM ATP (containing a trace amount of [γ-^{32}P]-ATP in a total volume of 25 μL in a 96-well microtitre plate. The reaction was stopped by placing the plate on ice for 2 min. Avidin (50 μg) was added to each well, and the plate was incubated at room temperature for 30 min. The samples were transferred to a 96-well p81 filterplate and washed (4x 200 μL per well) with 75 mM phosphoric acid. Microscint 40 scintillation liquid (50 μL) was added to each well, and the amount of ^{32}P incorporation for each sample was measured using a Packard TopCount microplate scintillation counter. IC_{50} values were calculated from dose response curves (GraphPad Prism curve-fitting software). The GSK3β assay was carried out by Upstate Discovery, Dundee, UK, essentially as described.[204] The ATP concentration used in the GSK3β assay was 10 μM.

5.3 General methods

5.3.1 General procedure S1

To a stirring solution of tributylphosphine (1.5 eq.), the alcohol (1.0 eq.) and the sulfonamide (1.5 eq.) in anhydrous benzene (3 mL), at 0 °C, TMAD (1.5 eq.) was added. The reaction was performed under an atmosphere of nitrogen. After 10 minutes the reaction mixture was allowed to warm to room temperature and stirred for a further 24 hours before being filtered and washed with hexane. The organic filtrate was concentrated *in vacuo* to afford a residue which was columned on silica (hexane: ethyl acetate 4:1). Appropriate fractions were combined and concentrated *in vacuo* to afford the title sulfonamide.

5.3.2 General procedure S2

To a stirring solution of the sulfonamide (1.0 eq.) in acetone (3.0 mL) was added the alkyl halide (5.0 eq.) followed by triethylamine (excess). The reaction mixture was irradiated in the Discover™ at 70 °C for 10 minutes, with active cooling of the sample. The reaction mixture was diluted with water (20 mL) and extracted with ethyl acetate (2 x 20 mL). The combined organics were washed with water (2 x 20 mL) before being concentrated *in vacuo* to afford a residue that was columned on silica. Appropriate fractions were combined and concentrated *in vacuo* to afford the title sulfonamide.

5.3.3 General procedure A1

To a solution of the aniline (1.0 eq.) in DCM (2.0 mL) was added the acid chloride (1.1 eq.). The reaction mixture was irradiated in the Discover™ at 110 °C for 5 minutes, with active cooling of the sample. The reaction mixture was concentrated in vacuo, and the residue diluted with ethyl acetate (10 mL) and washed with water (2 x 10 mL). The

organics were dried over anhydrous Na_2SO_4, filtered and concentrated *in vacuo* to afford the title amide that required no further purification.

5.3.4 General procedure A2

The acid chloride (1.2 eq.), amine (1.0 eq.) and morpholinomethyl-polystyrene resin (0.200 g, 3.7 mmole g^{-1}) in anhydrous DCM (2.0 mL) were stirred at room temperature for 48 hours before the addition of tris(aminoethyl)amine polystyrene resin (0.400 g, 4.4 mmole g^{-1}). The reaction mixture was allowed to stir at room temperature for a further 5 hours before being filtered and the resin washed with DCM (2 x 5.0 mL). The filtrate was concentrated *in vacuo* to afford the title amide that required no further purification.

5.3.5 General procedure P1

To a solution of 4,6-dichloropyrimidine (0.600 g, 4.00 mmole, 1.0 eq.) in acetonitrile (3 mL) was added 3-nitrophenyl boronic acid (0.673 g, 4.00 mmole, 1.0 eq.), Cs_2CO_3 (3.940 g, 12.00 mmole, 3.0 eq.), $Pd(OAc)_2$ (0.045 g, 0.20 mmole, 0.05 eq.) and triphenylphosphine (0.106 g, 0.40 mmole, 0.10 eq.). Water (0.3 mL) was added to solubilize the Cs_2CO_3. The reaction mixture was irradiated in the Discover™ at 110 °C for 15 minutes, with active cooling of the sample, before being divided into aliquots (3 x 1 mL). To one aliquot containing the Suzuki intermediate (1 mL, 1.30 mmole, 1.0 eq.) was added the aniline (1.30 mmole, 1.0 eq.) and HCl (2M, 2.6 mL, 4.0 eq.). The sample was irradiated on the Discover™ at 110 °C for 5 minutes, with active cooing. An aliquot (1 mL) of the reaction mixture was injected directly onto the Biotage Parallex Flex™ HPLC. Appropriate fractions were combined and concentrated *in vacuo* to afford the title pyrimidine.

5.3.6 General procedure P2

To a solution of 4,6-dichloropyrimidine (0.100 g, 0.67 mmole, 1.0 eq.) in acetonitrile (3 mL) was added the boronic acid (0.67 mmole, 1.0 eq.), Cs_2CO_3 (0.328 g, 1.00 mmole, 1.5 eq.), $Pd(OAc)_2$ (0.008 g, 0.05 eq.) and triphenylphosphine (0.018 g, 0.07 mmole, 0.10 eq.). Water (0.5 mL) was added to solubilize the Cs_2CO_3. The reaction mixture was irradiated in the Discover™ at 130 °C for 15 minutes, with active cooling of the sample, before the addition of the aniline (0.67 mmole, 1.0 eq.) and HCl (2M, 1.3 mL, 4.0 eq.). The reaction mixture was irradiated on the Discover™ at 110 °C for 5 minutes, with active cooling of the sample. Subsequently, an aliquot (1 mL) of the organic solvent was injected directly into the Biotage Parallex Flex™ HPLC. Appropriate fractions were combined and concentrated *in vacuo* to afford the title compound.

5.3.7 General procedure P3

To a solution of 4,6-dichloropyrimidine (0.100 g, 0.67 mmole, 1.0 eq.) in acetonitrile (3.0 mL) was added the boronic acid (0.67 mmole, 1.0 eq.), Cs_2CO_3 (0.328 g, 1.00 mmole, 1.5 eq.), $Pd(OAc)_2$ (0.008 g, 0.03 mmole, 0.05 eq.) and triphenylphosphine (0.018 g, 0.07 mmole, 0.10 eq.). Water (0.3 mL) was added to the reaction mixture to solubilise the Cs_2CO_3. The reaction mixture was irradiated in the Discover™ at 130 °C for 15 minutes, with active cooling of the sample, before the addition of the aniline (0.67 mmole, 1.0 eq.) and HCl (2M, 1.3 mL, 4.0 eq.). The reaction mixture was irradiated in the Discover™ at 110 °C for 5 minutes, with active cooling of the sample. Subsequently, the reaction mixture was divided into aliquots (3 x 1 mL) and injected directly into the Biotage Parallex Flex™ HPLC. Appropriate fractions were combined and concentrated *in vacuo* to afford the title compound.

5.3.8 General procedure P4

To a solution of the 4,6-dichloropyrimidine (0.50 mmole, 1.0 eq.) in THF (3.0 mL) was added the boronic acid (0.50 mmole, 1.0 eq.), Cs_2CO_3 (0.197 g, 0.60 mmole, 1.2 eq.), triphenylphosphine (0.013 g, 0.05 mmole, 0.1 eq.) and $Pd(OAc)_2$ (0.06 g, 0.05 mmole, 0.05 eq.). Water (0.3 mL) was added to the reaction mixture to dissolve the Cs_2CO_3. The reaction mixture was irradiated in the Discover™ at 110 °C for 25 minutes, with active cooling of the sample. The reaction mixture was separated into aliquots (3 x 1 mL) and to one aliquot was added the aniline (0.17 mmole, 1.0 eq.) and HCl (4M, 85 μL, 2.0 eq.). The reaction mixture was irradiated in the Discover™ at 110 °C for a further 25 minutes, with active cooling of the sample, before being injected directly onto the Biotage Parallex Flex™ HPLC. Appropriate fractions were combined and concentrated *in vacuo* to afford the title compound.

5.3.9 General procedure P5

To a solution of the 4,6-dichloropyrimidine (1.68 mmole, 1.0 eq.) in THF (5 mL) was added Cs_2CO_3 (0.660 g, 2.50 mmole, 1.5 eq.), $Pd(OAc)_2$ (0.020 g, 0.08 mmole, 0.05 eq.), triphenylphosphine (0.044 g, 0.17 mmole, 0.10 eq.) and the boronic acid (1.68 mmole, 1.0 eq.). The reaction mixture was irradiated in the Discover™ at 110 °C for 25 minutes, with active cooling of the sample, before being apportioned into aliquots (10 x 0.5 mL). To one aliquot containing the Suzuki intermediate (0.5 mL, 0.17 mmole, 1.0 eq.) was added the aniline (0.17 mmole, 1.0 eq.), HCl (4M, 163 μL, 4.0 eq.) and THF (0.5 mL). The reaction mixture was irradiated in the Discover™ at 110 °C for 25 minutes, with active cooling of the sample, before being injected directly onto the Biotage Parallex Flex™. Appropriate fractions were combined and concentrated *in vacuo* to afford the title compound.

5.3.10 General procedure L1

Reagent	No. Moles Dispensed (mmol)	Volume Dispensed (mL)	Solvent
Aniline	0.162	1.00	Pyridine
Sulfonyl chloride	0.147	1.00	Pyridine

Anilines

4-(Trifluoromethyl)aniline

4-Fluoroaniline

4-Chloroaniline

3,5-Dichloroaniline

3,5-Bis(trifluoromethyl)aniline

2,4,5-Trichloroaniline

Sulfonyl Chlorides

4,5-Dibromothiophene-2-sulfonyl chloride

5-Chlorothiophene-2-sulfonyl chloride

Experimental conditions for library L1

1. Stock solutions with concentration 0.162 M of each of the six anilines were prepared and loaded onto the reagent rack of the Bodhan Neptune™ MB Automated Workstation.
2. Stock solutions with concentration 0.147 M of each of the two sulfonyl chlorides were prepared and loaded onto the reagent rack of the Neptune.
3. Each sulfonyl chloride solution (1.0 mL) was dispensed to a horizontal line of 6 reaction tubes on a single MiniBlock™.
4. Each aniline solution (1.0 mL) was dispensed to a vertical line of 2 reaction tubes on a MiniBlock™, each tube containing either of the sulfonyl chlorides dispensed in Step 3.
5. The MiniBlock™ was covered and shaken on the MiniBlock™ High Capacity Shaking and Washing Station overnight.

6. The MiniBlock™ was transferred to the Allex™ Liquid/Liquid Extractor and each reaction mixture transferred to a boiling tube.
7. The Allex™ was used to dispense HCl (1M, 3 mL) into each boiling tube, followed by a mixture of ethyl acetate/ diethyl ether (1:1, 3 mL). The contents of each boiling tube were aspirated, and each organic layer extracted and transferred to a second boiling tube.
8. The Allex™ was used to dispense a saturated solution of brine (3 mL) to each boiling tube, and, after washing, the organics were transferred to a 48-well microtitre plate.
9. The 48-well plate containing the 12 samples were concentrated under reduced pressure using the Christ ALPHA-2-4 Freeze Dryer, BETA-RVC Ceramic Vacuum Measurement System (3 h, 25 °C, 20 mbar).
10. Samples **46** and **47** were used as test samples for mass directed purification on the ZMD 4000. Unfortunately, the molecular ions of the sulfonamides **46** and **47** were not detected and consequently, despite further attempts to identify **46** and **47** by electrospray mass spectrometry, it was decided to undertake further purifications on the Biotage Parallex Flex preparative HPLC system.

5.3.11 General procedure L2

Reagent	No. Moles Dispensed (mmol)	Volume Dispensed (mL)	Solvent
Aniline	0.220	1.00	Pyridine
Sulfonyl chloride	0.200	1.00	Pyridine

Anilines

Aniline
4-(Trifluoromethyl)aniline
4-Chloroaniline
4-Methylaniline
3,5-Dichloroaniline
4-Fluoroaniline
3,5-Bis(trifluoromethyl)aniline
2,4-Dichloroaniline

Sulfonyl Chlorides

5-[2-(Methylthio)pyrimidin-5-yl]-thiophene-2-sulfonyl chloride
4-(1,3-Oxazol-2-yl)benzenesulfonyl chloride
4-Bromo-5-chlorothiophene-2-sulfonyl chloride
5-Bromothiophene-2-sulfonyl chloride
3-Nitrobenzenesulfonyl chloride
5-(Phenylsulfonyl)thiophene-2-sulfonyl chloride

Experimental conditions for library L2

1. Stock solutions with concentration 0.220 M of each of the 8 anilines were prepared and loaded onto the reagent rack of the Bodhan Neptune™ MB Automated Workstation.
2. Stock solutions with concentration 0.200 M of each of the 6 sulfonyl chlorides were prepared and loaded onto the reagent rack of the Neptune.
3. Each sulfonyl chloride solution (1.0 mL) was dispensed to a horizontal line of 8 reaction tubes on a single MiniBlock™.

4. Each aniline solution (1.0 mL) was dispensed to a vertical line of 6 reaction tubes on a MiniBlock™, each tube containing one of the sulfonyl chlorides dispensed in Step 3.
5. The MiniBlock™ was covered and shaken on the MiniBlock™ High Capacity Shaking and Washing Station overnight.
6. The MiniBlock™ was transferred to the Allex™ Liquid/Liquid Extractor and each reaction mixture transferred to a boiling tube.
7. The Allex™ was used to dispense HCl (1M, 3mL) into each boiling tube, followed by a mixture of ethyl acetate/ diethyl ether (1:1, 3 mL). The contents of each boiling tube were aspirated, and each organic layer extracted and transferred to a second boiling tube.
8. The Allex™ was used to dispense a saturated solution of brine (3 mL) to each boiling tube, and, after washing, the organics were transferred to a 48-well microtitre plate.
9. The 48 samples were concentrated *in vacuo* using the Christ ALPHA-2-4 Freeze Dryer, BETA-RVC Ceramic Vacuum Measurement System (3 h, 25 °C, 20 mbar).
10. Samples **90** – **105** were used as test samples for mass directed purification on the ZMD 4000. Unfortunately, the molecular ions of the sulfonamides **90** - **105** were not detected and the majority of the samples were transferred to waste. Where some crude mixture had been recovered, and for subsequent samples **58** – **89**, the sample was dissolved in methanol (1 mL) and injected directly onto the Biotage Parallex Flex™ HPLC (Method R).

5.3.12 General procedure L2b

Reagent	No. Moles Dispensed (mmol)	Volume Dispensed (mL)	Solvent
Aniline	0.220	1.00	Pyridine
Sulfonyl Chloride	0.200	1.00	Pyridine

Aniline

Aniline

4-(Trifluoromethyl)aniline

4-Chloroaniline

4-Methylaniline

3,5-Dichloroaniline

4-Fluoroaniline

3,5-Bis(trifluoromethyl)aniline

2,4-Dichloroaniline

Sulfonyl Chlorides

3-Nitrobenzenesulfonyl chloride

5-(Phenylsulfonyl)thiophene-2-sulfonyl chloride

Experimental conditions for sulfonamide library L2b

1. The General procedure outlined for Sulfonamide Library **L2** was followed.
2. Prior to transferring the crude reaction mixtures to the Allex™, the contents of the MiniBlock™ were drained into a 48-well microtitre plate and concentrated *in vacuo* on the Christ ALPHA-2-4 Freeze Dryer, BETA-RVC Ceramic Vacuum Measurement System (3 h, 25 °C, 20 mbar), in order to remove the excess pyridine from the crude mixtures.
3. Using the Allex™, each sample contained in the 48-well plate was diluted with ethyl acetate (3 mL) and transferred to a boiling tube.

4. The Allex™ was used to dispense HCl (1M, 3mL) into each boiling tube, the contents of each boiling tube aspirated, and each organic layer extracted and transferred to a second boiling tube.
5. The Allex™ was used to dispense a saturated solution of brine (2 mL) to each boiling tube, and, after washing, the organics were transferred to a 48-well microtitre plate.
6. The 16 samples were concentrated *in vacuo* using the Christ ALPHA-2-4 Freeze Dryer, BETA-RVC Ceramic Vacuum Measurement System (3 h, 25 °C, 20 mbar).
7. Each sample was purified on silica (hexane: ethyl acetate, 1:1) and appropriate fractions combined and concentrated *in vacuo* to afford the sulfonamide.

5.3.13 General procedure L3

Reagent	No. Moles Dispensed (mmol)	Volume Dispensed (mL)	Solvent
Aniline	0.220	1.00	Pyridine
Sulfonyl Chloride	0.200	1.00	Pyridine

Aniline

3,5-Bis(trifluoromethyl)aniline

3-Chloroaniline

3-(Trifluoromethyl)aniline

3,4-Dichloroaniline

Sulfonyl Chlorides

5-Chlorothiophene-2-sulfonyl chloride

4,5-Dibromothiophene-2-sulfonyl chloride

4-Chloro-3-nitrobenzenesulfonyl chloride

Benzoyl chloride

Experimental conditions for library L3

1. The General procedure outlined for the resynthesis of Sulfonamide Library **L2** was followed.
2. Each sample was purified on silica (hexane: ethyl acetate, 1:1) and appropriate fractions combined and concentrated *in vacuo* to afford the title sulfonamide.

5.3.14 General procedure L4

Reagent	No. Moles Dispensed (mmol)	Volume Dispensed (mL)	Solvent
Aniline	0.440	1.00	DCM
Sulfonyl Chloride	0.400	1.00	DCM
Pyridine	0.400	1.00	DCM

Anilines

4-Chloroaniline

4-Chlorobenzylamine

(1*R*)-1-(4-Chlorophenyl)ethanamine

(1*S*)-1-(4-Chlorophenyl)ethanamine

3,5-Bis(trifluoromethyl)aniline

1-[3,4-Bis(trifluoromethyl)phenyl]-methanamine

4-(Trifluoromethyl)aniline

1-[4-(Trifluoromethyl)phenyl]-methanamine

Sulfonyl Chlorides

5-Chloro-3-methyl-1-benzothiophene-2-sulfonyl chloride

1-Benzothiophene-2-sulfonyl chloride

5-{[(4-Chlorobenzoyl)amino]methyl}thiophene-2-sulfonyl chloride

2,1,3-Benzothiadiazole-5-sulfonyl chloride

5-Pyridin-2-ylthiophene-2-sulfonyl chloride

4,5-Dibromothiophene-2-sulfonyl chloride

Experimental conditions for library L4

1. Stock solutions with concentration 0.440 M of each of the 8 anilines were prepared and loaded onto the reagent rack of the Bodhan Neptune™ MB Automated Workstation.

2. Stock solutions with concentration 0.400 M of each of the 6 sulfonyl chlorides were prepared and loaded onto the reagent rack of the Neptune.
3. Stock solutions (2 x 14 mL) with concentration 0.400 M of pyridine were prepared and loaded onto the reagent rack of the Neptune.
4. Each sulfonyl chloride solution (1 mL) was dispensed to a horizontal line of 8 reaction tubes on a single MiniBlock™.
5. Each aniline solution (1 mL) was dispensed to a vertical line of 6 reaction tubes on a MiniBlock™, each tube containing one of the sulfonyl chlorides dispensed in Step 3.
6. Pyridine (0.400 M, 1 mL) was dispensed to each of the 48 reaction tubes on a Miniblock™.
7. The MiniBlock™ was covered and shaken on the MiniBlock™ High Capacity Shaking and Washing Station overnight.
8. The MiniBlock™ was transferred to the Allex™ Liquid/Liquid Extractor and each reaction mixture transferred to a boiling tube.
9. The Allex™ was used to dispense HCl (1M, 3 mL) into each boiling tube, followed by a mixture of ethyl acetate/ diethyl ether (1:1, 3 mL). The contents of each boiling tube were aspirated, and each organic layer extracted and transferred to a second boiling tube.
10. The Allex™ was used to dispense a saturated solution of brine (3 mL) to each boiling tube, and, after washing, the organics were transferred to a 48-well microtitre plate.
11. The 48 samples were concentrated *in vacuo* using the Christ ALPHA-2-4 Freeze Dryer, BETA-RVC Ceramic Vacuum Measurement System (3 h, 25 °C, 20 mbar).
12. Each sample was purified on silica (hexane: ethyl acetate, 2:1) and appropriate fractions combined and concentrated *in vacuo* to afford the title sulfonamide.

5.4 Experimental for Chapter 2

N-Phenylthiophene-2-sulfonamide (26)[205]

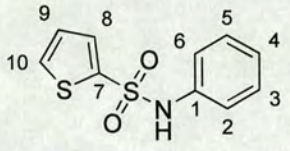

To a solution of aniline (5.36 mL, 58.9 mmole, 2.15 eq.) in methanol (45 mL), thiophene-2-sulfonyl chloride (5.0 g, 27.3 mmole, 1.00 eq.) was added and the reaction mixture allowed to stir overnight at room temperature, before being concentrated *in vacuo* to afford a brown residue which was washed with NaOH (40%) and extracted with ethyl acetate. The combined organic extracts were dried over anhydrous potassium carbonate and concentrated *in vacuo*. The residue was columned on silica (hexane: ethyl acetate 4:1, R_f 0.15) to afford sulfonamide **26** as a cream solid (4.907 g, 75%); LRMS EI^+ *m/z* 239 $(M)^+$; HRMS EI^+ *m/z* 239.00747 $(M)^+$ (calculated for $C_{10}H_9NO_2S_2$, 239.00747 (Dev – 0.02 ppm)); ν_{max} (film)/cm^{-1} 3204 (N-H), 3104 (thiophene C-H), 3090 (aryl C-H), 1596 (aryl C=C), 1332 (SO_2), 1150 (SO_2); δ_H (250 MHz, $CDCl_3$): 6.48 – 6.55 (m, 1H, *H*9), 6.84 – 6.98 (m, 5H, Ar*H*), 7.21 (d, 1H, *J* = 3.5 Hz, *H*8), 7.45 (d, 1H, *J* = 4.9 Hz, *H*10), δ_C (63 MHz, $(CD_3)_2SO$): 117.6 (CH_{Ar}), 121.7 (2 x CH_{Ar}), 127.0 (CH_{Ar}), 127.9 (CH_{Ar}), 128.2 (CH_{Ar}), 128.8 (2 x CH_{Ar}), 150.5 (C_{Ar}), 151.4 (C_{Ar}); Mpt. 99.5-100.0 °C (Lit. 100 °C).

N-Methyl-N-phenylthiophene-2-sulfonamide (27)[206]

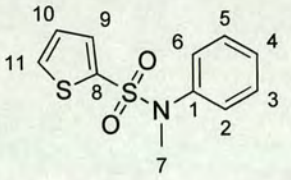

General procedure **S1** was followed using tributylphosphine (0.18 mL, 0.72 mmole, 1.5 eq.), methanol (19.4 μL, 0.48 mmole, 1.0 eq.), *N*-phenylthiophene-2-sulfonamide (0.172 g, 0.72 mmole, 1.5 eq.) and TMAD (0.124 g, 0.72 mmole, 1.5 eq.). Sulfonamide **27** was isolated as a white solid (0.036 g, 30%, R_f 0.20 (hexane: ethyl acetate, 4:1)); LRMS EI^+ *m/z* 253 $(M)^+$; HRMS EI^+ *m/z* 253.02359 $(M)^+$ (calculated for $C_{11}H_{11}NO_2S_2$, 253.02312 (Dev. 1.83 ppm)); ν_{max} (film)/cm^{-1} 3105 (thiophene C-H), 3096 (aryl C-H), 2926 (C-H), 1593 (aryl C=C), 1352 (SO_2), 1152 (SO_2); δ_H (200 MHz, $CDCl_3$): 3.28 (s, 3H, *H*7), 7.09 – 7.19 (m, 3H, Ar*H*), 7.28 – 7.40 (m, 4H, Ar*H*), 7.60 (d, 1H, *J* = 5.0 Hz, *H*11); δ_C (63 MHz, $CDCl_3$): 38.7 (*C*7), 127.1 (2 x CH_{Ar}), 127.7 (CH_{Ar}), 128.0 (CH_{Ar}), 129.4 (2 x CH_{Ar}), 132.5 (CH_{Ar}), 133.1 (CH_{Ar}), 137.1 (C_{Ar}), 141.6 (C_{Ar}); Mpt. 96.1 – 96.9 °C.

N-Ethyl-N-phenylthiophene-2-sulfonamide (28)

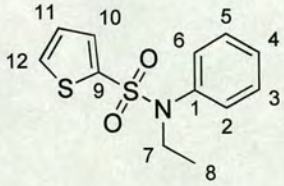

General procedure **S1** was followed using tributylphosphine (0.19 mL, 0.74 mmole, 1.5 eq.), ethanol (28.9 μL, 0.49 mmole, 1.0 eq.), *N*-phenylthiophene-2-sulfonamide (0.178 g, 0.74 mmole, 1.5 eq.) and TMAD (0.128 g, 0.74 mmole, 1.5 eq.). Sulfonamide **28** was isolated as a white solid (0.018 g, 14%, R_f 0.23 (hexane: ethyl acetate, 4:1)); LRMS EI^+ *m/z* 267 $(M)^+$; HRMS EI^+ *m/z* 267.03848 $(M)^+$ (calculated for $C_{12}H_{13}NO_2S_2$, 267.03877

(Dev. – 1.11 ppm)); ν_{max} (film)/cm^{-1} 3096 (thiophene C-H), 3086 (aryl C-H), 2965 (C-H), 1599 (aryl C=C), 1344 (SO_2), 1154 (SO_2); δ_H (200 MHz, $CDCl_3$): 1.17 (t, 3H, *J* = 7.0 Hz, *H*8), 3.73 (q, 2H, *J* = 7.0 Hz, *H*7), 7.04 – 7.20 (m, 2H, H10, *H*11), 7.23 – 7.39 (m, 5H, Ar*H*), 7.63 (d, 1H, *J* = 5.1 Hz, *H*12); Mpt. 98.6 – 99.7 °C.

_N_-Butyl-_N_-phenylthiophene-2-sulfonamide (29)

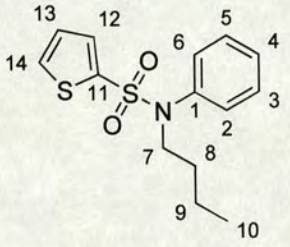

General procedure **S1** was followed using tributylphosphine (0.18 mL, 0.72 mmole, 1.5 eq.), butanol (43.5 μL, 0.48 mmole, 1.0 eq.), *N*-phenylthiophene-2-sulfonamide (0.171 g, 0.72 mmole, 1.5 eq.) and TMAD (0.124 g, 0.72 mmole, 1.5 eq.). The reaction was carried out at room temperature. Sulfonamide **29** was isolated as a white solid (0.030 g, 21%, R_f 0.23 (hexane: ethyl acetate, 4:1)); LRMS EI$^+$ *m/z* 295 (M)$^+$; HRMS EI$^+$ *m/z* 295.06978 (M)$^+$ (calculated for $C_{14}H_{17}NO_2S_2$, 295.07007 (Dev. – 0.98 ppm)); ν_{max} (film)/cm^{-1} 3096 (thiophene C-H), 3065 (aryl C-H), 2932 (C-H), 1594 (aryl C=C), 1350 (SO_2), 1156 (SO_2); δ_H (200 MHz, $CDCl_3$): 0.79 (t, 3H, *J* = 7.0 Hz, *H*10) 1.10 – 1.37 (m, 4H, *H*8, *H*9), 3.51 (t, 2H, *J* = 6.6 Hz, *H*7), 6.97 – 7.03 (m, 2H, H12, *H*13), 7.18 – 7.26 (m, 5H, Ar*H*), 7.49 (d, 1H, *J* = 4.8 Hz, *H*14); Mpt. 71.4 – 71.6 °C.

_N_-Benzyl-_N_-phenylthiophene-2-sulfonamide (30)

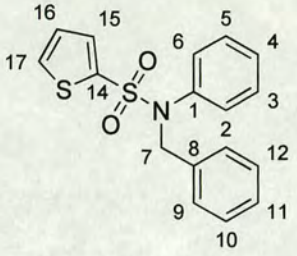

General procedure **S1** was followed using tributylphosphine (0.18 mL, 0.72 mmole, 1.5 eq.), benzyl alcohol (49.7 μL, 0.48 mmole, 1.0 eq.), *N*-phenylthiophene-2-sulfonamide (0.171 g, 0.72 mmole, 1.5 eq.) and TMAD (0.124 g, 0.72 mmole, 1.5 eq.). Sulfonamide **30** was isolated as a white solid (0.056 g, 35%, R_f 0.33 (hexane: ethyl acetate, 4:1)); LRMS EI^+ *m/z* 329 $(M)^+$; δ_H (200 MHz, $CDCl_3$): 4.61 (s, 2H, *H*7), 6.88 – 7.44 (m, 13H, Ar*H*).

_N_-Allyl-_N_-phenylthiophene-2-sulfonamide (31)

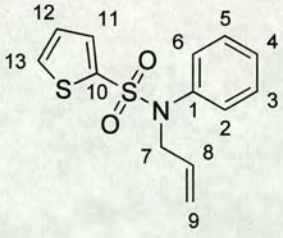

General procedure **S1** was followed using tributylphosphine (0.20 mL, 0.79 mmole, 1.5 eq.), allyl alcohol (36.0 μL, 0.53 mmole, 1.0 eq.), *N*-phenylthiophene-2-sulfonamide (0.190 g, 0.79 mmole, 1.5 eq.) and TMAD (0.137 g, 0.79 mmole, 1.5 eq.). The reaction was carried out at room temperature. Sulfonamide **31** was isolated as a white solid (0.097 g, 66%, R_f 0.31 (hexane: ethyl acetate, 4:1)); LRMS EI^+ *m/z* 279 $(M)^+$; HRMS EI^+ *m/z* 279.03886 $(M)^+$ (calculated for $C_{13}H_{13}NO_2S_2$, 279.03877 (Dev. 0.29 ppm)); ν_{max} (film)/cm^{-1} 3098 (thiophene C-H), 3088 (aryl C-H), 2924 (C-H), 1644 (C=C), 1595 (aryl

C=C), 1355 (SO_2), 1160 (SO_2); δ_H (200 MHz, $CDCl_3$): 4.30 (d, 2H, J = 6.3 Hz, *H*7), 5.13 (dd, 1H, J = 1.2, 3.5 Hz, $H9_{cis}$), 5.20 (dd, 1H, J = 1.2, 10.5 Hz, $H9_{trans}$), 5.74 – 5.94 (m, 1H, *H*8), 7.12 – 7.21 (m, 2H, *H*11, *H*12), 7.33 – 7.44 (m, 5H, Ar*H*), 7.66 (d, 1H, J = 4.7 Hz, *H*13); δ_C (75 MHz, $(CD_3)_2SO$): 54.0 (*C*7), 119.3 (*C*9), 127.6 (CH_{Ar}), 128.4 (CH_{Ar}), 129.0 (2 x CH_{Ar}), 129.3 (2 x CH_{Ar}), 132.3 (*C*8), 132.8 (C_{Ar}), 132.9 (CH_{Ar}), 139.0 (C_{Ar}); Mpt. 90.7 – 91.3 °C.

5-Chloro-*N*-(4-methoxyphenyl)thiophene-2-sulfonamide (37)[206]

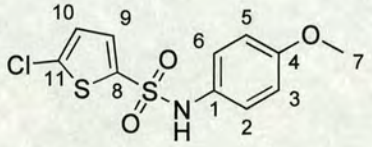

To a solution of *p*-anisidine (0.98 g, 8.0 mmole, 1.1 eq.) in THF (10 ml), 5-chlorothiophene-2-sulfonyl chloride (1.50 g, 7.3 mmole, 1.0 eq.) and DIPEA (1.27 mL) was added. The reaction mixture was allowed to stir overnight at room temperature before being concentrated *in vacuo* to afford a brown residue that was neutralized with HCl (conc.) and extracted into EtOAc. The organics were combined and concentrated *in vacuo* to afford sulfonamide **37** as a beige solid that required no further purification (2.24g, 99%); LRMS EI^+ *m/z* 303 $(M)^+$; HRMS EI^+ *m/z* 302.97925 $(M)^+$ (calculated for $C_{11}H_{10}{}^{35}ClNO_3S_2$, 302.97907 (Dev. 0.61 ppm)); ν_{max} (KBr)/cm^{-1} 3278 (N-H), 3117 (thiophene C-H), 3056 (aryl C-H), 1331 (SO_2), 1155 (SO_2); δ_H (250 MHz, $CDCl_3$): 3.78 (s, 3H, *H*7), 6.58 (bs, 1H, N*H*), 6.80 (d, 2H, J = 9.1 Hz, *H*2, *H*6), 6.82 (d, 1H, J = 4.0 Hz, *H*10), 7.04 (d, 2H, J = 9.1 Hz, *H*3, *H*5), 7.17 (d, 1H, J = 4.0 Hz, *H*9); δ_C (63 MHz, $CDCl_3$): 55.4 (*C*7), 114.5 (2 x CH_{Ar}), 125.7 (2 x CH_{Ar}), 126.6 (CH_{Ar}), 127.9 (C_{Ar}), 129.2 (CH_{Ar}), 137.1 (C_{Ar}), 137.6 (C_{Ar}), 158.4 (C_{Ar}).

N-Allyl-5-chloro-N-(4-methoxyphenyl)thiophene-2-sulfonamide (39)

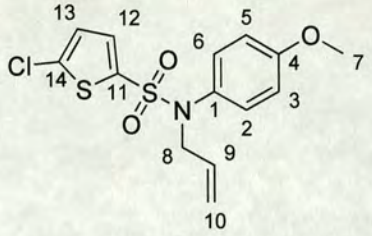

General procedure **S1** was followed using tributylphosphine (829 μL, 3.30 mmole, 1.5 eq.), allyl alcohol (300 μL, 6.60 mmole, 2.0 eq.), 5-chloro-*N*-(4-methoxyphenyl)thiophene-2-sulfonamide (1.009 g, 3.30 mmole, 1.5 eq.) in anhydrous benzene (15 mL), and TMAD (0.572 g, 3.30 mmole, 1.5 eq.). The reaction mixture left to stir at room temperature for 4 days. Sulfonamide **39** was isolated as a yellow solid (1.056 g, 92%, R_f 0.37 (hexane: ethyl acetate, 4:1)); LRMS EI^+ *m/z* 343 $(M)^+$; HRMS EI^+ *m/z* 343.01089 $(M)^+$ (calculated for $C_{14}H_{14}{}^{35}ClNO_3S_2$, 343.01037 (Dev. 1.53 ppm)); ν_{max} (film)/cm^{-1} 3098 (thiophene C-H), 3082 (aryl C-H), 3001 (C-H), 2962 (C-H), 2937 (C-H), 1646 (C=C), 1355 (SO_2), 1155 (SO_2); δ_H (360 MHz, $CDCl_3$): 3.81 (s, 3H, *H*7), 4.20 (dt, 2H, *J* = 6.3, 1.3 Hz, *H*8), 5.10 (dd, 1H, *J* = 10.0, 1.4 Hz, $H10_{cis}$), 5.13 (dd, 1H, *J* = 18.4, 1.4 Hz, $H10_{trans}$), 5.59 – 5.75 (m, 1H, *H*9), 6.86 (d, 2H, *J* = 6.8 Hz, *H*2, *H*6), 6.93 (d, 1H, *J* = 4.0 Hz, *H*12), 7.04 (d, 2H, *J* = 6.8 Hz, *H*3, *H*5), 7.16 (d, 1H, J = 4.0 Hz, *H*13); δ_C (63 MHz, $(CD_3)_2SO$): 53.8 (*C*8), 56.0 (*C*7), 114.9 (2 x CH_{Ar}), 119.8 (*C*10), 129.1 (CH_{Ar}), 130.6 (2 x CH_{Ar}), 131.2 (*C*), 133.4 (C_{Ar}), 133.6 (C_{Ar}), 136.2 (C_{Ar}), 136.9 (C_{Ar}), 159.5 (C_{Ar}); Mpt. 88.7 – 90.2 °C.

5-Chloro-*N*-[(5-chloro-2-thienyl)sulfonyl]-*N*-[4-(trifluoromethyl)phenyl]thiophene-2-sulfonamide (43)

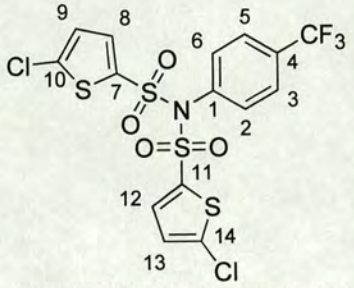

To a solution of 4-(trifluoromethyl)aniline (2.88 g, 23.0 mmole, 1.1 eq.) in THF (25 ml), 5-chlorothiophene-2-sulfonyl chloride (4.53 g, 20.8 mmole, 1.0 eq.) and DIPEA (3.63 mL) was added. The reaction mixture was allowed to stir overnight at room temperature before being concentrated *in vacuo* to afford a brown residue that was neutralized with HCl (conc.) and extracted into EtOAc. The organics were combined and concentrated *in vacuo* to afford a residue that was columned on silica (hexane: ethyl acetate, 4:1). Appropriate fractions were combined and concentrated *in vacuo* to afford a white solid (1.62 g, 23%); LRMS EI^+ *m/z* 520 $(M)^+$; HRMS EI^+ *m/z* 520.86684 $(M)^+$ ((calculated for $C_{15}H_8{}^{35}Cl_2F_3NO_4S_4$, 520.86653 (Dev. 0.60 ppm)); ν_{max} (film)/cm^{-1} 3111 (thiophene C-H), 3086 (aryl C-H), 1318 (SO_2), 1132 (SO_2); δ_H (250 MHz, $CDCl_3$): 7.00 (d, 2H, *J* = 4.0 Hz, *H*9, *H*13), 7.28 (d, 2H, *J* = 8.2 Hz, *H*2, *H*6), 7.56 (d, 2H, *J* = 4.0 Hz, *H*8, *H*12), 7.69 (d, 2H, *J* = 8.2 Hz, *H*3, *H*5); δ_C (63 MHz, $CDCl_3$): 123.6 (q, J_{CF} = 273 Hz, CF_3), 126.8 (q, J_{CF} = 4 Hz, *C*3, *C*5), 127.0 (2 x CH_{Ar}), 131.6 (2 x CH_{Ar}), 135.5 (2 x CH_{Ar}), 132.7 (q, J_{CF} = 33 Hz, C4), 135.9 (2 x C_{Ar}), 136.6 (*C*1), 140.9 (2 x C_{Ar}); Mpt. 221.5 – 222.4 °C.

4,5-Dibromo-*N*-[4-(trifluoromethyl)phenyl]thiophene-2-sulfonamide (46)

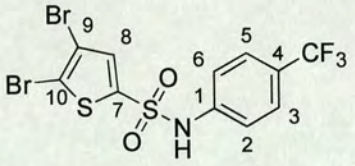

General procedure **L4** was followed. Sulfonamide **46** was isolated as a white solid (0.071 g, 38%, R_f 0.53 (hexane: ethyl acetate, 2:1)); LRMS FAB$^+$ *m/z* 466 $(MH)^+$; HRMS FAB$^+$ *m/z* 465.82124 $(MH)^+$ (calculated for $C_{11}H_7{}^{79}Br^{81}BrF_3NO_2S_2$, 465.82179 (Dev. –1.18 ppm)); ν_{max} (film)/cm^{-1} 3260 (N-H), 3106 (thiophene C-H), 3054 (aryl C-H), 1337 (SO_2), 1156 (SO_2); δ_H (250 MHz, $CDCl_3$): 7.20 (d, 2H, *J* = 8.4 Hz, *H*2, *H*6), 7.33 (s, 1H, *H*8), 7.35 (s, 1H, N*H*), 7.53 (d, 2H, *J* = 8.4 Hz, *H*3, *H*5);

4,5-Dibromo-*N*-(4-chlorophenyl)thiophene-2-sulfonamide (48)

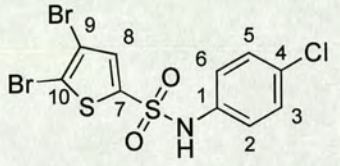

General procedure **L4** was followed. Sulfonamide **48** was isolated as a yellow solid (0.009 g, 5%, R_f 0.53 (hexane: ethyl acetate, 2:1)); LRMS FAB$^+$ *m/z* 432 $(MH)^+$; HRMS FAB$^+$ *m/z* 431.79633 $(MH)^+$ (calculated for $C_{10}H_7{}^{79}Br^{81}Br^{35}ClNO_2S_2$, 431.79543 (Dev. 2.08 ppm)); δ_H (250 MHz, $CDCl_3$): 6.91 (s, 1H, N*H*), 7.04 (d, 2H, *J* = 6.7 Hz, *H*2, *H*6), 7.23 (s, 1H, *H*8), 7.24 (d, 2H, *J* = 6.7 Hz, *H*3, *H*5).

4,5-Dibromo-*N*-(3,5-dichlorophenyl)thiophene-2-sulfonamide (49)

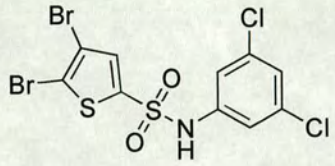

General procedure **L1** was followed. Sulfonamide **49** was isolated as a cream solid (0.001 g, 1 %, HPLC Method R, t_R 8.21 min); LRMS ES^- *m/z* 463.9 $(M-H)^-$.

***N*-[3,5-Bis(trifluoromethyl)phenyl]-4,5-dibromothiophene-2-sulfonamide (50)**

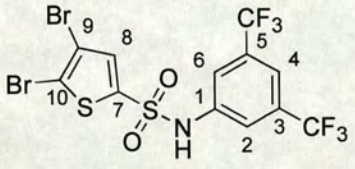

General procedure **L4** was followed. Sulfonamide **50** was isolated as a white solid (0.003 g, 1%, R_f 0.58 (hexane: ethyl acetate, 2:1)); LRMS FAB^+ *m/z* 534 $(MH)^+$; HRMS FAB^+ *m/z* 533.80129 $(MH)^+$ (calculated for $C_{12}H_6{}^{79}Br^{81}BrF_6NO_2S_2$, 533.80917 (Dev. 2.1 ppm)); δ_H (250 MHz, $CDCl_3$): 7.21 (s, 1H, N*H*), 7.34 (s, 1H, *H*8), 7.55 (s, 2H, *H*2, *H*6), 7.64 (s, 1H, *H*4).

4,5-Dibromo-*N*-(2,4,5-trichlorophenyl)thiophene-2-sulfonamide (51)

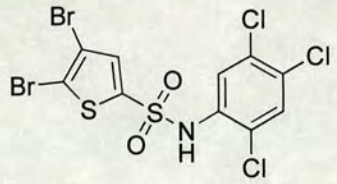

General procedure **L1** was followed. Sulfonamide **51** was isolated as a white solid (0.001 g, 1%, HPLC Method R, t_R 8.49 min). LRMS ES$^-$ *m/z* 497.9 $(M-H)^-$ assigned to $C_{10}H_3{}^{79}Br^{81}Br^{35}Cl_3NO_2S_2$.

5-Chloro-*N*-[4-(trifluoromethyl)phenyl]thiophene-2-sulfonamide (52)[207]

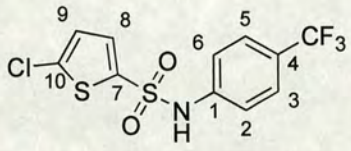

To a stirring solution of 4-(trifluoromethyl)aniline (0.498 g, 3.1 mmole, 1.1 eq.) in anhydrous pyridine (4 mL), a solution of 5-chlorothiophene-2-sulfonyl chloride (0.610 g, 2.8 mmole, 1.0 eq.) in anhydrous pyridine (2 mL) was added. The reaction mixture was allowed to stir at room temperature overnight before being washed with HCl (1M, 25 mL) and extracted into ethyl acetate (3 x 25 mL). The combined organics were washed with brine (2 x 25 mL) and dried over anhydrous magnesium sulfate before being concentrated *in vacuo* to afford a brown oil. The oil was purified on silica (hexane: ethyl acetate: DCM, 3:2:1). Appropriate fractions were combined and concentrated *in vacuo* to afford sulfonamide **52** as a white solid (0.682g, 71%, R_f 0.61(hexane: ethyl acetate: DCM, 3:2:1)); LRMS FAB$^+$ 342 $(MH)^+$; HRMS FAB$^+$ *m/z* 341.96464 $(MH)^+$ ((calculated for $C_{11}H_8{}^{35}ClF_3NO_2S_2$, 341.96371 (Dev. 2.72 ppm)); ν_{max} (film)/cm^{-1} 3261 (N-H), 3107 (thiophene C-H), 3011 (aryl C-H), 1342 (SO_2), 1162 (SO_2); δ_H (250 MHz, $CDCl_3$): 6.87 (d, 1H, *J* = 4.1 Hz, *H*9), 7.23 (bs, 1H, N*H*), 7.25 (d,

2H, J = 9.2 Hz, *H*2, *H*6), 7.36 (d, 1H, J = 4.1 Hz, *H*8), 7.55 (d, 2H, J = 9.2 Hz, *H*3, *H*5); δ_C (63 MHz, $CDCl_3$): 120.7 (2 x CH_{Ar}), 124.2 (q, J_{CF} = 272 Hz, CF_3), 127.3 (CH_{Ar}), 127.4 (2 x CH_{Ar}), 127.5 (q, J_{CF} = 35 Hz, *C*4), 133.3 (CH_{Ar}), 137.1 (C_{Ar}), 139.1 (C_{Ar}), 139.5 (C_{Ar}); Mpt. 97.5 – 97.7 °C.

5-Chloro-*N*-(4-chlorophenyl)thiophene-2-sulfonamide (54)[206]

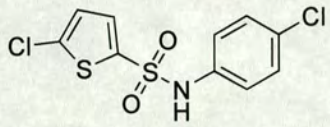

General procedure **L1** was followed. Sulfonamide **54** was isolated as a white solid (0.001 g, 1 %, HPLC Method R, t_R 8.45 min); LRMS ES^- *m/z* 306.1 $(M-H)^-$.

5-Chloro-*N*-(3,5-dichlorophenyl)thiophene-2-sulfonamide (55)

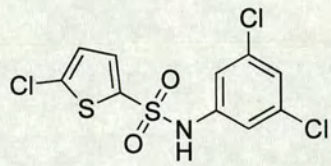

General procedure **L1** was followed. Sulfonamide **55** was isolated as a white solid (0.001 g, 1%, HPLC Method R, t_R = 8.09 min); LRMS ES^- *m/z* 340.0 $(M-H)^-$ assigned to $C_{10}H_5{}^{35}Cl_3NO_2S_2$.

N-[3,5,-Bis(trifluoromethyl)phenyl]-5-chlorothiophene-2-sulfonamide (56)

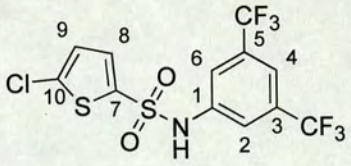

To a stirring solution of 3,5-bis(trifluoromethyl)aniline (396 μL, 2.50 mmole, 1.1 eq.) in pyridine (4 mL) a solution of 5-chlorothiophene-2-sulfonyl chloride (0.500 g, 2.30 mmole, 1.0 eq.) in pyridine (4 mL) was added. The reaction mixture was allowed to stir at room temperature for 24 hours before being concentrated *in vacuo* to afford a brown residue. The residue was dissolved in ethyl acetate (50 mL) and washed with HCl (1M, 2 x 50 mL); brine (50 mL) and concentrated *in vacuo* to afford a residue that was columned on silica (hexane: ethyl acetate) to afford sulfonamide **56** as a white solid (0.631 g, 67%, R_f 0.56 (hexane: ethyl acetate, 2:1)); LRMS ES^- *m/z* 408.0 $(M-H)^-$; δ_H (250 MHz, $CDCl_3$): 6.85 (d, 1H, *J* = 4.1 Hz, *H*9), 7.31 (s, 1H, N*H*), 7.34 (d, 1H, *J* = 4.1 Hz, *H*8), 7.54 (s, 2H, *H*2, *H*6), 7.60 (s, 1H, *H*4).

5-[2-(Methylthio)pyrimidin-5-yl]-*N*-phenylthiophene-2-sulfonamide (58)

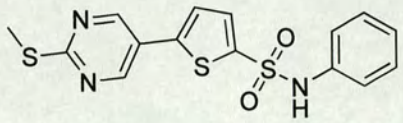

General procedure **L2** was followed. Sulfonamide **58** was isolated as a white solid (0.003 g, 4%, HPLC Method R, t_R 8.52 min); LRMS ES$^-$ *m/z* 362.0 $(M-H)^-$.

5-[2-(Methylthio)pyrimidin-5-yl]-*N*-[4-(trifluoromethyl)phenyl]thiophene-2-sulfonamide (59)

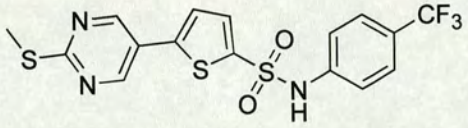

General procedure **L2** was followed. Sulfonamide **59** was isolated as a white solid (0.002 g, 2%, HPLC Method R, t_R 11.01 min); LRMS ES$^-$ *m/z* 430.1 $(M-H)^-$; ν_{max} (film)/cm^{-1} 3265 (N-H), 3056 (aryl C-H), 2929 (C-H), 1585 (aryl C=C), 1325 (SO_2), 1158 (SO_2).

***N*-(4-Chlorophenyl)-5-[2-(methylthio)pyrimidin-5-yl]thiophene-2-sulfonamide (60)**

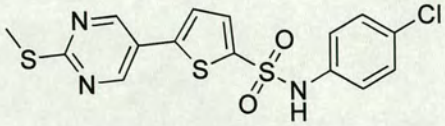

General procedure **L2** was followed. Sulfonamide **60** was isolated as a white solid (0.003 g, 4%, HPLC Method R, t_R 10.17 min); LRMS ES$^-$ *m/z* 395.9 $(M-H)^-$ calculated for $C_{15}H_{12}{}^{35}ClN_3O_2S_2$

N-(4-Methylphenyl)-5-[2-(methylthio)pyrimidin-5-yl]thiophene-2-sulfonamide (61)

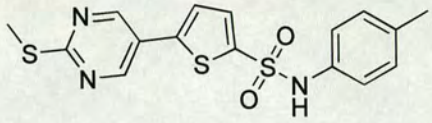

General procedure **L2** was followed. Sulfonamide **61** was isolated as a cream solid (0.001 g, 1%, HPLC Method R, t_R 9.38 min); LRMS ES$^-$ *m/z* 376.1 $(M-H)^-$.

N-(3,5-Dichorophenyl)-5-[2-(methylthio)pyrimidin-5-yl]thiophene-2-sulfonamide (62)

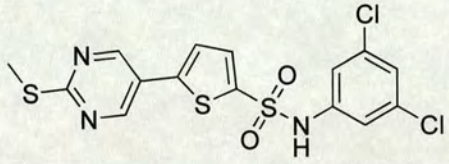

General procedure **L2** was followed. Sulfonamide **62** was isolated as a white solid (0.001 g, 1%, HPLC Method R, t_R 9.01 min); LRMS ES$^-$ *m/z* 429.9 $(M-H)^-$ assigned to $C_{15}H_{10}{}^{35}Cl_2N_3O_2S_3$.

N-(4-Fluorophenyl)-5-[2-(methylthio)pyrimidin-5-yl]thiophene-2-sulfonamide (63)

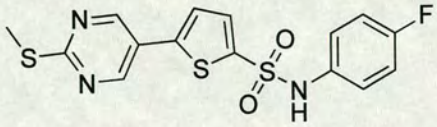

General procedure **L2** was followed. Sulfonamide **63** was isolated as a white solid (0.001 g, 1%, HPLC Method R, t_R 9.17 min); LRMS ES$^-$ *m/z* 380.1 $(M-H)^-$.

_N_-[3,5-Bis(trifluoromethyl)phenyl]-5-[2-(methylthio)pyrimidin-5-yl]thiophene-2-sulfonamide (64)

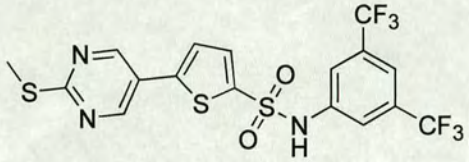

General procedure **L2** was followed. Sulfonamide **64** was isolated as a cream solid (0.002 g, 2%, HPLC Method R, t_R 8.31 min); LRMS ES$^-$ *m/z* 498.0 $(M-H)^-$.

_N_-(2,4-Dichloro-phenyl)-5-[2-(methylthio)pyrimidin-5-yl]thiophene-2-sulfonamide (65)

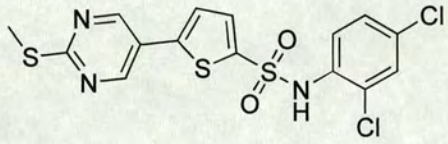

General procedure **L2** was followed. Sulfonamide **65** was isolated as a white solid (0.001 g, 1%, HPLC Method R, t_R 8.34 min); LRMS ES- *m/z* 429.9 $(M-H)^-$ assigned to $C_{15}H_{10}{}^{35}Cl_2N_3S_3O_2$.

4-(1,3-Oxazol-2-yl)-_N_-[4-(trifluoromethyl)phenyl]benzenesulfonamide (67)

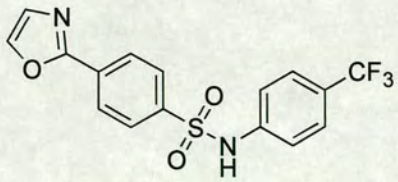

General procedure **L2** was followed. Sulfonamide **67** was isolated as a white solid (0.007 g, 10%, HPLC Method R, t_R 9.02 min); LRMS ES$^-$ *m/z* 367.1 $(M-H)^-$.

N-(4-Chlorophenyl)-4-(1,3-oxazol-2-yl)benzenesulfonamide (68)

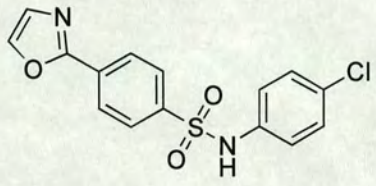

General procedure **L2** was followed. Sulfonamide **68** was isolated as a white solid (0.007 g, 10%, HPLC Method R, t_R 8.13 min); LRMS ES$^-$ *m/z* 333.1 $(M-H)^-$.

N-(4-Methylphenyl)-4-(1,3-oxazol-2-yl)benzenesulfonamide (69)

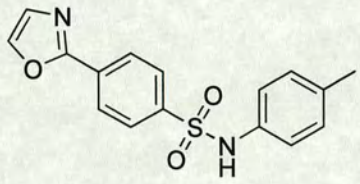

General procedure **L2** was followed. Sulfonamide **69** was isolated as a white solid (0.001 g, 1%, HPLC Method R, t_R 8.48 min); LRMS ES$^-$ *m/z* 313.2 $(M-H)^-$.

N-(3,5-Dichlorophenyl)-4-(1,3-oxazol-2-yl)benzenesulfonamide (70)

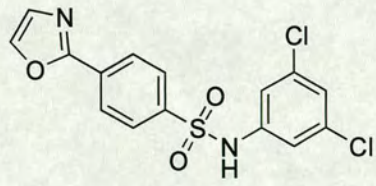

General procedure **L2** was followed. Sulfonamide **70** was isolated as a white solid (0.001 g, 1%, HPLC Method R, t_R 9.04 min); LRMS ES$^-$ *m/z* 367.0 $(M-H)^-$ assigned to $C_{15}H_9{}^{35}Cl_2N_2O_3S$.

N-(4-Fluorophenyl)-4-(1,3-oxazol-2-yl)benzenesulfonamide (71)

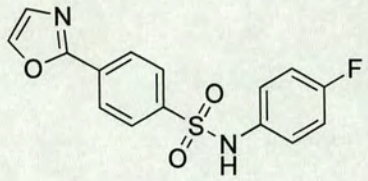

General procedure **L2** was followed. Sulfonamide **71** was isolated as a white solid (0.001 g, 2%, HPLC Method R, t_R 7.59 min); LRMS ES^- *m/z* 317.1 $(M-H)^-$.

N-[3,5-Bis(trifluoromethyl)phenyl]-4-(1,3-oxazol-2-yl)benzenesulfonamide (72)

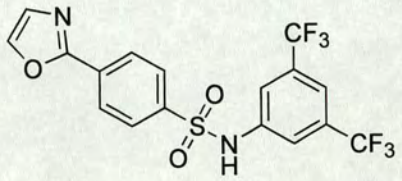

General procedure Library **L2** was followed. Sulfonamide **72** was isolated as a white solid (0.001 g, 1%, HPLC Method R, t_R 9.13 min); LRMS ES^- *m/z* 435.1 $(M-H)^-$.

4-Bromo-5-chloro-N-phenylthiophene-2-sulfonamide (74)

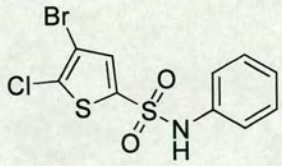

General procedure **L2** was followed. Sulfonamide **74** was isolated as a yellow solid (0.001 g, 1%, HPLC Method R, t_R 8.22 min); LRMS ES^- *m/z* 349.9 $(M-H)^-$ assigned to $C_{10}H_6{}^{79}Br^{35}ClNO_2S_2$.

4-Bromo-5-chloro-*N*-[4-(trifluoromethyl)phenyl]thiophene-2-sulfonamide (75)

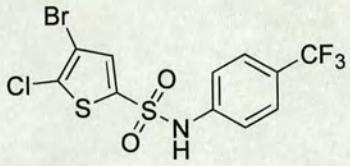

General procedure **L2** was followed. Sulfonamide **75** was isolated as a yellow solid (0.001 g, 1%, HPLC Method R, t_R 8.25 min); LRMS ES^- *m/z* 419.9 $(M-H)^-$ assigned to $C_{11}H_5{}^{79}Br^{35}ClF_3NO_2S_2$.

4-Bromo-5-chloro-*N*-(4-chlorophenyl)thiophene-2-sulfonamide (76)

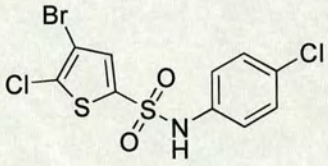

General procedure **L2** was followed. Sulfonamide **76** was isolated as a yellow solid (0.001 g, 1%, HPLC Method R, t_R 8.27 min); LRMS ES^- *m/z* 383.8 $(M-H)^-$ assigned to $C_{10}H_5{}^{79}Br^{35}Cl_2NO_2S_2$.

4-Bromo-5-chloro-*N*-(4-methylphenyl)thiophene-2-sulfonamide (77)

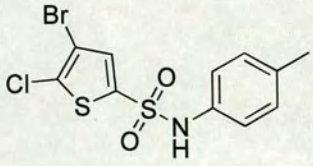

General procedure **L2** was followed. Sulfonamide **77** was isolated as a yellow solid (0.001 g, 2%, HPLC Method R, t_R 8.52 min); LRMS ES^- *m/z* 363.8 $(M-H)^-$ assigned to $C_{11}H_8{}^{79}Br^{35}ClNO_2S_2$.

_N_-[3,5-Bis(trifluoromethyl)phenyl]-4-bromo-5-chlorothiophene-2-sulfonamide (80)

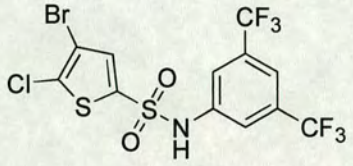

General procedure **L2** was followed. Sulfonamide **80** was isolated as a yellow solid (0.001 g, 1%, HPLC Method R, t_R 9.22 min); LRMS ES$^-$ *m/z* 485.9 $(M-H)^-$ assigned to $C_{12}H_4{}^{79}Br^{35}ClNO_2S_2$.

4-Bromo-5-chloro-_N_-(2,4-dichlorophenyl)thiophene-2-sulfonamide (81)

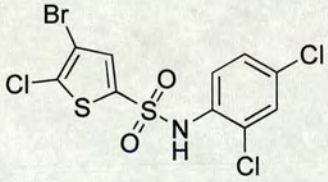

General procedure **L2** was followed. Sulfonamide **81** was isolated as a yellow solid (0.001 g, 1%, HPLC Method R, t_R 9.12 min); LRMS ES$^-$ *m/z* 417.9 $(M-H)^-$ assigned to $C_{10}H_4{}^{79}Br^{35}Cl_3NO_2S_2$.

5-Bromo-*N*-phenylthiophene-2-sulfonamide (82)[208]

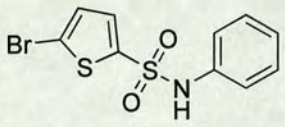

General procedure **L2** was followed. Sulfonamide **82** was isolated as a yellow solid (0.002 g, 3%, HPLC Method R, t_R 8.58 min); LRMS ES$^-$ *m/z* 315.9 $(M-H)^-$ assigned to $C_{10}H_8{}^{79}BrNO_2S_2$.

5-Bromo-N-[4-(trifluoromethyl)phenyl]thiophene-2-sulfonamide (83)[207]

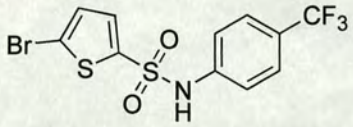

General procedure **L2** was followed. Sulfonamide **83** was isolated as a yellow solid (0.001 g, 1%, HPLC Method R, t_R 8.28 min); LRMS ES$^-$ *m/z* 385.9 $(M-H)^-$ assigned to $C_{10}H_6{}^{81}BrF_3NO_2S_2$.

Also prepared by an alternative method:

To a stirring solution of 5-bromothiophene-2-sulfonyl chloride (0.800 g, 3.06 mmole, 1.0 eq.) in DCM (10 mL) was added 4-(trifluoromethyl)aniline (420 µL, 3.37 mmole, 1.1 eq.) and pyridine (247 µL, 3.06 mmole, 1.0 eq.). The reaction mixture was allowed to stir at room temperature for 24 hours before being concentrated *in vacuo* to afford a brown residue. The residue was dissolved in ethyl acetate (50 mL) and washed with HCl (1M, 2 x 50 mL); brine (50 mL) and concentrated *in vacuo* to afford a pale yellow solid that was columned on silica (hexane: ethyl acetate, 2: 1) to afford sulfonamide **83** (1.055 g, 89%, R_f 0.51 (hexane: ethyl acetate, 2:1), ES$^-$ *m/z* 386.0 $(M-H)^-$) which was used

directly for the synthesis of sulfonamides **193**, **199**, **205**, **212** and **219** without further characterization.

5-Bromo- *N*-(4-chlorophenyl)thiophene-2-sulfonamide (84)

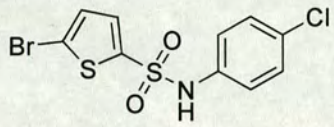

General procedure **L2** was followed. Sulfonamide **84** isolated as a yellow solid (0.001 g, 2%, HPLC Method R, t_R 8.50 min); LRMS ES$^-$ *m/z* 352.0 $(M-H)^-$ assigned to $C_{10}H_6{}^{79}Br^{35}ClNO_2S_2$.

5-Bromo-*N*-(4-methylphenyl)thiophene-2-sulfonamide (85)

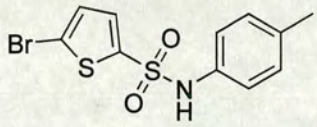

General procedure **L2** was followed. Sulfonamide **85** was isolated as a yellow solid (0.001 g, 1%, HPLC Method R, t_R 9.24 min); LRMS ES$^-$ *m/z* 329.9 $(M-H)^-$ assigned to $C_{11}H_{10}{}^{79}BrNO_2S_2$.

5-Bromo-*N*-(3,5-dichlorophenyl)thiophene-2-sulfonamide (86)

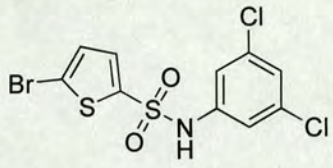

General procedure **L2** was followed. Sulfonamide **86** was isolated as a yellow solid (0.001 g, 1%, Method R, 8.49 min); LRMS ES$^-$ *m/z* 385.8 (M-H)$^-$ assigned to $C_{10}H_6{}^{81}Br^{35}Cl_2NO_2S_2$.

***N*-[3,5-Bis(trifluoromethyl)phenyl]-5-bromothiophene-2-sulfonamide (88)**

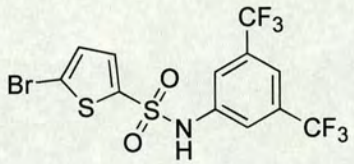

General procedure **L2** was followed. Sulfonamide **88** was isolated as a yellow solid (0.001 g, 1%, Method R, 8.07 min); LRMS ES$^-$ *m/z* 453.9 (M-H)$^-$.

Also prepared by an alternative method:

To a stirring solution of 5-bromothiophene-2-sulfonyl chloride (0.800 g, 3.06 mmole, 1.0 eq.) in DCM (10 mL) was added 3,5-bis(trifluoromethyl)aniline (476μL, 3.37 mmole, 1.1 eq.) and pyridine (247 μL, 3.06 mmole, 1.0 eq.). The reaction mixture was allowed to stir at room temperature for 24 hours before being concentrated *in vacuo* to afford a brown residue. The residue was dissolved in ethyl acetate (50 mL) and washed with HCl (1M, 2 x 50 mL); brine (50 mL) and concentrated *in vacuo* to afford a pale yellow solid that was columned on silica (hexane: ethyl acetate, 2: 1) to afford sulfonamide **88** (0.994 g, 72%, R_f 0.53 (hexane: ethyl acetate, 2:1), ES$^-$ *m/z* 453.8 (M-

H)⁻) which was used directly for the synthesis of sulfonamides **191**, **197**, **204**, **211** and **218** without further characterization.

5-Bromo-*N*-(2,4-dichlorophenyl)thiophene-2-sulfonamide (89)

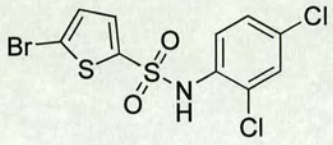

General procedure **L2** was followed. Sulfonamide **89** was isolated as a yellow solid (0.001 g, 1%, Method R, t_R 8.27 min); LRMS ES⁻ *m/z* 383.8 $(M-H)^-$ calculated for $C_{10}H_7{}^{79}Br^{35}Cl_2NO_2S_2$.

3-Nitro-*N*-phenylbenzenesulfonamide (90)[209]

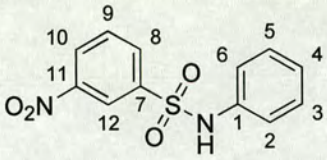

General procedure **L2b** was followed. Sulfonamide **90** was isolated as a white solid (0.016 g, 28%); LRMS ES⁻ *m/z* 277.0 $(M-H)^-$; δ_H (250 MHz, $CDCl_3$): 6.77 (s, 1H, NH), 7.00 – 7.22 (m, 5H, Ar*H*), 7.62 (t, 1H, *J* = 7.8 Hz, *H*9), 8.08 (ddd, 1H, *J* = 7.8, 1.9, 1.0 Hz, *H*10), 8.37 (ddd, 1H, *J* = 7.8, 2.2, 1.1 Hz, *H*8), 8.67 (t, 1H, *J* = 2.2 Hz, *H*12).

3-Nitro-*N*-[4-(trifluoromethyl)phenyl]benzenesulfonamide (91)[210]

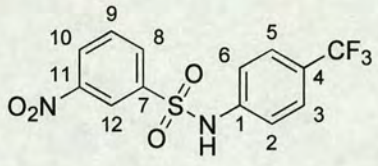

To a stirring solution of 3-nitrobenzenesulfonyl chloride (0.600 g, 2.71 mmole, 1.0 eq.) in DCM (10 mL), 4-(trifluoromethyl)aniline (374 μL, 2.98 mmole, 1.10 eq.) and pyridine (218 μL, 2.71 mmole, 1.0 eq.) were added. The reaction mixture was allowed to stir at room temperature for 24 hours before being concentrated *in vacuo*. The crude residue was columned on silica (Hexane: Ethyl acetate, 2:1) to afford sulfonamide **91** as a pink solid (0.562 g, 60%); LRMS ES^- *m/z* 345.0 $(M-H)^-$; HRMS FAB^+ *m/z* $(MH)^+$ 347.03189 (calculated for $C_{13}H_{10}F_3N_2O_4$, 347.03134 (Dev. 1.58 ppm)); ν_{max} (film)/cm^{-1} 3271 (N-H), 3093 (thiophene C-H), 1618 (aryl C=C), 1534 (NO_2), 1354 (NO_2), 1334 (SO_2), 1168 (SO_2); δ_H (250 MHz, $CDCl_3$): 7.18 (d, 2H, *J* = 8.4 Hz, *H*2, *H*6), 7.47 (d, 2H, *J* = 8.4 Hz, *H*3, *H*5), 7.58 (s, 1H, N*H*), 7.65 (t, 1H, *J* = 8.1 Hz, *H*9), 8.08 (ddd, 1H, *J* = 8.1, 1.9, 1.0 Hz, *H*10), 8.37 (ddd, 1H, *J* = 8.1, 2.1, 1.0 Hz, *H*8), 8.67 (dd, 1H, *J* = 2.1, 1.9 Hz, *H*12); δ_C (63 MHz, $CDCl_3$): 120.8 (2 x CH_{Ar}), 122.8 (CH_{Ar}), 124.1 (q, J_{CF} = 272 Hz, CF_3), 127.4 (2 x CH_{Ar}), 128.0 (q, J_{CF} = 33 Hz, *C*4), 128.4 (*C*10), 131.2 (CH_{Ar}), 133.1 (CH_{Ar}), 139.2 (C_{Ar}), 141.1 (C_{Ar}), 148.8 (C_{Ar}); Mpt 109.6 – 110.4 °C (Lit. 110.5-111.0 °C); Mpt. 114.8 – 116.2 °C.

***N*-(4-Chlorophenyl)-3-nitrobenzenesulfonamide (92)[209]**

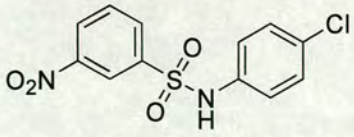

General procedure **L2b** was followed. Sulfonamide **92** was isolated as a brown solid (0.017 g, 30%); LRMS ES^- *m/z* 311.0 $(M-H)^-$.

_N_-(4-methylphenyl)-3-nitrobenzenesulfonamide (93)[211]

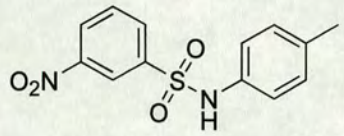

General procedure **L2b** was followed. Sulfonamide **93** was isolated as a yellow solid (0.017 g, 29%); LRMS ES$^-$ *m/z* 291.0 (M-H)$^-$.

_N_-(3,5-Dichlorophenyl)-3-nitrobenzenesulfonamide (94)

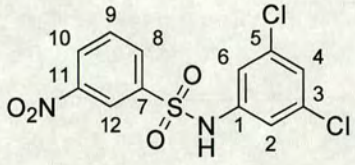

General procedure **L2b** was followed. Sulfonamide **94** was isolated as a yellow solid (0.021 g, 30%); LRMS ES$^-$ *m/z* 345.0 (M-H)$^-$ assigned to $C_{12}H_7{}^{35}Cl_2N_2O_4S$; δ_H (250 MHz, $CDCl_3$): 6.84 (s, 1H, NH), 6.98 (d, 2H, *J* = 1.8 Hz, *H*2, *H*6), 7.09 (t, 1H, *J* = 1.8 Hz, *H*4), 7.65 (t, 1H, *J* = 8.0 Hz, *H*9), 8.05 (ddd, 1H, *J* = 8.0, 1.8, 1.1 Hz, *H*10), 8.37 (ddd, 1H, *J* = 8.0, 1.8, 1.1 Hz, *H*8), 8.67 (t, 1H, *J* = 1.8 Hz, *H*12).

_N_-(4-Fluorophenyl)-3-nitrobenzenesulfonamide (95)

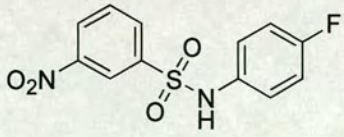

General procedure Library **L2b** was followed. Sulfonamide **95** was isolated as a yellow solid (0.017 g, 29%); LRMS ES$^-$ *m/z* 295.1 (M-H)$^-$.

_N_-[3,5-Bis(trifluoromethyl)phenyl]-3-nitrobenzenesulfonamide (96)

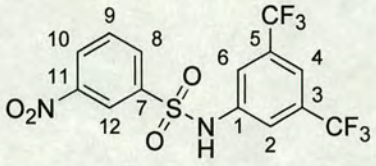

To a stirring solution of 3-nitrobenzenesulfonyl chloride (0.600 g, 2.71 mmole, 1.0 eq.) in DCM (10 mL), 3,5-bis(trifluoromethyl)aniline (463 μL, 2.98 mmole, 1.10 eq.) and pyridine (218 μL, 2.71 mmole, 1.0 eq.) were added. The reaction mixture was allowed to stir at room temperature for 24 hours before being concentrated *in vacuo*. The crude residue was columned on silica (Hexane: Ethyl acetate, 2:1) to afford sulfonamide **96** as a white solid (0.836 g, 77%); LRMS ES^- *m/z* 413.0 $(M-H)^-$; HRMS FAB^+ *m/z* 415.11893 $(MH)^+$ (calculated for $C_{14}H_9F_6N_2O_4S$, 415.01872 (Dev. 0.51 ppm)); ν_{max} (film)/cm^{-1} 3268 (N-H), 3102 (aryl C-H), 1608 (aryl C=C), 1537 (NO_2), 1377 (NO_2), 1354 (SO_2), 1132 (SO_2); δ_H (250 MHz, $CDCl_3$): 7.60 (s, 2H, *H*2, H6), 7.66 (s, 1H, N*H*), 7.67 (s, 1H, *H*4), 7.77 (t, 1H, *J* = 8.1 Hz, *H*9), 8.15 (dt, 1H, *J* = 8.1, 2.1 Hz, *H*10), 8.48 (dd, 1H, *J* = 8.1, 2.1 Hz, *H*8), 8.73 (t, 1H, *J* = 2.1 Hz, *H*12); δ_C (63 MHz, $CDCl_3$): 119.1 (CH_{Ar}), 120.4 (2 x CH_{Ar}), 122.4 (CH_{Ar}), 122.4 (q, J_{CF} = 273 Hz, CF_3), 128.2 (CH_{Ar}), 130.8 (CH_{Ar}), 132.3 (CH_{Ar}), 133.1 (q, J_{CF} = 34 Hz, *C*3, *C*5), 137.3 (C_{Ar}), 140.3 (C_{Ar}), 148.4 (C_{Ar}); Mpt. 133.8 – 134.2 °C.

N-(2,4-Dichlorophenyl)-3-nitrobenzenesulfonamide (97)[209]

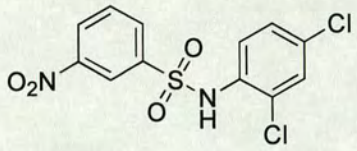

General procedure **L2b** was followed. Sulfonamide **97** was isolated as a yellow solid (0.004 g, 6%); LRMS ES$^-$ *m/z* 344.8 (M-H)$^-$ assigned to $C_{12}H_7{}^{35}Cl_2N_2O_2S$.

N-Phenyl-5-(phenylsulfonyl)thiophene-2-sulfonamide (98)

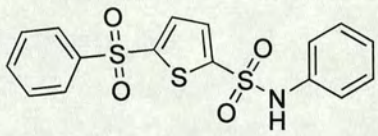

General procedure as set out for the resynthesis of Library **L2** was followed. Sulfonamide **98** was isolated as a beige solid (0.012 g, 16%); LRMS ES$^-$ *m/z* 378.0 (M-H)$^-$.

5-(Phenylsulfonyl)-N-[4-(trifluoromethyl)phenyl]thiophene-2-sulfonamide (99)

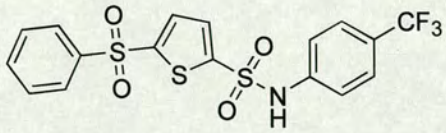

General procedure **L2b** was followed. Sulfonamide **99** was isolated as a yellow solid (0.005 g, 6%); LRMS ES$^-$ *m/z* 446.0 (M-H)$^-$.

N-(4-Chlorophenyl)-5-(phenylsulfonyl)thiophene-2-sulfonamide (100)

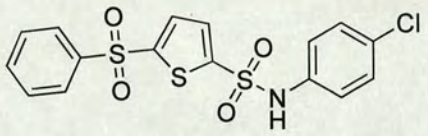

General procedure **L2b** was followed. Sulfonamide **100** was isolated as a yellow solid (0.006 g, 6%); LRMS ES$^-$ *m/z* 411.9 (M-H)$^-$.

N-(4-Methylphenyl)-5-(phenylsulfonyl)thiophene-2-sulfonamide (101)

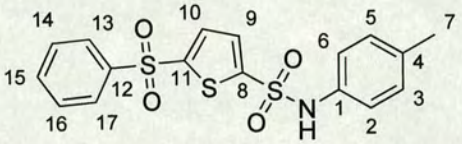

General procedure **L2b** was followed. Sulfonamide **101** was isolated as a yellow solid (0.010 g, 13%); LRMS ES$^-$ *m/z* 392.0 (M-H)$^-$; δ_H (250 MHz, $CDCl_3$): 2.26 (s, 3H, *H*7), 6.40 (s, 1H, N*H*), 6.90 (d, 2H, *J* = 8.4 Hz, *H*2, *H*6), 7.03 (d, 2H, *J* = 8.4 Hz, *H*3, *H*5), 7.23 (d, 1H, *J* = 4.0 Hz, thiophene *H*), 7.44 (d, 1H, *J* = 4.0 Hz, thiophene *H*), 7.46 – 7.55 (m, 3H, *H*14, *H*15, *H*16), 7.85 – 7.90 (m, 2H, *H*13, *H*17).

N-(3,5-Dichlorophenyl)-5-(phenylsulfonyl)thiophene-2-sulfonamide (102)

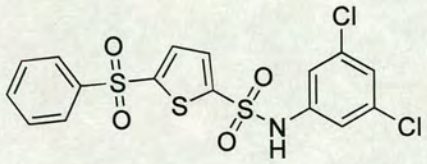

General procedure **L2b** was followed. Sulfonamide **102** was isolated as a brown solid (0.002 g, 2%); LRMS ES$^-$ *m/z* 446.0 (M-H)$^-$ assigned to $C_{16}H_{10}{}^{35}Cl_2NO_4S_3$.

N-(4-Fluorophenyl)-5-(phenylsulfonyl)thiophene-2-sulfonamide (103)

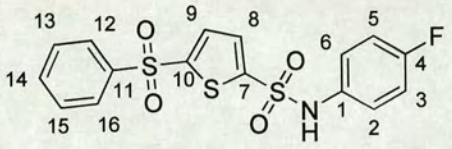

General procedure **L2b** was followed. Sulfonamide **103** was isolated as a yellow solid (0.015 g, 19%); LRMS ES$^-$ 396.1 (M-H)$^-$; δ_H (250 MHz, $CDCl_3$): 6.53 (s, 1H, N*H*), 6.89 – 7.05 (m, 4H, *Ar*H), 7.22 (d, 1H, J = 4.0 Hz, thiophene *H*), 7.45 (d, 1H, J = 4.0 Hz, thiophene *H*), 7.47 – 7.59 (m, 3H, *Ar*H), 7.84 – 7.90 (m, 2H, *Ar*H).

N-[3,5-Bis(trifluoromethyl)phenyl]-5-(phenylsulfonyl)thiophene-2-sulfonamide (104)

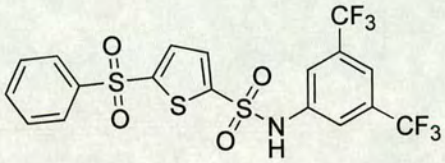

General procedure **L2b** was followed. Sulfonamide **104** was isolated as a yellow solid (0.003 g, 3%); LRMS ES$^-$ *m/z* 514.2 (M-H)$^-$.

N-(2,4-Dichlorophenyl)-5-(phenylsulfonyl)thiophene-2-sulfonamide (105)

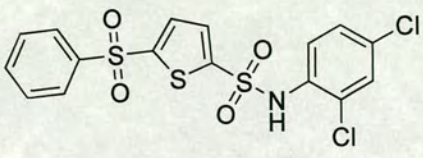

General procedure **L2b** was followed. Sulfonamide **105** was isolated as a brown solid (0.002 g, 3%); LRMS ES$^-$ *m/z* 446.0 (M-H)$^-$.

5-Chloro-*N*-(3-chlorophenyl)thiophene-2-sulfonamide (108)

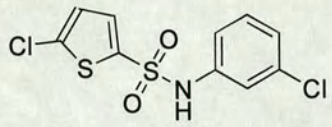

General procedure **L3** was followed. Sulfonamide **108** was isolated as a cream solid (0.008 g, 13%); LRMS ES$^-$ *m/z* 305.9 $(M-H)^-$.

5-Chloro-*N*-[3-(trifluoromethyl)phenyl]thiophene-2-sulfonamide (109)

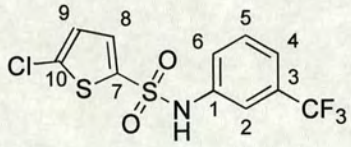

General procedure **L3** was followed. Sulfonamide 109 was isolated as a cream solid (0.026 g, 38%); LRMS ES$^-$ *m/z* 340.0 $(M-H)^-$; δ_H (250 MHz, $CDCl_3$): 6.87 (bs, 1H, N*H*), 6.88 (d, 1H, J = 4.0 Hz, *H*9), 7.32 (d, 1H, J = 4.0 Hz, *H*8), 7.33 – 7.37 (m, 1H, Ar*H*), 7.40 (s, 1H, *H*2), 7.45 – 7.47 (m, 2H, Ar*H*).

5-Chloro-*N*-(3,4-dichlorophenyl)thiophene-2-sulfonamide (110)

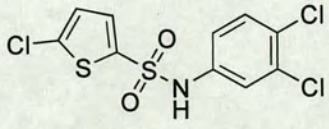

General procedure **L3** was followed. Sulfonamide **110** was isolated as a white solid (0.005 g, 7%); LRMS ES- *m/z* 339.8 $(M-H)^-$ assigned to $C_{10}H_5{}^{35}Cl_3NO_2S_2$.

4,5-Dibromo-*N*-[3-(trifluoromethyl)phenyl]thiophene-2-sulfonamide (112)

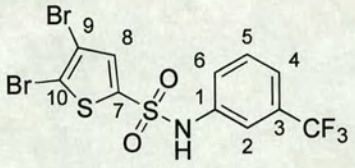

General procedure **L3** was followed. Sulfonamide **112** as a cream solid (0.011 g, 12%); LRMS ES$^-$ *m/z* 463.8 (M-H)$^-$ assigned to $C_{11}H_5{}^{79}Br^{81}BrF_3NO_2S_2$; ν_{max} (film)/cm^{-1} 3250 (N-H), 3107 (thiophene C-H), 2916 (C-H), 1328 (SO_2), 1156 (SO_2); δ_H (250 MHz, $CDCl_3$): 6.69 (s, 1H, N*H*), 7.26 (s, 1*H*, H8), 7.27 – 7.31 (m, 1H, Ar*H*), 7.33 (s, 1H, *H*2), 7.41 – 7.43 (m, 2H, Ar*H*); Mpt. 129.6 – 130.5 °C.

4,5-Dibromo-*N*-(3,4-dichlorophenyl)thiophene-2-sulfonamide (113)

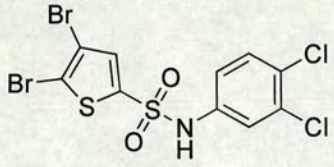

General procedure **L3** was followed. Sulfonamide **113** was isolated as a biege solid (0.007 g, 7%); LRMS ES$^-$ *m/z* 463.7 assigned to $C_{10}H_4{}^{79}Br^{81}Br^{35}Cl_2NO_2S_2$ (M-H)$^-$.

N-[3,5-Bis(trifluoromethyl)phenyl]-4-chloro-3-nitrobenzenesulfonamide (114)

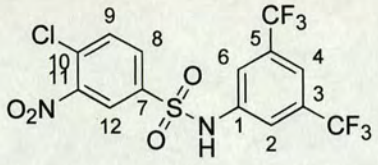

General procedure **L3** was followed. Sulfonamide **114** was isolated as a white solid (0.010 g, 11%); LRMS ES$^-$ *m/z* 447.0 $(M-H)^-$; ν_{max} (film)/cm^{-1} 3293 (N-H), 3083 (aryl C-H), 1534 (NO_2), 1375 (NO_2), 1355 (SO_2), 1162 (SO_2); δ_H (250 MHz, $CDCl_3$): 7.24 (s, 1H, N*H*), 7.60 (s, 2H, *H*2, *H*6), 7.70 (s, 1H, *H*4), 7.73 (d, 1H, *J* = 8.5 Hz, *H*9), 7.92 (dd, 1H, *J* = 2.3 Hz, 8.5Hz, *H*8), 8.35 (d, 1H, *J* = 2.3 Hz, *H*12); Mpt. 167.5 – 168.9 °C.

4-Chloro-*N*-(3-chlorophenyl)-3-nitrobenzenesulfonamide (115)

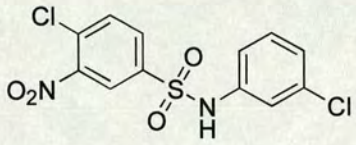

General procedure **L3** was followed. Sulfonamide **115** was isolated as a cream solid (0.004 g, 5%); LRMS ES$^-$ *m/z* 345.0 $(M-H)^-$;

4-Chloro-3-nitro-*N*-[3-(trifluoromethyl)phenyl]benzenesulfonamide (116)

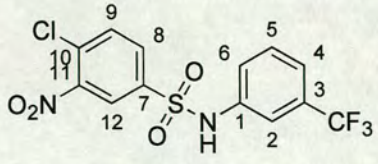

To a stirring solution of 4-chloro-3-nitrobenzenesulfonyl chloride (1.000 g, 3.9 mmole, 1.0 eq.) in DCM (10 mL), 3-(trifluoromethyl)aniline (575 μL, 4.3 mmole, 1.1 eq.) and

pyridine (315 μL, 4.3 mmole, 1.0 eq.) were added. The reaction mixture was allowed to stir at room temperature overnight before being washed with HCl (1M, 2 x 10 mL); H_2O (10 mL) and brine (10 mL) and concentrated *in vacuo* to afford a residue that was columned on silica (hexane: ethyl acetate, 1:1) to afford **116** as a pink solid (1.338 g, 90%); LRMS FAB^+ *m/z* 380 $(M)^+$; HRMS FAB^+ *m/z* 379.98582 $(M)^+$ (calculated for $C_{13}H_8{}^{35}ClF_3N_2O_4S$, 379.98454 (Dev. 3.38 ppm)); ν_{max} (film)/cm^{-1} 3272 (N-H), 3098 (aryl C-H), 1540 (NO_2), 1337 (NO_2), 1327 (SO_2), 1172 (SO_2); δ_H (250 MHz, $(CD_3)_2SO$): 7.43 – 7.57 (m, 4H, Ar*H*), 8.02 (s, 2H, Ar*H*), 8.48 (s, 1H, *H*12), 11.07 (s, 1H, N*H*); δ_C (63 MHz, $(CD_3)_2SO$): 116.4 (CH_{Ar}), 121.1 (CH_{Ar}), 123.4 (q, J_{CF} = 273 Hz, CF_3), 123.9 (CH_{Ar}), 124.0 (CH_{Ar}), 129.8 (q, J_{CF} = 32 Hz, *C*3), 130.1 (C_{Ar}), 130.7 (C_{Ar}), 131.0 (CH_{Ar}), 133.2 (CH_{Ar}), 137.5 (C_{Ar}), 138.8 (C_{Ar}), 147.2 (C_{Ar}); Mpt. 123.5 – 123.8 °C.

4-Chloro-*N*-(3,4-dichlorophenyl)-3-nitrobenzenesulfonamide (117)

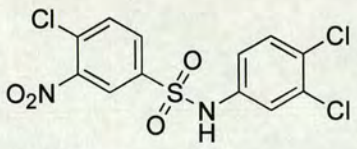

General procedure **L3** was followed. Sulfonamide **117** was isolated as a white solid (0.003 g, 4%); LRMS ES^- *m/z* 380.9 $(M-H)^-$ assigned to $C_{12}H_6{}^{37}Cl^{35}Cl_2N_2O_4S$.

***N*-[3,5-Bis(trifluoromethyl)phenyl]benzamide (118)**

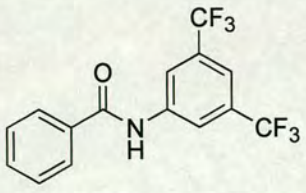

General procedure **L3** was followed. Amide **118** was isolated as a white solid (0.010 g, 15%); LRMS ES^+ *m/z* 334.1 $(MH)^+$.

N-(3-Chlorophenyl)benzamide (119)[212]

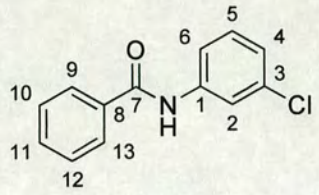

General procedure **L3** was followed. Amide **119** was isolated as a white solid (0.015 g, 31%); LRMS ES$^-$ *m/z* 229.9 (M-H)$^-$; δ_H (250 MHz, $CDCl_3$): 7.14 (d, 1H, *J* = 7.9 Hz, *H*4), 7.32 (d, 1H, *J* = 8.1 Hz, *H*6), 7.48 – 7.62 (m, 4H, Ar*H*, N*H*), 7.79 – 7.89 (m, 4H, Ar*H*).

N-[3-(Trifluoromethyl)phenyl]benzamide (120)

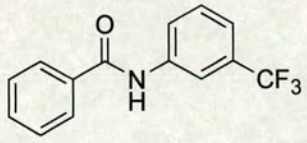

General procedure **L3** was followed. Amide **120** was isolated as a white solid (0.019 g, 36%); LRMS ES- *m/z* 264.0 (M-H)$^-$.

N-(3,4-Dichlorophenyl)benzamide (121)

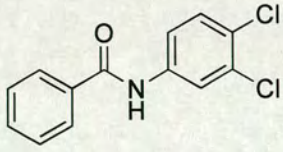

General procedure **L3** was followed. Amide 121 was isolated as a white solid (0.013 g, 24%); LRMS ES$^-$ *m/z* 264.0 (M-H)$^-$.

5-Chloro-*N*-(4-chlorophenyl)-3-methyl-1-benzothiophene-2-sulfonamide (122)

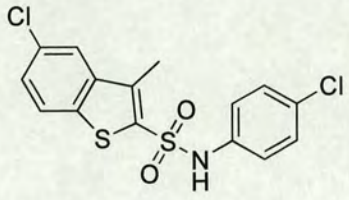

General procedure **L4** was followed. Sulfonamide **122** was isolated as a yellow solid (0.015 g, 10%, R_f 0.53 (hexane: ethyl acetate 2:1); LRMS FAB$^+$ *m/z* 371 $(M)^+$; HRMS FAB$^+$ *m/z* 370.96116 $(M)^+$ (calculated for $C_{15}H_{11}{}^{35}Cl_2NO_2S_2$, 370.96083 (Dev. 0.89 ppm)); δ_H (250 MHz, $CDCl_3$): 2,35 (s, 3H, C*H*$_3$), 6.89 (s, 1H, N*H*), 7.00 (d, 2H, *J* = 8.9 Hz, Ar*H*), 7.15 (d, 2H, Ar*H*), 7.38 (dd, 1H, *J* = 8.7, 1.9 Hz, benzothiophene *H*), 7.63 - 7.66 (m, 2H, benzothiophene *H*).

5-Chloro-*N*-[(1*R*)-1-(4-chlorophenyl)ethyl]-3-methyl-1-benzothiophene-2-sulfonamide (124)

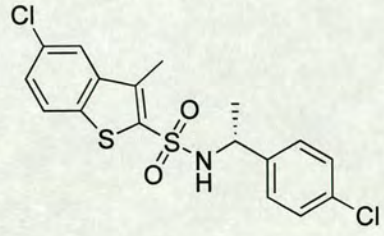

General procedure as set out for Library **L4** was followed. Sulfonamide **124** was isolated as a yellow solid (0.008 g, 5%, R_f 0.55 (hexane: ethyl acetate, 2:1)); LRMS FAB$^+$ *m/z* 399 $(M)^+$; HRMS FAB$^+$ *m/z* 398.99133 $(M)^+$ (calculated for $C_{17}H_{15}{}^{35}Cl_2NO_2S_2$, 398.99213 (Dev. – 2.01 ppm)); δ_H (250 MHz, $CDCl_3$): 1.39 (d, 3H, *J* = 6.9 Hz, CH(C*H*$_3$)), 1.52 (s, 3H, C*H*$_3$), 4.52 (dq, 1H, *J* = 6.9 Hz, C*H*(CH$_3$)), 5.00 (d, 1H, *J* = 6.9

Hz, N*H*), 6.99 (s, 4H, Ar*H*), 7.36 (dd, 1H, *J* = 8.6, 2.1 Hz, benzothiophene *H*), 7.61 – 7.66 (m, 2H, benzothiophene *H*).

_N_-[3,5-Bis(trifluoromethyl)phenyl]-5-chloro-3-methyl-1-benzothiophene-2-sulfonamide (126)

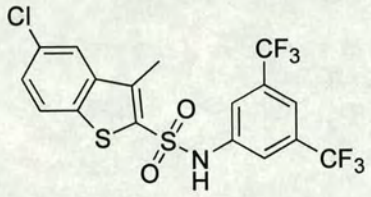

General procedure **L4** was followed. Sulfonamide **126** was isolated as a white solid (0.014 g, 7%, R_f 0.62 (hexane: ethyl acetate, 2:1)); LRMS FAB$^+$ *m/z* 474 $(MH)^+$; HRMS FAB$^+$ *m/z* 472.97412 $(MH)^+$ (calculated for $C_{17}H_{10}{}^{35}ClF_6NO_2S_2$, 472.97457 (Dev. – 0.83 ppm)); δ_H (250 MHz, $CDCl_3$): 2.51 (s, 3H, C*H*$_3$), 7.40 (dd, 1H, *J* = 8.7, 2.0 Hz, benzothiophene *H*), 7.51 (s, 1H, N*H*), 7.54 – 7.56 (m, 3H, benzothiophene *H*, Ar*H*), 7.67 (d, 1H, *J* = 8.7 Hz, benzothiophene *H*), 7.69 (s, 1H, Ar*H*).

_N_-[3,5-Bis(trifluoromethyl)benzyl]-5-chloro-3-methyl-1-benzothiophene-2-sulfonamide (127)

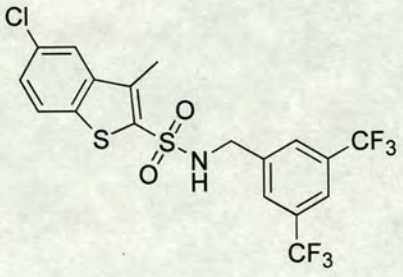

General procedure Library **L4** was followed. Sulfonamide **127** was isolated as a white solid (0.065 g, 33%, R_f 0.58 (hexane: ethyl acetate, 2:1)); LRMS FAB$^+$ *m/z* 488 $(MH)^+$; HRMS FAB$^+$ *m/z* 486.99120 $(MH)^+$ (calculated for $C_{18}H_{12}{}^{35}ClF_6NO_2S_2$, 486.99022

(Dev. 2.01 ppm)); δ_H (250 MHz, $CDCl_3$): 2.55 (s, 3H, C*H*$_3$), 4.36 (d, 2H, *J* = 6.4 Hz, C*H*$_2$NH), 5.30 (t, 1H, *J* = 6.4 Hz, N*H*), 7.40 (dd, 1H, *J* = 8.6, 2.0 Hz, benzothiophene *H*), 7.62 – 7.69 (m, 5H, Ar*H*).

5-Chloro-3-methyl-*N*-[4-(trifluoromethyl)phenyl]-1-benzothiophene-2-sulfonamide (128)

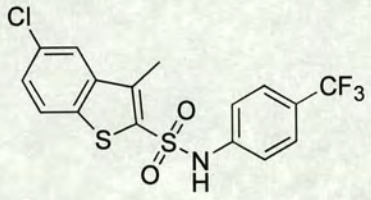

General procedure **L4** was followed. Sulfonamide **128** was isolated as a white solid (0.013 g, 8%, R_f 0.51 (hexane: ethyl acetate, 2:1)); LRMS FAB$^+$ *m/z* 406 $(MH)^+$; HRMS FAB$^+$ *m/z* 405.99450 $(MH)^+$ (calculated for $C_{16}H_{12}{}^{35}ClF_3NO_2S_2$, 405.99501 (Dev. – 1.25 ppm)); δ_H (250 MHz, $CDCl_3$): 2.46 (s, 3H, C*H*$_3$), 7.19 (d, 2H, *J* = 9.0 Hz, Ar*H*), 7.38 (dd, 1H, *J* = 8.6, 2.0 Hz, benzothiophene *H*), 7.46 (d, 2H, *J* = 9.0 Hz, Ar*H*), 7.63 – 7.68 (m, 2H, benzothiophene *H*).

***N*-(4-Chlorophenyl)-1-benzothiophene-2-sulfonamide (130)**

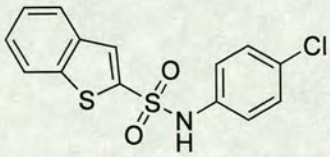

General procedure Library **L4** was followed. Sulfonamide **130** was isolated as a white solid (0.022 g, 17%, R_f 0.49 (hexane: ethyl acetate, 2:1)); LRMS FAB$^+$ *m/z* 324 $(MH)^+$; HRMS FAB$^+$ *m/z* 323.99185 $(MH)^+$ (calculated for $C_{14}H_{11}{}^{35}ClNO_2S_2$, 323.99198 (Dev. – 0.39 ppm)); δ_H (250 MHz, $CDCl_3$): 6.89 (d, 2H, *J* = 8.9 Hz, Ar*H*), 7.08 (d, 2H, *J* = 8.9

Hz, Ar*H*), 7.09 (s, 1H, N*H*), 7.37 – 7.41 (m, 2H, benzothiophene *H*), 7.77 – 7.82 (m, 1H, benzothiophene *H*), 8.07 – 8.11 (m, 2H, benzothiophene *H*).

_N_-(4-Chlorobenzyl)-1-benzothiophene-2-sulfonamide (131)

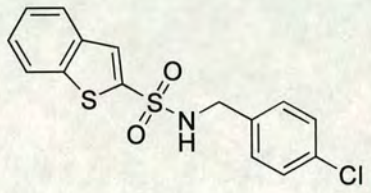

General procedure **L4** was followed. Sulfonamide **131** was isolated as a white solid (0.016 g, 12%, R_f 0.45 (hexane: ethyl acetate, 2:1)); LRMS FAB+ *m/z* 338 $(MH)^+$; HRMS FAB^+ *m/z* 338.00778 $(MH)^+$ (calculated for $C_{15}H_{13}{}^{35}ClNO_2S_2$, 338.00763 (Dev. 0.44 ppm)); δ_H (250 MHz, $CDCl_3$): 4.06 (d, 2H, *J* = 6.2 Hz, C*H*$_2$NH), 5.20 (t, 1H, *J* = 6.2 Hz, *N*H), 6.96 (d, 2H, *J* = 8.6 Hz, Ar*H*), 7.07 (d, 2H, *J*= 8.6 Hz, Ar*H*), 7.37 – 7.47 (m, 2H, benzothiophene *H*), 7.82 – 8.86 (m, 1H, benzothiophene *H*), 8.07 – 8.13 (m, 2H, benzothiophene *H*).

_N_-[(1*R*)-1-(4-chlorophenyl)ethyl]-1-benzothiophene-2-sulfonamide (132)

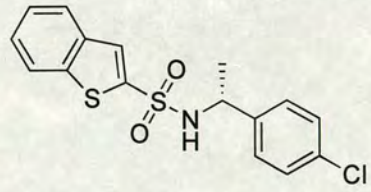

General procedure **L4** was followed. Sulfonamide **132** was isolated as a white solid (0.014 g, 10%, R_f 0.49 (hexane: ethyl acetate, 2:1)); LRMS FAB^+ *m/z* 352 $(MH)^+$; HRMS FAB^+ *m/z* 352.02293 $(MH)^+$ (calculated for $C_{16}H_{15}{}^{35}ClNO_2S_2$, 352.02328 (Dev. – 0.99 ppm)); δ_H (250 MHz, $CDCl_3$): 1.31 (d, 3H, *J* = 6.9 Hz, CH(C*H*$_3$)), 4.44 (dq, 1H, *J* = 6.9 Hz, C*H*(CH$_3$)), 5.14 (d, 1H, *J* = 6.9 Hz, N*H*), 6.80 (d, 2H, *J* = 8.5 Hz, Ar*H*), 6.88

(d, 2H, J = 8.5 Hz, Ar*H*), 7.36 – 7.40 (m, 2H, benzothiophene *H*), 7.75 – 7.79 (m, 1H, benzothiophene *H*), 7.90 (s, 1H, benzothiophene *H*), 8.00 – 8.04 (m, 1H, benzothiophene *H*).

_N_-[(1_S_)-1-(4-chlorophenyl)ethyl]-1-benzothiophene-2-sulfonamide (133)

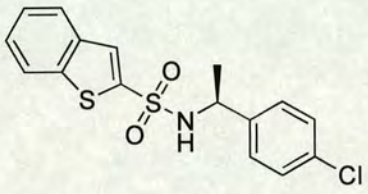

General procedure **L4** was followed. Sulfonamide **133** was isolated as a white solid (0.004 g, 3%, R_f 0.51 (hexane: ethyl acetate, 2:1)); LRMS FAB$^+$ *m/z* 352 $(MH)^+$; HRMS FAB$^+$ *m/z* 352.02254 $(MH)^+$ (calculated for $C_{16}H_{15}{}^{35}ClNO_2S_2$, 352.02328 (Dev. – 2.10 ppm)); δ_H (250 MHz, $CDCl_3$): 1.32 (d, 3H, J = 6.9 Hz, CH(C*H*$_3$)), 4.45 (dq, 1H, J = 6.9 Hz, C*H*(CH$_3$)), 4.89 (d, 1H, J = 6.9 Hz, N*H*), 6.80 (d, 2H, J = 8.4 Hz, Ar*H*), 6.89 (d, 2H, J = 8.4 Hz, Ar*H*), 7.37 – 7.42 (m, 2H, benzothiophene *H*), 7.76 – 7.79 (m, 1H, benzothiophene *H*), 7.89 (s, 1H, benzothiophene *H*), 7.98 – 8.02 (m, 1H, benzothiophene *H*).

_N_-[3,5-Bis(trifluoromethyl)phenyl]-1-benzothiophene-2-sulfonamide (134)

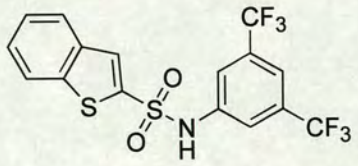

General procedure **L4** was followed. Sulfonamide **134** was isolated as a white solid (0.050 g, 29%, R_f 0.58 (hexane: ethyl acetate, 2:1)); LRMS FAB$^+$ *m/z* 426 $(MH)^+$; HRMS FAB$^+$ *m/z* 426.00487 $(MH)^+$ (calculated for $C_{16}H_{10}F_6NO_2S_2$, (Dev. – 1.98 ppm)); δ_H (250 MHz, $CDCl_3$): 7.27 (s, 1H, N*H*), 7.39 – 7.46 (m, 5H, benzothiophene *H*, Ar*H*),

7.82 – 7.84 (m, 1H, Ar*H*), 8.04 – 8.07 (m, 1H, benzothiophene *H*), 8.24 (s, 1H, benzothiophene *H*).

_N_-[3,5-Bis(trifluoromethyl)benzyl-1-benzothiophene-2-sulfonamide (135)

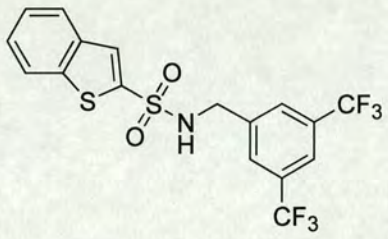

General procedure **L4** was followed. Sulfonamide **135** was isolated as a white solid (0.053g, 30%, R_f 0.53 (hexane: ethyl acetate, 2:1)); LRMS FAB$^+$ *m/z* 440 $(MH)^+$; HRMS FAB$^+$ *m/z* 440.02203 $(MH)^+$ (calculated for $C_{17}H_{12}F_6NO_2S_2$, 440.02137 (Dev. 1.51 ppm)); δ_H (250 MHz, $CDCl_3$): 4.26 (d, 2H, *J* = 6.4 Hz, CH_2NH), 5.28 (t, 1H, *J* = 6.4 Hz, N*H*); 7.40 – 7.45 (m, 2H, benzothiophene *H*), 7.49 (s, 2H, Ar*H*), 7.60 (s, 1H, Ar*H*), 7.80 – 7.84 (m, 1H, Ar*H*), 8.05 – 8.12 (m, 1H, benzothiophene *H*), 8.15 (s, 1H, benzothiophene *H*).

_N_-[4-(Trifluoromethyl)phenyl]-1-benzothiophene-2-sulfonamide (136)

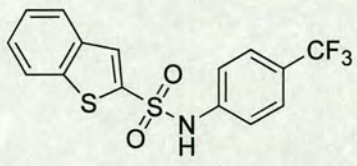

General procedure **L4** was followed. Sulfonamide **136** was isolated as a white solid (0.026 g, 18%, R_f 0.48 (hexane: ethyl acetate, 2:1)); LRMS FAB$^+$ *m/z* 358 $(MH)^+$; HRMS FAB$^+$ *m/z* 358.01782 $(MH)^+$ (calculated for $C_{15}H_{11}F_3NO_2S_2$, 358.01833 (Dev. – 1.42 ppm)); δ_H (250 MHz, $CDCl_3$): 7.09 (d, 2H, *J* = 8.3 Hz, Ar*H*), 7.22 (s, 1H, N*H*),

7.37 – 7.44 (m, 4H, Ar*H*, benzothiophene *H*), 7.80 – 7.84 (m, 1H, benzothiophene *H*), 8.08 – 8.12 (m, 1H, benzothiophene *H*), 8.20 (s, 1H, benzothiophene *H*).

_N_-[4-(Trifluoromethyl)benzyl]-1-benzothiophene-2-sulfonamide (137)

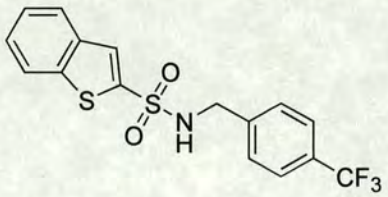

General procedure **L4** was followed. Sulfonamide **137** was isolated as a white solid (0.014 g, 9%, R_f 0.44 (hexane: ethyl acetate, 2:1)); LRMS FAB$^+$ *m/z* 372 $(MH)^+$; HRMS FAB$^+$ *m/z* 372.03359 $(MH)^+$ (calculated for $C_{16}H_{13}F_3NO_2S_2$, 372.03398 (Dev.- 1.06 ppm)); δ_H (250 MHz, $CDCl_3$): 4.17 (d, 2H, *J* = 6.3 Hz, C*H*$_2$NH), 5.09 (t, 1H, *J* = 6.3 Hz, N*H*), 7.15 (d, 2H, *J* = 8.0 Hz, Ar*H*), 7.34 (d, 2H, *J* = 8.0 Hz, Ar*H*), 7.40 – 7.44 (m, 2H, benzothiophene *H*), 7.81 – 7.85 (m, 1H, benzothiophene *H*), 8.06 – 8.10 (m, 1H, benzothiophene *H*), 8.14 (s, 1H, benzothiophene *H*).

_N_-(4-Chlorophenyl)-2,1,3-benzothiadiazole-5-sulfonamide (146)

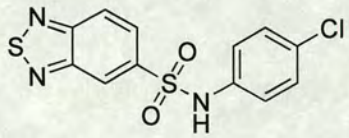

General procedure **L4** was followed. Sulfonamide **146** was isolated as a yellow solid (0.005 g, 4%, R_f 0.40 (hexane: ethyl acetate, 2:1)); LRMS FAB$^+$ *m/z* 326 $(MH)^+$; HRMS FAB$^+$ *m/z* 325.98212 $(MH)^+$ (calculated for $C_{12}H_9{}^{35}ClN_3O_2S_2$, 325.98247 (Dev. – 1.08 ppm)); δ_H (250 MHz, $CDCl_3$): 6.83 (s, 1H, N*H*), 7.00 (m, 2H, Ar*H*), 7.16 (m, 2H, Ar*H*), 7.79 (dd, 1H, *J* = 1.8Hz, 9.2 Hz, benzothiadiazole *H*), 8.03 (dd, 1H, *J* = 0.7 Hz, 9.2 Hz, benzothiadiazole *H*), 8.46 (dd, 1H, *J* = 0.7 Hz, 1.8 Hz, benzothiadiazole *H*).

N-(4-Chlorobenzyl)-2,1,3-benzothiadiazole-5-sulfonamide (147)

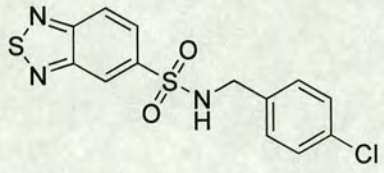

General procedure **L4** was followed. Sulfonamide **147** was isolated as a pale yellow solid (0.009 g, 7%, R_f 0.42 (hexane: ethyl acetate, 2:1)); LRMS FAB^+ *m/z* 340 $(MH)^+$; HRMS FAB^+ *m/z* 339.99880 $(MH)^+$ (calculated for $C_{13}H_{11}{}^{35}ClN_3O_2S_2$, 339.99812 (Dev. 1.99 ppm)); δ_H (250 MHz, $CDCl_3$): 4.15 (d, 2H, *J* = 6.2 Hz, CH_2NH), 5.00 (t, 1H, *J* = 6.2 Hz, N*H*), 7.06 (d, 2H, *J* = 10.4 Hz, Ar*H*), 7.12 (d, 2H, *J* = 10.4 Hz, Ar*H*), 7.86 (dd, 1H, *J* = 9.2, 0.8 Hz, benzothiadiazole *H*), 8.06 (dd, 1H, *J* = 9.2, 1.7 Hz, benzothiadiazole *H*), 8.48 (dd, 1H, *J* = 1.7, 0.8 Hz, benzothiadiazole *H*).

N-[(1*R*)-1-(4-Chlorophenyl)ethyl]-2,1,3-benzothiadiazole-5-sulfonamide (148)

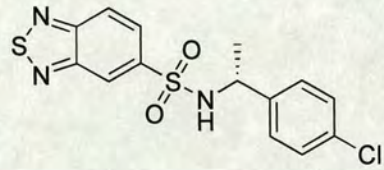

General procedure **L4** was followed. Sulfonamide **148** was isolated as pale yellow solid (0.007 g, 5%, R_f 0.38 (hexane: ethyl acetate, 2:1)); LRMS FAB^+ *m/z* 354 $(MH)^+$; HRMS FAB^+ *m/z* 354.01406 $(MH)^+$ (calculated for $C_{14}H_{13}{}^{35}ClN_3O_2S_2$, 354.01377 (Dev. 0.79 ppm)); δ_H (250 MHz, $CDCl_3$): 1.39 (d, 3H, *J* = 6.9 Hz, $CH(CH_3)$), 4.53 (dq, 1H, *J* = 6.9 Hz, $CH(CH_3)$), 5.00 (d, 1H, *J* = 6.9 Hz, N*H*), 6.93 (s, 4H, Ar*H*), 7.72 (dd, 1H, *J* = 9.2, 1.8 Hz, benzothiadiazole *H*), 7.94 (dd, 1H, *J* = 9.2, 0.8 Hz, benzothiadiazole *H*), 8.24 (dd, 1H, *J* = 1.8, 0.8 Hz, benzothiadiazole *H*).

N-[(1S)-1-(4-Chlorophenyl)ethyl]-2,1,3-benzothiadiazole-5-sulfonamide (149)

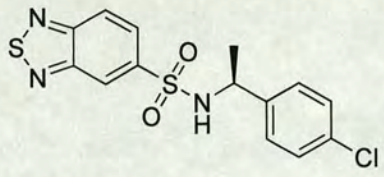

General procedure **L4** was followed. Sulfonamide **149** was isolated as a yellow solid (0.018 g, 13%, R_f 0.38 (hexane: ethyl acetate, 2:1)); LRMS FAB$^+$ *m/z* 354 $(MH)^+$; HRMS FAB$^+$ *m/z* 354.01447 $(MH)^+$ (calculated for $C_{14}H_{13}{}^{35}ClN_3O_2S_2$, 354.01377 (Dev. 1.96 ppm)); δ_H (250 MHz, $CDCl_3$): 1.38 (d, 3H, *J* = 6.9 Hz, CH(C*H*$_3$)), 4.53 (dq, 1H, *J* = 6.9 Hz, C*H*(CH$_3$)), 5.33 (d, 1H, *J* = 6.9 Hz, N*H*), 6.88 – 6.96 (m, H, Ar*H*), 7.73 (dd, 1H, *J* = 9.2, 1.8 Hz, benzothiadiazole *H*), 7.94 (dd, 1H, *J* = 9.2, 0.7 Hz, benzothiadiazole *H*), 8.25 (dd, 1H, *J* = 1.8, 0.7 Hz, benzothiadiazole *H*).

N-[3,5-Bis(trifluoromethyl)phenyl]-2,1,3-benzothiadiazole-5-sulfonamide (150)

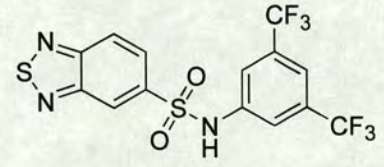

General procedure **L4** was followed. Sulfonamide **150** was isolated as a yellow solid (0.048 g, 28%, R_f 0.49, (hexane: ethyl acetate, 2:1)); LRMS FAB$^+$ *m/z* 428 $(MH)^+$; HRMS FAB$^+$ *m/z* 427.9960 $(MH)^+$ (calculated for $C_{14}H_8F_6N_3O_2S_2$, 427.99622 (Dev. – 0.44 ppm)); δ_H (250 MHz, $CDCl_3$): 7.43 (s, 1H, N*H*), 7.58 (s, 2H, Ar*H*), 7.84 (s, 1H, Ar*H*), 8.09 (dd, 1H, *J* = 9.2, 1.8 Hz, benzothiadiazole *H*), 8.03 (dd, 1H, *J* = 9.2, 0.7 Hz, benzothiadiazole *H*), 8.57 (dd, 1H, *J* = 1.8, 0.7 Hz, benzothiadiazole *H*).

N-[3,5-Bis(trifluoromethyl)benzyl]-2,1,3-benzothiadiazole-5-sulfon amide (151)

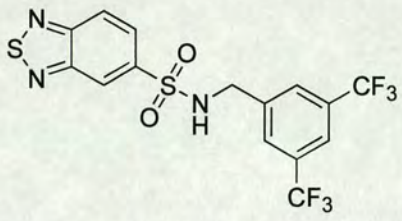

General procedure Library **L4** was followed. Sulfonamide **151** was isolated as a yellow solid (0.077 g, 44%, R_f 0.47 (hexane: ethyl acetate, 2:1)); LRMS FAB^+ *m/z* 442 $(MH)^+$; HRMS FAB^+ *m/z* 442.01195 $(MH)^+$ (calculated for $C_{15}H_{10}F_6N_3O_2S_2$, 442.01187 (Dev. 0.20 ppm)); δ_H (250 MHz, $CDCl_3$): 4.34 (d, 2H, *J* = 6.3 Hz, CH_2NH), 5.33 (t, 1H, *J* = 6.3 Hz, CH_2NH), 7.60 (s, 2H, Ar*H*), 7.63 (s, 1H, Ar*H*), 7.86 (dd, 1H, *J* = 9.2, 1.8 Hz, benzothiadiazole *H*), 8.07 (dd, *J* = 9.2, 0.8 Hz, benzothiadiazole *H*), 8.50 (dd, 1H, *J* = 1.8, 0.8 Hz, benzothiadiazole *H*).

N-[(4-(Trifluoromethyl)phenyl]-2,1,3-benzothiadiazole-5-sulfonamide (152)

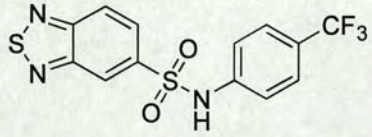

General procedure **L4** was followed. Sulfonamide **152** was isolated as a yellow solid (0.012 g, 8%, R_f 0.40 (hexane: ethyl acetate, 2:1)); LRMS FAB^+ *m/z* 360 $(MH)^+$; HRMS FAB^+ *m/z* 360.00804 $(MH)^+$ (calculated for $C_{13}H_9F_3N_3O_2S_2$, 360.00883 (Dev. –2.19 ppm)); δ_H (250 MHz, $CDCl_3$): 7.19 (d, 2H, Ar*H*), 7.41 – 7.45 (m, 3H, Ar*H*, N*H*), 7.87 (dd, 1H, *J* = 9.2, 1.8 Hz, benzothiadiazole *H*), 8.06 (dd, 1H, *J* = 9.2, 0.7 Hz, benzothiadiazole *H*), 8.58 (dd, 1H, *J* = 1.8, 0.7 Hz, benzothiadiazole *H*).

_N_-[4-(Trifluoromethyl)benzyl]-2,1,3-benzothiadiazole-5-sulfonamide (153)

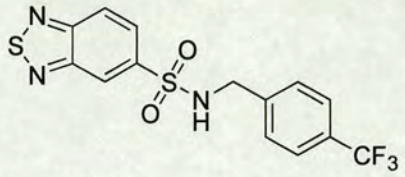

General procedure **L4** was followed. Sulfonamide **153** was isolated as a white solid (0.048 g, 32%, R_f 0.36 (hexane: ethyl acetate, 2:1)); LRMS FAB$^+$ *m/z* 374 $(MH)^+$; HRMS FAB$^+$ *m/z* 374.02405 $(MH)^+$ (calculated for $C_{14}H_{11}F_3N_3O_2S_2$, 374.02448 (Dev. – 1.15 ppm)); δ_H (250 MHz, $CDCl_3$): 4.25 (d, 2H, *J* = 6.2 Hz, C*H*$_2$NH), 5.07 (t, 1H, *J* = 6.2 Hz, CH_2N*H*), 7.28 (d, 2H, *J* = 8.1 Hz, Ar*H*), 7.42 (d, 2H, *J* = 8.1 Hz, Ar*H*), 7.88 (dd, 1H, *J* = 9.2, 1.8 Hz, benzothiadiazole *H*), 8.07 (dd, 1H, *J* = 9.2, 0.7 Hz, benzothiadiazole *H*), 8.50 (dd, 1H, *J* = 1.8, 0.7 Hz, benzothiadiazole *H*).

_N_-(4-Chlorophenyl)-5-pyridin-2-ylthiophene-2-sulfonamide (154)

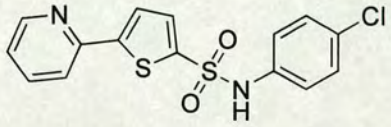

General procedure **L4** was followed. Sulfonamide **154** was isolated as a yellow solid (0.041 g, 29%, R_f 0.25 (hexane: ethyl acetate, 2:1)); LRMS FAB$^+$ *m/z* 351 $(MH)^+$; HRMS FAB$^+$ *m/z* 351.00241 $(MH)^+$ (calculated for $C_{15}H_{12}{}^{35}ClN_2O_2S_2$, 351.00288 (Dev. – 1.34 ppm)); δ_H (250 MHz, $CDCl_3$): 7.03 (d, 2H, *J* = 8.9 Hz, Ar*H*), 7.16 – 7.21 (m, 4H, pyridyl *H*, Ar*H*, N*H*), 7.33 (d, 2H, *J* = 4.0 Hz, thiophene *H*), 7.38 (d, 1H, *J* = 4.0 Hz, thiophene *H*), 7.56 – 7.68 (m, 2H, pyridyl *H*), 8.50 – 8.52 (m, 1H, pyridyl *H*).

_N_-(4-Chlorobenzyl)-5-pyridin-2-ylthiophene-2-sulfonamide (155)

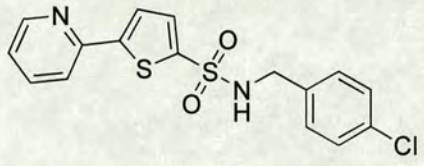

General procedure **L4** was followed. Sulfonamide **155** was isolated as a yellow solid (0.003 g, 2%, R_f 0.25 (hexane: ethyl acetate, 2:1)); LRMS FAB$^+$ *m/z* 365 $(MH)^+$; HRMS FAB$^+$ *m/z* 365.01790 $(MH)^+$ (calculated for $C_{16}H_{14}{}^{35}ClN_2O_2S_2$, 365.01853 (Dev. – 1.72 ppm)); δ_H (250 MHz, $CDCl_3$): 4.17 (d, 2H, *J* = 6.2 Hz, C*H*$_2$NH), 4.88 (t, 1H, *J* = 6.2 Hz, CH$_2$N*H*), 7.13 – 7.24 (m, 5H, ArH, pyridyl *H*), 7.42 (d, 1H, *J* = 4.0 Hz, thiophene *H*), 7.53 (d, 1H, *J* = 4.0 Hz, thiophene *H*), 7.61 – 7.74 (m, 2H, pyridyl *H*), 8.53 – 8.55 (m, 1H, pyridyl *H*).

_N_-[(1*R*)-1-(4-Chlorophenyl)ethyl]-5-pyridin-2-ylthiophene-2-sulfonamide (156)

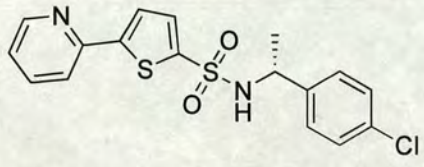

General procedure **L4** was followed. Sulfonamide **156** was isolated as a yellow solid (0.012 g, 8%, R_f 0.29 (hexane: ethyl acetate, 2:1)); LRMS FAB$^+$ *m/z* 379 $(MH)^+$; HRMS FAB$^+$ *m/z* 379.03451 $(MH)^+$ (calculated for $C_{17}H_{16}{}^{35}ClN_2O_2S_2$, 379.03418 (Dev. 0.88 ppm)); δ_H (250 MHz, $CDCl_3$): 1.40 (d, 3H, *J* = 6.9 Hz, CH(C*H*$_3$)), 4.52 (dq, 1H, *J* = 6.9 Hz, C*H*(CH$_3$)), 4.95 (d, 1H, *J* = 6.9 Hz, N*H*), 7.06 – 7.22 (m, 5H, Ar*H*), 7.30 (d, 1H, *J* = 4.0 Hz, thiophene *H*), 7.32 (d, 1H, *J* = 4.0 Hz, thiophene *H*), 7.57 – 7.71 (m, 2H, pyridyl *H*), 8.51 – 8.54 (m, 1H, pyridyl *H*).

_N_-[(1_S_)-1-(4-Chlorophenyl)ethyl]-5-pyridin-2-ylthiophene-2-sulfonamide (157)

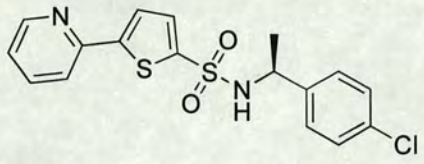

General procedure **L4** was followed. Sulfonamide **157** was isolated as a yellow solid (0.005 g, 3%, R_f 0.27 (hexane: ethyl acetate, 2:1)); LRMS FAB$^+$ *m/z* 379 $(MH)^+$; HRMS FAB$^+$ *m/z* 379.03367 $(MH)^+$ (calculated for $C_{17}H_{16}{}^{35}ClN_2O_2S_2$, 379.03418 (Dev. – 1.32 ppm)); δ_H (250 MHz, $CDCl_3$): 1.40 (d, 3H, *J* = 6.9 Hz, CH(C*H*$_3$)), 4.52 (dq, 1H, *J* = 6.9 Hz, C*H*(CH$_3$)), 4.87 (d, 1H, *J* = 6.9 Hz, N*H*), 7.06 – 7.22 (m, 5H, Ar*H*), 7.30 (d, 1H, *J* = 3.9 Hz, thiophene *H*), 7.32 (d, 1H, *J* = 3.9 Hz, thiophene *H*), 7.58 – 7.72 (m, 2H, pyridyl *H*), 8.52 – 8.54 (m, 1H, pyridyl *H*).

_N_-[3,5-Bis(trifluoromethyl)phenyl]-5-pyridin-2-ylthiophene-2-sulfonamide (158)

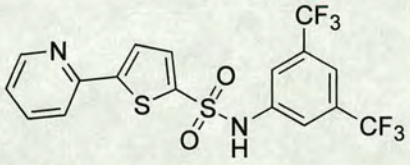

General procedure **L4** was followed. Sulfonamide **158** was isolated as a white solid (0.053 g, 29%, R_f 0.47 (hexane: ethyl acetate, 2:1)); LRMS FAB$^+$ *m/z* 453 $(MH)^+$; HRMS FAB$^+$ *m/z* 453.01639 $(MH)^+$ (calculated for $C_{17}H_{11}F_6N_2O_2$, 453.01662 (Dev – 0.50 ppm)); δ_H (250 MHz, $CDCl_3$): 7.20 – 7.22 (m, 1H, pyridyl *H*), 7.40 (d, 1H, *J* = 4.0 Hz, thiophene *H*), 7.52 – 7.54 (m, 3H, Ar*H*), 7.55 (d, 1H, J= 4.0 Hz, thiophene *H*), 7.58 – 7.62 (m, 1H, pyridyl *H*), 7.68 (m, 1H, pyridyl *H*), 7.80 (s, 1H, N*H*), 8.51 (m, 1H, pyridyl *H*).

_N_-[3,5-Bis(trifluoromethyl)benzyl]-5-pyridin-2-ylthiophene-2-sulfonamide (159)

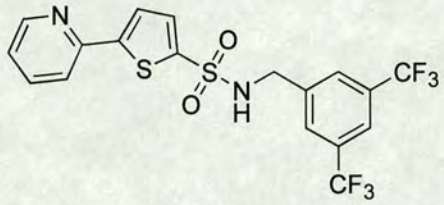

General procedure **L4** was followed. Sulfonamide **159** was isolated as a yellow solid (0.061 g, 33%, R_f 0.33 (hexane: ethyl acetate, 2:1)); LRMS FAB^+ *m/z* 467 $(MH)^+$; HRMS FAB^+ *m/z* 467.03259 $(MH)^+$ (calculated for $C_{18}H_{13}F_6N_2O_2S_2$, 467.03227 (Dev. 0.69 ppm)); δ_H (250 MHz, $CDCl_3$): 4.34 (d, 2H, *J* = 6.5 Hz, C*H*$_2$NH), 5.19 (t, 1H, *J* = 6.5 Hz, N*H*), 7.20 – 7.24 (m, 1H, pyridyl *H*), 7.40 (d, 1H, *J* = 4.0 Hz, thiophene *H*), 7.52 (d, 1H, *J* = 4.0 Hz, thiophene *H*), 7.60 – 7.74 (m, 5H, pyridyl *H*, Ar*H*), 8.51 – 8.53 (m, 1H, pyridyl *H*).

5-Pyridin-2-yl-_N_-[4-(trifluoromethyl)phenyl]thiophene-2-sulfonamide (160)

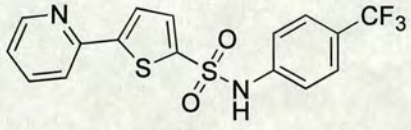

General procedure **L4** was followed. Sulfonamide **160** was isolated as a pale yellow solid (0.012 g, 8%, R_f 0.27 (hexane: ethyl acetate, 2:1)); LRMS FAB^+ *m/z* 385 $(MH)^+$; HRMS FAB^+ *m/z* 385.02921 $(MH)^+$ (calculated for $C_{16}H_{12}F_3N_2O_2S_2$, 385.02923 (Dev. – 0.05 ppm)); δ_H (250 MHz, $CDCl_3$): 7.18 – 7.22 (m, 4H, Ar*H*, pyridyl *H*), 7.36 (d, 1H, *J* = 4.0 Hz, thiophene *H*), 7.45 – 7.52 (m, 3H, Ar*H*), 7.55 – 7.70 (m, 2H, Ar*H*), 8.50 – 8.52 (m, 1H, pyridyl *H*); Mpt. 219.4 – 219.8 °C.

5-Pyridin-2-yl-_N_-[4-(trifluoromethyl)benzyl]thiophene-2-sulfonamide (161)

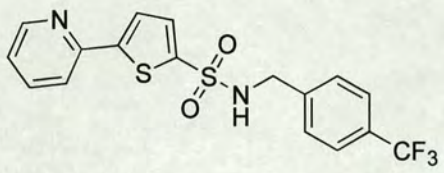

General procedure **L4** was followed. Sulfonamide **161** was isolated as a yellow solid (0.031 g, 19%, R_f 0.24 (hexane: ethyl acetate, 2:1)); LRMS FAB^+ *m/z* 399 $(MH)^+$; HRMS FAB^+ *m/z* 399.04554 $(MH)^+$ (calculated for $C_{17}H_{14}F_3N_2O_2S_2$, 399.04488 (Dev. 1.65 ppm)); δ_H (250 MHz, $CDCl_3$): 4.26 (d, 2H, *J* = 6.4 Hz, C*H*$_2$NH), 5.06 (t, 1H, *J* = 6.4 Hz, N*H*), 7.17 – 7.24 (m, 1H, pyridyl *H*), 7.34 (d, 2H, *J* = 8.1 Hz, Ar*H*), 7.40 (d, 1H, *J* = 4.0 Hz, thiophene *H*), 7.49 (d, 2H, *J* = 8.1 Hz, Ar*H*), 7.51 (d, 1H, *J* = 4.0 Hz, thiophene *H*), 7.60 – 7.74 (m, 2H, pyridyl *H*), 8.51 – 8.54 (m, 1H, pyridyl *H*).

4,5-Dibromo-*N*-(4-chlorobenzyl)thiophene-2-sulfonamide (162)

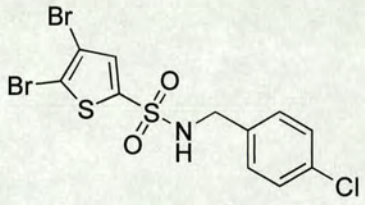

General procedure **L4** was followed. Sulfonamide **162** was isolated as a white solid (0.028 g, 16%, R_f 0.51(hexane: ethyl acetate, 2:1)); LRMS FAB^+ *m/z* 446 $(MH)^+$; HRMS FAB^+ *m/z* 445.81207 $(MH)^+$ (calculated for $C_{11}H_9{}^{79}Br^{81}Br^{35}ClNO_2S_2$, 445.81108 (Dev. 2.22 ppm)); δ_H (250 MHz, $CDCl_3$): 4.15 (d, 2H, *J* = 6.2 Hz, C*H*$_2$NH), 4.89 (t, 1H, *J* = 6.2 Hz, N*H*), 7.13 (d, 2H, *J* = 8.7 Hz, Ar*H*), 7.24 (d, 2H, *J* = 6.2 Hz, Ar*H*), 7.27 (s, 1H, thiophene *H*).

4,5-Dibromo-*N*-[(1*R*)-1-(4-chlorophenyl)ethyl]thiophene-2-sulfonamide (163)

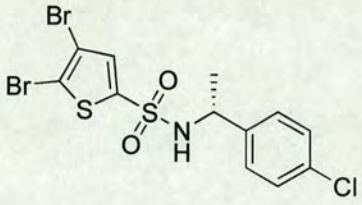

General procedure **L4** was followed. Sulfonamide **163** was isolated as a white solid (0.015 g, 8%, R_f 0.49 (hexane: ethyl acetate, 2:1)); LRMS FAB^+ *m/z* 460 $(MH)^+$; HRMS FAB^+ *m/z* 459.82693 $(MH)^+$ (calculated for $C_{12}H_{11}{}^{79}Br^{81}Br^{35}ClNO_2S_2$, 459.82673 (Dev. 0.42 ppm)); δ_H (250 MHz, $CDCl_3$): 1.48 (d, 3H, *J* = 6.9 Hz, CH(C*H*$_3$)), 4.56 (dq, 1H, *J* = 6.9 Hz, C*H*(CH$_3$)), 4.98 (d, 1H, *J* = 6.9 Hz, N*H*), 7.04 (s, 1H, thiophene *H*), 7.10 (d, 2H, *J* = 8.4 Hz, Ar*H*), 7.26 (d, 2H, *J* = 8.4 Hz, Ar*H*).

***N*-[3,5-Bis(trifluoromethyl)benzyl]-4,5-dibromothiophene-2-sulfonamide (165)**

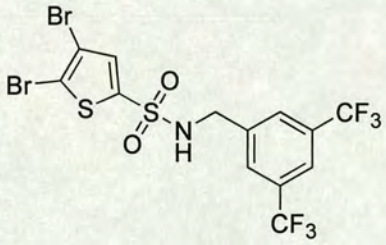

General procedure **L4** was followed. Sulfonamide **165** was isolated to afford **165** as a white solid (0.071 g, 33%, R_f 0.58 (hexane: ethyl acetate, 2:1)); LRMS FAB^+ *m/z* 548 $(MH)^+$; HRMS FAB^+ *m/z* 547.82464 $(MH)^+$ (calculated for $C_{13}H_8{}^{79}Br^{81}BrF_6NO_2S_2$, 547.82482 (Dev. – 0.34 ppm)); δ_H (250 MHz, $CDCl_3$): 4.40 (d, 2H, *J* = 6.4 Hz, C*H*$_2$NH), 5.30 (t, 1H, *J* = 6.4 Hz, N*H*), 7.33 (s, 1H, thiophene *H*), 7.74 (s, 2H, Ar*H*), 7.83 (s, 1H, Ar*H*).

4,5-Dibromo-*N*-[4-(trifluoromethyl)benzyl]thiophene-2-sulfonamide (166)

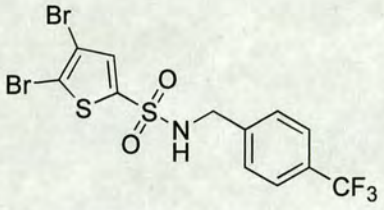

General procedure **L4** was followed. Sulfonamide **166** was isolated as a white solid (0.024 g, 13%, R_f 0.51 (hexane: ethyl acetate, 2:1)); LRMS FAB^+ *m/z* 480 $(MH)^+$; HRMS FAB^+ *m/z* 479.83798 $(MH)^+$ (calculated for $C_{12}H_9{}^{79}Br^{81}BrF_3NO_2S_2$, 479.83744 (Dev. 1.12 ppm)); δ_H (250 MHz, $CDCl_3$): 4.31 (d, 2H, *J* = 6.3 Hz, C*H*$_2$NH), 5.17 (t, 1H, *J* = 6.3 Hz, N*H*), 7.34 (s, 1H, thiophene *H*), 7.40 (d, 2H, *J* = 8.0 Hz, Ar*H*), 7.60 (d, 2H, *J* = 8.0 Hz, Ar*H*).

***N*-(4-Fluorophenyl)benzenesulfonamide (172)[213]**

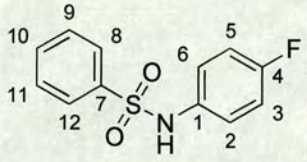

A solution of benzenesulfonyl chloride (54 μL, 0.42 mmole, 2.10 eq.) in DCM (1.5 mL, anhydrous) was added to PS-DMAP (570 mg, 0.20 mmole, 1.0 eq.) and allowed to stir for 2 hours at room temperature before the resin was washed five times with DCM. A solution of the 4-fluoroaniline (14 μL, 0.14 mmole, 0.70 eq.) in DCM (1.5 mL, anhydrous) was added to the resin and allowed to stir at room temperature for 72 hours. The resin was washed with DCM and the filtrate collected and concentrated *in vacuo* to a residue that was columned on silica (hexane: ethyl acetate, 1:1). Sulfonamide **172** was isolated as a white solid (0.008 g, 23 %, R_f 0.46 (hexane: ethyl acetate, 1:1)); LRMS ES^- *m/z* 250.0 $(M-H)^-$; δ_H (250 MHz, $CDCl_3$): 6.78 (bs, 1H, N*H*), 6.82 – 6.89 (m, 2H, *H*2,

*H*6), 6.94 – 7.00 (m, 2H, *H*3, *H*5), 7.33 – 7.42 (m, 2H, *H*9, *H*11), 7.45 – 7.52 (m, 1H, *H*10), 7.64 – 7.69 (m, 2H, *H*8, *H*12);

4-Chloro-*N*-(3,5-dichlorophenyl)-3-nitrobenzenesulfonamide (174)

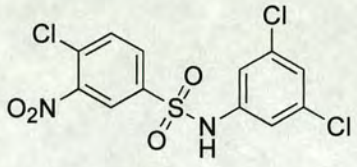

To a stirring solution of 4-chloro-3-nitrobenzenesulfonyl chloride (0.500 g, 1.95 mmole, 1.0 eq.), in DCM (5 mL) was added 3,5-dichloroaniline (0.348 g, 2.15 mmole, 1.1 eq.) and pyridine (158 μL, 1.95 mmole, 1.0 eq.). The reaction mixture was allowed to stir at room temperature for 24 hours before being concentrated *in vacuo* to afford a brown residue. The residue was dissolved in ethyl acetate (50 mL) and washed with HCl (1M, 2 x 50 mL); brine (50 mL) and concentrated *in vacuo* to afford a residue that was columned on silica (hexane: ethyl acetate, 2:1) to afford sulfonamide **174** as a white solid (0.552 g, 74%); LRMS ES^- *m/z* 379.0 $(M-H)^-$ assigned to $C_{12}H_7{}^{35}Cl_3N_2O_4$.

4-Chloro-*N*-(4-fluorophenyl)-3-nitrobenzenesulfonamide (175)

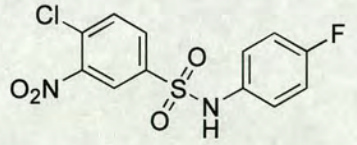

To a stirring solution 4-chloro-3-nitrobenzenesulfonyl chloride (0.500 g, 1.95 mmole, 1.0 eq.), in DCM (5 mL) was added 4-fluoroaniline (207 μL, 2.15 mmole, 1.1 eq.) and pyridine (158 μL, 1.95 mmole, 1.0 eq.). The reaction mixture was allowed to stir at room temperature for 24 hours before being concentrated *in vacuo* to afford a brown residue. The residue was dissolved in ethyl acetate (50 mL) and washed with HCl (1M, 2 x 50 mL); brine (50 mL) and concentrated *in vacuo* to afford a residue that was

columned on silica (hexane: ethyl acetate, 2:1) to afford sulfonamide **175** as a pink solid (0.555 g, 86%); LRMS ES$^-$ *m/z* 329.0 $(M-H)^-$.

N-[3,5-Bis(trifluoromethyl)phenyl]-5-chloro-N-methylthiophene-2-sulfonamide (192)

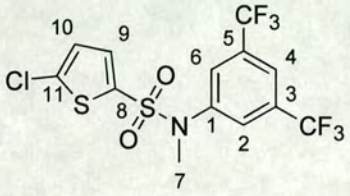

To a stirring solution of *N*-[3,5-bis(trifluoromethyl)phenyl]-5-chlorothiophene-2-sulfonamide (0.080 g, 0.19 mmole, 1.0 eq.) in acetone (3 mL), methyl iodide (61 μL, 0.98 mmole, 5.0 eq.) and triethylamine (27 μL, 0.19 mmole, 1.0 eq.) were added. The reaction mixture was allowed to stir at room temperature for 24 hours before being diluted with water (20 mL) and extracted into ethyl acetate (2 x 20 mL). The combined organics were washed with water (2 x 20 mL), dried over anhydrous $MgSO_4$, and concentrated *in vacuo* to afford a residue that was purified on silica (hexane: ethyl acetate 15:1). Appropriate fractions were combined and concentrated *in vacuo* to afford sulfonamide **192** as a white solid (0.010 g, 12%); δ_H (250 MHz, $CDCl_3$): 3.23 (s, 3H, *H*7), 6.90 (d, 1H, *J* = 4.0 Hz, *H*9), 7.09 (d, 1H, *J* = 4.0 Hz, *H*10), 7.57 (s, 2H, *H*2, *H*6), 7.75 (s, 2H, *H*4).

_N_-Allyl-_N_-[3,5-bis(trifluoromethyl)phenyl]-5-chlorothiophene-2-sulfonamide (205)

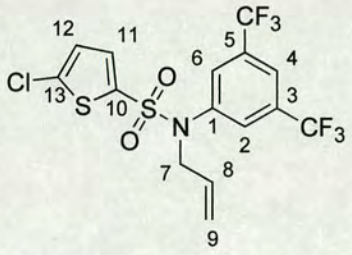

General procedure **S2** was followed using *N*-[3,5-bis(trifluoromethyl)phenyl]-5-chlorothiophene-2-sulfonamide (0.091 g, 0.22 mmole, 1.0 eq.), allyl bromide (96 μL, 1.10 mmole, 5.0 eq.) and triethylamine (300 μL, excess). The reaction mixture was irradiated in the Discover™ at 80 °C for 10 minutes. The crude reaction mixture was columned on silica (hexane: ethyl acetate 15:1) to afford sulfonamide **205** as a white solid (0.045 g, 45%); δ_H (250 MHz, $CDCl_3$): 4.19 (dt, 2H, *J* = 6.4, 1.3 Hz, *H*7), 5.07 (dd, 1H, *J* = 9.5, 1.3 Hz, $H9_{cis}$), 5.12 (dd, 1H, *J* = 16.3, 1.3 Hz, $H9_{trans}$), 5.58 – 5.72 (m, 1H, *H*8), 6.89 (d, 1H, *J* = 4.0 Hz, *H*11), 7.10 (d, 1H, *J* = 4.0 Hz, *H*12), 7.50 (s, 2H, *H*2, *H*6), 7.76 (s, 1H, *H*4).

4,5-Dibromo-_N_-methyl-_N_-[4-(trifluoromethyl)phenyl]thiophene-2-sulfonamide (196)

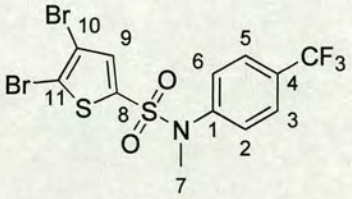

General procedure **S2** was followed using 4,5-dibromo-*N*-[4-(trifluoromethyl)-phenyl]thiophene-2-sulfonamide (0.104 g, 0.23 mmole, 1.0 eq.), methyl iodide (61 μL, 0.98 mmole, 4.4 eq.) and triethylamine (200 μL, excess). The reaction mixture was irradiated in the Discover™ at 150 °C for 5 minutes. The crude reaction mixture was columned on silica (hexane: ethyl acetate 15:1) to afford sulfonamide **196** as a white

solid (0.022 g, 20%); LRMS EI^+ *m/z* 479 $(M)^+$ calculated for $C_{12}H_8{}^{79}Br_2F_3NO_2S_2$; δ_H (250 MHz, $CDCl_3$): 3.21 (s, 3H, *H*7), 7.11 (s, 1H, *H*9), 7.27 (d, 2H, *J* = 7.5 Hz, *H*2, *H*6), 7.57 (d, 2H, *J* = 7.5 Hz, *H*3, *H*5).

_N_-Benzyl-_N_-[3,5-bis(trifluoromethyl)phenyl]-5-bromothiophene-2-sulfonamide (197)

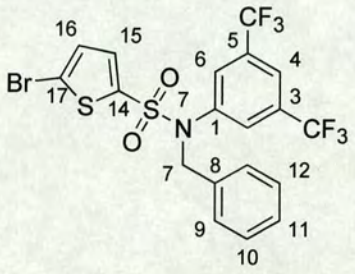

General procedure **S2** was followed using *N*-[3,5-bis(trifluoromethyl)phenyl]-5-bromothiophene-2-sulfonamide (0.100 g, 0.22 mmole, 1.0 eq.), benzyl bromide (131 μL, 1.10 mmole, 5.0 eq.) and triethylamine (300 μL, excess). The reaction mixture was irradiated in the Discover™ at 60 °C for 10 minutes. The crude reaction mixture was purified on silica (hexane: ethyl acetate 15:1) to afford sulfonamide **197** as a white solid (0.046 g, 38%, R_f 0.29 (hexane: ethyl acetate 15:1)); LRMS ES^+ *m/z* 566.0 $(M + Na)^+$ calculated for $C_{19}H_{12}{}^{79}BrF_6NO_2S_2$; ν_{max} (film)/cm^{-1} 3094 (thiophene C-H), 3034 (aryl C-H), 2922 (C-H), 1368 (SO_2), 1164 (SO_2); δ_H (250 MHz, $CDCl_3$): 4.72 (s, 2H, *H*7), 7.05 (d, 1H, *J* = 4.0 Hz, *H*15), 7.10 (d, 1H, *J* = 4.0 Hz, *H*16), 7.14 – 7.20 (m, 5H, *H*9, *H*10, *H*11, *H*12, *H*13), 7.41 (s, 2H, *H*2, *H*6), 7.67 (s, 1H, *H*4); Mpt. 109.4 – 110. 2 °C.

_N_-Benzyl-_N_-[3,5-bis(trifluoromethyl)phenyl]-5-chlorothiophene-2-sulfonamide (198)

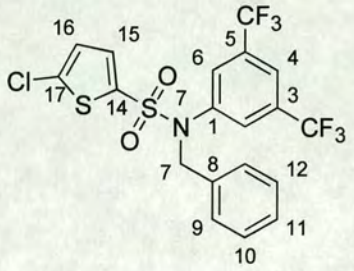

General procedure **S2** was followed using _N_-[3,5-bis(trifluoromethyl)phenyl]-5-chlorothiophene-2-sulfonamide (0.091 g, 0.22 mmole, 1.0 eq.), benzyl bromide (131 μL, 1.10 mmole, 5.0 eq.) and triethylamine (300 μL, excess). The reaction mixture was irradiated in the Discover™ at 60 °C for 10 minutes. The crude reaction mixture was columned on silica (hexane: ethyl acetate 15:1) to afford sulfonamide **198** as a white solid (0.052 g, 47%,, R_f 0.25 (hexane: ethyl acetate 15:1)); LRMS ES^+ *m/z* 522.0 $(M + Na)^+$; HRMS EI^+ *m/z* 498.98972 $(M)^+$ (calculated for $C_{19}H_{12}{}^{35}ClF_6NO_2S_2$, 498.99022 (Dev. – 1.01 ppm)); δ_H (250 MHz, $CDCl_3$): 4.73 (s, 2H, *H*7), 6.92 (d, 1H, *J* = 4.0 Hz, *H*16), 7.13 – 7.21 (m, 6H, *H*9, *H*10, *H*11, *H*12, *H*13, *H*15), 7.41 (s, 2H, *H*2, *H*6), 7.67 (s, 1H, *H*4).

_N_-Benzyl-5-bromo-_N_-[4-(trifluoromethyl)phenyl]thiophene-2-sulfonamide (199)

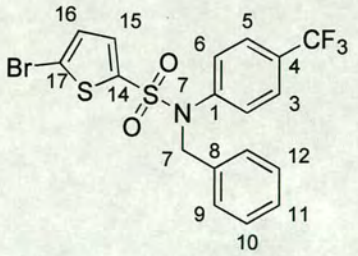

General procedure per **S2** was followed using 5-bromo-*N*-[4-(trifluoromethyl)phenyl]-thiophene-2-sulfonamide (0.085 g, 0.22 mmole, 1.0 eq.), benzyl bromide (131 μL, 1.10 mmole, 5.0 eq.) and triethylamine (300 μL, excess). The reaction mixture was irradiated in the Discover™ at 60 °C for 10 minutes. The crude reaction mixture was purified on silica (hexane: ethyl acetate 15:1) to afford sulfonamide **199** as a white solid (0.067 g, 64%, R_f 0.20 (hexane: ethyl acetate 15:1)); LRMS ES^+ *m/z* 498.0 $(M + Na)^+$; ν_{max} (film)/cm^{-1} 3094 (thiophene C-H), 3069 (aryl C-H), 2924 (C-H), 1325 (SO_2), 1164 (SO_2); δ_H (250 MHz, $CDCl_3$): 4.72 (s, 2H, *H*7), 7.02 (d, 1H, *J* = 4.0 Hz, *H*15), 7.08 (d, 2H, *J* = 4.0 Hz, *H*16), 7.11 – 7.20 (m, 7H, *H*2, *H*6, *H*9, *H*10, *H*11, *H*12, *H*13), 7.45 (d, 2H, *J* = 8.3 Hz, *H*3, *H*5); δ_C (63 MHz, $CDCl_3$): 54.6 (*C*7), 120.5 (C_{Ar}), 123.5 (q, J_{CF} = 272 Hz, CF_3), 126.1 (2 x CH_{Ar}), 128.0 (CH_{Ar}), 128.3 (2 x CH_{Ar}), 128.5 (2 x CH_{Ar}), 128.8 (2 x CH_{Ar}), 130.0 (q, J_{CF} = 33 Hz, *C*4), 130.5 (CH_{Ar}), 133.0 (CH_{Ar}), 134.6 (C_{Ar}), 139.1 (C_{Ar}), 141.5 (C_{Ar}); Mpt.103.2 –103.5 °C.

_N_-Benzyl-5-chloro-_N_-[4-(trifluoromethyl)phenyl]thiophene-2-sulfonamide (200)

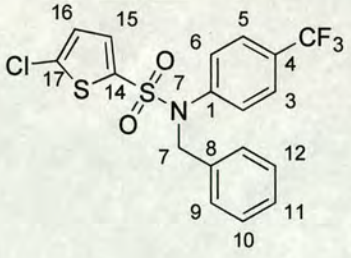

General procedure **S2** was followed using 5-chloro-*N*-[4-(trifluoromethyl)phenyl]-thiophene-2-sulfonamide (0.075 g, 0.22 mmole, 1.0 eq.), benzyl bromide (131 μL, 0.98 mmole, 5.0 eq.) and triethylamine (300 μL, excess). The reaction mixture was irradiated in the Discover™ at 60 °C for 10 minutes. The crude reaction mixture was columned on silica (hexane: ethyl acetate 15:1) to afford sulfonamide **200** as a pale yellow solid (0.083 g, 87%); LRMS ES^+ *m/z* 454.1 $(M + Na)^+$; ν_{max} (film)/cm^{-1} 3106 (thiophene C-H), 3094 (aryl C-H), 2923 (C-H), 1334 (SO_2), 1163 (SO_2); δ_H (250 MHz, $CDCl_3$): 4.73

(s, 2H, *H*7), 6.89 (d, 1H, *J* = 4.0 Hz, *H*15), 7.13 (d, 2H, *J* = 4.0 Hz, *H*16), 7.16 – 7.19 (m, 7H, *H*2, *H*6, *H*9, *H*10, *H*11, *H*12, *H*13), 7.47 (d, 2H, *J* = 8.4 Hz, *H*3, *H*5); Mpt. 112.9 – 113.3 °C.

_N_-Benzyl-_N_-[3,5-bis(trifluoromethyl)phenyl]-4,5-dibromothiophene-2-sulfonamide (201)

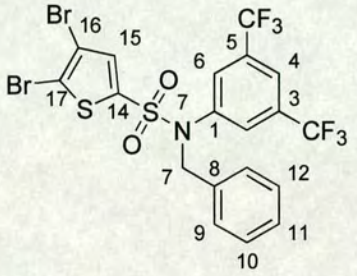

General procedure **S2** was followed using *N*-[3,5-bis(trifluoromethyl)phenyl]-4,5-dibromothiophene-2-sulfonamide (0.103 g, 0.19 mmole, 1.0 eq.), benzyl bromide (131 μL, 1.10 mmole, 5.0 eq.) and triethylamine (300 μL, excess). The reaction mixture was irradiated in the Discover™ at 60 °C for 10 minutes. The crude reaction mixture was columned on silica (hexane: ethyl acetate) to afford sulfonamide **201** as a cream solid (0.090 g, 75%); LRMS ES$^+$ *m/z* 578.0 (M + Na)$^+$ calculated $C_{19}H_{12}{}^{79}Br^{81}BrF_6NO_2S_2$; ν_{max} (film)/cm^{-1} 3082 (thiophene C-H), 3037 (aryl C-H), 2929 (C-H), 1358 (SO_2), 1134 (SO_2); δ_H (250 MHz, $CDCl_3$): 4.72 (s, 2H, *H*7), 7.13 – 7.22 (m, 6H, *H*9, *H*10, *H*11, *H*12, *H*13, *H*15), 7.43 (s, 2H, *H*2, *H*6), 7.71 (s, 1H, *H*4); Mpt. 137.7 – 138.4 °C.

_N_-Benzyl-4,5-dibromo-_N_-[4-(trifluoromethyl)phenyl]thiophene-2-sulfonamide (202)

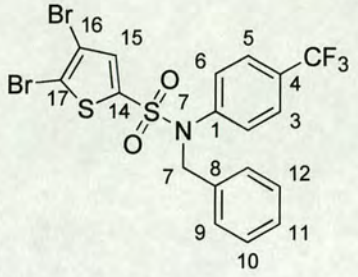

General procedure **S2** was followed using 4,5-dibromo-*N*-[4-(trifluoromethyl)phenyl]-thiophene-2-sulfonamide (0.075 g, 0.22 mmole, 1.0 eq.), benzyl bromide (131 μL, 1.10 mmole, 5.0 eq.) and triethylamine (300 μL, excess). The reaction mixture was irradiated in the Discover™ at 60 °C for 10 minutes. The crude reaction mixture was columned on silica (hexane: ethyl acetate 15:1) to afford sulfonamide **202** as a white solid (0.114 g, 81%); LRMS ES^+ *m/z* 646.1 $(M + Na)^+$ calculated for $C_{18}H_{12}{}^{79}Br^{81}BrF_3NO_2S_2$; δ_H (250 MHz, $CDCl_3$): 4.73 (s, 2H, *H*7), 7.14 – 7.20 (m, 1H, *J* = 4.0 Hz, *H*15), 7.13 (d, 2H, *J* = 4.0 Hz, *H*16), 7.16 – 7.19 (m, 8H, *H*2, *H*6, *H*9, *H*10, *H*11, *H*12, *H*13, *H*15), 7.49 (d, 2H, *J* = 8.3 Hz, *H*3, *H*5).

_N_-Benzyl-_N_-[3,5-bis(trifluoromethyl)phenyl]-5-[2-(methylthio)pyrimidin-5-yl]-thiophene-2-sulfonamide (203)

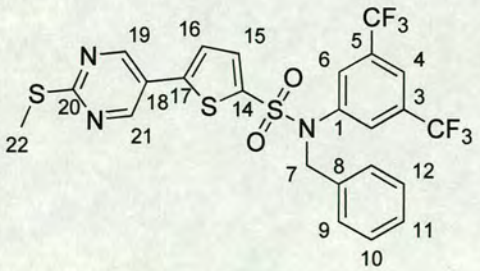

General procedure **S2** was followed using *N*-[3,5-bis(trifluoromethyl)phenyl]-5-[2-(methylthio)pyrimidin-5-yl]-thiophene-2-sulfonamide (0.110 g, 0.22 mmole, 1.0 eq.),

benzyl bromide (131 μL, 1.10 mmole, 5.0 eq.) and triethylamine (300 μL, excess). The reaction mixture was irradiated in the Discover™ at 60 °C for 10 minutes. The crude reaction mixture was columned on silica (hexane: ethyl acetate 15:1) to afford sulfonamide **203** as a yellow solid (0.074 g, 57%); LRMS ES^+ *m/z* 612.3 $(M + Na)^+$; ν_{max} (film)/cm^{-1} 3093 (aryl C-H), 2930 (C-H), 1355 (SO_2), 1137 (SO_2); δ_H (250 MHz, $CDCl_3$): 2.59 (s, 3H, *H*22), 4.83 (s, 2H, *H*7), 7.20 – 7.27 (m, 6H, *H*9, *H*10, *H*11, *H*12, *H*13, *H*19), 7.45 (d, 1H, *J* = 4.0 Hz, *H*15), 7.57 (s, 2H, *H*2, *H*6), 7.73 (d, 1H, *J* = 4.0 Hz, *H*16), 7.81 (s, 1H, *H*4), 8.65 (d, 1H, *J* = 5.2 Hz, *H*21); Mpt. 141.8 – 142.3.

_N_-Allyl-_N_-[3,5-bis(trifluoromethyl)phenyl]-5-bromothiophene-2-sulfonamide (204)

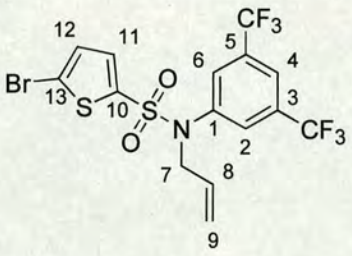

General procedure **S2** was followed using *N*-[3,5-bis(trifluoromethyl)phenyl]-5-bromothiophene-2-sulfonamide (0.100 g, 0.22 mmole, 1.0 eq.), allyl bromide (96 μL, 1.10 mmole, 5.0 eq.) and triethylamine (300 μL, excess). The reaction mixture was irradiated in the Discover™ at 60 °C for 10 minutes. The crude reaction mixture was columned on silica (heptane: hexane: ethyl acetate, 8:2:1) to afford sulfonamide **204** as a pale yellow solid (0.052 g, 48%, R_f 0.26 (heptane: hexane: ethyl acetate 8:2:1)); δ_H (250 MHz, $CDCl_3$): 4.19 (dt, 2H, *J* = 6.4, 1.3 Hz, *H*7), 5.08 (dd, 1H, *J* = 9.5, 1.3 Hz, $H9_{cis}$), 5.10 (dd, 1H, *J* = 17.6, 1.3 Hz, $H9_{trans}$), 5.58 – 5.74 (m, 1H, *H*8), 7.03 (d, 1H, *J* = 4.0 Hz, *H*12), 7.06 (d, 1H, *J* = 4.0 Hz, *H*11), 7.50 (s, 2H, *H*2, *H*6), 7.76 (s, 1H, *H*4).

_N_-Allyl-5-bromo-_N_-[4-(trifluoromethyl)phenyl]thiophene-2-sulfonamide (206)

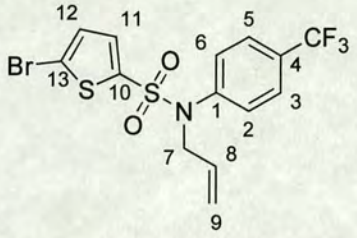

General procedure **S2** was followed using 5-bromo-*N*-[4-(trifluoromethyl)phenyl]-thiophene-2-sulfonamide (0.085 g, 0.22 mmole, 1.0 eq.), allyl bromide (96 μL, 1.10 mmole, 5.0 eq.) and triethylamine (300 μL, excess). The reaction mixture was irradiated in the Discover™ at 60 °C for 10 minutes. The crude reaction mixture was columned on silica (heptane: hexane: ethyl acetate, 8:2:1) to afford sulfonamide **206** as a white solid (0.054 g, 57%, R_f 0.14 (heptane: hexane: ethyl acetate, 8:2:1)); δ_H (250 MHz, $CDCl_3$): 4.18 (dt, 2H, *J* = 9.3, 1.3 Hz, *H*7), 5.04 (dd, 1H, *J* = 9.3, 1.3 Hz, $H9_{cis}$), 5.07 (dd, 1H, *J* = 16.6, 1.3 Hz, $H9_{trans}$), 5.59 – 5.75 (m, 1H, *H*8), 7.00 (d, 1H, *J* = 4.0 Hz, *H*12), 7.05 (d, 1H, *J* = 4.0 Hz, *H*11), 7.20 (d, 2H, *J* = 8.9 Hz, *H*2, *H*6), 7.55 (d, 2H, *J* = 8.9 Hz, *H*3, *H*5).

_N_-Allyl-5-chloro-_N_-[4-(trifluoromethyl)phenyl]thiophene-2-sulfonamide (207)

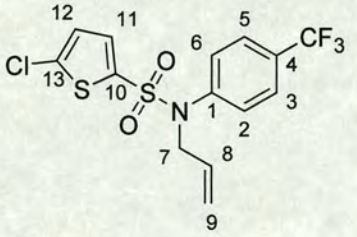

To a stirring solution of 5-chloro-*N*-[4-(trifluoromethyl)phenyl]thiophene-2-sulfonamide (0.118 g, 0.22 mmole, 1.0 eq.) in acetone (3.0 mL) was added allyl bromide (96 μL, 1.10 mmole, 5.0 eq.) followed by triethylamine (300 μL, excess). The reaction mixture was

irradiated in the Discover™ at 70 °C for 10 minutes, with active cooling of the sample. The reaction mixture was diluted with water (20 mL) and extracted with ethyl acetate (2 x 20 mL). The combined organics were washed with water (2 x 20 mL) before being concentrated *in vacuo* to afford a residue that was columned on silica (heptane: hexane: ethyl acetate, 8:2:1). Appropriate fractions were combined and concentrated *in vacuo* to afford sulfonamide **207** as a cream solid (0.074 g, 84%, R_f 0.16, (heptane: hexane: ethyl acetate, 8:2:1)); LRMS EI^+ *m/z* 381 $(M)^+$; HRMS EI^+ *m/z* 380.98640 $(M)^+$ (calculated for $C_{14}H_{11}{}^{35}ClF_3NO_2S_2$, 380.98719 (Dev. – 2.05 ppm)); δ_H (250 MHz, $CDCl_3$): 4.18 (dt, 2H, *J* = 6.3, 1.3 Hz, *H*7), 5.06 (dd, 1H, *J* = 9.8, 1.3 Hz, $H9_{cis}$), 5.08 (dd, 1H, *J* = 17.6, 1.3 Hz, $H9_{trans}$), 5.59 – 5.75 (m, 1H, *H*8), 6.86 (d, 1H, *J* = 4.0 Hz, *H*11), 7.09 (d, 1H, *J* = 4.0 Hz, *H*12), 7.20 (d, 2H, *J* = 8.4 Hz, *H*2, *H*6), 7.55 (d, 2H, *J* = 8.4 Hz, *H*3, *H*4); δ_C (63 MHz, $CDCl_3$): 53.4 (*C*7), 119.8 (*C*9), 123.5 (q, J_{CF} = 272 Hz, CF_3), 126.1 (2 x CH_{Ar}), 126.8 (CH_{Ar}), 128.7 (2 x CH_{Ar}), 131.0 (q, J_{CF} = 33 Hz, *C*4), 131.6 (*C*8), 132.2 (CH_{Ar}), 136.1 (C_{Ar}), 137.8 (C_{Ar}), 141.6 (C_{Ar}).

N-Allyl-N-[3,5-bis(trifluoromethyl)phenyl]-4,5-dibromothiophene-2-sulfonamide (208)

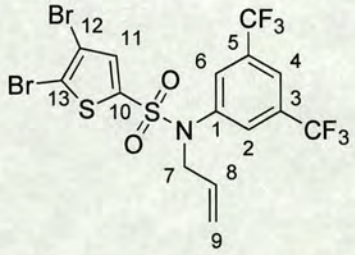

General procedure **S2** was followed using *N*-[3,5-bis(trifluoromethyl)phenyl]-4,5-dibromothiophene-2-sulfonamide (0.103 g, 0.19 mmole, 1.0 eq.), allyl bromide (96 µL, 1.10 mmole, 5.7 eq.) and triethylamine (300 µL, excess). The reaction mixture was irradiated in the Discover™ at 70 °C for 10 minutes. The crude reaction mixture was columned on silica (heptane: hexane: ethyl acetate, 8:2:1) to afford sulfonamide **208** as a white solid (0.040 g, 36%); δ_H (250 MHz, $CDCl_3$): 4.19 (dt, 2H, *J* = 6.4, 1.3 Hz, *H*7),

5.08 (dd, 1H, J = 9.3, 1.3 Hz, $H9_{cis}$), 5.13 (dd, 1H, J = 16.6, 1.3 Hz, $H9_{trans}$), 5.61 – 5.71 (m, 1H, $H8$), 7.12 (s, 1H, $H11$), 7.51 (s, 2H, $H2$, $H6$), 7.79 (s, 1H, $H4$).

N-Allyl-4,5-dibromo-N-[4-(trifluoromethyl)phenyl]thiophene-2-sulfonamide (209)

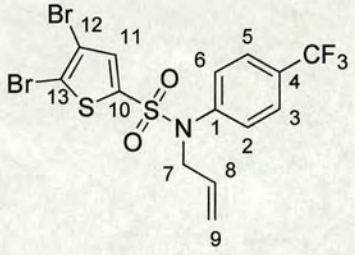

General procedure **S2** was followed using 4,5-dibromo-N-[4-(trifluoromethyl)phenyl]-thiophene-2-sulfonamide (0.104 g, 0.22 mmole, 1.0 eq.), allyl bromide (96 μL, 1.10 mmole, 5.0 eq.) and triethylamine (300 μL, excess). The reaction mixture was irradiated in the Discover™ at 70 °C for 10 minutes. The crude reaction mixture was columned on silica (heptane: hexane: ethyl acetate 8:2:1) to afford sulfonamide **209** as a white solid (0.043 g, 39%, R_f 0.30 (heptane: hexane: ethyl acetate 8:2:1)); ν_{max} (film)/cm^{-1} 3116 (thiophene C-H), 3089 (aryl C-H), 2927 (C-H), 1327 (SO_2), 1170 (SO_2); δ_H (250 MHz, $CDCl_3$): 4.18 (dt, 2H, J = 6.3, 1.3 Hz, $H7$), 5.06 (dd, 1H, J = 9.1, 1.3 Hz, $H9_{cis}$), 5.11 (dd, 1H, J = 16.6, 1.3 Hz, $H9_{trans}$), 5.61 – 5.72 (m, 1H, $H8$), 7.14 (s, 1H, $H11$), 7.22 (d, 2H, J = 8.9 Hz, $H2$, $H6$), 7.57 (d, 2H, J = 8.9 Hz, $H3$, $H5$); Mpt. 85.2 – 85.7 °C.

_N_-[3,5-Bis(trifluoromethyl)phenyl]-5-bromo-_N_-ethylthiophene-2-sulfonamide (211)

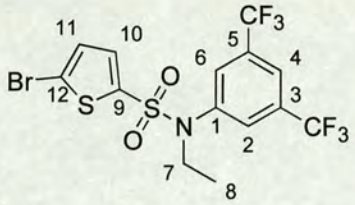

General procedure **S2** was followed using *N*-[3,5-bis(trifluoromethyl)phenyl]-5-bromothiophene-2-sulfonamide (0.100 g, 0.22 mmole, 1.0 eq.), ethyl iodide (88 μL, 1.10 mmole, 5.0 eq.) and triethylamine (300 μL, excess). The reaction mixture was irradiated in the Discover™ at 70 °C for 10 minutes. The crude reaction mixture was columned on silica (heptane: hexane: ethyl acetate 8:2:1) to afford sulfonamide **211** as a white solid (0.037 g, 35%); δ_H (250 MHz, $CDCl_3$): 1.16 (t, 3H, *J* = 7.2 Hz, *H*8), 3.71 (q, 2H, *J* = 7.2 Hz, *H*7), 7.08 – 7.12 (m, 2H, *H*10, *H*11), 7.58 (s, 2H, *H*2, *H*6), 7.87 (s, 1H, *H*4).

_N_-[3,5-Bis(trifluoromethyl)phenyl]-5-chloro-_N_-ethylthiophene-2-sulfonamide (212)

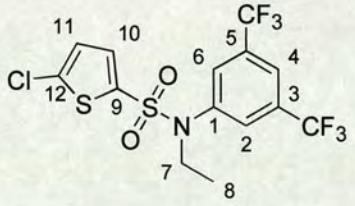

General procedure **S2** was followed using *N*-[3,5-bis(trifluoromethyl)phenyl]-5-chlorothiophene-2-sulfonamide (0.091 g, 0.22 mmole, 1.0 eq.), ethyl iodide (88 μL, 1.10 mmole, 5.0 eq.) and triethylamine (300 μL, excess). The reaction mixture was irradiated in the Discover™ at 70 °C for 10 minutes. The crude reaction mixture was columned on silica (heptane: hexane: ethyl acetate, 8:2:1) to afford sulfonamide **212** as a white solid (0.044 g, 46%, R_f 0.25 (heptane: hexane: ethyl acetate, 8:2:1)); δ_H (250 MHz, $CDCl_3$): 1.15 (t, 3H, *J* = 7.2 Hz, *H*8), 3.71 (q, 2H, *J* = 7.2 Hz, *H*7), 6.96 (d, 1H, *J* = 4.0 Hz, *H*11), 7.15 (d, 1H, *J* = 4.0 Hz, *H*10), 7.58 (s, 2H, *H*2, *H*6), 7.87 (s, 1H, *H*4); δ_C (63

MHz, $CDCl_3$): 13.9 (*C*8), 43.8 (*C*7), 121.9 (*C*4), 122.5 (q, J_{CF} = 273 Hz, CF_3), 126.9 (CH_{Ar}), 128.8 (2 x CH_{Ar}), 132.4 (CH_{Ar}), 132.6 (q, J_{CF} = 32 Hz, *C*3, *C*5), 135.3 (C_{Ar}), 138.3 (C_{Ar}), 135.3 (C_{Ar}), 140.2 (C_{Ar}).

5-Bromo-*N*-ethyl-*N*-[4-(trifluoromethyl)phenyl]thiophene-2-sulfonamide (213)

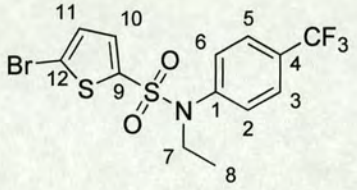

General procedure **S2** was followed using 5-bromo-*N*-[4-(trifluoromethyl)phenyl]-thiophene-2-sulfonamide (0.08 g, 0.22 mmole, 1.0 eq.), ethyl iodide (88 μL, 1.10 mmole, 5.0 eq.) and triethylamine (300 μL, excess). The reaction mixture was irradiated in the Discover™ at 70 °C for 10 minutes. The crude reaction mixture was columned on silica (hexane: ethyl acetate 8:1) to afford sulfonamide **213** as a white solid (0.046 g, 51%, R_f 0.19 (hexane: ethyl acetate 8:1)); δ_H (250 MHz, $CDCl_3$): 1.12 (t, 3H, *J* = 7.1 Hz, *H*8), 3.69 (q, 2H, *J* = 7.1 Hz, *H*7), 7.06 (d, 1H, *J* = 4.0 Hz, *H*11), 7.10 (d, 1H, *J* = 4.0 Hz, *H*10), 7.28 (d, 2H, *J* = 8.3 Hz, *H*2, *H*6), 7.63 (d, 2H, *J* = 8.3 Hz, *H*3, *H*5); δ_C (63 MHz, $CDCl_3$): 13.9 (*C*8), 45.7 (*C*7), 120.1 (C_{Ar}), 123.1 (q, J_{CF} = 272 Hz, CF_3), 126.3 (2 x CH_{Ar}), 128.8 (2 x CH_{Ar}), 130.1 (q, J_{CF} = 30 Hz, *C*4), 130.4 (CH_{Ar}), 132.7 (CH_{Ar}), 139.0 (C_{Ar}), 141.5 (C_{Ar}).

5-Chloro-*N*-ethyl-*N*-[4-(trifluoromethyl)phenyl]thiophene-2-sulfonamide (214)

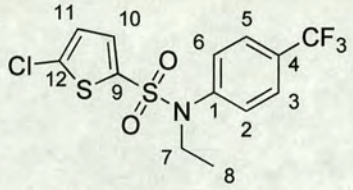

General procedure **S2** was followed using 5-chloro-*N*-[4-(trifluoromethyl)phenyl]-thiophene-2-sulfonamide (0.075 g, 0.22 mmole, 1.0 eq.), ethyl iodide (81 μL, 1.10 mmole, 5.0 eq.) and triethylamine (300 μL, excess). The reaction mixture was irradiated in the Discover™ at 70 °C for 10 minutes. The crude reaction mixture was columned on silica (hexane: ethyl acetate, 8:1) to afford sulfonamide **214** as a white solid (0.031 g, 38%); δ_H (250 MHz, $CDCl_3$): 1.13 (t, 3H, *J* = 7.1 Hz, *H*8), 3.69 (q, 2H, *J* = 7.1 Hz, *H*7), 6.73 (d, 1H, *J* = 4.0 Hz, *H*11), 7.14 (d, 1H, *J* = 4.0 Hz, *H*10), 7.29 (d, 2H, *J* = 8.3 Hz, *H*2, *H*6), 7.63 (d, 2H, *J* = 8.3 Hz, *H*3, *H*5).

***N*-[3,5-Bis(trifluoromethyl)phenyl]-4,5-dibromo-*N*-ethylthiophene-2-sulfonamide (215)**

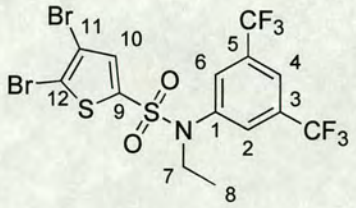

General procedure **S2** was followed using *N*-[3,5-bis(trifluoromethyl)phenyl]-4,5-dibromothiophene-2-sulfonamide (0.103 g, 0.19 mmole, 1.0 eq.), ethyl iodide (88 μL, 1.10 mmole, 5.8 eq.) and triethylamine (300 μL, excess). The reaction mixture was irradiated in the Discover™ at 70 °C for 10 minutes. The crude reaction mixture was columned on silica (hexane: ethyl acetate, 8:1) to afford a white solid (0.028 g, 26%); δ_H

(250 MHz, $CDCl_3$): 1.16 (t, 3H, *J* = 7.2 Hz, *H*8), 3.71 (q, 2H, *J* = 7.2 Hz, *H*7), 7.18 (s, 1H, *H*10), 7.60 (s, 2H, *H*2, *H*6), 7.90 (s, 1H, *H*4).

4,5-Dibromo-*N*-ethyl-*N*-[4-(trifluoromethyl)phenyl]thiophene-2-sulfonamide (216)

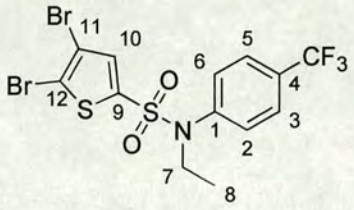

General procedure **S2** was followed using 4,5-dibromo-*N*-[4-(trifluoromethyl)phenyl]-thiophene-2-sulfonamide (0.118 g, 0.25 mmole, 1.0 eq.), ethyl iodide (88 μL, 1.10 mmole, 4.4 eq.) and triethylamine (300 μL, excess). The reaction mixture was irradiated in the Discover™ at 70 °C for 10 minutes. The crude reaction mixture was columned on silica (hexane: ethyl acetate 8:1) to afford sulfonamide **216** as a white solid (0.044 g, 35%); ν_{max} (film)/cm^{-1} 3117 (thiophene C-H), 3087 (aryl C-H), 2979 (C-H), 1332 (SO_2), 1169 (SO_2); δ_H (250 MHz, $CDCl_3$): 1.14 (t, 3H, *J* = 7.1 Hz, *H*8), 3.70 (q, 2H, *J* = 7.1 Hz, *H*7), 7.19 (s, 1H, *H*10), 7.30 (d, 2H, *J* = 8.8 Hz, *H*2, *H*6), 7.67 (d, 2H, *J* = 8.8 Hz, *H*3, *H*5); Mpt. 140.4 – 141.7 °C.

5-Chloro-*N*-isobutyl-*N*-[4-(trifluoromethyl)phenyl]thiophene-2-sulfonamide (221)

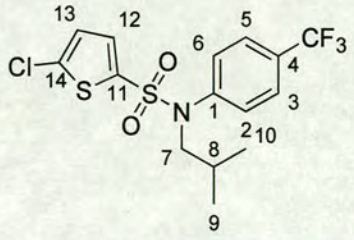

General procedure **S2** was followed using 5-chloro-*N*-[4-(trifluoromethyl)phenyl]-thiophene-2-sulfonamide (0.075 g, 0.22 mmole, 1.0 eq.), 1-iodo-2-methylpropane (131

μL, 1.10 mmole, 5.0 eq.) and triethylamine (300 μL, excess). The reaction mixture was irradiated in the Discover™ at 70 °C for 10 minutes. The crude reaction mixture was columned on silica (heptane: hexane: ethyl acetate 8:2:1) to afford sulfonamide **221** as a white solid (0.007 g, 8%); δ_H (250 MHz, $CDCl_3$): 0.85 (d, 6H, *J* = 6.7 Hz, *H*9, *H*10), 1.44 – 1.61 (m, 1H, *H*8), 3.32 (d, 2H, *J* = 7.4, *H*7), 6.85 (d, 1H, *J* = 4.0 Hz, *H*13), 7.03 (s, 1H, *J* =4.0 Hz, H12), 7.21 (d, 2H, *J* = 8.4 Hz, *H*2, *H*6), 7.55 (d, 2H, *J* = 8.4 Hz, *H*3, *H*5).

_N_-[3,5-Bis(trifluoromethyl)phenyl]-4,5-dibromo-_N_-isobutylthiophene-2-sulfonamide (222)

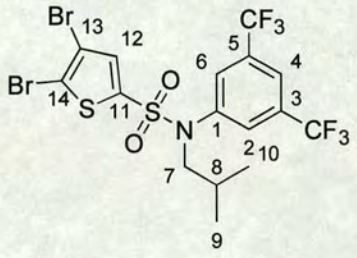

General procedure **S2** was followed using *N*-[3,5-bis(trifluoromethyl)phenyl]-4,5-dibromothiophene-2-sulfonamide (0.103 g, 0.19 mmole, 1.0 eq.), 1-iodo-2-methylpropane (131 μL, 0.98 mmole, 5.8 eq.) and triethylamine (300 μL, excess). The reaction mixture was irradiated in the Discover™ at 70 °C for 10 minutes. The crude reaction mixture was columned on silica (heptane: hexane: ethyl acetate, 8:2:1) to afford sulfonamide **222** as a white solid (0.003 g, 3%); δ_H (250 MHz, $CDCl_3$): 0.88 (d, 6H, *J* = 6.6 Hz, *H*9, *H*10), 1.44 – 1.61 (m, 1H, *H*8), 3.33 (d, 2H, *J* = 7.4 Hz, *H*7), 7.05 (s, 1H, *H*12), 7.52 (s, 2H, *H*2, *H*6), 7.81(s, 1H, *H*4).

4,5-Dibromo-*N*-isobutyl-*N*-[4-(trifluoromethyl)phenyl]thiophene-2-sulfonamide (223)

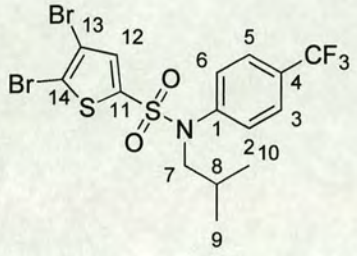

General procedure **S2** was followed using 4,5-dibromo-*N*-[4-(trifluoromethyl)phenyl]-thiophene-2-sulfonamide (0.118 g, 0.25 mmole, 1.0 eq.), 1-iodo-2-methylpropane (131 μL, 1.10 mmole, 4.4 eq.) and triethylamine (300 μL, excess). The reaction mixture was irradiated in the Discover™ at 70 °C for 10 minutes. The crude reaction mixture was columned on silica (heptane: hexane: ethyl acetate 8:2:1) to afford sulfonamide **223** as a white solid (0.008 g, 6%); δ_H (250 MHz, $CDCl_3$): 0.86 (d, 6H, J = 6.7 Hz, *H*9, *H*10), 1.45 – 1.62 (m, 1H, *H*8), 3.33 (d, 2H, J = 7.4, *H*7), 7.08 (s, 1H, *H*12), 7.24 (d, 2H, J = 8.3 Hz, *H*2, *H*6), 7.59 (d, 2H, J = 8.3 Hz, *H*3, *H*5).

***N*-[3,5-Bis(trifluoromethyl)phenyl]-4-chloro-3-nitrobenzamide (225)**

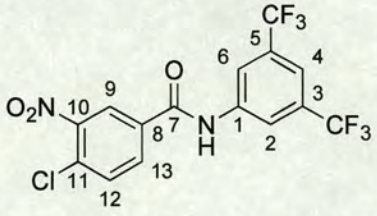

General procedure **A1** was followed using 3,5-(trifluoromethyl)aniline (141 μL, 0.91 mmole, 1.0 eq.) and 4-chloro-3-nitrobenzoyl chloride (0.220 g, 1.0 mmole, 1.1 eq.). Amide **225** was isolated as a white solid (0.298 g, 79%); LRMS FAB$^+$ *m/z* 413 $(MH)^+$; HRMS FAB$^+$ *m/z* 413.01316 $(MH)^+$ (calculated for $C_{15}H_8{}^{35}ClF_6N_2O_3$, 413.01276 (Dev. 0.97 ppm)); δ_H (250 MHz, $(CD_3)_2SO$): 7.87 (s, 1H, *H*4), 8.03 (d, 1H, J = 8.5 Hz, *H*12),

8.30 (dd, 1H, J = 8.5, 2.1 Hz, *H*13), 8.49 (s, 2H, *H*2, *H*6), 8.70 (d, 1H, J = 2.1 Hz, *H*9), 11.10 (s, 1H, N*H*); δ_C (63 MHz, $(CD_3)_2SO$): 116.8 (CH_{Ar}), 119.8 (*C*2, *C*6), 123.0 (q, J_{CF} = 273 Hz, CF_3), 124.7 (CH_{Ar}), 128.6 (C_{Ar}), 130.5 (q, J_{CF} = 33 Hz, *C*3, *C*5), 132.0 (CH_{Ar}), 132.7 (CH_{Ar}), 133.6 (C_{Ar}), 140.3 (C_{Ar}), 147.1 (C_{Ar}), 162.9 (*C*7).

4-Chloro-*N*-(3-chlorophenyl)-3-nitrobenzamide (226)

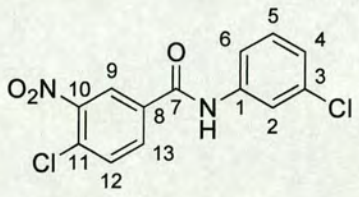

General procedure **A1** was followed using 3-chloroaniline (96 μL, 0.91 mmole, 1.0 eq.) and 4-chloro-3-nitrobenzoyl chloride (0.220 g, 1.0 mmole, 1.1 eq.). Amide **226** was isolated as a pale yellow solid (0.259 g, 92 %); LRMS EI^+ *m/z* 310 $(M)^+$; HRMS EI^+ *m/z* 309.99179 $(M)^+$ (calculated for $C_{13}H_8{}^{35}Cl_2N_2O_3$, 309.99120 (Dev. 1.92 ppm)); ν_{max} (KBr)/cm^{-1} 3310 (N-H), 3045 (aryl C-H), 1646 (C=O), 1530 (NO_2), 1350 (NO_2); δ_H (250 MHz, $(CD_3)_2SO$): 7.23 (ddd, 1H, J = 8.0, 1.2, 0.9 Hz, *H*4), 7.43 (t, 1H, J = 8.0 Hz, *H*5), 7.71 (ddd, 1H, J = 8.0, 1.2, 0.9 Hz, *H*6), 7.95 (t, 1H, J = 0.9 Hz, *H*2), 8.00 (d, 1H, J = 8.4 Hz, *H*12), 8.28 (dd, 1H, J = 8.4, 2.1 Hz, *H*13), 8.65 (d, 1H, J = 2.1 Hz, *H*9), 10.73 (s, 1H, N*H*); δ_C (63 MHz, $(CD_3)_2SO$): 118.6 (CH_{Ar}), 119.7 (CH_{Ar}), 123.7 (CH_{Ar}), 124.7 (CH_{Ar}), 128.1 (C_{Ar}), 130.3 (CH_{Ar}), 131.8 (CH_{Ar}), 132.7 (CH_{Ar}), 132.8 (C_{Ar}), 134.3 (C_{Ar}), 139.8 (C_{Ar}), 147.1 (C_{Ar}), 162.5 (*C*7); Mpt. 159.5 – 160.0 °C.

4-Chloro-*N*-(3,4-dichlorophenyl)-3-nitrobenzamide (227)

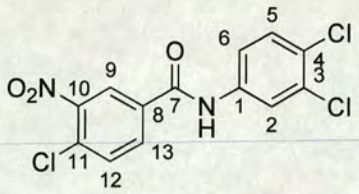

General procedure **A1** was followed using 3,4-dichloroaniline (0.147 □, 0.91 mmole, 1.0 eq.) and 4-chloro-3-nitrobenzoyl chloride (0.220 g, 1.0 mmole, 1.1 eq.). Amide **227** was isolated as a pale brown solid (0.224 g, 71 %); LRMS EI+ *m/z* 344 $(M)^+$; HRMS EI^+ *m/z* 343.95161 $(M)^+$ (calculated for $C_{13}H_7{}^{35}Cl_3N_2O_3$, 343.95223 (Dev. – 1.79 ppm)); ν_{max} (KBr)/cm^{-1} 3281 (N-H), 3096 (aryl C-H), 1655 (C=O), 1534 (NO_2), 1340 (NO_2); δ_H (250 MHz, $(CD_3)_2SO$): 7.65 (d, 1H, *J* = 8.8 Hz, *H*5), 7.74 (dd, 1H, *J* = 8.8, 2.4 Hz, *H*6), 7.99 (d, 1H, *J* = 8.4 Hz, *H*12), 8.12 (d, 1H, *J* =2.4 Hz, *H*2), 8.26 (dd, 1H, *J* = 8.4, 2.1 Hz, *H*13), 8.64 (d, 1H, *J* = 2.1 Hz, *H*9), 10.80 (s, 1H, N*H*); δ_C (63 MHz, $(CD_3)_2SO$): 120.2 (CH_{Ar}), 121.4 (CH_{Ar}), 124.7 (CH_{Ar}), 125.5 (C_{Ar}), 128.3 (C_{Ar}), 130.5 (CH_{Ar}), 130.7 (C_{Ar}), 131.9 (CH_{Ar}), 132.7 (CH_{Ar}), 134.0 (C_{Ar}), 138.5 (C_{Ar}), 147.1 (C_{Ar}), 162.5 (*C*7).

4-Chloro-3-nitro-*N*-[4-(trifluoromethyl)phenyl]benzamide (228)

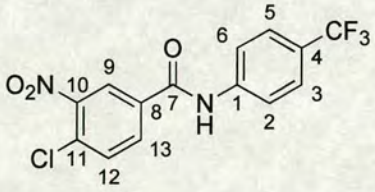

General procedure **A1** was followed using 4-(trifluoromethyl)aniline (114 μL, 0.91 mmole, 1.0 eq.) and 4-chloro-3-nitrobenzoyl chloride (0.220 g, 1.0 mmole, 1.1 eq.). Amide **228** was isolated as a cream solid (0.206 g, 66 %); LRMS EI^+ *m/z* 344 $(M)^+$; HRMS EI^+ *m/z* 344.01720 $(M)^+$ (calculated for $C_{14}H_8{}^{35}ClF_3N_2O_3$, 344.01755 (Dev. – 1.02 ppm)); ν_{max} (KBr)/cm^{-1} 3293 (N-H), 3084 (aryl C-H), 1654 (C=O), 1529 (NO_2),

1341 (NO_2); δ_H (250 MHz, $(CD_3)_2SO$): 7.78 (d, 2H, *J* = 8.8 Hz, *H*3, *H*5), 8.02 (d, 2H, *J* = 8.8 Hz, *H*2, *H*6), 8.02 (d, 1H, *J* = 8.4 Hz, *H*12), 8.30 (dd, 1H, *J* = 8.4, 2.1 Hz, *H*13), 8.68 (d, 1H, *J* = 2.1 Hz, *H*9), 10.88 (s, 1H, N*H*); δ_C (63 MHz, $(CD_3)_2SO$): 120.1 (2 x CH_{Ar}), 123.9 (q, J_{CF} = 32 Hz, *C*4), 124.1 (q, J_{CF} = 271 Hz, CF_3), 124.8 (CH_{Ar}), 125.9 (2 x CH_{Ar}), 128.2 (C_{Ar}), 131.8 (CH_{Ar}), 132.8 (CH_{Ar}), 134.2 (C_{Ar}), 142.0 (C_{Ar}), 147.2 (C_{Ar}), 162.8 (*C*7);

4-Chloro-*N*-(4-chlorophenyl)-3-nitrobenzamide (229)

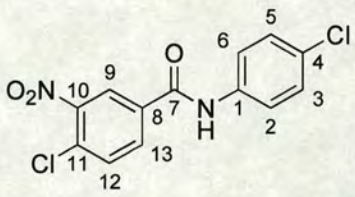

General procedure **A1** was followed using 4-chloroaniline (0.116 g, 0.91 mmole, 1.0 eq.) and 4-chloro-3-nitrobenzoyl chloride (0.220 g, 1.0 mmole, 1.1 eq.). Amide **229** was isolated as a pale yellow solid (0.234 g, 83%); LRMS FAB^+ *m/z* 311 $(MH)^+$; HRMS FAB^+ *m/z* 310.99868 $(MH)^+$ (calculated for $C_{13}H_9{}^{35}Cl_2N_2O_3$, 310.99902 (Dev. –1.11 ppm)); ν_{max} (film)/cm^{-1} 3285 (N-H), 3060 (aryl C-H), 2930 (C-H), 1648 (C=O), 1534 (NO_2), 1341 (NO_2); δ_H (250 MHz, $(CD_3)_2SO$): 7.46 (d, 2H, *J* = 8.8 Hz, *H*3, *H*5), 7.82 (d, 2H, *J* = 8.8 Hz, *H*2, *H*6), 8.00 (d, 1H, *J* = 8.4 Hz, *H*12), 8.28 (dd, 1H, *J* = 8.4, 2.1 Hz, *H*13), 8.65 (d, 1H, *J* = 2.1 Hz, *H*9), 10.71 (s, 1H,N*H*); δ_C (63 MHz, $(CD_3)_2SO$): 121.8 (2 x CH_{Ar}), 124.7 (CH_{Ar}), 127.6 (C_{Ar}), 128.0 (C_{Ar}), 128.4 (2 x CH_{Ar}), 131.8 (CH_{Ar}), 132.6 (CH_{Ar}), 134.4 (C_{Ar}), 137.3 (C_{Ar}), 147.1 (C_{Ar}), 162.3 (*C*7); Mpt. 187.8 – 188.2 °C.

4-Chloro-*N*-(4-fluorophenyl)-3-nitrobenzamide (230)

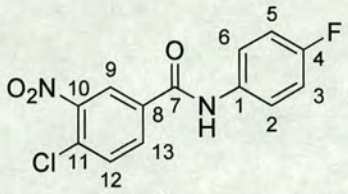

General procedure **A1** was followed using 4-fluoroaniline (87 μL, 0.91 mmole, 1.0 eq.) and 4-chloro-3-nitrobenzoyl chloride (0.220 g, 1.0 mmole, 1.1 eq.). Amide **230** was isolated as a grey solid (0.079 g, 30 %); LRMS EI^+ *m/z* 294 $(M)^+$; HRMS EI^+ *m/z* 294.01993 $(M)^+$ (calculated for $C_{13}H_8{}^{35}ClFN_2O_3$, 294.02075 (Dev.- 2.79 ppm)); ν_{max} (KBr)/cm^{-1} 3286 (N-H), 3075 (aryl C-H), 1651 (C=O), 1538 (NO_2), 1321 (NO_2); δ_H (250 MHz, $(CD_3)_2SO$): 7.24 (t, 2H, J = 8.9 Hz, J_{HF} = 8.9 Hz, *H*3, *H*5), 7.79 (dd, 2H, J = 8.9 Hz, J_{HF} = 5.0 Hz, *H*2, *H*6), 7.99 (d, 1H, J = 8.4 Hz, *H*12), 8.27 (dd, 1H, J = 8.4, 2.1 Hz, *H*13), 8.64 (d, 1H, J = 2.1 Hz, *H*9), 10.62 (s, 1H, N*H*); δ_C (63 MHz, $(CD_3)_2SO$): 115.2 (d, J_{CF} = 22 Hz, *C*3, *C*5), 122.2 (d, J_{CF} = 8 Hz, *C*2, *C*6), 124.6 (CH_{Ar}), 127.9 (C_{Ar}), 131.8 (CH_{Ar}), 132.6 (CH_{Ar}), 134.5 (C_{Ar}), 134.7 (C_{Ar}), 147.1 (C_{Ar}), 158.4 (d, J_{CF} = 241 Hz, *C*4), 162.2 (*C*7).

4-Chloro-*N*-(3,4-difluorophenyl)-3-nitrobenzamide (231)

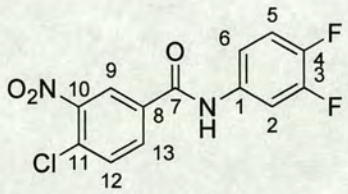

General procedure **A1** was followed using 3,4-difluoroaniline (87 μL, 0.91 mmole, 1.0 eq.) and 4-chloro-3-nitrobenzoyl chloride (0.220 g, 1.0 mmole, 1.1 eq.). Amide 231 was isolated as a white solid (0.041 g, 14 %); LRMS EI^+ *m/z* 312 $(M)^+$; HRMS EI^+ *m/z* 312.02421 $(M)^+$ (calculated for $C_{13}H_7{}^{35}ClF_2N_2O_3$, 312.01133 (Dev. 3.59 ppm)); ν_{max}

(KBr)/cm^{-1} 3291 (N-H), 3029 (aryl C-H), 1653 (C=O), 1518 (NO_2), 1336 (NO_2); δ_H (250 MHz, $(CD_3)_2SO$): 7.42 – 7.59 (m, 2H, H2, H5), 7.93 (ddd, 1H, J = 7.7, 2.3 Hz, J_{HF} = 13.1 Hz, *H*6), 8.01 (d, 1H, J = 8.6 Hz, *H*12), 8.27 (dd, 1H, J = 8.6, 2.1 Hz, *H*13), 8.64 (d, 1H, J =2.1 Hz, *H*9), 10.76 (s, 1H, N*H*); δ_C (63 MHz, $(CD_3)_2SO$): 109.3 (d, J_{CF} = 22 Hz, CH_{Ar}), 116.6 (CH_{Ar}), 117.3 (d, J_{CF} = 18 Hz, CH_{Ar}), 124.7 (CH_{Ar}), 128.2 (C_{Ar}), 131.8 (CH_{Ar}), 132.6 (CH_{Ar}), 134.1 (C_{Ar}), 135.3 (d, J_{CF} = 6 Hz, *C*1), 145.7 (dd, J_{CF} = 243, 13 Hz, C_{Ar}), 147.1 (C_{Ar}), 148.6 (dd, J_{CF} = 244, 13 Hz, C_{Ar}), 162.4 (*C*7).

4-Chloro-*N*-(3-fluorophenyl)-3-nitrobenzamide (232)

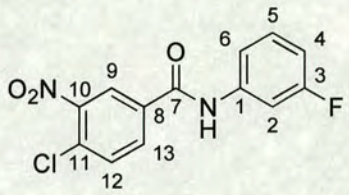

General procedure **A1** was followed using 3-fluoroaniline (87 μL, 0.91 mmole, 1.0 eq.) and 4-chloro-3-nitrobenzoyl chloride (0.220 g, 1.0 mmole, 1.1 eq.). Amide **232** was isolated as a white solid (0.176 g, 66 %); LRMS EI$^+$ *m/z* 294 (M)$^+$; HRMS EI$^+$ *m/z* 294.02074 (M)$^+$ (calculated for $C_{13}H_8ClFN_2O_3$, 294.02075 (Dev. – 0.02 ppm)); ν_{max} (KBr)/cm^{-1} 3278 (N-H), 3085 (aryl C-H), 1650 (C=O), 1539 (NO_2), 1358 (NO_2); δ_H (250 MHz, $(CD_3)_2SO$): 6.96 – 7.04 (m, 1H, *H*4), 7.44 (dt, 1H, J_{HF} = 6.7 Hz, J = 8.0 Hz, *H*5), 7.56 (ddd, 1H, J = 8.0, 2.3, 1.0 Hz, *H*6), 7.75 (dt, 1H, J_{HF} = 11.7 Hz, J = 2.3 Hz, *H*2), 8.00 (d, 1H, J = 8.4 Hz, *H*12), 8.28 (dd, 1H, J = 8.4, 2.1 Hz, *H*13), 8.65 (d, 1H, J = 2.1 Hz, *H*9), 10.74 (s, 1H, N*H*); δ_C (63 MHz, $(CD_3)_2SO$): 107.0 (d, J_{CF} = 26 Hz, CH_{Ar}), 110.5 (d, J_{CF} = 21 Hz, CH_{Ar}), 116.0 (CH_{Ar}), 124.7 (CH_{Ar}), 128.1 (C_{Ar}), 130.2 (d, J_{CF} = 9 Hz, *C*5), 131.8 (CH_{Ar}), 132.7 (CH_{Ar}), 134.3 (C_{Ar}), 140.1 (d, J_{CF} = 11 Hz, C_{Ar}), 147.1 (C_{Ar}), 161.8 (d, J_{CF} = 242 Hz, *C*3), 162.5 (*C*7).

4-Chloro-*N*-(2,4-dichlorophenyl)-3-nitrobenzamide (233)

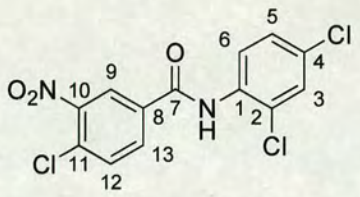

General procedure **A1** was followed using 2,4-dichloroaniline (0.147 g, 0.91 mmole, 1.0 eq.) and 4-chloro-3-nitrobenzoyl chloride (0.220 g, 1.0 mmole, 1.1 eq.). Amide **233** was isolated as a white solid (0.290 g, 92 %); LRMS EI+ *m/z* 344 $(M)^+$; HRMS EI^+ *m/z* 343.95204 $(M)^+$ (calculated for $C_{13}H_7{}^{35}Cl_3N_2O_3$, 343.95223 (Dev. – 0.55 ppm)); ν_{max} (KBr)/cm^{-1} 3406 (N-H), 3081 (aryl C-H), 1686 (C=O), 1537 (NO_2), 1357 (NO_2); δ_H (250 MHz, $(CD_3)_2SO$): 7.52 (dd, 1H, *J* = 8.6, 2.3 Hz, *H*5), 7.63 (d, 1H, *J* = 8.6 Hz, *H*6), 7.77 (d, 1H, *J* = 2.3 Hz, *H*3), 8.00 (d, 1H, *J* = 8.4 Hz, *H*12), 8.28 (dd, 1H, *J* = 8.4 , 2.1 Hz, *H*13), 8.66 (d, 1H, *J* = 2.1 Hz, *H*9), 10.57 (s, 1H, N*H*); δ_C (63 MHz, $(CD_3)_2SO$): 124.8 (CH_{Ar}), 127.6 (CH_{Ar}), 128.4 (C_{Ar}), 129.0 (CH_{Ar}), 129.6 (CH_{Ar}), 130.4 (C_{Ar}), 131.1 (C_{Ar}), 132.0 (CH_{Ar}), 132.6 (CH_{Ar}), 133.4 (C_{Ar}), 133.8 (C_{Ar}), 147.2 (C_{Ar}), 162.5 (*C*7); Mpt. 166.8 – 167.5 °C.

4-Chloro-*N*-(3,5-dichlorophenyl)-3-nitrobenzamide (234)

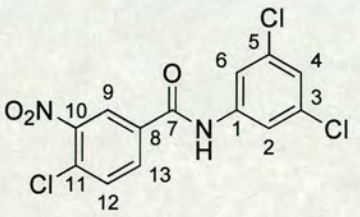

General procedure **A1** was followed using 3,5-dichloroaniline (147 □, 0.91 mmole, 1.0 eq.) and 4-chloro-3-nitrobenzoyl chloride (0.220 g, 1.0 mmole, 1.1 eq.). Amide **234** was isolated as a cream solid (0.291 g, 93 %); LRMS EI^+ *m/z* 344 $(M)^+$; HRMS EI^+ *m/z* 343.95139 $(M)^+$ (calculated for $C_{13}H_7{}^{35}Cl_3N_2O_3$, 343.95223 (Dev. –2.43 ppm)); ν_{max}

(KBr)/cm^{-1} 3283 (N-H), 3079 (aryl C-H), 1667 (C=O), 1532 (NO_2), 1340 (NO_2); δ_H (250 MHz, $(CD_3)_2SO$): 7.39 (t, 1H, J = 1.8 Hz, *H*4), 7.88 (d, 2H, J = 1.8 Hz, *H*2, *H*6), 8.01 (d, 1H, J = 8.4 Hz, *H*12), 8.26 (dd, 1H, J = 8.4, 2.1 Hz, *H*13), 8.65 (d, 1H, J = 2.1 Hz, *H*9), 10.82 (s, 1H, N*H*); δ_C (63 MHz, $(CD_3)_2SO$): 118.2 (*C*2, *C*6), 123.2 (CH_{Ar}), 124.7 (CH_{Ar}), 128.4 (C_{Ar}), 131.9 (CH_{Ar}), 132.7 (CH_{Ar}), 133.8 (3 x C_{Ar}), 140.7 (C_{Ar}), 147.1 (C_{Ar}), 162.7 (*C*7); Mpt. 207.4 – 207.8 °C.

4-Chloro-3-nitro-*N*-(2,4,5-trichlorophenyl)benzamide (235)

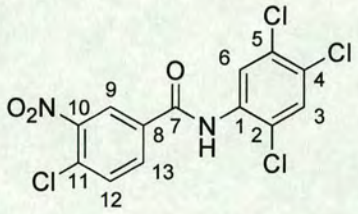

General procedure **A1** was followed using 2,4,5-trichloroaniline (0.179 g, 0.91 mmole, 1.0 eq.) and 4-chloro-3-nitrobenzoyl chloride (0.220 g, 1.0 mmole, 1.1 eq.). Amide **235** was isolated as a grey solid (0.215 g, 62 %); LRMS EI$^+$ *m/z* 378 $(M)^+$; HRMS EI$^+$ *m/z* 377.91319 $(M)^+$ (calculated for $C_{13}H_6{}^{35}Cl_4N_2O_3$, 377.91325 (Dev. – 0.17 ppm)); ν_{max} (KBr)/cm^{-1} 3413 (N-H), 3113 (aryl C-H), 3082 (aryl C-H), 1697 (C=O), 1536 (NO_2), 1354 (NO_2); δ_H (250 MHz, $(CD_3)_2SO$): 8.01 (s, 1H, *H*3), 8.03 (d, 1H, J = 8.0 Hz, *H*12), 8.04 (s, 1H, *H*6), 8.28 (dd, 1H, J = 8.0, 2.1 Hz, *H*13), 8.66 (d, 1H, J = 2.1 Hz, *H*9), 10.67 (s, 1H, N*H*); δ_C (63 MHz, $(CD_3)_2SO$): 124.9 (CH_{Ar}), 128.5 (C_{Ar}), 128.8 (C_{Ar}), 129.1 (CH_{Ar}), 129.3 (C_{Ar}), 129.7 (C_{Ar}), 130.6 (CH_{Ar}), 132.0 (CH_{Ar}), 132.7 (CH_{Ar}), 133.8 (C_{Ar}), 134.5 (C_{Ar}), 147.1 (C_{Ar}), 162.7 (*C*7).

4-Chloro-3-nitro-*N*-[4-(trifluoromethyl)benzyl]benzamide (236)

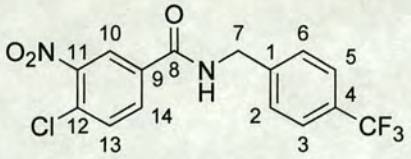

General procedure **A1** was followed using 1-[4-(trifluoromethyl)phenyl]methanamine (130 μL, 0.91 mmole, 1.0 eq.) and 4-chloro-3-nitro-benzoylchloride (0.220 g, 1.0 mmole, 1.1 eq.). Amide **236** was isolated as a cream solid (0.306 g, 94 %); LRMS EI^+ *m/z* 358 $(M)^+$; HRMS EI^+ *m/z* 358.03389 $(M)^+$ (calculated for $C_{15}H_{10}{}^{35}ClF_3N_2O_3$, 358.03320 (Dev. 1.93 ppm)); ν_{max} (KBr)/cm^{-1} 3274 (N-H), 3073 (aryl C-H), 2940 (C-H), 2878 (C-H), 1640 (C=O), 1536 (NO_2), 1329 (NO_2); δ_H (250 MHz, $(CD_3)_2SO$): 4.60 (d, 2H, *J* = 5.7 Hz, *H*7), 7.58 (d, 2H, *J* = 8.0 Hz, *H*2, *H*6), 7.72 (d, 2H, *J* = 8.0 Hz, *H*3, *H*5), 7.95 (d, 1H, *J* = 6.3 Hz, *H*13), 8.22 (dd, 1H, *J* = 6.3, 2.1 Hz, *H*14), 8.59 (d, 1H, *J* = 2.1 Hz, *H*10), 9.54 (t, 1H, *J* = 5.7 Hz, N*H*); δ_C (63 MHz, $(CD_3)_2SO$): 42.4 (*C*7), 124.1 (q, *J* = 272 Hz, *C*F_3), 124.4 (*C*H_{Ar}), 125.0 (d, J_{CF} = 4 Hz, *C*3, *C*5), 127.4 (q, J_{CF} = 32 Hz, *C*4), 127.7 (*C*2, *C*6), 127.8 (C_{Ar}), 131.8 (*C*H_{Ar}), 132.2 (*C*H_{Ar}), 133.8 (C_{Ar}), 143.7 (C_{Ar}), 147.1 (C_{Ar}), 163.2 (*C*8);

***N*-[3,5-Bis(trifluoromethyl)benzyl]-4-chloro-3-nitrobenzamide (237)**

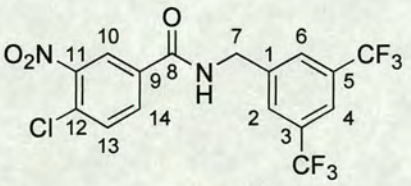

General procedure **A1** was followed was using 1-[3,5-bis(trifluoromethyl)phenyl]-methanamine (0.221 g, 0.91 mmole, 1.0 eq.) and 4-chloro-3-nitrobenzoyl chloride (0.220 g, 1.0 mmole, 1.1 eq.). Amide **237** was isolated as a cream solid (0.226 g, 58 %); LRMS EI^+ *m/z* 426 $(M)^+$; HRMS EI^+ *m/z* 426.02084 $(M)^+$ (calculated for

$C_{16}H_9{}^{35}ClF_6N_2O_3$, 426.02059 (Dev. 0.59 ppm)); δ_H (250 MHz, CD_3OD): 4.78 (s, 2H, *H*7), 7.87 (d, 1H, *J* = 8.7 Hz, *H*13), 8.14 (s, 1H, *H*4), 8.18 (dd, 1H, *J* = 2.1, 8.7 Hz, *H*14), 8.20 (s, 2H, *H*2, *H*6), 8.51 (d, 1H, *J* = 2.1 Hz, *H*10).

4-Chloro-*N*-(4-chlorobenzyl)-3-nitrobenzamide (238)

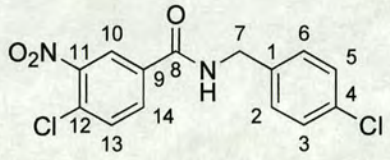

General procedure **A1** was followed using 1-[(4-chlorophenyl)phenyl]methanamine (111 μL, 0.91 mmole, 1.0 eq.) and 4-chloro-3-nitrobenzoyl chloride (0.220 g, 1.0 mmole, 1.1 eq.). Amide **238** was isolated as a white solid (0.217 g, 74 %); LRMS EI^+ *m/z* 324 $(M)^+$; HRMS EI^+ *m/z* 324.00712 $(M)^+$ (calculated for $C_{14}H_{10}{}^{35}Cl_2N_2O_3$, 324.00685 (Dev. 0.85 ppm)); ν_{max} (KBr)/cm^{-1} 3270 (N-H), 3071 (aryl C-H), 1635 (C=O), 1538 (NO_2), 1362 (NO_2); δ_H (250 MHz, $(CD_3)_2SO$): 4.50 (d, 2H, *J* = 5.8 Hz, *H*7), 7.37 (d, 2H, *J* = 8.8 Hz, *H*2, *H*6), 7.41 (d, 2H, *J* = 8.8 Hz, *H*3, *H*5), 7.93 (d, 1H, *J* = 8. 4 Hz, *H*13), 8.20 (dd, 1H, *J* = 8.4, 2.1 Hz, *H*14), 8.57 (d, 1H, *J* = 2.1 Hz, *H*10), 9.46 (t, 1H, *J* = 5.8 Hz, N*H*); δ_C (63 MHz, $(CD_3)_2SO$): 42.1 (*C*7), 124.3 (CH_{Ar}), 127.8 (C_{Ar}), 128.1 (2 x CH_{Ar}), 129.0 (2 x CH_{Ar}), 131.3 (C_{Ar}), 131.8 (CH_{Ar}), 132.2 (CH_{Ar}), 133.9 (C_{Ar}), 137.8 (C_{Ar}), 147.1 (C_{Ar}), 163.1 (*C*8);

_N_-[3,5-Bis(trifluoromethyl)phenyl]-3,5-dinitrobenzamide (239)[214]

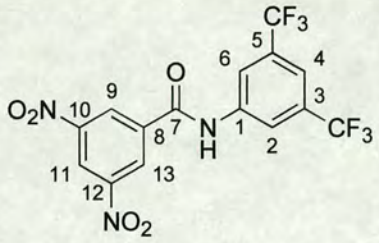

General procedure **A2** was followed using 3,5-dinitrobenzoyl chloride (0.139 g, 0.60 mmole 1.2 eq.) and 3,5-bis(trifluoromethyl)aniline (78 μL, 0.50 mmole, 1.0 eq.). Amide **239** was isolated as a cream solid (0.049 g, 23%); LRMS FAB$^+$ *m/z* 424 $(MH)^+$; HRMS FAB$^+$ *m/z* 424.03658 $(MH)^+$ (calculated for $C_{15}H_8F_6N_3O_5$, 424.03682 (Dev. – 0.54 ppm)); ν_{max} (KBr)/cm^{-1} 3293 (N-H), 3099 (aryl C-H), 1657 (C=O), 1544 (NO_2), 1348 (NO_2); δ_H (250 MHz, $(CD_3)_2SO$): 7.93 (s, 1H, *H*4), 8.51 (s, 2H, *H*2, *H*6), 9.05 (t, 1H, *J* = 1.9 Hz, *H*11), 9.21 (d, 2H, *J* = 1.9 Hz, *H*9, *H*13), 11.37 (s, 1H, N*H*); δ_C (63 MHz, $(CD_3)_2SO$): 117.2 (C_{Ar}), 120.2 (*C*2, *C*6), 120.2 (*C*11), 123.0 (q, J_{CF} = 273 Hz, CF_3), 127.9 (*C*9, *C*13), 130.6 (q, J_{CF} = 33.0 Hz, *C*3, *C*5), 136.2 (C_{Ar}), 140.1 (C_{Ar}), 148.0 (*C*10, *C*12), 161.9 (*C*7); Mpt. 237.1 – 238.6 °C.

_N_-(4-Chlorophenyl)-3,5-dinitrobenzamide (240)

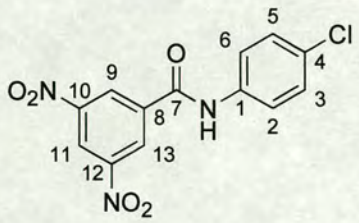

General procedure **A2** was followed using 3,5-dinitrobenzoyl chloride (0.139 g, 0.60 mmole, 1.2 eq.) and 4-chloroaniline (0.064 g, 0.50 mmole, 1.0 eq.) Amide **240** was isolated as a cream solid (0.042 g, 26 %); LRMS FAB$^+$ *m/z* 322 $(MH)^+$; HRMS FAB$^+$ *m/z* 322.02362 $(MH)^+$ (calculated for $C_{13}H_9{}^{35}ClN_3O_5$, 322.02307 (Dev. 1.70 ppm)); ν_{max}

(film)/cm^{-1} 3292 (N-H), 3092 (aryl C-H), 2928 (C-H), 1653 (C=O), 1535 (NO_2), 1340 (NO_2); δ_H (250 MHz, $(CD_3)_2SO$): 7.48 (d, 2H, J = 8. 8 Hz, *H*3, *H*5), 7.84 (d, 2H, J = 8.9 Hz, *H*2, *H*6), 9.02 (t, 1H, J = 2.0 Hz, *H*11), 9.17 (d, 2H, J = 2.0 Hz, *H*9, *H*13), 10.97 (s, 1H, N*H*); δ_C (63 MHz, $(CD_3)_2SO$): 121.0 (*C*11), 122.0 (2 x CH_{Ar}), 127.8 (*C*9, *C*13), 128.0 (C_{Ar}), 128.5 (2 x CH_{Ar}), 136.9 (C_{Ar}), 137.0 (C_{Ar}), 147.9 (*C*10, *C*12), 161.2 (*C*7); Mpt. 241.6 – 242.2 °C.

_N_-[3,5-Bis(trifluoromethyl)phenyl]-4-methyl-3-nitrobenzamide (241)

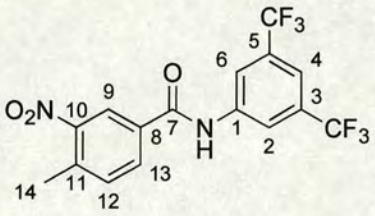

General procedure **A2** was followed using 4-methyl-3-nitrobenzoyl chloride (76 μL, 0.60 mmole 1.2 eq.) and 3,5-bis(trifluoromethyl)aniline (0.064 g, 0.50 mmole, 1.0 eq.). Amide **241** was isolated as a white solid (0.078 g, 40%); LRMS FAB$^+$ *m/z* 393 $(MH)^+$; HRMS FAB$^+$ *m/z* 393.06681 $(MH)^+$ (calculated for $C_{16}H_{11}F_6N_2O_3$, 393.06739 (Dev. – 1.46 ppm)); ν_{max} (film)/cm^{-1} 3316 (N-H), 3081 (aryl C-H), 2934 (C-H), 1644 (C=O), 1530 (NO_2), 1326 (NO_2); δ_H (250 MHz, CD_3OD): 2.70 (s, 3H, *H*14), 7.68 (d, 1H, J = 8.0 Hz, *H*12), 7.77 (s, 1H, *H*4), 8.23 (dd, 1H, J = 1.9, 8.0 Hz, *H*13), 8.48 (s, 2H, *H*2, *H*6), 8.65 (d, 1H, J = 1.9 Hz, *H*9); δ_C (63 MHz, CD_3OD): 19.5 (*C*14), 116.6 (CH_{Ar}), 119.9 (2 x CH_{Ar}), 123.0 (q, J_{CF} = 273 Hz, CF_3), 123.5 (CH_{Ar}), 130.5 (q, J_{CF} = 33 Hz, *C*3, *C*5), 132.1 (CH_{Ar}), 132.5 (C_{Ar}), 133.1 (CH_{Ar}), 136.9 (C_{Ar}), 140.5 (C_{Ar}), 148.6 (C_{Ar}), 163.7 (*C*7).

N-(3-Chlorophenyl)-4-methyl-3-nitrobenzamide (242)

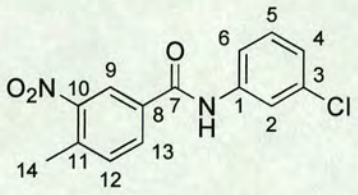

General procedure **A2** was followed using 4-methyl-3-nitrobenzoyl chloride (76 μL, 0.60 mmole, 1.2 eq.) and 3-chloroaniline (53 μL, 0.50 mmole, 1.0 eq.). Amide **242** was isolated as a pale cream solid (0.117 g, 81%); LRMS FAB$^+$ *m/z* 291 $(MH)^+$; HRMS FAB$^+$ *m/z* 291.05364 $(MH)^+$ (calculated for $C_{14}H_{12}{}^{35}ClN_2O_3$, 291.05365 (Dev. – 0.03 ppm)); ν_{max} (film)/cm^{-1} 3297 (N-H), 3081 (aryl C-H), 1654 (C=O), 1530 (NO_2), 1346 (NO_2); δ_H (250 MHz, $(CD_3)_2SO$): 2.62 (s, 3H, *H*14), 7.21 (ddd, 1H, *J* = 8.2, 1.2, 1.1 Hz, *H*4), 7.43 (t, 1H, *J* = 8.2 Hz, *H*5), 7.69 – 7.75 (m, 2H, H6, *H*12), 7.97 (d, 1H, *J* = 1.1 Hz, *H*2), 8.22 (dd, 1H, *J* = 8.0, 0.9 Hz, *H*13), 8.59 (d, 1H, *J* = 0.9 Hz, *H*9), 10.63 (s, 1H, N*H*); δ_C (63 MHz, $(CD_3)_2SO$): 19.4 (*C*14), 118.6 (CH_{Ar}), 119.7 (CH_{Ar}), 123.4 (CH_{Ar}), 123.5 (CH_{Ar}), 130.2 (CH_{Ar}), 132.0 (CH_{Ar}), 132.8 (C_{Ar}), 132.9 (CH_{Ar}), 133.0 (C_{Ar}), 133.1 (C_{Ar}), 136.4 (C_{Ar}), 148.5 (C_{Ar}), 163.2 (*C*7); Mpt. 161.0 – 161.3 °C.

4-Methyl-3-nitro-N-[3-(trifluoromethyl)phenyl]benzamide (243)

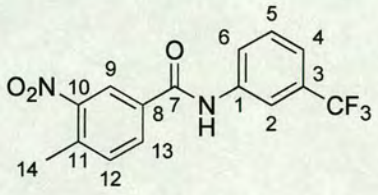

General procedure **A2** was followed using 4-methyl-3-nitrobenzoyl chloride (76 μL, 0.60 mmole, 1.2 eq.) and 3-(trifluoromethyl)aniline (63 μL, 0.50 mmole, 1.0 eq.). Amide **243** was isolated as a pale yellow solid (0.096 g, 59%); LRMS FAB$^+$ *m/z* 325 $(MH)^+$; HRMS FAB$^+$ *m/z* 325.07967 $(MH)^+$ (calculated for $C_{15}H_{12}N_2O_3F_3$, 325.08000 (Dev. –

1.02 ppm)); δ_H (250 MHz, $(CD_3)_2SO$): 2.62 (s, 3H, *H*14), 7.50 (d, 1H, *J* = 8.0 Hz, *H*4), 7.64 (t, 1H, *J* = 8.0 Hz, *H*5), 7.72 (d, 1H, *J* = 8.2 Hz, *H*12), 8.09 (d, 1H, *J* = 8.0 Hz, *H*6), 8.22 – 8.27 (m, 2H, H2, *H*13), 8.63 (d, 1H, *J* = 1.8 Hz, *H*9), 10.77 (s, 1H, N*H*); δ_C (63 MHz, $(CD_3)_2SO$): 19.40 (*C*14), 116.34 (d, J_{CF} = 4.0 Hz, CH_{Ar}), 120.1 (CH_{Ar}), 123.4 (CH_{Ar}), 123.7 (CH_{Ar}), 123.9 (q, J_{CF} = 272 Hz, CF_3), 129.4 (q, J_{CF} = 32 Hz, *C*3), 129.7 (CH_{Ar}), 132.0 (CH_{Ar}), 133.0 (CH_{Ar}), 133.0 (C_{Ar}), 136.5 (C_{Ar}), 139.3 (C_{Ar}), 148.6 (C_{Ar}), 163.3 (*C*7).

4-Methyl-3-nitro-*N*-[4-(trifluoromethyl)phenyl]benzamide (244)

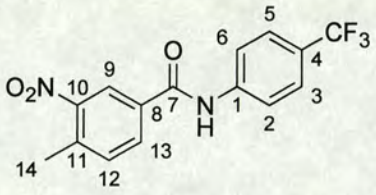

General procedure **A2** was followed using 4-methyl-3-nitrobenzoyl chloride (76 μL, 0.60 mmole, 1.2 eq.) and 4-(trifluoromethyl)aniline (63 μL, 0.50 mmole, 1.0 eq.). Amide **244** was isolated as a white solid (0.095 g, 59%); LRMS FAB^+ *m/z* 325 $(MH)^+$; HRMS FAB^+ *m/z* 325.07980 $(MH)^+$ (calculated for $C_{15}H_{11}N_2O_3F_3$, 325.08000 (Dev. – 0.63 ppm)); δ_H (250 MHz, $(CD_3)_2SO$): 2.62 (s, 3H, *H*14), 7.72 (d, 1H, *J* = 8.0 Hz, *H*12), 7.77 (d, 2H, *J* = 8.8 Hz, *H*3, *H*5), 8.04 (d, 2H, *J* = 8.8 Hz, *H*2, *H*6), 8.25 (dd, 1H, *J* = 8.0, 1.8 Hz, *H*13), 8.62 (d, 1H, *J* = 1.8 Hz, *H*9), 10.80 (s, 1H, N*H*); δ_C (63 MHz, $(CD_3)_2SO$): 19.4 (*C*14), 120.1 (2 x CH_{Ar}), 123.5 (CH_{Ar}), 123.8 (q, J_{CF} = 31 Hz, *C*4), 124.1 (q, J_{CF} = 271 Hz, CF_3), 126.0 (2 x CH_{Ar}), 132.1 (CH_{Ar}), 133.0 (C_{Ar}), 133.1 (C_{Ar}), 136.5 (C_{Ar}), 142.2 (C_{Ar}), 148.5 (C_{Ar}), 163.5 (*C*7).

_N_-(4-Chlorophenyl)-4-methyl-3-nitrobenzamide (245)

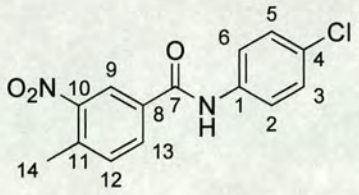

General procedure **A2** was followed using 4-methyl-3-nitrobenzoyl chloride (76 μL, 0.60 mmole 1.2 eq.) and 4-chloroaniline (0.064 g, 0.50 mmole, 1.0 eq.). Amide **245** was isolated as a white solid (0.088 g, 61%); LRMS FAB^+ *m/z* 291 $(MH)^+$; HRMS FAB^+ *m/z* 291.05355 $(MH)^+$ (calculated for $C_{14}H_{12}{}^{35}ClN_2O_3$, 291.05365 (Dev. – 0.32 ppm)); δ_H (250 MHz, $(CD_3)_2SO$): 2.61 (s, 3H, *H*14), 7.45 (d, 2H, *J* = 8.8 Hz, *H*3, *H*5), 7.70 (d, 1H, *J* = 8.1 Hz, *H*12), 7.83 (d, 2H, *J* = 8.8 Hz, *H*2, *H*6), 8.22 (dd, 1H, *J* = 8.1, 1.8 Hz, *H*13), 8.58 (d, 1H, *J* = 1.8 Hz, *H*9), 10.61 (s, 1H, N*H*); δ_C (63 MHz, $(CD_3)_2SO$): 19.4 (*C*14), 121.8 (2 x CH_{Ar}), 123.4 (CH_{Ar}), 127.5 (C_{Ar}), 128.4 (2 x CH_{Ar}), 132.0 (CH_{Ar}), 132.9 (CH_{Ar}), 133.3 (C_{Ar}), 136.3 (C_{Ar}), 137.5 (C_{Ar}), 148.5 (C_{Ar}), 163.1 (*C*7);

_N_-(4-Fluorophenyl)-4-methyl-3-nitrobenzamide (246)

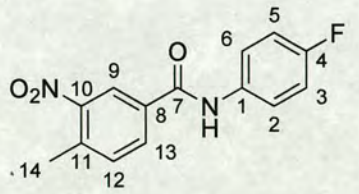

General procedure **A2** was followed using 4-methyl-3-nitrobenzoyl chloride (76 μL, 0.60 mmole, 1.2 eq.) and 4-fluoroaniline (48 μL, 0.50 mmole, 1.0 eq.). Amide **246** was isolated as a yellow solid (0.072 g, 53%); LRMS FAB^+ *m/z* 275 $(MH)^+$; HRMS FAB^+ *m/z* 275.08359 $(MH)^+$ (calculated for $C_{14}H_{12}FN_2O_3$, 275.08320 (Dev. 1.42 ppm)); δ_H (250 MHz, $(CD_3)_2SO$): 2.63 (s, 3H, *H*14), 7.25 (d, 2H, *J* = 8.8 Hz, J_{HF} = 8.8 Hz, *H*3, *H*5), 7.70 (d, 1H, *J* = 8.1 Hz, *H*12), 7.95 (dd, 2H, *J* = 8.8 Hz, J_{HF} = 5.1 Hz, *H*2, *H*6),

8.24 (dd, 1H, J = 8.0, 1.9 Hz, *H*13), 8.60 (d, 1H, J = 1.9 Hz, *H*9), 10.55 (s, 1H, N*H*); δ_C (63 MHz, $(CD_3)_2SO$): 19.4 (*C*14), 115.1 (d, J_{CF} = 14 Hz, *C*3, *C*5), 122.2 (d, J_{CF} = 9 Hz, *C*2, *C*6), 123.3 (CH_{Ar}), 131.9 (CH_{Ar}), 132.9 (CH_{Ar}), 133.4 (C_{Ar}), 134.9 (d, J_{CF} = 3 Hz, *C*1), 136.2 (C_{Ar}), 148.5 (C_{Ar}), 154.0 (d, J_{CF} = 230 Hz, *C*4), 162.9 (*C*7).

N-(3,4-Difluorophenyl)-4-methyl-3-nitrobenzamide (247)

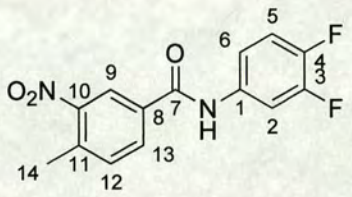

General procedure **A2** was followed using 4-methyl-3-nitrobenzoyl chloride (76 μL, 0.60 mmole, 1.2 eq.) and 3,4-difluoroaniline (50 μL, 0.50 mmole, 1.0 eq.). Amide **247** was isolated as a white solid (0.089 g, 61%); LRMS FAB^+ *m/z* 293 $(MH)^+$; HRMS FAB^+ *m/z* 293.07302 $(MH)^+$ (calculated for $C_{14}H_{11}F_2N_2O_3$, 293.07377 (Dev. – 2.57 ppm)); δ_H (250 MHz, $(CD_3)_2SO$): 2.62 (s, 3H, *H*14), 7.41 – 7.59 (m, 2H, Ar*H*), 7.72 (d, 1H, J = 8.1 Hz, *H*12), 7.95 (ddd, 1H, J = 13.2, 7.5. 2.3 Hz, Ar*H*), 8.22 (dd, 1H, J = 8.0, 1.9 Hz, *H*13), 8.59 (d, 1H, J = 1.9 Hz, *H*9), 10.67 (s, 1H, N*H*); δ_C (63 MHz, $(CD_3)_2SO$): 19.4 (*C*14), 109.3 (d, J_{CF} = 22 Hz, CH_{Ar}), 116.6 (d, J_{CF} = 5.9 Hz, CH_{Ar}), 117.2 (d, J_{CF} = 18 Hz, CH_{Ar}), 123.4 (CH_{Ar}), 131.9 (CH_{Ar}), 133.0 (CH_{Ar}), 133.0 (C_{Ar}), 135.5 (d, J_{CF} = 6 Hz, *C*1), 136.4 (C_{Ar}), 145.5 (dd, J_{CF} = 242, 13 Hz, C_{Ar}), 148.5 (C_{Ar}), 148.6 (dd, J_{CF} = 243, 13 Hz, C_{Ar}), 163.1 (*C*7).

_N_-(3,5-Dichlorophenyl)-4-methyl-3-nitrobenzamide (248)

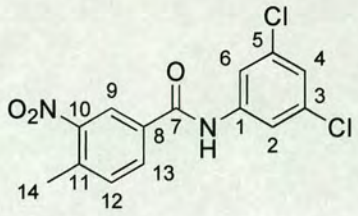

General procedure **A2** was followed using 4-methyl-3-nitrobenzoyl chloride (76 μL, 0.60 mmole, 1.2 eq.) and 3,5-dichloroaniline (0.081 g, 0.50 mmole, 1.0 eq.). Amide **248** was isolated as a white solid (0.055 g, 34%); LRMS FAB^+ *m/z* 325 $(MH)^+$; HRMS FAB^+ *m/z* 325.01465 $(MH)^+$ (calculated for $C_{14}H_{11}{}^{35}Cl_2N_2O_3$, 425.01467 (Dev. – 0.09 ppm)); δ_H (250 MHz, $(CD_3)_2SO$): 2.61 (s, 3H, *H*14), 7.36 (t, 1H, *J* = 1.8 Hz, *H*4), 7.71 (d, 1H, *J* = 8.1 Hz, *H*12), 7.89 (d, 2H, *J* = 1.8 Hz, *H*2, *H*6), 8.20 (dd, 1H, *J* = 8.1, 1.8 Hz, *H*13), 8.58 (d, 1H, *J* = 1.8 Hz, *H*9), 10.71 (s, 1H, N*H*); δ_C (63 MHz, $(CD_3)_2SO$): 19.4 (*C*14), 118.2 (*C*2, *C*6), 123.0 (CH_{Ar}), 123.4 (CH_{Ar}), 132.0 (CH_{Ar}), 132.7 (C_{Ar}), 133.0 (CH_{Ar}), 133.8 (*C*3, *C*5), 136.7 (C_{Ar}), 140.9 (C_{Ar}), 148.5 (C_{Ar}), 163.4 (*C*7).

4-Methyl-3-nitro-_N_-[4-(trifluoromethyl)benzyl]benzamide (249)

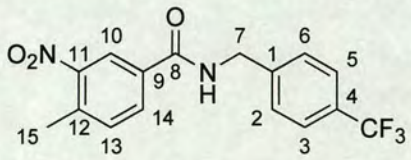

General procedure **A2** was followed using 4-methyl-3-nitrobenzoyl chloride (76 μL, 0.60 mmole, 1.2 eq.) and 1-[4-(trifluoromethyl)phenyl]methanamine (71 μL, 0.50 mmole, 1.0 eq.). Amide **249** was isolated as a white solid (0.129 g, 76%); LRMS FAB^+ *m/z* 339 $(MH)^+$; HRMS FAB^+ *m/z* 339.09599 $(MH)^+$ (calculated for $C_{16}H_{13}F_3N_2O_3$, 339.09565 (Dev. 1.00 ppm)); δ_H (250 MHz, $(CD_3)_2SO$): 2.59 (s, 3H, *H*15), 4.59 (d, *J* = 5.6 Hz, 2H, *H*7), 7.56 (d, 2H, *J* = 8. 2 Hz, *H*2, *H*6), 7.66 (d, 1H, *J* = 8.0 Hz, *H*13), 7.72

(d, 2H, J = 8.2 Hz, *H*3, *H*5), 8.15 (dd, 1H, J = 8.0, 1.4 Hz, *H*14), 8.53 (d, 1H, J = 1.4 Hz, *H*10), 9.44 (t, 1H, J = 5.6 Hz, N*H*); δ_C (63 MHz, $(CD_3)_2SO$): 19.4 (*C*15), 42.3 (*C*7), 123.0 (CH_{Ar}), 124.1 (q, J_{CF} = 272 Hz, CF_3), 125.0 (d, J_{CF} = 4 Hz, *C*3, *C*5), 127.4 (q, J_{CF} = 32 Hz, *C*4), 127.8 (*C*2, *C*6), 131.5 (CH_{Ar}), 132.8 (C_{Ar}), 133.0 (CH_{Ar}), 136.0 (C_{Ar}), 143.9 (C_{Ar}), 148.6 (C_{Ar}), 164.0 (*C*8); Mpt. 136.8 – 137.5 °C.

_N_-[3,5-Bis(trifluoromethyl)benzyl]-4-methyl-3-nitrobenzamide (250)

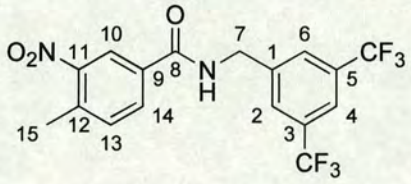

General procedure **A2** was followed using 4-methyl-3-nitrobenzoyl chloride (76 µL, 0.60 mmole, 1.2 eq.) and 1-[3,5-bis(trifluoromethyl)phenyl]methanamine (0.122 g, 0.50 mmole, 1.0 eq.). Amide **250** was isolated as a white solid (0.149 g, 73%); LRMS FAB^+ *m/z* 407 $(MH)^+$; HRMS FAB^+ *m/z* 407.08266 $(MH)^+$ (calculated for $C_{17}H_{13}F_6N_2O_3$, 407.08304 (Dev. – 0.92 ppm)); δ_H (250 MHz, $(CD_3)_2SO$): 2.58 (s, 3H, *H*15), 4.69 (d, 1H, J = 5.8 Hz, *H*7), 7.66 (d, 1H, J = 8.0 Hz, *H*13), 8.02 (s, 1H, *H*4), 8.05 (s, 2H, *H*2, *H*6), 8.15 (dd, 1H, J = 8.0, 1.8 Hz, *H*14), 8.51 (d, 1H, J = 1.8 Hz, *H*10), 9.48 (t, 1H, J = 5.8 Hz, N*H*); δ_C (63 MHz, $(CD_3)_2SO$): 19.4 (*C*15), 42.0 (*C*7), 120.6 (CH_{Ar}), 123.0 (CH_{Ar}), 123.1 (q, J_{CF} = 273 Hz, CF_3), 128.1 (*C*2, *C*6), 130.0 (q, J_{CF} = 33 Hz, *C*3, *C*5), 131.6 (CH_{Ar}), 132.5 (C_{Ar}), 133.0 (CH_{Ar}), 136.1 (C_{Ar}), 142.6 (C_{Ar}), 164.2 (*C*8).

N-(4-Chlorobenzyl)-4-methyl-3-nitrobenzamide (251)

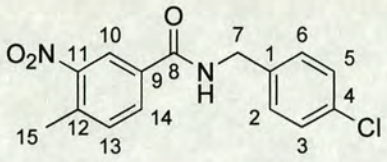

General procedure **A2** was followed using 4-methyl-3-nitrobenzoyl chloride (76 μL, 0.60 mmole, 1.2 eq.) and 1-(4-chlorophenyl)methanamine (61 μL, 0.50 mmole, 1.0 eq.) Amide **251** was isolated as a white solid (0.118 g, 78 %); LRMS FAB^+ *m/z* 305 $(MH)^+$; HRMS FAB^+ *m/z* 305.06879 $(MH)^+$ (calculated for $C_{15}H_{14}{}^{35}ClN_2O_3$, 305.06930 (Dev. – 1.64 ppm)); ν_{max} (KBr)/cm^{-1} 3294 (N-H), 3066 (aryl C-H), 2866 (C-H), 1639 (C=O), 1525 (NO_2), 1353 (NO_2); δ_H (250 MHz, $(CD_3)_2SO$): 2.59 (s, 3H, *H*15), 4.50 (d, 2H, *J* = 5.8 Hz, *H*7), 7.37 (d, 2H, *J* = 8.7 Hz, *H*2, *H*6), 7.42 (d, 2H, *J* = 8.7 Hz, *H*3, *H*5), 7.65 (d, 1H, *J* = 8.0 Hz, *H*13), 8.14 (dd, 1H, *J* = 8.0, 1.0 Hz, *H*14), 8.52 (d, 1H, *J* = 1.0 Hz, *H*10), 9.37 (t, 1H, *J* = 5.8 Hz, N*H*); δ_C (63 MHz, $(CD_3)_2SO$): 19.4 (*C*15), 42.0 (*C*7), 123.0 (CH_{Ar}), 128.1 (2 x CH_{Ar}), 129.0 (2 x CH_{Ar}), 131.3 (C_{Ar}), 131.5 (CH_{Ar}), 132.9 (CH_{Ar}), 132.9 (C_{Ar}), 135.9 (C_{Ar}), 138.1 (C_{Ar}), 148.5 (C_{Ar}), 163.9 (*C*8); Mpt. 156.7 – 157.2 °C.

N-[(1*R*)-1-(4-Chlorophenyl)ethyl]-4-methyl-3-nitrobenzamide (252)

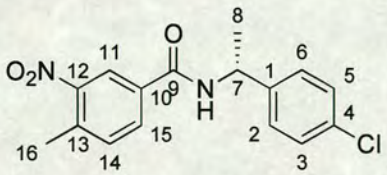

General procedure **A2** was followed using 4-methyl-3-nitrobenzoyl chloride (76 μL, 0.60 mmole, 1.2 eq.) and (1*R*)-1-(4-chlorophenyl)ethanamine (70 μL, 0.50 mmole, 1.0 eq.). Amide **252** was isolated as a white solid (0.097 g, 61%); LRMS FAB^+ *m/z* 319 $(MH)^+$; HRMS FAB^+ *m/z* 319.08501 $(MH)^+$ (calculated for $C_{16}H_{16}{}^{35}ClN_2O_3$, 319.08495

(Dev. 0.21 ppm)); ν_{max} (KBr)/cm^{-1} 3261 (N-H), 3056 (aryl C-H), 2977 (C-H), 2931 (C-H), 2871 (C-H), 1635 (C=O), 1523 (NO_2), 1340 (NO_2); δ_H (250 MHz, $(CD_3)_2SO$): 1.49 (d, 3H, *J* = 7.1 Hz, H8), 2.58 (s, 3H, H16), 5.17 (quintet, *J* = 7.1 Hz, H7), 7.32 – 7.45 (m, 4H, *H*2, *H*3, *H*5, *H*6), 7.63 (d, 1H, *J* = 8.1 Hz, *H*14), 8.14 (dd, 1H, *J* = 8.1, 1.8 Hz, *H*15), 8.52 (d, 1H, *J* = 1.8 Hz, *H*11), 9.12 (d, 1H, *J* = 7.1 Hz, N*H*); δ_C (63 MHz, $(CD_3)_2SO$): 19.3 (*C*16), 21.7 (*C*8), 48.1 (*C*7), 123.0 (CH_{Ar}), 127.8 (2 x CH_{Ar}), 128.0 (2 x CH_{Ar}), 131.0 (C_{Ar}), 131.7 (CH_{Ar}), 132.8 (CH_{Ar}), 133.0 (C_{Ar}), 135.8 (C_{Ar}), 143.4 (C_{Ar}), 148.5 (C_{Ar}), 163.1 (*C*9).

N-[(1*S*)-1-(4-Chlorophenyl)ethyl]-4-methyl-3-nitrobenzamide (253)

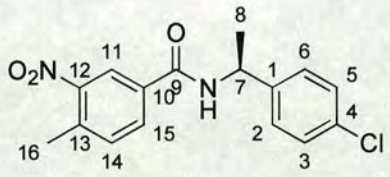

General procedure **A2** was followed using 4-methyl-3-nitrobenzoyl chloride (76 μL, 0.60 mmole, 1.2 eq.) and (1*S*)-1-(4-chlorophenyl)ethanamine (70 μL, 0.50 mmole, 1.0 eq.). Amide **253** was isolated as a pale yellow solid (0.096 g, 60%); LRMS FAB$^+$ *m/z* 319 (MH)$^+$; HRMS FAB$^+$ *m/z* 319.08465 (MH)$^+$ (calculated for $C_{16}H_{16}{}^{35}ClN_2O_3$, 319.08495 (Dev. – 0.94 ppm)); ν_{max} (KBr)/cm^{-1} 3298 (N-H), 3073 (aryl C-H), 2978 (C-H), 2932 (C-H), 2874 (C-H), 1632 (C=O), 1524 (NO_2), 1344 (NO_2); δ_H (250 MHz, $(CD_3)_2SO$): 1.49 (d, 3H, *J* = 7.1 Hz, H8), 2.57 (s, 3H, H16), 5.17 (quintet, *J* = 7.1 Hz, H7), 7.32 – 7.45 (m, 4H, *H*2, *H*3, *H*5, *H*6), 7.63 (d, 1H, *J* = 8.1 Hz, *H*14), 8.14 (dd, 1H, *J* = 8.1, 1.8 Hz, *H*15), 8.52 (d, 1H, *J* = 1.8 Hz, *H*11), 9.11 (d, 1H, *J* = 7.1 Hz, N*H*); δ_C (63 MHz, $(CD_3)_2SO$): 19.3 (*C*16), 21.7 (*C*8), 48.1 (*C*7), 123.0 (CH_{Ar}), 127.8 (2 x CH_{Ar}), 128.0 (2 x CH_{Ar}), 131.0 (C_{Ar}), 131.7 (CH_{Ar}), 132.8 (CH_{Ar}), 133.0 (C_{Ar}), 135.8 (C_{Ar}), 143.4 (C_{Ar}), 148.5 (C_{Ar}), 163.1 (*C*9).

_N_-[3,5-Bis(trifluoromethyl)phenyl]-5-chloro-4-nitrothiophene-2-carboxamide (254)

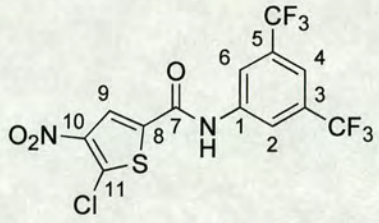

General procedure **A2** was followed using 5-chloro-4-nitrothiophene-2-carbonyl chloride (0.680 g, 3.00 mmole, 1.2 eq.), 3,5-bis(trifluoromethyl)aniline (389 μL, 2.50 mmole, 1.0 eq.), morpholinomethyl-polystyrene resin (1.000 g, 3.7 mmole g^{-1}) and tris-(2-aminoethyl)-polystyrene resin (2.000 g, 4.4 mmole g^{-1}). Amide **254** was isolated as a yellow solid (0.176 g, 17%); LRMS ES^- *m/z* 416.9 $(M-H)^-$ assigned to $C_{13}H_4{}^{35}ClF_6N_2O_3S$; HRMS FAB^+ *m/z* 418.9546992 $(MH)^+$ (calculated for $C_{13}H_6{}^{35}ClF_6N_2O_3S$, 416.95408 (Dev. 1.77 ppm)); ν_{max} (film)/cm^{-1} 3305 (N-H), 3112 (thiophene C-H), 3105 (aryl C-H), 1652 (C=O), 1536 (NO_2), 1332 (NO_2); δ_H (250 MHz, CD_3OD): 7.77 (s, 1H, *H*4), 8.41 (s, 2H, *H*2, *H*6), 8.55 (s, 1H, *H*9); δ_C (75 MHz, $(CD_3)_2SO$): 117.3 (CH_{Ar}), 119.9 (2 x CH_{Ar}), 123.5 (q, J_{CF} = 272 Hz, CF_3), 124.6 (CH_{Ar}), 132.2 (q, J_{CF} = 33 Hz, *C*3, *C*5), 135.4 (C_{Ar}), 137.1 (C_{Ar}), 140.2 (C_{Ar}), 143.3 (C_{Ar}), 158.9 (*C*7); Mpt. 218.2 – 218.9 °C.

5-Chloro-4-nitro-_N_-[4-(trifluoromethyl)phenyl]thiophene-2-carboxamide (255)

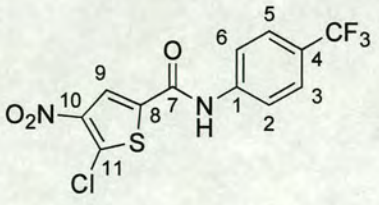

General procedure **A2** was followed using 5-chloro-4-nitrothiophene-2-carbonyl chloride (0.136 g, 0.60 mmole, 1.2 eq.) and 4-(trifluoromethyl)aniline (63 μL, 0.50

mmole, 1.0 eq.). Amide **255** was isolated as a white solid (0.048 g, 27%); LRMS ES$^-$ *m/z* 349.0 (M-H)$^-$; δ_H (250 MHz, $(CD_3)_2SO$): 7.78 (d, 2H, *J* = 8.9 Hz, *H*3, *H*5), 7.96 (d, 2H, *J* = 8.9 Hz, *H*2, *H*6), 8.75 (s, 1H, *H*9), 10.93 (s, 1H, N*H*).

5-Chloro-*N*-(4-chlorophenyl)-4-nitrothiophene-2-carboxamide (256)

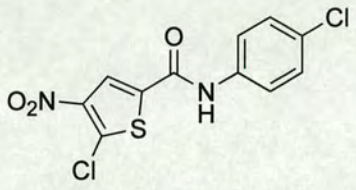

General procedure **A2** was followed using 5-chloro-4-nitrothiophene-2-carbonyl chloride (0.680 g, 3.00 mmole, 1.2 eq.), 4-chloroaniline (0.319 g, 2.50 mmole, 1.0 eq.), morpholinomethyl-polystyrene resin (1.000 g, 3.7 mmole g^{-1}) and tris-(2-aminoethyl)-polystyrene resin (2.000 g, 4.4 mmole g^{-1}). Amide **256** was isolated as a yellow solid (0.238 g, 30%; LRMS ES$^-$ *m/z* 314.8 (M-H)$^-$; HRMS FAB$^+$ *m/z* 316.95613 (MH)$^+$ (calculated for $C_{11}H_7{}^{35}Cl_2N_2O_3S$, 316.95544 (Dev. 2.18 ppm)); ν_{max} (film)/cm^{-1} 3294 (N-H), 3120 (thiophene C-H), 2928 (C-H), 1644 (C=O), 1548 (NO_2), 1335 (NO_2); δ_H (250 MHz, $(CD_3)_2SO$): 7.64 (d, 2H, *J* = 8.9 Hz, Ar*H*), 7.94 (d, 2H, *J* = 8.9 Hz, Ar*H*), 8.88 (s, 1H, thiophene *H*), 10.92 (s, 1H, N*H*); δ_C (75 MHz, $(CD_3)_2SO$): 122.5 (2 x CH_{Ar}), 125.3 (CH_{Ar}), 128.9 (C_{Ar}), 120.5 (2 x CH_{Ar}), 136.5 (C_{Ar}), 136.8 (C_{Ar}), 137.6 (C_{Ar}), 143.4 (C_{Ar}), 158.3 (*C*O); Mpt. 264.4 – 264.6 °C.

5-Chloro-*N*-(4-fluorophenyl)-4-nitrothiophene-2-carboxamide (257)

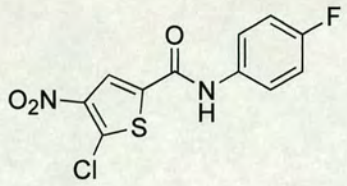

General procedure **A2** was followed using 5-chloro-4-nitrothiophene-2-carbonyl chloride (0.136 g, 0.60 mmole, 1.2 eq.) and 4-fluoroaniline (48 μL, 0.50 mmole, 1.0 eq.). Amide **257** was isolated as a white solid (0.032 g, 21%); LRMS ES$^-$ *m/z* 416.9 $(M-H)^-$.

5-Chloro-4-nitro-*N*-[4-(trifluoromethyl)benzyl]thiophene-2-carboxamide (258)

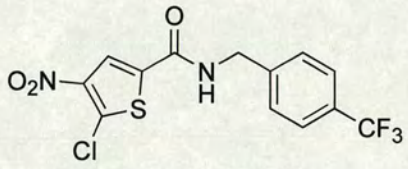

General procedure **A2** was followed using 5-chloro-4-nitrothiophene-2-carbonyl chloride (0.136 g, 0.60 mmole, 1.2 eq.) and 1-[4-(trifluoromethyl)phenyl]methanamine (71 μL, 0.50 mmole, 1.0 eq.). Amide **258** was isolated as a white solid (0.088 g, 48%); LRMS ES$^-$ *m/z* 363.0 $(M-H)^-$.

5-Chloro-*N*-(4-chlorobenzyl)-4-nitrothiophene-2-carboxamide (259)

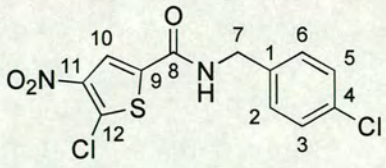

General procedure **A2** was followed using 5-chloro-4-nitrothiophene-2-carbonyl chloride (0.136 g, 0.60 mmole, 1.2 eq.) and 1-(4-chlorophenyl)methanamine (61 μL, 0.50 mmole, 1.0 eq.). Amide **259** was isolated as a white solid (0.097 g, 58%); LRMS ES^- *m/z* 328.9 $(M-H)^-$; δ_H (250 MHz, $(CD_3)_2SO$): 4.47 (d, 2H, *J* = 5.8 Hz, *H*7), 7.36 (d, 2H, *J* = 8.4 Hz, *H*2, *H*6), 7.43 (d, 2H, *J* = 8.4 Hz, *H*3, *H*5), 8.48 (s, 1H, *H*10), 9.54 (t, 1H, *J* = 5.8 Hz, N*H*).

_N_-[3,5-Bis(trifluoromethyl)phenyl]-1-benzothiophene-2-carboxamide (260)

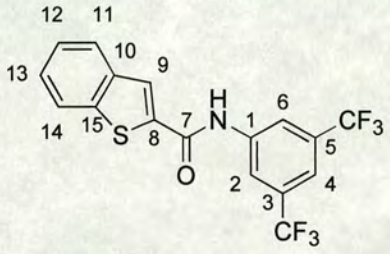

General procedure **A2** was followed using 1-benzothiophene-2-carbonyl chloride (0.118 g, 0.60 mmole, 1.2 eq.) and 3,5-bis(trifluoromethyl)aniline (78 μL, 0.50 mmole, 1.0 eq.). Amide **260** was isolated as a pale yellow solid (0.116 g, 60%); LRMS FAB^+ *m/z* 390 $(MH)^+$; HRMS FAB^+ *m/z* 390.03772 $(MH)^+$ (calculated for $C_{17}H_{10}F_6NOS$, 390.03873 (Dev. –2.59 ppm)); δ_H (250 MHz, $(CD_3)_2SO$): 7.44 – 7.57 (m, 2H, *H*12, *H*13), 7.85 (s, 1H, *H*4), 8.02 – 8.13 (m, 2H, *H*11, *H*14), 8.42 (s, 1H, *H*9), 8.50 (s, 2H, *H*2, *H*6), 11.09 (s, 1H, N*H*); δ_C (63 MHz, $(CD_3)_2SO$): 118.7 (q, J_{CF} = 272 Hz, CF_3), 119.4 (CH_{Ar}), 122.7 (CH_{Ar}), 125.0 (2 x CH_{Ar}), 125.5 (2 x CH_{Ar}), 126.7 (2 x CH_{Ar}), 130.5 (q, J_{CF} = 33 Hz, *C*3, *C*5), 138.5 (C_{Ar}), 138.7 (C_{Ar}), 140.4 (C_{Ar}), 140.6 (C_{Ar}), 160.9 (*C*7).

_N_-[3-(trifluoromethyl)phenyl]-1-benzothiophene-2-carboxamide (261)

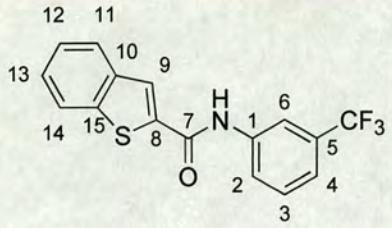

General procedure **A2** was followed using 1-benzothiophene-2-carbonyl chloride (0.118 g, 0.60 mmole, 1.2 eq.) and 3-(trifluoromethyl)aniline (63 μL, 0.50 mmole, 1.0 eq.). Amide **261** was isolated as a yellow solid (0.156 g, 97%); LRMS FAB^+ *m/z* 322 $(MH)^+$; HRMS FAB^+ *m/z* 322.05108 $(MH)^+$ (calculated for $C_{16}H_{11}F_3NOS$, 322.05135 (Dev. – 0.84 ppm)); δ_H (250 MHz, $(CD_3)_2SO$): 7.46 – 7.54 (m, 3H, Ar*H*), 7.65 (t, 1H, *J* = 7.9 Hz, *H*3), 8.04 – 8.13 (m, 3H, Ar*H*), 8.26 (s, 1H, *H*6), 8.42 (s, 1H, *H*9), 10.85 (s, 1H, N*H*); δ_C (63 MHz, $(CD_3)_2SO$): 116.1 (CH_{Ar}), 120.0 (CH_{Ar}), 121.7 (q, J_{CF} = 272 Hz, CF_3), 122.7 (CH_{Ar}), 123.5 (CH_{Ar}), 124.9 (CH_{Ar}), 125.3 (CH_{Ar}), 126.2 (CH_{Ar}), 126.5 (CH_{Ar}), 129.3 (q, J_{CF} = 32 Hz, *C*5), 129.8 (CH_{Ar}), 138.8 (C_{Ar}), 139.1 (C_{Ar}), 139.2 (C_{Ar}), 140.4 (C_{Ar}), 160.5 (*C*7); Mpt. 141.1 – 141.9 °C.

_N_-[4-(trifluoromethyl)phenyl]-1-benzothiophene-2-carboxamide (262)

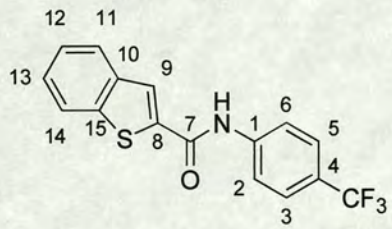

General procedure **A2** was followed using 1-benzothiophene-2-carbonyl chloride (0.118 g, 0.60 mmole, 1.2 eq.) and 4-(trifluoromethyl)aniline (63 μL, 0.50 mmole, 1.0 eq.). Amide **262** was isolated as an off-white solid (0.055 g, 34%); LRMS FAB^+ *m/z* 322 $(MH)^+$; HRMS FAB^+ *m/z* 322.05161 $(MH)^+$ (calculated for $C_{16}H_{11}F_3NOS$, 322.05135

(Dev. 0.81 ppm)); δ_H (250 MHz, $(CD_3)_2SO$): 7.42 – 7.57 (m, 2H, aromatic), 7.77 (d, 2H, J = 8.8 Hz, *H*2, *H*6), 8.02 – 8.11 (m, 4H, aromatic), 8.44 (s, 1H, *H*9), 10.87 (s, 1H, N*H*); δ_C (63 MHz, $(CD_3)_2SO$): 119.9 (2 x CH_{Ar}), 122.0 (q, J_{CF} = 273 Hz, CF_3), 122.7 (CH_{Ar}), 123.6 (q, J_{CF} = 32 Hz, *C*4), 124.9 (CH_{Ar}), 125.4 (CH_{Ar}), 125.9 (2 x CH_{Ar}), 126.3 (CH_{Ar}), 126.5 (CH_{Ar}), 138.8 (C_{Ar}), 139.2 (C_{Ar}), 140.5 (C_{Ar}), 142.1 (C_{Ar}), 160.6 (*C*7).

_N_-(4-Chlorophenyl)-1-benzothiophene-2-carboxamide (263)

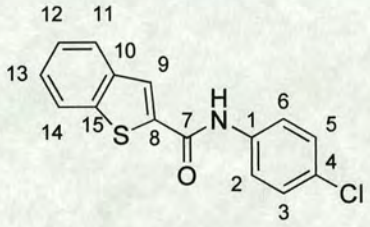

General procedure **A2** was followed using 1-benzothiophene-2-carbonyl chloride (0.118 g, 0.60 mmole, 1.2 eq.) and 4-chloroaniline (0.064 g, 0.50 mmole, 1.0 eq.). Amide **263** was isolated as a cream solid (0.073 g, 51%); LRMS FAB^+ *m/z* 288 $(MH)^+$; HRMS FAB^+ *m/z* 288.02503 $(MH)^+$ (calculated for $C_{15}H_{11}{}^{35}ClNOS$, 288.02499 (Dev. 0.13 ppm)); ν_{max} (KBr)/cm^{-1} 3362 (N-H), 3054 (aryl C-H), 1646 (C=O); δ_H (250 MHz, $(CD_3)_2SO$): 7.48 (d, 2H, J = 8.9 Hz, *H*3, *H*5), 7.50 – 7.58 (m, 2H, *H*12, *H*13), 7.86 (d, 2H, J = 8.9 Hz, *H*2, *H*6), 8.04 – 8.14 (m, 2H, *H*11, *H*14), 8.41 (s, 1H, *H*9), 10.70 (s, 1H, N*H*); δ_C (63 MHz, $(CD_3)_2SO$): 121.6 (2 x CH_{Ar}), 122.7 (CH_{Ar}), 124.9 (CH_{Ar}), 125.3 (CH_{Ar}), 125.8 (CH_{Ar}), 126.4 (CH_{Ar}), 127.4 (C_{Ar}), 128.5 (2 x CH_{Ar}), 137.4 (C_{Ar}), 138.8 (C_{Ar}), 139.5 (C_{Ar}), 140.3 (C_{Ar}), 160.2 (*C*7).

N-(4-Fluorophenyl)-1-benzothiophene-2-carboxamide (264)

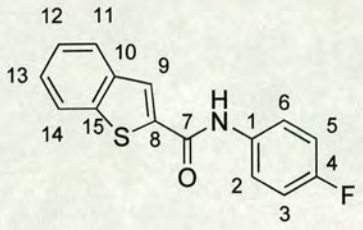

General procedure **A2** was followed using 1-benzothiophene-2-carbonyl chloride (0.118 g, 0.60 mmole, 1.2 eq.) and 4-fluoroaniline (48 μL, 0.50 mmole, 1.0 eq.). Amide **264** was isolated as a cream solid (0.079 g, 55%); LRMS FAB$^+$ *m/z* 272 $(MH)^+$; HRMS FAB$^+$ *m/z* 272.05459 $(MH)^+$ (calculated for $C_{15}H_{11}FNOS$, 272.05454 (Dev 0.20 ppm)); ν_{max} (KBr)/cm^{-1} 3393 (N-H), 3067 (aryl C-H), 1642 (C=O); δ_H (250 MHz, $(CD_3)_2SO$): 7.25 (t, 2H, J = 8.9 Hz, J_{HF} = 8.9 Hz, *H*3, *H*5), 7.46 – 7.56 (m, 2H, *H*12, *H*13), 7.82 (dd, 2H, J = 9.1 Hz, J_{HF} = 5.0 Hz, 5.7 Hz, *H*2, *H*6), 8.02 – 8.12 (m, 2H, *H*11, *H*14), 8.37 (s, 1H, *H*9), 10.62 (s, 1H, N*H*); δ_C (63 MHz, $(CD_3)_2SO$): 115.2 (d, J_{CF} = 22 Hz, *C*3, *C*5), 122.0 (d, J_{CF} = 8 Hz, *C*2, *C*6), 122.7 (CH_{Ar}), 124.9 (CH_{Ar}), 125.2 (CH_{Ar}), 125.6 (CH_{Ar}), 126.3 (CH_{Ar}), 134.7 (d, J_{CF} = 2 Hz, *C*1), 138.9 (C_{Ar}), 139.6 (C_{Ar}), 140.3 (C_{Ar}), 158.2 (d, J_{CF} = 241 Hz, *C*4), 160.0 (C7).

N-(3,4-Difluorophenyl)-1-benzothiophene-2-carboxamide (265)

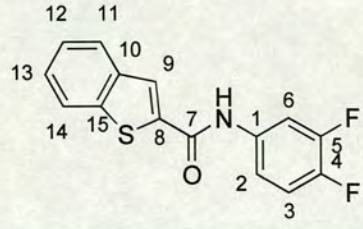

General procedure **A2** was followed using 1-benzothiophene-2-carbonyl chloride (0.118 g, 0.60 mmole, 1.2 eq.) and 3,4-difluoroaniline (50 μL, 0.50 mmole, 1.0 eq.). Amide **265** was isolated as a beige solid (0.075 g, 52%); LRMS FAB$^+$ *m/z* 290 $(MH)^+$; HRMS FAB$^+$

m/z 290.04555 $(MH)^+$ (calculated for $C_{15}H_{10}F_2NOS$, 290.04512 (Dev. 1.48 ppm)); δ_H (250 MHz, $(CD_3)_2SO$): 7.45 – 7.57 (m, 4H, aromatic), 7.91 – 8.12 (m, 3H, aromatic), 8.38 (s, 1H, *H*9), 10.75 (s, 1H, N*H*); δ_C (63 MHz, $(CD_3)_2SO$): 109.1 (d, J_{CF} = 22 Hz, CH_{Ar}), 116.4 (CH_{Ar}), 117.3 (d, J_{CF} = 18 Hz, CH_{Ar}), 122.7 (CH_{Ar}), 124.9 (CH_{Ar}), 125.3 (CH_{Ar}), 126.0 (CH_{Ar}), 126.5 (CH_{Ar}), 135.5 (C_{Ar}), 138.8 (C_{Ar}), 139.1 (C_{Ar}), 140.4 (C_{Ar}), 145.5 (dd, J_{CF} = 242, 13 Hz, *C*4), 148.8 (dd, J_{CF} = 243, 13 Hz, C*5*), 160.3 (*C*7).

_N_-[4-(Trifluoromethyl)benzyl]-1-benzothiophene-2-carboxamide (266)

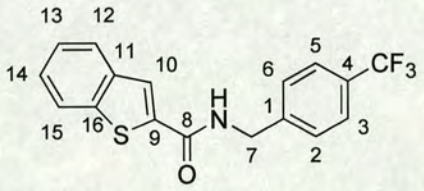

General procedure **A2** was followed using 1-benzothiophene-2-carbonyl chloride (0.118 g, 0.60 mmole, 1.2 eq.) and 1-[4-(trifluoromethyl)phenyl]methanamine (71 µL, 0.50 mmole, 1.0 eq.). Amide **266** was isolated as a white solid (0.121 g, 72%); LRMS FAB^+ *m/z* 336 $(MH)^+$; HRMS FAB^+ *m/z* 336.06738 $(MH)^+$ (calculated for $C_{17}H_{13}F_3NOS$, 336.06700 (Dev 1.14 ppm)); ν_{max} (KBr)/cm^{-1} 3296 (N-H), 3077 (aryl C-H), 2917 (C-H), 1628 (C=O); δ_H (250 MHz, $(CD_3)_2SO$): 4.61 (d, 2H, *J* = 5.9 Hz, *H*7), 7.43 – 7.53 (m, 2H, *H*13, *H*14), 7.59 (d, 2H, *J* = 8.1 Hz, *H*2, *H*6), 7.75 (d, 2H, *J* = 8.1 Hz, *H*3, *H*5), 7.95 – 8.07 (m, 2H, *H*12, *H*15), 8.18 (s, 1H, *H*10), 9.48 (t, 1H, *J* = 5.9 Hz, N*H*); δ_C (63 MHz, $(CD_3)_2SO$): 42.1 2 (*C*7), 122.6 (CH_{Ar}), 124.1 (q, J_{CF} = 272 Hz, CF_3), 125.0 (3 x CH_{Ar}), 125.1 (2 x CH_{Ar}), 126.1 (CH_{Ar}), 127.1 (q, J_{CF} = 32 Hz, *C*4), 127.6 (2 x CH_{Ar}), 138.9 (C_{Ar}), 139.3 (C_{Ar}), 140.0 (C_{Ar}), 143.9 (C_{Ar}), 161.5 (*C*8); Mpt. 192.0 – 193.2 °C.

_N_-(4-Chlorobenzyl)-1-benzothiophene-2-carboxamide (267)

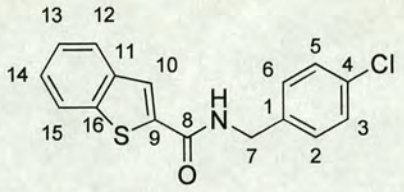

General procedure **A2** was followed using 1-benzothiophene-2-carbonyl chloride (0.118 g, 0.60 mmole, 1.2 eq.) and 1-(4-chlorophenyl)methanamine (61 μL, 0.50 mmole, 1.0 eq.). Amide **267** was isolated as a pale yellow solid (0.070 g, 46%); LRMS FAB^+ *m/z* 302 $(MH)^+$; HRMS FAB^+ *m/z* 302.04094 $(MH)^+$ (calculated for $C_{16}H_{13}{}^{35}ClNOS$, 302.04064 (Dev. 1.01 ppm)); ν_{max} (KBr)/cm^{-1} 3291 (N-H), 3083 (aryl C-H), 2922 (C-H), 1628 (C=O); δ_H (250 MHz, $(CD_3)_2SO$): 4.59 (d, 2H, *J* = 5.9 Hz, *H*7), 7.35 – 7.53 (m, 6H, Ar*H*), 7.92 – 8.09 (m, 2H, Ar*H*), 8.17 (s, 1H, *H*10), 9.41 (t, 1H, *J* = 5.9 Hz, N*H*); δ_C (63 MHz, $(CD_3)_2SO$): 41.8 (*C*7), 122.6 (CH_{Ar}), 124.7 (2 x CH_{Ar}), 125.0 (CH_{Ar}), 126.0 (CH_{Ar}), 128.1 (2 x CH_{Ar}), 129.0 (2 x CH_{Ar}), 131.3 (C_{Ar}), 138.8 (C_{Ar}), 138.9 (C_{Ar}), 139.4 (C_{Ar}), 140.0 (C_{Ar}), 161.4 (*C*8); Mpt. 223.6 – 224.0 °C.

_N_-[3,5-Bis(trifluoromethyl)phenyl]-5-(4-chlorophenyl)-2-methyl-3-furamide (268)

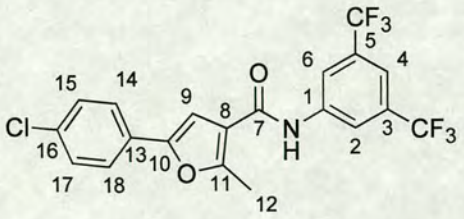

General procedure **A2** was followed using 5-(4-chlorophenyl)-2-methyl-3-furoyl chloride (0.153 g, 0.60 mmole, 1.2 eq.) and 3,5-bis(trifluoromethyl)aniline (78 μL, 0.50 mmole, 1.0 eq.). Amide **268** was isolated as a cream solid (0.166 g, 74%); LRMS FAB^+ *m/z* 448 $(MH)^+$; HRMS FAB^+ *m/z* 448.05331 $(MH)^+$ (calculated for $C_{20}H_{13}{}^{35}ClF_6NO_2$,

448.05390 (Dev. –1.33 ppm)); δ_H (250 MHz, $(CD_3)_2SO$): 2.67 (s, 3H, *H*12), 7.51 (s, 1H, *H*9), 7.56 (d, 2H, *J* = 8.5 Hz, *H*15, *H*17), 7.70 (d, 2H, *J* = 8.5 Hz, *H*14, *H*18), 7.82 (s, 1H, *H*4), 8.49 (s, 2H, *H*2, *H*6), 10.44 (s, 1H, N*H*); δ_C (63 MHz, $(CD_3)_2SO$): 13.4 (*C*12), 105.1 (CH_{Ar}), 116.4 (CH_{Ar}), 117.3 (C_{Ar}), 119.3, (2 x CH_{Ar}), 121.9 (q, J_{CF} = 272 Hz, CF_3), 124.7 (2 x CH_{Ar}), 128.0 (C_{Ar}), 129.0 (2 x CH_{Ar}), 130.4 (q, J_{CF} = 32 Hz, *C*3, *C*5), 132.1 (C_{Ar}), 140.7 (C_{Ar}), 149.4 (C_{Ar}), 157.9 (C_{Ar}), 161.9 (*C*7).

5-(4-Chlorophenyl)-2-methyl-*N*-[4-(trifluoromethyl)phenyl]-3-furamide (269)

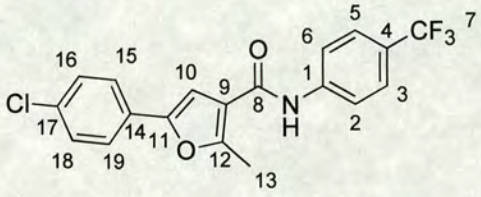

General procedure **A2** was followed using 5-(4-chlorophenyl)-2-methyl-3-furoyl chloride (0.153 g, 0.60 mmole, 1.2 eq.) and 4-(trifluoromethyl)aniline (63 μL, 0.50 mmole, 1.0 eq.). Amide **269** was isolated as a white solid (0.133 g, 70%); LRMS FAB^+ *m/z* 380 $(MH)^+$; HRMS FAB^+ *m/z* 380.06648 $(MH)^+$ (calculated for $C_{19}H_{14}{}^{35}ClF_3NO_2$, 380.06652 (Dev. – 0.09 ppm)); ν_{max} (KBr)/cm^{-1} 3286 (N-H), 3114 (Furan C-H), 3029 (aryl C-H), 2925 (C-H), 1649 (C=O); δ_H (250 MHz, $(CD_3)_2SO$): 2.65 (s, 3H, *H*13), 7.53 (s, 1H, *H*10), 7.55 (d, 2H, *J* = 8.5 Hz, *H*16, *H*18), 7.70 (d, 2H, *J* = 8.5 Hz, *H*15, *H*19), 7.84 (d, 2H, *J* = 8.3 Hz, *H*2, *H*6), 8.00 (d, 2H, *J* = 8.3 Hz, *H*3, *H*5), 10.18 (s, 1H, N*H*); δ_C (63 MHz, $(CD_3)_2SO$): 13.3 (*C*13), 105.4 (CH_{Ar}), 117.8 (C_{Ar}), 122.0 (q, J_{CF} = 273 Hz, *C*7), 119.6 (2 x CH_{Ar}), 123.5 (q, J_{CF} = 32 Hz, *C*4), 124.7 (2 x CH_{Ar}), 125.7 (2 x CH_{Ar}), 128.2 (C_{Ar}), 128.9 (2 x CH_{Ar}), 131.9 (C_{Ar}), 142.4 (C_{Ar}), 149.2 (C_{Ar}), 157.3 (C_{Ar}), 161.6 (*C*8).

N,5-Bis(4-chlorophenyl)-2-methyl-3-furamide (270)

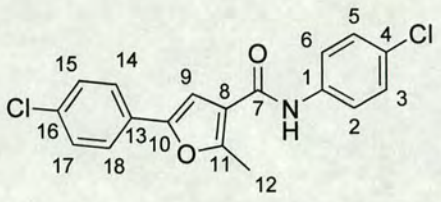

General procedure **A2** was followed using 5-(4-chlorophenyl)-2-methyl-3-furoyl chloride (0.153 g, 0.60 mmole, 1.2 eq.) and 4-chloroaniline (0.064 g, 0.50 mmole, 1.0 eq.). Amide **270** was isolated as a white crystalline solid (0.114 g, 66%); LRMS FAB^+ *m/z* 346 $(MH)^+$; HRMS FAB^+ *m/z* 346.04010 $(MH)^+$ (calculated for $C_{18}H_{14}{}^{35}Cl_2NO_2$, 346.04016 (Dev. – 0.17 ppm)); ν_{max} (KBr)/cm^{-1} 3272 (N-H), 3031 (aryl C-H), 1643 (C=O); δ_H (250 MHz, $(CD_3)_2SO$): 2.63 (s, 3H, *H*12), 7.42 (d, 2H, *J* = 8.8 Hz, *H*3, *H*5), 7.49 (s, 1H, *H*9), 7.54 (d, 2H, *J* = 8.5 Hz, *H*15, *H*17), 7.68 (d, 2H, *J* = 8.5 Hz, *H*14, *H*18), 7.79 (d, 2H, *J* = 8.8 Hz, *H*2, *H*6), 9.98 (s, 1H, N*H*); δ_C (63 MHz, $(CD_3)_2SO$): 13.3 (*C*12), 105.5 (CH_{Ar}), 117.9 (C_{Ar}), 121.4 (2 x CH_{Ar}), 124.6 (2 x CH_{Ar}), 126.9 (C_{Ar}), 128.2 (C_{Ar}), 128.3 (2 x CH_{Ar}), 128.9 (2 x CH_{Ar}), 131.9 (C_{Ar}), 137.7 (C_{Ar}), 149.1 (C_{Ar}), 157.0 (C_{Ar}), 161.3 (*C*7).

5-(4-Chlorophenyl)-*N*-(4-fluorophenyl)-2-methyl-3-furamide (271)

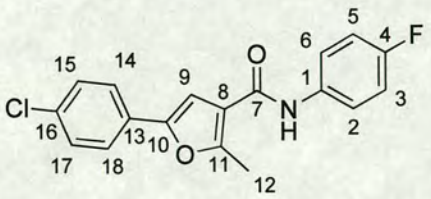

General procedure **A2** was followed using 5-(4-chlorophenyl)-2-methyl-3-furoyl chloride (0.153 g, 0.60 mmole, 1.2 eq.) and 4-fluoroaniline (48 μL, 0.50 mmole, 1.0 eq.). Amide **271** was isolated as a pale brown solid (0.136 g, 83%); LRMS FAB^+ *m/z* 330 $(MH)^+$; HRMS FAB^+ *m/z* 330.07038 $(MH)^+$ (calculated for $C_{18}H_{14}{}^{35}ClFNO_2$,

330.06971 (Dev. 1.73 ppm)); ν_{max} (KBr)/cm^{-1} 3288 (N-H), 3142 (Furan C-H), 3056 (aryl C-H), 2925 (C-H), 1639 (C=O); δ_H (250 MHz, $(CD_3)_2SO$): 2.64 (s, 3H, *H*12), 7.21 (t, 2H, J = 8.8 Hz, J_{HF} = 8.8 Hz, *H*3, *H*5), 7.49 (s, 1H, *H*9), 7.55 (d, 2H, J = 8.5 Hz, *H*15, *H*17), 7.70 (d, 2H, J = 8.5 Hz, *H*14, *H*18), 7.77 (dd, 2H, J = 8.8 Hz, J_{HF} = 5.0 Hz, *H*2, *H*6), 9.98 (s, 1H, N*H*); δ_C (63 MHz, $(CD_3)_2SO$): 13.3 (*C*12), 105.5 (CH_{Ar}), 115.0 (d, J_{CF} = 22 Hz, *C*3, *C*5), 118.0 (C_{Ar}), 121.8 (d, J_{CF} = 8 Hz, *C*2, *C*6), 124.6 (2 x CH_{Ar}), 128.3 (C_{Ar}), 128.9 (2 x CH_{Ar}), 131.9 (C_{Ar}), 135.1 (d, J_{CF} = 2 Hz, *C*1), 149.1 (C_{Ar}), 156.7 (C_{Ar}), 158.0 (d, J_{CF} = 240 Hz, *C*4), 161.1 (*C*7); Mpt. 183.9 – 185.4 °C.

5-(4-Chlorophenyl)-2-methyl-*N*-[4-(trifluoromethyl)benzyl]-3-furamide (272)

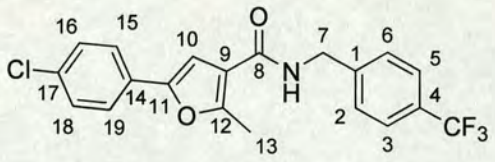

General procedure **A2** was followed using 5-(4-chlorophenyl)-2-methyl-3-furoyl chloride (0.153 g, 0.60 mmole, 1.2 eq.) and 1-[4-(trifluoromethyl)phenyl]methanamine (71 µL, 0.50 mmole, 1.0 eq.). Amide **272** was isolated as a white solid (0.138 g, 70%); LRMS FAB$^+$ *m/z* 394 (MH)$^+$; HRMS FAB$^+$ *m/z* 394.08259 (MH)$^+$ (calculated for $C_{20}H_{16}{}^{35}ClF_3NO_2$, 394.08217 (Dev. 1.07 ppm)); ν_{max} (KBr)/cm^{-1} 3302 (N-H), 3064 (aryl C-H), 2961 (C-H), 2925 (C-H), 1643 (C=O); δ_H (250 MHz, $(CD_3)_2SO$): 2.53 (s, 3H, *H*13), 4.54 (d, 2H, J = 5.8 Hz, *H*7), 7.37 (s, 1H, *H*10), 7.54 (d, 2H, J = 8.4 Hz, *H*2, *H*6), 7.57 (d, 2H, J = 8.5 Hz, *H*16, *H*18), 7.66 (d, 2H, J = 8.4 Hz, *H*3, *H*5), 7.74 (d, 2H, J = 8.5 Hz, *H*15, *H*19), 8.78 (t, J = 5.8 Hz, N*H*); δ_C (63 MHz, $(CD_3)_2SO$): 13.1 (*C*13), 41.5 (*C*7), 105.2 (CH_{Ar}), 117.5 (C_{Ar}), 122.0 (q, J_{CF} = 272 Hz, CF_3), 124.6 (2 x CH_{Ar}), 125.0 (2 x CH_{Ar}), 127.0 (q, J_{CF} = 32 Hz, *C*4), 127.7 (2 x CH_{Ar}), 128.3 (C_{Ar}), 128.9 (2 x CH_{Ar}), 131.8 (C_{Ar}), 144.4 (C_{Ar}), 149.1 (C_{Ar}), 156.0 (C_{Ar}), 162.5 (*C*8); Mpt. 184.7 - 185.7 °C.

_N_-(4-Chlorobenzyl)-5-(4-chlorophenyl)-2-methyl-3-furamide (273)

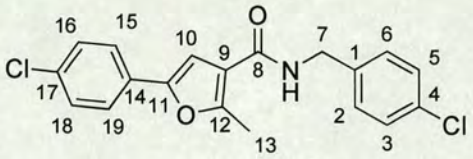

General procedure **A2** was followed using 5-(4-chlorophenyl)-2-methyl-3-furoyl chloride (0.153 g, 0.60 mmole, 1.2 eq.) and 1-(4-chlorophenyl)methanamine (61 μL, 0.50 mmole, 1.0 eq.). Amide **273** was isolated as a white solid (0.149 g, 83%); LRMS FAB^+ *m/z* 360 $(MH)^+$; HRMS FAB^+ *m/z* 360.05603 $(MH)^+$ (calculated for $C_{19}H_{16}{}^{35}Cl_2NO_2$, 360.05581 (Dev. 0.60 ppm)); ν_{max} (KBr)/cm^{-1} 3262 (N-H), 3048 (aryl C-H), 2918 (C-H), 2873 (C-H), 1632 (C=O); δ_H (250 MHz, $(CD_3)_2SO$): 2.60 (s, 3H, *H*13), 4.42 (d, 2H, *J* = 6.0 Hz, *H*7), 7.35 (d, 2H, *J* = 8.5 Hz, *H*2, *H*6), 7.43 (s, 1H, *H*10), 7.41 (d, 2H, *J* = 8.5 Hz, *H*3, *H*5), 7.52 (d, 2H, *J* = 8.6 Hz, *H*16, *H*18), 7.63 (d, 2H, *J* = 8.6 Hz, *H*15, *H*19), 8.68 (t, *J* = 6.0 Hz, N*H*); δ_C (63 MHz, $(CD_3)_2SO$): 13.1 (*C*13), 41.2 (*C*7), 105.2 (CH_{Ar}), 117.5 (C_{Ar}), 124.6 (2 x CH_{Ar}), 128.0 (2 x CH_{Ar}), 128.3 (C_{Ar}), 128.9 (4 x CH_{Ar}), 131.1 (C_{Ar}), 131.8 (C_{Ar}), 138.5 (C_{Ar}), 149.0 (C_{Ar}), 156.0 (C_{Ar}), 162.4 (*C*8).

_N_-[3,5-Bis(trifluoromethyl)phenyl]-5-nitrothiophene-2-carboxamide (278)

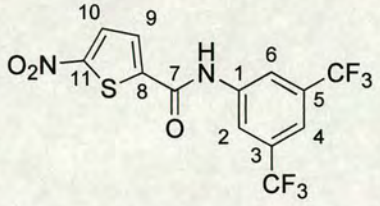

General procedure **A2** was followed using 5-nitrothiophene-2-carbonyl chloride (0.115 g, 0.60 mmole, 1.2 eq.) and 3,5-bis(trifluoromethyl)aniline (78 μL, 0.50 mmole, 1.0 eq.). Amide **278** was isolated as a green solid (0.035 g, 18%); LRMS ES^+ *m/z* 384 $(M)^+$; δ_H

(250 MHz, $(CD_3)_2SO$): 7.87 (s, 1H, *H*4), 7.97 (s, 1H, N*H*), 8.05 (d, 1H, *J* = 4.4 Hz, *H*9), 8.25 (d, 1H, *J* = 4.4 Hz, *H*10), 8.43 (s, 2H, H2, *H*6).

N-(3-Chlorophenyl)-5-nitrothiophene-2-carboxamide (279)

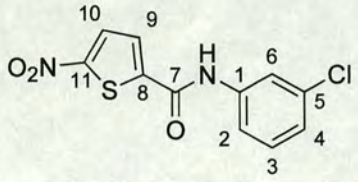

General procedure **A2** was followed using 5-nitrothiophene-2-carbonyl chloride (0.115 g, 0.60 mmole, 1.2 eq.) and 3-chloroaniline (53 μL, 0.50 mmole, 1.0 eq.). Amide **279** was isolated as a brown solid (0.083 g, 59%); LRMS EI^+ *m/z* 282 $(M)^+$; ν_{max} (KBr)/cm^{-1} 3399 (N-H), 3107 (thiophene C-H), 3055 (aryl C-H), 1677 (C=O), 1541 (NO_2), 1351 (NO_2); δ_H (250 MHz, $(CD_3)_2SO$): 7.27 (ddd, 1H, *J* = 8.0, 2.0, 0.9 Hz, *H*4), 7.46 (t, 1H, *J* = 8.0 Hz, *H*3), 7.72 (ddd, 1H, *J* = 8.0, 2.0, 0.9 Hz, *H*2), 7.94 (t, 1H, *J* = 2.0 Hz, *H*6), 8.13 (d, 1H, *J* = 4.4 Hz, *H*9), 8.25 (d, 1H, *J* = 4.4 Hz, *H*10), 10.86 (s, 1H, N*H*); δ_C (91 MHz, CD_3OD): 118.1 (CH_{Ar}), 119.8 (CH_{Ar}), 123.9 (CH_{Ar}), 126.9 (CH_{Ar}), 127.9 (CH_{Ar}), 129.4 (CH_{Ar}), 133.6 (C_{Ar}), 138.7 (C_{Ar}), 144.9 (C_{Ar}), 154.0 (C_{Ar}), 158.7 (*C*7).

5-Nitro-N-[3-(trifluoromethyl)phenyl]thiophene-2-carboxamide (280)

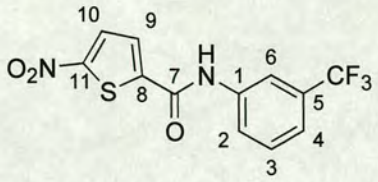

General procedure **A2** was followed using 5-nitrothiophene-2-carbonyl chloride (0.115 g, 0.60 mmole, 1.2 eq.) and 3-(trifluoromethyl)aniline (63 μL, 0.50 mmole, 1.0 eq.). Amide **280** was isolated as a yellow solid (0.075 g, 48%); LRMS EI^+ *m/z* 316 $(M)^+$; δ_H

(250 MHz, $(CD_3)_2SO$): 7.81 (d, 1H, J = 8.0 Hz, *H*4), 8.07 (t, 1H, J = 8.0 Hz, *H*3), 8.49 (d, 1H, J = 8.0 Hz, *H*2), 8.52 (d, 1H, J = 4.4 Hz, *H*9), 8.66 (d, 1H, J = 4.4 Hz, *H*10), 11.36 (s, 1H, N*H*).

5-Nitro-*N*-[4-(trifluoromethyl)phenyl]thiophene-2-carboxamide (281)

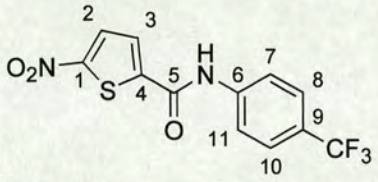

General procedure **A2** was followed using 5-nitrothiophene-2-carbonyl chloride (0.115 g, 0.60 mmole, 1.2 eq.) and 4-(trifluoromethyl)aniline (63 μL, 0.50 mmole, 1.0 eq.). Amide **281** was isolated as a brown solid (0.071 g, 45%); LRMS EI^+ *m/z* 316 $(M)^+$; HRMS EI^+ *m/z* 316.01348 $(M)^+$ (calculated for $C_{12}H_7F_3N_2O_3S$, 316.01295 (Dev. 1.68 ppm)); ν_{max} (KBr)/cm^{-1} 3329 (N-H), 3122 (thiophene C-H), 3056 (aryl C-H), 1655 (C=O), 1538 (NO_2), 1328 (NO_2); δ_H (250 MHz, $(CD_3)_2SO$): 7.58 (d, 2H, J = 8.9 Hz, *H*8, *H*10), 7.79 (d, 2H, J = 8.9 Hz, *H*7, *H*11), 7.93 (d, 1H, J = 4.5 Hz, *H*3), 8.05 (d, 1H, J = 4.5 Hz, *H*2), 10.77 (s, 1H, N*H*); δ_C (63 MHz, $(CD_3)_2SO$): 121.2 (2 x CH_{Ar}), 121.9 (q, J_{CF} = 272 Hz, CF_3), 124.2 (q, J_{CF} = 33 Hz, *C*9), 125.9 (2 x CH_{Ar}), 128.7 (CH_{Ar}), 129.9 (CH_{Ar}), 141.4 (C_{Ar}), 145.3 (C_{Ar}), 153.5 (C_{Ar}), 158.5 (*C*5); Mpt. 195.9 – 196.8 °C.

***N*-(4-Chlorophenyl)-5-nitrothiophene-2-carboxamide (282)**

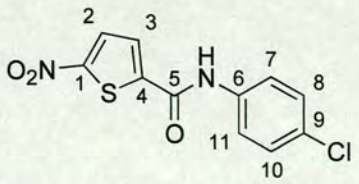

General procedure **A2** was followed using 5-nitrothiophene-2-carbonyl chloride (0.115 g, 0.60 mmole, 1.2 eq.) and 4-chloroaniline (0.064 g, 0.50 mmole, 1.0 eq.). Amide **282**

was isolated as a brown solid (0.044 g, 31%); LRMS EI^+ *m/z* 292 $(M)^+$; δ_H (250 MHz, $(CD_3)_2SO$): 7.28 (d, 2H, *J* = 6.9 Hz, *H*8, *H*10), 7.60 (d, 2H, *J* = 6.9 Hz, *H*7, *H*11) 7.88 (d, 1H, *J* = 4.4 Hz, *H*3), 8.03 (d, 1H, *J* = 4.4 Hz, *H*2), 10.61 (s, 1H, N*H*); δ_C (63 MHz, $(CD_3)_2SO$): 121.9 (2 x CH_{Ar}), 128.2 (C_{Ar}), 128.4 (CH_{Ar}), 128.7 (2 x CH_{Ar}), 130.0 (CH_{Ar}), 136.6 (C_{Ar}), 145.7 (C_{Ar}), 153.3 (C_{Ar}), 158.1 (*C*5).

_N_-(4-Fluorophenyl)-5-nitrothiophene-2-carboxamide (283)

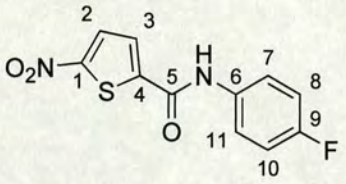

General procedure **A2** was followed using 5-nitrothiophene-2-carbonyl chloride (0.115 g, 0.60 mmole, 1.2 eq.) and 4-fluoroaniline (48 μL, 0.50 mmole, 1.0 eq.). Amide **283** was isolated as a yellow solid (0.079 g, 59%); LRMS EI^+ *m/z* 266 $(M)^+$; HRMS EI^+ *m/z* 266.01634 $(M)^+$ (calculated for $C_{11}H_7FN_2O_3S$ 266.01614, Dev. 0.75 ppm); ν_{max} (film)/cm^{-1} 3292 (N-H), 3107 (thiophene C-H), 2928 (C-H), 1646 (C=O), 1540 (NO_2), 1338 (NO_2); δ_H (250 MHz, $(CD_3)_2SO$): 7.43 – 7.52 (m, 2H, *H*8, *H*10), 7.97 – 8.02 (m, 2H, *H*7, *H*11), 8.30 (d, 1H, *J* = 4.4 Hz, *H*3), 8.44 (d, 1H, *J* = 4.4 Hz, *H*2), 10.97 (s, 1H, N*H*); δ_C (63 MHz, $(CD_3)_2SO$): 115.3 (d, J_{CF} = 22 Hz, *C*8, *C*10), 122.3 (d, J_{CF} = 8 Hz, *C*7, *C*11), 128.1 (CH_{Ar}), 129.9 (CH_{Ar}), 134.0 (C_{Ar}), 146.0 (C_{Ar}), 153.1 (C_{Ar}), 156.7 (d, J_{CF} = 242 Hz, *C*9), 157.9 (*C*5); Mpt. 194.7 – 195.2 °C.

N-(3,4-Difluorophenyl)-5-nitrothiophene-2-carboxamide (284)

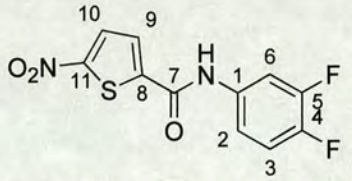

General procedure **A2** was followed using 5-nitrothiophene-2-carbonyl chloride (0.115 g, 0.60 mmole, 1.2 eq.) and 3,4-difluoroaniline (50 μL, 0.50 mmole, 1.0 eq.). Amide **284** was isolated as a yellow solid (0.072 g, 51%); LRMS EI^+ *m/z* 284 $(M)^+$; ν_{max} (KBr)/cm^{-1} 3377 (N-H), 3112 (thiophene C-H), 3047 (aryl C-H), 1668 (C=O), 1552 (NO_2), 1340 (NO_2); δ_H (250 MHz, $(CD_3)_2SO$): 7.46 – 7.54 (m, 2H, *H*2, *H*6), 7.84 – 7.97 (m, 1H, *H*3), 8.06 (d, 1H, *J* = 4.4 Hz, *H*9), 8.23 (d, 1H, *J* = 4.4 Hz, *H*10), 10.86 (s, 1H, N*H*).

N-(3,5-Dichlorophenyl)-5-nitrothiophene-2-carboxamide (285)

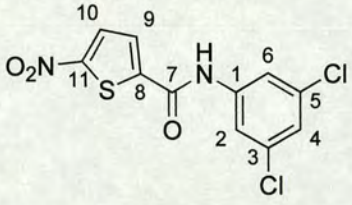

General procedure **A2** was followed using 5-nitrothiophene-2-carbonyl chloride (0.115 g, 0.60 mmole, 1.2 eq.) and 3,5-dichloroaniline (0.081 □, 0.50 mmole, 1.0 eq.). Amide **285** was isolated as a brown solid (0.068 g, 43%); LRMS ES^+ *m/z* 316 $(M)^+$; HRMS FAB^+ *m/z* 316.95445 $(MH)^+$ (calculated for $C_{11}H_7{}^{35}Cl_2N_2O_3S$, 315.95544 (Dev. - 3.12 ppm)); ν_{max} (KBr)/cm^{-1} 3370 (N-H), 3102 (thiophene C-H), 3089 (aryl C-H), 1666 (C=O), 1541 (NO_2), 1337 (NO_2); δ_H (250 MHz, $(CD_3)_2SO$): 7.49 (s, 1H, *H*4), 7.84 (s, 2H, *H*2, *H*6), 8.07 (d, 1H, *J* = 4.3 Hz, *H*9), 8.22 (d, 1H, *J* =4.3 Hz, *H*10), 10.91 (s, 1H, N*H*); δ_C (63 MHz, $(CD_3)_2SO$): 118.3 (*C*2, *C*6), 123.5 (CH_{Ar}), 128.8 (CH_{Ar}), 130.0

(CH_{Ar}), 133.8 (*C*3, *C*5), 140.1 (C_{Ar}), 144.9 (C_{Ar}), 153.6 (C_{Ar}), 158.5 (*C*7); Mpt. 217.6 – 218.3 °C.

_N_-[3,5-Bis(trifluoromethyl)benzyl]-5-nitrothiophene-2-carboxamide (286)

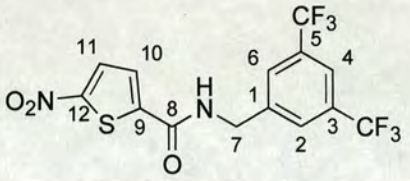

General procedure **A2** was followed using 5-nitrothiophene-2-carbonyl chloride (0.115 g, 0.60 mmole, 1.2 eq.) and 1-[3,5-bis(trifluoromethyl)phenyl]methanamine (0.122 g, 0.50 mmole, 1.0 eq.). Amide **286** was isolated as a green solid (0.151 g, 76%); LRMS EI^+ *m/z* 398 $(M)^+$; δ_H (250 MHz, $(CD_3)_2SO$): 4.70 (d, 2H, *J* = 5.8 Hz, *H*7), 4.28 (d, 1H, *J* = 4.4 Hz, *H*10), 8.04 (s, 1H, *H*4), 8.10 (s, 2H, *H*2, *H*6), 8.17 (d, 1H, *J* = 4.4 Hz, *H*11), 9.71 (t, 1H, *J* = 5.8 Hz, N*H*); δ_C (63 MHz, $(CD_3)_2SO$): 41.9 (*C*7), 120.7 (CH_{Ar}), 123.1 (q, J_{CF} = 273 Hz, CF_3), 127.6 (CH_{Ar}), 128.2 (*C*2, *C*6), 129.9 (CH_{Ar}), 130.1 (q, J_{CF} = 33 Hz, *C*3, *C*5), 142.0 (C_{Ar}), 145.3 (C_{Ar}), 152.9 (C_{Ar}), 159.7 (*C*8).

_N_-(4-Chlorobenzyl)-5-nitrothiophene-2-carboxamide (287)

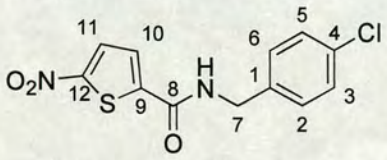

General procedure **A2** was followed using 5-nitrothiophene-2-carbonyl chloride (0.115 g, 0.60 mmole, 1.2 eq.) and 1-(4-chlorophenyl)methanamine (61 µL, 0.50 mmole, 1.0 eq.). Amide **287** was isolated as a brown solid (0.035 g, 47%); LRMS EI^+ *m/z* 296 $(M)^+$; δ_H (250 MHz, $(CD_3)_2SO$): 4.49 (d, 2H, *J* = 5.9 Hz, *H*7), 7.36 (d, 2H, *J* = 8.4 Hz, *H*2, *H*6), 7.43 (d, 2H, *J* = 8.4 Hz, *H*3, *H*5), 7.86 (d, 1H, *J* = 4.4 Hz, *H*10), 8.16 (d, 1H, *J*

=4.4 Hz, *H*11), 9.59 (t, 1H, *J* = 5.9 Hz, N*H*); δ_C (63 MHz, $(CD_3)_2SO$): 42.0 (*C*7), 127.3 (CH_{Ar}), 128.2 (2 x CH_{Ar}), 129.1 (2 x CH_{Ar}), 130.0 (CH_{Ar}), 131.5 (C_{Ar}), 137.5 (C_{Ar}), 145.8 (C_{Ar}), 152.8 (C_{Ar}), 159.39 (*C*8).

N-[(1*R*)-1-(4-Chlorophenyl)ethyl]-5-nitrothiophene-2-carboxamide (288)

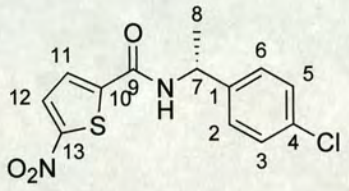

General procedure **A2** was followed using 5-nitrothiophene-2-carbonyl chloride (0.115 g, 0.60 mmole, 1.2 eq.) and (1*R*)-1-(4-chlorophenyl)ethanamine (70 µL, 0.50 mmole, 1.0 eq.). Amide **288** was isolated as a biege solid (0.116 g, 74%); LRMS EI^+ *m/z* 310 $(M)^+$; δ_H (250 MHz, CD_3OD): 1.61 (d, 3H, *J* = 7.1 Hz, *H*8), 5.23 (q, 1H, *J* = 7.1 Hz, *H*7), 7.38 (d, 2H, *J* = 8.9 Hz, *H*2, *H*6), 7.43 (d, 2H, *J* = 8.9 Hz, *H*3, *H*5), 7.79 (d, 1H, *J* = 4.4 Hz, *H*11), 8.01 (d, 1H, *J* = 4.4 Hz, *H*12); Mpt. 162.0 – 162.6 °C.

N-[(1*S*)-(4-Chlorophenyl)ethyl]-5-nitrothiophene-2-carboxamide (289)

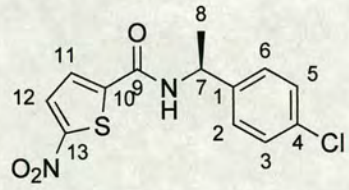

General procedure **A2** was followed using 5-nitrothiophene-2-carbonyl chloride (0.115 g, 0.60 mmole, 1.2 eq.) and (1*S*)-1-(4-chlorophenyl)ethanamine (70 µL, 0.50 mmole, 1.0 eq.). Amide **289** was isolated as a beige solid (0.107 g, 69%); LRMS EI^+ *m/z* 310 $(M)^+$; HRMS FAB^+ *m/z* 311.75645 $(MH)^+$ (calculated for $C_{13}H_{12}{}^{35}ClN_2O_3S$, 311.02598 (Dev. 0.87 ppm)); ν_{max} (film)/cm^{-1} 3297 (N-H), 3105 (thiophene C-H), 3086 (aryl C-H), 2978

(C-H), 2932 (C-H), 1628 (C=O), 1546 (NO_2), 1341 (NO_2); δ_H (250 MHz, $(CD_3)_2SO$): 1.50 (d, 3H, J = 7.0 Hz, *H*8), 5.13 (quintet, 2H, J = 7.0 Hz, *H*7), 7.42 (s, 4H, *H*2, *H*3, *H*5, *H*6), 7.97 (d, 1H, J = 4.4 Hz, *H*11), 8.17 (d, 1H, J = 4.4 Hz, *H*12), 9.36 (d, 1H, J = 7.0 Hz, N*H*); δ_C (63 MHz, $(CD_3)_2SO$): 21.5 (*C*8), 48.3 (*C*7), 127.4 (CH_{Ar}), 127.8 (2 x CH_{Ar}), 128.1 (2 x CH_{Ar}), 129.9 (CH_{Ar}), 131.3 (C_{Ar}), 142.7 (C_{Ar}), 146.0 (C_{Ar}), 152.8 (C_{Ar}), 158.6 (*C*9); Mpt. 154.7 – 155.2 °C.

5-Chloro-4-nitrothiophene-2-carboxylic acid (291)[215]

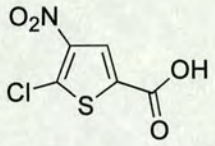

To a stirring suspension of 5-chlorothiophene-2-carboxylic acid (8.13 g, 50 mmole) in acetic anhydride (15 mL) a mixture of fuming nitric acid (16 mL) in glacial acetic acid (25 mL) was added over a period of 1 hour whilst maintaining the temperature of the reaction mixture below 30 °C. The reaction mixture was then stirred at room temperature for 2 hours before the dropwise addition of acetic acid (75 mL) over a period of 30 minutes, again whilst maintaining the temperature of the reaction mixture below 30 °C. The reaction mixture was then stirred at room temperature for 19 hours before being neutralised with NaOH pellets. The reaction mixture was diluted with H_2O (200 mL) and extracted into Et_2O (200 mL). The organic layer was washed with H_2O (2 x 100 mL) and brine (2 x 100 mL) before being dried over anhydrous $MgSO_4$ and concentrated *in vacuo* to afford a pale yellow solid (3.08 g, 30 %); LRMS ES^- *m/z* 205.8 $(M-H)^-$; HRMS FAB^+ *m/z* 207.94756 $(MH)^+$ (calculated for $C_5H_3{}^{35}ClNO_4S$, 207.94713 (Dev. 2.07 ppm)); δ_H (500 MHz, $(CD_3)_2SO$): 8.52 (s, 1H, thiophene *H*), 10.92 (bs, 1H, O*H*); Mpt 156.0 – 157.6 °C.

5-Chloro-4-nitrothiophene-2-carbonyl chloride (292)

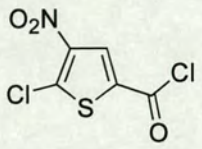

To a stirring suspension of 5-chloro-4-nitrothiophene-2-carboxylic acid (1.21 g, 5.8 mmole, 1.0 eq.) in DCM (15 mL, anhydrous) was added oxalyl chloride (610 mL, 7.0 mmole, 1.2 eq.) followed by two drops of DMF. The reaction mixture was left to stir at room temperature for 24 hours before being concentrated *in vacuo* to afford a brown residue that was used directly for the synthesis of amides **254** – **259**.

5-Nitrothiophene-2-carboxylic acid (294)[216]

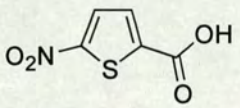

To a stirring suspension of silver oxide, produced *in situ* from the addition of NaOH pellets (4.00 g) to $AgNO_3$ (10.30 g) in water (200 mL), a solution of 5-nitrothiophene-2-carbaldehyde (4.52 g, 28.8 mmole) in ethanol (50 mL) was added. The free silver was removed by filtration, washed with water (2 x 50 mL) and the filtrate was acidified with HCl. The white precipitate was filtered and dried in air to afford carboxylic acid **294** as a white solid (1.57g, 26 %, LRMS ES^- *m/z* 171.5 $(M-H)^-$) which was converted to 5-nitrothiophene-2-carbonyl chloride, using standard procedure reported for compound **292**, and used for the synthesis of amides **278** - **289**.

4-Nitro-*N*-[4-(trifluoromethyl)phenyl]benzamide (296)[210]

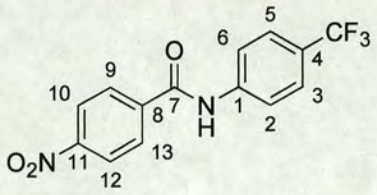

To a sample of 4-nitrobenzoic acid (0.200 g, 1.2 mmole, 1.0 eq.) was added 4-trifluoromethylaniline (211 μL, 1.8 mmole, 1.5 eq.). Under solvent free conditions, the reaction mixture was irradiated in the Discover™ at 160 °C for 15 minutes, with active cooling of the sample. The reaction mixture was diluted with EtOAc (30 mL), washed with HCl (1M, 20 mL) and neutralized with $NaHCO_3$ (saturated) before being dried over anhydrous Na_2SO_4, filtered and concentrated *in vacuo* to afford a pale yellow solid (0.053 g, 15 %) which required no further purification; LRMS *m/z* 311.1 $(MH)^+$; HRMS FAB$^+$ *m/z* 311.06472 $(MH)^+$ (calculated for $C_{14}H_{10}F_3N_2O_3$, 311.06435 (Dev. 1.19 ppm)); ν_{max} (KBr)/cm^{-1} 3413 (N-H), 3113 (thiophene C-H), 3078 (aryl C-H), 1685 (C=O), 1536 (NO_2), 1320 (NO_2); δ_H (250 MHz, $(CD_3)_2SO$): 7.56 (d, 2H, *J* = 8.5 Hz, *H*3, *H*5), 7.82 (d, 2H, *J* = 8.5 Hz, *H*2, *H*6), 8.01 (d, 2H, *J* = 8.5 Hz, *H*9, *H*13), 8.19 (d, 2H, *J* = 8.5 Hz, *H*10, *H*12), 10.66 (s, 1H, N*H*); δ_C (75 MHz, $(CD_3)_2SO$): 120.4 (2 x CH_{Ar}), 121.0 (2 x CH_{Ar}), 124.3 (2 x CH_{Ar}), 125.6 (q, J_{CF} = 272 Hz, CF_3), 130.1 (2 x CH_{Ar}), 131.4 (C_{Ar}), 140.8 (C_{Ar}), 143.1 (C_{Ar}), 150.1 (C_{Ar}), 165.1 (*C*7); Mpt. 228.9 – 231.2 °C.

5.5 Experimental for Chapter 4

_N_-(4-methylphenyl)-6-phenylpyrimidin-4-amine (388)

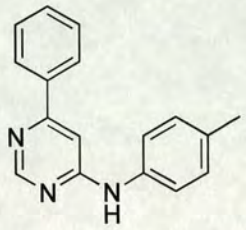

To a solution of 4,6-dichloropyrimidine (0.200 g, 1.34 mmole, 1.0 eq.) in NaOH (2M, 2.6 mL, 4.0 eq.), 4-methylaniline (0.144 g, 1.34 mmole, 1.0 eq.) was added. The reaction mixture was irradiated in the Discover™ at 110 °C for 5 minutes during which time a grey precipitate formed. The precipitate was filtered and washed with water and dried in air to afford 6-chloro-_N_-(4-methylphenyl)pyrimidin-4-amine (0.217 g, 85%); LRMS ES^+ *m/z* 219.8 $(MH)^+$.

To a solution of 6-chloro-_N_-(4-methylphenyl)pyrimidin-4-amine (0.217 g, 0.99 mmole, 1.0 eq.) in THF (3 mL) was added phenylboronic acid (0.120 g, 0.99 mmole, 1.0 eq.), Cs_2CO_3 (0.964 g, 2.97 mmole, 3.0 eq.), $Pd(OAc)_2$ (0.011 g, 0.05 mmole, 0.05 eq.) and triphenylphosphine (0.026 g, 0.10 mmole, 0.10 eq.). Water (0.3 mL) was added to solubilize the Cs_2CO_3. The reaction mixture was irradiated in the Discover™ at 110 °C for 15 minutes. An aliquot (1 mL) of the reaction mixture was injected directly onto the Biotage Parallex Flex™ HPLC (Method C, t_R = 7.35 min.). Appropriate fractions were combined and concentrated *in vacuo* to afford pyrimidine **388** as a white solid (0.001 g, 1 %); LRMS ES^+ *m/z* 261.9 $(MH)^+$.

N-[3,5-Bis(trifluoromethyl)phenyl]-6-phenylpyrimidin-4-amine (389)

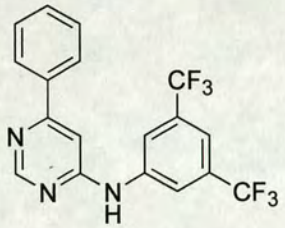

To a stirring solution of 4,6-dichloropyrimidine (0.200 g, 1.34 mmole, 1.0 eq.) in NaOH (2M, 2.6 mL, 4.0 eq.), 3,5-bis(trifluoromethyl)aniline (209 μL, 1.34 mmole, 1.0 eq.) was added. The reaction mixture was irradiated in the Discover™ at 110 °C for 5 minutes during which time a precipitate formed. The precipitate was filtered and washed with water and dried in air to afford *N*-[3,5-bis(trifluoromethyl)phenyl]-6-chloropyrimidin-4-amine (0.366 g, 80%); LRMS ES^+ *m/z* 341.9 $(MH)^+$.

To a solution of *N*-[3,5-bis(trifluoromethyl)phenyl]-6-chloropyrimidin-4-amine (0.366 g, 1.10 mmole, 1.0 eq.) in THF (3 mL) was added phenylboronic acid (0.131 g, 1.10 mmole, 1.0 eq.), Cs_2CO_3 (1.050 g, 3.30 mmole, 3.0 eq.), $Pd(OAc)_2$ (0.012 g, 0.05 mmole, 0.05 eq.) and triphenylphosphine (0.028 g, 0.11 mmole, 0.10 eq.). Water (0.3 mL) was added to solubilize the Cs_2CO_3. The reaction mixture was irradiated in the Discover™ at 110 °C for 15 minutes. An aliquot (1 mL) of the reaction mixture was injected onto the Biotage Parallex Flex™ HPLC (Method C, t_R = 18.47 min.). Appropriate fractions were combined and concentrated *in vacuo* to afford pyrimidine **389** as a cream solid (0.001 g, 1 %); LRMS ES^+ *m/z* 384.0 $(MH)^+$.

N-[3,5-Bis(trifluoromethyl)phenyl]-6-(3-nitrophenyl)pyrimidin-4-amine (392)

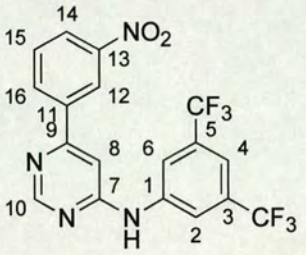

General procedure **P1** was followed using 3,5-bis(trifluoromethyl)aniline (203 μL, 1.30 mmole, 1.0 eq.). Pyrimidine **392** was isolated as a white solid (HPLC Method C, t_R = 19.49 min., 0.003 g, 1 %); LRMS ES^+ *m/z* 429.1 $(MH)^+$; δ_H (250 MHz, CD_3OD): 7.35 (d, 1H, *J* = 1.1 Hz, *H*8), 7.61 (s, 1H, *H*4), 7.82 (t, 1H, *J* = 7.9 Hz, *H*15), 8.40 – 8.44 (m, 2H, *H*14, *H*16), 8.48 (s, 2H, *H*2, *H*6), 8.83 (d, 1H, *J* = 1.1 Hz, *H*10), 8.94 (t, 1H, *J* = 1.8 Hz, *H*12).

N-(4-Chlorophenyl)-6-(3-nitrophenyl)pyrimidin-4-amine (393)

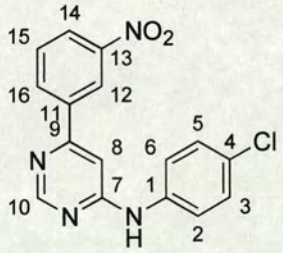

General procedure **P1** was followed using 4-chloroaniline (0.166 g, 1.30 mmole, 1.0 eq.). Pyrimidine **393** was isolated as yellow solid (HPLC Method C, t_R = 15.06 min., 0.002 g, 1%); LRMS ES^+ 327.0 $(MH)^+$; HRMS FAB^+ *m/z* 327.06499 $(MH)^+$ (calculated for $C_{16}H_{12}{}^{35}ClN_4O_2$, 327.06488 (Dev. 0.34 ppm)); ν_{max} (film)/cm^{-1} 3392 (N-H), 3085 (aryl C-H), 2929 (C-H), 1623 (C=C), 1588 (aryl C=C), 1524 (NO_2), 1507 (C=N), 1360 (NO_2); Mpt. 219.8 – 220.8 °C.

Also synthesized using an alternative procedure:

To a solution of 4,6-dichloropyrimidine (0.075 g, 0.50 mmole, 1.0 eq.) in THF (3.0 mL) was added 3-nitrophenylboronic acid (0.084 g, 0.50 mmole, 1.0 eq.), Cs_2CO_3 (0.197 g, 0.60 mmole, 1.2 eq.), $Pd(OAc)_2$ (0.006 g, 0.03 mmole, 0.05 eq.) and triphenylphosphine (0.013 g, 0.05 mmole, 0.10 eq.). Water (0.3 mL) was added to the reaction mixture to solubilise the Cs_2CO_3. The reaction mixture was irradiated in the Discover™ at 110 °C for 25 minutes with active cooling of the sample. To an aliquot (1 mL) of the crude reaction mixture was added 4-chloroaniline (0.022 g, 0.17 mmole, 1.0 eq.) followed by HCl (4M, 85 μL, 2.0 eq.) and the sample was irradiated in the Discover™ at 110 °C for a further 25 minutes. The sample was then injected directly onto the Biotage Parallex Flex™ HPLC (Method E, t_R 17.32 min.). Appropriate fractions were combined and concentrated *in vacuo* to afford pyrimidine **393** as a biege solid (0.017 g, 31 %); LRMS ES^+ *m/z* 327.0 $(MH)^+$ assigned to $C_{16}H_{11}{}^{35}ClN_4O_2$; δ_H (250 MHz, $(CD_3)_2SO$): 7.40 (s, 1H, *H*8),7.43 (d, 2H, J = 8.9 Hz, *H*2, *H*6), 7.80 (d, 2H, *J* = 8.9 Hz, *H*3, *H*5), 7.87 (t, 1H, *J* = 8.2 Hz, *H*15), 8.39 (dd, 1H, *J* = 8.2, 1.7 Hz, *H*16), 8.48 (d, 1H, *J* = 8.2 Hz, *H*14), 8.81 (s, 1H, *H*10), 8.85 (d, 1H, *J* = 1.7 Hz, *H*12), 9.98 (s, 1H, N*H*).

N-(4-Methylphenyl)-6-(3-nitrophenyl)-pyrimidin-4-amine (395)

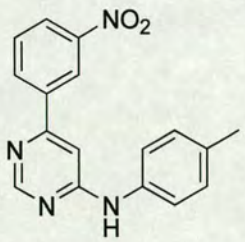

General procedure **P1** was followed using 4-methylaniline (0.139 g, 1.30 mmole, 1.0 eq.). Pyrimidine **395** was isolated as a yellow solid (HPLC Method C, t_R = 11.26 min, 0.001 g, 1 %); LRMS ES^+ *m/z* 307.0 $(MH)^+$.

6-(3-Nitrophenyl)-*N*-[4-(trifluoromethyl)phenyl]pyrimidin-4-amine (396)

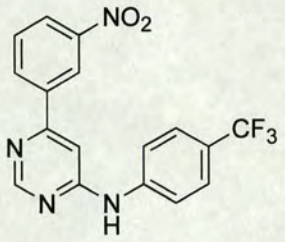

General procedure **P1** was followed using 4-(trifluoromethyl)aniline (0.139 g, 1.30 mmole, 1.0 eq.). Pyrimidine **396** was isolated as a cream solid (HPLC Method C, t_R = 23.46 min., 0.002 g, 1 %); LRMS ES^+ *m/z* 361.1 $(MH)^+$.

6-(2,5-Difluorophenyl)-*N*-phenylpyrimidin-4-amine (401)

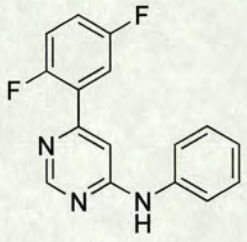

To a solution of 4,6-dichloropyrimidine (1.000 g, 6.70 mmole, 1.0 eq.) in acetonitrile (5 mL) was added 2,5-difluorophenylboronic acid (1.059 g, 6.70 mmole, 1.0 eq.), Cs_2CO_3 (3.280 g, 10.00 mmole, 1.5 eq.), $Pd(OAc)_2$ (0.075 g, 0.34 mmole, 0.05 eq.) and triphenylphosphine (0.176 g, 0.67 mmole, 0.10 eq.). Water (0.5 mL) was added to solubilize the Cs_2CO_3. The reaction mixture was irradiated in the Discover™ at 130 °C for 15 minutes before being divided into aliquots (5 x 1 mL). To one aliquot containing the Suzuki intermediate (1 mL, 1.34 mmole, 1.0 eq.) was added aniline (122 µL, 1.34 mmole, 1.0 eq.) and *p*-toluenesulfonic acid (0.510 g, 2.68 mmole, 2.0 eq.) and the sample was irradiated on the Discover™ at 110 °C for 5 minutes. The reaction mixture was injected directly onto the Biotage Parallex Flex™ HPLC (Method C, t_R = 22.13

min). Appropriate fractions were combined and concentrated *in vacuo* to afford pyrimidine **401** as a cream solid (0.002 g, 1 %); LRMS ES^+ *m/z* 284.0 $(MH)^+$.

N-[3,5-Bis(trifluoromethyl)phenyl)-6-(2,5-difluorophenyl)pyrimidin-4-amine (402)

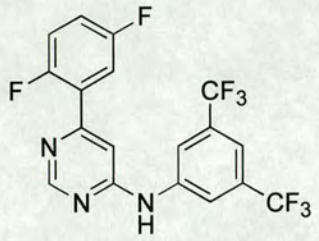

General procedure **P2** was followed using 2,5-difluorophenylboronic acid (0.106 g, 0.67 mmole, 1.0 eq.) followed by 3,5-bis(trifluoromethyl)aniline (102 μL, 0.67 mmole, 1.0 eq.). Pyrimidine **402** was isolated as a white solid (HPLC Method L, t_R = 24.21 min., 0.002 g, 1 %); LRMS ES^+ *m/z* 420.0 $(MH)^+$; ν_{max} (film)/cm^{-1} 3307 (N-H), 3116 (aryl C-H), 1636 (C=C), 1601 (aryl C=C), 1515 (C=N).

6-(2,5-Difluorophenyl)-N-[4-(trifluoromethyl)phenyl]pyrimidin-4-amine (403)

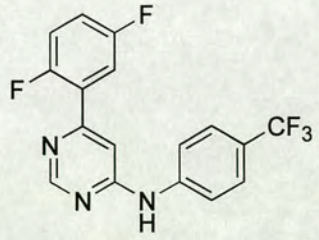

General procedure **P2** was followed using 2,5-difluorophenylboronic acid (0.106 g, 0.67 mmole, 1.0 eq.) followed by 4-(trifluoromethyl)aniline (82 μL, 0.67 mmole, 1.0 eq.). Pyrimidine **403** was isolated as a cream solid (HPLC Method L, t_R = 19.33 min., 0.005 g, 2 %); LRMS ES^+ *m/z* 352.1 $(MH)^+$.

N-[3,5-Bis(trifluoromethyl)phenyl]-6-(5-fluoro-2-methoxyphenyl)pyrimidin-4-amine (404)

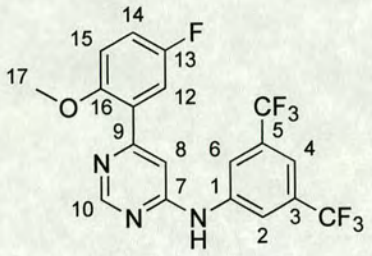

General procedure **P2** was followed using 5-fluoro-2-methoxyphenylboronic acid (0.114 g, 0.67 mmole, 1.0 eq.) followed by 3,5-bis(trifluoromethyl)aniline (102 μL, 0.67 mmole, 1.0 eq.). Pyrimidine **404** was isolated as a white solid (HPLC Method L, t_R = 16.54 min., 0.003 g, 1 %); LRMS ES^+ *m/z* 432.0 $(MH)^+$; ν_{max} (film)/cm^{-1} 3392 (N-H), 2917 (C-H), 2850 (O-CH_3), 1646 (C=C), 1602 (aryl C=C), 1507 (C=N); δ_H (250 MHz, CD_3OD): 3.96 (s, 3H, *H*17), 7.21 – 7.26 (m, 2H, *H*14, *H*15), 7.54 (d, 1H, *J* = 1.2 Hz, *H*8), 7.61 (s, 1H, *H*4), 7.69 (dd, 1H, *J* = 3.0 Hz, J_{HF} = 9.5 Hz, *H*12), 8.48 (s, 2H, *H*2, *H*6), 8.85 (d, 1H, *J* = 1.2 Hz, *H*10).

6-(5-Fluoro-2-methoxyphenyl)-N-[4-(trifluoromethyl)phenyl]pyrimidin-4-amine (405)

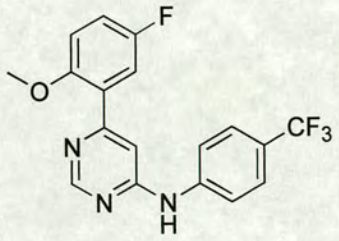

General procedure **P2** was followed using 5-fluoro-2-methoxyphenylboronic acid (0.114 g, 0.67 mmole, 1.0 eq.) followed by 4-(trifluoromethyl)aniline (82 μL, 0.67 mmole, 1.0

eq.). Pyrimidine **405** was isolated as a white solid (HPLC Method L, t_R = 11.08 min., 0.002 g, 1 %); LRMS ES^+ *m/z* 364.0 $(MH)^+$.

N-[3,5-Bis(trifluoromethyl)phenyl]-6-[3-(trifluoromethyl)phenyl]pyrimidin-4-amine (406)

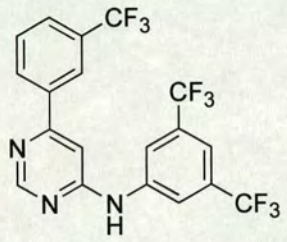

General procedure **P2** was followed using 3-(trifluoromethyl)phenylboronic acid (0.284 g, 0.67 mmole, 1.0 eq.) followed by 3,5-bis(trifluoromethyl)aniline (102 μL, 0.67 mmole, 1.0 eq.). Pyrimidine **406** was isolated as a pale yellow solid (HPLC Method L, t_R = 24.18 min., 0.003 g, 1 %); LRMS ES^+ *m/z* 452.1 $(MH)^+$.

6-[3-(Trifluoromethyl)phenyl]-N-[4-(trifluoromethyl)phenyl]pyrimidin-4-amine (407)

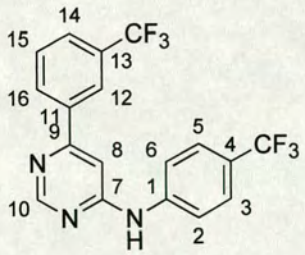

General procedure **P2** was followed using 3-(trifluoromethyl)phenylboronic acid (0.284 g, 0.67 mmole, 1.0 eq.) followed by 4-(trifluoromethyl)aniline (82 μL, 0.67 mmole, 1.0 eq.). Pyrimidine **407** was isolated as a pale yellow solid (HPLC Method L, t_R = 20.08 min., 0.003 g, 1 %); LRMS ES^+ *m/z* 384.2 $(MH)^+$; ν_{max} (film)/cm^{-1} 3308 (N-H), 3116

(aryl C-H), 2925 (C-H), 1645 (C=C), 1584 (aryl C=C), 1520 (C=N); δ_H (250 MHz, CD_3OD): 7.34 (d, 1H, *J* = 1.1 Hz, *H*8), 7.70 (d, 2H, *J* = 8.6 Hz, *H*2, *H*6), 7.80 (t, 1H, *J* = 7.9 Hz, *H*15), 7.91 (d, 1H, *J* = 7.9 Hz, *H*14), 8.01 (d, 2H, *J* = 8.6 Hz, *H*3, *H*5), 8.28 (d, 1H, *J* = 7.9 Hz, *H*16), 8.36 (s, 1H, *H*12), 8.86 (d, 1H, *J* = 1.1 Hz, *H*10); Mpt. 151.2 – 152.6 °C.

N-[3,5-Bis(trifluoromethyl)phenyl]-6-(4-fluorophenyl)pyrimidin-4-amine (408)

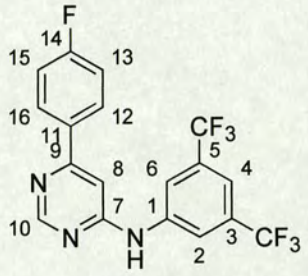

General procedure **P3** was followed using 4-fluorophenylboronic acid (0.094 g, 0.67 mmole, 1.0 eq.) followed by 3,5-bis(trifluoromethyl)aniline (102 μL, 0.67 mmole, 1.0 eq.). Pyrimidine **408** was isolated as a cream solid (HPLC Method L, t_R = 20.45 min., 0.022 g, 8 %); LRMS ES^+ *m/z* 402.0 $(MH)^+$; HRMS FAB^+ *m/z* 402.08447 $(MH)^+$ (calculated for $C_{18}H_{11}F_7N_3$, 402.08412 (Dev. 0.87 ppm)); ν_{max} (film)/cm^{-1} 3419 (N-H), 3102 (aryl C-H), 2917 (C-H), 1645 (C=C), 1602 (aryl C=C), 1515 (C=N); δ_H (250 MHz, CD_3OD): 7.28 (d, 1H, *J* = 1.0 Hz, *H*8), 7.37 (t, 2H, *J* = 8.7 Hz, J_{HF} = 8.7 Hz, *H*13, *H*15), 7.73 (s, 1H, *H*4), 8.05 (dd, 2H, *J* = 8.7 Hz, J_{HF} = 5.2 Hz, *H*12, *H*16), 8.45 (s, 2H, *H*2, *H*6), 8.94 (d, 1H, *J* = 1.0 Hz, *H*10); Mpt. 171.6 – 173.2 °C.

N-[3,5-Bis(trifluoromethyl)phenyl]-6-(3,5-dimethylphenyl)pyrimidin-4-amine (409)

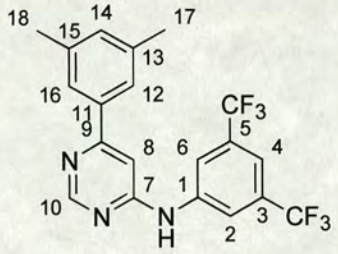

General procedure **P3** was followed using 3,5-dimethylphenylboronic acid (0.101 g, 0.67 mmole, 1.0 eq.) followed by 3,5-bis(trifluoromethyl)aniline (102 μL, 0.67 mmole, 1.0 eq.). Pyrimidine **409** was isolated as a yellow solid (HPLC Method L, t_R = 16.01 min., 0.064 g, 23 %); LRMS ES^+ *m/z* 412.0 $(MH)^+$; δ_H (250 MHz, CD_3OD): 2.41 (s, 3H, *H*18), 2.43 (s, 3H, *H*17), 7.09 (d, 1H, *J* = 1.0 Hz, *H*8), 7.33 (s, 1H, *H*14), 7.34 (s, 2H, *H*12, *H*16), 7.80 (s, 1H, *H*4), 8.48 (s, 2H, *H*2, *H*6), 9.00 (d, 1H, *J* = 1.0 Hz, *H*10).

N-[3,5-Bis(trifluoromethyl)phenyl]-6-[4-(trifluoromethyl)phenyl]pyrimidin-4-amine (410)

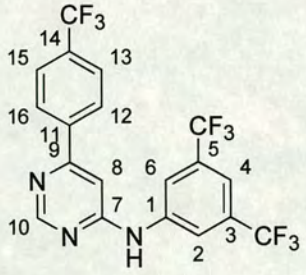

General procedure **P3** was followed using 4-(trifluoromethyl)phenylboronic acid (0.128 g, 0.67 mmole, 1.0 eq.) followed by 3,5-bis(trifluoromethyl)aniline (102 μL, 0.67 mmole, 1.0 eq.). Pyrimidine **410** was isolated as a white solid (HPLC Method K, t_R = 23.45 min., 0.029 g, 10 %); LRMS ES^+ *m/z* 452.1 $(MH)^+$; ν_{max} (film)/cm^{-1} 3248 (N-H), 3108 (aryl C-H), 2927 (C-H), 1637 (C=C), 1592 (aryl C=C), 1519 (C=N); δ_H (250 MHz,

CD_3OD): 7.26 (d, 1H, J = 1.1 Hz, *H*8), 7.60 (s, 1H, *H*4), 7.84 (d, 2H, J = 8.1 Hz, *H*12, *H*16), 8.19 (d, 2H, J = 8.1 Hz, *H*13, *H*15), 8.44 (s, 2H, *H*2, *H*6), 8.87 (d, 1H, J = 1.1 Hz, *H*10); Mpt. 192.0 – 192.5 °C.

_N_-[3,5-Bis(trifluoromethyl)phenyl]-6-(2-nitrophenyl)pyrimidin-4-amine (411)

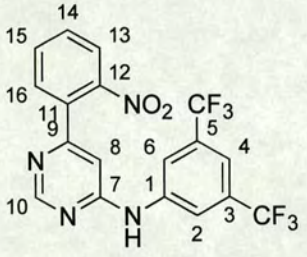

General procedure **P3** was followed using 2-nitrophenylboronic acid (0.112 g, 0.67 mmole, 1.0 eq.) followed by 3,5-bis(trifluoromethyl)aniline (102 µL, 0.67 mmole, 1.0 eq.). Pyrimidine **411** was isolated as a brown oil (HPLC Method L, t_R = 21.11 min., 0.002 g, 1 %); LRMS ES^+ *m/z* 429.1 $(MH)^+$; ν_{max} (film)/cm^{-1} 3371 (N-H), 3108 (aryl C-H), 2919 (C-H), 1636 (C=C), 1589 (aryl C=C), 1523 (NO_2), 1508 (C=N), 1379 (NO_2); δ_H (250 MHz, CD_3OD): 7.04 (d, 1H, J = 1.1 Hz, *H*8), 7.64 (s, 1H, *H*4), 7.73 – 7.79 (m, 2H, *H*14, *H*15), 7.85 (dd, 1H, J =1.4, 7.4 Hz, *H*16), 8.09 (dd, 1H, J = 1.6, 8.0 Hz, *H*13), 8.49 (s, 2H, *H*3, *H*5), 8.80 (d, 1H, J = 1.1 Hz, *H*10).

4-(6-{[3,5-Bis(trifluoromethyl)phenyl]amino}pyrimidin-4-yl)phenol (412)

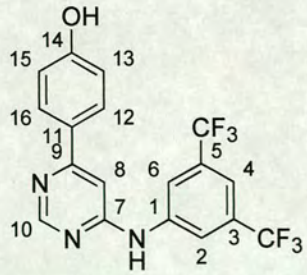

General procedure **P3** was followed using 4-hydroxyphenylboronic acid (0.093 g, 0.67 mmole, 1.0 eq.) followed by 3,5-bis(trifluoromethyl)aniline (102 μL, 0.67 mmole, 1.0 eq.). Pyrimidine **412** was isolated as a yellow oil (HPLC Method J, t_R = 13.40 min., 0.008 g, 3 %); LRMS ES^+ *m/z* 399.9 $(MH)^+$; δ_H (250 MHz, CD_3OD): 7.26 (m, 1H, Ar*H*), 7.45 (d, 1H, *J* = 0.9 Hz, *H*8), 7.55 – 7.63 (m, 3H, Ar*H*), 7.94 (s, 1H, *H*4), 8.63 (s, 2H, *H*2, *H*6), 9.12 (d, 1H, *J* = 0.9 Hz, *H*10).

N-[3,5-Bis(trifluoromethyl)phenyl]-6-(4-methoxyphenyl)pyrimidin-4-amine (413)

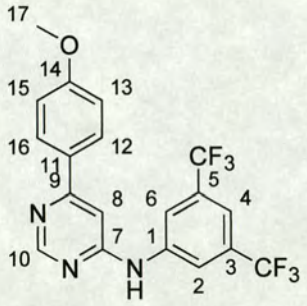

General procedure **P3** was followed using 4-methoxyphenylboronic acid (0.102 g, 0.67 mmole, 1.0 eq.) followed by 3,5-bis(trifluoromethyl)aniline (102 μL, 0.67 mmole, 1.0 eq.). Pyrimidine **413** was isolated as a pale cream solid (HPLC Method K, t_R = 15.14 min., 0.018 g, 6 %); LRMS ES^+ *m/z* 413.9 $(MH)^+$; ν_{max} (film)/cm^{-1} 3307 (N-H), 2927 (C-H), 2844 (O-CH_3), 3054 (aryl C-H), 1636 (C=C), 1593 (aryl C=C), 1515 (C=N); δ_H (250 MHz, CD_3OD): 3.94 (s, 3H, *H*17), 7.20 (d, 2H, *J* = 9.0 Hz, *H*13, *H*15), 7.28 (d, 1H, *J* = 0.9 Hz, *H*8), 7.78 (s, 1H, *H*4), 7.95 (d, 2H, *J* = 9.0 Hz, *H*12, *H*16), 8.45 (s, 2H, *H*2, *H*6), 8.94 (d, 1H, *J* = 0.9 Hz, *H*10); Mpt. 180.9 – 181.7 °C.

6-(3-Aminophenyl)-*N*-[3,5-bis(trifluoromethyl)phenyl]pyrimidin-4-amine (414)

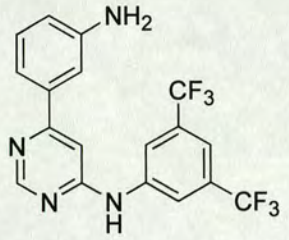

General procedure **P3** was followed using 3-aminophenylboronic acid (0.125 g, 0.67 mmole, 1.0 eq.) followed by 3,5-bis(trifluoromethyl)aniline (102 μL, 0.67 mmole, 1.0 eq.). Pyrimidine **414** was isolated as a brown oil (HPLC Method J, t_R = 10.27 min., 0.002 g, 1 %); LRMS ES^+ *m/z* 399.1 $(MH)^+$.

6-(4-Fluorophenyl)-*N*-[4-(trifluoromethyl)phenyl]pyrimidin-4-amine (415)

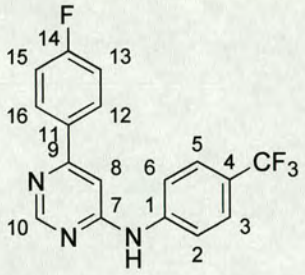

General procedure **P3** was followed using 4-fluorophenylboronic acid (0.094 g, 0.67 mmole, 1.0 eq.) followed by 4-(trifluoromethyl)aniline (82 μL, 0.67 mmole, 1.0 eq.). Pyrimidine **415** was isolated as a pale brown solid (HPLC Method L, t_R = 14.37 min., 0.019 g, 9 %); LRMS ES^+ *m/z* 334.0 $(MH)^+$; ν_{max} (film)/cm^{-1} 3250 (N-H), 2995 (C-H), 1647 (C=C), 1602 (aryl C=C), 1513 (C=N); δ_H (250 MHz, CD_3OD): 7.24 (d, 1H, *J* = 1.0 Hz, *H*8), 7.34 (t, 2H, *J* = 8.7 Hz, J_{HF} = 8.7 Hz, *H*13, *H*15), 7.70 (d, 2H, *J* = 9.1 Hz, *H*2, *H*6), 7.97 (s, 2H, *J* = 9.1 Hz, *H*3, *H*5), 8.03 (dd, 2H, *J* = 8.7 Hz, J_{HF} = 5.2 Hz, *H*12, *H*16), 8.81 (d, 1H, *J* = 1.0 Hz, *H*10); Mpt. 202.8 – 204.0 °C.

N-[3,5-Bis(trifluoromethyl)phenyl)-6-(2-bromophenyl)pyrimidin-4-amine (416)

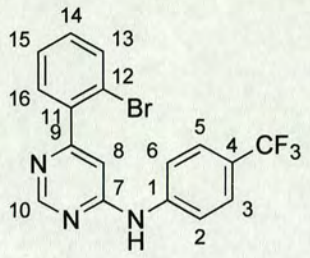

General procedure **P3** was followed using 2-bromophenylboronic acid (0.135 g, 0.67 mmole, 1.0 eq.) followed by 4-(trifluoromethyl)aniline (82 μL, 0.67 mmole, 1.0 eq.). Pyrimidine **416** was isolated as a brown oil (HPLC Method L, t_R = 14.48 min., 0.019 g, 7 %); LRMS ES^+ *m/z* 396.1 $(MH)^+$ assigned to $C_{18}H_{10}{}^{81}BrF_6N_3$; δ_H (250 MHz, CD_3OD): 7.16 (d, 1H, *J* = 0.9 Hz, *H*8), 7.52 – 7.66 (m, 3H, *H*14, *H*15, *H*16), 7.77 (d, 2H, *J* = 8.6 Hz, *H*2, *H*6), 7.88 (dd, 1H, *J* = 0.9, 7.5 Hz, *H*13), 8.02 (d, 2H, *J* = 8.6 Hz, *H*3, *H*5), 9.95 (d, 1H, *J* = 0.9 Hz, *H*10).

6-(3,5-Dimethylphenyl)-*N*-[4-(trifluoromethyl)phenyl]pyrimidin-4-amine (417)

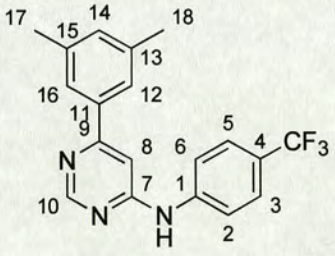

General procedure **P3** was followed using 3,5-dimethylphenylboronic acid (0.101 g, 0.67 mmole, 1.0 eq.) followed by 4-(trifluoromethyl)aniline (82 μL, 0.67 mmole, 1.0 eq.). Pyrimidine **417** was isolated as a white solid (HPLC Method L, t_R = 24.08 min., 0.041 g, 18 %); LRMS ES^+ *m/z* 344.0 $(MH)^+$; ν_{max} (film)/cm^{-1} 3306 (N-H), 2927 (C-H), 1646 (C=C), 1586 (aryl C=C), 1508 (C=N); δ_H (250 MHz, CD_3OD): 2.41 (s, 3H, *H*18),

2.43 (s, 3H, *H*17), 7.04 (s, 1H, *H*8), 7.32 (s, 1H, *H*14), 7.35 (s, 2H, *H*12, *H*16), 7.77 (d, 2H, J = 8.6 Hz, *H*2, *H*6), 8.01 (d, 2H, J = 8.6 Hz, *H*3, *H*5), 8.91 (s, 1H, *H*10).

_N_,6-Bis-[4-(Trifluoromethyl)phenyl]pyrimidin-4-amine (418)

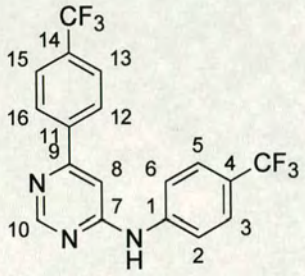

General procedure **P3** was followed using 4-(trifluoromethyl)phenylboronic acid (0.128 g, 0.67 mmole, 1.0 eq.) followed by 4-(trifluoromethyl)aniline (82 μL, 0.67 mmole, 1.0 eq.). Pyrimidine **418** was isolated as a cream solid (HPLC Method L, t_R = 21.09 min., 0.017 g, 7 %); LRMS ES$^+$ *m/z* 384.0 (MH)$^+$; ν_{max} (film)/cm^{-1} 3237 (N-H), 3052 (aryl C-H), 2992 (C-H), 1612 (C=C), 1593 (aryl C=C), 1525 (C=N); δ_H (250 MHz, CD_3OD): 7.27 (d, 1H, J = 1.1 Hz, *H*8), 7.64 (d, 2H, J = 8.4 Hz, *H*2, *H*6), 7.84 (d, 2H, J = 8.2 Hz, *H*12, *H*16), 7.97 (d, 2H, J = 8.4 Hz, *H*3, *H*5), 8.19 (d, 2H, J = 8.2 Hz, *H*13, *H*15), 8.79 (d, 1H, J = 1.1 Hz, *H*10); Mpt. 222.2 – 222.8 °C.

6-(2-Nitrophenyl)-_N_-[4-(trifluoromethyl)phenyl]pyrimidin-4-amine (419)

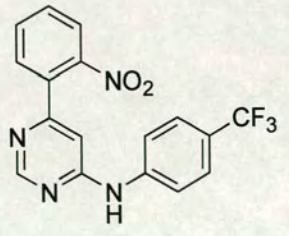

General procedure **P3** was followed using 2-nitrophenylboronic acid (0.112 g, 0.67 mmole, 1.0 eq.), followed by 4-(trifluoromethyl)aniline (82 μL, 0.67 mmole, 1.0 eq.).

Pyrimidine **419** was isolated as a brown oil (HPLC Method L, t_R = 16.14 min., 0.005 g, 2 %); LRMS ES^+ *m/z* 361.1 $(MH)^+$.

4-(6-{[4-(Trifluoromethyl)phenyl]amino}pyrimidin-4-yl)-phenol (420)

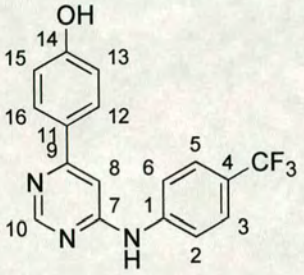

General procedure **P3** was followed using 4-hydroxyphenylboronic acid (0.093 g, 0.67 mmole, 1.0 eq.), followed by 4-(trifluoromethyl)aniline (82 μL, 0.67 mmole, 1.0 eq.). Pyrimidine **420** was isolated as a yellow oil (HPLC Method L, t_R = 11.49 min., 0.018 g, 8 %); LRMS ES^+ *m/z* 332.0 $(MH)^+$; δ_H (250 MHz, CD_3OD): 6.67 – 6.71 (m, 1H, Ar*H*), 7.24 (d, 1H, *J* = 0.7 Hz, *H*8), 7.35 – 7.47 (m, 3H, Ar*H*), 7.62 (d, 2H, *J* = 8.4 Hz, *H*2, *H*6), 7.98 (d, 2H, *J* = 8.4 Hz, *H*3, *H*5), 8.84 (d, 1H, *J* = 0.7 Hz, *H*10).

6-(4-Methoxyphenyl)-*N*-[4-(trifluoromethyl)phenyl]pyrimidin-4-amine (421)

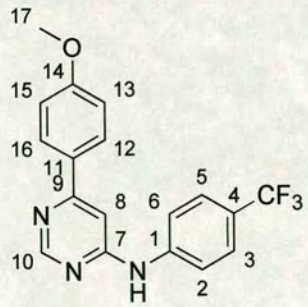

General procedure **P3** was followed using 4-methoxyphenylboronic acid (0.102 g, 0.67 mmole, 1.0 eq.) followed by 4-(trifluoromethyl)aniline (82 μL, 0.67 mmole, 1.0 eq.). Pyrimidine **421** was isolated as a cream solid (HPLC Method K, t_R = 10.16 min., 0.034

g, 15 %); LRMS ES^+ *m/z* 345.9 $(MH)^+$; δ_H (250 MHz; $(CD_3)_2SO$) 3.87 (s, 3H, *H*17), 7.15 (d, 2H, *J* = 8.9 Hz, *H*2, *H*6), 7.29 (s, 1H, *H*8), 7.74 (d, 2H, *J* = 8.7 Hz, *H*13, *H*15) 7.98 (d, 2H, *J* = 8.7 Hz, *H*12, *H*16), 8.03 (d, 2H, *J* = 8.9 Hz, *H*3, *H*5), 8.83 (s, 1H, *H*10), 10.35 (s, 1H, N*H*).

6-(3-Aminophenyl)-*N*-[4-(trifluoromethyl)phenyl]pyrimidin-4-amine (422)

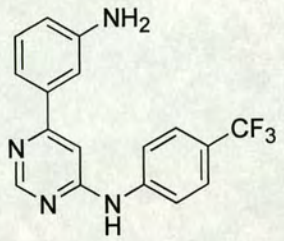

General procedure **P3** was followed using 3-aminophenylboronic acid (0.125 g, 0.67 mmole, 1.0 eq.) followed by 4-(trifluoromethyl)aniline (82 μL, 0.67 mmole, 1.0 eq.). Pyrimidine **422** was isolated as a brown oil (HPLC Method K, t_R = 6.46 min., 0.003 g, 1 %); LRMS ES^+ *m/z* 331.0 $(MH)^+$.

5-(6-{[4-(Trifluoromethyl)phenyl]amino}pyrimidin-4-yl)-thiophene-2-carbaldehyde (423)

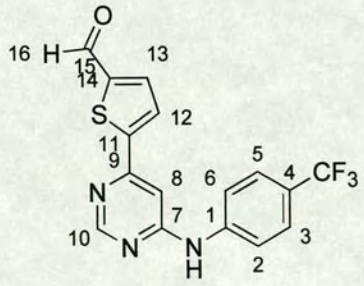

General procedure **P3** was followed using 5-formylthiophene-2-boronic acid (0.105 g, 0.67 mmole, 1.0 eq.) followed by 4-(trifluoromethyl)aniline (82 μL, 0.67 mmole, 1.0 eq.). Pyrimidine **423** was isolated as a yellow solid (HPLC Method L, t_R = 22.10 min.,

0.005 g, 2 %); LRMS ES^+ *m/z* 350.0 $(MH)^+$; δ_H (250 MHz, CD_3OD): 7.30 (d, 1H, *J* = 0.9 Hz, *H*8), 7.67 (d, 2H, *J* = 8.8 Hz, *H*2, *H*6), 7.95 (d, 1H, *J* = 4.2 Hz, *H*12), 7.98 (d, 2H, *J* = 8.8 Hz, *H*3, *H*5), 7.01 (d, 1H, *J* = 4.2 Hz, *H*13), 8.72 (d, 1H, *J* = 0.9 Hz, *H*10), 9.99 (s, 1H, *H*16).

4-{[6-(3-Nitrophenyl)pyrimidin-4-yl]amino}phenol (424)

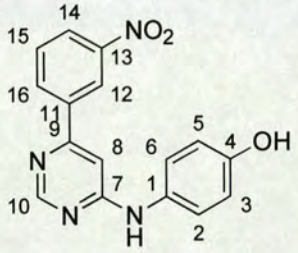

To a solution of 4,6-dichloropyrimidine (0.100 g, 0.67 mmole, 1.0 eq.) in dioxane (3.0 mL) was added 3-nitrophenylboronic acid (0.112 g, 0.67 mmole, 1.0 eq.), Cs_2CO_3 (0.656 g, 1.00 mmole, 3.0 eq.), $Pd(OAc)_2$ (0.008 g, 0.03 mmole, 0.05 eq.) and triphenylphosphine (0.018 g, 0.07 mmole, 0.10 eq.). Water (0.3 mL) was added to the reaction mixture to solubilise the Cs_2CO_3. The reaction mixture was irradiated in the Discover™ at 130 °C for 20 minutes with active cooling of the sample. To an aliquot (1 mL) of the crude reaction mixture was added 4-aminophenol (0.026 g, 0.24 mmole, 1.0 eq.) followed by HCl (4M, 222 μL, 4.0 eq.) and the sample irradiated in the Discover™ at 130 °C for a further 20 minutes, with active cooling of the sample, before being injected directly onto the Biotage Parallex Flex™ HPLC (Method E, t_R = 16.01 min.). Appropriate fractions were combined and concentrated *in vacuo* to afford pyrimidine **424** as a yellow solid (0.011 g, 15 %); LRMS ES^+ *m/z* 309.0 $(MH)^+$; HRMS FAB^+ *m/z* 309.09932 $(MH)^+$ (calculated for $C_{16}H_{13}N_4O_3$, 309.09877 (Dev. 1.78 ppm)); ν_{max} (film)/cm^{-1} 3392 (O-H), 3250 (N-H), 2918 (C-H), 1636 (C=C), 1522 (NO_2), 1507 (C=N), 1346 (NO_2); δ_H ($(CD_3)_2SO$): 6.81 (d, 2H, *J* = 8.9 Hz, *H*2, *H*6), 7.25 (s, 1H, *H*8), 7.45 (d, 2H, *J* = 8.9 Hz, *H*3, *H*5), 7.86 (t, 1H, *J* = 8.1 Hz, *H*15), 8.38 – 8.44 (m, 2H,

*H*14, *H*16), 8.73 (s, 1H, *H*10), 8.81 (t, 1H, *J* = 1.9 Hz, *H*12), 9.80 (s, 1H, O*H*); Mpt. 188.4 – 189.0 °C.

4-{[6-(2-Naphthyl) pyrimidin-4-yl]amino}phenol (425)

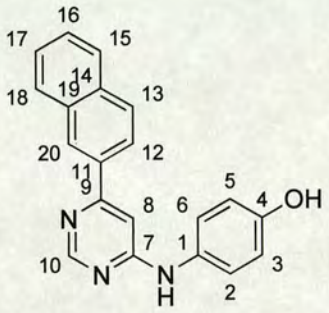

To a solution of 4,6-dichloropyrimidine (0.050 g, 0.34 mmole, 1.0 eq.) in acetonitrile (1.0 mL) was added 2-naphthylboronic acid (0.058 g, 0.34 mmole, 1.0 eq.), Cs_2CO_3 (0.164 g, 0.50 mmole, 1.5 eq.) and $Pd(OAc)_2$ (0.04 g, 0.02 mmole, 0.05 eq.). Water (0.3 mL) was added to the reaction mixture to dissolve the Cs_2CO_3. The reaction mixture was irradiated in the Discover™ at 130 °C for 15 minutes, with active cooling of the sample, before the addition of 4-hydroxyaniline (0.037 g, 0.34 mmole, 1.0 eq.) and *p*-toluenesulfonic acid (0.128 g, 0.67 mmole, 2.0 eq.). The reaction mixture was irradiated in the Discover™ at 110 °C for a further 5 minutes before being injected directly onto the Biotage Parallex Flex™ HPLC (Method E t_R = 20.17 min) to afford **425** as a yellow solid (0.002 g, 2 %); LRMS ES^+ *m/z* 313.9 $(MH)^+$; HRMS FAB^+ *m/z* 314.12878 $(MH)^+$ (calculated for $C_{20}H_{16}N_3O$, 314.12934 (Dev. - 1.78 ppm)); ν_{max} (film)/cm^{-1} 3392 (O-H), 2921 (C-H), 1636 (C=C), 1576 (aryl C=C), 1507 (C=N); δ_H (250 MHz, CD_3OD): 7.55 – 7.66 (m, 2H, *H*16, *H*17), 7.89 – 8.06 (m, 3H, *H*12, *H*15, *H*18), 8.19 (d, 1H, *J* = 1.1 Hz, *H*8), 8.23 (dd, 1H, *J* = 1.9, 8.7 Hz, *H*13), 8.73 (dd, 1H, *J* = 0.7, 1.4 Hz, *H*20), 9.03 (d, 1H, *J* = 1.1 Hz, *H*10); Mpt. 233.0 – 233.5 °C.

6-(2-Naphthyl)-*N*-(4-nitrophenyl)pyrimidin-4-amine (426)

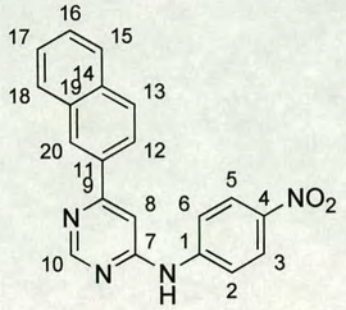

General procedure **P4** was followed using 4,6-dichloropyrimidine (0.075 g, 0.50 mmole, 1.0 eq.) and 2-naphthylboronic acid (0.087 g, 0.50 mmole, 1.0 eq.) followed by 4-nitroaniline (0.023 g, 0.17 mmole, 1.0 eq.). Pyrimidine **426** was isolated as a yellow solid (HPLC Method E, t_R = 18.21 min., 0.019 g, 33 %); LRMS ES$^+$ *m/z* 343.1 $(MH)^+$; HRMS FAB$^+$ *m/z* 343.11989 $(MH)^+$ (calculated for $C_{20}H_{15}N_4O_2$ 343.11950, Dev. 1.15 ppm); ν_{max} (film)/cm^{-1} 3325 (N-H), 3063 (aryl C-H), 2920 (C-H), 1635 (C=C), 1576 (aryl C=C), 1545 (NO_2), 1504 (C=N), 1347 (NO_2); δ_H (250 MHz, $(CD_3)_2SO$): 7.61 – 7.68 (m, 3H, Ar*H*), 8.00 – 8.04 (m, 1H, Ar*H*), 8.09 – 8.18 (m, 3H, Ar*H*), 8.10 (d, 2H, *J* = 9.3 Hz, *H*2, *H*6), 8.27 (d, 2H, *J* = 9.3 Hz, *H*3, *H*5), 8.71 (s, 1H, *H*10), 8.93 (s, 1H, Ar*H*), 10.83 (s, 1H, N*H*);

***N*-(3-{[6-(3,5-Dimethoxyphenyl)amino]pyrimidin-4-yl}phenyl)acetamide (427)**

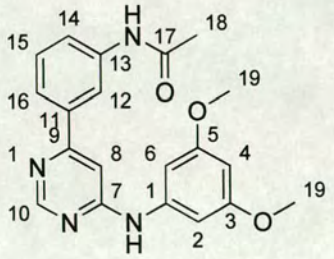

General procedure **P4** was followed using 4,6-dichloropyrimidine (0.075 g, 0.50 mmole, 1.0 eq.) and 3-acetamidophenylboronic acid (0.090 g, 0.50 mmole, 1.0 eq.) followed by

3,5-dimethoxyaniline (0.019 g, 0.17 mmole, 1.0 eq.). Pyrimidine **427** was isolated as a brown solid (HPLC Method E, t_R 18.07 min., 0.004 g, 6%); LRMS ES^+ *m/z* 365.0 $(MH)^+$; HRMS FAB^+ *m/z* 365.16203 $(MH)^+$ (calculated for $C_{20}H_{21}N_4O_3$, 365.16137 (Dev. 1.82 ppm)); ν_{max} (film)/cm^{-1} 3306 (N-H), 2930 (C-H), 2842 (O-CH_3), 1636 (C=C), 1592 (aryl C=C), 1508 (C=N); δ_H (250 MHz, CD_3OD): 2.38 (s, 3H, *H*18), 4.02 (s, 6H, *H*19), 6.60 (t, 1H, *J* = 2.2 Hz, *H*4), 7.09 (d, 2H, *J* = 2.2 Hz, *H*2, *H*6), 7.35 (d, 1H, *J* = 0.9 Hz, *H*8), 7.75 – 7.86 (m, 3H, Ar*H*), 8.49 (m, 1H, Ar*H*), 8.99 (d, 1H, *J* = 0.9 Hz, *H*10).

3-{[6-(3-Nitrophenyl)pyrimidin-4-yl]amino}phenol (428)

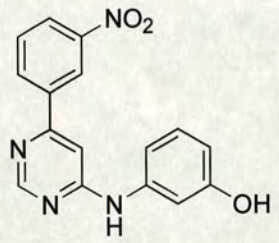

To an aliquot (1 mL) of the crude Suzuki intermediate **424** was added 3-aminophenol (0.026 g, 0.24 mmole, 1.0 eq.) followed by HCl (4M, 222 μL, 4.0 eq.). The sample was irradiated in the Discover™ at 130 °C for a further 20 minutes before being injected directly onto the Biotage Parallex Flex™ HPLC (Method G, t_R = 7.16 min.). Appropriate fractions were combined and concentrated *in vacuo* to afford pyrimidine **429** as a yellow oil (0.011 g, 15 %); LRMS ES^+ *m/z* 309.5 $(MH)^+$.

3-{6-[(3-Hydroxyphenyl)amino]pyrimidin-4-yl}phenol (429)

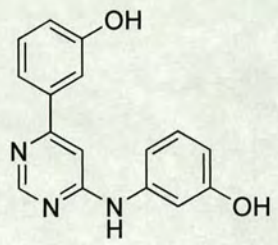

General procedure **P4** was followed using 4,6-dichloropyrimidine (0.075 g, 0.50 mmole, 1.0 eq.) and 3-hydroxyphenylboronic acid (0.076 g, 0.5 mmole, 1.0 eq.) 3-hydroxyaniline (0.019 g, 0.17 mmole, 1.0 eq.). Pyrimidine **429** was isolated as a yellow oil (HPLC Method A, t_R = 11.36 min., 0.015 g, 32 %); LRMS ES^+ *m/z* 280.0 $(MH)^+$.

5-{[6-(2,5-Difluorophenyl)pyrimidin-4-yl]amino}-2-methoxyphenol (430)

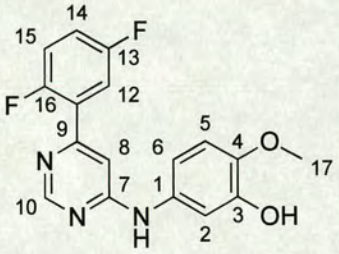

General procedure **P5** was followed using 4,6-dichloropyrimidine (0.250 g, 1.67 mmole, 1.0 eq.) and 2,5-difluorophenylboronic acid (0.265 g, 1.67 mmole, 1.0 eq.) followed by 3-hydroxy-4-methoxyaniline (0.024 g, 0.17 mmole, 1.0 eq.). Pyrimidine **430** was isolated as a brown solid (HPLC Method G, t_R = 10.48 min, 0.005 g, 9 %); LRMS ES^+ *m/z* 330.0 $(MH)^+$; δ_H (250 MHz, CD_3OD): 3.92 (s, 3H, *H*17), 7.00 – 7.19 (m, 4H, *H*2, *H*5, *H*6, *H*8), 7.41 – 7.51 (m, 2H, *H*14, *H*15), 7.57 – 7.65 (m, 1H, *H*12), 8.80 (d, 1H, *J* = 0.8 Hz, *H*10).

6-(2,5-Difluorophenyl)-*N*-(3,4-dimethoxyphenyl)pyrimidin-4-amine (431)

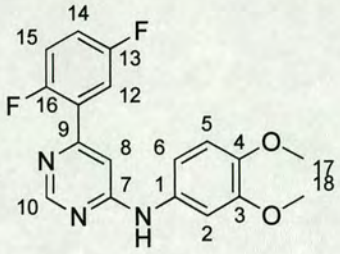

General procedure **P5** was followed using 4,6-dichloropyrimidine (0.250 g, 1.67 mmole, 1.0 eq.) and 2,5-difluorophenylboronic acid (0.265 g, 1.67 mmole, 1.0 eq.) followed by 3,4-dimethoxyaniline (0.026 g, 0.17 mmole, 1.0 eq.). Pyrimidine **431** was isolated as a yellow solid (HPLC Method G, t_R = 11.16 min, 0.017 g, 29 %); LRMS ES^+ *m/z* 344.2 $(MH)^+$; ν_{max} (film)/cm^{-1} 3420 (N-H), 3078 (aryl C-H), 2940 (C-H), 1646 (C=C), 1589 (aryl C=C), 1507 (C=N); δ_H (250 MHz, CD_3OD): 3.92 (s, 6H, *H*17, *H*18), 7.08 (d, 1H, *J* = 8.7 Hz, H6), 7.17 – 7.37 (m, 3H, *H*2, *H*5, *H*8), 7.45 – 7.53 (m, 2H, *H*14, *H*15), 7.60 – 7.68 (m, 1H, *H*12), 8.85 (d, 1H, *J* = 0.9 Hz, *H*10); Mpt. 180.2 – 180.7 °C.

3-{[6-(2,5-Difluorophenyl)pyrimidin-4-yl]amino}phenol (432)

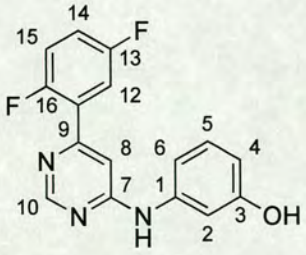

General procedure **P5** was followed using 4,6-dichloropyrimidine (0.250 g, 1.67 mmole, 1.0 eq.) and 2,5-difluorophenylboronic acid (0.265 g, 1.67 mmole, 1.0 eq.) followed by 4-aminophenol (0.019 g, 0.17 mmole, 1.0 eq.). Pyrimidine **432** was isolated as a cream solid (HPLC Method G, t_R = 10.19 min, 0.035 g, 63 %); LRMS ES^+ *m/z* 330.0 $(MH)^+$; ν_{max} (film)/cm^{-1} 3392 (O-H), 2917 (C-H), 1636 (C=C), 1508 (C=N); δ_H (250 MHz,

CD_3OD): 6.72 (ddd, 1H, J = 0.9, 2.4, 8.1 Hz, H6), 7.07 – 7.13 (ddd, 1H, J = 0.9, 2.4, 8.1 Hz, H4), 7.21 –7.25 (m, 2H, H2, H8), 7.27 (t, 1H, J = 8.1 Hz, H5), 7.41 – 7.47 (m, 2H, H14, H15), 7.60 – 7.68 (m, 1H, *H*12), 8.82 (d, 1H, J = 0.9 Hz, *H*10); Mpt. 176.6 – 178.5 °C.

4-{[6-(2,5-Difluorophenyl)pyrimidin-4-yl]amino}phenol (433)

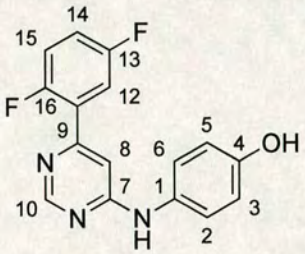

General procedure **P5** was followed using 4,6-dichloropyrimidine (0.250 g, 1.67 mmole, 1.0 eq.) and 2,5-difluorophenylboronic acid (0.265 g, 1.67 mmole, 1.0 eq.) followed by 4-aminophenol (0.019 g, 0.17 mmole, 1.0 eq.). Pyrimidine **433** was isolated as a yellow solid (HPLC Method G, t_R = 10.12 min, 0.011 g, 22 %); LRMS ES^+ *m/z* 300.1 $(MH)^+$; ν_{max} (film)/cm^{-1} 3392 (O-H), 2918 (C-H), 1636 (C=C), 1508 (C=N); δ_H (250 MHz, CD_3OD); 6.92 (d, 2H, J = 8.9 Hz, *H*2, *H*6), 7.11 (d, 1H, J = 0.8 Hz, *H*8), 7.46 – 7.53 (m, 4H, *H*3, *H*5, *H*14, *H*15), 7.58 – 7.67 (m, 1H, *H*12), 8.79 (d, 1H, J = 0.8 Hz, *H*10); Mpt. 213.2 – 213.8 °C.

6-(3-Aminophenyl)-*N*-(3,5-dimethoxyphenyl)pyrimidin-4-amine (434)

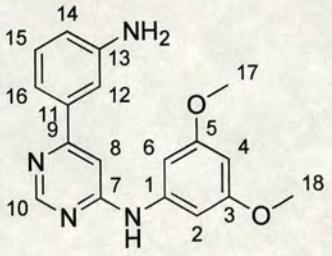

General procedure **P5** was followed using 4,6-dichloropyrimidine (0.250 g, 1.67 mmole, 1.0 eq.) and 3-acetamidophenylboronic acid (0.300 g, 1.67 mmole, 1.0 eq.) followed by 3,5-dimethoxyaniline (0.026 g, 0.17 mmole, 1.0 eq.). Pyrimidine **434** was isolated as a brown solid (HPLC Method G, t_R = 10.01 min, 0.009 g, 16 %); LRMS ES^+ *m/z* 323.1 $(MH)^+$; δ_H (250 MHz, CD_3OD): 3.85 (s, 6H, *H*17, *H*18), 6.47 (t, 1H, *J* = 2.2 Hz, *H*4), 6.92 (d, 2H, *J* = 2.2 Hz, *H*2, *H*6), 7.19 (d, 1H, *J* = 0.9 Hz, *H*8), 7.24 (ddd, 1H, *J* = 1.1, 2.2, 8.2 Hz, *H*14), 7.38 – 7.41 (m, 2H, *H*12, *H*16), 7.52 (t, 1H, *J* = 8.2 Hz, *H*15), 8.84 (d, 1H, *J* = 0.9 Hz, *H*10).

6-(2,5-Difluorophenyl)-*N*-(3,5-dimethoxyphenyl)pyrimidin-4-amine (435)

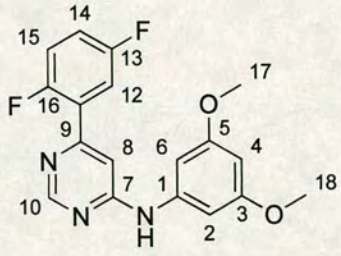

General procedure **P5** was followed using 4,6-dichloropyrimidine (0.250 g, 1.67 mmole, 1.0 eq.) and 2,5-difluorophenylboronic acid (0.265 g, 1.67 mmole, 1.0 eq.) followed by 3,5-dimethoxyaniline (0.026 g, 1.67 mmole, 1.0 eq.). Pyrimidine **435** was isolated as a biege solid (HPLC Method G, t_R = 19.02 min, 0.012 g, 20 %); LRMS ES^+ *m/z* 344.1 $(MH)^+$; HRMS FAB^+ *m/z* 344.12198 $(MH)^+$ (calculated for $C_{18}H_{16}F_2N_3O_2$, 344.12106

(Dev. 2.67 ppm)); ν_{max} (film)/cm^{-1} 3250 (N-H), 2928 (C-H), 2840 (O-CH_3), 1625 (C=C), 1585 (aryl C=C), 1507 (C=N); δ_H (250 MHz, CD_3OD): 3.86 (s, 6H, *H*17, *H*18), 6.42 (t, 1H, *J* = 2.2 Hz, *H*4), 6.94 (d, 2H, *J* = 2.2 Hz, *H*2, *H*6), 7.27 (d, 1H, *J* = 0.9 Hz, *H*8), 7.41 – 7.47 (m. 1H, *H*14), 7.57 - 7.75 (m, 2H, *H*12, *H*15), 8.84 (d, 1H, *J* = 0.9 Hz, *H*10); Mpt. 200.2 – 200.7 °C.

3-(6-Anilinopyrimidin-4-yl)phenol (436)

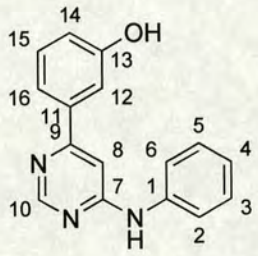

To a solution of 4,6-dichloropyrimidine (0.175 g, 1.18 mmole, 1.0 eq.) in acetonitrile (3.0 mL) was added 3-hydroxyphenylboronic acid (0.162 g, 1.18 mmole, 1.0 eq.), Cs_2CO_3 (0.462 g, 1.42 mmole, 1.2 eq.), $Pd(OAc)_2$ (0.014 g, 0.06 mmole, 0.05 eq.) and tri-*o*-tolylphosphine (0.036 g, 0.12 mmole, 0.10 eq.). Water (0.5 mL) was added to the reaction mixture to solubilise the Cs_2CO_3. The reaction mixture was irradiated in the Discover™ at 110 °C for 25 minutes, with active cooling of the sample. The sample was then divided into aliquots (7 x 0.5 mL, **436a**). To one aliquot containing the Suzuki intermediate (0.17 mmole, 1.0 eq.) was added aniline (16 μL, 0.17 mmole, 1.0 eq.) followed by HCl (4M, 168 μL, 4.0 eq.) and the sample irradiated in the Discover™ at 110 °C for a further 25 minutes. The sample was then injected directly onto the Biotage Parallex Flex™ HPLC (Method A, t_R 11.07 min.). Appropriate fractions were combined and concentrated *in vacuo* to afford pyrimidine **436** as a white solid (0.014 g, 31%); LRMS ES$^+$ *m/z* 262.9 (MH)$^+$; δ_H (500 MHz, CD_3OD): 7.12 (s, 1H, *H*8), 7.28 (d, 1H, *J* = 7.9 Hz, *H*16), 7.31 – 7.34 (m, 2H, Ar*H*), 7.46 (t, 1H, *J* = 7.9 Hz, *H*15), 7.48 – 7.58 (m, 5H, Ar*H*), 8.77 (s. 1H, *H*10), 7.57 - 7.75 (m, 2H, *H*12, *H*15), 8.84 (d, 1H, *J* = 0.9 Hz, *H*10);

3-{6-[(3-Nitrophenyl)amino]pyrimidin-4-yl}phenol (437)

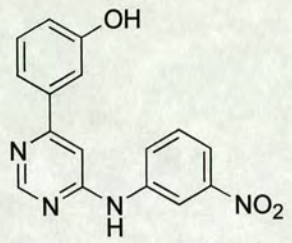

To one aliquot (0.5 mL) containing the Suzuki intermediate **436a** (0.17 mmole, 1.0 eq.) was added 3-nitroaniline (0.024 g, 0.17 mmole, 1.0 eq.) followed by HCl (4M, 168 μL, 4.0 eq.). The reaction mixture was irradiated in the Discover™ at 110 °C for a further 25 minutes before being injected directly onto the Biotage Parallex Flex™ HPLC (Method A, t_R 15.19 min.). Appropriate fractions were combined and concentrated *in vacuo* to afford pyrimidine **437** as a brown solid (0.008 g, 15%); LRMS ES^+ *m/z* 309.1 $(MH)^+$.

3-{6-[(3-Fluorophenyl)amino]pyrimidin-4-yl}phenol (438)

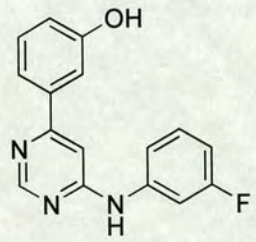

To one aliquot (0.5 mL) containing the Suzuki intermediate **436a** (0.17 mmole, 1.0 eq.) was added 3-nitroaniline (0.024 g, 0.17 mmole, 1.0 eq.) followed by HCl (4M, 168 μL, 4.0 eq.). The reaction mixture was irradiated in the Discover™ at 110 °C for a further 25 minutes before being injected directly onto the Biotage Parallex Flex™ HPLC (Method A, t_R 13.48 min.). Appropriate fractions were combined and concentrated *in vacuo* to afford pyrimidine **438** as a brown solid (0.006 g, 13%); LRMS ES^+ *m/z* 282.1 $(MH)^+$.

(3-{[6-(2,5-Dimethylphenyl)pyrimidin-4-yl]amino}phenyl)methanol (439)

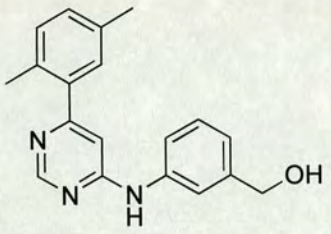

To a solution of 4,6-dichloropyrimidine (0.175 g, 1.18 mmole, 1.0 eq.) in acetonitrile (3.0 mL) was added 2,5-dimethylphenylboronic acid (0.176 g, 1.18 mmole, 1.0 eq.), Cs_2CO_3 (0.462 g, 1.42 mmole, 1.2 eq.), $Pd(OAc)_2$ (0.014 g, 0.06 mmole, 0.05 eq.) and tri-*o*-tolylphosphine (0.036 g, 0.12 mmole, 0.10 eq.). Water (0.5 mL) was added to the reaction mixture to solubilise the Cs_2CO_3. The reaction mixture was irradiated in the Discover™ at 110 °C for 25 minutes, with active cooling of the sample. The sample was then divided into aliquots (7 x 0.5 mL). To one aliquot containing the Suzuki intermediate (0.17 mmole, 1.0 eq.) was added (3-aminophenyl)methanol (0.024 g, 0.17 mmole, 1.0 eq.) followed by HCl (4M, 168 μL, 4.0 eq.) and the sample irradiated in the Discover™ at 110 °C for a further 25 minutes. The sample was then injected directly onto the Biotage Parallex Flex™ HPLC (Method A, t_R 10.54 min.). Appropriate fractions were combined and concentrated *in vacuo* to afford pyrimidine **439** as a brown oil (0.002 g, 4%); LRMS ES^+ *m/z* 306.3 $(MH)^+$.

6-(2,5-Dimethylphenyl)-*N*-(3-fluorophenyl)pyrimidin-4-amine (440)

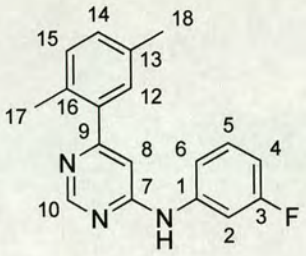

To a solution of 4,6-dichloropyrimidine (0.025 g, 0.17 mmole, 1.0 eq.) in toluene (1.0 mL) was added 2,5-dimethylphenylboronic acid (0.026 g, 0.17 mmole, 1.0 eq.), Cs_2CO_3 (0.082 g, 0.25 mmole, 1.5 eq.), KF (0.015 g, 0.25 mmole, 1.5 eq), $Pd(OAc)_2$ (0.002 g, 0.01 mmole, 0.05 eq.) and triphenylphosphine (0.005 g, 0.17 mmole, 0.10 eq.). Water (0.1 mL) was added to the reaction mixture to solubilise the Cs_2CO_3. The reaction mixture was irradiated in the Discover™ at 130 °C for 15 minutes, with active cooling of the sample before being filtered and injected directly onto the Flex™ HPLC (Method P, t_R14.28 min). Appropriate fractions were combined and concentrated *in vacuo* to afford a brown residue (0.011g) that was dissolved in dioxane (1.0 mL) and to which was added 3-fluoroaniline (6 μL, 0.05 mmole, 1.0 eq., calculation based on recovered Suzuki intermediate) and HCl (4M, 51 μL, 4.0 eq.). The reaction mixture was irradiated in the Discover™ at 110 °C for 25 minutes, with stirring and active cooling of the sample, before being injected directly onto the Biotage Parallex Flex™ HPLC (Method A, t_R = 14.50 min.). Appropriate fractions were combined and concentrated *in vacuo* to afford pyrimidine **440** as a yellow solid (0.004 g, 8 %); LRMS ES^+ *m/z* 294.2 $(MH)^+$; δ_H (250 MHz, CD_3OD): 6.69 (d, 1H, *J* = 0.8 Hz, *H*8), 7.28 (s, 1H, *H*12), 7.29 – 7.36 (m, 2H, *H*14, *H*15), 7.69 – 7.76 (m, 1H, Ar*H*), 7.72 (d, 1H, *H*6), 8.14 – 8.15 (m, 1H, Ar*H*), 8.17 – 8.21 (m, 1H, Ar*H*), 9.05 (d, 1H, *J* = 0.8 Hz, *H*10).

4-{[2-Amino-6-(3,5-dimethylphenyl)pyrimidin-4-yl]amino}phenol (444)

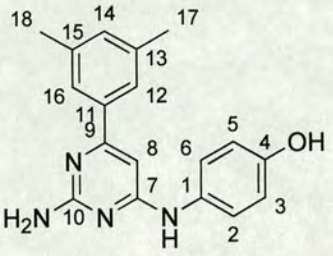

General procedure **P4** was followed using 2-amino-4,6-dichloropyrimidine (0.083 g, 0.50 mmole, 1.0 eq.) and 3,5-dimethylphenylboronic acid (0.062 g, 0.50 mmole, 1.0 eq.) followed by 4-hydroxyaniline (0.019 g, 0.17 mmole, 1.0 eq.). Pyrimidine **444** was isolated as a white solid (HPLC Method E, t_R = 17.46 min., 0.020 g, 39%); LRMS ES^+ *m/z* 307.0 $(MH)^+$; ν_{max} (film)/cm^{-1} 3307 (O-H), 2928 (C-H), 1636 (C=C), 1616 (aryl C=C), 1508 (C=N); δ_H (250 MHz, CD_3OD): 2.39 (s, 3H, *H*18), 2.41 (s, 3H, *H*17), 6.19 (s, 1H, *H*8), 6.87 (d, 2H, *J* = 8.8 Hz, *H*2, *H*6), 7.27 (s, 1H, *H*14), 7.33 (s, 2H, *H*12, *H*16), 7.47 – 7.41 (m, 2H, *H*3, *H*5).

N^4-(4-Chlorophenyl)-6-(3,5-dimethylphenyl)pyrimidine-2,4-diamine (445)

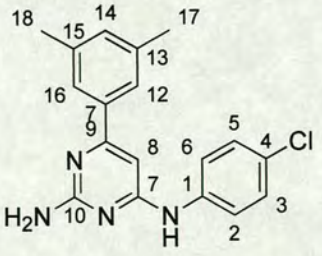

General procedure **P4** was followed using 2-amino-4,6-dichloropyrimidine (0.083 g, 0.50 mmole, 1.0 eq.) and 3,5-dimethylphenylboronic acid (0.062 g, 0.50 mmole, 1.0 eq.) followed by 4-chloroaniline (0.022 g, 0.17 mmole, 1.0 eq.). Pyrimidine **445** was isolated as a brown solid (HPLC Method E, t_R = 22.45 min., 0.021 g, 38%); LRMS ES^+ *m/z* 325.0 $(MH)^+$; ν_{max} (film)/cm^{-1} 3487 (N-H), 3298 (N-H), 3154 (aryl C-H), 2928 (C-H),

1636 (C=C), 1605 (aryl C=C), 1506 (C=N); δ_H (250 MHz, CD_3OD): 2.40 (s, 3H, *H*18), 2.42 (s, 3H, *H*17), 6.08 (s, 1H, *H*8), 7.30 (s, 1H, *H*14), 7.34 (s, 2H, *H*12, *H*16), 7.44 (d, 2H, J = 8.9 Hz, *H*2, *H*6), 7.83 (d, 2H, J = 8.9 Hz, *H*3, *H*5); Mpt. 236.1 – 236.7 °C.

_N_-(3-{2-Amino-6-[(3,5-dimethoxyphenyl)amino]pyrimidin-4-yl}phenyl)acetamide (446)

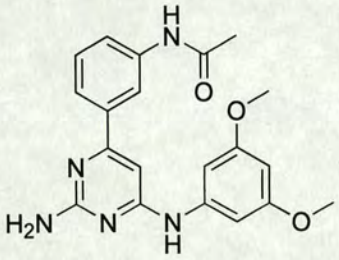

General procedure **P4** was followed using 2-amino-4,6-dichloropyrimidine (0.083 g, 0.50 mmole, 1.0 eq.) and 3-acetamidophenylboronic acid (0.090 g, 0.50 mmole, 1.0 eq.) followed by 3,5-dimethoxyaniline (0.026 g, 0.17 mmole, 1.0 eq.). Pyrimidine **446** was isolated as a yellow solid (HPLC Method E, t_R = 15.48 min., 0.012 g, 19%); LRMS ES^+ *m/z* 379.0 $(MH)^+$.

_N_-(3-{2-Amino-6-[(3-nitrophenyl)amino]pyrimidin-4-yl}phenyl)acetamide (447)

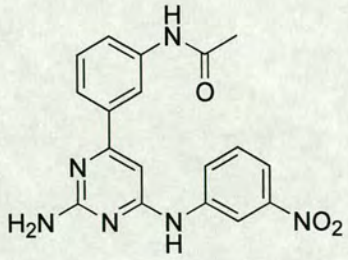

General procedure **P4** was followed using 2-amino-4,6-dichloropyrimidine (0.083 g, 0.50 mmole, 1.0 eq.) and 3-acetamidophenylboronic acid (0.090 g, 0.50 mmole, 1.0 eq.) followed by 3-nitroaniline (0.026 g, 0.17 mmole, 1.0 eq.). Pyrimidine **447** was isolated

as a yellow oil (HPLC Method E, t_R = 15.30 min., 0.009 g, 15%); LRMS ES^+ *m/z* 365.3 $(MH)^+$.

3-{[2-Amino-6-[3-nitrophenyl)pyrimidin-4-yl]amino}phenol (448)

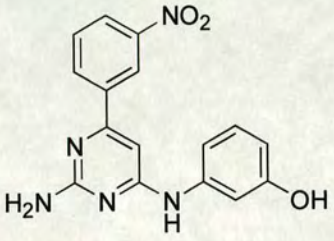

General procedure **P4** was followed using 2-amino-4,6-dichloropyrimidine (0.083 g, 0.50 mmole, 1.0 eq.) and 3-nitrophenylboronic acid (0.084 g, 0.50 mmole, 1.0 eq.) in followed by 3-hydroxyaniline (0.019 g, 0.17 mmole, 1.0 eq.) to an aliquot (1.0 mL, 0.17 mmole, 1.0 eq.). Pyrimidine **448** was isolated as a yellow solid (HPLC Method A, t_R = 13.37 min., 0.008 g, 16 %); LRMS ES^+ *m/z* 323.9 $(MH)^+$; ν_{max} (film)/cm^{-1} 3392 (O-H), 2928 (C-H), 1636 (C=C), 1527 (NO_2), 1350 (NO_2).

3-{[2-Amino-6-(3-nitrophenyl)amino]pyrimidin-4-yl]-phenol (449)

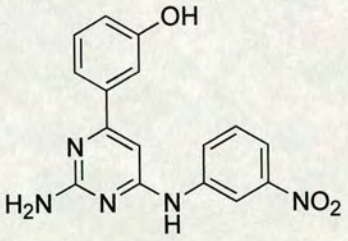

General procedure **P4** was followed using 2-amino-4,6-dichloropyrimidine (0.083 g, 0.50 mmole, 1.0 eq.) and 3-hydroxyphenylboronic acid (0.069 g, 0.50 mmole, 1.0 eq.) followed by 3-nitroaniline (0.023 g, 0.17 mmole, 1.0 eq.). Pyrimidine **449** was isolated as a cream solid (HPLC Method A, t_R = 15.31 min., 0.003 g, 5 %); LRMS ES^+ *m/z* 323.9 $(MH)^+$.

3-{2-Amino-6-[(3-hydroxyphenyl)amino]pyrimidin-4-yl}phenol (450)

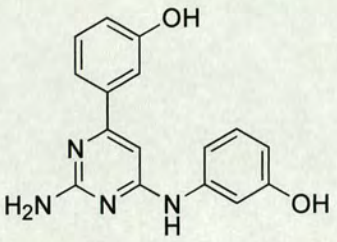

General procedure **P4** was followed using 2-amino-4,6-dichloropyrimidine (0.083 g, 0.50 mmole, 1.0 eq.) and 3-hydroxyphenylboronic acid (0.069 g, 0.50 mmole, 1.0 eq.) followed by 3-hydroxyaniline (0.019 g, 0.17 mmole, 1.0 eq.). Pyrimidine **450** was isolated as a yellow solid (HPLC Method A, t_R = 12.59 min., 0.011 g, 22 %); LRMS ES^+ *m/z* 294.8 $(MH)^+$; ν_{max} (film)/cm^{-1} 3392 (O-H), 2928 (C-H), 1636 (C=C), 1585 (aryl C=C), 1506 (C=N).

6-(2,5-Dimethylphenyl)-N^4-(3-nitrophenyl)pyrimidine-2,4-diamine (451)

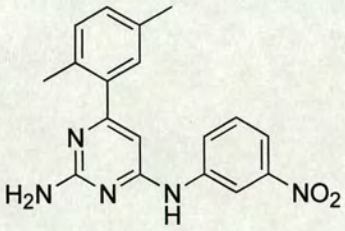

General procedure **P4** was followed using 2-amino-4,6-dichloropyrimidine (0.083 g, 0.50 mmole, 1.0 eq.) and 2,5-dimethylphenylboronic acid (0.076 g, 0.50 mmole, 1.0 eq.) followed by 3-nitroaniline (0.023 g, 0.17 mmole, 1.0 eq.). Pyrimidine **451** was isolated as a white solid (HPLC Method A, t_R = 17.06 min., 0.004 g, 7 %); LRMS ES^+ *m/z* 336.0 $(MH)^+$.

3-{[2-Amino-6-(2,5-dimethylphenyl)pyrimidin-4-yl]amino}phenol (452)

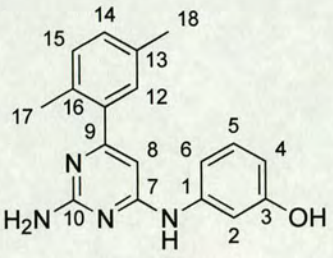

General procedure **P4** was followed using 2-amino-4,6-dichloropyrimidine (0.083 g, 0.50 mmole, 1.0 eq.) and 2,5-dimethylphenylboronic acid (0.076 g, 0.50 mmole, 1.0 eq.) followed by 3-hydroxyaniline (0.023 g, 0.17 mmole, 1.0 eq.). Pyrimidine **452** was isolated as a yellow oil (HPLC Method A, t_R = 14.43 min., 0.005 g, 10 %); LRMS ES^+ *m/z* 307.0 $(MH)^+$; δ_H (250 MHz, CD_3OD): 2.63 (s, 3H, *H*18), 2.65 (s, 3H, *H*17), 6.50 (s, 1H, *H*8), 6.90 – 6.94 (m, 1H, *H*2), 7.40 – 7.56 (m, 6H, Ar*H*).

6-(2,5-Difluorophenyl)-N^4-(3,5-dinitrophenyl)pyrimidine-2,4-diamine (453)

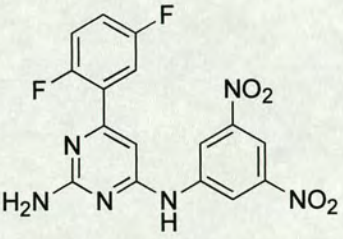

General procedure **P4** was followed using 2-amino-4,6-dichloropyrimidine (0.083 g, 0.50 mmole, 1.0 eq.) and 2,5-difluorophenylboronic acid (0.079 g, 0.5 mmole, 1.0 eq.) followed by 3,5-dinitroaniline (0.031 g, 0.17 mmole, 1.0 eq.). Pyrimidine **453** was isolated as a yellow solid (HPLC Method G, t_R = 19.48 min., 0.015 g, 23%); LRMS ES^+ *m/z* 388.9 $(MH)^+$.

6-(2,5-Difluorophenyl)-N^4-pyridin-3-ylpyrimidine-2,4-diamine (454)

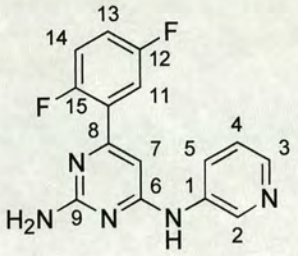

General procedure **P4** was followed using 2-amino-4,6-dichloropyrimidine (0.083 g, 0.50 mmole, 1.0 eq.) and 2,5-difluorophenylboronic acid (0.079 g, 0.50 mmole, 1.0 eq.) followed by 3-aminopyridine (0.016 g, 0.17 mmole, 1.0 eq.). Pyrimidine **454** was isolated as a yellow solid (HPLC Method I, t_R = 7.38 min., 0.010 g, 20 %); LRMS ES^+ *m/z* 299.9 $(MH)^+$; δ_H (250 MHz, CD_3OD): 6.70 (s, 1H, *H*7), 7.48 – 7.54 (m, 2H, *H*5, *H*13), 7.60 – 7.69 (m, 1H, *H*14), 7.79 (dd, 1H, J_{HF} = 8.4, 5.2 Hz, *H*11), 8.53 – 8.59 (m, 2H, *H*3, *H*4), 9.10 (d, 1H, *J* = 2.3 Hz, *H*2).

6-(2,5-Difluorophenyl)-N^4-(3,5-dimethoxyphenyl)pyrimidine-2,4-diamine (455)

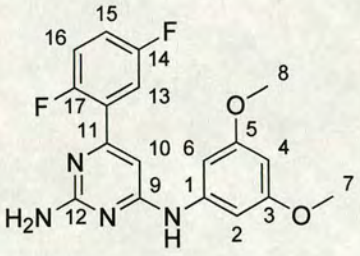

General procedure **P4** was followed using 2-amino-4,6-dichloropyrimidine (0.083 g, 0.50 mmole, 1.0 eq.) and 2,5-difluorophenylboronic acid (0.079 g, 0.5 mmole, 1.0 eq.) followed by 3,5-dimethoxyaniline (0.026 g, 0.17 mmole, 1.0 eq.). Pyrimidine **455** was isolated as a yellow solid (HPLC Method I, t_R = 15.12 min., 0.019 g, 32%); LRMS ES^+ *m/z* 358.9 $(MH)^+$; HRMS FAB^+ *m/z* 359.13204 $(MH)^+$ (calculated for $C_{18}H_{17}F_2N_4O_2$, 359.13196 (Dev. 0.22 ppm)); ν_{max} (film)/cm^{-1} 3308 (N-H), 2926 (C-H), 2840 (O-CH_3),

1646 (C=C), 1507 (C=N); δ_H (250 MHz, CD_3CN): 3.83 (s, 6H, *H*7, *H*8), 6.39 (t, 1H, J = 2.0 Hz, *H*4), 6.51 (s, 1H, *H*10), 6.95 (d, 2H, J = 2.0 Hz, *H*2, *H*6), 7.33 – 7.39 (m, 2H, *H*15, *H*16), 7.50 – 7.55 (m, 1H, *H*13), 8.92 (s, 1H, N*H*); Mpt. 203.2 – 204.0 °C.

4-Chloro-6-phenylpyrimidine (456 – Table 4.6 Entry 2)[217]

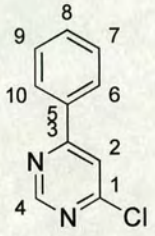

To a solution of 4,6-dichloropyrimidine (0.025 g, 0.17 mmole, 1.0 eq.) in acetonitrile (1.0 mL) was added phenylboronic acid (0.021 g, 0.17 mmole, 1.0 eq.), Cs_2CO_3 (0.066 g, 0.20 mmole, 1.2 eq.) and $Pd(PPh_3)_4$ (0.020 g, 0.02 mmole, 0.10 eq.). Water (0.1 mL) was added to the reaction mixture to solubilise the Cs_2CO_3. The reaction mixture was irradiated in the Discover™ at 110 °C for 25 minutes with active cooling of the sample, before being injected directly onto the Biotage Parallex Flex™ HPLC (Method A, t_R = 18.12 min). Pyrimidine **456** was isolated as a biege solid (0.010 g, 30%); LRMS ES^+ *m/z* 191.1 $(MH)^+$; δ_H (250 MHz, $CDCl_3$): 7.52 – 7.57 (m, 3H, *H*7, *H*8, *H*9), 7.77 (d, 1H, J = 1.1 Hz, *H*2), 8.07 – 8.11 (m, 2H, *H*6, *H*10), 9.05 (d, 1H, J = 1.1 Hz, *H*4).

4,6-Diphenylpyrimidine (457 – Table 4.6 Entry 2)[218]

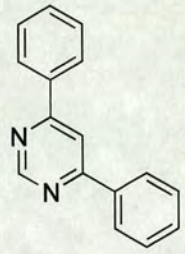

Isolated during the synthesis of pyrimidine **457** (HPLC Method A, t_R = 20.59 min.) as a brown solid (0.001 g, 5%); LRMS ES^+ *m/z* 233.1 $(MH)^+$.

6-(4-Methoxyphenyl)-*N*-(3-nitrophenyl)pyrimidin-4-amine (460)

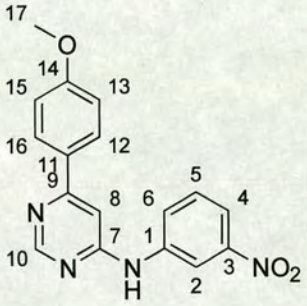

To a solution of 4,6-dichloropyrimidine (0.100 g, 0.67 mmole, 1.0 eq.) in dioxane (3 mL) was added was added 3-nitroaniline (0.093 g, 0.67 mmole, 1.0 eq.) and HCl (4M, 670 μL, 4.0 eq.). The reaction mixture was irradiated in the Discover™ at 130 °C for 30 minutes before being injected, in 3 x 1 mL aliquots, onto the Biotage Parallex Flex™ HPLC (Method B, t_R = 14.26 min.). Appropriate fractions were combined and concentrated *in vacuo* to afford a residue (**460a**) that was dissolved in a mixture of toluene/ethanol (3 mL, 4:1) and divided into aliquots (3 x 1 mL). To one aliquot containing the anilino intermediate (1 mL, 0.17 mmole, 1.0 eq.) was added 4-methoxyphenyl boronic acid (0.048 g, 0.17 mmole, 1.0 eq.), K_2CO_3 (0.122 g, 0.68 mmole, 2.0 eq.) and $Pd(PPh_3)_4$ (0.010 g, 0.01 mmole, 0.04 eq.). Water (0.2 mL) was

added to solubilize the K_2CO_3 and the reaction mixture was irradiated in the Discover™ at 140 °C for 15 minutes before being injected directly onto the Biotage Parallex Flex™ HPLC (Method S, t_R = 7.17 min). Appropriate fractions were combined and concentrated *in vacuo* to afford pyrimidine **460** as a yellow solid (0.007 g, 10%); LRMS ES^+ *m/z* 322.6 $(MH)^+$; ν_{max} (film)/cm^{-1} 3328 (N-H), 3096 (aryl C-H), 2930 (C-H), 2839 (O-CH_3), 1625 (C=C), 1526 (NO_2), 1361 (NO_2); δ_H (500 MHz, CD_3OD): 3.92 (s, 3H, *H*17), 7.01 (dd, 1H, *J* = 8.1, 1.5 Hz, *H*6), 7.03 (s, 1H, *H*8), 7.16 (d, 2H, *J* = 8.7 Hz, *H*13, *H*15), 7.27 (t, 1H, *J* = 8.1 Hz, *H*5), 7.44 (dd, 1H, *J* = 8.1, 1.5 Hz, *H*4), 7.67 (t, 1H, *J* = 1.5 Hz, *H*2), 7.84 (d, 2H, *J* = 8.7 Hz, *H*12, *H*16), 8.69 (s, 1H, *H*10); Mpt. 179.1 - 180.7 °C.

4-{[6-(4-Methoxyphenyl)pyrimidin-4-yl]amino}phenol (461)

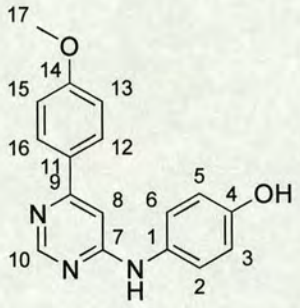

To a solution of **523** (0.15 mmole, 1.0 eq.) in toluene/ethanol (1 mL, 4:1) was added 4-methoxyphenylboronic acid (0.032 g, 0.21 mmole, 1.4 eq.), K_2CO_3 (0.083 g, 0.60 mmole, 4.0 eq.) and $Pd(PPh_3)_4$ (0.07 g, 0.01 mmole, 0.04 eq.). The reaction mixture was irradiated in the Discover™ at 140 °C for 15 minutes, before being injected directly onto the Biotage Parallex Flex™ HPLC (Method S, t_R = 6.44 min). Appropriate fractions were combined and concentrated *in vacuo* to afford pyrimidine **461** as a yellow solid (0.005 g, 11%); LRMS ES^+ *m/z* 293.6 $(MH)^+$; HRMS FAB^+ *m/z* 294.12453 $(MH)^+$ (calculated for $C_{17}H_{16}N_3O_2$, 294.12425 (Dev. 0.97 ppm)); ν_{max} (film)/cm^{-1} 3388 (O-H), 2928 (C-H), 2834 (O-CH_3), 1633 (C=C), 1579 (aryl C=C), 1505 (C=N); δ_H (250 MHz; CD_3OD) 3.95 (s, 3H, *H*17), 6.92 (d, 2H, *J* = 8.8 Hz, *H*2, *H*6), 7.01 (s, 1H, *H*8), 7.20 (d,

2H, J = 8.9 Hz, *H*13, *H*15), 7.44 (d, 2H, J = 8.8 Hz, *H*3, *H*5), 7.84 (d, 2H, J = 8.9 Hz, *H*12, *H*16), 8.70 (s, 1H, *H*10); δ_C (75 MHz; CD_3OD) 56.6 (*C*17), 111.2 (CH_{Ar}), 116.5 (2 x CH_{Ar}), 116.6 (2 x CH_{Ar}), 116.7 (2 x CH_{Ar}), 117.4 (C_{Ar}), 117.5 (C_{Ar}), 124.0 (2 x CH_{Ar}), 130.3 (C_{Ar}), 130.5 (CH_{Ar}), 133.6 (C_{Ar}), 148.0 (C_{Ar}), 165.3 (CH_{Ar}); Mpt. 227.2 – 227.8 °C.

3-[{6-(4-Methoxyphenyl)pyrimidin-4-yl]amino}phenol (462)

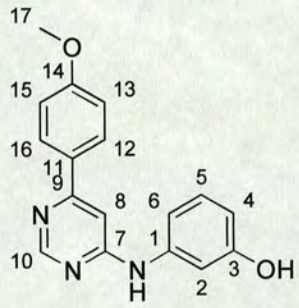

To a solution of **460a** (0.23 mmole, 1.0 eq.) in a mixture of toluene/ethanol (1.0 mL, 4:1) was added 4-methoxyphenylboronic acid (0.048 g, 0.32 mmole, 1.4 eq.), $Pd(PPh_3)_4$ (0.010 g, 0.01 mmole, 0.04 eq.), K_2CO_3 (0.122 g, 0.91 mmole, 4.0 eq.) and water (0.1 mL). The reaction mixture was irradiated in the Discover™ at 140 °C for 15 minutes before being injected directly onto the Biotage Parallex Flex™ HPLC (Method S, t_R = 8.12 min.). Appropriate fractions were combined and concentrated *in vacuo* to afford pyrimidine **462** as a white solid (0.013 g, 20%); LRMS ES^+ *m/z* 293.6 $(MH)^+$; ν_{max} (film)/cm^{-1} 3352 (O-H), 2929 (C-H), 2841 (O-CH_3), 1635 (C=C), 1592 (aryl C=C), 1509 (C=N); δ_H (250 MHz, CD_3OD): 4.04 (s, 3H, *H*17), 6.85 (dd, 1H, J = 8.1, 2.3 Hz, *H*6), 7.19 (dd, 1H, J = 8.1, 2.2 Hz, *H*4), 7.23 (s, 1H, *H*8), 7.28 (m, 1H, *H*8), 7.30 (d, 2H, J = 8.9 Hz, *H*13, *H*15), 7.39 (t, 1H, J = 8.1 Hz, *H*5), 7.96 (d, 2H, J = 8.9 Hz, *H*12, *H*16), 8.85 (s, 1H, *H*10); Mpt. 190.4 – 192.0 °C.

6-(3-Methoxyphenyl)-*N*-pyridin-2-yl pyrimidin-4-amine (463)

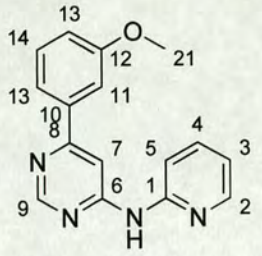

To a solution of **525** (0.015 g, 0.08 mmole, 1.0 eq.) in toluene/ethanol (1 mL, 4:1) was added 3-methoxyphenylboronic acid (0.016 g, 0.11 mmole, 1.4 eq.), K_2CO_3 (0.040 g, 0.32 mmole, 4.0 eq.) and $Pd(PPh_3)_4$ (0.04 g, 0.01 mmole, 0.04 eq.). The reaction mixture was irradiated in the Discover™ at 140 °C for 15 minutes, before being injected directly onto the Biotage Parallex Flex™ HPLC (Method S, t_R = 7.39 min). Appropriate fractions were combined and concentrated *in vacuo* to afford pyrimidine **463** as a white solid (0.009 g, 43%); LRMS ES^+ *m/z* 278.7 $(MH)^+$; ν_{max} (film)/cm^{-1} 3258 (N-H), 3028 (aryl C-H), 2929 (C-H), 2840 (O-CH_3), 1658 (C=C), 1602 (aryl C=C), 1496 (C=N); δ_H (250 MHz; CD_3OD) 3.93 (s, 3H, *H*21), 7.20 – 7.23 (m, 1H, *H*13), 7.42 – 7.59 (m, 3H, Ar*H*), 7.67 – 7.70 (m, 1H, Ar*H*), 7.70 (s, 1H, *H*11), 7.77 (s, 1H, *H*7), 8.27 – 8.34 (m, 1H, Ar*H*), 8.48 – 8.51 (m, 1H, Ar*H*), 9.05 (s, 1H, *H*9); Mpt. 176.0 –177.0 °C.

4-{[6-(3-Methoxyphenyl)pyrimidin-4-yl]amino}phenol (466)

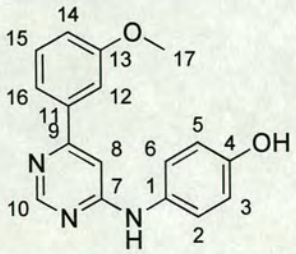

To a solution of 4,6-dichloropyrimidine (0.110 g, 0.74 mmole, 1.1 eq.) in 2-propanol (3 mL), 4-aminophenol (0.078 g, 0.67 mmole, 1.0 eq.) and *N*,*N*-diisopropylethylamine (117

μL, 1.34 mmole, 2.0 eq.) were added. The reaction mixture was irradiated in the Discover™ at 120 °C for 30 minutes, with active cooling of the sample, and then divided into 3 x 1 mL aliquots. To one aliquot containing the Suzuki intermediate (1 mL, 0.23 mmole, 1.0 eq.) was added 3-methoxy-phenyl boronic acid (0.048 g, 0.32 mmole, 1.4 eq.), K_2CO_3 (0.122g, 0.92 mmole, 4.0 eq.) and $Pd(PPh_3)_4$ (0.10 g, 0.02 mmole, 0.1 eq.). The reaction mixture was irradiated in the Discover™ at 140 °C for 15 minutes, before being injected directly onto the Biotage Parallex Flex™ HPLC (Method S, t_R = 6.46 min). Appropriate fractions were combined and concentrated *in vacuo* to afford pyrimidine **466** as a yellow solid (0.044 g, 68%); LRMS ES^+ *m/z* 293.5 $(MH)^+$; ν_{max} (film)/cm^{-1} 3397 (O-H), 2841 ($O-CH_3$), 2918 (C-H), 1636 (C=C), 1578 (aryl C=C), 1508 (C=N); δ_H (250 MHz, CD_3OD): 3.93 (s, 3H, *H*17), 6.91 (d, 2H, *J* = 8.9 Hz, *H*2, *H*6), 7.07 (s, 1H, *H*8), 7.27 (ddd, 1H, *J* = 8.4, 2.5, 0.8 Hz, *H*14), 7.39 – 7.48 (m, 4H, *H*3, *H*5, *H*12, *H*16), 7.58 (t, 1H, *J* = 8.4 Hz, *H*15), 8.74 (s, 1H, *H*10); Mpt. 205.3 – 207.0 °C.

6-(3-Methoxyphenyl)-*N*-phenylpyrimidin-4-amine (467)

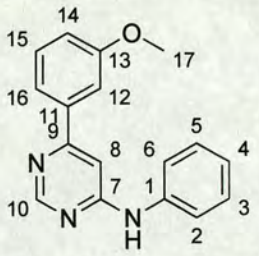

To a stirring solution of **526** (0.045 g, 0.22 mmole, 1.0 eq.) in 2-propanol (1.0 mL) was added 3-methoxyphenylboronic acid (0.047 g, 0.31 mmole, 1.4 eq.), $Pd(PPh_3)_4$ (0.010 g, 0.01 mmole, 0.04 eq.) and K_2CO_3 (0.121 g, 0.88 mmole, 4.0 eq.). The reaction mixture was irradiated in the Discover™ at 140 °C for 15 minutes, with active cooling of the sample. The reaction mixture was injected directly onto the Biotage Parallex Flex™ (Method S, t_R = 12.45 min.). Appropriate fractions were combined and concentrated *in vacuo* to afford pyrimidine **467** as a yellow solid (0.019 g, 31%); LRMS ES^+ *m/z* 277.6

$(MH)^+$; δ_H (250 MHz; CD_3OD) 3.94 (s, 3H, *H*17), 7.07 (s, 1H, H8), 7.31 – 7.35 (m, 2H, Ar*H*), 7.42 – 7.61 (m, 6H, Ar*H*), 7.69 – 7.73 (m, 2H, Ar*H*), 8.83 (s, 1H, *H*10).

4-{[6-(3,4-Dimethoxyphenyl)pyrimidin-4-yl]amino}phenol (469)

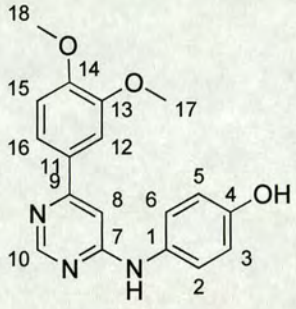

To a solution of **523** (0.046 g, 0.21 mmole, 1.0 eq.) in toluene/ethanol (1 mL, 4:1) was added 3,4-dimethoxyphenylboronic acid (0.053 g, 0.29 mmole, 1.4 eq.), K_2CO_3 (0.116 g, 0.84 mmole, 4.0 eq.) and $Pd(PPh_3)_4$ (0.10 g, 0.01 mmole, 0.04 eq.). The reaction mixture was irradiated in the Discover™ at 140 °C for 15 minutes, before being injected directly onto the Biotage Parallex Flex™ HPLC (Method S, t_R = 6.28 min). Appropriate fractions were combined and concentrated *in vacuo* to afford pyrimidine **469** as a yellow solid (0.021 g, 31%); LRMS ES^+ *m/z* 323.7 $(MH)^+$; ν_{max} (film)/cm^{-1} 3391 (O-H), 3253 (N-H), 2939 (C-H), 2839 (O-CH_3), 1636 (C=C), 1599 (aryl C=C), 1500 (C=N); δ_H (250 MHz; CD_3OD) 3.96 (s, 3H, *H*17), 3.97 (s, 3H, *H*18), 6.91 (d, 2H, *J* = 8.9 Hz, *H*2, *H*6), 7.03 (s, 1H, *H*8), 7.20 (d, 1H, *J* = 8.4 Hz, *H*15), 7.42 – 7.50 (m, 4H, *H*3, *H*5, *H*12, *H*16), 8.70 (s, 1H, *H*10); Mpt. 223.5 – 224.5 °C.

3-{[6-(3,4-Dimethoxyphenyl)pyrimidin-4-yl]amino}phenol (470)

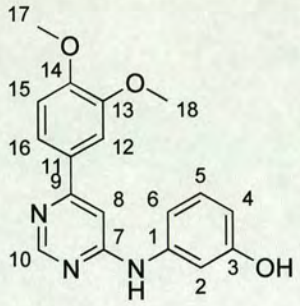

To a solution of **460a** (0.23 mmole, 1.0 eq.) in a mixture of toluene/ethanol (1.0 mL, 4:1) was added 3,4-dimethoxyphenylboronic acid (0.058 g, 0.32 mmole, 1.4 eq.), $Pd(PPh_3)_4$ (0.010 g, 0.01 mmole, 0.04 eq.) and K_2CO_3 (0.122 g, 0.92 mmole, 4.0 eq.). The reaction mixture was irradiated in the Discover™ at 140 °C for 15 minutes, with active cooling of the sample. The reaction mixture was injected directly onto the Biotage Parallex Flex™ (Method S, t_R = 7.07 min.). Appropriate fractions were combined and concentrated in vacuo to afford pyrimidine **470** as a yellow solid (0.014 g, 19%); LRMS ES^+ *m/z* 323.7 $(MH)^+$; δ_H (250 MHz, CD_3OD): 3.97 (s, 3H, *H*17), 3.98 (s, 3H, *H*18), 6.73 - 6.78 (m, 1H, Ar*H*), 7.10 (ddd, 1H, Ar*H*), 7.16 (s, 1H, *H*8), 7.21 (t, 1H, *J* = 2.1 Hz, *H*2), 7.22 (d, 1H, *J* = 8.4 Hz, *H*15), 7.29 (t, 1H, 8.1 Hz, *H*5), 7.46 (d, 1H, *J* = 2.2 Hz, *H*12), 7.52 (dd, 1H, *J* = 8.4, 2.2 Hz, *H*16), 8.77 (s, 1H, *H*10).

6-Chloro-*N*-(3-fluorophenyl)pyrimidin-4-amine (471)

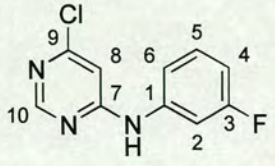

To a solution of 4,6-dichloropyrimidine (0.020 g, 0.13 mmole, 1.0 eq.) was added 3-fluoroaniline (0.018 g, 0.13 mmole, 1.0 eq.) followed by *p*-toluenesulfonic acid (0.051 g, 0.26 mmole, 2.0 eq.). The reaction mixture was irradiated in the Discover™ at 100 °C

for 15 minutes before being injected directly onto the Biotage Parallex Flex™ HPLC (Method I, t_R = 20.19 min.). Pyrimidine **471** was isolated as a white solid (0.008 g, 27 %); LRMS ES^+ *m/z* 223.5 $(MH)^+$; δ_H (250 MHz, $CDCl_3$): 6.58 (s, 1H, *H*8), 6.73 – 6.80 (m, 1H, *H*5), 6.93 (dd, 1H, *J* = 8.1, 1.1 Hz, *H*6), 7.04 (dt, 1H, J_{HF} = 7.9 Hz, *J* = 2.2 Hz, *H*2), 7.17 – 7.25 (m, 2H, *H*4, N*H*), 8.35 (s, 1H, *H*10).

Also prepared following a similar protocol to that described for the synthesis of pyrimidine **522** using 3-fluoroaniline (69 μL, 0.67 mmole, 1.0 eq.). Pyrimidine **471** was isolated as a white solid (HPLC Method A, t_R = 12.21 min, 0.030 g, 20%); LRMS ES^+ *m/z* 223.6 $(MH)^+$.

3-{[6-(3-Methoxyphenyl)pyrimidin-4-yl]amino}phenol (480)

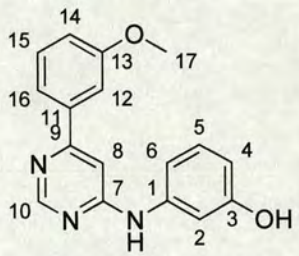

To a solution of **522** (0.23 mmole, 1.0 eq.) in a mixture of toluene/ethanol (1.0 mL, 4:1) was added 3-methoxyphenylboronic acid (0.048 g, 0.32 mmole, 1.4 eq.), $Pd(PPh_3)_4$ (0.010 g, 0.01 mmole, 0.04 eq.) and K_2CO_3 (0.122 g, 0.92 mmole, 4.0 eq.). The reaction mixture was irradiated in the Discover™ at 140 °C for 15 minutes, with active cooling of the sample. The reaction mixture was injected directly onto the Biotage Parallex Flex™ (Method S, t_R = 8.20 min.). Appropriate fractions were combined and concentrated in vacuo to afford pyrimidine **480** as a yellow solid (0.010 g, 15%); LRMS ES^+ *m/z* 293.5 $(MH)^+$; ν_{max} (film)/cm^{-1} 3307 (O-H), 2918 (C-H), 2840 (O-CH_3), 1646 (C=C), 1595 (aryl C=C), 1508 (C=N); δ_H (250 MHz, CD_3OD): 4.13 (s, 3H, *H*17), 6.94 (ddd, 1H, *J* = 8.2, 2.3, 0.9 Hz, Ar*H*), 7.27 – 7.32 (m, 1H, Ar*H*), 7.38 (s, 1H, *H*8), 7.42 – 7.47 (m, 2H,

Ar*H*), 7.48 (t, 1H, *J* = 8.2 Hz, *H*5), 7.62 – 7.66 (m, 2H, Ar*H*), 7.77 (t, 1H, *J* = 8.2 Hz, *H*15), 8.99 (s, 1H, *H*10).

_N_-(3,4-Dimethoxyphenyl)-6-(3-methoxyphenyl)pyrimidin-4-amine (485)

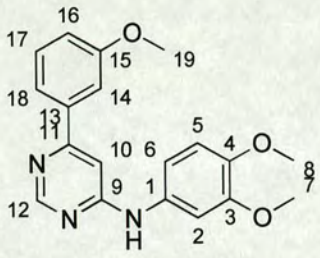

To a solution of **524** (0.23 mmole, 1.0 eq.) in a mixture of toluene/ethanol (1.0 mL, 4:1) was added 3-methoxyphenylboronic acid (0.048 g, 0.32 mmole, 1.4 eq.), $Pd(PPh_3)_4$ (0.010 g, 0.01 mmole, 0.04 eq.) and K_2CO_3 (0.122 g, 0.92 mmole, 4.0 eq.). The reaction mixture was irradiated in the Discover™ at 140 °C for 15 minutes, with active cooling of the sample. The reaction mixture was injected directly onto the Biotage Parallex Flex™ (Method S, t_R = 7.45 min.). Appropriate fractions were combined and concentrated *in vacuo* to afford pyrimidine **485** as a yellow oil (0.056 g, 72%); LRMS ES^+ *m/z* 337.8 $(MH)^+$; ν_{max} (film)/cm^{-1} 3235 (N-H), 2925 (C-H), 1645 (C=C), 1586 (aryl C=C), 1506 (C=N); δ_H (250 MHz; $CDCl_3$): 3.91 (s, 6H, *H*7, *H*8), 3.98 (s, 3H, *H*19), 7.08 (d, 1H, *J* = 8.6 Hz, *H*5), 7.15 (s, 1H, *H*10), 7.18 – 7.40 (m, 5H, Ar*H*), 7.60 (t, 1H, *J* = 8.4 Hz, *H*17), 8.81 (s, 1H, *H*12).

N-(3,4-Dimethoxyphenyl)-6-(4-methoxyphenyl)pyrimidin-4-amine (486)

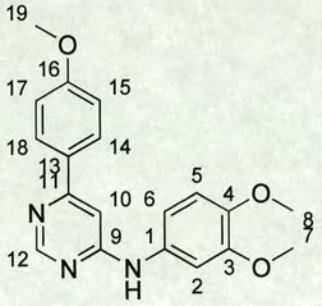

To a solution of **524** (0.23 mmole, 1.0 eq.) in a mixture of toluene/ethanol (1.0 mL, 4:1) was added 4-methoxyphenylboronic acid (0.048 g, 0.32 mmole, 1.4 eq.), $Pd(PPh_3)_4$ (0.010 g, 0.01 mmole, 0.04 eq.) and K_2CO_3 (0.122 g, 0.92 mmole, 4.0 eq.). The reaction mixture was irradiated in the Discover™ at 140 °C for 15 minutes, with active cooling of the sample. The reaction mixture was injected directly onto the Biotage Parallex Flex™ (Method S, t_R = 8.34 min.). Appropriate fractions were combined and concentrated *in vacuo* to afford pyrimidine **486** as a yellow solid (0.022 g, 29%); LRMS ES^+ *m/z* 337.8 $(MH)^+$; δ_H (250 MHz, CD_3OD): 3.77 (s, 6H, 2 x CH_3), 3.95 (s, 3H, CH_3), 7.07 (s, 1H, *H*2), 7.08 (d, 1H, *J* = 8.6 Hz, *H*6), 7.19 – 7.25 (m, 3H, *H*5, *H*15, *H*17), 7.32 (s, 1H, *H*10), 7.85 (d, 2H, *J* = 8.9 Hz, *H*14, *H*18), 8.76 (s, 1H, *H*12);

N,6-Bis-(3,4-dimethoxyphenyl) pyrimidin-4-amine (487)

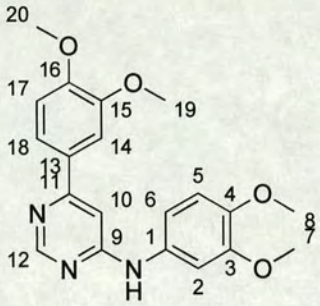

To a solution of **524** (0.23 mmole, 1.0 eq.) in a mixture of toluene/ethanol (1.0 mL, 4:1) was added 4-methoxyphenylboronic acid (0.048 g, 0.32 mmole, 1.4 eq.), $Pd(PPh_3)_4$ (0.010 g, 0.01 mmole, 0.04 eq.) and K_2CO_3 (0.122 g, 0.92 mmole, 4.0 eq.). The reaction mixture was irradiated in the Discover^{TM} at 140 °C for 15 minutes, with active cooling of the sample. The reaction mixture was injected directly onto the Biotage Parallex Flex^{TM} (Method S, t_R = 7.26 min.). Appropriate fractions were combined and concentrated *in vacuo* to afford pyrimidine **487** as a yellow solid (0.033 g, 41%); LRMS ES^+ *m/z* 367.6 $(MH)^+$; ν_{max} (film)/cm^{-1} 3392 (N-H), 2926 (C-H), 2840 (O-CH_3), 1637 (C=C), 1585 (aryl C=C), 1507 (C=N); δ_H (500 MHz; CD_3OD) 3.89 (s, 6H, 2 x C*H*$_3$), 6.94 (s, 6H, 2 x C*H*$_3$), 7.04 (s, 1H, *H*2), 7.07 (d, 1H, *J* = 8.0 Hz, *H*6), 7.16 – 7.20 (m, 2H, *H*5, *H*17), 7.32 (s, 1H, *H*10), 7.44 (s, 1H, *H*14), 7.48 (d, 1H, *J* = 8.4 Hz, *H*18), 8.72 (s, 1H, *H*12); Mpt. 203.2 – 204.2 °C.

N-(3-Fluorophenyl)-6-(3-methoxyphenyl)pyrimidin-4-amine (489)

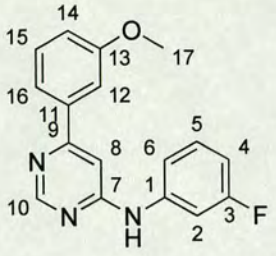

To a solution of **471** (0.029 g, 0.13 mmole, 1.0 eq.) in toluene/ethanol (1 mL, 4:1) was added 3-methoxyphenylboronic acid (0.028 g, 0.18 mmole, 1.4 eq.), K_2CO_3 (0.072 g, 0.32 mmole, 4.0 eq.) and $Pd(PPh_3)_4$ (0.06 g, 0.01 mmole, 0.04 eq.). The reaction mixture was irradiated in the Discover™ at 140 °C for 15 minutes, before being injected directly onto the Biotage Parallex Flex™ HPLC (Method S, t_R = 14.15 min). Appropriate fractions were combined and concentrated *in vacuo* to afford pyrimidine **489** as a white solid (0.011 g, 29%); LRMS ES^+ *m/z* 295.6 $(MH)^+$; δ_H (250 MHz; CD_3OD) 3.89 (s, 3H, *H*17, *H*18), 6.94 (m, 1H, Ar*H*), 7.19 (s, 1H, *H*8), 7.19 – 7.23 (m, 1H, Ar*H*), 7.39 – 7.45 (m, 4H, Ar*H*), 7.49 –7.52 (m, 1H, Ar*H*), 7.70 – 7.75 (m, 1H, Ar*H*), 8.90 (s, 1H, *H*10).

3-{[6-(2,5-Dimethylphenyl)pyrimidin-4-yl]amino}phenol (490)

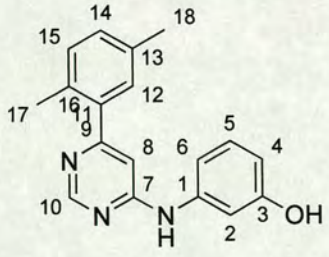

To a stirring solution of **522** (0.056 g, 0.25 mmole, 1.0 eq.) in 2-propanol (1.0 mL) was added 2,5-dimethylphenylboronic acid (0.053 g, 0.35 mmole, 1.4 eq.), $Pd(PPh_3)_4$ (0.013 g, 0.01 mmole, 0.04 eq.) and K_2CO_3 (0.140 g, 1.00 mmole, 4.0 eq.). The reaction mixture was irradiated in the Discover™ at 140 °C for 15 minutes, with active cooling of

the sample. The reaction mixture was injected directly onto the Biotage Parallex Flex™ (Method S, t_R = 11.28 min.). Appropriate fractions were combined and concentrated in vacuo to afford pyrimidine **490** as a yellow solid (0.051 g, 70%); LRMS ES^+ *m/z* 291.7 $(MH)^+$; ν_{max} (film)/cm^{-1} 3410 (O-H), 2926 (C-H), 1646 (C=C), 1586 (aryl C=C), 1504 (C=N); δ_H (250 MHz; CD_3OD) 2.42 (s, 3H, *H*17), 2.45 (s, 3H, *H*18), 6.78 (dd, 1H, *J* = 8.1, 1.5 Hz, *H*6), 6.95 (s, 1H, *H*8), 7.14 (d, 1H, *J* = 7.6 Hz, *H*4), 7.24 (m, 1H, *H*2), 7.31 (t, 1H, *J* = 8.1 Hz, *H*5), 7.33 (s, 1H, *H*12), 7.38 – 7.43 (m, 2H, *H*14, *H*15), 8.85 (s, 1H, *H*10); δ_C (75 MHz; CD_3OD) 18.2 (CH_3), 19.6 (CH_3), 110.0 (C_{Ar}), 113.5 (C_{Ar}), 120.1 (CH_{Ar}), 120.9 (C_{Ar}), 128.6 (C_{Ar}), 129.4 (CH_{Ar}), 130.0 (CH_{Ar}), 131.2 (C_{Ar}), 131.3 (CH_{Ar}), 132.1 (CH_{Ar}), 133.2 (CH_{Ar}), 134.7 (C_{Ar}), 136.7 (CH_{Ar}), 142.0 (C_{Ar}), 152.4 (CH_{Ar}), 158.4 (CH_{Ar}); Mpt. 174.1 – 175.2 °C.

3-[(6-Phenylpyrimidin-4-yl)amino]phenol (491)

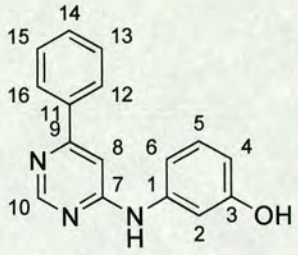

To a stirring solution of **522** (0.053 g, 0.24 mmole, 1.0 eq.) in 2-propanol (1.0 mL) was added phenylboronic acid (0.041 g, 0.34 mmole, 1.4 eq.), $Pd(PPh_3)_4$ (0.012 g, 0.01 mmole, 0.04 eq.) and K_2CO_3 (0.133 g, 0.96 mmole, 4.0 eq.). The reaction mixture was irradiated in the Discover™ at 140 °C for 15 minutes, with active cooling of the sample. The reaction mixture was injected directly onto the Biotage Parallex Flex™ (Method S, t_R = 8.44 min.). Appropriate fractions were combined and concentrated *in vacuo* to afford pyrimidine **491** as a yellow solid (0.042 g, 67%); LRMS ES^+ *m/z* 263.7 $(MH)^+$; HRMS FAB^+ *m/z* 264.11452 $(MH)^+$ (calculated for $C_{16}H_{14}N_3O$, 264.11369 (Dev. 3.14 ppm)); ν_{max} (film)/cm^{-1} 3420 (O-H), 1646 (C=C), 1586 (aryl C=C), 1506 (C=N); δ_H (250 MHz; CD_3OD) 6.74 (dd, 1H, *J* = 6.5, 1.6 Hz, *H*6), 7.09 (d, 1H, *J* = 8.0 Hz, *H*4), 7.17 (s,

1H, *H*8), 7.19 – 7.20 (m, 1H, *H*2), 7.26 (t, 1H, *J* = 8.0 Hz, *H*5), 7.64 – 7.71 (m, 3H, *H*13, *H*14, *H*15), 7.85 (dd, 2H, *J* = 6.4, 1.9 Hz, *H*12, *H*16), 8.79 (s, 1H, *H*10); Mpt. 188.4 – 190.0 °C.

3-{6-[(4-Hydroxyphenyl)amino]pyrimidin-4-yl}phenol (492)

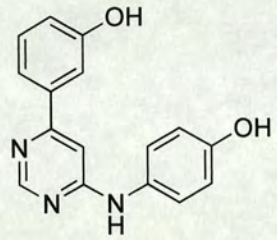

To a stirring solution of **523** (0.050 g, 0.23 mmole, 1.0 eq.) in 2-propanol (1.0 mL) was added 3-hydroxyphenylboronic acid (0.043 g, 0.32 mmole, 1.4 eq.), $Pd(PPh_3)_4$ (0.011 g, 0.01 mmole, 0.04 eq.) and K_2CO_3 (0.125 g, 0.92 mmole, 4.0 eq.). The reaction mixture was irradiated in the Discover™ at 140 °C for 15 minutes, with active cooling of the sample. The reaction mixture was injected directly onto the Biotage Parallex Flex™ (Method S, t_R = 7.55 min.). Appropriate fractions were combined and concentrated *in vacuo* to afford **492** as a white solid (0.001 g, 2%); LRMS ES^+ *m/z* 279.6 $(MH)^+$.

4-{[6-(2,5-Dimethylphenyl)pyrimidin-4-yl]amino}phenol (493)

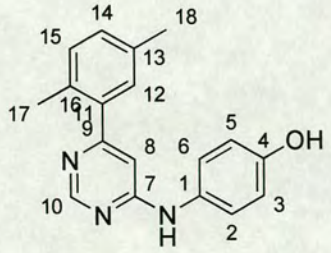

To a stirring solution of **523** (0.050 g, 0.23 mmole, 1.0 eq.) in 2-propanol (1.0 mL) was added 2,5-dimethylphenylboronic acid (0.050 g, 0.32 mmole, 1.4 eq.), $Pd(PPh_3)_4$ (0.011

g, 0.01 mmole, 0.04 eq.) and K_2CO_3 (0.125 g, 0.92 mmole, 4.0 eq.). The reaction mixture was irradiated in the Discover™ at 140 °C for 15 minutes, with active cooling of the sample. The reaction mixture was injected directly onto the Biotage Parallex Flex™ (Method S, t_R = 10.42 min.). Appropriate fractions were combined and concentrated *in vacuo* to afford pyrimidine **493** as a yellow solid (0.016 g, 24%); LRMS ES^+ *m/z* 291.7 $(MH)^+$; δ_H (250 MHz; CD_3OD) 2.35 (s, 6H, *H*17, *H*18), 6.82 – 6.84 (m, 3H, *H*8, *H*14, *H*15), 7.25 – 7.30 (m, 4H, *H*2, *H*3, *H*5, *H*6), 7.48 – 7.51 (m, 1H, *H*12), 8.69 (s, 1H, *H*10).

6-(4-Methoxyphenyl)-*N*-phenylpyrimidin-4-amine (496)

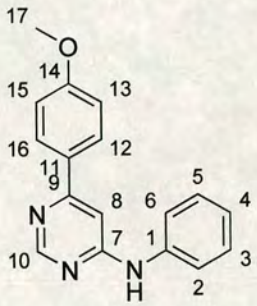

To a stirring solution of **526** (0.045 g, 0.22 mmole, 1.0 eq.) in 2-propanol (1.0 mL) was added 4-methoxyphenylboronic acid (0.047 g, 0.31 mmole, 1.4 eq.), $Pd(PPh_3)_4$ (0.010 g, 0.01 mmole, 0.04 eq.) and K_2CO_3 (0.121 g, 0.88 mmole, 4.0 eq.). The reaction mixture was irradiated in the Discover™ at 140 °C for 15 minutes, with active cooling of the sample. The reaction mixture was injected directly onto the Biotage Parallex Flex™ (Method S, t_R = 12.04 min.). Appropriate fractions were combined and concentrated *in vacuo* to afford pyrimidine **496** as a white solid (0.038 g, 62%); LRMS ES^+ *m/z* 277.6 $(MH)^+$; HRMS FAB^+ *m/z* 278.12920 $(MH)^+$ (calculated for $C_{17}H_{16}N_3O$, 278.12934 (Dev. - 0.50 ppm)); ν_{max} (film)/cm^{-1} 3420 (N-H), 2929 (C-H), 2840 (O-CH_3), 1645 (C=C), 1578 (aryl C=C), 1506 (C=N); δ_H (250 MHz; CD_3OD): 3.67 (s, 3H, *H*17), 7.15 (s, 1H, H8), 7.22 (d, 2H, *J* = 8.9 Hz, H13, H15), 7.35 (t, 1H, *J* = 7.5 Hz, H4), 7.52 (t,

2H, J = 7.5 Hz, H3, H5), 7.70 (d, 2H, J = 7.5 Hz, H2, H6), 7.87 (d, 2H, J = 8.9 Hz, H12, H16), 8.80 (s, 1H, *H*10); Mpt. 182.8 – 183.3 °C.

_N_-(3,4-Dimethoxyphenyl)-6-(2,5-dimethylphenyl)pyrimidin-4-amine (497)

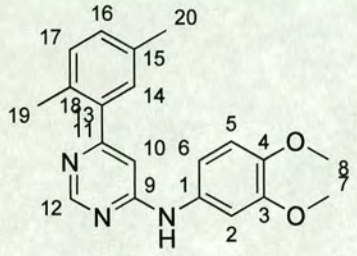

To a stirring solution of **524** (0.083 g, 0.31 mmole, 1.0 eq.) in 2-propanol (1.0 mL) was added 2,5-dimethylphenylboronic acid (0.066 g, 0.44 mmole, 1.4 eq.), $Pd(PPh_3)_4$ (0.015 g, 0.01 mmole, 0.04 eq.) and K_2CO_3 (0.173 g, 1.25 mmole, 4.0 eq.). The reaction mixture was irradiated in the Discover™ at 140 °C for 15 minutes, with active cooling of the sample. The reaction mixture was injected directly onto the Biotage Parallex Flex™ (Method S, t_R = 11.26 min.). Appropriate fractions were combined and concentrated *in vacuo* to afford pyrimidine **497** as a yellow oil (0.039 g, 37%); LRMS ES^+ *m/z* 335.8 $(MH)^+$; δ_H (250 MHz; CD_3OD): 2.40 (s, 3H, *H*20), 2.43 (s, 3H, *H*19), 3.91 (s, 6H, *H*7, *H*8), 6.91 (s, 1H, *H*10), 7.08 (d, 1H, J = 8.1 Hz, *H*6), 7.33 – 7.38 (m, 4H, *H*2, *H*6, *H*16, *H*17), 7.49 (s, 1H, *H*14), 8.95 (s, 1H, *H*12).

3-{6-[(3,4-Dimethoxyphenyl)amino]pyrimidin-4-yl}phenol (498)

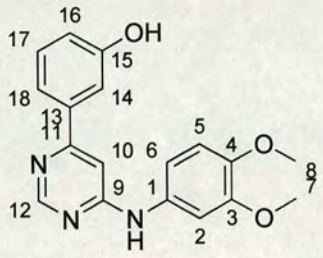

To a stirring solution of **524** (0.072 g, 0.27 mmole, 1.0 eq.) in 2-propanol (1.0 mL) was added 3-hydroxyphenylboronic acid (0.052 g, 0.38 mmole, 1.4 eq.), $Pd(PPh_3)_4$ (0.013 g, 0.01 mmole, 0.04 eq.) and K_2CO_3 (0.150 g, 1.25 mmole, 4.0 eq.). The reaction mixture was irradiated in the Discover™ at 140 °C for 15 minutes, with active cooling of the sample. The reaction mixture was injected directly onto the Biotage Parallex Flex™ (Method S, t_R = 8.03 min.). Appropriate fractions were combined and concentrated *in vacuo* to afford pyrimidine **498** as a yellow solid (0.052 g, 59%); LRMS ES^+ *m/z* 323.7 $(MH)^+$; ν_{max} (film)/cm^{-1} 3310 (O-H), 3118 (N-H), 3054 (aryl C-H), 2928 (C-H), 2840 ($O\text{-}CH_3$), 1646 (C=C), 1578 (aryl C=C), 1506 (C=N); δ_H (250 MHz; CD_3OD) 3.91 (s, 6H, *H*8, *H*9), 7.05 – 7.15 (m, 4H, Ar*H*), 7.25 – 7.32 (m, 3H, Ar*H*), 7.49 (t, 1H, *J* = 8.0 z, H17), 8.79 (s, 1H, *H*12); δ_C (63 MHz, $(CD_3)_2SO$): 55.5 (2 x CH_3), 111.1 (C_{Ar}), 112.0 (C_{Ar}), 112.1 (2 x C_{Ar}), 113.7 (CH_{Ar}), 117.9 (2 x CH_{Ar}), 119.6 (CH_{Ar}), 130.9 (2 x CH_{Ar}), 131.7 (CH_{Ar}), 152.0 (C_{Ar}), 152.9 (C_{Ar}), 158.8 (C_{Ar}); Mpt. 198.5 – 199.5 °C.

N-(4-Fluoro-3-methylphenyl)-6-(3-methoxyphenyl)pyrimidin-4-amine (499)

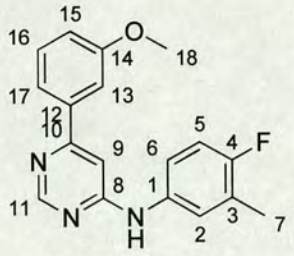

To a solution of 4,6-dichloropyrimidine (0.147 g, 1.0 mmole, 1.1 eq.) in 2-propanol (4 mL), 4-fluoro-3-methylaniline (0.113 g, 0.9 mmole, 1.0 eq.) and *N,N*-diisopropylethylamine (172 μL, 1.8 mmole, 2.0 eq.) were added. The reaction mixture was irradiated in the Discover™ at 120 °C for 30 minutes, with active cooling of the sample, and then split into 4 x 1 mL aliquots. To one aliquot was added 3-methoxyphenylboronic acid (0.048 g, 0.32 mmole, 1.4 eq.), potassium carbonate (0.122g, 0.9 mmole, 4.0 eq.) and $Pd(PPh_3)_4$ (0.10 g, 0.02 mmole, 0.1 eq.). The reaction mixture was irradiated in the Discover™ at 140 °C for 15 minutes, before being injected directly onto the Biotage Parallex Flex™ HPLC (Method S, t_R = 14.34 min) Appropriate fractions were combined and concentrated *in vacuo* to afford pyrimidine **499** as a yellow solid (0.040g, 57%); LRMS ES^+ *m/z* 309.7 $(MH)^+$; HRMS FAB^+ *m/z* 310.13642 $(MH)^+$ (calculated for $C_{18}H_{17}FN_3O$, 310.13556 (Dev. 2.77 ppm)); ν_{max} (film)/cm^{-1} 3299 (N-H), 2931 (C-H), 2841 (O-CH_3), 1646 (C=C), 1586 (aryl C=C), 1506 (C=N); δ_H (250 MHz, CD_3OD): 2.37 (d, 3H, J_{HF} = 2.0 Hz, *H*7), 3.94 (s, 3H, *H*18), 7.17 (s, 1H, *H*9), 7.18 (t, 1H, *J* = 9.1 Hz, J_{HF} = 9.1 Hz, *H*5), 7.30 (ddd, 1H, *J* = 8.2, 2.5, 0.8 Hz, *H*15), 7.42 (d, 1H, *J* = 1.7 Hz, *H*17), 7.44 (dd, 1H, *J* = 2.5, 0.8 Hz, *H*13), 7.51 – 7.63 (m, 3H, *H*2, *H*6, *H*15), 8.82 (s, 1H, *H*11); Mpt. 145.6 – 145.8 °C.

2-Methoxy-5-{[6-(3-methoxyphenyl)-pyrimidin-4-yl]amino}phenol (502)

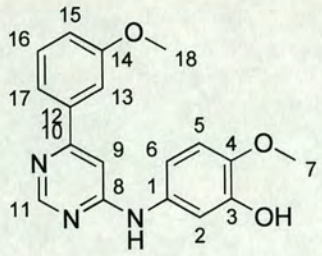

To a solution of 4,6-dichloropyrimidine (0.147 g, 1.0 mmole, 1.1 eq.) in 2-propanol (4 mL), 3-hydroxy-4-methoxyaniline (0.125 g, 0.9 mmole, 1.0 eq.) and *N*,*N*-diisopropylethylamine (172 μL, 1.8 mmole, 2.0 eq.) were added. The reaction mixture was irradiated in the Discover™ at 120 °C for 30 minutes, with active cooling of the sample, and then split into 4 x 1 mL aliquots. To one aliquot was added 3-methoxyphenylboronic acid (0.048 g, 0.32 mmole, 1.4 eq.), potassium carbonate (0.122g, 0.9 mmole, 4.0 eq.) and $Pd(PPh_3)_4$ (0.10 g, 0.02 mmole, 0.1 eq.). The reaction mixture was irradiated in the Discover™ at 140 °C for 15 minutes, before being injected directly onto the Biotage Parallex Flex™ HPLC (Method S, t_R = 7.32 min) Appropriate fractions were combined and concentrated *in vacuo* to afford pyrimidine **502** as a yellow solid (0.049 g, 67%); LRMS ES^+ *m/z* 323.6 $(MH)^+$; ν_{max} (film)/cm^{-1} 3392 (O-H), 2938 (C-H), 2835 (O-CH_3), 1646 (C=C), 1582 (aryl C=C), 1510 (C=N); δ_H (250 MHz, CD_3OD): 3.92 (s, 3H, *H*7), 3.94 (s, 3H, *H*18), 7.05 – 7.19 (m, 4H, *H*2, *H*5, *H*6, *H*9), 7.28 (ddd, 1H, *J* = 8.1, 2.4, 0.7 Hz, *H*15), 7.39 (d, 1H, *J* = 0.7 Hz, *H*13), 7.40 (dd, 1H, *J* = 8.1, 0.7 Hz, *H*17), 7.62 (t, 1H, *J* = 8.1 Hz, *H*16), 8.77 (d, 1H, *J* = 0.4 Hz, *H*11); Mpt. 184.7 – 185.4 °C.

N-(3,5-Dimethoxyphenyl)-6-(3-methoxyphenyl)pyrimidin-4-amine (503)

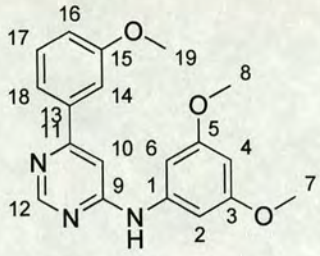

To a solution of 4,6-dichloropyrimidine (0.147 g, 1.0 mmole, 1.1 eq.) in 2-propanol (4 mL), 3,5-dimethoxyaniline (0.137 g, 0.9 mmole, 1.0 eq.) and *N*,*N*-diisopropylethylamine (172 μL, 1.8 mmole, 2.0 eq.) were added. The reaction mixture was irradiated in the Discover™ at 120 °C for 30 minutes, with active cooling of the sample, and then split into 4 x 1 mL aliquots. To one aliquot was added 3-methoxyphenylboronic acid (0.048 g, 0.32 mmole, 1.4 eq.), potassium carbonate (0.122g, 0.9 mmole, 4.0 eq.) and $Pd(PPh_3)_4$ (0.10 g, 0.02 mmole, 0.1 eq.). The reaction mixture was irradiated in the Discover™ at 140 °C for 15 minutes, before being injected directly onto the Biotage Parallex Flex™ HPLC (Method S, t_R = 14.15 min) Appropriate fractions were combined and concentrated *in vacuo* to afford pyrimidine **503** as a yellow solid (0.018 g, 24%); LRMS ES^+ *m/z* 337.7 $(MH)^+$; HRMS FAB^+ *m/z* 338.15089 $(MH)^+$ (calculated for $C_{19}H_{20}N_3O_3$, 338.15047 (Dev. 1.24 ppm)); ν_{max} (film)/cm^{-1} 3391 (N-H), 3051 (aryl C-H), 2942 (C-H), 2840 (O-CH_3), 1646 (C=C), 1592 (aryl C=C), 1519 (C=N); δ_H (250 MHz, CD_3OD): 3.85 (s, 6H, *H*7, *H*8), 3.94 (s, 3H, *H*19), 6.46 (t, 1H, *J* = 2.2 Hz, *H*4), 6.93 (d, 2H, *J* = 2.2 Hz, *H*2, *H*6), 7.20 (d, 1H, *J* = 0.8 Hz, *H*10), 7.29 (ddd, 1H, *J* = 8.2, 2.5, 0.9 Hz, *H*16), 7.43 (d, 1H, *J* = 2.5 Hz, *H*14), 7.44 (dd, *J* = 8.2, 0.9 Hz, *H*18), 7.58 (t, 1H, *J* = 8.2 Hz, *H*17), 8.84 (d, 1H, *J* = 0.8 Hz, *H*12); Mpt. 143.2 – 143.8 °C.

N-(4-Fluoro-3-methylphenyl)-6-(4-methoxyphenyl)pyrimidin-4-amine (504)

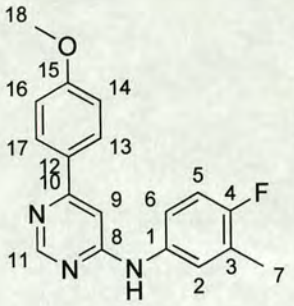

To a solution of 4,6-dichloropyrimidine (0.147 g, 1.0 mmole, 1.1 eq.) in 2-propanol (4 mL), 4-fluoro-3-methylaniline (0.113 g, 0.9 mmole, 1.0 eq.) and *N,N*-diisopropylethylamine (172 μL, 1.8 mmole, 2.0 eq.) were added. The reaction mixture was irradiated in the Discover™ at 120 °C for 30 minutes, with active cooling of the sample, and then split into 4 x 1 mL aliquots. To one aliquot was added 4-methoxyphenylboronic acid (0.048 g, 0.32 mmole, 1.4 eq.), potassium carbonate (0.122g, 0.9 mmole, 4.0 eq.) and $Pd(PPh_3)_4$ (0.10 g, 0.02 mmole, 0.1 eq.). The reaction mixture was irradiated in the Discover™ at 140 °C for 15 minutes, before being injected directly onto the Biotage Parallex Flex™ HPLC (Method S, t_R = 13.58 min) Appropriate fractions were combined and concentrated *in vacuo* to afford pyrimidine **504** as a yellow solid (0.046 g, 66%); LRMS ES^+ *m/z* 309.7 $(MH)^+$; HRMS FAB^+ *m/z* 310.13589 $(MH)^+$ (calculated for $C_{18}H_{17}FN_3O$, 310.13556 (Dev. 1.09 ppm)); ν_{max} (film)/cm^{-1} 3306 (N-H), 3053 (aryl C-H), 2936 (C-H), 2842 (O-CH_3), 1646 (C=C), 1592 (aryl C=C), 1516 (C=N); δ_H (250 MHz, CD_3OD): 2.35 (d, 3H, J_{HF} = 2.0 Hz, *H*7), 3.95 (s, 3H, *H*18), 7.09 (d, 1H, *J* = 0.7 Hz, *H*9), 7.17 (t, 1H, *J* = 8.9 Hz, J_{HF} = 8.9 Hz, *H*5), 7.21 (d, 2H, *J* = 8.9 Hz, *H*14, *H*16), 7.48 – 7.56 (m, 2H, *H*2, *H*6), 7.86 (d, 2H, *J* = 8.9 Hz, *H*13, *H*17), 8.77 (d, 1H, *J* = 0.7 Hz, *H*11); δ_C (75 MHz; CD_3OD) 13.5 (*C*7), 55.1 (*C*18), 102.3 (C_{Ar}), 111.2 (C_{Ar}), 115.1 (2 x CH_{Ar}), 115.2 (2 x CH_{Ar}), 122.5 (CH_{Ar}), 128.9 (2 x CH_{Ar}), 132.9 (C_{Ar}), 133.0 (C_{Ar}), 140.1 (C_{Ar}), 152.7 (CH_{Ar}), 154.7 (C_{Ar}), 162.1 (C_{Ar}), 163.7 (CH_{Ar}); Mpt. 179.9 – 180.7 °C.

4-{[6-(4-Methoxyphenyl)pyrimidin-4-yl]amino}-3-nitrophenol (505)

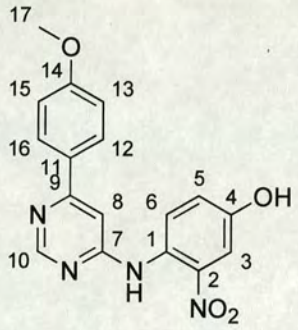

To a solution of 4,6-dichloropyrimidine (0.147 g, 1.0 mmole, 1.1 eq.) in 2-propanol (4 mL), 4-hydroxy-2-nitroaniline (0.138 g, 0.9 mmole, 1.0 eq.) and *N*,*N*-diisopropylethylamine (172 μL, 1.8 mmole, 2.0 eq.) were added. The reaction mixture was irradiated in the Discover™ at 120 °C for 30 minutes, with active cooling of the sample, and then split into 4 x 1 mL aliquots. To one aliquot was added 4-methoxyphenylboronic acid (0.048 g, 0.32 mmole, 1.4 eq.), potassium carbonate (0.122g, 0.9 mmole, 4.0 eq.) and $Pd(PPh_3)_4$ (0.10 g, 0.02 mmole, 0.1 eq.). The reaction mixture was irradiated in the Discover™ at 140 °C for 15 minutes, before being injected directly onto the Biotage Parallex Flex™ HPLC (Method S, t_R = 8.44 min) Appropriate fractions were combined and concentrated *in vacuo* to afford pyrimidine **505** as a red oil (0.023 g, 30%); LRMS ES^+ *m/z* 338.7 $(MH)^+$.

2-Methoxy-5-{[6-(4-methoxyphenyl)pyrimidin-4-yl]amino}phenol (507)

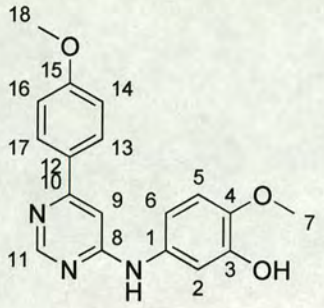

To a solution of 4,6-dichloropyrimidine (0.147 g, 1.0 mmole, 1.1 eq.) in 2-propanol (4 mL), 3-hydroxy-4-methoxyaniline (0.125 g, 0.9 mmole, 1.0 eq.) and *N,N*-diisopropylethylamine (172 μL, 1.8 mmole, 2.0 eq.) were added. The reaction mixture was irradiated in the Discover™ at 120 °C for 30 minutes, with active cooling of the sample, and then split into 4 x 1 mL aliquots. To one aliquot was added 4-methoxyphenylboronic acid (0.048 g, 0.32 mmole, 1.4 eq.), potassium carbonate (0.122g, 0.9 mmole, 4.0 eq.) and $Pd(PPh_3)_4$ (0.10 g, 0.02 mmole, 0.1 eq.). The reaction mixture was irradiated in the Discover™ at 140 °C for 15 minutes, before being injected directly onto the Biotage Parallex Flex™ HPLC (Method S, t_R = 7.26 min) Appropriate fractions were combined and concentrated *in vacuo* to afford pyrimidine **507** as a yellow solid (0.027 g, 37%); LRMS *m/z* 324.1 $(MH)^+$; ν_{max} (film)/cm^{-1} 3400 (O-H), 2929 (C-H), 2842 (O-CH_3), 1636 (C=C), 1576 (aryl C=C), 1507 (C=N); δ_H (250, MHz, CD_3OD): 3.92 (s, 3H, *H*7), 3.93 (s, 3H, *H*18), 7.03 (m, 3H, *H*2, *H*5, *H*6), 7.14 (s, 1H, *H*9), 7.18 (d, 2H, *J* = 8.8 Hz, *H*14, *H*16), 7.82 (d, 2H, *J* = 8.8 Hz, *H*13, *H*17), 8.69 (s, 1H, *H*11); Mpt. 226.5 – 227.0 °C.

N-(3,5-Dimethoxyphenyl)-6-(4-methoxyphenyl)pyrimidin-4-amine (508)

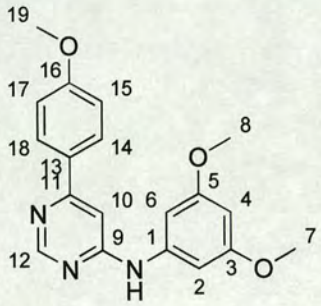

To a solution of 4,6-dichloropyrimidine (0.147 g, 1.0 mmole, 1.1 eq.) in 2-propanol (4 mL), 3,5-dimethoxyaniline (0.137 g, 0.9 mmole, 1.0 eq.) and *N*,*N*-diisopropylethylamine (172 μL, 1.8 mmole, 2.0 eq.) were added. The reaction mixture was irradiated in the Discover™ at 120 °C for 30 minutes, with active cooling of the sample, and then split into 4 x 1 mL aliquots. To one aliquot was added 4-methoxyphenylboronic acid (0.048 g, 0.32 mmole, 1.4 eq.), potassium carbonate (0.122g, 0.9 mmole, 4.0 eq.) and $Pd(PPh_3)_4$ (0.10 g, 0.02 mmole, 0.1 eq.). The reaction mixture was irradiated in the Discover™ at 140 °C for 15 minutes, before being injected directly onto the Biotage Parallex Flex™ HPLC (Method S, t_R = 11.33 min) Appropriate fractions were combined and concentrated *in vacuo* to afford pyrimidine **508** as a cream solid (0.011 g, 14%); LRMS ES^+ *m/z* 337.8 $(MH)^+$; ν_{max} (film)/cm^{-1} 3248 (N-H), 3058 (aryl C-H), 2933 (C-H), 1654 (C=C), 1595 (aryl C=C), 1508 (C=N); δ_H (250 MHz, CD_3OD): 4.04 (s, 6H, *H*7, *H*8), 4.14 (s, 3H, *H*19), 6.65 (t, 1H, *J* = 2.2 Hz, *H*4), 7.10 (d, 2H, *J* = 2.2 Hz, *H*2, *H*6), 7.34 (d, 1H, *J* = 0.9 Hz, *H*10), 7.40 (d, 2H, *J* =9.0 Hz, *H*15, *H*17), 8.98 (d, 1H, *J* = 0.9 Hz, *H*12); Mpt. 196.7 – 197.2 °C.

6-(2,5-Dimethylphenyl)-*N*-(4-fluoro-3-methylphenyl)pyrimidin-4-amine (509)

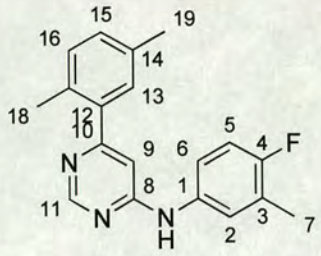

To a solution of 4,6-dichloropyrimidine (0.147 g, 1.0 mmole, 1.1 eq.) in 2-propanol (4 mL), 4-fluoro-3-methylaniline (0.113 g, 0.9 mmole, 1.0 eq.) and *N*,*N*-diisopropylethylamine (172 μL, 1.8 mmole, 2.0 eq.) were added. The reaction mixture was irradiated in the Discover™ at 120 °C for 30 minutes, with active cooling of the sample, and then split into 4 x 1 mL aliquots. To one aliquot was added 2,5-dimethylphenylboronic acid (0.047 g, 0.32 mmole, 1.4 eq.), potassium carbonate (0.122g, 0.9 mmole, 4.0 eq.) and $Pd(PPh_3)_4$ (0.10 g, 0.02 mmole, 0.1 eq.). The reaction mixture was irradiated in the Discover™ at 140 °C for 15 minutes, before being injected directly onto the Biotage Parallex Flex™ HPLC (Method S, t_R = 13.07 min) Appropriate fractions were combined and concentrated *in vacuo* to afford pyrimidine **509** as a white solid (0.037 g, 54%); LRMS ES^+ *m/z* 307.4 $(MH)^+$; HRMS FAB^+ *m/z* 308.15689 $(MH)^+$ (calculated for $C_{19}H_{19}FN_3$, 308.15630 (Dev. 1.91 ppm)); ν_{max} (film)/cm^{-1} 3244 (N-H), 3054 (aryl C-H), 2929 (C-H), 2863 (O-CH_3), 1640 (C=C), 1590 (aryl C=C), 1504 (C=N); δ_H (250 MHz, CD_3OD): 2.36 (d, 3H, J_{HF} = 2.0 Hz, *H*7), 2.40 (s, 3H, *H*19), 2.43 (s, 3H, *H*18), 6.91 (s, 1H, *H*9), 7.18 (t, 1H, *J* = 9.0 Hz, J_{HF} = 9.0 Hz, *H*5), 7.32 (s, 1H, *H*13), 7.36 (d, 1H, *J* = 8.4 Hz, *H*15), 7.40 (d, 1H, *J* = 8.4 Hz, *H*16), 7.43 – 7.59 (m, 2H, *H*2, *H*6), 8.83 (s, 1H, *H*11); Mpt. 115.0 – 115.4 °C.

5-{[6-(2,5-Dimethylphenyl)pyrimidin-4-yl]amino}-2-methoxyphenol (512)

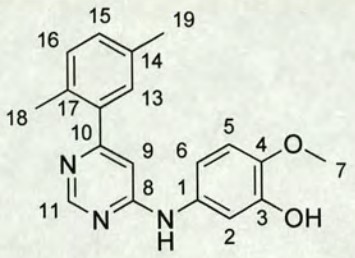

To a solution of 4,6-dichloropyrimidine (0.147 g, 1.0 mmole, 1.1 eq.) in 2-propanol (4 mL), 3-hydroxy-4-methoxyaniline (0.125 g, 0.9 mmole, 1.0 eq.) and *N*,*N*-diisopropylethylamine (172 μL, 1.8 mmole, 2.0 eq.) were added. The reaction mixture was irradiated in the Discover™ at 120 °C for 30 minutes, with active cooling of the sample, and then split into 4 x 1 mL aliquots. To one aliquot was added 2,5-dimethylphenylboronic acid (0.047 g, 0.32 mmole, 1.4 eq.), potassium carbonate (0.122g, 0.9 mmole, 4.0 eq.) and $Pd(PPh_3)_4$ (0.10 g, 0.02 mmole, 0.1 eq.). The reaction mixture was irradiated in the Discover™ at 140 °C for 15 minutes, before being injected directly onto the Biotage Parallex Flex™ HPLC (Method S, t_R = 7.10 min) Appropriate fractions were combined and concentrated *in vacuo* to afford pyrimidine **512** as a yellow solid (0.015 g, 21%); LRMS ES^+ *m/z* 321.7 $(MH)^+$; δ_H (250 MHz, CD_3OD): 2.39 (s, 3H, *H*18), 2.43 (s, 3H, *H*19), 3.93 (s, 3H, *H*7), 6.86 (s, 1H, *H*9), 7.02 – 7.11 (m, 3H, *H*2, *H*5, *H*6), 7.31 (s, 1H, *H*13), 7.35 (d, 2H, *J* = 8.7 Hz, *H*15), 7.39 (d, 2H, *J* = 8.7 Hz, *H*16), 8.79 (s, 1H, *H*11).

N-(3,5-Dimethoxyphenyl)-6-(2,5-dimethylphenyl)pyrimidin-4-amine (513)

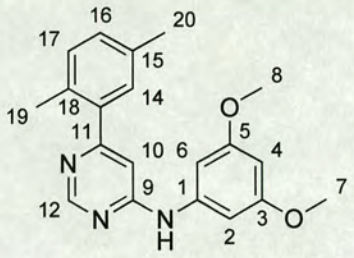

To a solution of 4,6-dichloropyrimidine (0.147 g, 1.0 mmole, 1.1 eq.) in 2-propanol (4 mL), 3,5-dimethoxyaniline (0.137 g, 0.9 mmole, 1.0 eq.) and *N*,*N*-diisopropylethylamine (172 μL, 1.8 mmole, 2.0 eq.) were added. The reaction mixture was irradiated in the Discover™ at 120 °C for 30 minutes, with active cooling of the sample, and then split into 4 x 1 mL aliquots. To one aliquot was added 2,5-dimethylphenylboronic acid (0.047 g, 0.32 mmole, 1.4 eq.), potassium carbonate (0.122 g, 0.9 mmole, 4.0 eq.) and $Pd(PPh_3)_4$ (0.10 g, 0.02 mmole, 0.1 eq.). The reaction mixture was irradiated in the Discover™ at 140 °C for 15 minutes, before being injected directly onto the Biotage Parallex Flex™ HPLC (Method S, t_R = 12.58 min) Appropriate fractions were combined and concentrated *in vacuo* to afford pyrimidine **513** as a white solid (0.015 g, 20%); LRMS ES^+ *m/z* 335.8 $(MH)^+$; δ_H (250 MHz, CD_3OD): 2.40 (s, 3H, *H*19), 2.43 (s, 3H, *H*20), 3.86 (s, 6H, *H*7, *H*8), 6.48 (t, 1H, *J* = 2.2 Hz, *H*4), 6.93 (d, 2H, *J* = 2.2 Hz, *H*2, *H*6), 6.95 (s, 1H, *J* = 0.9 Hz, *H*10), 7.32 (s, 1H, *H*14), 7.35 (d, 1H, *J* = 8.5 Hz, *H*16), 7.39 (d, 1H, *J* = 8.5 Hz, *H*15), 8.86 (d, 1H, *J* = 0.9 Hz, *H*12).

3-{6-[(4-Fluoro-3-methylphenyl)amino]pyrimidin-4-yl}phenol (514)

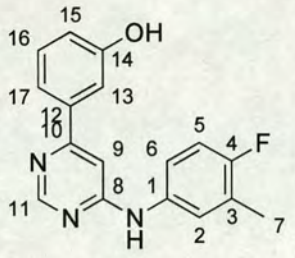

To a solution of 4,6-dichloropyrimidine (0.147 g, 1.0 mmole, 1.1 eq.) in 2-propanol (4 mL), 4-fluoro-3-methylaniline (0.113 g, 0.9 mmole, 1.0 eq.) and *N*,*N*-diisopropylethylamine (172 μL, 1.8 mmole, 2.0 eq.) were added. The reaction mixture was irradiated in the Discover™ at 120 °C for 30 minutes, with active cooling of the sample, and then split into 4 x 1 mL aliquots. To one aliquot was added 3-hydroxyphenylboronic acid (0.044 g, 0.32 mmole, 1.4 eq.), potassium carbonate (0.122 g, 0.9 mmole, 4.0 eq.) and $Pd(PPh_3)_4$ (0.10 g, 0.02 mmole, 0.1 eq.). The reaction mixture was irradiated in the Discover™ at 140 °C for 15 minutes, before being injected directly onto the Biotage Parallex Flex™ HPLC (Method S, t_R = 10.43 min) Appropriate fractions were combined and concentrated *in vacuo* to afford pyrimidine **514** as a yellow solid (0.030 g, 45%); LRMS ES^+ *m/z* 295.7 $(MH)^+$; HRMS FAB^+ *m/z* 296.12073 $(MH)^+$ (calculated for $C_{17}H_{15}FN_3O$, 296.11991 (Dev. 2.77 ppm)); ν_{max} (film)/cm^{-1} 3309 (N-H), 3157 (O-H), 3058 (aryl C-H), 2928 (C-H), 2840 (O-CH_3), 1647 (C=C), 1636 (aryl C=C), 1507 (C=N); δ_H (250 MHz, CD_3OD): 2.35 (d, 3H, *J* = 2.0 Hz, *H*7), 7.11 (d, 1H, *J* = 0.7 Hz, *H*9), 7.11 – 7.14 (m, 1H, *H*15), 7.16 (t, 1H, *J* = 9.1 Hz, J_{HF} = 9.1 Hz, *H*5), 7.27 (t, 1H, *J* = 1.9 Hz, *H*13), 7.29 – 7.34 (m, 1H, *H*17), 7.48 (t, 1H, *J* = 7.9 Hz, *H*16), 7.49 – 7.59 (m, 2H, *H*2, *H*6), 8.78 (d, 1H, *J* = 0.7 Hz, *H*11); δ_C (75 MHz; CD_3OD) 13.7 (*C*7), 103.2 (C_{Ar}), 112.5 (C_{Ar}), 113.7 (CH_{Ar}), 117.9 (CH_{Ar}), 119.4 (CH_{Ar}), 122.2 (C_{Ar}), 124.6 (CH_{Ar}), 126.7 (CH_{Ar}), 128.9 (CH_{Ar}), 130.8 (CH_{Ar}), 130.9 (C_{Ar}), 132.3 (C_{Ar}), 151.2 (C_{Ar}), 153.1 (CH_{Ar}), 155.1 (C_{Ar}), 158.7 (C_{Ar}); Mpt. 237.9 – 238.4 °C.

3-{[6-(3-Hydroxyphenyl)pyrimidin-4-yl]amino}benzonitrile (516)

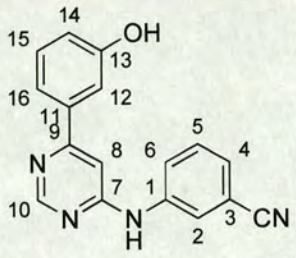

To a solution of 4,6-dichloropyrimidine (0.147 g, 1.0 mmole, 1.1 eq.) in 2-propanol (4 mL), 3-aminobenzonitrile (0.106 g, 0.9 mmole, 1.0 eq.) and *N*,*N*-diisopropylethylamine (172 μL, 1.8 mmole, 2.0 eq.) were added. The reaction mixture was irradiated in the Discover™ at 120 °C for 30 minutes, with active cooling of the sample, and then split into 4 x 1 mL aliquots. To one aliquot was added 3-hydroxyphenylboronic acid (0.044 g, 0.32 mmole, 1.4 eq.), potassium carbonate (0.122 g, 0.9 mmole, 4.0 eq.) and $Pd(PPh_3)_4$ (0.10 g, 0.02 mmole, 0.1 eq.). The reaction mixture was irradiated in the Discover™ at 140 °C for 15 minutes, before being injected directly onto the Biotage Parallex Flex™ HPLC (Method S, t_R = 10.36 min) Appropriate fractions were combined and concentrated *in vacuo* to afford pyrimidine **516** a white solid (0.002 g, 3%); LRMS ES^+ *m/z* 288.7 $(MH)^+$; δ_H (250 MHz, CD_3OD): 7.30 – 7.34 (ddd, 1H, *J* = 8.0, 2.4, 1.3 Hz, *H*14), 7.45 (d, *J* = 1.0 Hz, *H*8), 7.55 (t, 1H, *J* = 1.9 Hz, *H*2), 7.58 (dd, 1H, *J* = 8.0, 1.3 Hz, *H*16), 7.69 (t, 1H, *J* = 8.0 Hz, *H*15), 7.81 (dt, 1H, *J* = 1.9 Hz, *H*6), 7.86 (t, 1H, *J* = 7.6 Hz, *H*5), 8.16 (dt, 1H, *J* = 7.6, 1.9 Hz, *H*4), 8.54 – 8.55 (m, 1H, *H*12), 9.10 (d, 1H, *J* = 1.0 Hz, *H*10).

5-{[6-(3-Hydroxyphenyl) pyrimidin-4-yl]amino}-2-methoxyphenol (517)

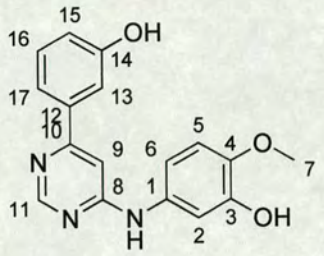

To a solution of 4,6-dichloropyrimidine (0.147 g, 1.0 mmole, 1.1 eq.) in 2-propanol (4 mL), 3-hydroxy-4-methoxyaniline (0.125 g, 0.9 mmole, 1.0 eq.) and *N*,*N*-diisopropylethylamine (172 μL, 1.8 mmole, 2.0 eq.) were added. The reaction mixture was irradiated in the Discover™ at 120 °C for 30 minutes, with active cooling of the sample, and then split into 4 x 1 mL aliquots. To one aliquot was added 3-hydroxy-phenyl boronic acid (0.044 g, 0.32 mmole, 1.4 eq.), potassium carbonate (0.122 g, 0.9 mmole, 4.0 eq.) and $Pd(PPh_3)_4$ (0.10 g, 0.02 mmole, 0.1 eq.). The reaction mixture was irradiated in the Discover™ at 140 °C for 15 minutes, before being injected directly onto the Biotage Parallex Flex™ HPLC (Method S, t_R = 6.27 min) Appropriate fractions were combined and concentrated *in vacuo* to afford pyrimidine **517** as a yellow solid (0.004 g, 6%); LRMS ES^+ *m/z* 309.7 $(MH)^+$; δ_H (250 MHz, CD_3OD): 3.68 (s, 1H, *H*7), 7.02 – 7.18 (m, 5H, *H*2, *H*5, *H*6, *H*13, *H*15), 7.24 (s, 1H, *H*9), 7.29 (d, 1H, *J* = 7.8 Hz, *H*17), 7.48 (t, 1H, *J* = 7.8 Hz, *H*16), 8.75 (s, 1H, *H*11).

3-{6-[(3,5-Dimethoxyphenyl)amino]pyrimidin-4-yl}phenol (518)

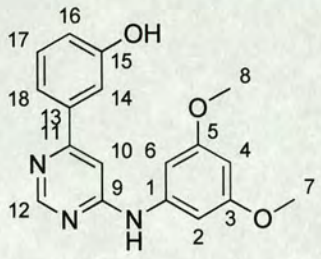

To a solution of 4,6-dichloropyrimidine (0.147 g, 1.0 mmole, 1.1 eq.) in 2-propanol (4 mL), 3,5-dimethoxyaniline (0.137 g, 0.9 mmole, 1.0 eq.) and *N*,*N*-diisopropylethylamine (172 μL, 1.8 mmole, 2.0 eq.) were added. The reaction mixture was irradiated in the Discover™ at 120 °C for 30 minutes, with active cooling of the sample, and then split into aliquots (4 x 1 mL). To one aliquot was added 3-hydroxyphenylboronic acid (0.044 g, 0.32 mmole, 1.4 eq.), potassium carbonate (0.122 g, 0.9 mmole, 4.0 eq.) and $Pd(PPh_3)_4$ (0.10 g, 0.02 mmole, 0.1 eq.). The reaction mixture was irradiated in the Discover™ at 140 °C for 15 minutes, before being injected directly onto the Biotage Parallex Flex™ HPLC (Method S, t_R = 9.02 min) Appropriate fractions were combined and concentrated *in vacuo* to afford pyrimidine **518** as a cream solid (0.006 g, 8%); LRMS ES^+ *m/z* 354.6 $(MH)^+$; δ_H (250 MHz, CD_3OD): 3.84 (s, 6H, *H*7, *H*8), 6.47 (t, 1H, *J* = 2.1 Hz, *H*4), 6.91 (bs, 2H, H2, *H*6), 7.13 (ddd, 1H, *J* = 8.3, 2.1, 0.8 Hz, *H*16), 7.17 (s, 1H, *H*10), 7.24 – 7.32 (m, 3H, *H*14, N*H*, O*H*), 7.49 (t, 1H, *J* = 8.3 Hz, *H*17), 7.74 (d, 1H, *J* = 8.3 Hz, *H*18), 8.83 (s, 1H, *H*12).

Synthesis of 6-anilino-4-chloropyrimidine intermediates

3-[(6-Chloropyrimidin-4-yl)amino]phenol (522)

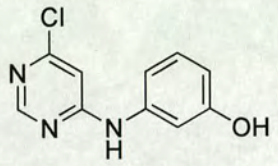

To a solution of 4,6-dichloropyrimidine (0.110 g, 0.74 mmole, 1.1 eq.) in 2-propanol (3 mL) was added 3-hydroxyaniline (0.078 g, 0.67 mmole, 1.0 eq.) followed by DIPEA (117 μL, 1.34 mmole, 2.0 eq.). The reaction mixture was irradiated in the Discover™ at 120 °C for 30 minutes before being injected directly, in 3 x 1 mL aliquots, on the Biotage Parallex Flex™ HPLC (Method A, t_R = 14.24 min.). Pyrimidine **533** was isolated as a white solid (0.109 g, 73%); LRMS ES^+ *m/z* 221.6 $(MH)^+$.

4-[(6-Chloropyrimidin-4-yl)amino]phenol (523)

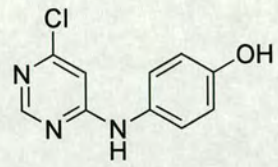

The general procedure for pyrimidine **522** was followed using 4-hydroxyaniline (0.078 g, 0.67 mmole, 1.0 eq.). Pyrimidine **523** was isolated as a white solid (HPLC Method A, t_R = 12.42 min, 0.100 g, 67%); LRMS ES^+ *m/z* 221.5 $(MH)^+$.

6-Chloro-*N*-(3,4-dimethoxyphenyl)pyrimidin-4-amine (524)

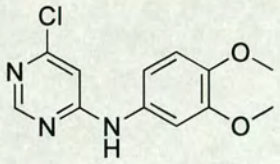

The general procedure for pyrimidine **522** was followed using 3,4-dimethoxyaniline (0.105 g, 0.67 mmole, 1.0 eq.). Pyrimidine **524** was isolated as a white solid (HPLC Method A, t_R = 14.09 min, 0.155 g, 87%); LRMS ES^+ *m/z* 265.6 $(MH)^+$.

6-Chloro-*N*-pyridin-2-ylpyrimidin-4-amine (525)

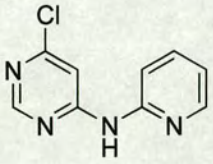

The general procedure for pyrimidine **522** was followed using 2-aminopyridine (0.066 g, 0.67 mmole, 1.0 eq.). Pyrimidine **525** was isolated as a white solid (HPLC Method A, t_R = 8.16 min, 0.015 g, 11%); LRMS ES^+ *m/z* 206.4 $(MH)^+$.

6-Chloro-*N*-phenylpyrimidin-4-amine (526)[219]

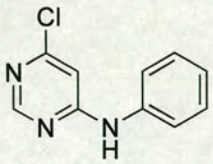

The general procedure for pyrimidine **522** was followed using aniline (0.069 g, 0.67 mmole, 1.0 eq.). Pyrimidine **526** was isolated as a white solid (HPLC Method A, t_R = 17.16 min, 0.090 g, 65%); LRMS ES^+ *m/z* 205.4, 207.4 $(MH)^+$.

1. Hunter, T.; Pines, J.; *Cell* **1994**, 79, 573; Pines, J.; *Cancer Biology*, **1995**, 6, 63; Hartwell, L. H.; Kastan, M. B.; *Science,* **1994**, 266, 1821.
2. Morgan, D. O.; *Nature*, **1995**, 374, 131.
3. Collins, K.; Jacks, T.; Pavletich, N. P.; *Proc. Natl. Acad. Sci. U.S.A.*, **1997**, 94, 2776.
4. Elledge, S.J.; *Science*, **1996**, 274, 1664.
5. Li, J.-M.; Brooks, G.; *European Heart Journal*, **1999**, 20, 406.
6. Sherr, C.J.; *Science*, **1996**, 274, 1672.
7. Aaronson, S. A.; *Science*, **1991**, 254, 1146.
8. Lane, D. P.; Crawford, L. V.; *Nature*, **1979**, 278, 261.
9. Ko, L. J.; Pives, C.; *Genes Dev.*, **1996**, 10, 1054.
10. Kastan, M. B.; Onyekwere, O.; Sidransky, D.; Vogelstein, B.; Craig, R. W.; *Cancer Res.*, **1991**, 51, 6304.
11. Graeber, T. G.; Osmanian, C; Jacks, T.; Housman, D. E.; Koch, C. J.; Lowe, S. W.; Giaccia, A. J.; *Nature*, **1996**, 379, 88.
12. Oren, M.; *J. Biol. Chem.*, **1999**, 274, 36031.
13. Chène, P.; *Nat. Rev. Cancer*, **2003**, 3, 102.
14. el-Deiry, W. S.; Tokino, T.; Velculescu, V. E.; Levy, D. B.; Parsons, R.; Trent, J. M.; Lin, D.; Mercer, W. E.; Kinzler, K. W.; Vogelstein, B.; *Cell*, **1993**, 75, 817.
15. Stewart, Z. A.; Pietenpol, J. A.; *Chem. Res. Toxicol.*, **2001**, 14, 243.
16. Peng, C. Y.; Graves, P. R.; Thoma, R. S.; Wu, Z. Q.; Shaw, A. S.; Piwnica-Worms, H.; *Science*, **1997**, 277, 1501.
17. Hirao, A.; Kong, Y. Y.; Matsuoka, S.; Wakeham, A.; Ruland, J.; Yoshida, H.; Liu, D.; Elledge, S.J.; Mak, T. W.; *Science*, **2000**, 287, 1824.
18. Lopez-Girona, A.; Fumari, B.; Mondesert, O.; Russell, P.; *Nature*, **1999**, 397, 172.
19. Hainuat, P.; Hollstein, M.; *Adv. Cancer Res.*, **2000**, 77, 81.
20. Lane, D. P.; Hupp, T. R.; *Drug Discovery Today*, **2003**, 8, 347.
21. Donehower, L. A.; *Semin. Cancer Biol.*, **1996**, 7, 269.

22. el-Deiry, W. S.; Kern, S. E.; Pietenpol, J. A.; Kinzler, K. W.; Vogelstein, B.; *Nat. Genet.*, **1992**, 1, 45.

23. Pietenpol, J. A.; Tokino, T.; Thiagalingam, S; el-Deiry, W. S.; Kinzler, K. W.; Vogelstein, B.; *Proc. Natl. Acad. Sci. U.S.A.*, **1994**, 91, 1998.

24. Fields, S.; Jang, S. K.; *Science*, **1990**, 249, 1046.

25. Pavletich, N. P.; Chambers, K. A.; Pabo, C. O.; *Genes Dev.*, **1993**, 7, 2556.

26. Clore, G. M.; Ernst, J.; Clubb, R.; Omichinski, J. G.; Kennedy, W. M.; Sakaguchi, K.; Appella, E.; Gronenborn, A. M.; *Nat. Struct. Biol.*, **1995**, 2, 321.

27. Hupp, T. R.; Sparks, A.; Lane, D. P.; *Cell*, **1995**, 83, 237.

28. Cho, Y.; Gorina, S.; Jeffrey, P. D.; Pavletich, N. P.; *Science*, **1994**, 265, 346.

29. Kubbutat, M. H.; Vousden, K. H.; *Molecular Medicine Today*, **1998**, 250.

30. Fakharzadeh, S. S.; Trusko, S. P.; George, D. L.; *EMBO J.*, **1991**, 10, 1565.

31. Momand, J.; Zambetti, G. P.; Olson, D. C.; George, D.; Levine, A. J.; *Cell*, **1992**, 69, 1237.

32. Mayo, L. D.; Turchi, J. J.; Berberich, S. J.; *Cancer Res.*, **1997**, 57, 5013.

33. Oliner, J. D.; Kinzler, K. W.; Meltzer, P. S.; George, D. L.; Vogelstein, B.; *Nature*, **1992**, 358, 80.

34. Picksley, S. M.; Vojtesek, B.; Sparks, A.; Lane, D. P.; *Oncogene*, **1994**, 9, 2523.

35. Balint, E. E.; Vousden, K. H.; *Br. J. Cancer*, **2001**, 85, 1813.

36. Brachmann, R. K.; Yu, K.; Eby, Y.; Pavletich, N. P.; Boeke, J. D.; *EMBO J.*, **1998**, 17, 1847.

37. Ball, K. L.; Lain, S.; Fahraeus, R.; Smythe, C.; Lane, D. P.; *Curr Biol.*, **1997**, 7, 71.

38. Zheleva, D. I.; Lane, D. P.; Fischer, P. M.; *Mini Reviews in Medicinal Chemistry*, **2003**, 3, 167.

39. Oliner, J. D.; Pietenpol, J. A.; Thiagalingam, S.; Gyuris, J.; Kinzler, K. W.; Vogelstein, B.; *Nature*, **1993**, 362, 857.

40. Wu, X.; Bayle, J. H.; Olsen, D.; Levine, A. J.; *Genes Dev.*, **1993**, 7, 1126.

41. Roth, J.; Dobbelstein, M.; Freedman, D. A.; Shenk, T.; Levine, A. J.; *EMBO J.*, **1998**, 17, 554.

42. Tao, W.; Levine, A. J.; *Proc. Natl. Acad. Sci. U.S.A.*, **1999**, 96, 3077.

43. Honda, R.; Tanaka, H.; Yasuda, H.; *FEBS Lett.*, **1997**, 420, 25.

44. Haupt, Y.; Maya, R. Kazaz, A.; Oren, M.; *Nature*, **1997**, 387, 296; Kubbutat, M. H.; Jones, S. N.; Vousden, K. H.; *Nature*, **1997**, 387, 299.

45. Lane, D. P.; Hall, P. A.; *Trends Biochem. Sci.*, **1997**, 22, 372.

46. Montes de Oca Luna, R.; Wagner, D. S.; Lozano, G.; *Nature*, **1995**, 378, 203.

47. Chen, J.; Wu, X.; Lin, J.; Levine, A. J.; *Mol. Cell Biol.*, **1996**, 16, 2445.

48. Schon, O.; Friedler, A.; Bycroft, M.; Freund, S. M. V.; Ferscht, A. R.; *J. Mol. Biol.*, **2002**, 323, 491.

49. Eischen, M. D.; Weber, J. D.; Roussel, M. F.; Sherr, C. J.; Cleveland, J. L.; *Genes Dev.*, **1999**, 13, 2658; Palmero, I.; Pantoja, C.; Serrano, M.; *Nature*, **1998**, 395, 125.

50. Xiao, Z. X.; Chen, J.; Levine, A. J.; Modjtahedi, N.; Xing, J.; Sellers, W. R.; Livingston, D. M.; *Nature*, **1995**, 375, 694.

51. Leveillard, T.; Wasylyk, B.; *J. Biol. Chem.*, **1997**, 272, 30651.

52. Chen, J.; Marechal, V.; Levine, A. J.; *Mol. Cell Biol.*, **1993**, 13, 4107.

53. Lin, J.; Chen, J.; Elenbaas, B.; Levine, A. J.; *Genes Dev.*, **1994**, 8, 1235.

54. Kussie, P. H.; Gorina, S.; Marechal, V.; Elenbaas, B.; Moreau, J.; Levine, A. J.; Pavletich, N. P.; *Science*, **1996**, 274, 948.

55. Massova, I.; Kollman, P. A.; *J. Am. Chem. Soc.*, **1999**, 121, 8133.

56. Blommers, M. J. J.; Fendrich, G.; Garcia-Echeverria, C.; Chène, P.; *J. Am. Chem. Soc.*, **1997**, 119, 3425.

57. Pavletich, N. P.; Chambers, K. A.; Pabo, C. O.; *Genes Dev.*, **1993**, 7, 2556

58. Böttger, A.; Böttger, V.; Garcia-Echeverria, C.; Chene, P.; Hochkeppel, H. K.; Sampson, W.; Ang, K.; Howard, S. F.; Picksley, S. M.; Lane, D. P.; *J. Mol. Biol.*, **1997**, 269, 744.

59. Wasylyk, C.; Salvi, R.; Argentini, M.; Durelli, C.; Delumeau, I.; Abecassis, J.; Debussche, L.; Wasylyk, B.; *Oncogene*, **1999**, 18, 1921.

60. Blaydes, J. P.; Gire, V.; Rowson, J. M.; Wynford-Thomas, D.; *Oncogene*, **1997**, 14, 1859.

61. Blaydes, J. P.; Wynford-Thomas, J. P.; *Oncogene*, **1998**, 16, 3317.

62. Kanovsky, M.; Raffo, A.; Drew, L.; Rosal, R.; Do, T.; Friedman, F. K.; Rubinstein, P.; Visser, J.; Robinson, R.; Brandt-Rauf, P. W.; Michl, J.; Fine, R. L.; Pincus, M. R.; *Proc. Natl. Acad. Sci. U.S.A.*, **2001**, 98, 12438.

63. Yang, A.; McKeon, F.; *Nat. Rev. Mol. Cell Biol.*, **2000**, 1, 199.

64. Levrero, M.; De Laurenzi, V.; Costanzo, A.; Sabatini, S.; Gong, J.; Wang, J. Y. J.; Melino, G.; *J. Cell. Sci.*, **2000**, 113, 1661.

65. Shvarts, A.; Steegenga, W. T.; Ritco, N.; van Laar, T.; Dekker, P.; Bazuine, M.; van Ham, R. C.; van der Houven van Oordt, W.; Hateboer, G.; van der Eb, A. J.; Jochemsen, A. G.; *EMBO J.*, **1996**, 15, 5349.

66. Ongkeko, W. M.; Wang, X. Q.; Sui, W. Y.; Lau, A. W.; Yamashita, K.; Harris, A. L.; Cox, L. S.; Poon, R. Y.; *Curr. Biol.*, **1999**, 9, 829.

67. Kadakia, M.; Slader, C.; Berberich, S. J.; *DNA Cell Biol.*, **2001**, 20, 321.

68. Böttger, A.; Böttger, V.; Garcia-Echeverria, C.; Ramos, Y. F. M.; van der Eb, A. J.; Jochemsen, A. G.; Lane, D. P.; *Oncogene*, **1999**, 18, 189.

69. Garcia-Echeverria, C.; Chene, P.; Blommers, M. J.; Furet, P.; *J. Med. Chem.*, **2000**, 43, 3205.

70. Duncan, S. J.; Gruschow, S.; Williams, D. H.; McNicholas, C.; Purewal, R.; Hajek, M.; Gerlitz, M.; Martin, S.; Wrigley, S. K.; Moore, M.; *J. Am. Chem. Soc.*, **2001**, 123, 554.

71. Zhao, J.; Wang, M.; Chen, J.; Luo, A.; Wang, X.; Wu, M.; Yin, D.; Liu, Z.; *Cancer Lett.*, **2002**, 183, 69.

72. Stoll, R.; Renner, C.; Hansen, S.; Palme, S.; Klein, C.; Belling, A.; Zeslawski, W.; Kamionka, M.; Rehm, T.; Muhlhahn, P.; Schumaker, R.; Hesse, F.; Kaluza, B.; Voelter, W.; Holak, T. A.; *Biochemistry*, **2001**, 40, 336.

73. Stoll, R.; Renner, C.; Muhlhahn, P.; Hansen, S.; Schumaker, R.; Hesse, F.; Kaluza, B.; Engh, R. A.; Voelter, W.; Holak, T. A.; *J. Biomol. NMR*, **2000**, 17, 91.

74. Vassilev, L. T.; Binh, T. V.; Graves, B.; Carvajal, D.; Podlaski, F.; Filipovic, Z.; Kong, N.; Kammlott, U.; Lukacs, C.; Klein, C.; Fotouhi, N.; Liu, E. A.; *Science*, **2004**, 303, 844.

75. Walkinshaw, M.D.; Weber, H. P.; Widmer, A., *Triangle*, **1986**, 25, 131.

76. Gubernator, K.; Boehm, M., *Methods Princ. Med. Chem.*, 1998, **6**, 1.

77. Tsunoda, T.; Otsuka, J.; Yamamiya, Y.; Ito, S.; *Chem. Letters*, **1994**, 539; Tsunoda, T.; Yamamiya, Y.; Ito, S.; *Tetrahedron. Lett.*, **1993**, 1639.

78. Gajda, T.; Zwierzak, A.; *Synthesis*, **1981**, 1005.

79. Mitsunobu, O.; *Bull. Chem. Soc. Jpn.*, **1967**, 40, 4235.

80. Mitsunobu, O.; *Synthesis*, **1981**, 1.

81. Hughes, D. L.; Reamer, R. A.; *J. Org. Chem.*, **1996**, 61, 2967.

82. Koppel, I.; Koppel, J.; Degerbeck, F.; Grehn, L.; Ragnarsson, U., *J. Org. Chem.*, **1991**, 56, 7172.

83. Arcoria, A.; Maccarone, E.; Musumara, G.; Tomaselli, G., A.; *J. Org. Chem.*, **1973**, 38, 2457.

84. Barnish, I., T.; Cross, P., E.; Dickinson, R., P.; Parry, M., J.; Randall, M., J.; *J. Med. Chem.*, **1981**, 24, 959.

85. Park, Y. J.; Shin, H. H.; Kim, Y. H.; *Chem. Lett.*, **1992**, 1483.

86. Shai, Y.; Jacobsen, K. A.; Patchornik, A.; *J. Am. Chem. Soc.*, **1985**, 107, 4249.

87. Borch, R. F.; Bernstein, M. D.; Durst, H. D.; *J. Am. Chem. Soc.*, **1971**, 93, 2897.

88. Fu, M.; Nikolic, D.; Van Breemen, R. B.; Silverman, R. B.; *J. Am. Chem. Soc.*, **1999**, 121, 7751.

89. Satonaka, H.; *Bull. Chem. Soc. Jpn.*, **1983**, 56, 2463.

90. Booth, R. J.; Hodges, J.C.; *J. Am. Chem. Soc.*, **1997**, 119, 4882.

91. Perreux, L. P.; Loupy, A.; Volatron, F.; *Tetrahedron*, **2002**, 58, 2155.

92. Galvez, C.; Garcia, F.; Garcia, J.; Soldevila, J.; *J. Heterocyclic Chem.*, **1986**, 23, 1103.

93. Curtius, T.; *Ber. Dtsch. Chem. Ges.*, **1890**, 23, 3023.

94. Hunter, T.; *Cell* **2000**, 100, 113; Blume-Jensen, P.; Hunter, T.; *Nature*, **2001**, 411, 355.

95. Fabbro, D.; Ruetz, S.; Buchdunger, E.; Cowan-Jacob, S. W.; Fendrich, G.; Liebetanz, J.; Mestan, J.; O'Reilly, T.; Traxler, P.; Chaudhuri, B.; Fretz, H.; Zimmermann, J.; Meyer, T.; Caravatti, G.; Furet, P.; Manley, P. W.; *Pharmacology & Therapeutics*, **2002**, 93, 79.

96. International Human Genome Sequencing Consortium; *Nature*, **2001**, 409, 860.

97. Marshall, J. C.; *Curr. Opin. Cell Biol.*, **1996**, 8, 197.

98. Sherr, C. J.; *Cancer Res.*, **2000**, 60, 3689.

99. Yarden, Y.; Sliwkowski, M. X.; *Nat. Rev. Mol. Cell Biol.*, **2001**, 2, 127.

100. Sasaki, S.; Hashimoto, T.; Obana, N.; Yasuda, H.; Uehara, Y.; Maeda, M.; *Bioorg. Med. Chem. Lett.*, **1998**, 8, 1019.

101. Dalgarno, D. C.; Metcalf, C. A.; Shakespeare, W. C.; Sawyer, T. K.; *Curr. Opin. Drug Discov. Devel.*, **2000**, 3, 549.

102. Pines, J.; *Adv. Cancer Res.*, **1995**, 55, 181.

103. Hunter, T.; Pines, J.; *Cell*, **1994**, 79, 573.

104. Dowdy, S. F.; Hinds, P. W.; Louie, K.; Reed, S. I.; Arnold, A.; Weinberg, R. A.; *Cell*, **1993**, 73, 499.

105. Dyson, N.; *Genes Dev.*, **1998**, 12, 2245.

106. Sherr, C. J.; *Science*, **1996**, 274, 1672

107. Reviewed in Fry, D. W.; Garrett, M. D.; *Curr. Opin. Oncol. Endocrine Metab. Invest. Drugs*, **2000**, 2, 40.

108. Kaldis, P.; *Cell Mol. Life Sci.*, **1999**, 55, 284.

109. Knockaert, M.; Greengard, P.; Meijer, L.; *Trends Pharmacol. Sci.*, **2002**, 9, 417.

110. Morgan, D. O.; *Nature*, **1995**, 374, 131.

111. Espinoza, F. H.; Farrell, A.; Erdjument-Bromage, H.; Tempst, P.; Morgan, D. O.; *Science*, **1996**, 273, 1714.

112. Russo, A. A.; Jeffrey, P. D.; Pavletich, N. P.; *Nature Struct. Biol.*, **1996**, 3, 696.

113. Serrano, M.; *Exp. Cell Res.*, **1997**, 237, 7.

114. Sherr, C. J.; Roberts, J. M.; *Genes Dev.*, **1995**, 1149.

115. Johnson, L. N.; Lewis, R.: *Chem. Rev.*, **2001**, 101, 2209.

116. De Bondt, H. L.; Rosenblatt, J.; Jancarik, J.; Jones, H. D.; Morgan, D. O.; Kim, S. H.; *Nature*, **1993**, 363, 595.

117. Jeffrey, P. D.; Russo, A. A.; Polyak, K.; Gibbs, E.; Hurwitz, J.; Massague, J.; Pavletic, N. P.; *Nature*, **1995**, 376, 313.

118. Kim, S. H.; *Pure Appl. Chem.*, **1998**, 70, 555.

119. Schulze-Gahmen, U.; De Bondt, H. L.; Kim, S. H.; *J. Med. Chem.*, **1996**, 39, 4540.

120. Kim, K. S.; Sack, J. S.; Tokarski, J. S.; Qian, L.; Chao, S. T.; Leith, L.; Kelly, Y. F.; Misra, R. N.; Hunt, J. T.; Kimball, S. D.; Humphreys, W. G.; Wautlet, B. S.; Mulheron, J. G.; Webster, K. R.; *J. Med. Chem.*, **2000**, 43, 4126.

121. Wu, S. Y.; McNae, I.; Kontopidis, G.; McClue, S. J.; McInnes, C.; Stewart, K. J.; Wang, S.; Zheleva, D. I.; Marriage, H.; Lane, D. P.; Taylor, P.; Walkinshaw, M. D.; *Structure*, **2003**, 11, 399.

122. Gray, N. S.; Wodicka, L.; Thunissen, A. –M. W. H.; Norman, T. C.; Kwon, S.; Espinoza, F. H.; Morgan, D. O.; Barnes, G.; LeClerc, S.; Meijer, L.; Kim, S. H.; Lockhart, D. J.; Schultz, P. G.; *Science*, **1998**, 281, 533.

123. De Azevedo, W. F.; LeClerc, S.; Meijer, L.; Havlicek, L.; Strnad, M.; Kim, S. H.; Eur. *J. Biochem.*, **1997**, 243, 518.

124. Legraverend, M.; Tunnah, P; Noble, M.; Ducrot, P.; Ludwig, O.; Grierson, D. S.; Leost, M.; Meijer, L.; Endicott, J.; *J. Med. Chem.* **2000**, 43, 1282.

125. Noble, M. E. M.; Endicott, J. A.; *Pharmacol. Ther.*, **1999**, 82, 269.

126. Davies, T. G.; Tunnah, P.; Meijer, L.; Marko, D.; Eisenbrand, G.; Endicott, J. A.; Noble, M. E. M.; *Structure*, **2001**, 9, 389.

127. Furusaki, A.; Hashiba, N.; Matsumoto, T.; Hirano, A.; Iwai, Y.; Omura, S.; *Bull. Chem. Soc. Jpn.*, **1982**, 55, 3681.

128. Gadbois, D.; Hamaguchi, J. R.; Swank, R. A.; Bradbury, E. M.; *Biochem. Biophys. Res. Commun.*, **1992**, 184. 80.

129. Meijer, L.; *Progress in Cell Cycle Research*, **1995**, 1, 351.

130. Lawrie, A. M.; Noble, M. E. M.; Tunnah, P.; Brown, N. R.; Johnson, L. N.; Endicott, J. A.; *Nat. Struc. Biol.*, **1997**, 4, 796.

131. Newell, D. R.; *Clin. Cancer Res.*, **2001**, 7(Suppl.), 3822s.

132. Engler, T. A.; Furness, K.; Malhotra, S.; Sanchez-Martinez, C.; Shih, C.; Xie, W.; Guoxin, Z.; Zhou, X.; Conner, S.; Faul, M. M.; Sullivan, K. A.; Kolis, S. P.; Brooks, H. B.; Patel, B.; Schultz, R. M.; DeHahn, T. B.; Kirmani, K.; Spencer, C. D.; Watkins, S. A.; Considine, E. L.; Dempsey, J. A.; Ogg, C. A.; Stamm, N. B.; Anderson, B. D.; Campbell, R. M.; Vasudevan, V.; Lytle, M. L.; *Bioorg. Med. Chem. Lett.*, **2003**, 13, 2261.

133. Ranelleti, F. O.; Ricci, R.; Larocca, L. M.; Maggiano, N.; Capelli, A.; Scamibia, G.; Benedett-Pancini, P.; Mancuso, S.; Rumi, C.; Piantelli, M.; *Int. J. Cancer*, **1992**, 50, 486.

134. Losiewicz, M. D.; Carlson, B. A.; Kaur, G.; Sausville, E. A.; Worland, P. J.; *Biochem. Biophys. Res. Commun.*, **1994**, 201, 589.

135. Carlson, B. A.; Dubay, M. M.; Sausville, E. A.; Brizuela, L.; Worland, P. J.; *Cancer Res.*, **1996**, 56, 2973.

136. Schwartz, G. K.; Farsi, D.; Greaney, C.; Werner, J.; Kelsen, D. K.; *Prog. Gastric Res.*, **1997**, 1, 627.

137. De Azevedo, W. F. Jr.; Meuller-Dieckmann, H.; Schulze-Gahmen, U.; Worland. P. J.; Sausville, E.; Kim, S.; *Proc. Natl. Acad. Sci. U.S.A.*, **1996**, 93, 2735.

138. Paull, K. D.; Hamel, E.; Malspeis, L.; In *Cancer Chemotherapeutic Agents*, American Chemical Society Books, **1995**, 9.

139. Zaharevitz, D. W.; Gussio, R.; Leost, M.; Senderowicz, A. M.; Lahusen, T.; Kunick, C.; Meijer, L.; Sausville, E. A.; *Cancer Res.*, **1999**, 59, 2566.

140. Schultz, C.; Link, A.; Leost, M.; Zaharevitz, D. W.; Gussio, R.; Sausville, E. A.; Meijer, L.; Kunick, C.; *J. Med. Chem.*, **1999**, 42, 2909.

141. Kunick, C.; Schultz, C.; Lemcke, T.; Zaharevitz, D. W.; Gussio, R.; Jalluri, R. K.; Sausville, E. A.; Leost, M.; Meijer, L.; *Bioorg. Med. Chem. Lett.*, **2000**, 10, 567.

142. Leost, M.; Schultz, C.; Link, A.; Wu, Y. –Z.; Biernat, J.; Mandelkow, E. –M.; Bibb, J. A.; Snyder, G. L.; Greengard, P.; Zaharevitz, D. W.; Gussio, R.; Senderowicz, A. M.; Sausville, E. A.; Kunick, C.; Meijer, L.; *Eur. J. Biochem.*, **2000**, 267, 5983.

143. Larner, A. W.; *Exp. Opin. Ther. Patents*, **1999**, 9, 1359.

144. Vesely, J.; Havlicek, L.; Strnad, M.; Blow, J. J.; Donella-Deana, A.; Pinna, L.; Letham, D. S.; Kato, J. Y.; Detivaud, L.; LeClerc, S.; Meijer, L.; *Eur. J. Biochem.*, **1994**, 224, 771.

145. Davies, T. G.; Pratt, D. J.; Endicott, J. A.; Johnson, L. N.; Noble, M. E. M.; *Pharmacology & Therapeutics*, **2002**, 92, 125.

146. Furet, P; Zimmerman, J.; Capraro, H. –G.; Meyer, T.; Imbach, P.; *J. Comput. Aided Mol. Des.*, **2000**, 14, 403.

147. Dreyer, M. K.; Borcherding, D. R.; Dumont, J. A.; Peet, N. P.; Tsay, J. T.; Wright, P. S.; Bitonti, A. J.; Shen, J.; Kim, S. H.; *J. Med. Chem.*, **2001**, 44, 524.

148. Hajduch, M.; Havlicek, L.; Vesely, J.; Novotny, R.; Mihal, V.; Strnad, M.; *Adv. Exp. Med. Biol.*, **1999**, 457, 341.

149. Schow, S. R.; Mackmam, R. L.; Blum, C. L.; Brooks, E.; Horsma, A. G.; Joly, A.; Kerwar, S. S.; Lee, G.; Shiffman, D.; Nelson, M. G.; Wang, X.; Wick, M. M.; Zhang, X.; Lum, R. T.; *Bioorg. Med. Chem. Lett.*, **1997**, 7, 2697.

150. Legraverend, M.; Ludwig, O.; Bisagni, E.; Leclerc, S.; Meijer, L.; *Bioorg. Med. Chem. Lett.*, **1998**, 8, 793.

151. Moravec, J.; Krystof, V.; Hanus, J.; Havlicek, L.; Moracova, D.; Fuksova, K.; Kuzma, M.; Lenobel, R.; Otyepka, M; Strnad, M.; *Bioorg. Med. Chem. Lett.*, **2003**, 13, 2993.

152. Ortega, M. A.; Montoya, M. E.; Zarranz, B.; Jaso, A.; Aldana, I.; LeClerc, S.; Meijer, L.; Monge, A.; *Bioorg. Med. Chem.*, **2002**, 10, 2177.

153. Kent, L. L.; Hull-Campbell, N. E.; Lau, T.; Wu, J. C.; Thompson, S. A.; Nori, M.; *Biochem. Biophys. Res. Commun.*, **1999**, 260, 768.

154. Cheung, M.; Glennon, K. C.; Lackey, K. E.; Peel, M. R.; PCT. Int. Appl. WO9921859 A1 990506.

155. Bramson, H. N.; Corona, J.; Davis, S. T.; Dickerson, S. H.; Edelstein, M.; Frye, S. V.; Gampe, R. T.; Harris, P. A.; Hassel, A.; Holmes, W. D.; Hunter, R. N.; Lackey, K. E.; Lovejoy, B.; Luzzio, M. J.; Montana, V.; Rocque, W. J.; Rusnak, D.; Shewchuk, L.; Veal, J. M.; Walker, D. H.; Kuyper, L. F.; *J. Med. Chem.*, **2001**, 44, 4339.

156. Nugiel, D. A.; Vidwans, A.; Etzkorn, A. –M.; Rossi, K. A.; Benfield, P. A.; Burton, C. R.; Cox, S.; Doleniak, D.; Seitz, S. P.; *J. Med. Chem.*, **2002**, 45, 5224.

157. Yue, E. W.; Higley, C. A.; DiMeo, S. V.; Carini, D. J.; Nugiel, D. A.; Benware, C.; Benfield, P. A.; Burton, C. R.; Cox, S.; Grafstrom, R. H.; Sharp, D. M.; Sisk, L. M.; Boylan, J. F.; Muckelbauer, J. K.; Smallwood, A. M.; Chen, H.; Chang, C. –H.; Seitz, S. P.; Trainor, G. L.; *J. Med. Chem.*, **2002**, 45, 5233.

158. Tang, J.; Shewchuk, L. M.; Sato, H.; Hasegawa, M.; Washio, Y.; Nishigaki, N.; *Bioorg. Med. Chem. Lett.*, **2003**, 13, 2985.

159. Arris, C. E.; Boyle, F. T.; Calvert, A. H.; Curtin, N. J.; Endicott, J. A.; Garmen, E. F.; Gibson, A. E.; Golding, T. E.; Grant, S.; Griffen, R. J.; Jewsbury, P.; Johnson, L. N.; Lawrie, A. M.; Newell, D. R.; Noble, M. E. M.; Sausville, E. A.; Schultz, R.; Yu, W.; *J. Med. Chem.*, **2000**, 43, 2797.

160. Gibson, A. E.; Arris, C. E.; Bentley, J.; Boyle, F. T.; Curtin, N. J.; Davies, T. G.; Endicott, J. A.; Golding, B. T.; Grant, S.; Griffen, R. J.; Jewsbury, P.;

Johnson, L. N.; Mesguiche, V.; Newell, D. R.; Noble, M. E. M.; Tucker, J. A.; Whitfield, H. J.; *J. Med. Chem.*, **2002**, 45, 3381.

161. Sayle, K. L.; Bentley, J.; Boyle, F. T.; Calvert, A. H.; Cheng, Y.; Curtin, N. J.; Endicott, J. A.; Golding, B. T.; Hardcastle, I. R.; Jewsbury, P.; Mesguiche, V.; Newell, D. R.; Noble, M. E. M.; Parsons, R. J.; Pratt, D. J.; Wang, L. Z.; Griffen, R. J.; *Bioorg. Med. Chem. Lett.*, **2003**, 13, 3079.

162. Moracova, D.; Krystof, V.; Havlicek, L.; Moravec, J.; Lenobel, R.; Strnad, M.; *Bioorg. Med. Chem. Lett.*, **2003**, 13, 2989.

163. Barvain, M.; Boschelli, D. H.; Cossrow, J.; Dobrusin, E.; Fattaey, A.; Fritsch, A.; Fry, D.; Harvey, P.; Keller, P.; Garrett, M.; La, F.; Leopold, W.; McNamara, D.; Quin, M.; Trumpp-Kallmeyer, S.; Toogood, P.; Wu, Z.; Zhang, E.; *J. Med. Chem.*, **2000**, 43, 4606.

164. Anderson, M.; Beattie, J. F.; Breault, G. A.; Breed, J.; Byth, K. F.; Culshaw, J. D.; Ellston, R. P. A.; Green, S.; Minshull, C. A.; Norman, R. A.; Paupit, R. A.; Stanway, J.; Thomas, A. P.; Jewsbury, P. J.; *Bioorg. Med. Chem. Lett.*, **2003**, 13, 3021.

165. Wang, S.; Meades, C.; Wood, G.; Osnowski, A.; Anderson, S.; Yuill, R.; Thomas, M.; Mezna, M.; Jackson, W.; Midgley, C.; Griffiths, G.; Fleming, I.; Green, S.; McNae, I.; Wu, S. –Y.; McInnes, C.; Zheleva, D.; Walkinshaw, M. D.; Fischer, P. M.; *J. Med. Chem.*, **2004**, 47, 1662.

166. McInnes, C.; Wang, S.; Anderson, S.; O'Boyle, J.; Jackson, W.; Kontopidis, G.; Meades, C.; Mezna, M.; Thomas, M.; Wood, G.; Lane, D. P.; Fischer, P. M.; *Chem. Biol.*, **2004**, 11, 525.

167. Beattie, J. F.; Breault, G. A.; Ellston, R. P. A.; Green, S.; Jewsbury, P. J.; Midgley, C. J.; Naven, R. T.; Minshull, C. A.; Paupit, R. A.; Tucker, J. A.; Pease, J. E.; *Bioorg. Med. Chem. Lett.*, **2003**, 13, 2955.

168. Breault, G. A.; Ellston, R. P. A.; Green, S.; James, S. R.; Jewsbury, P. J.; Midgley, C. J.; Paupit, R. A.; Minshull, C. A.; Tucker, J. A.; Pease, J. E.; *Bioorg. Med. Chem. Lett.*, **2003**, 13, 2961.

169. Meijer, L.; Skaltsounis, A. –L.; Magiatis, P.; Polychronopoulos, P.; Knockaert, M.; Leost, M.; Ryan, X. P.; Vonica, C. A.; Brivanlou, A.; Dajani, R.; Crovace, C.; Tarricone, C.; Musacchio, A.; Roe, M.; Pearl, L.; Greengard, P.; *Chem. Biol.*, **2003**, 10, 1255.

170. Cyclacel Ltd., *Unpublished work.*

171. Miyaura, N.; Suzuki, A.; *Chem. Rev.*, **1995**, 95, 2457.

172. Milstein, D.; Stille, J. K.; *J. Am. Chem. Soc.*, **1978**, 100, 3636.

173. Negishi, E.; King, A. O.; Okukado, N.; *J. Org. Chem.*, **1977**, 42, 1821.

174. Heck, R. F.; Dieck, H. A.; *J. Am. Chem. Soc.*, **1974**, 96, 1133.

175. Tamao, K.; Sumitani, K.; Kumada, M.; *J. Am. Chem. Soc.*, **1972**, 94, 4374.

176. Sonogashira, K.; Tohda, Y.; Hagihara, N.; *Tetrahedron Lett.*, **1975**, 16, 4467.

177. Hatanaka, Y.; Hiyama, T.; *J. Org. Chem.*, **1988**, 53, 918.

178. Miyaura, N.; *Adv. Met. Org. Chem.*, **1998**, 6, 187.

179. Grushin, V. V.; Alper, H.; *Chem. Rev.*, **1994**, 94, 1047.

180. For examples see; a) Ishikura, M.; Kumada, M.; Terashima, M.; *Synthesis*, **1984**, 936; b) Mitchell, M. B.; Wallbank, P. J.; *Tetrahedron Lett.*, **1991**, 32, 2273; c) Ali, N. M.; McKillop, A.; Mitchell, M. B.; Rebelo, R. A.; Wallbank, P. J.; *Tetrahedron*, **1992**, 48, 8117; d) Cocuzza, A. J.; Chidester, D. R.; Culp, S.; Fitzgerald, L.; Gilligan, P.; *Bioorg. Med. Chem. Lett.*, **1999**, 9, 1063; e) Ciufolini, M. A.; Mitchell, J. W.; Roschangar, F.; *Tetrahedron Lett.*, **1996**, 37, 8281; f) Alcock, N. W.; Brown, J. M.; Hulmes, D. I.; *Tetrahedron: Asymmetry*, **1993**, 4, 743; g) Chapouland, V. G.; Audoux, J.; Plé, N.; Turck, G.; Quéguiner, G.; *Tetrahedron*, **1999**, 40, 9005; h) Havelkova, M.; Hocek, M.; Cesnek, M.; Dvorak, D.; *Synlett.*, **1999**, 1145.

181. Shen, W.; *Tetrahedron Lett.*, **1997**, 38, 5575.

182. Gronowitz, S.; Hoenfeldt, A.-B.; Kristjannson, V.; Musil, T.; *Chem. Scr.*, **1986**, 26, 305.

183. Jiang, B.; Yang, C.-g.; *Heterocycles*, **2000**, 53, 1489.

184. Gong, Y.; Pauls, H. W.; *Synlett.*, **2000**, 829.

185. Schomaker, J. M.; Delia, T. J.; *J. Org. Chem.*, **2001**, 66, 7125.

186. Cocuzza, A. J.; Chidester, D. R.; Culp, S.; Fitzgerald, L.; Gilligan, P.; *Bioorg. Med. Chem. Lett.*, **1999**, 9, 1063.

187. Lidström, P.; Tierney, J.; Wathey, B.; Westman, J.; *Tetrahedron*, **2001**, 57, 9225.

188. Binner, J. G. P.; Hassine, N. A.; Cross, T. E.; *J. Mater. Sci.*, **1995**, 30, 5389.

189. Berlan, J.; Giboreau, P.; Lefeuvre, S.; Marchand, C; *Tetrahedron Lett.*, **1991**, 32, 2363.

190. Varma, R. S.; *J. Heterocycl. Chem.*, **1999**, 36, 1565.

191. Loupy, A.; Petit, A.; Hamelin, J.; Texier-Boullet, F.; Jacquault, P.; Mathé, D.; *Synthesis*, **1998**, 1213.

192. Deshayes, S.; Liagre, M.; Loupy, A.; Luche, J. –L.; Petit, A.; *Tetrahedron*, **1999**, 55, 10851.

193. de la Hoz, A.; Díaz-Ortis, A.; Moreno, A.; Langa, F.; *Eur. J. Org. Chem.*, **2000**, 3659.

194. Kaiser, N. –F. K.; Bremberg, U.; Larhed, M.; Moberg, C.; Hallberg, A.; *Angew. Chem.*, **2000**, 112, 3742.

195. Kappe, C. O.; *Curr. Opin. Chem. Biol.*, **2002**, 6, 314.

196. Stadler, A.; Kappe, C. O.; *J. Comb. Chem.*, **2001**, 3, 624.

197. Causton, A. S.; Turner, N. J.; *Unpublished work.*

198. Qing, F. –L.; Wang, R.; Li, B.; Zheng, X.; Meng, W. –D.; *J. Flourine. Chem.*, **2003**, 120, 21.

199. Anderson, C. B.; Burreson, B. J.; Michalowski, T. J.; *J. Org. Chem.*, **1976**, 41, 1990.

200. Dina, S.; Grav, N. S.; Wu, X.; Dina, Q.; Schultz, P. G.; *J. Am. Chem. Soc.*, **2002**, 124, 1594.

201. Wade, J. V.; Krueger, C. A.; *J. Comb. Chem.* **2003**, 5, 267.

202. Luo, G.; Chen, L.; Poindexter, G. S.; *Tetrahedron Lett*, **2002**, 43, 5739.

203. Harris, R. L. N.; *Synthesis*, **1981**, 11, 907.

204. Davies, S. P.; Reddy, H.; Caivano, M.; Cohen, P.; *Biochem. J.*, **2000**, 351, 95.

205. Acoria, A.; Maccarone, E.; Musumarra, G.; Tomaselli, G. A.; *J. Org. Chem.*, **1973**, 14, 2457.

206. Obafemi, C. A.; *Phosphorus, Sulfur Relat. Elem.*; **1980**, 2, 201.

207. Edwards, L. H.; *U.S. Patent 3991081*, **1976**.

208. Ballistreri, A.; Maccarone, E.; Musumarra, G.; *J. Chem. Soc., Perkin Trans.2*, **1977**, 7, 984.

209. Mikhailova, V. N.; *Zh. Obshch. Khim.*, **1976**, 46, 879.

210. Burger, A.; Hornbaker, E. D.; *J. Org. Chem.*; **1953**, 18, 192.

211. Gerasimova, T. N.; *Zh. Obshch. Khim.*, **1965**, 1, 1667.

212. El-Sheikh, M. I.; *J. Org. Chem.*, **1981**, 46, 3256.

213. Gowda, B. T.; *Spectrochim. Acta, Part A*, **2004**, 60A, 1225.

214. Welch, D. E.; Baron, R. R.; *J. Med. Chem.*, **1969**, 12, 957.

215. Hurd, C. D.; Kreuz, K. L.; *J. Am. Chem. Soc.*, **1952**, 74, 2695.

216. Marques, M. A.; Doss, R. M.; Urbach, A. R.; Dervan, P. B.; *Helv. Chim. Acta*, **2002**, 85, 4485.

217. van der Plas, H. C.; *Recl. Trav. Chim. Pays-Bas*, **1965**, 84, 1101.

218. Bredereck, H.; Gompper, R.; Herlinger, H.; *Chem. Ber.*, **1958**, 91, 2830.

219. Higashino, T.; Hayashi, E.; Matsuda, H.; Katori, T.; *Heterocycles*, **1981**, 15, 483.